1-1-2013

Chiral Binaphthoquinones: Versatile Precursors for the Synthesis of Natural Products and Ligands for Asymmetric Catalysis

Erin Podlesny
University of Pennsylvania, podler01@gmail.com

Chiral Binaphthoquinones: Versatile Precursors for the Synthesis of Natural Products and Ligands for Asymmetric Catalysis

Abstract
The efforts described in this dissertation initially focus on the asymmetric synthesis of axially chiral binaphtho-*para*- and binaphtho-*ortho*-quinones, followed by an exploration of their utility in natural product synthesis, development of ligands for asymmetric catalysis, and development as potential sensors. Axially chiral binaphtho-*para*- and *in-in*-binaphtho-*ortho*-quinones were synthesized through a concerted route involving the enantioselective coupling of a hindered 8-substituted 2-naphthol, with a diaza-*cis*-decalin copper catalyst developed previously by the Kozlowski group. The coupling was achieved in 62% yield and 87% ee (a single trituration produced material of >99% ee). Subsequent transformations led to an 8,8'-hydroxylated binaphthol, which was selectively oxidized to a binaphtho-*para*-quinone using a Co-salen catalyst or transformed to the *in-in*-binaphtho-*ortho*-quinone with *o*-iodoxybenzoic acid (IBX). Similarly, the *out-out*-binaphtho-*ortho*-quinone was synthesized from a 6,6'-hydroxylated binaphthol, using IBX.

Binaphtho-*para*-quinones were used as key intermediates for the synthesis of the bisanthraquinone natural product (*S*)-bisoranjidiol. (*S*)-Bisoranjidiol was synthesized from a 6,6'-dibrominated binaphtho-*para*-quinone and mixed vinyl ketene acetal, through

a regioselective tandem Diels-Alder/aromatization reaction. This transformation was achieved in 80% yield (~95% per transformation). The synthesis of (*S*)-bisoranjidiol was completed in 4% yield over 12 steps, and >99% ee. In addition, the synthesis of a reported binaphthalene tetraol natural product was achieved through reduction of an *out-out*-binaphtho-*ortho*-quinone. This synthesis led to the structural reassignment of the proposed compound to a tetrabrominated diphenyl ether. Condensation of various phenylenediamines with binaphtho-*ortho*-quinones led to bisbenzo[*a*]phenazines, which represent BINOL derivatives with electron-withdrawing groups (pyrazine ring). The *in-in*-bisbenzo[*a*]phenazines performed better than BINOL, but did not offer improvements over the electron-deficient BINOL based catalysts/ligands reported for those reactions. The bisbenzo[*a*]phenazines, in particular the tetrachlorinated derivatives, also displayed a series of interesting properties and colorimetric responses to various stimuli (chromism), which may lead to the development of colorimetric sensors. The properties include mechanochromism, thermochromism, solvatochromism, vapochromism, acidochromism, and fluorescence.

Degree Type
Dissertation

Degree Name
Doctor of Philosophy (PhD)

Graduate Group
Chemistry

First Advisor
Marisa C. Kozlowski

Keywords
binaphthoquinone, bisanthraquinone, bisbenzo[a]phenazine, bisoranjidiol, Diels-Alder, enantioselective

Subject Categories
Organic Chemistry

CHIRAL BINAPHTHOQUINONES:

VERSATILE PRECURSORS FOR THE SYNTHESIS OF NATURAL PRODUCTS AND LIGANDS FOR ASYMMETRIC CATALYSIS

Erin E. Podlesny

A DISSERTATION

in

Chemistry

Presented to the Faculties of the University of Pennsylvania

in

Partial Fulfillment of the Requirements for the

Degree of Doctor of Philosophy

2013

Supervisor of Dissertation	Graduate Group Chairperson
_____	_____
Marisa C. Kozlowski Professor of Chemistry	Gary A. Molander Hirschmann-Makineni Professor of Chemistry

Dissertation Committee:

Madeleine M. Joullié, Professor of Chemistry
Amos B. Smith III, Rhodes-Thompson Professor of Chemistry
William P. Dailey, Associate Professor of Chemistry

To my family, for all of their love and support

ACKNOWLEDGMENTS

Many people have provided assistance and suggestions for the research presented in this thesis and have supported me throughout graduate school. For starters, I would like to thank my advisor, Marisa C. Kozlowski, for her guidance and suggestions. I have always felt a certain degree of freedom to pursue my ideas and to help steer the projects into other directions. In addition, I would also like to thank Marisa for encouraging me to apply for fellowships, which has provided me with practical experience in writing proposals. I have received two fellowships during my time here, first a NIH Chemistry-Biology training fellowship and later a NIH NRSA predoctoral fellowship. I am truly gratefully for the support provided by these fellowships for research, travel to conferences, and the overall development of my career.

I am grateful to have been a part of the Kozlowski group. Past and present, I could not ask for a better group of friends and coworkers to work with. Ryan, Scott, and Trung have been my friends since the beginning of graduate school. It has been quite a journey over the years, after all, we became the most senior current members of the group by our third year. I appreciate everyone's suggestions and input they have provided towards my research, practice presentations, Scott for proof reading many reports and presentations, Trung for his unreserved willingness to help, and Rosaura for being such a good and supportive friend over the years. The phenazine project will be left in good hands with Alison. I am grateful to past group members as well. In particular, I want to acknowledge Dr. Joshua Dickstein for teaching/training me when I was beginning, and Dr. Barbara Morgan for her research advice and contributions toward the biaryl coupling of C-8 substituted naphthols.

My committee members, Professors Madeleine Joullié, Amos Smith III, and William Dailey have provided much insight and suggestions for my projects during my annual committee meetings. The phenazine project developed from one of these suggestions. Helpful discussions with Professor David Chenoweth, in particular his suggestion to investigate the mechanochromism of the phenazine derivatives, have helped in the development of the phenazine project. The facilities provided by the Chemistry Department here at the University of Pennsylvania have been instrumental in contributing to my research. Dr. Patrick Carroll has solved seven crystal structures for me and has built a packing diagram for the tetrachlorophenazine derivative. Dr. George Furst and Dr. Jun Gu are acknowledged for their help obtaining 2D NMR spectra and ^{13}C spectra on small quantities of sample and Dr. Rakesh Kohli is thanked for obtaining high-resolution mass spectra. Other members of the department are also gratefully acknowledged for their assistance. Danielle Reifsnyder (Murray group) obtained the XRPD results, Pawaret (Kla) Leowanawat (Percec group) obtained CD spectra, and Jacob Goldberg assisted in measuring fluorescence.

Finally, I would like to acknowledge all of my family and friends, especially my parents, whose love and support helped me get through graduate school and complete my degree.

ABSTRACT

CHIRAL BINAPHTHOQUINONES: VERSATILE PRECURSORS FOR THE SYNTHESIS OF NATURAL PRODUCTS AND LIGANDS FOR ASYMMETRIC CATALYSIS

Erin E. Podlesny

Professor Marisa C. Kozlowski

The efforts described in this dissertation initially focus on the asymmetric synthesis of axially chiral binaphtho-*para*- and binaphtho-*ortho*-quinones, followed by an exploration of their utility in natural product synthesis, development of ligands for asymmetric catalysis, and development as potential sensors. Axially chiral binaphtho-*para*- and *in*-*in*-binaphtho-*ortho*-quinones were synthesized through a concerted route involving the enantioselective coupling of a hindered 8-substituted 2-naphthol, with a diaza-*cis*-decalin copper catalyst developed previously by the Kozlowski group. The coupling was achieved in 62% yield and 87% ee (a single trituration produced material of >99% ee). Subsequent transformations led to an 8,8'-hydroxylated binaphthol, which was selectively oxidized to a binaphtho-*para*-quinone using a Co-salen catalyst or transformed to the *in*-*in*-binaphtho-*ortho*-quinone with *o*-iodoxybenzoic acid (IBX). Similarly, the *out*-*out*-binaphtho-*ortho*-quinone was synthesized from a 6,6'-hydroxylated binaphthol, using IBX.

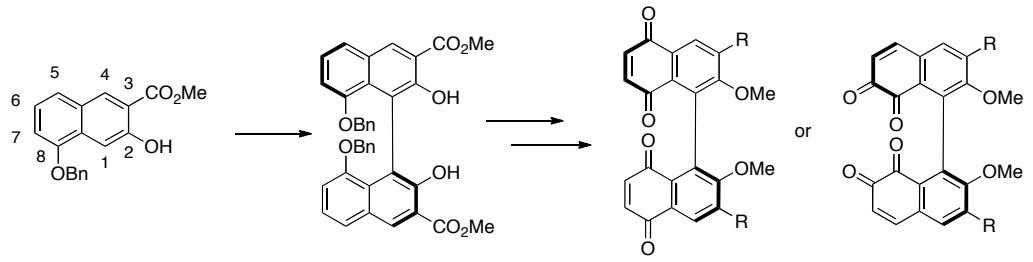

Binaphtho-*para*-quinones were used as key intermediates for the synthesis of the bisanthraquinone natural product (*S*)-bisoranjidiol. (*S*)-Bisoranjidiol was synthesized from a 6,6'-dibrominated binaphtho-*para*-quinone and mixed vinyl ketene acetal, through a regioselective tandem Diels-Alder/aromatization reaction. This transformation was achieved in 80% yield (~95% per transformation). The synthesis of (*S*)-bisoranjidiol was completed in 4% yield over 12 steps, and >99% ee. In addition, the synthesis of a reported binaphthalene tetraol natural product was achieved through reduction of an *out-out*-binaphtho-*ortho*-quinone. This synthesis led to the structural reassignment of the proposed compound to a tetrabrominated diphenyl ether.

Condensation of various phenylenediamines with binaphtho-*ortho*-quinones led to bisbenzo[*a*]phenazines, which represent BINOL derivatives with electron-withdrawing groups (pyrazine ring). The *in-in*-bisbenzo[*a*]phenazines performed better than BINOL, but did not offer improvements over the electron-deficient BINOL based catalysts/ligands reported for those reactions. The bisbenzo[*a*]phenazines, in particular the tetrachlorinated derivatives, also displayed a series of interesting properties and colorimetric responses to various stimuli (chromism), which may lead to the development of colorimetric sensors. The properties include mechanochromism, thermochromism, solvatochromism, vapochromism, acidochromism, and fluorescence.

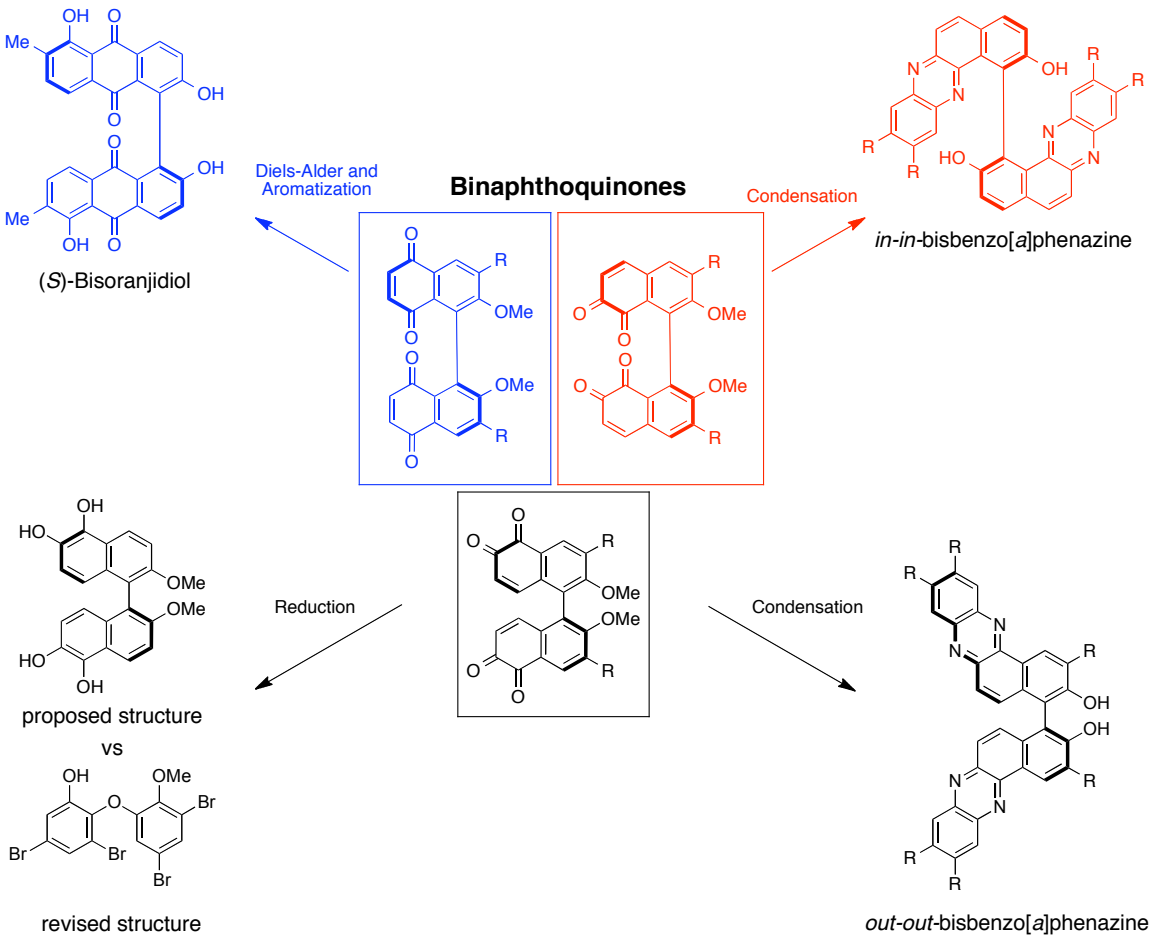
(S)-Bisoranjidiol
Diels-Alder and Aromatization
Binaphthoquinones
Condensation
in-in-bisbenzo[a]phenazine
Reduction
Condensation
proposed structure
vs
revised structure
out-out-bisbenzo[a]phenazine

TABLE OF CONTENTS

CHAPTER 1: Asymmetric Binaphthol Coupling for the Synthesis of Chiral Binaphthoquinones

1.1 Chiral Binaphthoquinones: Significance and Retrosynthesis

Naphthoquinones are oxidized derivatives of naphthalene, containing either a *para*-quinone (1,4-quinone) or an *ortho*-quinone (1,2-quinone) fused to a benzene ring (Figure 1.1). The occurrence of these structural motifs is widespread. They can be found in an abundance of bioactive natural products,[1] as well as in the byproducts of fuel combustion.[1f,2] A majority of the attention gained by naphthoquinones and their derivatives stems from their reactivity as electrophiles, being good dienophiles or Michael acceptors, and other properties, such as their redox activity. Interest in these attributes has led to a wide range of applications for both naphthoquinones and their derivatives. For example, the redox properties of anthraquinones have been used in industry for the production of hydrogen peroxide.[3] Quinones have been used as dyes,[4]

(1) For reviews, including refs therein, on naphthoquinone natural products, biosynthesis and bioactivity/toxicity see: (a) Thomson, R. H. *Naturally Occurring Quinones III: Recent Advances*, 3rd ed.; Chapman and Hall: New York, 1987. (b) O'Brien, P. J. "Molecular Mechanisms of Quinone Cytotoxicity" *Chem.-Biol. Interact.* **1991**, *80*, 1–41. (c) Medentsev, A. G.; Akimenko, V. K. "Naphthoquinone Metabolites of the Fungi" *Phytochemistry* **1998**, *47*, 935–959. (d) Pinto, A. V.; de Castro, S. L. "The Trypanocidal Activity of Naphthoquinones: A Review" *Molecules* **2009**, *14*, 4570–4590. (e) Sunassee, S. N.; Davies-Coleman, M. T. "Cytotoxic and Antioxidant Marine Prenylated Quinones and Hydroquinones" *Nat. Prod. Rep.* **2012**, *29*, 513–535. (f) Kumagai, Y.; Shinkai, Y.; Miura, T.; Cho, A. K. "The Chemical Biology of Naphthoquinones and its Environmental Implications" *Ann. Rev. Pharmacol. Toxicol.* **2012**, *52*, 221–247.

(2) Cho, A. K., Di Stefano, E.; You, Y.; Rodriguez, C. E.; Schmitz, D. A.; Kumagai, Y.; Miguel, A. H.; Eiguren-Fernandez, A.; Kobayashi, T.; Avol, E.; Froines, J. R. "Determination of Four Quinones in Diesel Exhaust Particles SRM 1649a, and Atmospheric $PM_{2.5}$" *Aerosol. Sci. Tech.* **2004**, *38*, 68–81.

(3) Campos-Martin, J. M.; Blanco-Brieva, G.; Fierro, J. L. G. "Hydrogen Peroxide Synthesis: An Outlook Beyond the Anthraquinone Process" *Angew. Chem. Int. Ed.* **2006**, *45*, 6962–6984.

oxidants (e.g. DDQ) and synthons in organic synthesis, and as medicinal agents (natural and synthetic) for the treatment of diseases such as malaria[5] and cancer.[6]

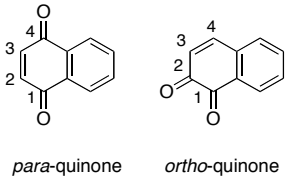

para-quinone *ortho*-quinone

Figure 1.1 Naphthoquinones.

Consequently, we were interested in exploiting the properties of the quinone functional group by incorporating naphthoquinones onto a BINOL-type scaffold. Specifically, we targeted chiral binaphtho-*para*-quinones (**1.3**, Scheme 1.1) and binaphtho-*ortho*-quinones with the 1,2-dicarbonyls directed inward (*in-in,* **1.4**, Scheme 1.1) or outwards (*out-out*, **1.9**, Scheme 1.2). These chiral binaphthoquinones could serve as key intermediates in natural product synthesis and lead to the development of ligands for asymmetric catalysis, redox-active ligands, and chiral oxidants.

Retrosynthetically, both *para*-quinone **1.3** and *ortho*-quinone **1.4** could be formed selectively from common intermediate **1.5**, possessing 8,8'-hydroxyls (Scheme 1.1). This chiral binaphthol could be formed via an oxidative enantioselective biaryl coupling reaction of the hindered 8-substituted 2-naphthol **1.6**. The targeted binaphtho-*para*- and

---

(4) (a) Bien, H.-S.; Stawitz, J.; Wunderlich, K. "Anthraquinone Dyes and Intermediates" *Ullmann's Encyclopedia of Industrial Chemistry*, Electronic Release, Wiley-VCH, Weinheim Jun. 2000. (b) Griffiths, J. "Benzoquinone and Naphthoquinone Dyes" *Ullmann's Encyclopedia of Industrial Chemistry*, Electronic Release, Wiley-VCH, Weinheim Jan. 2006.

(5) Fotie, J. "Quinones and Malaria." *Anti-Infect. Agents Med. Chem.* **2006**, *5*, 357–366.

(6) For examples see: (a) Asche, C. "Antitumour Quinones" *Mini-Rev. Med. Chem.* **2005**, *5*, 449–467. (b) Rodrigues de Almeida, E. "Preclinical and Clinical Studies of Lapachol and Beta-Lapachone" *The Open Natural Products Journal* **2009**, *2*, 42–47. (c) Kizek, R.; Adam, V.; Hrabeta, J.; Eckschlager, T.; Smutny, S.; Burda, J. V.; Frei, E.; Stiborova, M. "Anthracyclines and Ellipticines as DNA-damaging Anticancer Drugs: Recent Advances" *Pharmacology and Therapeutics* **2012**, *133*, 26–39.

binaphtho-*ortho*-quinones could then be used to access chiral bisanthraquinone natural products and analogs (**1.1**, see Chapters 3–4) through Diels-Alder/aromatization reactions or to access chiral *in*-*in*-bisbenzo[*a*]phenazines (**1.2**, see Chapter 6) through condensation with phenylenediamines (Scheme 1.1).

Scheme 1.1 Retrosynthesis for binaphtho-*para*- and *in*-*in*-binaphtho-*ortho*-quinones.

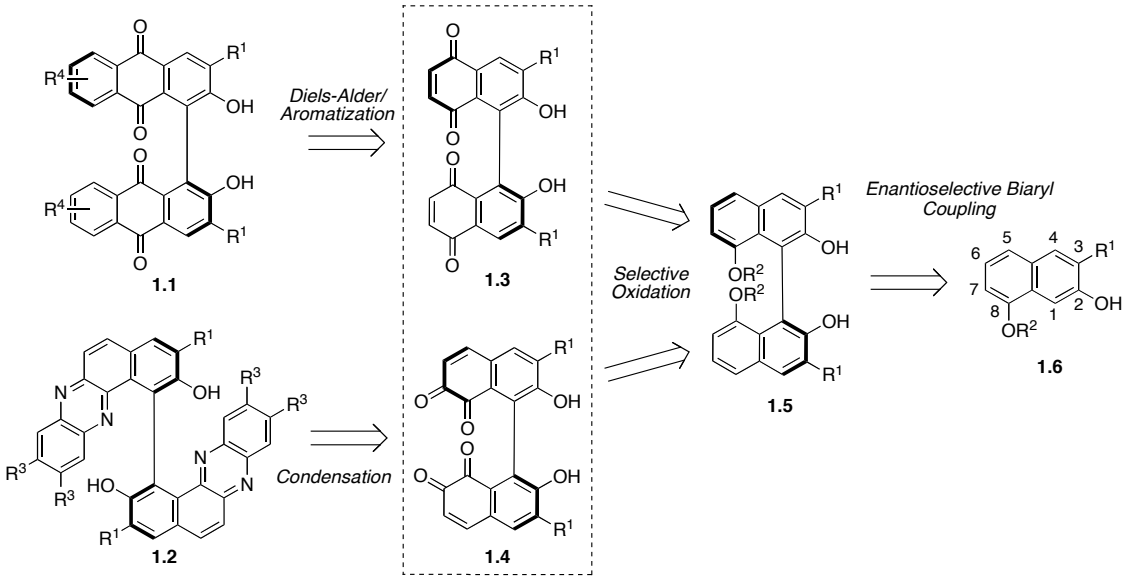

out-*out*-Binaphtho-*ortho*-quinone **1.9** could be accessed via a separate, but similar route, from 6-substituted 2-naphthols, and likewise could be used to access *out*-*out*-bisbenzo[*a*]phenazines (**1.7**, see Chapter 6) or natural products, such as the reported binaphthalenetetraol **1.8** (Scheme 1.2, see also Chapter 5).

Scheme 1.2 Retrosynthesis for *out-out*-binaphtho-*ortho*-quinones.

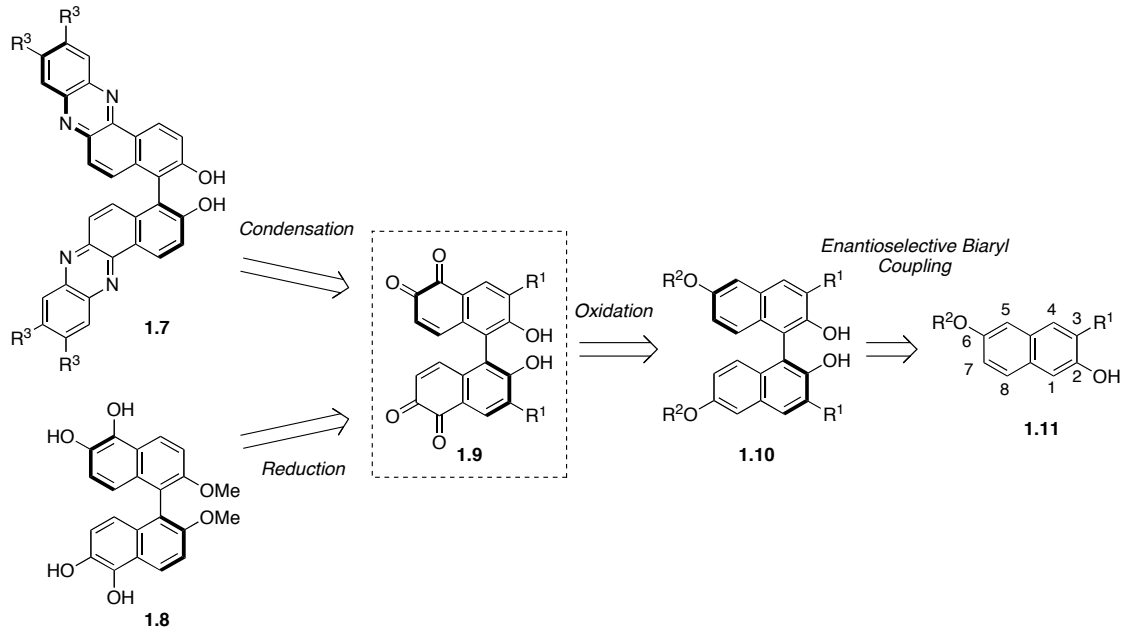

1.2 Introduction to Enantioselective Binaphthol Coupling: Cu vs V Catalysts

The first critical transformation outlined in the retrosynthesis of binaphthoquinones **1.3**, **1.4**, and **1.9** is an oxidative enantioselective biaryl coupling reaction of functionalized 2-naphthols. Presently there is no general method for coupling naphthols, however, a number of different metal-based catalysts have been developed with complementary reactivity, such as copper catalysts, dinuclear vanadium catalysts, and salen-based catalysts.[7] In particular, the diaza-*cis*-decalin copper catalyst **1.12** (Table 1.1)[8] developed by our group a number of years ago has proved to be an effective and

(7) (a) Kozlowski, M. C.; Morgan, B. J.; Linton, E. C. "Total Synthesis of Chiral Biaryl Natural Products by Asymmetric Biaryl Coupling" *Chem. Soc. Rev.* **2009**, *38,* 3193–3207. (b) Bringmann, G.; Gulder, T.; Gulder, T. A. M.; Breuning, M. "Atroposelective Total Synthesis of Axially Chiral Biaryl Natural Products" *Chem. Rev*. **2011**, *111*, 563–639.

(8) (a) Li, X.; Yang, J.; Kozlowski, M. C. "Enantioselective Oxidative Biaryl Coupling Reactions Catalyzed by 1,5-Diazadecalin Metal Complexes" *Org. Lett.* **2001**, *3,* 1137–1140. (b) Kozlowski, M. C.; Li, X.; Carroll, P. J.; Xu, Z. "Copper(II) Complexes of Novel 1,5-Diaza-cis-decalin Diamine Ligands: An Investigation of Structure and Reactivity" *Organometallics* **2002**, *21,* 4513–4522. (c) Li, X.; Hewgley, J. B.; Mulrooney, C. A.; Yang, J.; Kozlowski, M. C. "Enantioselective Oxidative Biaryl Coupling Reactions

tolerant catalyst for asymmetric binaphthol coupling. The use of **1.12** is generally limited to 2-naphthols bearing electron-deficient coordinating groups at the 3-position, such as a methyl ester. However, the catalyst is also capable of coupling highly functionalized naphthols (see Table 1.1).[9,10] Without any additional substituents, a 2-naphthol with a 3-methyl ester can be coupled by **1.12** under oxygen to yield the corresponding 1,1'-binaphthol in high yield and selectivity (85% yield, 93% ee, entry 1). Functionality at the 4-, 6-, and 7-positions is well tolerated (up to 72% yield, 90% ee, entry 3). However, if the electron density on the naphthol is too high, stabilization of the benzylic radical intermediate results in rapid reaction and poor enantioselectivity. This result is due to oxidation of the product by the catalyst, which causes atropisomerization (entry 2). Substitution can be incorporated at the 5-position of the naphthol, however, if there is also a substituent at the 4-position, steric interactions interfere with the formation of a coplanar methyl ester and hydroxyl. Since coordination of the methyl ester to the copper is important, lower selectivities and slower reactions were observed when this interaction was compromised (entries 4 and 5). This problem can be circumvented by constraining either the 4- and 5-functional groups with a cyclic protecting group, or by constraining the coordinating ester carbonyl into a fixed position (entries 6 and 7).

Catalyzed by 1,5-Diazadecalin Metal Complexes: Efficient Formation of Chiral Functionalized BINOL Derivatives" *J. Org. Chem*. **2003**, *68,* 5500–5511. (d) Hewgley, J. B.; Stahl, S. S.; Kozlowski, M. C. "Mechanistic Study of Asymmetric Oxidative Biaryl Coupling: Evidence for Self-processing of the Copper Catalyst to Achieve Control of Oxidase vs. Oxygenase Activity" *J. Am. Chem. Soc.* **2008**, *130,* 12232–12233.

(9) Mulrooney, C. A.; Li, X.; DiVirgilio, E. S.; Kozlowski, M. C. "General Approach for the Synthesis of Chiral Perylenequinones via Catalytic Enantioselective Oxidative Biaryl Coupling" *J. Am. Chem. Soc.* **2003**, *125,* 6856–6857.

Table 1.1 Copper catalyzed asymmetric binaphthol coupling.

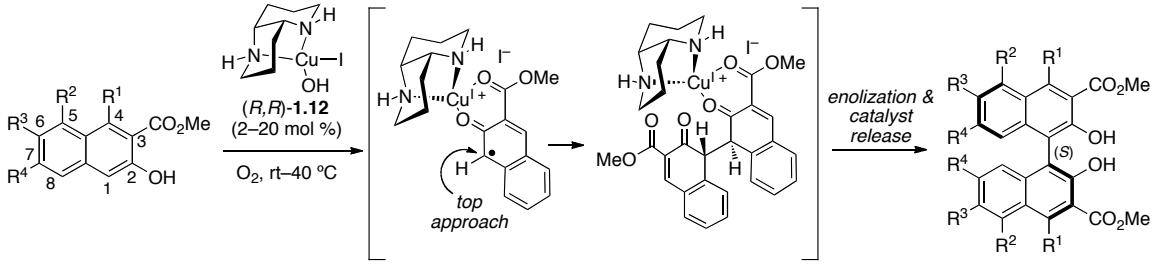

Entry	R^1	R^2	R^3	R^4	Catalyst	Yield (%)	ee (%)
1	H	H	H	H	(*S,S*)	85	93 (*R*)
2	OMe	H	OMe	OMe	(*S,S*)	83	3 (*R*)
3	OAc	H	OMe	OMe	(*R,R*)	72	90 (*S*)
4	OAc	OMe	OMe	OMe	(*S,S*)	41	27 (*R*)
5	OAc	OMe	H	OMe	(*S,S*)	75	45 (*R*)
6	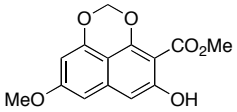				(*S,S*)	96[a]	66 (*R*)
7	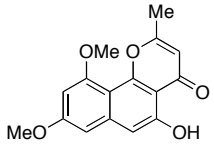				(*S,S*)	60[b]	80 (*R*)

[a] % conv., [b] 100 mol % catalyst

The resolution of the problems caused by 4- and 5-substituents led to the successful synthesis of the binaphthopyrone natural products nigerone and *ent*-nigerone.[10] In addition to binaphthopyrones, catalyst **1.12** has been successfully used for the total syntheses of helically chiral perylenequinone natural products and analogs,[11] including

(10) (a) DiVirgilio, E. S.; Dugan, E. C.; Mulrooney, C. A.; Kozlowski, M. C. "Asymmetric Total Synthesis of Nigerone" *Org. Lett.* **2007**, *9*, 385–388. (b) Kozlowski, M. C.; Dugan, E. C.; DiVirgilio, E. S.; Maksimenka, K.; Bringmann, G. "Asymmetric Total Synthesis of Nigerone and *ent*-Nigerone: Enantioselective Oxidative Biaryl Coupling of Highly Hindered Naphthols" *Adv. Synth. Catal.* **2007**, *349*, 583–594.

(11) Mulrooney, C. A.; O'Brien, E. M.; Morgan, B. J.; Kozlowski, M. C. "Perylenequinones: Isolation, Synthesis and Biological Activity" *Eur. J. Org. Chem*. **2012**, 3887–3904.

cercosporin,[12] hypocrellin A,[13] and others.[14]

Soon after the Kozlowski group reported diaza-*cis*-decalin based copper catalyzed enantioselective binaphthol couplings, both Sasai[15] and Gong[16] published the asymmetric coupling of binaphthols using chiral vanadium catalysts, such as **V1** and **V2** (Table 1.2). Unlike the diaza-*cis*-decalin copper catalyst, the vanadium catalysts are capable of selectively coupling electron-rich 2-naphthols lacking substitution at the 3-position (Table 1.2). Simple 2-naphthol is coupled in quantitative yield and up to 90% ee (entry 1). Similarly, 2-naphthols substituted at the 4-, 6-, and 7-positions provide good

(12) (a) Morgan, B. J.; Dey, S.; Johnson, S. W.; Kozlowski, M. C. "Total Synthesis of Cercosporin and New Photodynamic Perylenequinones: Inhibition of the Protein Kinase C Regulatory Domain" *J. Am. Chem. Soc.* **2009**, *131,* 9413–9425. (b) Morgan, B. J.; Mulrooney, C. A.; Kozlowski, M. C. "Perylenequinone Natural Products: Evolution of the Total Synthesis of Cercosporin" *J. Org. Chem.* **2010**, *75,* 44–56.

(13) (a) O'Brien, E. M.; Morgan, B. J.; Mulrooney, C. A.; Carroll, P. J.; Kozlowski, M. C. "Perylenequinone Natural Products: Total Synthesis of Hypocrellin A" *J. Org. Chem.* **2010**, *75*, 57–68. (b) O'Brien, E. M.; Morgan, B. J.; Kozlowski, M. C. "Dynamic Stereochemistry Transfer in a Transannular Aldol Reaction: Total Synthesis of Hypocrellin A" *Angew. Chem. Int. Ed.* **2008**, *47*, 6877–6880.

(14) (a) Mulrooney, C. A.; Morgan, B. J.; Li, X.; Kozlowski, M. C. "Perylenequinone Natural Products: Asymmetric Synthesis of the Oxidized Pentacyclic Core" *J. Org. Chem.* **2010**, *75,* 16–29. (b) Morgan, B. J.; Mulrooney, C. A.; O'Brien, E. M.; Kozlowski, M. C. "Perylenequinone Natural Products: Total Synthesis of the Diastereomers (+)-Phleichrome and (+)-Calphostin D by Assembly of Centrochiral and Axial Chiral Fragments" *J. Org. Chem.* **2010**, *75,* 30–43. (c) O'Brien, E. M.; Li, J.; Carroll, P. J.; Kozlowski, M. C. "Synthesis of the Cores of Hypocrellin and Shiraiachrome: Diastereoselective 1,8-Diketone Aldol Cyclization" *J. Org. Chem.* **2010**, *75*, 69–73.

(15) (a) Somei, H.; Asano, Y.; Yoshida, T.; Takizawa, S.; Yamataka, H.; Sasai, H. "Dual Activation in a Hemolytic Coupling Reaction Promoted by an Enantioselective Dinuclear Vanadium(IV) Catalyst." *Tetrahedron Lett.* **2004**, *45,* 1841–1844. (b) Takizawa, S.; Katayama, T.; Sasai, H. "Dinuclear Chiral Vanadium Catalysts for Oxidative Coupling of 2-Naphthols *via* a Dual Activation Mechanism" *Chem. Commun.* **2008**, 4113–4122. (c) Takizawa, S.; Katayama, T.; Somei, H.; Asano, Y.; Yoshida, T.; Kameyama, C.; Rajesh, D.; Onitsuka, K.; Suzuki, T.; Mikami, M.; Yamataka, H.; Jayaprakash, D.; Sasai, H. "Dual Activation in Oxidative Coupling of 2-Naphthols Catalyzed by Chiral Dinuclear Vanadium Complexes" *Tetrahedron* **2008**, *64,* 3361–3371. (d) Takizawa, S.; Katayama, T.; Kameyama, C.; Onitsuka, K.; Suzuki, T.; Yanagida, T.; Kawai, T.; Sasai, H. "Chiral Dinuclear Vanadium(V) Catalysts for Oxidative Coupling of 2-Naphthols" *Chem. Commun.* **2008**, 1810–1812.

(16) Guo, Q.-X.; Wu, Z.-J.; Luo, Z.-B.; Liu, Q.-Z.; Ye, J.-L.; Luo, S.-W.; Cun, L.-F.; Gong, L.-Z. "Highly Enantioselective Oxidative Couplings of 2-Naphthols Catalyzed by Chiral Bimetallic Oxovanadium Complexes with Either Oxygen or Air as Oxidant" *J. Am. Chem. Soc.* **2007**, *129*, 13927–13938.

selectivity (80–92% ee, entries 2–5). Having both 4- and 5-substitution is also readily tolerated by the dinuclear vanadium catalysts and was recently utilized in the total synthesis of the binaphthopyranone, (–)-viriditoxin.[17] Functionality at the 3-position results in both low yields and selectivity, especially for electron-poor substituents (entries 7 and 8). As a result, these catalysts are orthogonal to copper catalyst **1.12**.

Table 1.2 Vanadium catalyzed asymmetric binaphthol coupling.

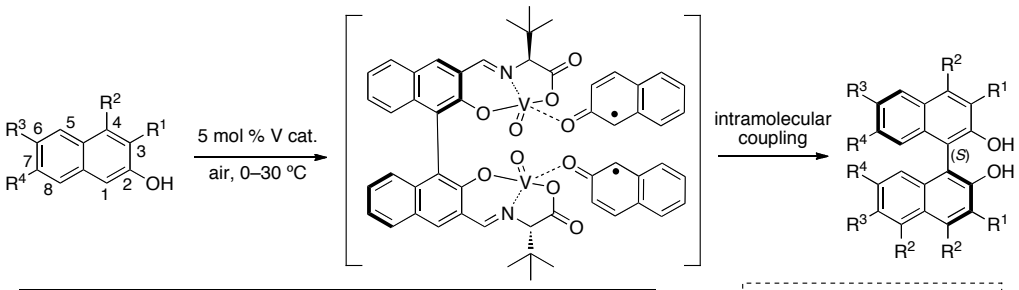

Entry	R^1	R^2	R^3	R^4	Yield (%)	ee (%)
1	H	H	H	H	quant.	90
2	H	H	OBn	H	94	80
3	H	H	Br	H	83	81
4	H	H	H	OMe	98	86
5	H	H	H	OMOM	51	92[a]
6	H	Br	H	H	35	86[a]
7	CO_2Me	H	H	H	10	4
8	OMe	H	H	H	35	48

[a] with **V2** cat.

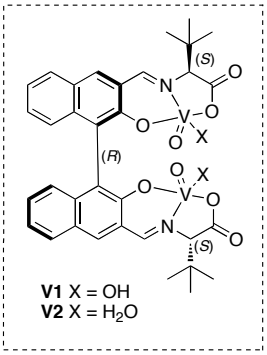

Choosing the appropriate catalyst for the enantioselective biaryl coupling and subsequent synthesis of binaphtho-*para*-quinone **1.3** and binaphtho-*ortho*-quinones **1.4** and **1.9** focused on two criteria: First, *ortho*-quinone formation of the 2-hydroxyl, although disfavored due to loss of aromaticity in both rings, was an unproductive reaction pathway which would lead to side products. Having a substituent in the 3-position during

(17) (a) Park, Y. S.; Grove, C. I.; González-López, M.; Urgaonkar, S.; Fettinger, J. C.; Shaw, J. T. "Synthesis of (–)-Viriditoxin: A 6,6'-Binaphthopyran-2-one that Targets the Bacterial Cell Division Protein FtsZ" *Angew. Chem. Int. Ed.* **2011**, *50*, 3730–3733. (b) Grove, C. I.; Fettinger, J. C.; Shaw, J. T. "Second-Generation Synthesis of (–)-Viriditoxin" *Synthesis*, **2012**, *44*, 362–371.

the selective oxidation step could prevent this side reaction. An electron withdrawing group, such as an ester at the 3-position, would also reduce the potential for oxidation of the ring containing the biaryl linkage, favoring reactivity with the 8,8'-hydroxyls on the adjacent ring. Secondly, a substituent in the 3-position provides quick access to a number of electronically and sterically variable derivatives. Since the vanadium catalysts do not tolerate any substitution at the 3-position, we chose to use the diaza-*cis*-decalin copper catalyst (**1.12**).

1.3 Coupling of Naphthols with Substitution at the 8-position[18,19]

Precedent for the enantioselective coupling of a 2-naphthol with substitution at the 8-position is not well studied. While a few examples of the racemic couplings of hindered 8-substituted 2-naphthols and subsequent chiral resolutions have been reported,[20] there is only one example of an enantioselective reaction. In 2007, Karnik and coworkers reported the enantioselective synthesis of a BINOL derivative containing furan rings fused to the 7,8 and 7',8'-positions (**1.14**, Scheme 1.3).[21]

---

(18) Portions of these sections were published previously: Podlesny, E. E.; Kozlowski, M. C. "Enantioselective Total Synthesis of (*S*)-Bisoranjidiol, an Axially Chiral Bisanthraquinone" *Org. Lett.* **2012**, *14*, 1408–1411.

(19) Portions of these sections were published previously: Podlesny, E. E.; Kozlowski, M. C. "A Divergent Approach to the Bisanthraquinone Natural Products: Total Synthesis of (*S*)-Bisoranjidiol and Derivatives From Binaphtho-*para*-quinones" *J. Org. Chem.* Submitted for review.

(20) For examples see: (a) Yamamoto, K.; Noda, K.; Okamoto, Y. "Synthesis and Chiral Recognition of Optically Active Crown Ethers Incorporating a 4,4'-Biphenanthryl Moiety as the Chiral Centre" *J. Chem. Soc., Chem. Commun.* **1985**, 1065–1066. (b) Nakano, K.; Hidehira, Y.; Takahashi, K.; Hiyama, T.; Nozaki, K. "Stereospecific Synthesis of Hetero[7]helicenes by Pd-Catalyzed Double *N*-Arylation and Intramolecular *O*-Arylation" *Angew. Chem. Int. Ed.* **2005**, *44*, 7136–7138.

(21) Upadhyay, S. I.; Karnik, A. V. "Enantioselective Synthesis of (*R*) and (*S*)-[9,9']Bi[naphtha(2,1-*b*)furanyl]-8,8'-diol: A Furo-Fused BINOL Derivative" *Tetrahedron Lett.* **2007**, *48*, 317–318.

Scheme 1.3 Prior asymmetric synthesis of 8,8'-substituted binaphthols.

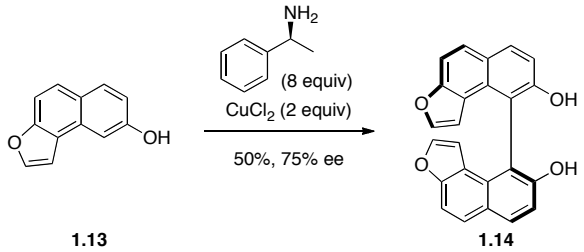

1.13 **1.14**

No example of a *catalyzed* asymmetric reaction of hindered 8-substituted naphthols have been reported, so it was necessary to gauge the ability of the diaza-*cis*-decalin copper catalyst and vanadium catalysts to tolerate this type of substitution pattern.

We briefly investigated the coupling of **1.16a** and **1.16b**, which were synthesized from commercially available diol **1.15** via either a monobenzylation or diacetylation followed by monodeprotection (Scheme 1.4). Formation of the racemate was achieved in low yield (39%) for the benzyl substrate, **1.17a**, using $VO(acac)_2$ and 59% yield for the acetoxy substrate, **1.17b**, using CuCl(OH)TMEDA. An initial screen of the coupling of either monomer **1.16a** or **1.16b** using chiral vanadium catalysts was performed by Scott Allen. Only low conversions and low selectivities (38-56% ee) were observed, which further supported the decision to use a copper catalyst for the biaryl coupling step.

Scheme 1.4 Synthesis of 8,8'-substituted biaryls without 3,3'-substitution.

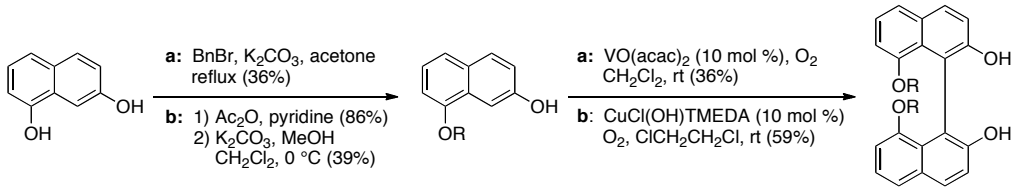

1.15 **1.16a**, R = Bn
b, R = Ac
1.17a, R = Bn
b, R = Ac

Dr. Barbara Morgan showed that compound **1.20**, which was synthesized via a Fischer esterification of **1.18** followed by selective methylation, couples with high selectivity and good yield (59% yield, 90% ee) using the diaza-*cis*-decalin copper catalyst (Scheme 1.5). The racemate was also easily formed (87% yield) using catalytic CuCl(OH)TMEDA under an oxygen atmosphere.

Scheme 1.5 Precedent for asymmetric biaryl coupling of 8-substituted 2-naphthols with a diaza-*cis*-decalin copper catalyst.

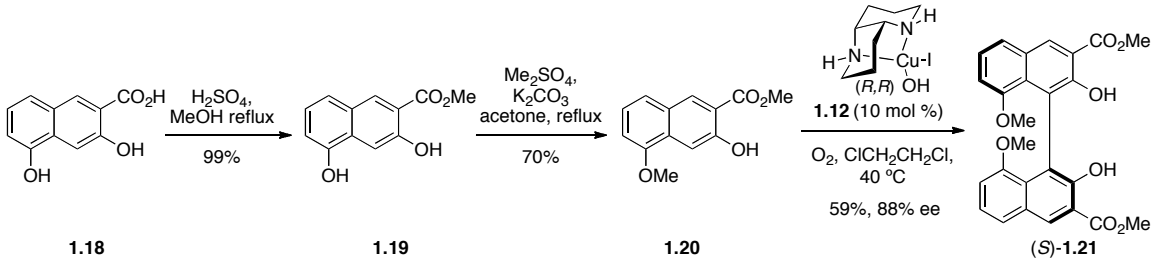

Although the selective coupling of **1.20** by copper catalyst **1.12** proved feasible, the presence of the 8,8'-dimethoxy groups was less than ideal because they could not be selectively deprotected without affecting protecting groups on the 2,2'-dihydroxyl groups and/or the ester groups. To avoid this problem, a benzyl protecting group was chosen instead. The 8-benzyloxy substrate, **1.22**, was synthesized from **1.19** via a selective alkylation of the 8-hydroxyl group, which is more nucleophilic than the 2-hydroxyl group. Like the methoxy substrate, the benzyl substrate coupled in good yield and high selectivity (62% yield and 87% ee) to generate biaryl (*S*)-**1.23** (Scheme 1.6). The enantiopurity could be enhanced to >99% ee with a single trituration. The racemate, *rac*-**1.23**, was also synthesized in 91% yield with catalytic CuCl(OH)TMEDA.

The formation of (*S*)-**1.21** and (*S*)-**1.23** represent the most selective couplings of 8-substituted 2-naphthols and to the best of our knowledge, also the first catalytic coupling of 2-naphthols containing functionality *peri* to the site of C–C bond formation.

Scheme 1.6 Asymmetric synthesis of an 8,8'-substituted binaphthol.

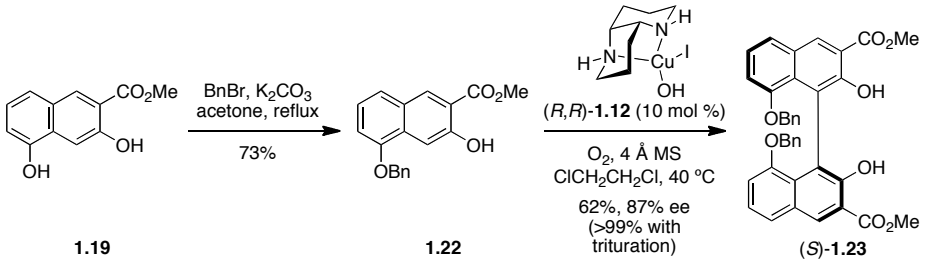

1.19 **1.22** (*S*)-**1.23**

CHAPTER 2: Selective Synthesis of Chiral Binaphthoquinones and Bis-spironaphthalenones From 8,8'-Hydroxylated Binaphthols

2.1 Introduction to Selective Formation of *Ortho*- or *Para*-Naphthoquinones

The regioselective transformation of a naphthol to either a *para*- or *ortho*-naphthoquinone is dependent upon both the oxidant and the absence or presence of other functionality. The oxidation of hydroquinones, methoxynaphthols, and dimethoxynaphthalenes can occur regioselectively, involving a single oxidation with loss of protons and/or demethylation (Scheme 2.1A).[22] On the other hand, the oxidation of naphthols, particularly 1-naphthols, without substitution in the *para* or *ortho* positions presents a different challenge, as these transformations require regioselective oxygenation followed by oxidation to the quinone (Scheme 2.1B), constituting a double oxidation of the naphthol.

Scheme 2.1 Regioselective *para*- or *ortho*-quinone formation.

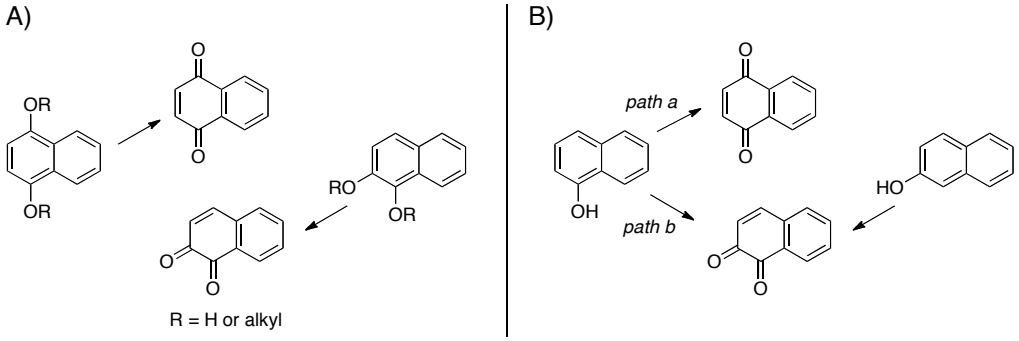

(22) For examples see: (a) Ali, M. H.; Niedbalski, M.; Bohnert, G.; Bryant, D. "Silica-Gel-Supported Ceric Ammonium Nitrate (CAN): A Simple and Efficient Solid-Supported Reagent for Oxidation of Oxygenated Aromatic Compounds to Quinones" *Synth. Commun.* **2006**, *36*, 1751–1759. (b) Pouységu, L.; Sylla, T.; Garnier, T.; Rojas, L. B.; Charris, J.; Deffieux, D.; Quideau, S. "Hypervalent Iodine-Mediated Oxygenative Phenol Dearomatization Reactions" *Tetrahedron* **2010**, *66*, 5908–5917.

Oxidants such as the hypervalent iodide reagents, phenyliodonium diacetate (PIDA) and phenyliodonium bis(trifluoroacetate) (PIFA) have been reported to selectively form *para*-quinones from phenols.[23,24] One of the standard oxidants for oxidizing phenols to *para*-quinones is $(KSO_3)_2NO$ (potassium nitrosodisulfonate), better known as Fremy's radical.[25] This reagent has been reported to be unstable though, and acid or nitrite impurities from preparation can accelerate its decomposition with explosive consequences. In the past half century, the use of a cobalt-salen (Co-salen or salcomine) catalyst with molecular oxygen as a stoichiometric oxidant has gained popularity. Co-salen and derivatives bind oxygen reversibly to give mixtures of Co-superoxo and dimeric peroxo complexes.[26] The Co-superoxo complex is responsible for the catalytic activity. Co-salen is an important catalyst for the oxidation of *para*-unsubstituted phenols to *para*-quinones (path a, Scheme 2.1B).[27] If both *ortho*- and *para*-positions of the phenol are unsubstituted, generally formation of the *para*-quinone is favored. However, sometimes mixtures of *para*- and *ortho*-quinones are obtained.

---

(23) Barret, R.; Daudon, M. "Oxidation of Phenols to Quinones by Bis(trifluoroacetoxy)iodobenzene" *Tetrahedron Lett.* **1990**, *31*, 4871–4872.

(24) Pelter, A.; Ward, R. S. "Two-Electron Phenolic Oxidations Using Phenyliodonium Dicarboxylates" *Tetrahedron* **2001**, *57*, 273–282.

(25) Zimmer, H.; Lankin, D. C.; Horgan, S. W. "Oxidations with Potassium Nitrosodisulfonate (Fremy's Radical). The Teuber Reaction" *Chem. Rev.* **1971**, *71*, 229–246.

(26) Bozell, J. J.; Hames, B. R.; Dimmel, D. R. "Cobalt-Schiff Base Complex Catalyzed Oxidation of *Para*-Substituted Phenolics. Preparation of Benzoquinones" *J. Org. Chem.* **1995**, *60,* 2398–2404.

(27) (a) Van Dort, H. M.; Guersen, H. J. "Salcomine-Catalyzed Oxidations of Some Phenols: A New Method for the Preparation of a Number of *Para*-Benzoquinones" *Recl. Trav. Chim. Pays-Bas* **1967**, *86*, 520–526. (b) Wakamatsu, T.; Nishi, T.; Ohnuma, T.; Ban, Y. "A Convenient Synthesis of Juglone Via Neutral Salcomine Oxidation" *Synth. Commun.* **1984**, *14*, 1167–1173. (c) Uliana, M. P.; Vieira, Y. W.; Donatoni, M. C.; Corrêa, A. G.; Brocksom, U.; Brocksom, T. J. "Oxidation of Mono-Phenols to *Para*-Benzoquinones: A Comparative Study" *J. Braz. Chem. Soc.* **2008**, *19*, 1484–1489.

Methods for the selective formation of the *ortho*-quinone from a phenol without *para*-blocking groups or *ortho*-alkoxy groups are not common. In 2002, Pettus and co-workers reported the regioselective oxidation of phenols to *ortho*-quinones using *ortho*-iodoxybenzoic acid (IBX).[28] This process reportedly involves an intramolecular oxygenation from the I^V reagent, rearrangement of substrate to a catechol intermediate, and subsequent oxidation by the I^{III} species to the *ortho*-quinone.

2.2 Synthesis of Chiral Binaphtho-*para*- and Binaphtho-*ortho*-quinones[18,29]

Various examples of binaphtho-*para*-quinone syntheses have appeared in the literature over the past few decades, involving non-stereoselective oxidative dimerizations.[30] For example, Takeya and coworkers have shown that $SnCl_4$ can be used to mediate the oxidative coupling of 1-naphthols to produce 2,2'-binaphthoquinones.[31]

---

(28) Magdziak, D.; Rodriguez, A. A.; Van De Water, R. W.; Pettus, T. R. R. "Regioselective Oxidation of Phenols to *o*-Quinones with *o*-Iodoxybenzoic Acid" *Org. Lett.* **2002**, *4*, 285–288.

(29) Portions of these sections were published previously: Podlesny, E. E.; Carroll, P. J.; Kozlowski, M. C. "Selective Oxidation of 8,8'-Hydroxylated Binaphthols to Bis-spironaphthalenones or Binaphtho-*para*- and Binaphtho-*ortho*-quinones" *Org. Lett.* **2012**, *14*, 4862–4865.

(30) For examples see: (a) Cameron, D. W.; Chan, H. W.-S. "Colouring Matters of the Aphididae. Part XXVIII. A Coupling Reaction Involving Phenols and Quinones. Reconstruction of the Protoaphins, and Synthesis of the Chrysoaphin Chromophore" *J. Chem. Soc. C* **1966**, 1825–1832. (b) Cameron, D. W.; Chan, H. W.-S.; Hildyard, E. M. "Colouring Matters of the Aphididae. Part XXIX. Partial Synthesis of Erythroaphin and Related Systems by Oxidative Coupling" *J. Chem. Soc. C* **1966**, 1832–1836. (c) Blackburn, G. M.; Cameron, D. W.; Chan, H. W.-S. "Colouring Matters of the Aphididae. Part XXX. Coupling Reactions Involving the Quinone A Derived by Reduction of Protoaphin-*fb*" *J. Chem. Soc. C* **1966**, 1836–1842. (d) Banks, H. J.; Cameron, D. W.; Crossley, M. J.; Samuel, E. L. "Synthesis of 5,7-Dihydroxynaphthoquinone Derivatives and Their Reactions with Nucleophiles: Nitration of 2,3-Dimethylnaphthalene and Subsequent Transformations" *Aust. J. Chem.* **1976**, *29,* 2247–2256. (e) Laatsch, H. "Synthese von Maritonon und Anderen 8,8'-Bijuglomen" *Liebigs Ann. Chem.* **1985**, 2420–2442. (f) Takeya, T.; Otsuka, T.; Okamoto, I.; Kotani, E. "Semiconductor-Mediated Oxidative Dimerization of 1-Naphthols with Dioxygen and *o*-Demethylation of the Enol-Ethers by SnO_2 Without Dioxygen" *Tetrahedron* **2004**, *60,* 10681–10693.

(31) (a) Okamoto, I.; Doi, H.; Kotani, E.; Takeya, T. "The Aryl-Aryl Coupling Reaction of 1-Naphthol With $SnCl_4$ for 2,2'-Binaphthol Synthesis and its Application to the Biomimetic Synthesis of Binaphthoquinone Isolated From *Plumbago zeylanica*" *Tetrahedron Lett.* **2001**, *42,* 2987–2989. (b) Takeya, T.; Doi, H.; Ogata, T.; Okamoto, I.; Kotani, E. "Aerobic Oxidative Dimerization of 1-Naphthols to

The proposed selective oxidation of a binaphthol to either the binaphtho-*ortho*- or binaphtho-*para*-quinone, however, had not been described. To explore regioselective quinone formation, the 8,8'-hydroxylated binaphthol **2.3** was synthesized in two steps via methylation of **1.23** followed by hydrogenolysis of the benzyl groups (Scheme 2.2). A number of oxidants were screened, including ceric ammonium nitrate (CAN), DDQ, PIDA, PIFA, and Co-salen. Co-salen provided the most efficient and cleanest reactions. Compound **2.3** was oxidized to the binaphtho-*para*-quinone **2.4** in 57% yield. An unsymmetrical binaphtho-*ortho,para*-quinone was also formed in 23% yield, but was easily removed from the desired product.

Scheme 2.2 Precedent for selective binaphtho-*para*-quinone formation.

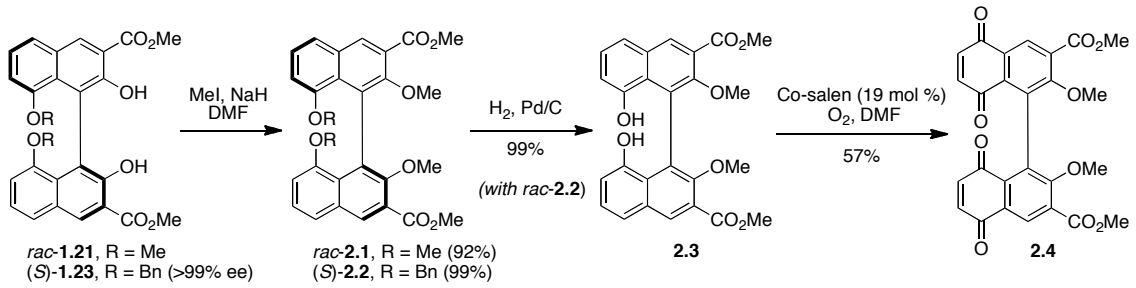

Once it was established that selective formation of the *para*-quinones was possible, I began exploring different 3,3'-functional groups. Removal or reduction of the 3,3'-diester groups from **2.4** was not attempted due to the reactivity of the quinones. Instead this transformation was carried out before formation of the quinone. To remove the ester groups, reaction conditions were initially screened with the more robust 8,8'-methoxy substrate, *rac*-**2.1**, which was synthesized via methylation of *rac*-**1.21** (Scheme 2.2). Hydrolysis of the ester group using LiOH in dioxane/water formed the 3,3'-diacid,

2,2'-Binaphthoquinones Mediated by $SnCl_4$ and its Application to Natural Product Synthesis" *Tetrahedron* **2004**, *60,* 9049–9060.

which could be decarboxylated at 180 °C with Cu and $CuCO_3$ in quinoline to yield *rac*-**2.5** (Scheme 2.3) in up to 74% yield. However, the decarboxylation was not reliable, often resulting in complete decomposition. Other decarboxylation conditions, including palladium or silver catalyzed reactions[32] were also unsuccessful. Fortunately, a three-step DIBAL-H reduction, IBX-mediated oxidation, and decarbonylation with Wilkinson's catalyst was found to be milder, more reliable, and higher yielding, forming **2.5** in 93% yield over three steps (Scheme 2.3). This protocol for removal of the ester group could then be applied to the 8,8'-benzyloxy substrate, (*S*)-**2.2**, to yield (*S*)-**2.6** in 63% yield over three steps. Hydrogenolysis of the benzyl groups and selective oxidation of the 8,8'-dihydroxyls led to binaphtho-*para*-quinone (*S*)-**2.8** in 63% yield without degradation of the enantiopurity.

Scheme 2.3 Synthesis of a chiral binaphtho-*para*-quinone.

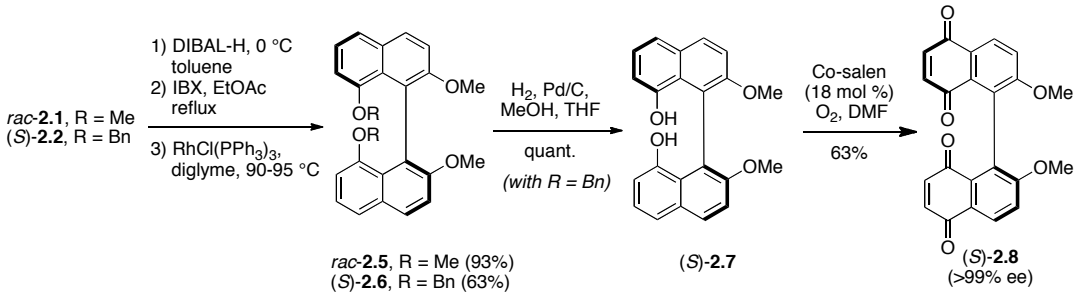

Finally, a 3,3'-dimethyl substrate was investigated in the selective oxidation step. The esters of compound *rac*-**2.2** were reduced to the benzylic alcohols with DIBAL-H. Hydrogenolysis of both the primary alcohols and benzyl protecting groups provided **2.9** in near quantitative yield (Scheme 2.4). As with substrates **2.3** and **2.7**, Co-salen

(32) (a) Dickstein, J. S.; Mulrooney, C. A.; O'Brien, E. M.; Morgan, B. J.; Kozlowski, M. C. "Development of a Catalytic Aromatic Decarboxylation Reaction" *Org. Lett.* **2007**, *9*, 2441-2444. (b) Cornella, J.; Sanchez, C.; Banawa, D.; Larrosa, I. "Silver-Catalysed Protodecarboxylation of *Ortho*-Substituted Benzoic Acids" *Chem. Commun.* **2009**, 7176–7178.

selectively oxidizes **2.9** to the binaphtho-*para*-quinone in 62% yield. In addition to *para*-quinone formation, the common intermediate, **2.9**, could also be selectively oxidized to the binaphtho-*ortho*-quinone using two equivalents of IBX in 74% yield (Scheme 2.4).

Scheme 2.4 Selective *para*- and *ortho*-quinone formation from an 8,8'-hydroxylated binaphthol.

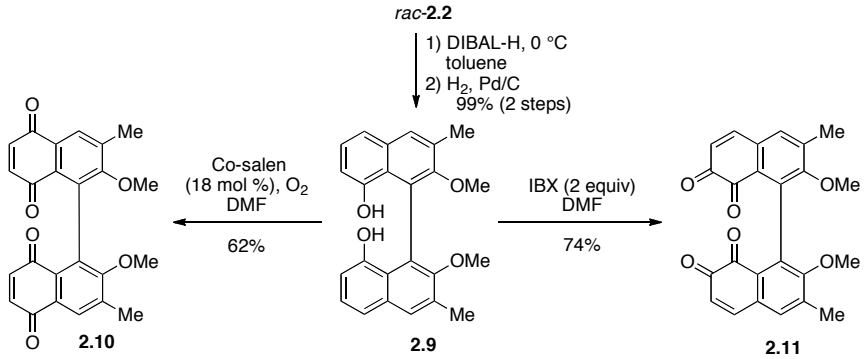

Unfortunately, deprotection of the 2,2'-dimethyl ethers of the binaphtho-*para*-quinone was unsuccessful, generally leading to decomposition. Since the binaphthoquinones could not be efficiently deprotected, selective oxidations of the unprotected tetraols **2.12**, **2.13** and **2.14** were explored. Formation of **2.12** and **2.13** was achieved in good yields (83–93%) via a similar sequence as **2.3** and **2.9** (Scheme 2.5). The 3,3'-unfunctionalized substrate, **2.14**, was synthesized in 70% yield via a global deprotection of **2.6** with BBr_3. Deprotection of the tetramethoxy derivative, **2.5**, provides **2.4** in higher yield (91%, Scheme 2.5).

Scheme 2.5 Synthesis of tetraols.

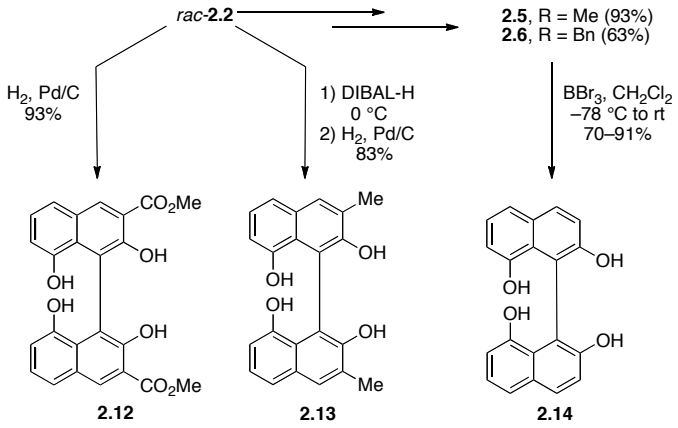

Selective oxidation of the unprotected **2.12**, **2.13**, and **2.14** with Co-salen, under oxygen atmosphere in DMF, led successfully to the corresponding binaphtho-*para*-quinones (*Q*, Scheme 2.6). However, it was observed via ^{1}H NMR spectroscopy that these quinones exist in equilibrium with the bishemiketals (*HK*). This behavior has been reported previously for a bisanthraquinone, but only upon treatment with acid.[33] Methylation of the mixture with Ag_2O and MeI confirmed the identity of the compounds as the binaphtho-*para*-quinone and bishemiketal. The quinone form was trapped as the previously synthesized compound, **2.8**, and the bishemiketal was captured as the bisketal *rac*-**2.18**. The structure of the bisketal was confirmed via X-ray crystallography (Scheme 2.6). Interestingly, the *Q*:*HK* ratio is dependent upon both the 3,3'-functionality and the solvent. Electron-poor groups at the 3,3'-positions favor the binaphtho-*para*-quinone, while the more electron-rich 3,3'-dimethyl binaphtho-*para*-quinone (**2.16**) forms the bishemiketal almost completely in DMSO-d_6 (Scheme 2.6). These results indicate that

(33) Tanaka, O. "Metabolic Products of Fungi. XIV. The Structure of Skyrin. (3). On Pseudoskyrin" *Chem. Pharm. Bull.* **1958**, *6,* 203–208.

the nucleophilicity of the 2,2'-hydroxyls control the internal attack onto the carbonyl. Compound **2.17**, with no 3,3'-substitution, exists as a 2.1:1 mixture in DMSO-d_6, but favors *HK* (1:2.8) in THF-d_8.

Scheme 2.6 Synthesis of binaphtho-*para*-quinones and bishemiketal formation.

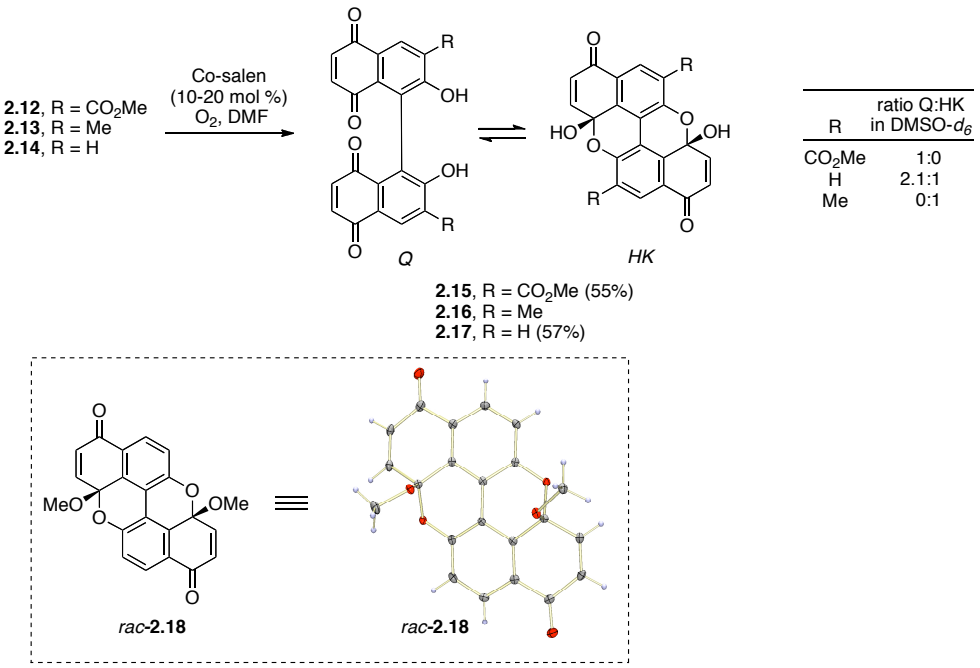

The ability to selectively oxidize 8,8'-hydroxylated binaphthols lacking 3,3'-substituents to the corresponding binaphtho-*para*-quinones was significant because it meant that chiral vanadium catalysts could be used under certain circumstances. With the exception of 8-substituted 2-naphthols, which did not couple well with vanadium catalysts (see Chapter 1), asymmetric vanadium catalyzed coupling could be easily used to form 6,6'- or 7,7'- dihydroxy binaphthols. This approach results in a shorter, more efficient route to binaphtho-*ortho*-quinones that lack substituents at the 3,3'-positions (see Chapters 5 and 6).

2.3 Synthesis of Bis-spironaphthalenones[29]

While screening other oxidation conditions for the synthesis of **2.17** (Scheme 2.6), the formation of an unusual spirocyclic compound was observed. When DMF was replaced with MeCN for the Co-salen catalyzed oxidation of **2.14**, the bis-spironaphthalenone **2.19** was isolated as the major product instead of the binaphtho-*para*-quinone (Scheme 2.7). An X-ray structure determination identified the architecturally complex compound, which formed via an intramolecular oxidative cyclization of the 8,8'-dihydroxyls onto the carbons bearing the biaryl bond.

Scheme 2.7 Synthesis of a bis-spironaphthalenone.

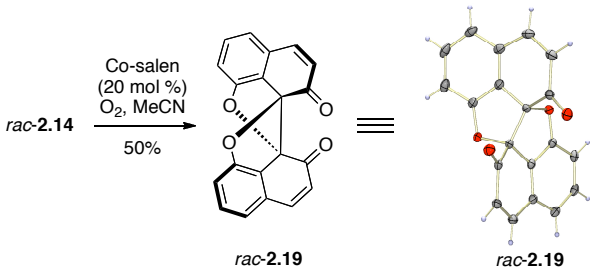

Synthetic or naturally occurring compounds containing this type of structural framework have not been reported in the literature. However, there are relevant natural products, such as grandidone D[34] and spiroxins A-E,[35] which possess one of the

(34) (a) Uchida, M.; Miyase, T.; Yoshizaki, F.; Bieri, J. H.; Rüedi, P.; Eugster, C. H. "14-Hydroxytaxodion als Hauptditerpen in *Plectranthus grandiden tatus* GÜRKE; Isolierung von Sieben Neuen Dimeren Diterpenen aus *P. grandidentatus, P. myrianthus* BRIQ. und *Coleus carnosus* HASSK.: Strukturen der Grandidone A, 7-Epi-A, B, 7-Epi-B, C, D und 7-Epi-D" *Helv. Chim. Acta* **1981**, *64*, 2227–2250. (b) Rüedi, P.; Uchida, M.; Eugster, C. H. "Partialsynthese der Grandidone A, B, 7-Epi-B, C, D und 7-Epi-D aus 14-Hydroxytaxodion" *Helv. Chim. Acta* **1981**, *64*, 2251–2256.

(35) McDonald, L. A.; Abbanat, D. R.; Barbieri, L. R.; Bernan, V. S.; Discafani, C. M.; Greenstein, M.; Janota, K.; Korshalla, J. D.; Lassota, P.; Tischler, M.; Carter, G. T. "Spiroxins, DNA Cleaving Antitumor Antibiotics From a Marine-Derived Fungus" *Tetrahedron Lett.* **1999**, *40*, 2489–2492.

spirofurans (Figure 2.1). In addition, calixarenes[36] and spironaphthalenones[37] have been reported, which contain a carbonyl adjacent to a spirodihydrobenzofuran (Figure 2.1). Due to the unique structure of **2.19**, derivatization and investigation of its reactivity was pursued.

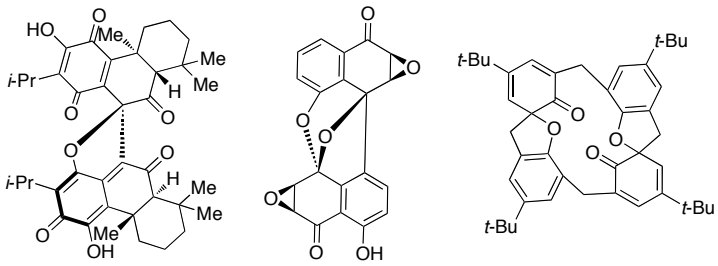

Figure 2.1 Examples of related spirocyclic compounds.

Although **2.19** has the simplest framework, its synthesis required removal of the ester group. This process was either unreliable with Cu/quinoline decarboxylation or expensive with Rh-mediated decarbonylation. Therefore, a more efficient synthesis of the 3,3'-dimethyl derivative was pursued. Similar to **2.19**, Co-salen catalyzed oxidation of **2.13** in MeCN also led to the bis-spironaphthalenone as the major product. Other oxidants were also found to promote this cyclization more efficiently. The hypervalent iodide reagent, PIDA, effectively induced the oxidative dearomatization, forming **2.20** in 75% yield. Reagents, such as PIDA, PIFA, IBX and SIBX, are known to promote

(36) (a) Litwak, A. M.; Grynszpan, F.; Aleksiuk, O.; Chen, S.; Biali, S. E. "Preparation, Stereochemistry, and Reactions of the Bis(spirodienone) Derivatives of *p-tert*-Butylcalix[4larene" *J. Org. Chem.* **1993**, *58*, 393–402. (b) Georghiou, P. E.; Ashram, M.; Clase, H. J.; Bridson, J. N. "Spirodienone and Bis(spirodienone) Derivatives of Calix[4]naphthalenes" *J. Org. Chem.* **1998**, *63,* 1819–1826.

(37) (a) Kasturi, T. R.; Sattigeri, J. A.; Pragnacharyulu, P. V. P. "Reaction of Spironaphthalenones with Hydroxylamine Hydrochloride: Part IV" *Tetrahedron*, **1995**, *51*, 3051–3060. (b) Khoramabadi-zad, A.; Yavari, I.; Shiri, A.; Bani, A. "Oxidation of Bisnaphthols to Spironaphthalenones, Revisited" *J. Heterocyclic Chem*. **2008**, *45,* 1351–1358.

oxidative dearomatizations.[22b,24] Bis-spironaphthalenone **2.20** could be transformed to diol **2.21** (77% yield) via a diastereoselective reduction using $NaBH_4$ (Scheme 2.8). The newly formed alcohols were oriented *anti* to each other and *cis* to the adjacent furan oxygens. These relationships were confirmed via X-ray crystallography.

Scheme 2.8 Synthesis and selective reduction of a bis-spironaphthalenone.

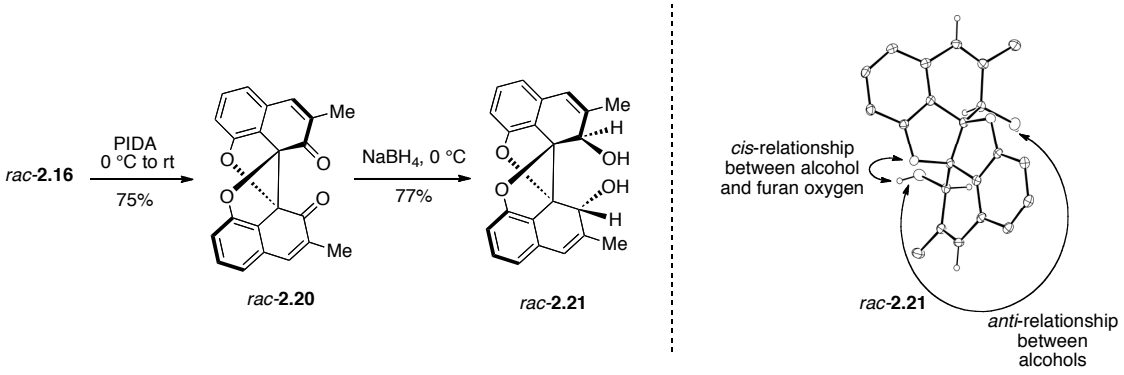

Preliminary studies with alkyl lithiums, such as MeLi, also showed reactivity with the carbonyls, but a large number of side products were observed. Attempts to functionalize **2.20** or **2.21** further were unsuccessful. Partial or complete elimination of the furan oxygens with rearomatization to **2.16** or to the monospirocyclic compound, **2.22 (**Figure 2.2**)**, was highly favored. This result was observed with reductants, such as L-selectride, Stryker's reagent ($[(PPh_3)CuH]_6$), and Pd/C under H_2 atmosphere. Other transformations, such as imine formation, led to complex mixtures composed of partial or complete rearomatization of **2.20**. Many of the rearomatized products also contained substitution at the 5,5'-positions (Figure 2.2). For example, when **2.20** was treated with $NH_2OH{\cdot}HCl$ and conc. HCl in EtOH/THF, instead of oxime formation, dichloro compound **2.23** was produced along with compounds resulting from the addition of

EtOH. Similar reactivity was reported for a calixarene containing a spironaphthalenone (as in Figure 2.1), in which treatment with HCl resulted in chloride addition to the arene ring despite a large *t*-butyl group.[36a]

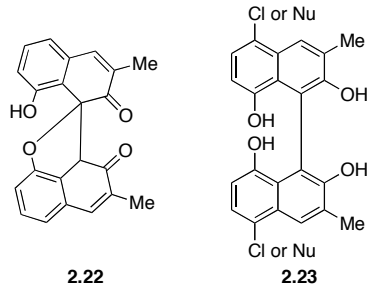

2.22 **2.23**

Figure 2.2 Typical side products.

CHAPTER 3: Background - (*S*)-Bisoranjidiol and Other Bisanthraquinone Natural Products

3.1 Isolation and Structural Determination

Natural products containing the *para*-naphthoquinone structure are extensive. Although many of the naturally occurring naphthoquinones and related derivatives are monomeric, several classes of biologically active unsymmetrical and symmetrical dimers have also been identified.[1a] These dimeric compounds include the binaphthoquinones, bisanthraquinones, and extended quinones such as the perylenequinones and gymnochromes (Figure 3.1). We were interested in the enantioselective synthesis of axially chiral bisanthraquinones, in particular (*S*)-bisoranjidiol.

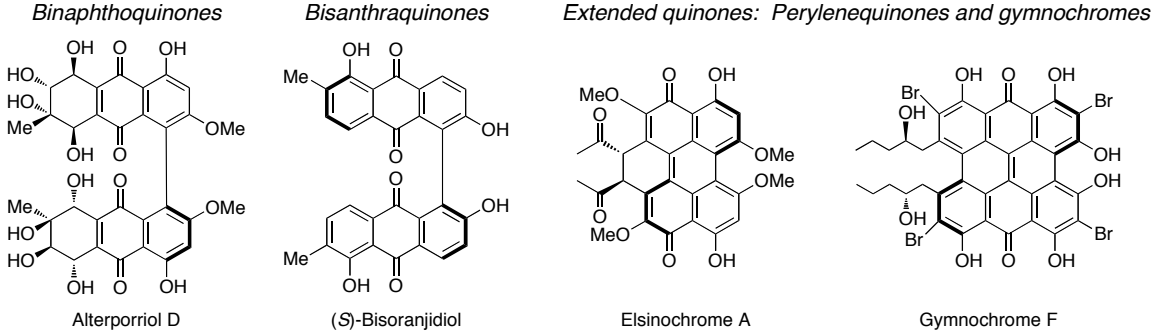

Figure 3.1 Quinone natural products.

Bisanthraquinone natural products are a structurally diverse class of compounds with variation to both the substituents on the anthraquinone rings, as well as the linkage point(s) between them. One subset of these bisanthraquinones contain a 1,1'-biaryl linkage, which creates an axially chiral symmetrical dimer. Several of these compounds have been isolated and identified from fungi, lichen, and shrubs. The first example is

skyrin (**3.1**, Figure 3.2), which was isolated in 1954 from *Penicillum islandicum*[38] and later from different sources of fungi.[39] Other examples include trachypone,[40] bislunatin,[41] disolorinic acid,[42] hinakurin,[43] etc.[44] One commonality between these eight bisanthraquinones is the *meta*-substitution pattern on the distal rings, as well as polyoxygenation with hydroxyls or ethers at the 2,2'-, 4,4'-, and 5,5'-positions.

In 2006, a previously unknown symmetrical bisanthraquinone was isolated from the leaves of the South American shrub, *Heterophyllaea pustulata* (genera Rubiaceae), which grows in mountainous regions of Argentina and Bolivia.[45] This compound, designated (*S*)-bisoranjidiol (**3.9**, Figure 3.2), fits into the family of symmetrical bisanthraquinones, but lacks the 4,4'-hydroxyls and contains an *ortho*-substituted distal

---

(38) Howard, B. H.; Raistrick, H. "Studies in Biochemistry of Microorganisms. The Colouring Matters of *Penicillum islandicum* Sopp. Part 3. Skyrin and Flavoskyrin" *Biochem. J.* **1954**, *56*, 56–65.

(39) Gill, M.; Gimenez, A.; McKenzie, R. W. "Pigments of Fungi, Part 8. Bianthraquinones From *Dermocybe Austroveneta*" *J. Nat. Prod.* **1988**, *51*, 1251-1256.

(40) Delle Monache, F.; D'Albuquerque, I. L.; De Andrade Chiappeta, A.; De Mello, J. F. "A Bianthraquinone and 4'-O-Methyl-*Ent*-gallocatechin from *Cassia Trachypus*" *Phytochemistry* **1992**, *31*, 259–261.

(41) Agusta, A.; Ohashi, K.; Shibuya, H. "Bisanthraquinone Metabolites Produced by the Endophytic Fungus *Diaporthe* sp" *Chem. Pharm. Bull.* **2006**, *54*, 579–582.

(42) (a) Steglich, W.; Jedtke, K.-F. "Novel Anthraquinone Pigments from *Solorina crocea*" *Z. Naturforsch.* **1976**, *31C*, 197–198. (b) Okuyama, E.; Hossain, C. F.; Yamazaki, M. "Monomine Oxidase Inhibitors from a Lichen, *Solorina crocea* (L.) ACH" *Shoyakugaku Zasshi*, **1991**, *45*, 159–162.

(43) Fujitake, N.; Suzuki, T.; Fukumoto, M.; Oji, Y. "Predomination of Dimers Over Naturally Occurring Anthraquinones in Soil" *J. Nat. Prod*. **1998**, *61*, 189–192.

(44) (a) Santesson, J. "Anthraquinonoid Pigments of *Trypetheliopsis boninensis* and *Ocellularia domingensis*" *Acta Chem. Scand.* **1970**, *24*, 3331–3334. (b) Singh, J.; Singh, J. "A Bianthraquinone and a Triterpenoid From the Seeds of *Cassia Hirsuta*" *Phytochemistry*, **1986**, *25*, 1985–1987. (c) Singh, V.; Singh, J.; Sharma, J. P. "Anthraquinones From Heartwood of *Cassia Siamea*" *Phytochemistry* **1992**, *31*, 2176–2177.

(45) Núñez Montoya, S. C.; Agnese, A. M.; Cabrera, J. L. "Anthraquinone Derivatives from *Heterophyllaea pustulata*" *J. Nat. Prod.* **2006**, *69*, 801–803.

ring. The structure was identified by spectroscopic analyses of the biaryl and, following reductive cleavage of the biaryl bond, by comparison of the monomer to soranjidiol. In addition, a positive Cotton effect in the CD spectrum established the (*S*)-configuration of the biaryl.[45]

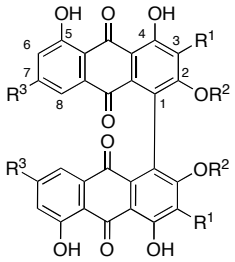

Compound	R^1	R^2	R^3
3.1 (*S*) and (*R*)-skyrin	H	H	Me
3.2 skyrinol	H	H	CH_2OH
3.3 (*S*)-bislunatin	H	H	OMe
3.4 hinakurin	H	Me	Me
3.5	Me	H	OMe
3.6	Me	H	OMe w/ 5,5'-OMe
3.7 trachypone	Me	Me	Me
3.8 disolorinic acid	COC_5H_{11}	H	OMe

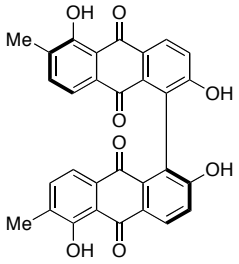

3.9, (*S*)-bisoranjidiol

Figure 3.2 Bisanthraquinone natural products.

3.2 Biological Activity

(*S*)-Bisoranjidiol is reported to have photosensitizing properties, meaning that the compound is able to interact with molecular oxygen upon irradiation with light to generate electronically excited singlet oxygen and the ground state radical anion.[46] The photosensitizing properties of bisoranjidiol and other compounds are responsible for the

(46) Comini, L. R.; Núñez Montoya, S. C.; Sarmiento, M.; Cabrera, J. L.; Argüello, G. A. "Characterizing Some Photophysical, Photochemical, and Photobiological Properties, of Photosensitizing Anthraquinones" *J. Photochem. Photobiol., A* **2007**, *188*, 185–191.

phototoxicity of the shrub from which it was isolated. Grazing livestock that have ingested the plant can suffer from dermatitis, keratoconjunctivitis (which may lead to blindness), and behavioral changes, such as restlessness and photophobia.[47] As a result of these photosensitizing properties (*S*)-bisoranjidiol is found to be photodynamically active against cancer cells,[48] bacteria,[49] and may have potential applications in photodynamic therapy.[50]

Other bisanthraquinones from this family of natural products are also biologically active, however, most biological assays have only been conducted on skyrin or close derivatives. These compounds have been shown to be active against cancer,[51] are glucagon antagonists (useful for exploring antidiabetics),[52] and have shown potential for

(47) (a) Aguirre, D. H.; Neumann, R. A. "Intoxicación por 'Cegadera' (*Heterophyllaea pustulata*) en Caprinos del Noroeste Argentino" *Med. Vet.* **2001**, *18*, 487–490. (b) Núñez Montoya, S. C.; Comini, L. R.; Rumie Vittar, B.; Fernández, I. M.; Rivarola, V. A.; Cabrera, J. L. "Phototoxic Effects of *Heterophyllaea pustulata* (Rubiaceae)" *Toxicon* **2008**, *51*, 1409–1415.

(48) Fernández, I.; Comini, L.; Nigra, A.; Núñez, S.; Rumie Vittar, B.; Cabrera, J.; Rivarola, V. A. "Photodynamic Action and Localization of Anthraquinones in Cancerous Cells" *Biocell* **2009**, *33*, A266.

(49) Comini, L. R.; Núñez Montoya, S. C.; Páez, P. L.; Argüello, G. A.; Albesa, I.; Cabrera, J. L. "Antibacterial Activity of Anthraquinone Derivatives From *Heterophyllaea pustulata*" *J. Photochem. Photobiol., B* **2011**, *102*, 108–114.

(50) (a) Dougherty, T. J.; Gomer, C. J.; Henderson, B. W.; Jori, G.; Kessel, D; Korbelik, M.; Moan, J.; Peng, Q. "Photodynamic Therapy" *J. Natl. Cancer Inst.* **1998**, *90*, 889–905. (b) Dolmans, D. E.; Fukumara, D.; Jain, R. K. "Photodynamic Therapy for Cancer" *Nat. Rev. Cancer* **2003**, *3*, 380–387. (c) Hamblin, M. R.; Hasan, T. "Photodynamic Therapy: A New Antimicrobial Approach to Infectious Disease?" *Photochem. Photobiol. Sci.* **2004**, *3*, 436–450. (d) Yano, S.; Hirohara, S.; Obata, M.; Hagiya, Y.; Ogura, S.; Ikeda, A.; Kataoka, H.; Tanaka, M.; Joh, T. J. "Current States and Future Views in Photodynamic Therapy" *Photochem. Photobiol., C* **2011**, *12*, 46–67.

(51) Lin, L.-C.; Chou, C.-J.; Kuo, Y.-C. "Cytotoxic Principles from *Ventilago leiocarpa*" *J. Nat. Prod.* **2001**, *64*, 674–676.

(52) Parker, J. C.; McPherson, R. K.; Andrews, K. M.; Levy, C. B.; Dubins, J. S.; Chin, J. E.; Perry, P. V.; Hulin, B.; Perry, D. A.; Inagaki, T.; Dekker, K. A.; Tachikawa, K.; Sugie, Y.; Treadway, J. L. "Effects of Skyrin, a Receptor-Selective Glucagon Antagonist, in Rat and Human Hepatocytes" *Diabetes* **2000**, *49*, 2079–2086.

the treatment of depression[53] and hepatitis B.[54] Skyrin has also been reported to display antioxidant behavior comparable to vitamins C and E.[55]

3.3 Prior and Related Syntheses

One of the earliest examples of a bisanthraquinone synthesis was reported by Scholl and co-workers in 1910 (Scheme 3.1A).[56] Their synthesis involved addition of two equivalents of an isobenzofuran-1,3-dione to a biphenyl intermediate. Following the isolation of skyrin as a natural product several decades later, there was an interest in the biomimetic syntheses of these types of compounds. The biomimetic syntheses involved oxidative coupling of anthraquinones or anthrones (Scheme 3.1B). However, the yields were low (0.28 – 35% yield) and the reactions were accompanied by side products such as unsymmetrical bisanthraquinones or extended quinone systems.[57] A different approach, concentrating on the Ullman coupling of brominated anthraquinones has led to moderate to good yields (58–83%) of 1,1'-linked bisanthraquinones, but requires harsh

---

(53) Wirz, A.; Simmen, U.; Heilmann, J.; Calis, I.; Meier, B.; Sticher, O. "Bisanthraquinone Glycosides of *Hypericum perforatum* With Binding Inhibition to CRH-1 Receptors" *Phytochemistry* **2000**, *55*, 941–947.

(54) Don, M.-J.; Huang, Y.-J.; Huang, R.-L.; Lin, Y.-L. "New Phenolic Principles From *Hypericum sampsonii*" *Chem. Pharm. Bull.* **2004**, *52*, 866–869.

(55) Vargas, F.; Rivas, C.; Zoltan, T.; Lopez, V.; Ortega, J.; Izzo, C.; Pineda, M.; Medina, J.; Medina, E.; Rosales, L. "Antioxidant and Scavenging Activity of Skyrin on Free Radical and Some Reactive Oxygen Species" *Avances en Química* **2008**, *3*, 7–14.

(56) Scholl, R.; Liese, K.; Michelson, K.; Grunewald, E. "Eine neue Synthese des 4,4'-Dimethyl-pyranthrons" *Ber.* **1910**, *43*, 512–518.

(57) (a) Ikekawa, T. "Isoskyrin" *Chem. Pharm. Bull.* **1963**, *11*, 749–751. (b) Franck, B.; Chahin, R.; Eckert, H.-G.; Langenberg, R.; Radtke, V. ""Natural Products From Fungi. 27. Biomimetic Synthesis of Skyrin" *Angew. Chem., Int. Ed.* **1975**, *14*, 819–820. (c) Banks, H. J.; Cameron, D. W.; Raverty, W. D. "Chemistry of Coccoidea II. Condensed Polycyclic Pigments from Two Australian Pseudococcids (Hemiptera)" *Aust. J. Chem.* **1976**, *29*, 1509–1521. (d) Cameron, D. W.; Edmonds, J. S.; Raverty, W. D. "Oxidation of Emodin Anthrone and Stereochemistry of Emodin Bianthrone" *Aust. J. Chem.* **1976**, *29*, 1535–1548.

reaction conditions (225–240 °C, Scheme 3.1C).[58] Both of these approaches were used to complete racemic syntheses of the natural products skyrin and hinakurin. More recently, syntheses of related bisanthraquinone natural products have been reported. For example, the 2,2'-linked biaryl named biphyscion, and the skyrin derivatives, 2,2'-epi-cytoskyrin and rugulosin, which possess cage-like "skyrane" motifs, have been synthesized.[59,60] However, none of these prior efforts have led to an enantioselective synthesis of a bisanthraquinone. In addition, no synthesis of bisoranjidiol had been reported.

Scheme 3.1 Prior synthetic approaches.

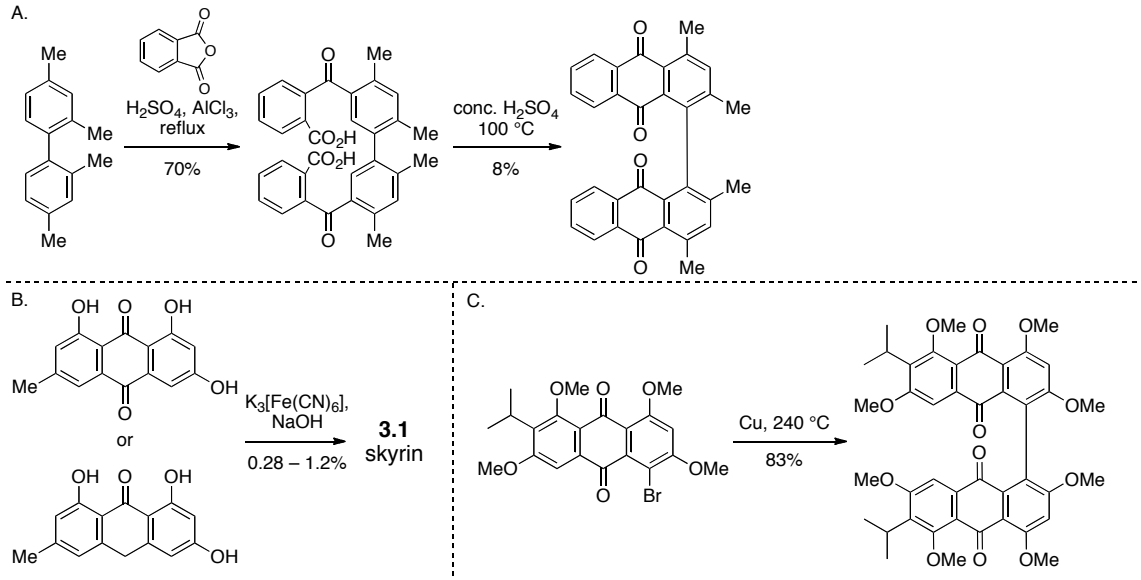

(58) (a) Shibata, S.; Tanaka, O.; Kitagawa, I. "Metabolic Products of Fungi V. The Structure of Skyrin" *Pharm. Bull.* **1955**, *3*, 278–283. (b) Tanaka, O.; Kaneko, C. "Metabolic Products of Fungi. VI. The Structure of Skyrin. II. Synthesis of Skyrin Beta, Beta'-Dimethyl Ether" *Pharm. Bull.* **1955**, *3*, 284–286. (c) Tanaka, O. "Metabolic Products of Fungi. XIV. The Structure of Skyrin (3). On Pseudoskyrin" *Chem. Pharm. Bull.* **1958**, *2*, 203–208. (d) Iio, H.; Zenfuku, K.; Tokoroyama, T. "A Facile Synthesis of Stentorin, the Photoreceptor of *Stentor coeruleus*" *Tetrahedron Lett.* **1995**, *36*, 5921–5924.

(59) Hauser, F. M.; Gauuan, P. J. F. "Total Synthesis of (+/-)-Biphyscion" *Org. Lett.* **1999**, *1*, 671–672.

(60) (a) Nicolaou, K. C.; Papageorgiou, C. D.; Piper, J. L.; Chadha, R. K. "The Cytoskyrin Cascade: A Facile Entry into Cytoskyrin A, Deoxyrubroskyrin, Rugulin, Skyrin, and Flavoskyrin Model Systems" *Angew. Chem. Int. Ed.* **2005**, *44*, 5846–5851. (b) Nicolaou, K. C.; Lim, Y. H.; Piper, J. L.; Papageorgiou, C. D. "Total Syntheses of 2,2 '-*Epi*-Cytoskyrin A, Rugulosin, and the Alleged Structure of Rugulin" *J. Am. Chem. Soc.* **2007**, *129*, 4001–4013.

3.4 Retrosynthetic Analysis[18,19]

For the synthesis of (*S*)-bisoranjidiol, we initially envisioned a biomimetic synthesis involving a late stage oxidative asymmetric biaryl coupling of an anthraquinone with a chiral copper catalyst. Enantioselective biaryl couplings have been used extensively by the Kozlowski group to access a number of helically chiral perylenequinone natural products and derivatives.[7a,11] However, for this project preliminary results suggested that a biomimetic approach would not work because of the resistance of the anthraquinone to further oxidation. It was previously shown by the Kozlowski group that the coupling of **3.10** using the diaza-*cis*-decalin copper catalyst **1.12** did not proceed (Scheme 3.2).

Scheme 3.2 Attempted biaryl coupling of an anthraquinone.

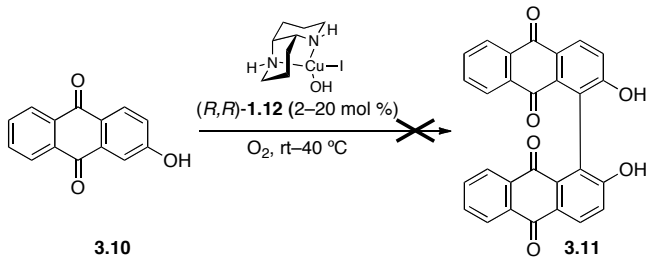

The retrosynthesis was revised to include the asymmetric oxidative coupling of 2-naphthols instead, with the goal of using a chiral binaphtho-*para*-quinone to access both (*S*)-bisoranjidiol and a number of analogs (Scheme 3.3). We envisioned forming (*S*)-bisoranjidiol through a tandem regioselective Diels-Alder/aromatization reaction between an alkyl trimethylsilylvinyl ketene acetal and binaphtho-*para*-quinone. Likewise, several analogs could also be generated from the same or similar binaphtho-*para*-quinone intermediate via Diels-Alder reactions with different dienes, followed by aromatization.

The chiral binaphtho-*para*-quinones, in turn, could be generated via an enantioselective biaryl coupling reaction of an 8-substituted 2-naphthol, followed by a selective oxidation of an 8,8'-hydroxylated binaphthol (see Chapters 1 and 2).

Scheme 3.3 Retrosynthetic analysis of bisanthraquinones.

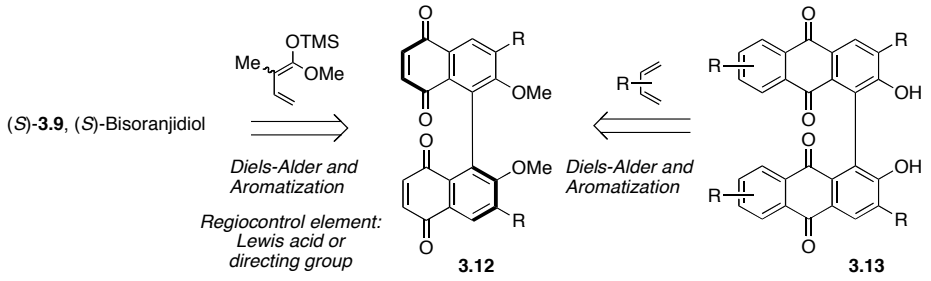

CHAPTER 4: Total Synthesis of (*S*)-Bisoranjidiol and Analogs Through Tandem Diels-Alder/Aromatization Reactions[18,19]

4.1 Introduction to Regioselectivity in the Diels-Alder Reaction

The Diels-Alder reaction between a 1,3-diene and a naphtho- or benzoquinone is well represented in the literature. Often, the [4+2] cycloaddition is followed by aromatization of the cycloadduct to produce anthraquinones or naphthoquinones. When considering only the formation of anthraquinones containing *peri*-hydroxyl substituents, as is a key component of all the 1,1'-linked symmetrical bisanthraquinone natural products (see Chapter 3), the choice of diene can be important. A very simple silyl- or alkoxy butadiene (**4.1**) or a more reactive diene such as the Danishefsky diene (**4.2**)[61] could be used for this transformation, however, loss of the siloxy or alkoxy protecting group during aromatization is typical (**4.6** and **47**, Figure 4.1). Other types of dienes, such as 2-pyrones or cyclohexadienes have also been employed because they undergo the favorable loss of carbon dioxide or ethylene during aromatization, but frequently, Brassard-type dienes (alkyl-, silyl- or mixed vinylketene acetals, **4.3**–**4.5,** Figure 4.1) are used to obtain *peri*-hydroxyl or alkoxy functionality upon aromatization (**4.8** or **4.9**).

(61) Danishefsky, S.; Kitaharai, T. "Useful Diene for the Diels-Alder Reaction" *J. Am. Chem. Soc.* **1974**, *96,* 7807–7808.

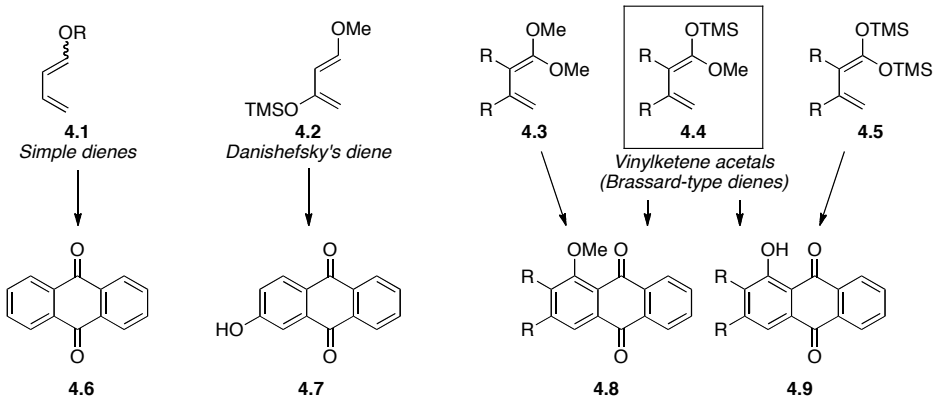

Figure 4.1 Dienes and corresponding anthraquinones after aromatization.

In a general reaction, the Brassard-type diene reacts with a *para*-naphthoquinone electrophile in a [4+2] process (Scheme 4.1). The newly formed cycloadduct can then undergo an acid or base mediated aromatization, upon which the silyl group is lost, followed by elimination of one of the RO-groups, tautomerization, and reoxidation to the anthraquinone. Alkyl vinylketene acetals (**4.3**),[62] silyl vinylketene acetals (**4.5**),[63] and more frequently, mixed vinylketene acetals (**4.4**) containing both a siloxy and alkoxy substituent at one of its termini have been used (Figure 4.1). One drawback of the mixed vinylketene acetals is that during aromatization loss of either the siloxy or alkoxy group from the cycloadduct is possible, though typically loss of MeOH is favored. Loss of

(62) Examples: (a) Banville, J.; Grandmaison, J.- L.; Lang, G.; Brassard, P. "Reactions of Keten Acetals. Part I. A Simple Synthesis of Some Naturally Occurring Anthraquinones" *Can. J. Chem*. **1974**, *52*, 80–87. (b) Brisson, C.; Brassard, P. "Regiospecific Reactions of Some Vinylogous Ketene Acetals with Haloquinones and Their Regioselective Formation by Dienolization" *J. Org. Chem*. **1981**, *46*, 1810–1814.

(63) (a) Roberge, G.; Brassard, P. "Reactions of Ketene Acetals. 12. A Regiospecific Synthesis of Anthragallols" *Synthesis* **1981**, 381–384. (b) Khan, A. T.; Blessing, B.; Schmidt, R. R. "An Expedient and Efficient Synthesis of Naturally Occurring Hydroxy Substituted Anthraquinones" *Synthesis* **1994**, 254–257.

TMSOH would produce an anthraquinone with a *peri*-methoxy group (**4.8**) instead of the desired hydroxyl group (**4.9**, Figure 4.1).[64,65]

Scheme 4.1 General Diels-Alder/aromatization reaction.

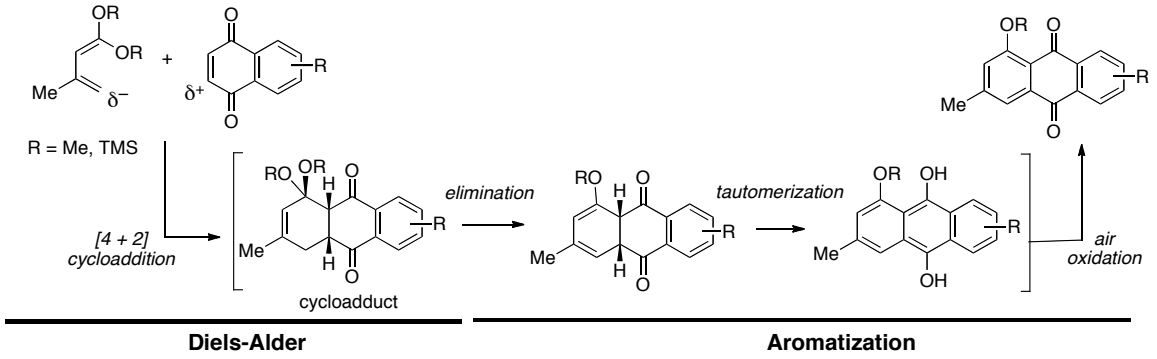

Unlike the generalized reaction illustrated in Scheme 4.1, most naphthoquinone substrates are not symmetrical, making control over the regiochemical outcome of the cycloaddition a challenge. Boeckman and coworkers have suggested, from their studies with juglone derivatives, that the polarization of the diene affects the regioselectivity of the reaction to a greater degree than the dienophile.[66] This means that the quinone is only weakly polarized and approximating the regioselection through evaluation of the quinone is not sufficient on its own.[66] In the cases of strongly polarized dienes, however, the regiochemical outcome of the reaction becomes more predictable based on the polarization of the dienophile, as illustrated with charge affinity patterns. For juglone

(64) Savard, J.; Brassard, P. "Reactions of Ketene Acetals-14. The Use of Simple Mixed Vinylketene Acetals in the Annulation of Quinones" *Tetrahedron* **1984**, *40*, 3455–3464.

(65) Motoyoshiya, J.; Masue, Y.; Nishi, Y.; Aoyama, H. "Synthesis of Hypericin via Emodin Anthrone Derived From a Two-Fold Diels-Alder Reaction of 1,4-Benzoquinone" *Nat. Prod. Commun.* **2007**, *2*, 67–70.

(66) Boeckman, R. K.; Dolak, T. M.; Culos, K. O. "Diels-Alder Cycloaddition of Juglone Derivatives: Elucidation of Factors Influencing Regiochemical Control" *J. Am. Chem. Soc.* **1978**, *100*, 7098–7100.

derivatives like **4.10** (Figure 4.2), the *peri*-4-hydroxyl of the naphthoquinone acts as an "internal Lewis acid" through hydrogen bonding to the carbonyl. This intramolecular hydrogen bond polarizes the quinone and favors attack at the 7-carbon. Without this interaction, nucleophilic attack is favored at the 6-carbon, due to the donation of electron density into the 5-carbonyl (Figure 4.2).[66]

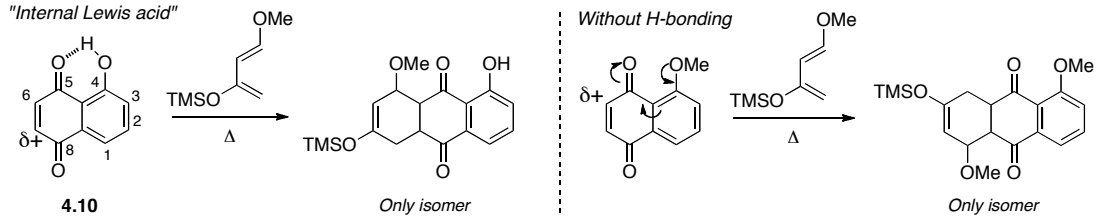

Figure 4.2 Regioselectivity with juglone derivatives.

Where hydrogen bonding is not possible, such as at the 2-position, substituents can still polarize the quinone through resonance, affecting regioselection (Figure 4.3A).[67] For these monomers, two possible regioisomers could be produced by the Diels-Alder reaction. Following aromatization of the cycloadducts, the *peri*-hydroxyl could be oriented either *syn* relative to the 2-alkoxy group or *anti*. Considering that the resonance contribution from the electron-donating group (EDG) is to the 5-carbonyl of the naphthoquinone, in this example, the 8-carbonyl is more electrophilic and formation of the *syn*-isomer is favored (Figure 4.3A). This outcome is further illustrated in the reaction of **4.11** with diene **4.12**. This example also pertains to our proposed synthesis of bisoranjidiol, as binaphtho-*para*-quinone **3.12** contains analogous groups (Scheme 3.3). Thus, a similar argument about regioselection can be made for binaphtho-*para*-quinone

(67) Kelly, T. R. "Regiochemical Control in the Diels Alder Reactions of Substituted Naphthoquinones: Orientational Manipulation in the Synthesis of Anthraquinones" *Tetrahedron Lett.* **1978**, *19*, 1387–1390. (b) Kelly, T. R.; Parekh, N. D. "Regiochemical Control in the Diels-Alder Reaction of Substituted Naphthoquinones. The Directing Effects of C-6 Oxygen Substituents" *J. Org. Chem.* **1982**, *47,* 5009–5013.

3.12, meaning the bis-*syn*-adduct (*in*-*in*-bisanthraquinone isomer) will predominate in the reaction. However, bisoranjidiol is effectively an *out*-*out*-isomer (see Figure 4.3B) and requires formation of a bis-*anti*-adduct. Thus, a means of controlling the regioselection of the cycloaddition reaction is required.

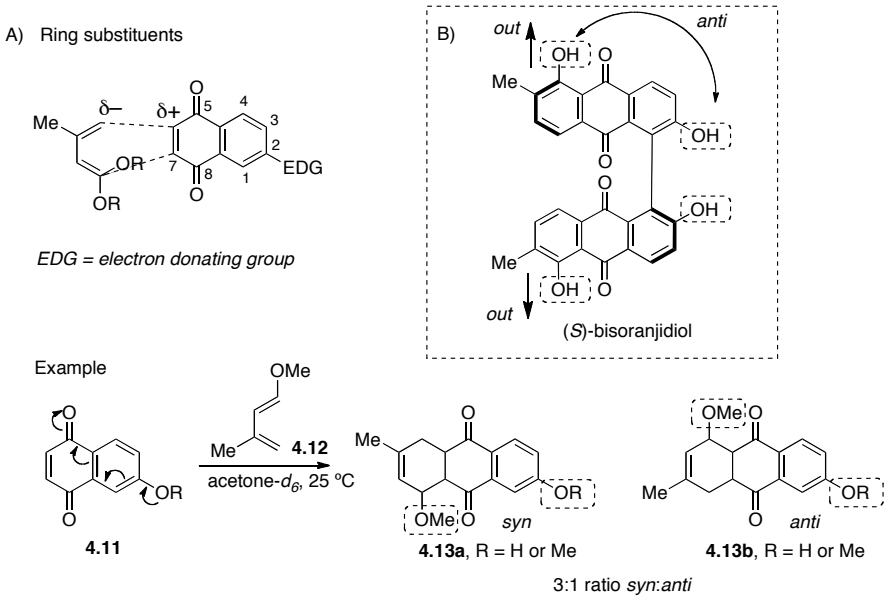

Figure 4.3 Substituent effects on regioselectivity.

Two methods for reversing the selectivity are to use Lewis acids (LA) or to install directing groups. The LA coordinates to the more basic carbonyl, resulting in a more electrophilic 7-carbon and formation of the *anti*-isomer (Figure 4.4A). Lewis acids, such as $ZnCl_2$, $BF_3{\cdot}OEt_2$, $AlCl_3$, etc. have been reported to improve selectivities.[66,68,69] For example, in the synthesis of 11-deoxydaunomycinone, the addition of $ZnCl_2$ improved

(68) Motoyoshiya, J.; Kameda, T; Asari, M.; Miyamoto, M.; Narita, S.; Aoyama, H.; Hayashi, S. "Importance of the Role of Secondary Orbital Interactions in the Diels–Alder Reaction. Regioselectivity in the Catalyzed and Uncatalyzed Reactions of Juglone and Aliphatic Dienes" *J. Chem. Soc., Perkin Trans. 2* **1997**, 1845–1850.

(69) Kraus, G. A.; Woo, S. H. "Total Synthesis of 11-Deoxydaunomycinone and Analogs by a Tandem Claisen-Diels-Alder Strategy" *J. Org. Chem*. **1987**, *52*, 4841–4846.

the selectivity between **4.14** and 1-(trimethylsilyloxy)-1,3-butadiene from a 4:3 ratio to a 50:1 ratio of regioisomers (**4.15**, Figure 4.4A).[69] Aside from Lewis acids, directing groups have also been used to control the regioselection of the Diels-Alder. Typically halogens, such as chloro[64,70-72] or bromo[71] substituents, have been used, but other groups, such as sulfoxides[73] or acetoxy[72] groups can provide a similar result (Figure 4.4B). For example, the reaction of bromoquinone **4.16** with vinylketene acetal **4.17** provided only the desired anthraquinone regioisomer (**4.18**) in high yield (Figure 4.4B).[71b]

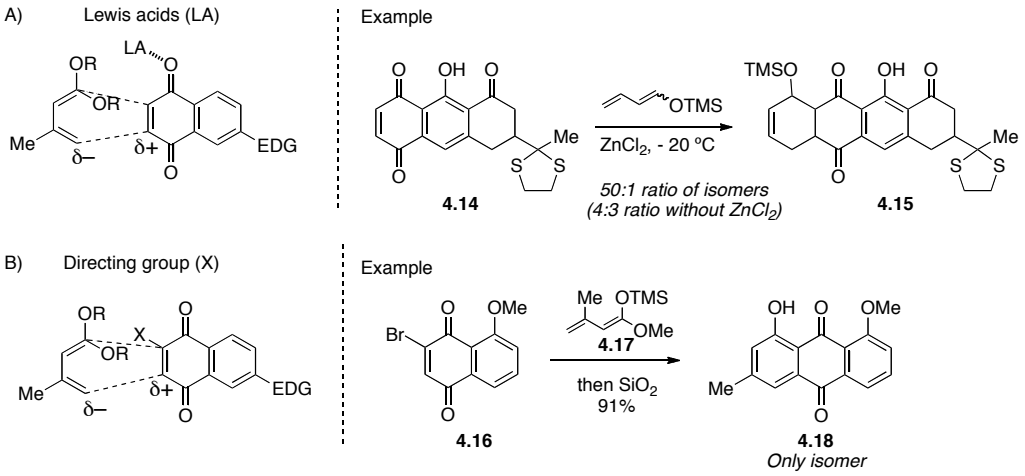

Figure 4.4 Methods of regiocontrol.

(70) (a) Savard, J.; Brassard, P. "Regiospecific Syntheses of Quinones Using Vinylketene Acetals Derived From Unsaturated Esters" *Tetrahedron Lett.* **1979**, *20*, 4911–4914. (b) Danishefsky, S.; Uang, B. J.; Quallich, G. "Total Synthesis of Vineomycinone B2 Methyl Ester" *J. Am. Chem. Soc.* **1985**, *107*, 1285–1293.

(71) (a) Grandmaison, J.-L.; Brassard, P. "Reactions of Ketene Acetals. 10. Total Syntheses of the Anthraquinones Rubrocomatulin Pentamethyl Ether, 2-Acetylemodin, 2-Acetyl-5-hydroxyemodin Tetramethyl Ether, and Xanthorin" *J. Org. Chem.* **1978**, *43*. 1435–1438. (b) Tietz, L. F.; Gericke, K. M.; Schuberth, I. "Synthesis of Highly Functionalized Anthraquinones and Evaluation of Their Antitumor Activity" *Eur. J. Org. Chem.* **2007**, 4563–4577.

(72) Cameron, D. W.; Riches, A. G. "Reaction of 2-Acetoxy-3-chloro and 2,3-Diacetoxy Naphthoquinones with 1,3-Dioxy and 1,1,3-Trioxy Butadienes" *Aust. J. Chem.* **1999**, *52*, 1165–1171.

(73) Iwao, M.; Kuraishi, T. "Utilization of Sulfide, Sulfoxide, and Sulfone Groups as Regiochemical Control Elements in the Diels–Alder Reaction of Naphthoquinones" *Bull. Chem. Soc. Jpn.* **1987**, *60*, 4051–4060.

4.2 Thermal Reactions and Effects of Lewis Acids in the Diels-Alder Reaction

To complete the synthesis of (*S*)-bisoranjidiol (**3.9**), we proposed that the anthraquinone scaffold could evolve from the regioselective Diels-Alder/aromatization reactions of a vinylketene acetal with a binaphtho-*para*-quinone (see Chapter 3, Scheme 3.3). As this task effectively meant conducting four transformations on one molecule in a regioselective manner, we chose to explore the tandem reaction initially with simple dienes and the racemic binaphtho-*para*-quinone **2.4** (Scheme 4.2). When **2.4** was treated with commercially available 1-(trimethylsilyloxy)-1,3-butadiene (**4.20**), the major product isolated was the monocycloadduct **4.19** (less than 10% biscycloadduct) after two days at room temperature. Moving to a more reactive diene such as the Danishefsky diene, **4.2**, established that the biscycloadduct would form and aromatize on silica to produce a bisanthraquinone in 41% yield. At this stage, attempts were not made to establish which regioisomer had formed, but based on the influence of the substituents on the quinone (see section 4.1) it is likely that formation of **4.21** was favored.

Scheme 4.2 Preliminary Diels-Alder reactions.

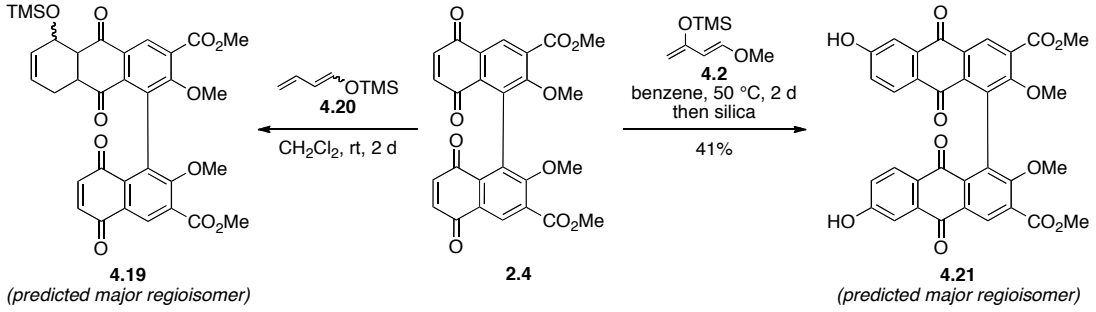

After establishing that a bisanthraquinone could be readily generated via this strategy, evaluation of the regioselectivity of the Diels-Alder reaction was the next

challenge to the synthesis of (*S*)-bisoranjidiol. Initially, a *meta*-substituted diene (**4.17**) was chosen for analysis, rather than the *ortho*-substituted diene necessary for the synthesis of bisoranjidiol because the *meta*-substituted diene is more stable and can be stored for longer periods of time.[64] Following a known procedure,[74] diene **4.17**, was synthesized via LDA deprotonation of ester **4.22** and subsequent trapping of the enolate with TMSCl (Scheme 4.3). Treatment of binaphtho-*para*-quinone **2.4** with diene **4.17**, followed by aromatization on silica produced a mixture of three regioisomers **4.23a-c** in 56–66% yield.

Scheme 4.3 Regioselectivity with a Lewis acid.

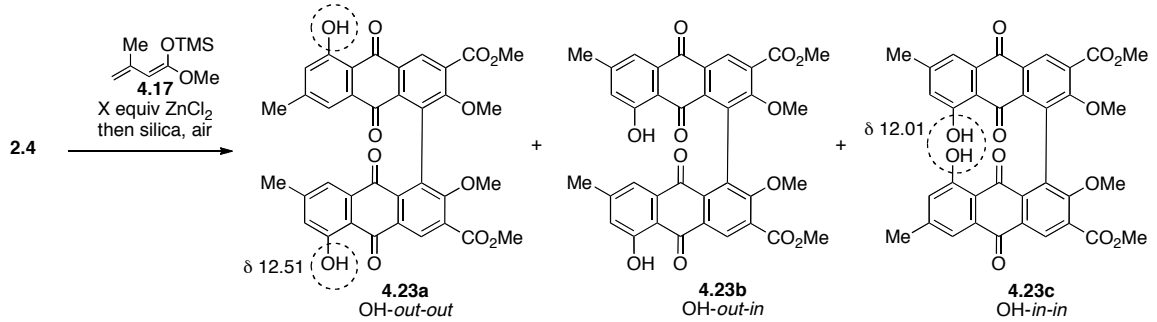

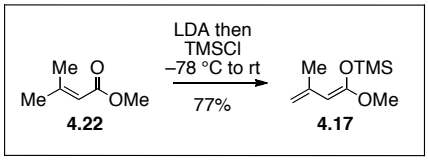

Equiv $ZnCl_2$	Ratio (**a**:**b**:**c**)	Mixture yield (%)
0	4:22:74	66[a]
2	13:37:50	<10
4	80:20:–	<10

[a]includes *peri*-methoxy derivatives

To measure the selectivity of this thermal reaction, regioisomeric assignments were made by comparing the relative ^{1}H NMR chemical shifts of the newly produced *peri*-hydroxyl groups (highlighted in Scheme 4.3). For this substrate, the chemical shifts

(74) Tietz, L. F.; Gericke, K. M.; Singidi, R. R.; Schuberth, I. "Novel Strategies for the Synthesis of Anthrapyran Antibiotics: Discovery of a New Antitumor Agent and Total Synthesis of (*S*)-Espicufolin" *Org. Biomol. Chem.* **2007**, *5*, 1191–1200.

of the *out*- or *in-peri*-hydroxyls differed by 0.5 ppm. Since the *peri*-hydroxyl group that is hydrogen-bonded to the more basic carbonyl is more deshielded, it is expected to shift downfield relative to the other regioisomer. According to this analysis, *out-out*-isomer, **4.23a**, should correspond to the compound displaying a shift of 12.51 ppm, while *in-in*-isomer, **4.23c**, corresponds to the compound with showing a chemical shift of 12.01 ppm. Likewise the unsymmetrical isomer, **4.23b**, exhibits two peaks similar to **4.23a** and **4.23c** (12.52 ppm and 11.99 ppm). A crystal structure of an analogous monomer, **4.24b** (Figure 4.5, see Table 4.1 for synthesis), which is shifted 0.2 ppm upfield from the *anti*-isomer, **4.24a**, later confirmed that the regioisomers were assigned correctly.

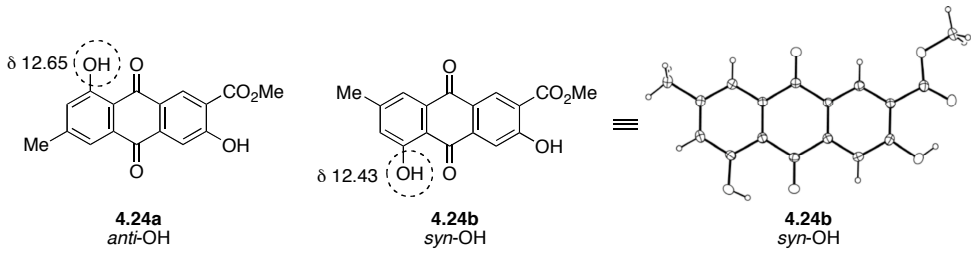

Figure 4.5 Confirmation of regioisomeric assignments.

Once assignment of the *out-out* and *in-in*-bisanthraquinone regioisomers was made, the selectivity of the thermal cycloaddition reaction of **2.4** with diene **4.17** was measured from the integration of the peaks in the ^{1}H NMR and calculated to be 4:22:74 for **4.23a:4.23b:4.23c** (Scheme 4.3). The observed favorable formation of *in-in*-isomer **4.23c** was the expected result based on the charge affinity patterns of binaphtho-*para*-quinone **2.4**. Unfortunately, the *out-out*-regioisomer is required for bisoranjidiol and it was necessary to explore different methods of regiocontrol that will favor reaction of the diene in the appropriate orientation. The first method explored was the use of a Lewis

acid. Two equivalents of $ZnCl_2$ moderately improved the regioselectivity, while four equivalents of $ZnCl_2$ produced *out-out*-isomer **4.23a** as the major regioisomer (Scheme 4.3). None of the *in-in*-isomer **4.23c** was observed, however, the overall yields were consistently poor (<10%) due to formation of numerous byproducts and decomposition. Other Lewis acids, such as $BF_3 \cdot OEt_2$, were equally detrimental to the yields, so I decided to optimize conditions on the monomer.

Two naphthoquinones were successfully synthesized from compound **1.19** (Scheme 4.4). Quinone **4.25**, was synthesized in 52% yield, followed by methylation to afford quinone **4.26** in 79% yield.

Scheme 4.4 Synthesis of naphthoquinone monomers.

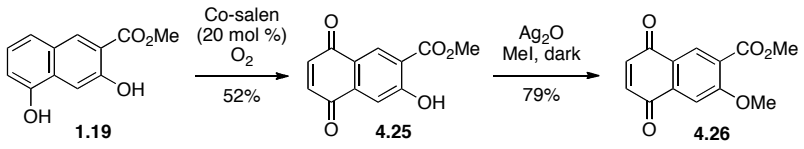

With both naphthoquinones in hand, each was treated with diene **4.17**. Without a Lewis acid present, anthraquinones **4.24a-b** and **4.27a-b** were produced in good yield (62–78%, entries 1-3, Table 4.1) with a preference for the undesired *syn*-isomer, as had been observed with the dimer. Significant amounts of anthraquinones containing *peri*-methoxy groups instead of *peri*-hydroxyl groups, such as compound **4.28**, were also isolated. The yields in Table 4.1 include these isomers. These products are the result of an aromatization in which loss of the trimethylsiloxy group rather than the methoxy group of the newly formed cycloadduct occurs. Deprotection of these compounds with BCl_3 confirmed that the regioisomeric ratios were identical with the isolated *peri*-

hydroxy-substituted anthraquinones. Thus, measurement of the ratios of *peri*-hydroxyl anthraquinones was sufficient to determine the overall selectivity of the reaction. Reaction preference for **4.24a** was not improved adequately by Lewis acids, such as $ZnCl_2$ and $Ti(OMe)_4$ (entries 4 and 5). Yields were low due to decomposition and byproducts. For example, the addition of $ZnCl_2$ resulted in 33% yield of an undesired product (**4.29**) resulting from conjugate addition of the diene onto the quinone. Overall, Lewis acids did not provide both good selectivities and yields, so we chose to explore directing groups as an alternate method of controlling the regioselectivity.

Table 4.1 Evaluation of Diels-Alder reaction selectivity on a monomeric system.

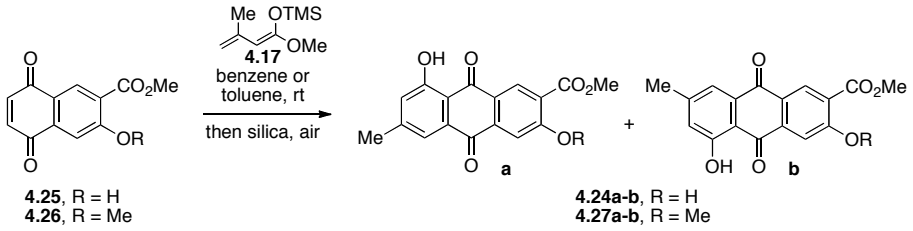

4.25, R = H
4.26, R = Me

4.24a-b, R = H
4.27a-b, R = Me

Entry	R	Lewis acid	Mixture yield (%)	Ratio (**a**:**b**)
1	H	—	65[a]	9:91
2	Me	—	62[a]	13:87
3[b]	Me (no ester)	—	78	24:76
4	H	$ZnCl_2$ (2 equiv)	17	19:81
5	H	$Ti(OMe)_4$ (2 equiv)	38	12:88

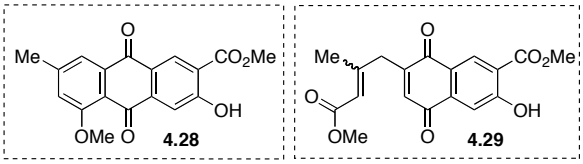

[a] Includes *peri*-methoxy yield
[b] Benzene reflux then O_2, 5% aq NaOH; reference 73

4.3 Synthesis of Bromoquinones and Effects of Directing Groups in the Diels-Alder Reaction

Since Lewis acids did not provide satisfactory yields in the Diels-Alder reaction, the synthesis of a binaphtho-*para*-quinone containing bromo-directing groups was

explored. Two approaches for bromination were investigated on the monomer. The first method involved bromination of **4.25**, followed by dehydrobromination to yield **4.30a** and **4.30b** as an inseparable 25:75 mixture of regioisomers. Pleasingly, this ratio was retained in the Diels-Alder reaction (25:75), producing anthraquinones **4.24a** and **4.24b** in 84% yield. Besides bromination with Br_2, another method has been reported, which involves hydrobromination of the quinone with HBr. Monomer **4.26** was treated with HBr, followed by oxidation of the brominated hydroquinones to quinones **4.31a** and **4.31b** in a favorable 93:7 ratio and 56% yield.

Scheme 4.5 Synthesis of bromoquinone monomers.

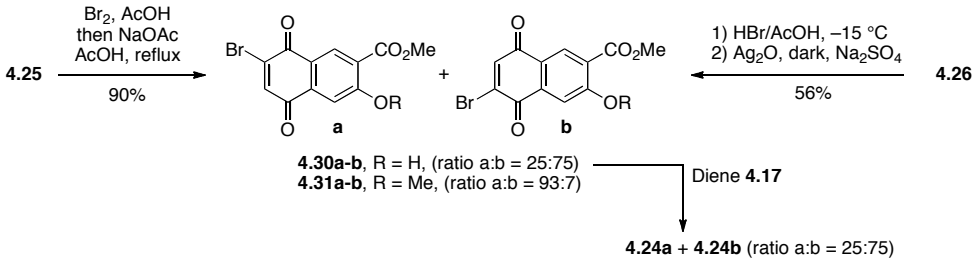

Unfortunately, this hydrobromination reaction did not translate well to the biaryl system, **2.4**. While preference for formation of the desired regioisomer was observed (66:33:<1), the yield was poor (30%) and the reactions were incomplete, with a significant amount of monobrominated species (entry 1, Table 4.2). More forcing conditions led to undesired demethylation of the methoxy groups and a complex mixture. Bromination, followed by dehydrobromination proved to be more promising for the dimers. Notably, the other substituents on the quinone and the conditions for the dehydrohalogenation influenced the ratio of regioisomers. For example, the protecting group or lack thereof on the 2,2'-hydroxyls produced the desired regioisomer in 18%

yield for the unprotected quinone (R^1 = H) and a more favorable 39% for the quinone with the 2,2'-methoxy groups (entries 2 and 3). Encouragingly, this regioisomer ratio was retained in the Diels-Alder reaction with diene **4.17**, as had been observed with the monomer.

Table 4.2 Bromination of binaphtho-*para*-quinones.

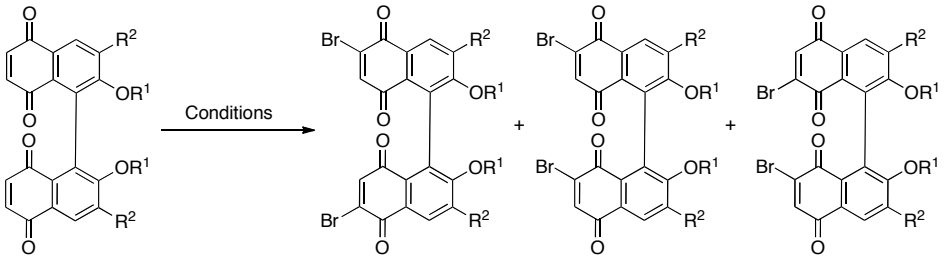

Entry	Product	R^1	R^2	Conditions	Mixture yield (%)	Ratio (**a**:**b**:**c**)
1	**4.32**	Me	CO_2Me	A	30[a]	66:33:<1
2	**4.33**	H	CO_2Me	B	–	18:58:24
3	**4.32**	Me	CO_2Me	B	87	37:50:13
4	**4.34**	Me	H	B	95 (75)[b]	43:47:10
5	**4.35**	Me	Me	B	–	60:35:5
6	**4.34**	Me	H	C	–	32:47:21

Conditions:
A = 1) HBr/AcOH, –15 °C, 2) Ag_2O, Na_2SO_4, dark
B = Br_2, AcOH then NaOAc, AcOH, reflux
C = Br_2, CH_2Cl_2 then NEt_3, rt
[a] Incomplete rxn; longer times result in demethylation
[b] After semi-prep HPLC

Further investigation of the bromination revealed that the R^2 substituent also influenced the selectivity, with electron poor groups producing less favorable ratios (39% for R^2 = CO_2Me compared with 60% for R^2 = Me, entries 3-5, Table 4.2). The use of hindered amine bases instead of NaOAc either provided less favorable ratios (NEt_3, entry 6) or led to decomposition (DBU). Ultimately, entry 4 provided the best opportunity to synthesize bisoranjidiol (95% yield, 43:47:10 ratio of **4.34a**:**4.34b**:**4.34c**). It also

contributed to our ability to synthesize potentially bioactive derivatives, since the reaction also generated a significant amount of the unsymmetrical regioisomer **4.34b**. This unsymmetrical regioisomer and the minor amount of **4.34c** could be used to generate unnatural regioisomers of bisoranjidiol.

4.4 Completion of the Synthesis of (*S*)-Bisoranjidiol

As it appeared that bromo groups on the quinone behaved successfully as directing groups, we focused on completion of the synthesis of (*S*)-bisoranjidiol and its unnatural regioisomer. *ortho*-Substituted diene **4.37** was synthesized from methyl tiglate, **4.36**, via deprotonation and trapping of the enolate with TMSCl (Scheme 4.2).[75] Knowing that the Diels-Alder reaction between **4.32a-c** and diene **4.17** proceeded with retention of the isomeric ratio, it was anticipated that comparable results would be obtained once **4.34a-c** was treated with diene **4.37**. However, treatment of **4.34a-c** with diene **4.37**, followed by aromatization on silica or with NaOH under O_2, led to almost no product formation and a complex mixture. This result was puzzling because the cycloaddition reaction appeared to be successful as judged by thin-layer chromatography (TLC). Namely, the new products that formed turned very bright yellow on TLC after a few hours, seeming to indicate anthraquinone formation. In fact, when these materials were isolated from the TLC plate they contained product. After realizing that the aromatization worked well on the TLC plate, silica obtained from a TLC plate (Silicycle) was used for this transformation rather than the bulk silica gel (Silicycle, 40–63 μm).

(75) Kim, G. T.; Wenz, M.; Park, J. I.; Hasserodt, J.; Janda, K. D. "Polyene Substrates With Unusual Methylation Patterns to Probe the Active Sites of Three Catalytic Antibodies" *Bioorg. Med. Chem.* **2002**, *10*, 1249–1262.

With this adjustment bisanthraquinone products **4.38** were successfully isolated, however, the distribution of bisanthraquinone products did not reflect the regioisomeric ratios of the starting material (Scheme 4.6). Rather, *out-out*-bisanthraquinone **4.38a** was isolated predominantly. The overall yield (52%) suggested that there was a reactivity problem in the cycloaddition reaction. This problem was believed to be centered around the change to *ortho*-substituted diene **4.37**, since the ester substrate **4.32** showed the same problem. The change in product distribution could, in part, be due to poor reactivity of **4.34b** and **4.34c** or their monocycloadducts towards diene **4.37**, and/or decomposition of those isomers. The *ortho*-methyl substitution on diene **4.37** does make the diene more hindered compared to the *meta*-methyl substituted diene **4.17**.

Scheme 4.6 Reactivity differences in the Diels-Alder reaction.

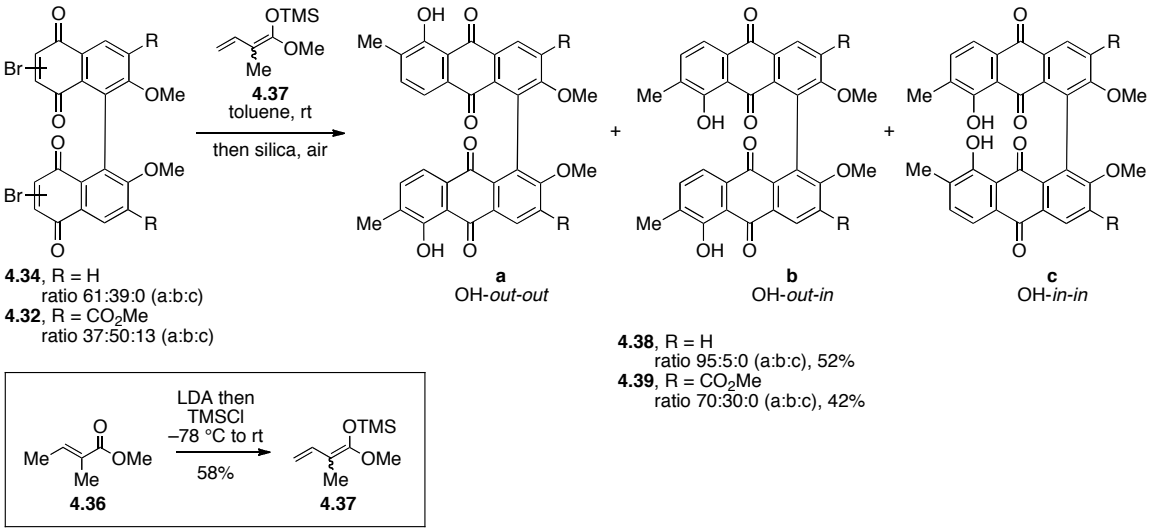

In order to investigate these reactivity differences, the bromoquinone regioisomers **4.34a-c** were separated via semi-preparative HPLC[76] and treated separately

(76) I thank the Joullié group for use of their HPLC and the Smith group for use of a semi-prep column.

with diene **4.37** (Scheme 4.7). Formation of *out*-*out*-bisanthraquinone, (*S*)-**4.38a**, proceeded well, affording the natural product precursor in 80% yield. Notably, this yield is the result of four transformations per molecule, which breaks down to a highly efficient ~95% yield per transformation. Formation of the unsymmetrical regioisomer, *out*-*in*-bisanthraquinone (*S*)-**4.38b** was nearly three times slower, due to a stalling of the Diels-Alder reaction at the monocycloadduct intermediate. Increased decomposition also contributed to lower yields of (*S*)-**4.38b**. Decomposition was the most prominent result from the reaction between (*S*)-**4.34c** and **4.37** to form the sterically congested *in*-*in*-bisanthraquinone, (*S*)-**4.38c**, so this regioisomer was not pursued further.

Scheme 4.7 Synthesis of (*S*)-bisoranjidiol and regioisomer.

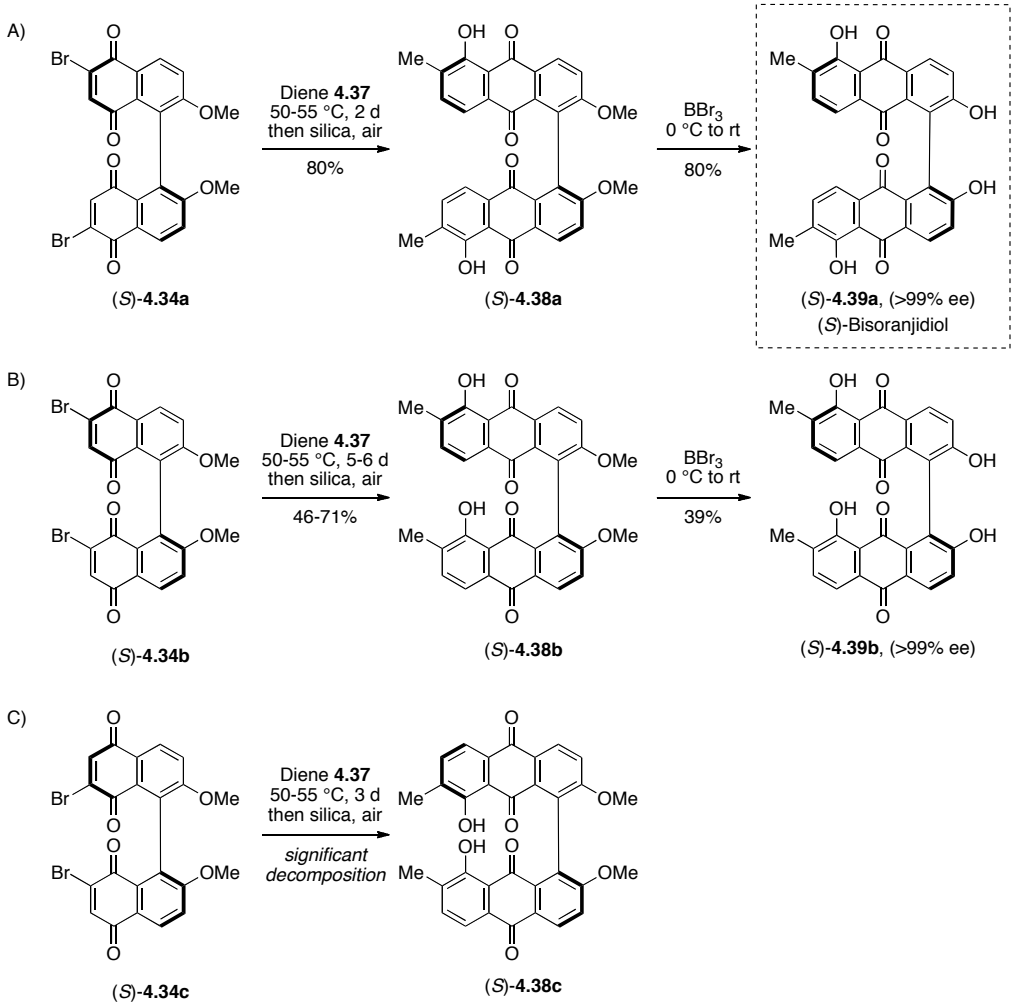

Following a BBr_3 deprotection, (*S*)-bisoranjidiol [(*S*)-**4.39a**] and its unnatural regioisomer [(*S*)-**4.39b**] were obtained in 80% and 39% yield respectively, without altering the enantiomeric excess (>99% ee, Scheme 4.7). The NMR spectroscopic data of (*S*)-**4.39a** matched the reported values of the natural product (Table 4.3).[45] The overall yield for the synthesis of (*S*)-bisoranjidiol is 4% over 12 steps. Notably, with racemic material it is possible to run the first four reactions and three other reactions without column chromatography.

Table 4.3 Comparison of ^{1}H and ^{13}C NMR data for literature and synthetic (*S*)-bisoranjidiol.

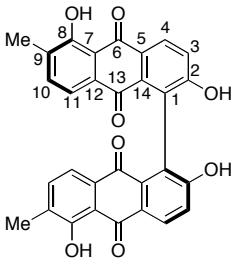

^{1}H NMR Data

Position	Literature[a] (DMSO-d_6) δ_H	Synthetic (DMSO-d_6) δ_H
3	7.32, d	7.34, d
4	8.23, d	8.25, d
10	7.30, d	7.31, d
11	7.53, d	7.54, d
Me	2.25, d	2.26, d
2-OH	– –	10.79, s
8-OH	13.14, s	13.15, s

[a]Chemical shifts adjusted from 2.54 ppm to 2.49 ppm for DMSO-d_6 reference peak.

^{13}C NMR Data

Position	Literature (DMSO-d_6) δ_C	Synthetic (DMSO-d_6) δ_C
1	127.1	127.2
2	161.5	161.5
3	125.2	125.2
4	128.6	128.6
5	120.1	120.1
6	187.8	187.8
7	114.4	114.4
8	159.6	159.6
9	133.4	133.4
10	136.9	136.9
11	118.4	118.4
12	131.6	131.6
13	182.3	182.3
14	132.5	132.5
Me	15.5	15.6

To confirm that the natural stereoisomer of bisoranjidiol is of the (*S*)-configuration, a CD spectrum of the synthetic material was measured (see Appendix), however, comparison with the CD spectrum provided by Dr. Cabrera was inconclusive. Dr. Cabrera kindly provided us with an authentic sample of bisoranjidiol for chiral HPLC analysis.[77] Surprisingly, only 5% ee (*S*) was measured for the natural product isolate. Concurrently, we discovered that while the enantiopurity of bisoranjidiol did not change when stored as a solid, it eroded upon standing in MeOH over the same length of time. The enantiopurity of the sample in MeOH degraded from >99% ee to 71% ee after 26 days (Figure 4.6). A potential pathway for the observed racemization of bisoranjidiol is through the formation of strained enone **4.40** (Scheme 4.8). Similar strained compounds,

(77) I thank Dr. Cabrera for providing us with an authentic sample of the natural product isolate.

such as binaphthone **4.43**,[14a] have been isolated and reported to be atropisomerically unstable due to rapid equilibration between twisted and stacked conformations.[7879] Enone **4.40** may proceed through similar conformations to produce the opposite enantiomer, (*R*)-**4.39a**. The half-life for the racemization is 3.8 months at 25 °C or 1.8 h at 80 °C (Figure 4.6). This short half-life at 80 °C is significant because isolation of the natural product involved heating to 80 °C, as well as exposure to acid and base. Thus, it is possible that any naturally occurring enantiomeric excess was eroded during isolation.

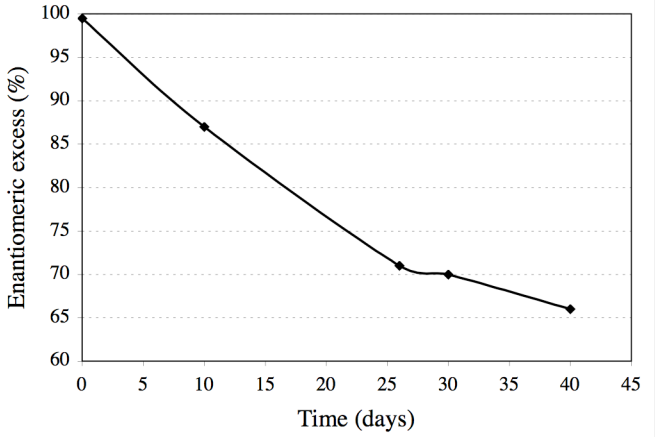

t (°C)	t (°K)	$t_{1/2}$
25	298	3.8 months
50	323	3 d
60	333	19.5 h
70	343	5.8 h
80	353	1.8 h
100	373	13 min

$\Delta G^{\ddagger}$(rt) = 27.20 kcal/mol

Figure 4.6 Atropisomerization of (*S*)-**4.39a** in MeOH (25 °C).

(78) For bianthrone examples: (a) Tapuhi, Y.; Kalisky, O.; Agranat, I. "Thermochromism and Thermal E,Z Isomerizations in Bianthrones" *J. Org. Chem.* **1979**, *44*, 1949–1952. (b) Evans, D. H.; Fitch, A. "Measurement of the Thermochromic Equilibrium Constant of a Nonthermochromic Compound: 1,1'-Dimethylbianthrone" *J. Am. Chem. Soc.* **1984**, *106*, 3039–3041.

(79) (a) Nakano, D.; Hirano, R.; Yamaguchi, M.; Kabuto, C. "Synthesis of Optically Active Bihelicenols" *Tetrahedron Lett.* **2003**, *44*, 3683–3686. (b) Karikomi, M.; Yamada, M.; Ogawa, Y.; Houjou, H.; Seki, K.; Hiratani, K.; Haga, K.; Uyehara, T. "Novel Synthesis of a Unique Helical Quinone Derivative by Coupling Reaction of 2-Hydroxybenzo[c]phenanthrene" *Tetrahedron Lett.* **2005**, *46*, 5867–5870.

Scheme 4.8 Proposed pathway for racemization.

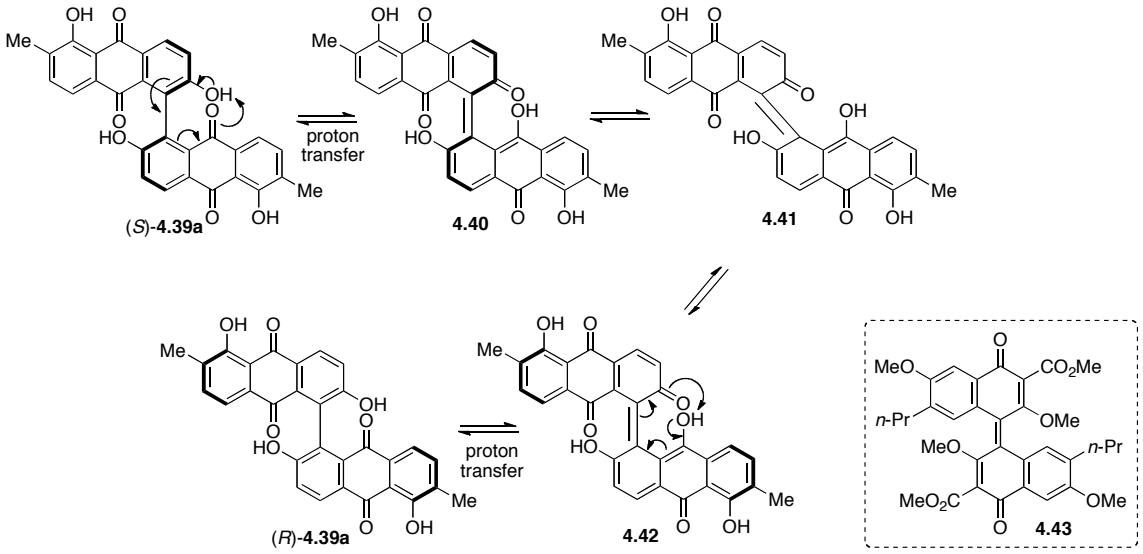

Potential second generation syntheses of bisoranjidiol were also briefly evaluated during the course of the natural product synthesis. These efforts were focused completely on selective formation of bromoquinone **4.32a** or **4.34a**. For example, since direct bromination of arene **2.1** favors the *para*-position, it was reasoned that subsequent installation of a 5,5'-hydroxyl group through a Buchwald hydroxylation[80] could provide both a director for *ortho*-bromination of the binaphthalene ring at the 6,6'-positions while also providing a completely *para*-selective oxidation to the binaphtho-*para*-quinone Scheme 4.9). Bromination of biaryl **2.1** was selective to the *para*-position, however in the next step, reaction of the ester groups rather than hydroxylation was observed. The biaryl lacking the ester groups, **2.5**, could also be brominated selectively at the 5,5'-positions using NBS, to afford **4.44b** in 80% yield. The subsequent hydroxylation

(80) Anderson, K. W.; Ikawa, T.; Tundel, R. E.; Buchwald, S. L. "The Selective Reaction of Aryl Halides With KOH: Synthesis of Phenols, Aromatic Ethers, and Benzofurans" *J. Am. Chem. Soc.* **2006**, *128*, 10694–10695.

reaction to produce **4.45b** was successful, however, yields were low due to formation of arene (reduction of Br to H) byproducts and instability of **4.45b**. The instability of the product dissuaded further pursuit of this route.

Scheme 4.9 Buchwald hydroxylation route.

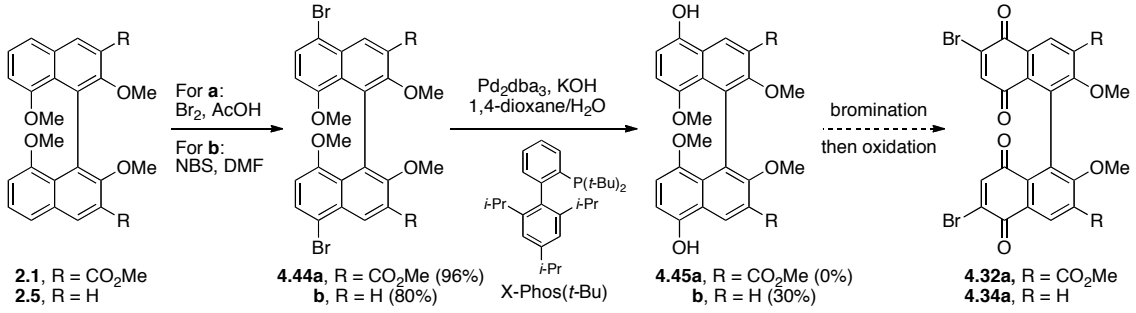

A second approach stemming from an *out-out*-binaphtho-*ortho*-quinone may be a more promising route for a second-generation synthesis of bisoranjidiol or derivatives (Scheme 4.10). This proposal is centered around transforming an *ortho*-quinone to a hydroxy-*para*-quinone, followed by exchanging the hydroxyl group for a chloro-substituent. Beginning with compound **6.23** (the synthesis of this compound will be discussed in Chapter 6), a transesterification to the more hindered *iso*-propyl ester was carried out in good yield with Ti(O*i*-Pr)$_4$. This transformation was done to prevent hydrolysis of the ester groups during a later step. Removal of the benzyl groups and oxidation to the *out-out*-binaphtho-*ortho*-quinone (**4.48**) was achieved in 98% yield. Direct conversion of *out-out*-binaphtho-*ortho*-quinone, **4.48**, to hydroxyquinone **4.51** was unsuccessful due to a rapid intramolecular oxidation to form perylenequinone **4.49**. It is notable, that transformation of the methyl ester to the isopropyl ester was necessary to prevent reaction of the ester during this oxidation step. While these conditions did not

produce the desired bishydroxyquinone, **4.51**, a potentially biologically active perylenequinone, **4.49**, was produced in good yield (70%). The solution to this intramolecular oxidation, was to use a Thiele-Winter acetoxylation reaction[81] to produce the hexaacetoxy biaryl **4.50**. This substrate could potentially be oxidized to hydroxy quinone **4.51**, and the hydroxyl group exchanged for a chloro substituent using $SOCl_2$, as has been reported in the literature.[82]

Scheme 4.10 Synthesis of a perylenequinone and proposed synthesis of a dihydroxy-binaphtho-*para*-quinone from a binaphtho-*ortho*-quinone.

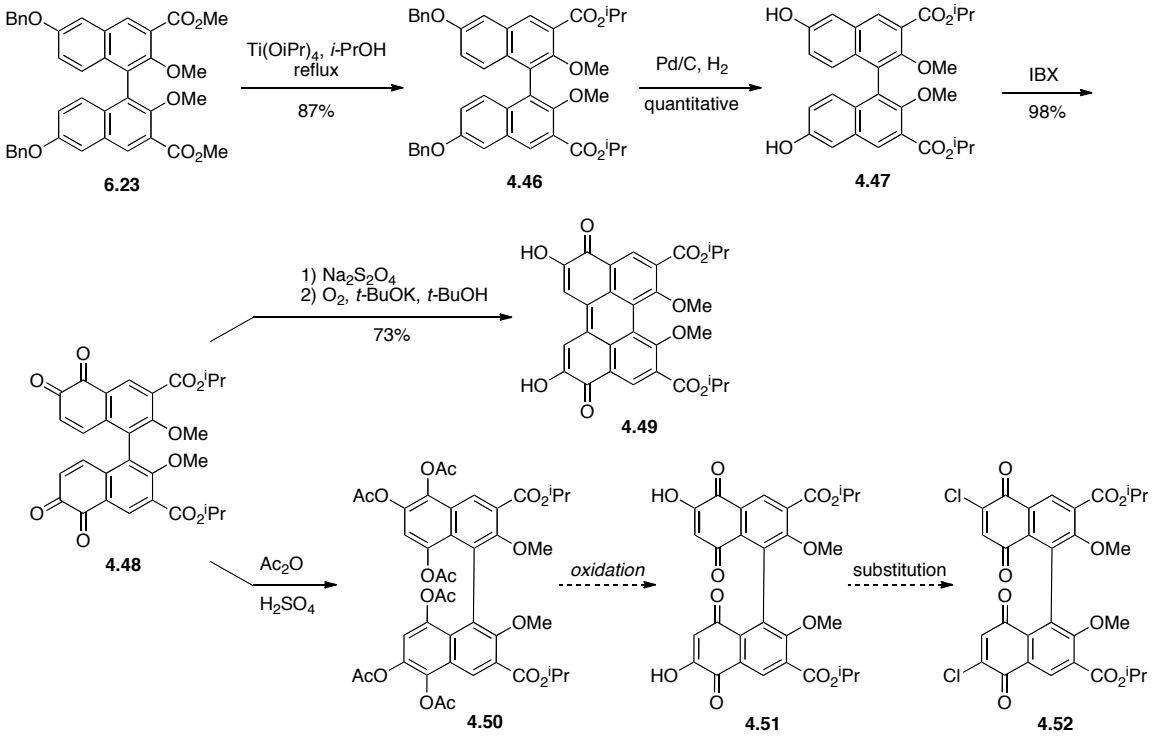

(81) (a) McOmie, J. F. W.; Blatchly, J. M. The Thiele-Winter Acetoxylation of Quinones. In *Organic Reactions*, Wiley: New York, **1972**, 19, 199–203. (b) Spyroudis, S. "Hydroxyquinones: Synthesis and Reactivity" *Molecules* **2000**, *5*, 1291–1330.

(82) Sucunza, D.; Dembkowski, D.; Neufeind, S.; Velder, J.; Lex, J.; Schmalz, H.- G. "Synthesis of a Mumbaistatin Analogue Through Cross-Coupling" *Synlett* **2007**, 2569–2573.

4.5 Synthesis of Analogs

Aside from bisoranjidiol, I synthesized several bisanthraquinone analogs. Binaphtho-*para*-quinone **4.35** was treated with commercially available dienes **4.20** and **4.55**. Following completion of the cycloaddition, the cycloadducts were treated with NEt_3 to generate bisanthraquinones **4.53** and **4.56** in good yield. Deprotection with BCl_3 provided analogs **4.54** and **4.57** in 80-88% yield. In addition, an extended bisanthraquinone **4.60** could also be synthesized from binaphtho-*para*-quinone **4.32a-c**, using an exocyclic diene that is generated *in situ* from sultine **4.58**. Deprotection of the resulting bisanthraquinone provided analog **4.60** in 45% yield over 2 steps.

Scheme 4.11 Synthesis of bisanthraquinone analogs.

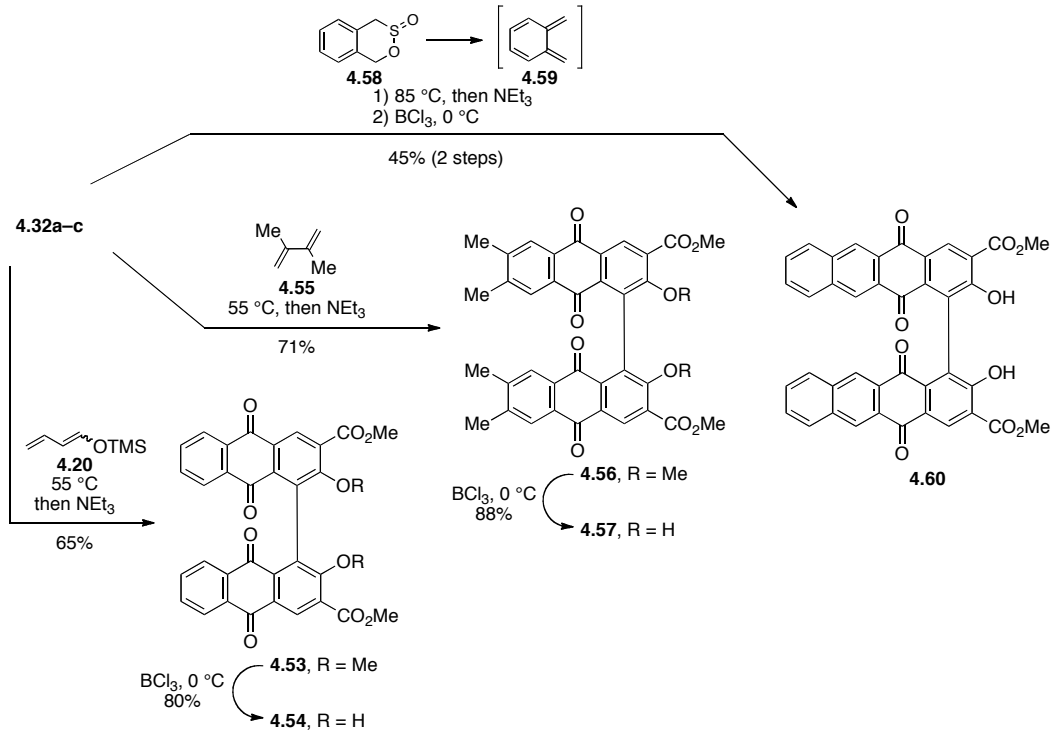

CHAPTER 5: Structural Reassignment of a Marine Natural Product[83]

5.1 Binaphthol Natural Product: Isolation and Retrosynthesis

In 2007, (*S*)-2,2'-dimethoxy-1,1'-binaphthyl-5,5',6,6'-tetraol [(*S*)-5.1, Scheme 5.1] was reportedly isolated from an Indonesian *Lendenfeldia* sp. sponge and displayed inhibitory activity against the activation of hypoxia-inducible factor-1 (HIF-1) in tumor cells.[84] The simple binaphthol structure was identified from the analysis of the NMR spectroscopic data (^{1}H, ^{13}C, COSY, HSQC, and HMBC) and by HRMS. The compound was reported to be optically active ($[\alpha]_{D}^{25}$ +10.4) and assigned an absolute (*S*)-configuration based on the CD spectrum.

Scheme 5.1 Retrosynthesis.

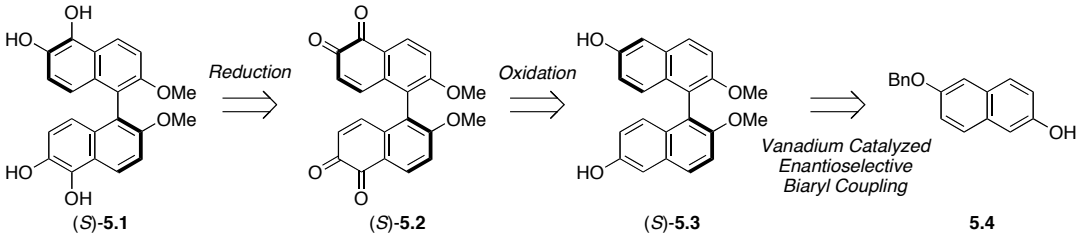

As we were interested in synthesizing *out-out*-binaphtho-*ortho*-quinones (see Chapters 1 and 2), the proposed structure of the natural product isolate, the (*S*)-configuration, optical activity, and biological activity made **5.1** an interesting target. I envisioned forming (*S*)-**5.1** through reduction of target binaphtho-*ortho*-quinone (*S*)-**5.2**

(83) Portions of these sections were published previously: Podlesny, E. E.; Kozlowski, M. C. "Structural Reassignment of a Marine Metabolite from a Binaphthalenetetrol to a Tetrabrominated Diphenyl Ether" *J. Nat. Prod*. **2012**, *75*, 1125–1129.

(84) Dai, J.; Liu, Y.; Zhou, Y.-D.; Nagle, D. G. "Cytotoxic Metabolites From an Indonesian Sponge *Lendenfeldia* sp" *J. Nat. Prod.* **2007**, *70,* 1824–1826.

(Scheme 5.1). This binaphthoquinone could be formed from oxidation of the 6,6'-dihydroxylated binaphthol (*S*)-**5.3**. Formation of the biaryl bond of (*S*)-**5.3** could be achieved through an asymmetric vanadium catalyzed biaryl coupling.

5.2 Synthesis of a Reported Binaphthol Natural Product Through a Binaphtho-*ortho*-quinone

Commencing with naphthol **5.4**, an enantioselective biaryl coupling with chiral dinuclear vanadium catalyst **V1** successfully produced known binaphthol,[15] (*S*)-**5.5**, in 82% yield and good selectivity (81% ee, Scheme 5.2). The enantiopurity of (*S*)-**5.5** could be enhanced to 98% ee following trituration. A racemic sample was also prepared via catalytic oxidative coupling of **5.4** using $VO(acac)_2$. Methylation of the 2,2'-dihydroxyls and hydrogenolysis of the benzyl protecting groups provided (*S*)-**5.3** in good yield. Using two equivalents of IBX, (*S*)-**5.3** was successfully oxidized to the *out-out*-binaphtho-*ortho*-quinone (*S*)-**5.2**. The structure of *rac*-**5.2** was confirmed via X-ray crystallography (Figure 5.1). Finally, reduction of the binaphthoquinone with sodium dithionite yielded the targeted natural product, (*S*)-**5.1** (from hereon out referred to as synthetic-**5.1**).

Scheme 5.2 Synthesis of reported binaphthalenetetraol natural product.

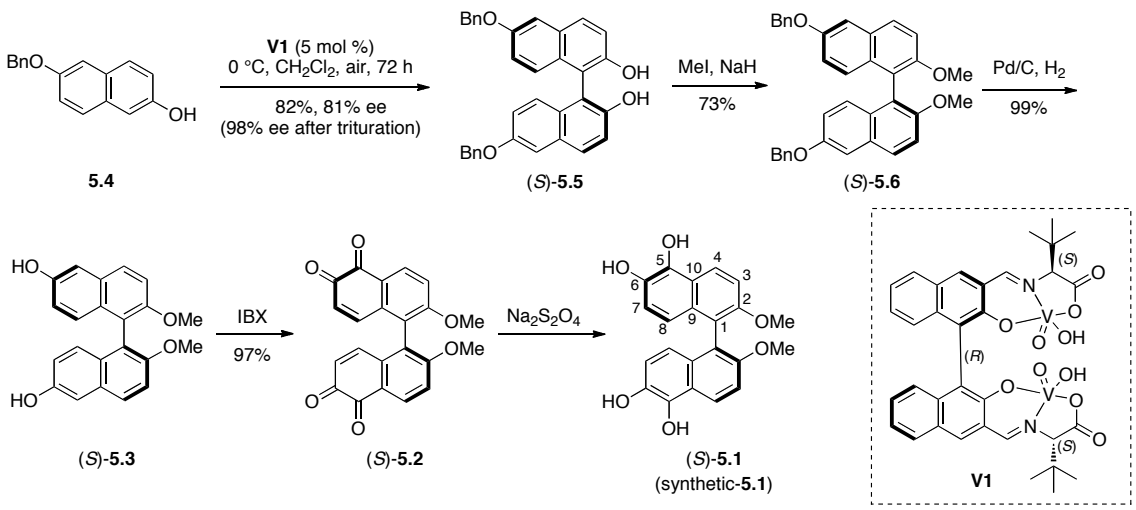

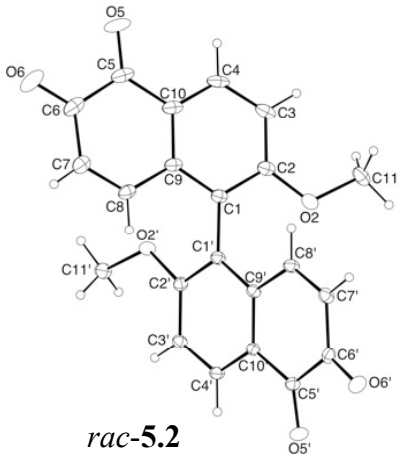

Figure 5.1 Crystal structure of binaphtho-*ortho*-quinone, *rac*-**5.2**.

Immediately, major discrepancies between the published data for the natural product isolate and the physical properties/spectroscopic data from synthetic-**5.1** were observed. Synthetic-**5.1** was oxidatively sensitive, unstable on silica, and had poor solubility in $CDCl_3$. These properties were incongruous with those reported for the natural product isolate, which was purified using silica gel chromatography (2:1 hexanes–

EtOAc) and dissolved in $CDCl_3$ for all NMR spectra. Therefore, the NMR spectroscopic data for synthetic-**5.1** were obtained in acetone-d_6 and in $CDCl_3$ containing EtOAc to enhance solubility. The observed ^1H and ^{13}C spectra for synthetic-**5.1**, were in stark contrast with the published data (Table 5.1). In the ^1H spectrum, the chemical shifts of all peaks differed by at least 0.53 ppm and all splitting patterns were clearly visible for synthetic-**5.1**, while peaks, which should be doublets based on the proposed structure, were reported as broad singlets for the natural product isolate. The lack of splitting could be explained if the original ^1H NMR sample had been very concentrated. The ^{13}C spectroscopic data is also considerably different between the published data and the data for synthetic-**5.1**. For example, the methoxy peak appeared at 56.7 ppm for synthetic-**5.1**, compared with 61.5 ppm for the natural product isolate (Table 5.1). Since the structure of the direct precursor to synthetic-**5.1** was confirmed via X-ray crystallography, it was concluded that the structure proposed for the natural product isolate was incorrect.

Table 5.1 Comparison of ^1H and ^{13}C NMR Data For Natural Product Isolate and Synthetic 5.1.

^1H NMR Data

Compd **5.1** position[a]	Nagle ($CDCl_3$) δ_H	Synthetic ($CDCl_3$ + EtOAc) δ_H	Synthetic (acetone-d_6) δ_H (J in Hz)
3	6.70, br s	7.29, d	7.45, d (9.3)
4	7.39, br s	8.13, d	8.25, d (9.3)
7	7.16, br s	6.44, d	6.45, d (9.3)
8	7.32, br s	6.79, d	6.90, d (9.0)
OH	–	6.98, s	8.00, s
OH	–	6.31, s	7.65, s
OMe	4.02, s	3.62, s	3.68, s

[a] See Scheme 5.2 for numbering.

^{13}C NMR Data

Compd **5.1** position[a]	Nagle ($CDCl_3$) δ_C	Synthetic (acetone-d_6) δ_C
1	117.4	120.9
2	145.0	139.0
3	118.2	114.6
4	130.2	122.9
5	150.5	154.3
6	138.5	138.5
7	120.2	117.6
8	127.4	119.2
9	119.9	130.9
10	118.5	122.6
OMe	61.5	56.7 (56.9)[b]

[a] See Scheme 5.2 for numbering.
[b] Recorded in $CDCl_3$ + EtOAc.

5.3 Structural Reassignment to a Tetrabrominated Diphenyl Ether

The proposed natural product structure was self-consistent with the data provided in the initial publication, particularly with the HMBC analysis.[84] An alternate structure could not be proposed which would correspond to the reported correlations and mass. No original spectra of the natural product isolate were available in the supporting information for the publication, but D. Nagle kindly provided copies of the original proton and carbon spectra of the natural product isolate, as well as an authentic sample of the natural product.[85] Copies of the original 2D NMR spectra, mass spectrum, etc. could not be procured. The first major problem discovered was that the number of carbons had been miscounted in the ^{13}C NMR spectrum from the natural product isolate. There were clearly 13 peaks labeled in the original spectrum, not 11 carbons as was published. These two extra peaks were adjacent to peaks at 117.4 ppm and 150.4 ppm (highlighted in Figure 5.3b).

In light of this error, full analysis and identification of the authentic sample of the natural product was undertaken. The chemical shifts in the ^{1}H and ^{13}C NMR spectra observed for this authentic sample (labeled Kozlowski, see Figure 5.2a and Figure 5.3a) matched the original spectra provided by Nagle (see Figure 5.2b and Figure 5.3b) as well as the published data. This confirmed that there was no accidental mix-up of samples or spectra and that we were indeed analyzing the correct natural product sample. The Kozlowski ^{1}H NMR spectrum of the natural product revealed small coupling constants consistent with *meta*-protons on an aromatic ring. This splitting was absent from the

(85) I thank Dr. Nagle for providing original spectra and an authentic sample of the natural product isolate.

spectra provided by Nagle because the sample was very concentrated (Figure 5.2). In addition, the Kozlowski ^{13}C NMR spectrum of the natural product was identical to the spectrum provided by Nagle, revealing that there are in fact 13 carbons, not 11 (Figure 5.3).

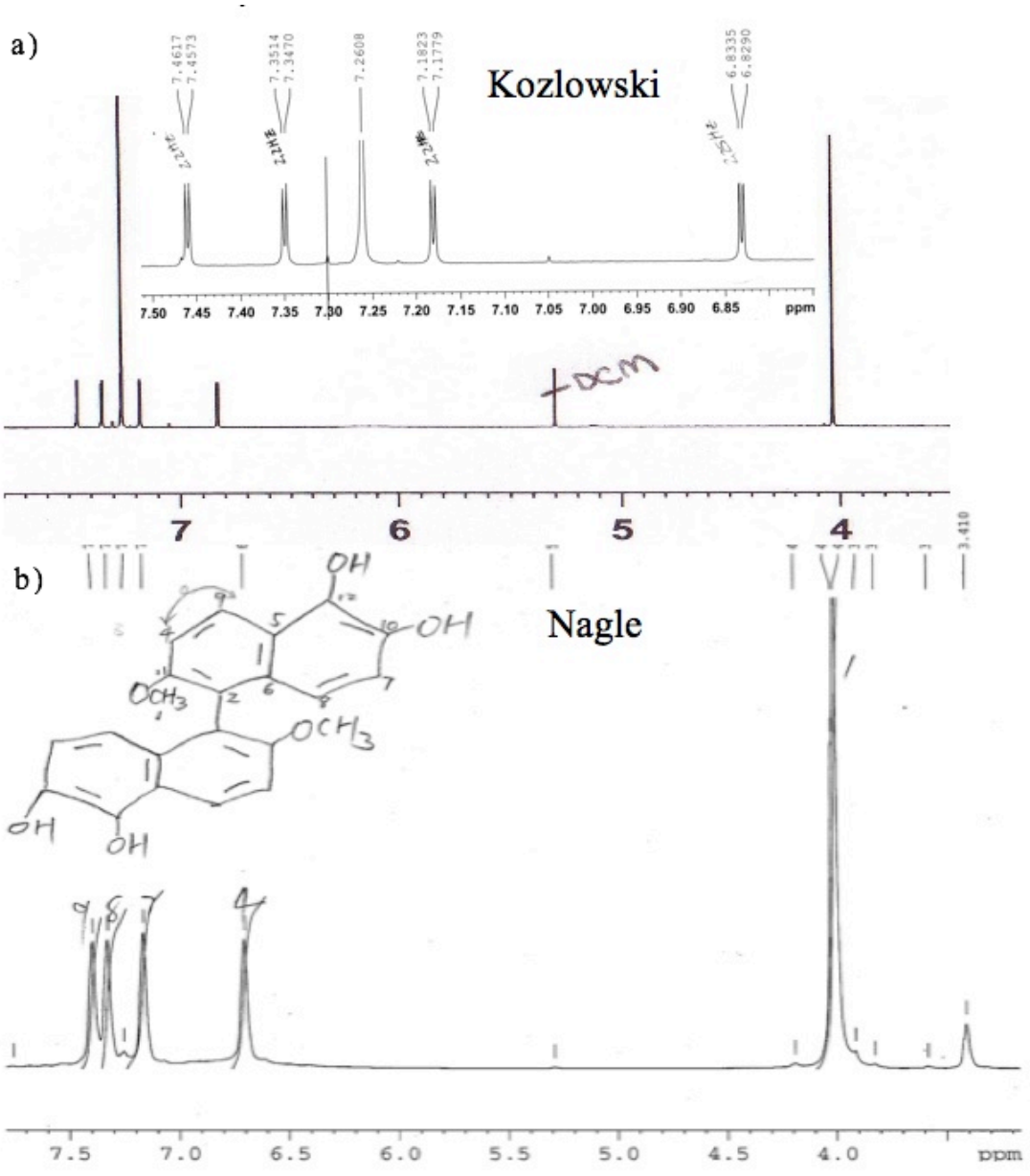

Figure 5.2 Comparison of Kozlowski and Nagle ^{1}H NMR spectra of natural product isolate in $CDCl_3$.

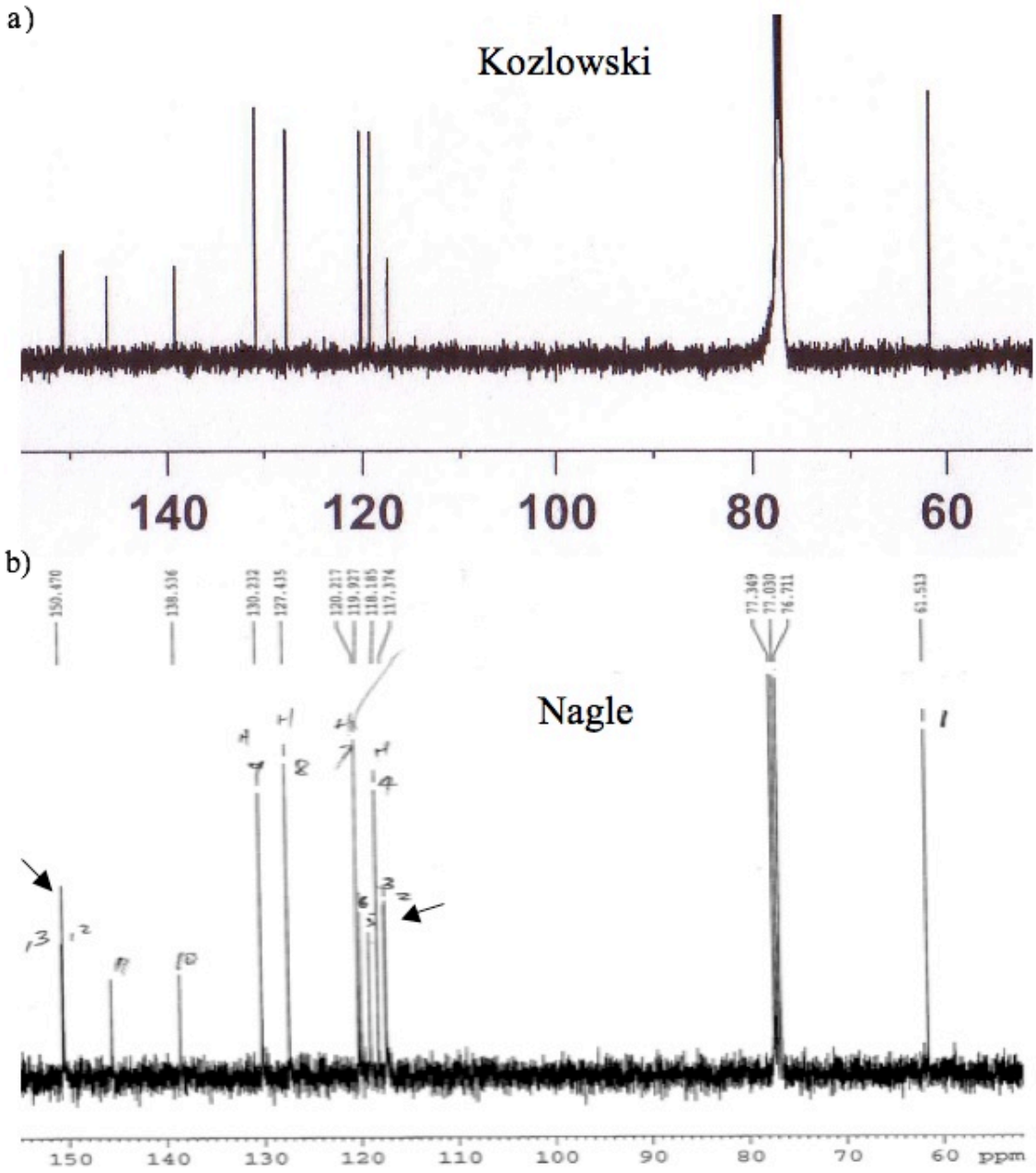

Figure 5.3 Comparison of Kozlowski and Nagle ^{13}C NMR spectra of natural product isolate in $CDCl_3$.

Surprisingly the (–)-HRMS (ES) spectrum of the natural product sample that we had obtained revealed a cluster of peaks consistent with the presence of four bromines. It

suggested a molecular formula of $C_{13}H_8Br_4O_3$ ($[M–H]^-$ *m/z* 526.7119). This meant that the mass of *m/z* 378.1105 and proposed molecular formula of $C_{22}H_{18}O_6$ from the natural product report were also incorrect.[84] With an accurate molecular formula in hand, a series of 2D NMR experiments were performed to establish the structure. The COSY correlation data revealed two distinct spin systems in the molecule where H-2 was coupled to H-4 and H-10 coupled to H-12 (Table 5.2). Together with the molecular formula, interpretation of the HSQC and HMBC data suggested that the natural product was a tetrabrominated diphenyl ether, with two bromines on each aromatic ring and the methoxy and hydroxyl groups on separate rings (Table 5.2).

Table 5.2 Comparison of observed data (Kozlowski) with published data for compound **5.7.**

	Kozlowski ($CDCl_3$)			Nagle[b] ($CDCl_3$)		Hattori[c] ($CDCl_3$)	Norton[d] (CD_3OD)	Kozlowski (CD_3OD)
position	δ_C, type	δ_H (*J* in Hz)	HMBC[a]	δ_C	δ_H	δ_C	δ_H	δ_H
1	150.9, C			150.5		152.9		
2	119.1, CH	6.83, d (2.3)	*1, 3, 4, 6*	118.2	6.70	118.0	6.53	6.50
3	117.5, C			117.4		117.4		
4	130.8, CH	7.46, d (2.2)	*3, 6*	130.2	7.40	129.7	7.30	7.39
5	119.2, C			119.0		119.8		
6	146.2, C			145.0		147.1		
7	61.8, CH_3	4.03, s	*6*	61.5	4.01	61.5	3.96	3.99
8	139.3, C			138.5		140.0		
9	150.6, C			150.5		153.6		
10	120.2, CH	7.18, d (2.2)	*8, 9, 11, 12*	120.2	7.16	121.1	7.10	7.13
11	120.1, C			119.9		120.4		
12	127.6, CH	7.35, d (2.2)	*8, 10, 13*	127.4	7.33	127.1	7.25	7.34
13	117.4, C			117.4		119.4		

[a] HMBC correlations indicate the protons in column 3 coupling to the carbon entry in column 2.
[b] Values taken from hard copies of original spectra.
[c] Reference 86.
[d] Reference 87.

Not all HMBC correlations were observed (three are missing), but eight possible structures could be proposed based on the correlation data (Figure 5.4). The chemical

shifts of all eight possible structures were calculated and compared with the observed ^{13}C NMR data. Based on the differences between calculated and observed values, structure **5.7** was the closest match and the proposed identity of the natural product. A literature search of the molecular formula revealed that **5.7** was a known compound. None of the other proposed compounds in Figure 5.4 are currently known. Comparison of the NMR data of the natural product observed by Kozlowski, data from the original spectra provided by Nagle, and that reported by Hattori[86] and Norton[87] indicated that **5.7** was a reasonable match. Slight variations in chemical shift are likely due to concentration dependence in the NMR, which was observed during analysis. Notably, the sample of **5.7** reported by Hattori was isolated from a Palauan collection of the same sponge genus as Nagle's sample, a marine *Lendenfeldia* sponge.[86,88] In conclusion, the evidence supports the structural reassignment of the natural product from the reported binaphthol **5.1** to the tetrabrominated diphenyl ether **5.7**. The reported optical rotation and interpretation of a CD spectrum were puzzling as **5.7** does not contain a stereocenter or chiral axis. It was reasoned that these results reported by Nagle could be the result of an optically active impurity.

(86) Hattori, T.; Konno, A.; Adachi, K.; Shizuri, Y. "Four New Bioactive Bromophenols From the Palauan Sponge *Phyllospongia dendyi*" *Fisheries Sci.* **2001**, *67,* 899–903.

(87) Norton, R. S.; Croft, K. D.; Wells, R. J. "Polybrominated Oxydiphenol Derivatives From the Sponge *Dysidea herbacea*" *Tetrahedron* **1981**, *37,* 2341–2349.

(88) Compound **5.7** was reported from the sponge *Phyllospongia dendyi*. This sponge has been taxonomically reclassified as *Lendenfeldia dendyi*: Bergquist, P. R. "A Revision of the Supraspecific Classification of the Orders Dictyoceratida, Dendroceratida and Verongida (Class Demospongiae)" *New Zeal. J. Zool.* **1980**, *7*, 443–503.

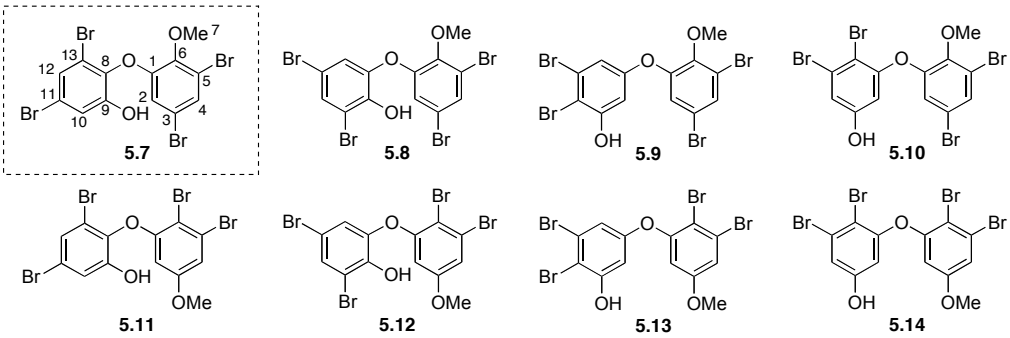

Figure 5.4 Tetrabrominated diphenyl ethers.

Table 5.3 Differences between observed ^{13}C NMR data (Kozlowski) of natural product isolate and calculated[a] values for **5.7**-**5.14**.

	Kozlowski	$\Delta\delta_C$							
position	δ_C	**5.7**	**5.8**	**5.9**	**5.10**	**5.11**	**5.12**	**5.13**	**5.14**
1	150.9	0.5	0.5	0.5	0.5	–6.3	–6.3	–6.3	–6.3
2	119.1	3.8	3.8	3.8	3.8	14.3	14.3	14.3	14.3
3	117.5	7.8	7.8	7.8	7.8	6.0	6.0	6.0	6.0
4	130.8	2.0	2.0	2.0	2.0	17.9	17.9	17.9	17.9
5	119.2	5.1	5.1	5.1	5.1	–7.4	–7.4	–7.4	–7.4
6	146.2	–1.7	–1.7	–1.7	–1.7	–15.3	–15.3	–15.3	–15.3
7	61.8	0.9	0.9	0.9	0.9	6.0	6.0	6.0	6.0
8	139.3	0.9	–4.7	–20.3	–20.1	0.9	–4.7	–20.3	–20.1
9	150.6	–1.5	5.6	–7.9	–7.0	–1.5	5.6	–7.9	–7.0
10	120.2	2.3	4.5	4.6	5.7	2.3	4.5	4.6	5.7
11	120.1	2.1	10.1	9.4	8.3	2.1	10.1	9.4	8.3
12	127.6	0.6	–1.6	21.2	21.2	0.6	–1.6	21.2	21.2
13	117.4	–1.6	6.3	–9.6	–9.6	–1.6	6.3	–9.6	–9.6
Avg. $\lvert\Delta\delta_C\rvert$		2.4	4.2	7.3	7.2	6.3	8.2	11.2	11.2

[a] Chemical shifts were calculated using CambridgeSoft ChemBioDraw.

CHAPTER 6: Bisbenzo[*a*]phenazines

6.1 Introduction to Phenazines and Potential Application as Ligands

At the outset of this project, one of our goals was to synthesize chiral binaphthoquinones possessing a BINOL-type scaffold for the purpose of developing ligands for asymmetric catalysis and potentially redox active ligands. To date, many BINOL derivatives have been synthesized, which offer improvements in yield or selectivity over BINOL.[89] A majority of these ligands possess a 3,3'-disubstituted scaffold with sterically influential groups at these positions, while another category of BINOL ligands have electron withdrawing groups at the 6,6'-positions. Binaphthoquinones were envisioned as a novel group of BINOL derivatives possessing electron-withdrawing groups in the form of a *para- or ortho*-quinone. The core structure would also enable facile incorporation of bulky substituents at the 3,3'-positions or augmentation through the quinone moiety. A few years ago, Dötz and coworkers reported the synthesis of BINOL ligands containing *para*-quinone functionality, however, the quinone groups were attached at the 3,3'- or 6,6'-positions through either a single C-C bonds or annulation to the naphthol (Figure 6.1). Some of these ligands showed activity in enantioselective zinc-mediated epoxidation.[90,91] Due to limited stability of our

(89) (a) Pu, L. "1,1'-Binaphthyl Dimers, Oligomers, and Polymers: Molecular Recognition, Asymmetric Catalysis, and New Materials." *Chem. Rev.* **1998**, *98*, 2405–2494. (b) Chen, Y.; Yekta, S.; Yudin, A. K. "Modified BINOL Ligands in Asymmetric Catalysis." *Chem. Rev.* **2003**, *103*, 3155–3211. (c) Brunel, J. M. "BINOL: A Versatile Chiral Reagent." *Chem. Rev.* **2005**, *105*, 857–897.

(90) Minatti, A.; Dötz, K. H. "Quinoid BINOL-type Compounds as a Novel Class of Chiral Ligands." *Tetrahedron: Asymmetry* **2005**, *16*, 3256–3267.

(91) Schneider, J. F.; Nieger, M.; Nättinen, K.; Lewall, B.; Niecke, E.; Dötz, K. H. "Novel [6]- and

binaphthoquinone BINOL derivatives we chose to transform the quinone groups to phenazines, which are also electron-deficient due to the heterocyclic nitrogens.

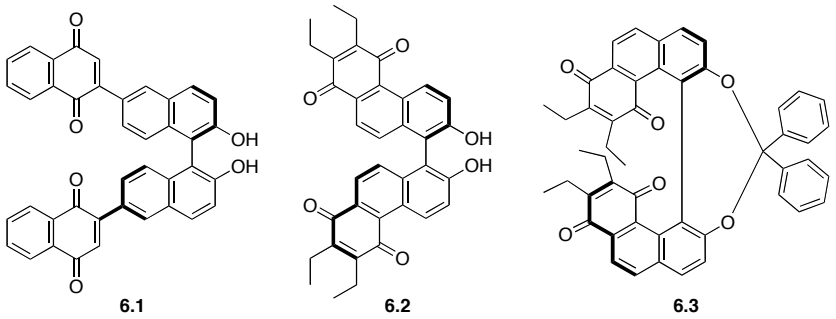

Figure 6.1 Related quinone-based BINOL derivatives.

Phenazine is a planar anthracenyl ring system containing a pyrazine core (**6.4**, Figure 6.2). There are two types of benzo-fused systems: the bent form, **6.5**, is called a benzo[*a*]phenazine and the linear form, **6.6**, is called a benzo[*b*]phenazine. The phenazine moiety is found in a number of biologically active natural products and synthetic compounds, with antibiotic, antimalarial, antiparasitic, antitumor, and trypanocidal activities, having also been shown to intercalate with DNA and to inhibit topoisomerase I and II enzymes.[92-94] Besides their biological activity, the heterocycle is an important component in materials chemistry. Phenazines and related pyrazine

---

[7]Helicene-Like Quinones via Mono- and Bidirectional Chromium-Templated Benzannulation of Bridged Binaphthyl Carbene Complexes." *Eur. J. Org. Chem*. **2005**, 1541–1560.

(92) Laursen, J. B.; Nielsen, J. "Phenazine Natural Products: Biosynthesis, Synthetic Analogues, and Biological Activity." *Chem. Rev*. **2004**, *104*, 1663–1685.

(93) Makgatho, M. E.; Anderson, R.; O'Sullivan, J. F.; Egan, T. J.; Freese, J. A.; Cornelius, N.; van Rensburg, C. E. J. "Tetramethylpiperidine-substituted Phenazines as Novel Anti-plasmodial Agents. *Drug Dev. Res.* **2000**, *50*, 195–202.

(94) Dai, J.; Punchihewa, C.; Mistry, P.; Ooi, A. T.; Yang, D. "Novel DNA Bis-intercalation by MLN944, a Potent Clinical Bisphenazine Anticancer Drug." *J. Biol. Chem.* **2004**, *279*, 46096–46103.

heterocycles have found applications as dyes,[95] organogelators,[96] and sensors,[97] such as anion sensors[98] and biosensors.[99] Other applications include fluorescent probes and organic-light emitting diodes (OLEDs), [100] semiconductors,[101] and electrogenerated bases.[102]

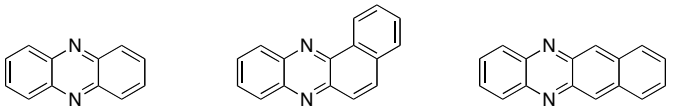

phenazine, **6.4** benzo[*a*]phenazine, **6.5** benzo[*b*]phenazine, **6.6**

Figure 6.2 Types of phenazines.

(95) Berneth, H. "Azine Dyes." *Ullmann's Encyclopedia of Industrial Chemistry*, Electronic Release, Wiley-VCH, Weinheim Jun. 2000.

(96) (a) Pozzo, J.-L.; Clavier, G. M.; Desvergne, J. P. "Rational Design of New Acid-Sensitive Organogelators." *J. Mater. Chem*. **1998**, *8*, 2575–2577. (b) Lee, D.-C.; Cao, B.; Jang, K.; Forster, P. M. "Self-Assembly of Halogen Substituted Phenazines." *J. Mater. Chem*. **2010**, *20*, 867–873. (c) Jang, K.; Brownell, L. V.; Forster, P. M.; Lee, D.-C. "Self-Assembly of Pyrazine-Containing Tetrachloroacenes." *Langmuir* **2011**, *27*, 14615–14620.

(97) Thomas III, S.W.; Joly, G. D.; Swager, T. M. "Chemical Sensors Based on Amplifying Fluorescent Conjugated Polymers." *Chem. Rev.* **2007**, *107*, 1339–1386.

(98) Aldakov, D.; Palacios, M. A.; Anzenbacher, Jr., P. "Benzothiadiazoles and Dipyrrolyl Quinoxalines with Extended Conjugated Chromophores-Fluorophores and Anion Sensors." *Chem. Mater.* **2005**, *17*, 5238–5241.

(99) Pauliukaite, R.; Ghica, M. E.; Barsan, M. M.; Brett, C. M. A. "Phenazines and Polyphenazines in Electrochemical Sensors and Biosensors." *Anal. Lett.* **2010**, 1588–1608.

(100) (a) Son, H.-O.; Han, W.-S.; Wee, K.-R.; Yoo, D.-H.; Lee, J.-H.; Kwon, S. N.; Ko, J.; Kang, S. O. "Turning on Fluorescent Emission from C-Alkylation on Quinoxaline Derivatives." *Org. Lett*. **2008**, *10*, 5401–5404. (b) Son, H.-O.; Han, W.-S.; Yoo, D.-H.; Min, K.-T.; Kwon, S.-N.; Ko, J.; Kang, S. O. "Fluorescence Control on Panchromatic Spectra via C-Alkylation on Arylated Quinoxalines." *J. Org. Chem*. **2009**, *74*, 3175–3178.

(101) Murphy, A. R.; Fréchet, J. M. J. "Organic Semiconducting Oligomers for Use in Thin Film Transistors." *Chem. Rev.* **2007**, *107*, 1066–1096.

(102) Alonso, A. M.; Horcajada, R.; Motevalli, M.; Utley, J. H.; Wyatt, P. B. "The Reactivity, as Electrogenerated Bases, of Chiral and Achiral Phenazine Radical-anions, Including Application in Asymmetric Deprotonation." *Org. Biomol. Chem*. **2005**, *3*, 2842–2847.

Incorporation of phenazines onto the BINOL scaffold may offer opportunities for other applications as well, including redox-active ligands.[103] Two regioisomeric sets of phenazines were synthesized initially to evaluate their utility as electron-deficient ligands for asymmetric catalysis (discussed in section 6.5), however, the observation of some interesting properties/chromism warranted further evaluation of their physical properties for potential applications in materials and sensing (discussed in section 6.6).

6.2 Related Systems and Retrosynthesis

Commonly, phenazines have been synthesized directly through a cyclization process or indirectly by cyclization to phenazine N-oxides, followed by reduction. Methods such as the Wohl-Aue reaction, Beirut reaction, palladium catalyzed cyclizations, and condensation reactions between diamines and quinones have been used. Generally, if highly functionalized systems are desired, often these substituents need to be incorporated prior to heterocycle formation, due to the electron poor nature of the ring system and resistance to electrophilic substitution.[92,104] Both *ortho*- and *para*-quinones have been used to synthesize phenazines, the latter leading to formation of a hydroxy phenazine (**6.11**, Scheme 6.1). For example, this method has been used recently to synthesize a series of amine-substituted and heterocycle-annulated

(103) (a) Chirik, P. J.; Wieghardt, K. *Science* **2010**, *327*, 794-795. (b) Shultz, D. A. "Structure-Property Relationships in New Serniquinone-Type Ligands: Past, Present, and Future Research Efforts" *Comments Inorg. Chem*. **2002**, *23,* 1-21. (c) Evangelio, E.; Ruiz-Molina, D. "Valence Tautomerism: New Challenges for Electroactive Ligands" *Eur. J. Inorg. Chem*. **2005**, 2957-2971. (d) Blackmore, K. J.; Ziller, J. W.; Heyduk, A. F. ""Oxidative Addition" to a Zirconium(IV) Redox-Active Ligand Complex " *Inorg. Chem.* **2005**, *44,* 5559-5561.

(104) Urleb, U. Phenazines. In *Houben-Weyl Methods of Organic Chemistry* **1998**, Vol. E 9b2; pp 266–303.

benzo[*a*]phenazines.[105,106]

Scheme 6.1 Synthesis of phenazines from quinones.

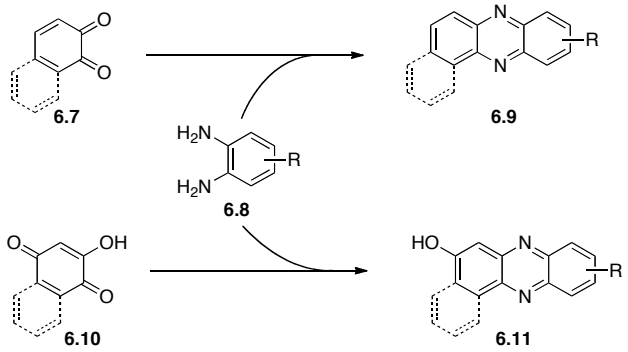

We chose to use the condensation reaction strategy to synthesize both *in-in*-bisbenzo[*a*]phenazines (**6.12**) and *out-out*- bisbenzo[*a*]phenazines (**6.15**) by treatment of their corresponding binaphtho-*ortho*-quinones (see also Chapters 1, 2 and 5) with various phenylenediamines (Scheme 6.2). Similar axially chiral structures have not been reported, with the exception of some carbon-based homologs.[20b,79b,107] Some bisphenazine-based helicenes **6.17** and **6.18**,[108] bisphenazine-based biaryls **6.16**,[109] and

(105) Singh, P.; Baheti, A.; Thomas, K. R. J. "Synthesis and Optical Properties of Acidochromic Amine-Substituted Benzo[*a*]phenazines." *J. Org. Chem.* **2011**, *76*, 6134–6145.

(106) Khurana, J. M.; Chaudhary, A.; Lumb, A.; Nand, B. "An Expedient Four-Component Domino Protocol for the Synthesis of Novel Benzo[*a*]phenazine Annulated Heterocycles and Their Photophysical Studies." *Green Chem.* **2012**, *14*, 2321–2327.

(107) (a) Yamamoto, K.; Noda, K.; Okamoto, Y. "Synthesis and Chiral Recognition of Optically Active Crown Ethers incorporating a 4,4'-Biphenanthryl Moiety as the Chiral Centre" *J. Chem. Soc., Chem. Commun.* **1985**, 1065–1066. (b) Yamamura, K.; Ono, S.; Ogoshi, H.; Masuda, H.; Kuroda, Y. "Chiral Liquid Crystal Mesogens. Synthesis and Determination of Absolute Configuration of Mesogens with 4,4'-Biphenanthryl Cores" *Synlett*, **1989**, 18–19. (c) Gingras, M.; Dubois, F. "Synthesis of Carbohelicenes and Derivatives by 'Carbenoid Couplings'" *Tetrahedron Lett.* **1999**, *40*, 1309–1312.

(108) Fox, J. M.; Katz, T. J. "Conversion of a [6]Helicene into an [8]Helicene and a Helical 1,10-Phenanthroline Ligand." *J. Org. Chem.* **1999**, *64*, 302–305.

(109) Hussain, H.; Specht, S.; Sarite, S. R.; Saeftel, M.; Hoerauf, A.; Schulz, B.; Krohn, K. "A New Class of Phenazines with Activity against a Chloroquine Resistant Plasmodium falciparum Strain and Antimicrobial Activity." *J. Med. Chem.* **2011**, *54*, 4913–4917.

the axially chiral bisacridine-based biaryl,[110] **6.19**, are other relevant examples (Figure 6.3).

Scheme 6.2 Retrosynthesis.

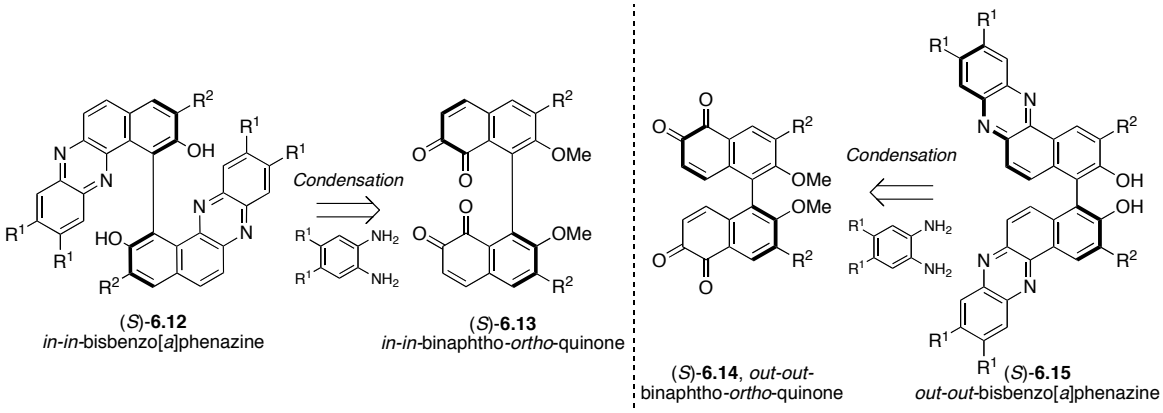

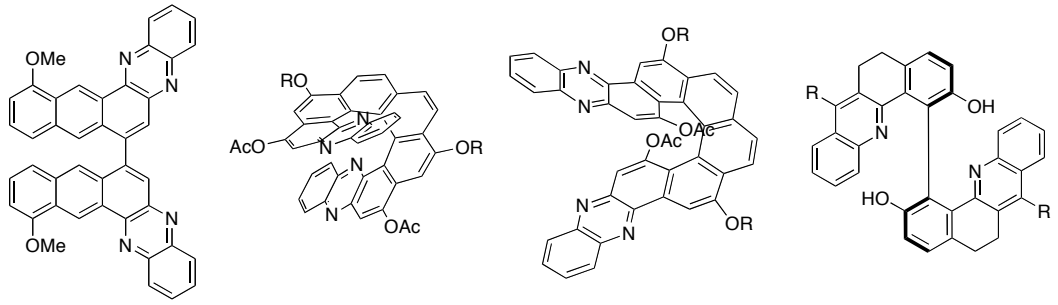

Figure 6.3 Related compounds to the bisbenzo[*a*]phenazines.

6.3 Synthesis of *out-out*-Bisbenzo[*a*]phenazines

Although, the synthesis of a simple *out-out*-binaphtho-*ortho*-quinone is discussed in Chapter 5, we first began our investigation into these types of compounds through a

(110) Jierry, L.; Harthong, S.; Aronica, C.; Mulatier, J.-C.; Guy, L.; Guy, S. "Efficient Dibenzo[c]acridine Helicene-like Synthesis and Resolution: Scaleup, Structural Control, and High Chiroptical Properties." *Org. Lett.* **2012**, *14*, 288–291.

copper catalyzed coupling route, involving naphthol substrates with 3,3'-methyl esters (Scheme 6.3). The biaryl coupling substrate, **6.21**, was synthesized from the commercially available acid, via a Fischer esterification, followed by selective benzylation. The esterification often suffered from substitution of a methoxy group for the 6-hydroxy group. Use of a different acid, such as HCl, would resolve this issue. Oxidative coupling of **6.21**, using the chiral diaza-*cis*-decalin copper catalyst **1.12** provided biaryl (*R*)-**6.22** in 60% yield and 83% ee (racemate was synthesized using achiral CuCl(OH)TMEDA in 87% yield). Unfortunately, the enantiomeric excess could not be enhanced at this stage. Following methylation in 98% yield, reduction of the esters with DIBAL-H and hydrogenolysis of the benzylic alcohols and ethers provided diol **6.24** in 93% yield over two steps. Preliminary investigations on small quantities of material suggested that it may be possible to enhance the enantiomeric excess at this stage via recrystallization. Further investigations were carried out with racemic material. Formation of the *out*-*out*-binaphtho-*ortho*-quinone was achieved in 83% yield with IBX as the oxidant. Subsequent formation of the *out*-*out*-bisbenzo[*a*]phenazine in 96% yield, followed by successful deprotection to produce compound **6.28** as a stable entity was encouraging. At this point, however, we decided that formation of the *in*-*in*-regioisomers could be more interesting due to the added hindrance imposed by the fused ring at the 8,8'-positions, and would revisit this system at a later time (see section 6.6).

Scheme 6.3 Synthesis of 3,3'-substituted *out-out*-bisbenzo[*a*]phenazine.

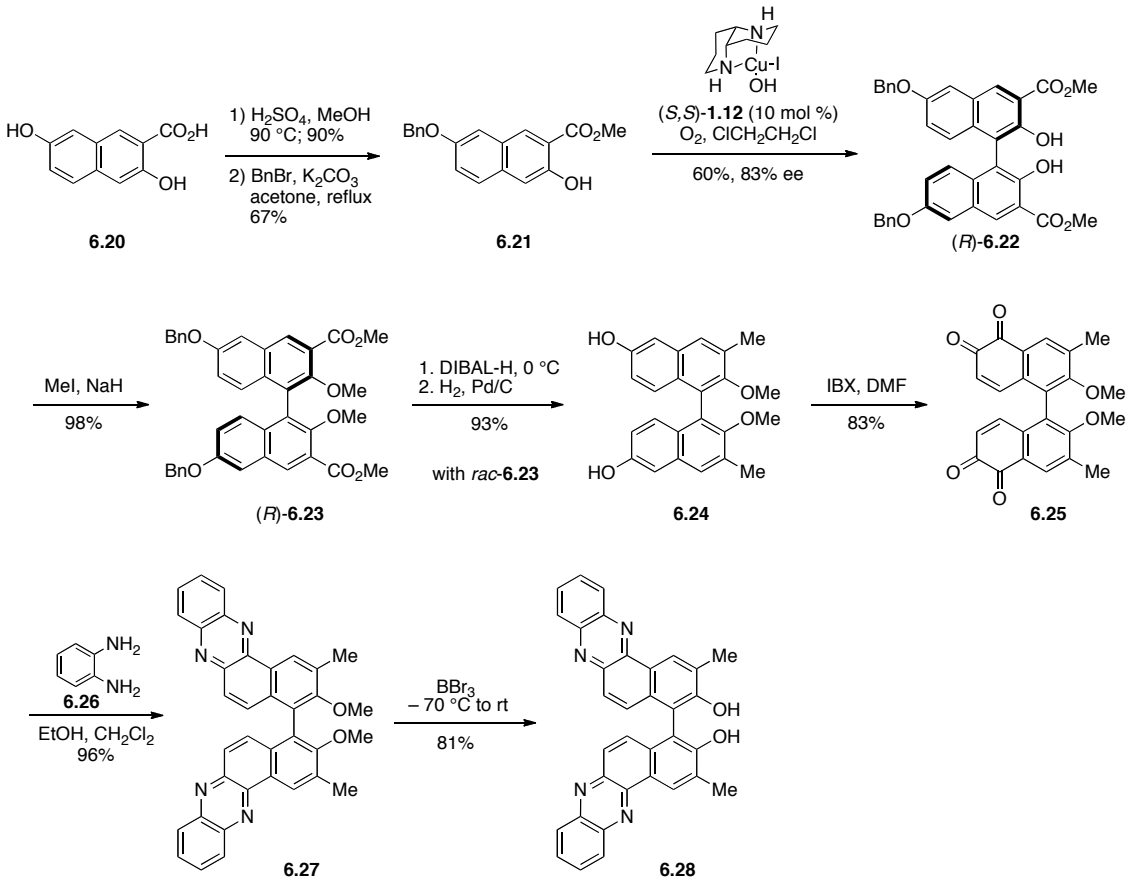

6.4 Synthesis of *in-in*-Bisbenzo[*a*]phenazines

In choosing to focus mainly on the synthesis of chiral *in-in*-bisbenzo[*a*]phenazines as potential ligands, we decided initially to only synthesize the simplest forms, without 3,3'-substitution. While a viable synthesis was already established for selectively synthesizing *in-in*-binaphtho-*ortho*-quinones from 8,8'-hydroxylated binaphthols (see Chapters 1 and 2), that route was better suited for development of more functionalized analogs and required extra steps to remove functionality at the 3,3'-positions. Thus, a shorter route was adopted which began with MOM protected naphthol **6.30** (Scheme 6.4). In addition, the use of a 7-substituted

naphthol rather than one with substitution at the 8-position was necessary because 8-substituted naphthols do not couple well with vanadium catalysts (see Chapter 1). According to Sasai, naphthol **6.30** can be coupled with chiral vanadium catalyst **V2** (see Table 1.2 in Chapter 1) under air for 72 h in 51% yield and 92% ee.[15b] We obtained similar results, using catalyst **V1** under O_2 for a shorter duration and in higher yield of (*S*)-**6.31**, but with lower selectivity (75% ee, 81% yield; Scheme 6.4). The enantiopurity, however, could be enhanced through triturations to yield material of 99% ee. Subsequent methylation and removal of the MOM groups with strong acid proceeded readily to generate diol (*S*)-**6.33** in high yield. Oxidation of this substrate to the binaphtho-*ortho*-quinone, (*S*)-**6.34**, was achieved in 93% yield. Compound (*S*)-**6.34** was treated with three different phenylenediamines containing either no substituents, electron-donating groups (R = Me), or electron-withdrawing groups (R = Cl) generating the corresponding *in*-*in*-bisbenzo[*a*]phenazines, (*S*)-**6.35a-c**, in 79-85% yields. Notably, changing the solvent for this reaction from EtOH/CH_2Cl_2 to AcOH dramatically improved yields (by >30%). A crystal structure of the racemate of **6.35a** confirmed the quinone and phenazine regiochemistry (Scheme 6.4). Finally, deprotection of the methoxy groups provided phenazines **36a-c** in 85%, 64%, and 81% yields respectively.

Scheme 6.4 Synthesis of *in-in*-bisbenzo[*a*]phenazines.

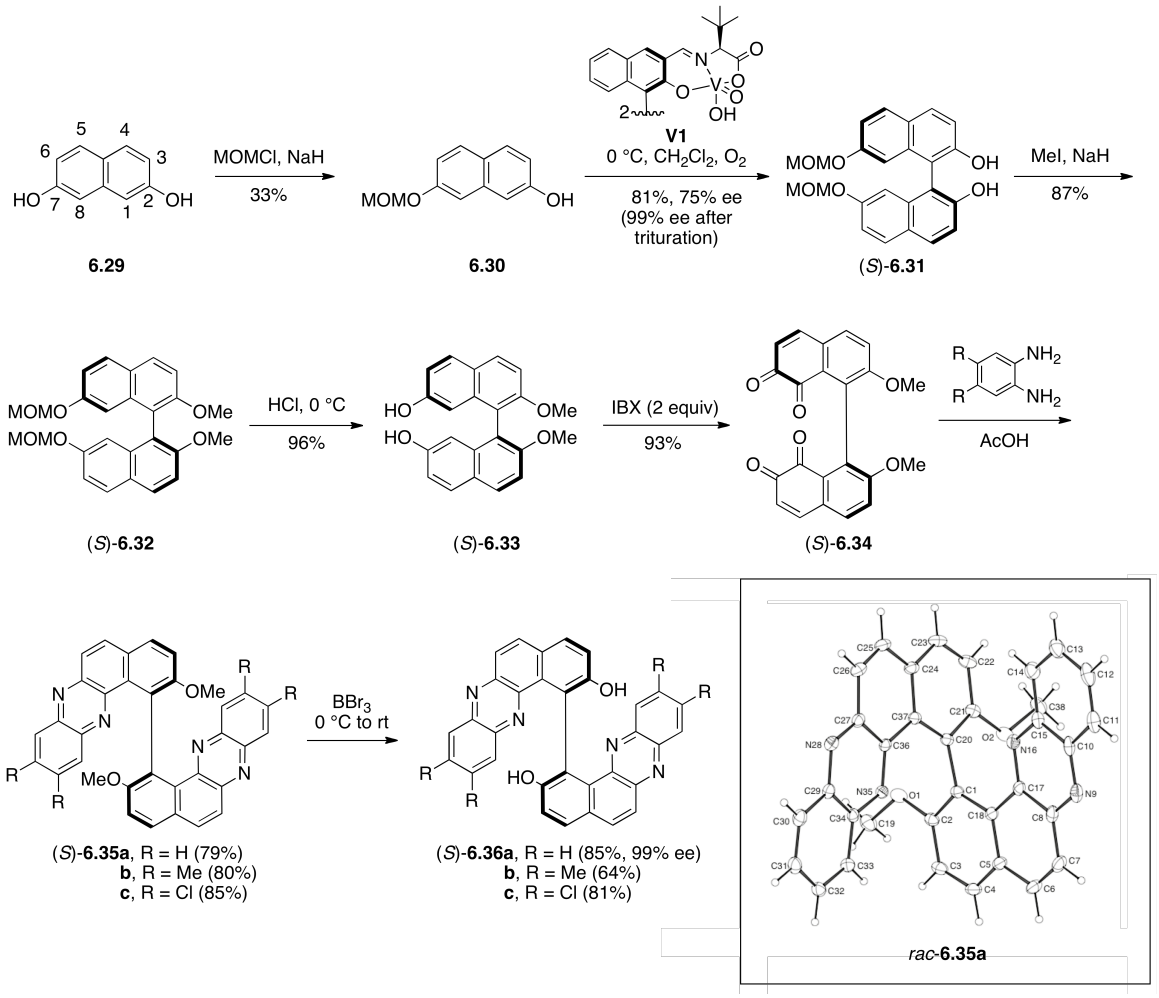

6.5 Utility as Ligands for Asymmetric Catalysis

Initially, the *in-in*-bisbenzophenazines were evaluated as chiral ligands in a titanium catalyzed sulfide oxidation reaction (Table 6.1). This reaction has been reported by Yudin and coworkers to be improved by electron-deficient F_8-BINOL compared to standard BINOL, in terms of both reactivity and selectivity.[111] After 18 h, F_8-BINOL gave the product in 55% yield (80% ee), while BINOL gave 69% yield after 42 h and

(111) Martyn, L. J. P.; Pandiaraju, S.; Yudin, A. K. "Catalytic Applications of F_8BINOL: Asymmetric Oxidation of Sulfides to Sulfoxides." *J. Organomet. Chem.* **2000**, *603*, 98–104.

only 3% ee.[111] When the phenazine ligand (*S*)-**6.36a** was tested in this reaction, using BINOL as a control, preliminary results suggested that the phenazine ligand behaved differently than BINOL (Table 6.1). The low selectivity of the BINOL control (0-7% ee) compared favorably with the literature, and the selectivity with the phenazine ligand was improved to 35-41% ee. However, the conversions were quite variable between different runs and compared to the literature, which made assessing the reactivity difficult.

Table 6.1 Titanium catalyzed sulfide oxidation.

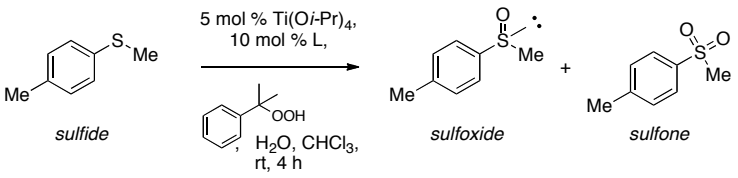

Entry	L	ee (%)	Conversion (%)* (sulfide:sulfoxide:sulfone)
1	(*S*)-BINOL	7 (*R*)	54:36:10
2	(*S*)-BINOL	0	17:77:6
3	(*S*)-**6.36a**	35 (*R*)	16:58:26
4	(*S*)-**6.36a**	41 (*R*)	31:60:9

*Conversions not reproducible

Allylboration of acetophenone was explored next (Table 6.2). Schaus and coworkers have shown that 15 mol % of 3,3'-dibromo-BINOL in toluene provided better yields and selectivity (82% yield, 66% ee) compared to BINOL (35% yield, 44% ee) in an unoptimized catalyst screen.[112] In addition, they saw that 6,6'-dibromo-BINOL gave 72% yield, but selectivity comparable to BINOL (36% ee). They suggested that substitution at the 3,3'-positions is important for selectivity. As substituents at 3,3' have a large influence on the selectivity and phenazines (*S*)-**6.36a-c** lack this feature, we were

(112) Lou, S.; Moquist, P. N.; Schaus, S. E. "Asymmetric Allylboration of Ketones Catalyzed by Chiral Diols." *J. Am. Chem. Soc.* **2006**, *128*, 12660–12661.

focused on the reactivity of the phenazines. Phenazine (*S*)-**6.36a** showed comparable conversion to BINOL with toluene as solvent, however, it was not homogeneous (Table 6.2). It was necessary to change solvents to CH_2Cl_2 and to lower the loading of catalyst due to the reduced solubility of (*S*)-**6.36a-c** compared to BINOL. With methylene chloride as solvent, phenazine ligands (*S*)-**6.36a**, (*S*)-**6.36b**, and (*S*)-**6.36c** were compared to BINOL, as well as 6,6'-dibromo-BINOL. Overall the phenazine ligands, with the exception of the chloro derivative appeared to have comparable reactivity to 6,6'-dibromo-BINOL (31-42% conversion versus 35% conversion). The conversion for the chloro phenazine derivative (*S*)-**6.36c** was the highest, at 54%. This result was encouraging.

Table 6.2 Allylboration of ketones.

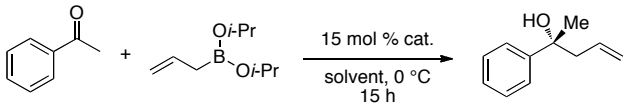

Entry	Catalyst	Solvent	Conversion (%)
1	none	Toluene	28
2	(*R*)-BINOL	Toluene	43
3	(*S*)-**6.36a**	Toluene	40
4	none	CH_2Cl_2	3
5	(*R*)-BINOL	CH_2Cl_2	20-25
6	(*S*)-**6.36a**	CH_2Cl_2	31
7	(*S*)-**6.36b**	CH_2Cl_2	42
8	(*S*)-**6.36c**	CH_2Cl_2	54
9	6,6'-dibromo-BINOL	CH_2Cl_2	35

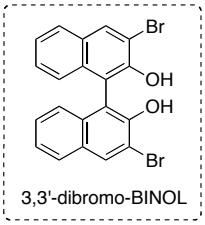

3,3'-dibromo-BINOL

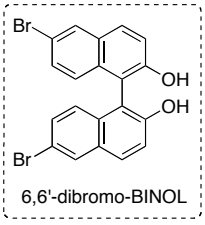

6,6'-dibromo-BINOL

The conjugate arylboration of α,β-unsaturated ketones, which Chong and coworkers found could be catalyzed by BINOL derivatives bearing electron-withdrawing

groups (Table 6.3), was also examined.[113] 3,3'-Dichloro-BINOL, in particular, provided the best selectivities and yield combination (65-90% yield, 78-98% ee). Reactions were sluggish, however, requiring high temperatures (120 °C) and extended reaction times (72 h). Chong *et al.* reported that 3,3'-dicyano-BINOL improved reactivity of the catalyst, but selectivities dropped. Interestingly, BINOL was reported to provide the same selectivity as the 3,3'-dichloro-BINOL, but with significantly reduced reactivity.[113] This result appeared encouraging for the phenazine system, since in their current state they also lack substitution at the 3,3'-positions, but the electron-withdrawing nature of the phenazine should make them more active catalysts. Even so, when both the unsubstituted and chloro-substituted phenazines (*S*)-**6.36a** and (*S*)-**6.36c** were used to catalyze the conjugate arylboration, only poor conversions were observed (Table 6.3).

Table 6.3 Arylboration of α,β-unsaturated ketones.

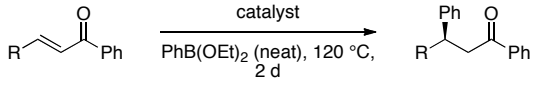

Entry	Catalyst	mol %	Conversion (%)
1	(*R*)-BINOL	200	6
2	3,3'-dichloro-BINOL	20	77
3	(*S*)-**6.36a**	20	11
4	(*S*)-**6.36c**	20	3

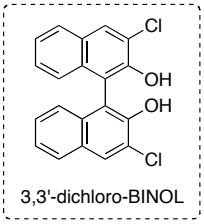

3,3'-dichloro-BINOL

Overall, the *in-in*-bisbenzo[*a*]phenazines showed improvements in reactivity and selectivity over BINOL for the tested reactions, but were not sufficient to improve upon the reported catalysts without further optimization. Application as the chiral phosphoric acids was also considered, however, substituents at the 3,3'-positions are usually

(113) Turner, H. M.; Patel, J.; Niljianskul, N.; Chong, J. M. "Binaphthol-Catalyzed Asymmetric Conjugate Arylboration of Enones." *Org. Lett.* **2011**, *13*, 5796–5799.

necessary for selectivity with those catalysts. It should be noted that the *out-out*-bisbenzo[*a*]phenazines ligands were never examined in these contexts. They may be more reactive than the *in-in*-bisbenzo[a]phenazines based on the location of the electron-withdrawing pyrazine ring relative to the phenols.

6.6 Evaluation of Properties: Chromism

Currently, many 'chromism' terms have been developed to describe color changes encountered with inorganic and organic compounds in response to a stimulus.[114] Generally the term refers to the stimuli causing the color change. Many of these responses have interesting applications in the development of sensors and materials. Both the *in-in*- and *out-out*-bisbenzo[*a*]phenazines were found to respond to different stimuli including heat (thermochromism), solvent (solvatochromism), vapors (vapochromism), acid (acidochromism), and mechanical action (mechanochromism).

Solid State Structure, Mechanochromism and Thermochromism

For many of the biaryls, including the phenazines, it was helpful to precipitate the compound out of EtOAc with hexanes in order to obtain an easily handled solid, rather than a resin. All of the phenazines were obtained as yellow to yellow-orange solids in this manner, however, while handling the tetrachloro-*in-in*-bisbenzo[*a*]phenazine, (*S*)-**6.36c**, an interesting phenomenon was observed. Compound (*S*)-**6.36c**, displayed a fast (less than a minute) color change between orange and yellow after hexanes was added to

(114) Bamfield, P.; Hutchings, M. G. *Chromic Phenomena. Technological Applications of Colour Chemistry,* 2nd ed., The Royal Society of Chemistry: Cambridge, UK, 2010.

the EtOAc solution. This transition was documented with a solution containing 11.4 mg (*S*)-**6.36c** in EtOAc (0.3 mL). The solution was initially homogeneous and orange in color (Figure 6.4A). Upon addition of hexanes (1 mL) the solution immediately became a nontransparent, cloudy yellow-orange solution, which changed quickly to a deep red-orange color directly before the formation of distinct bright orange solid (Figure 6.4B-D). The solution at this point appears to become more cloudy yellow-orange in color as the orange solid forms. This solid does not remain orange in color, however, and also turns yellow (Figure 6.4E). This phenomenon was not observed with any of the other phenazines synthesized, but following removal of the solvent, could be repeatedly demonstrated with (*S*)-**6.36c**. Pentane could also induce these color changes, however, no transitions were observed if EtOAc was replaced with acetone; only yellow solid (**Y**) formed. Orange solid (**O**), like that which forms at t = 32 in Figure 6.4D, can also be isolated by rotary evaporation from MeOH. Interestingly, **O** can be converted to **Y** simply by suspending it in hexanes or pentane and leaving the sample stand for a couple of hours.

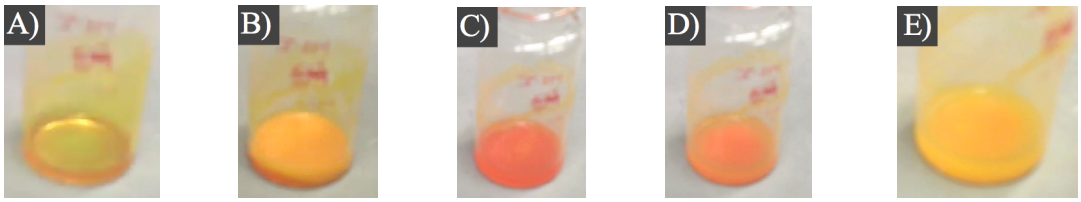

Figure 6.4 Color changes of (*S*)-**6.36c** in EtOAc/hexanes.

In an effort to explain this phenomenon, I also found that (*S*)-**6.36c**, the same compound, possesses reversible mechanochromism and thermochromism.[115] Both **Y** and **O** forms of (*S*)-**6.36c** were tested for mechanochromism by shearing the sample between two pieces of glass. The **Y** form showed a change from yellow to orange upon shearing (Figure 6.5A-B), while shearing the **O** form did not cause a visual change. This sheared sample could be reverted back to **Y** by submerging the sample in hexanes or pentane or by exposing it to the vapors of these solvents (Figure 6.5C). Analysis of the ^{1}H NMR spectra before and after shearing did not reveal any structural change to the phenazine, and our initial hypothesis is that the orange solid which forms during shearing is the same as the **O** form obtained by rotary evaporation from MeOH.

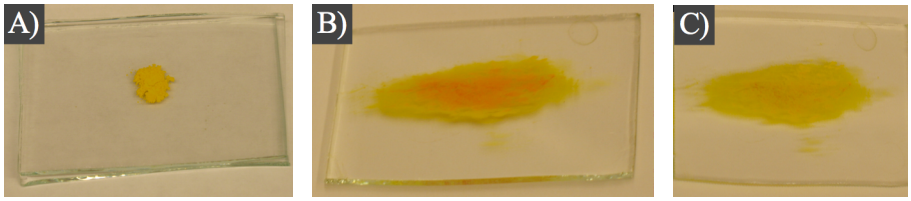

Figure 6.5 Mechanochromism of (*S*)-**6.36c**.

It was reasoned that **Y** and **O** could be different polymorphs of (*S*)-**6.36c**. This possibility was supported by the fact that there are examples of mechanochromic crystals where color can be restored upon exposure to solvent or solvent vapor.[116] Polymorphism is the ability of a compound to form different crystal structures and it is particularly

(115) Dr. David M. Chemoweth is gratefully acknowledged for helpful conversations and suggestions, in particular, his suggestion to check the compound for mechanochromism.

(116) Mataka, S.; Moriyama, H.; Sawada, T.; Takahashi, K.; Sakashita, H.; Tashiro, M. "Conformational Polymorphism of Mechanochromic 5,6-Di(*p*-chlorobenzoyl)-1,3,4,7-tetraphenylbenzo[*c*]thiophene." *Chem. Lett.* **1996**, 363–364.

important to the pharmaceutical industry. Although the chemical composition of each polymorph is the same, the molecules can have different packing arrangements or conformations, which influence their properties. Sometimes these differences in structure are accompanied by differences in morphology (e.g. plates versus needles) or color (color polymorphism), which may arise from differences in conformation or hydrogen bonding.[117-119] For example, the different crystal colors, which accompanied the seven conformational polymorphs of a nitroaniline-derived compound, were related to the degree of π-conjugation. This conjugation was, in turn, affected by the torsion angle of the conformer.[118]

To determine if different polymorphs were present, both **Y** and **O** samples were analyzed by powder X-ray diffraction (XRPD; see Figure 6.6).[120] The sample of **Y** (from acetone/pentane) displayed peaks characteristic of a crystalline solid. The **O** sample (from MeOH) displayed no sharp peaks and appeared to be amorphous, lacking long-range order. These results suggest that the mechanochromic behavior arises from a transition between crystalline and amorphous forms. The intermolecular or intramolecular interactions that were being disrupted by this action were unclear. Thus,

---

(117) Long, S.; Parkin, S.; Siegler, M. A.; Cammers, A.; Li, T. "Polymorphism and Phase Behaviors of 2-(Phenylamino)nicotinic Acid." *Cryst. Growth Des.* **2008**, *8*, 4006–4013.

(118) Yu, L. "Color Changes Caused by Conformational Polymorphism: Optical-Crystallography, Single-Crystal Spectroscopy, and Computational Chemistry." *J. Phys. Chem. A.* **2002**, *106*, 544–550.

(119) Sheth, A. R.; Lubach, J. W.; Munson, E. J.; Muller, F. X.; Grant, D. J. W. "Mechanochromism of Piroxicam Accompanied by Intermolecular Proton Transfer Probed by Spectroscopic Methods and Solid-Phase Changes." *J. Am. Chem. Soc.* **2005**, *127*, 6641–6651.

(120) The XRPD results were obtained by Danielle Reifsnyder of Dr. Christopher Murray's group, on their X-ray diffractometer, located at the Laboratory for Research on the Structure of Matter (LRSM). Her help with this analysis is gratefully acknowledged.

attempts were made to grow single crystals both to confirm the structure of (*S*)-**6.36c** and to discern what types of interactions could be present in the yellow crystalline form.

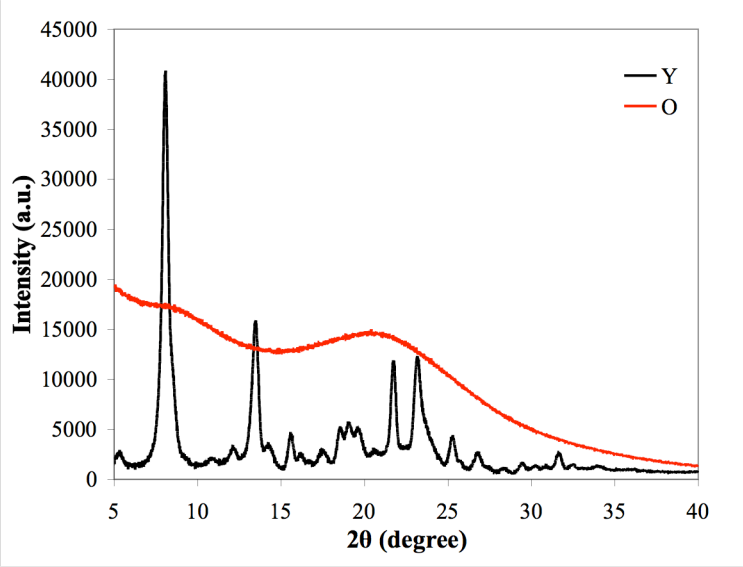

Figure 6.6 XRPD patterns of **Y** and **O** forms of (*S*)-**6.36c**.

Slow vapor diffusion of hexanes into a THF solution of (*S*)-**6.36c** produced yellow to light yellow-orange crystals suitable for single crystal X-ray diffraction analysis. The crystal structure, solved by Dr. Patrick Carroll, contained a total of four symmetry independent molecules (A, B, C, D) in the asymmetric unit of the crystal. Two of the molecules (A and B or C and D) in the asymmetric unit are able to form pores with a single molecule of hexane trapped inside (Figure 6.7).

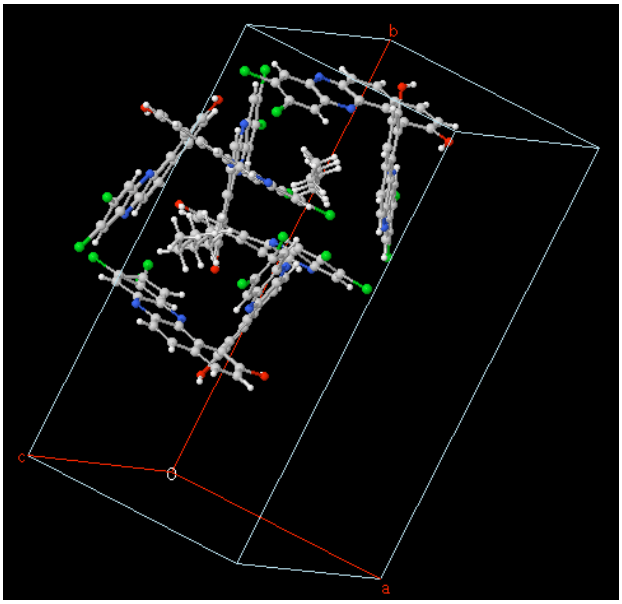

Figure 6.7 Asymmetric unit of the crystal structure of (*S*)-**6.36c**, containing pores that incorporate hexane.

Further analysis of the packing revealed a network of intermolecular O-H···Cl and O-H···N hydrogen bonding (Figure 6.8). The network of O-H···Cl interactions (d = 2.70–2.88 Å; θ = 130.5–140.0°) is isolated to individual molecules in the asymmetric unit, meaning A is only hydrogen bonded to other molecules of A, B to B, etc. However, the OH···N hydrogen bonding (d = 2.03–2.37 Å; θ = 112.9–159.3°) occurs between two symmetry independent molecules, such that A/B share O-H···N interactions and C/D share O-H···N interactions. Also, A/B and C/D form separate layers in the packing diagram.

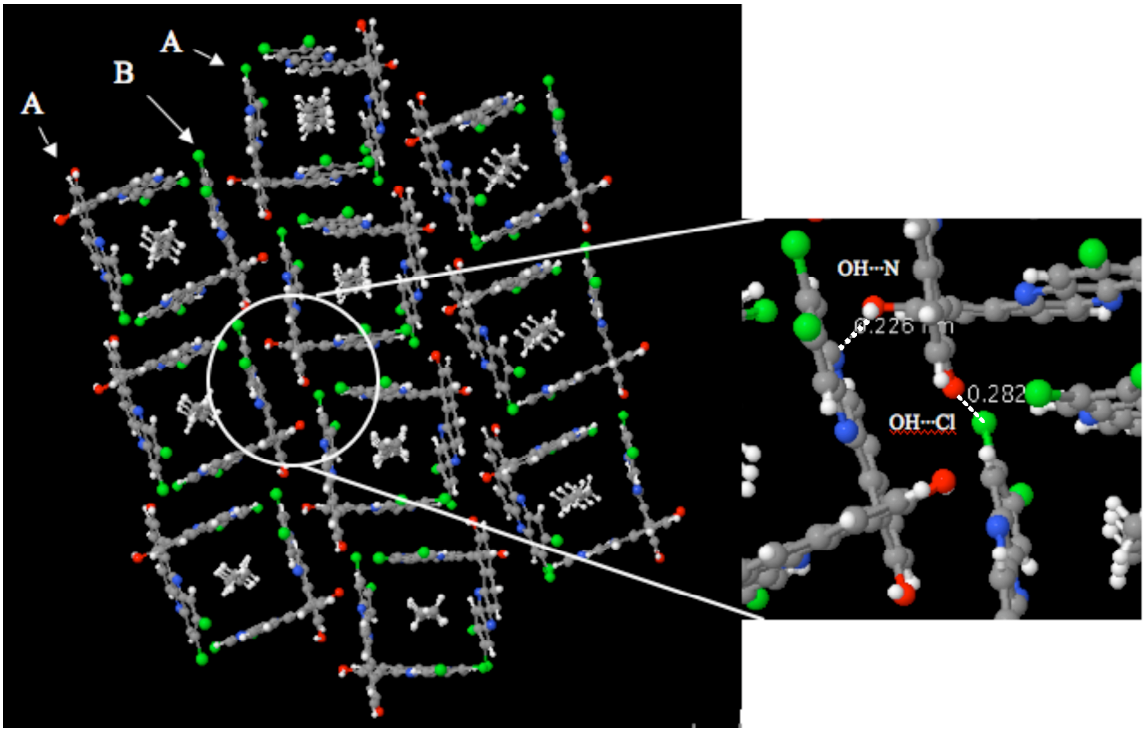

Figure 6.8 Network of intermolecular O-H···Cl and O-H···N hydrogen bonding for the A/B molecule layer in a crystal of (*S*)-**6.36c**.

Notably, the intermolecular O-H···Cl-C interactions found in the crystal structure of (*S*)-**6.36c** are not common. A CSD (Cambridge Structural Database) study from 2003, found only 68 intermolecular and 115 intramolecular O-H···Cl-C interactions out of 1277 total compounds containing both O-H and Cl-C groups.[122] Typically, chlorines bonded to carbon (Cl-C) are much weaker acceptors than chloride ions or activated chlorines bound to metals.[121,122] Weak hydrogen bonds have been generally characterized by H···A (A = acceptor) bond lengths >2.2 Å, θ = >90 °, and dissociation energy of 0.5–4 kcal/mol.

(121) Aullón, G.; Bellamy, D.; Brammer, L.; Bruton, E. A.; Orpen, A. G. "Metal-Bound Chlorine Often Accepts Hydrogen Bonds" Chem. Commun., 1998 653–654.

(122) Banerjee, R.; Desiraju, G. R.; Mondal, R.; Howard, J. A. K. "Organic Chlorine as a Hydrogen-Bridge Acceptor: Evidence for the Existence of Intramolecular O–H···Cl–C Interactions in Some *gem*-Alkynols" *Chem. Eur. J.* **2004**, *10*, 3373–3383.

Hydrogen bonds of moderate strength, such as O-H···O, O-H···N, and N-H···O interactions, are characterized by H···A bond lengths of 1.5–2.2 Å, θ = >130 °, and dissociation energy of 4–15 kcal/mol.[123] Due to the rarity and weakness of O-H···X-C (X = F, Cl, Br, I), it has been suggested that the interactions occur because of forced contacts or from close packing in the crystal. However, Banerjee and coworkers have suggested that H···Cl interactions are attractive and stabilizing, based on the intramolecular O-H···Cl-C interactions described in a series of *gem*-alkynols.[122]

Together with the results from XRPD, a plausible explanation for the mechanochromism can be proposed. The **Y** form of (*S*)-**6.36c** is crystalline, as a solvate of hexanes or pentane. The mechanical action from shearing causes the hydrogen bonds to break, disrupting the crystal lattice and leading to the amorphous **O** form. It appears that hexane or pentane is needed to facilitate crystallization of this enantiopure material, most likely by nucleating/filling the pores. Further support of this analysis was provided during an evaluation of (*S*)-**6.36c** for thermochromism. When a sample of **Y** (from acetone/pentane) was placed under high vacuum at room temperature for an extended period of time (15 h) nothing happened to the color, as some amount of pentane remained in the sample. The presence of pentane was observed by ^{1}H NMR spectroscopy. Upon heating the solid in an oil bath under vacuum, the solid turned slightly orange in color beginning at ~110°C and remained this color until 200 °C, when it turned the same color as the **O** form (Figure 6.9). ^{1}H NMR spectroscopic data indicated that all of the pentane in the sample was gone at this stage.

(123) Steiner, T. "The Hydrogen Bond in the Solid State" *Angew. Chem. Int. Ed.* **2002**, *41*, 48–76.

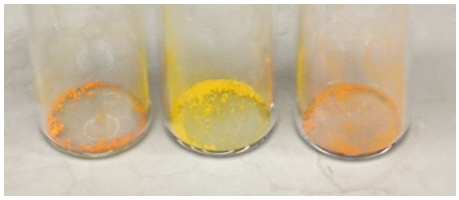

Figure 6.9 Thermochromism of (*S*)-**6.36c**.
Left to right: **Y** after heating to 200 °C under high vacuum, **Y** after high vacuum at rt, **O** after high vacuum at rt.

Interestingly, crystals could be grown from THF/MeCN, which were a similar yellow-orange color, but too small for analysis. These crystals were also mechanochromic. Red crystals were grown from CH_2Cl_2 (Figure 6.10), but X-ray quality crystals could not be obtained.

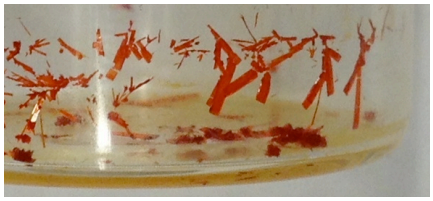

Figure 6.10 Red crystals from CH_2Cl_2.

In light of the current information, it is possible that the color changes observed in EtOAc/hexanes solutions (Figure 6.4) is related to phase transitions in the solid state. Addition of hexanes (or pentane) to a solution of (*S*)-**6.36c** in EtOAc initially causes rapid solid formation in the form of a very fine suspension. The possibility of (*S*)-**6.36c** oiling out seems unlikely, because the compound has a high melting point. Since the appearance in color is much redder in Figure 6.4C than in Figure 6.4D, perhaps this is a short-lived amorphous phase, similar to the resin that can be formed from some solvents, or related to the red crystals observed from dichloromethane. Aggregation of (*S*)-**6.36c**

then leads to formation of distinct **O** solid (Figure 6.4D). Since hexane is present, the phenazine can cocrystallize and transition to the **Y** form and a yellow color.

Analysis of the other bisbenzo[*a*]phenazines for mechanochromism revealed some necessary structural features. The chlorines and unprotected 2,2'-hydroxyls are necessary, as (*S*)-**6.36a** and (*S*)-**6.35c** do not display this behavior. The biaryl structure appears to be important as well, since the monomer (**6.38**) also does not change color upon shearing, nor does commercially available phenazine. The corresponding "*in*"-monomer was synthesized from **6.29**, by oxidation and condensation with 4,5-dichlorobenzene-1,2-diamine (Scheme 6.5A). The yields were low due to dimerization of naphthoquinone intermediate during the oxidation and work-up. In addition, the *out-out*-regioisomer was synthesized from (*S*)-**5.2** in 92% yield over two steps (Scheme 6.5B). This compound had some interesting properties of its own (discussed in the next subsection), but did not change colors with shearing; it remained yellow. Thus, the inward orientation of the phenazine rings also appears to be necessary. It was reasoned, due to the presence of OH···Cl hydrogen bonds in the crystal structure of (*S*)-**6.36c**, that more electronegative fluoro groups could form stronger hydrogen bonds in the solid state[124] and that these crystals could also be mechanochromic. The fluoro compound, (*S*)-**6.36d**, was synthesized in two steps from 4,5-difluorobenzene-1,2-diamine in 89% and 80% yield respectively (Scheme 6.5C). However, this compound also was not mechanochromic. At this point, after analyzing many different phenazines, it was determined that the mechanochromism and observed phenomenon with EtOAc/hexanes

(124) Wang, D.-Y.; Wang, J.-L.; Zhang, D.-W.; Li, Z.-T. "NH···X (X = F, Cl, Br, and I) hydrogen bonding in aromatic amide derivatives in crystal structures" *Sci. China Chem.* **2012**, *55*, 2018–2026.

solution appeared to be a property visualized only with compound **6.36c**. Enantiopurity, however, was not a requirement. Compound *rac*-**6.36c**, a yellow solid, was also mechanochromic. By comparison though, it formed more stable crystals, since no thermochromism, nor melting was observed up to 250 °C. Evaluation of the color changes from EtOAc/hexanes was difficult due to poor solubility. The poor solubility of *rac*-**6.36c** generally made the compound difficult to handle. In addition, although the methylated tetrachloro derivative, (*S*)-**6.35c**, was not mechanochromic it was reversibly thermochromic. Similar to (*S*)-**6.36c**, the 2,2'-dimethoxy derivative began turning pale orange at approximately 100-110 °C and was orange by 195 °C. However, this compound did not require solvent for reversal. It quickly returned to a yellow color upon cooling (Figure 6.11).

Scheme 6.5 Synthesis of other phenazine derivatives.

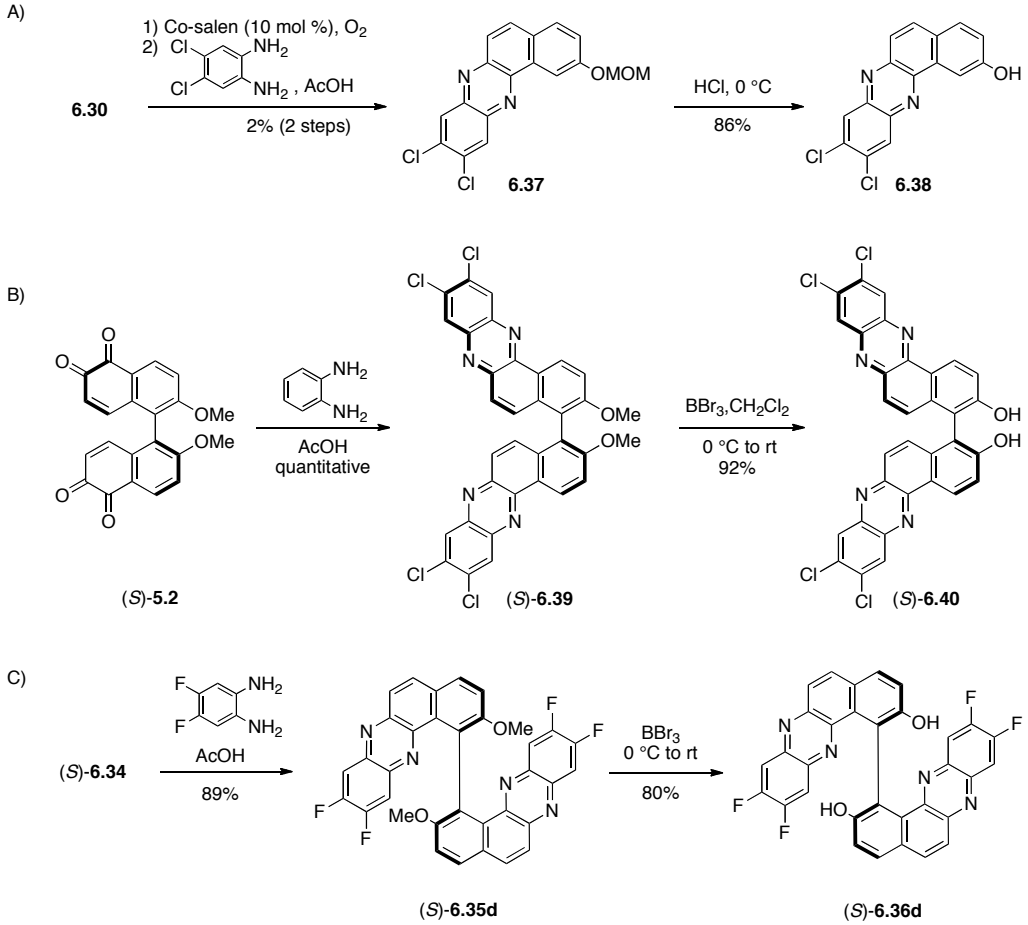

Before heat Heated to 195 °C After cooling

Figure 6.11 Thermochromism of (*S*)-**6.35c**.

Acidochromism, Vapochromism, Solvatochromism, and Fluorescence

For all the bisbenzo[*a*]phenazines synthesized, formation of red to dark purple solutions and solids were observed during the final BBr_3 deprotection. Addition of base

to neutralize the HBr returned the color of the solution to yellow, suggesting that these phenazines were acidochromic (color change due to acid), as had been demonstrated with a similar monomeric system.[105] This observation suggested that protonation with strong acid is accompanied by a color change, which could be demonstrated upon addition of trifluoroacetic acid (TFA, pK_a = –0.25) to a solution of (*S*)-**6.36c** in CH_2Cl_2. The addition of TFA caused the color of the solution to change from yellow to red. Quenching the acid with triethylamine reverted the color back to yellow. A weaker acid such as AcOH (pK_a = 4.76) did not cause any color change. Drop-cast thin films of (*S*)-**6.36c** from CH_2Cl_2, exhibited a rapid colorimetric response to TFA vapors (vapochromism). The color of the film changed from a yellow-orange to a very dark purple/black color on exposure to the acid (Figure 6.12). Subsequent exposure of the film to NH_3 vapors from NH_4OH reverted the film back to its original color. This cycle could be repeated. The UV/Vis spectrum[125] indicated that the color change of the thin film was accompanied by formation of a new band at 563 nm (Figure 6.12). Vapochromism is useful for the direct visual detection of volatile compounds. For example, recently a riboflavin-based polymer showing vapochromic behavior was found to be useful for the detection of volatile primary and secondary amines, whose selective detection is limited mostly to fluorescence-based sensors.[126]

---

(125) The assistance of Adrienne Pesce and Dr. Robert Rarig of the Chenoweth group are acknowledged for help using their group's UV/Vis instrument.

(126) Iida, H.; Iwahana, S.; Mizoguchi, T.; Yashima, E. "Main-Chain Optically Active Riboflavin Polymer for Asymmetric Catalysis and Its Vapochromic Behavior." *J. Am. Chem. Soc.* **2012**, *134*, 15103–15113.

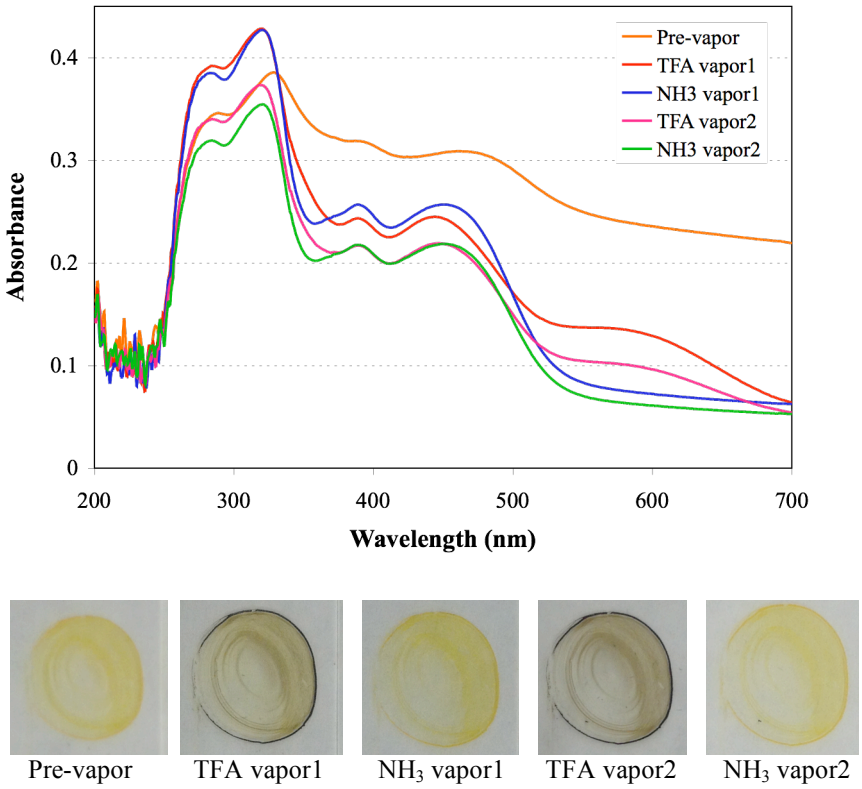

Figure 6.12 Vapochromism of (*S*)-**6.36c**.

In addition to the colorimetric response of (*S*)-**6.36c** to acid, different solvents also caused color changes (solvatochromism). Initially, it appeared that increased polarity of the solvent caused a shift in the absorbance of the UV/Vis spectrum toward longer wavelengths (red or bathochromic shift) since the compound formed yellow solutions with solvents such as benzene and methylene chloride, but much redder solutions in more polar solvents such as acetone and methanol. Further analysis by UV/Vis spectroscopy revealed, however, that other polar solvents, such as nitromethane and acetonitrile (Figure 6.13 and Figure 6.14), did not follow this trend. Reevaluation of the data was undertaken using the solvatochromatic parameters, α, β, and π^*, developed

by Kamlet and Taft.[127,128] The π* scale is a measure of solvent dipolarity/polarizability. The α scale is a measure of the ability of a solvent to act as a hydrogen-bond donor to a solute, while the β scale measures the ability of a solvent to act as a hydrogen-bond acceptor from a solute (scale of solvent basicities). The β values are the result of an average of multiple normalized values determined from a diverse set of indicators, such as UV/Vis spectral data of 4-nitroaniline and N,N-diethyl-4-nitroaniline.[127,128] Together these scales are part of the solvatochromic comparison method, in which the parameters are used independently or in combination to correlate and rationalize multiple interacting solvent effects and determine which property of a solvent had the greatest influence.[127,128]

Comparison of the longest maximum wavelength of absorbance of (*S*)-**6.36c** in various solvents to α, β, and π* parameters revealed a correlation to the *β* solvatochromic scale (Figure 6.13 and Figure 6.14). This correlation indicates that solvents with greater abilities to hydrogen bond to the OH of (*S*)-**6.36c** cause the longest λ_{max} to red shift in the UV/Vis spectrum. The red shift (to longer wavelengths/lower energy) indicates that the solvents with greater hydrogen-bond acceptor ability are able to stabilize the excited state. The electronic transition of the visible π → π* absorption band is likely associated with intramolecular charge-transfer, since the structure of (*S*)-**6.36c** contains an electron-donating group (OH) linked by a conjugated system to an electron acceptor group

(127) Reichardt, C.; Welton, T. *Solvents and Solvent Effects in Organic Chemistry*, 4th ed.; Wiley-VCH: Germany, 2011.

(128) (a) Kamlet, M. J.; Taft, R. W. "The solvatochromic comparison method. I. The .beta.-scale of solvent hydrogen-bond acceptor (HBA) basicities." *J. Am. Chem. Soc.* **1976**, *98*, 377–383. (b) Kamlet, M. J.; Abboud, J.-L. M.; Abraham, M. H.; Taft, R. W. "Linear Solvation Energy Relationships. 23. A Comprehensive Collection of the Solvatochromic Parameters, π*, α, and β, and Some Methods for Simplifying the Generalized Solvatochromic Equation." *J. Org. Chem.* **1983**, *48*, 2877–2887.

(pyrazine group).[127] Only the solvatochromism of (*S*)-**6.36c** had been evaluated, but it is possible the other phenazines generated in this study exhibit similar behaviors.

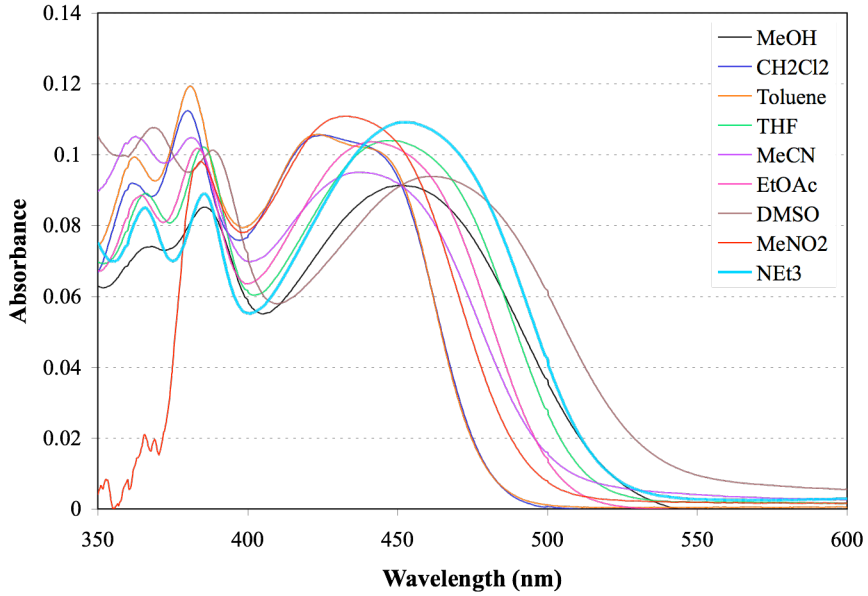

Figure 6.13 UV/Vis spectrum of (*S*)-**6.36c** in various solvents (0.01 mM).

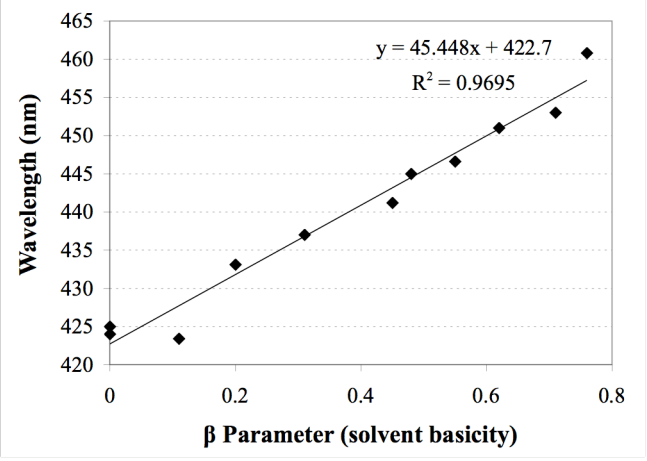

Entry	Solvent	λ (nm)	β parameter[a]
1	DMSO	461	0.76
2	NEt_3	453	0.71
3	MeOH	451	0.62
4	THF	447	0.55
5	Acetone	445	0.48
6	EtOAc	441	0.45
7	MeCN	437	0.31
8	$MeNO_2$	433	0.20[b]
9	Toluene	423	0.11
10	CH_2Cl_2	425	0.00
11	$CHCl_3$	424	0.00

[a] Reference 128, [b] Reference 129

Figure 6.14 Solvatochromism correlated with solvent basicity (β parameter).

(129) Taft, R. W.; Abboud, J.-L. M.; Kamlet, M. J. "Linear Solvation Energy Relationships. 28. An Analysis of Swain's Solvent 'Acity' and 'Basity' Scales." *J. Org. Chem.* **1984**, *49*, 2001–2005.

The absorption spectra for a few other phenazines were also measured to see the effect of structural changes relative to (*S*)-**6.36c**. The *in*-*in*-bisbenzo[*a*]phenazines, (*S*)-**6.36a** (no Cl groups) and (*S*)-**6.35c** (2,2'-hydroxyl groups replaced with methoxy groups), had similarly shaped absorption bands, but the introduction of chlorines (as in (*S*)-**6.36c** and (*S*)-**6.35c**) led to a red shift and increased absorption. Protection of the 2,2'-hydroxyl groups as methoxy substituents [(*S*)-**6.35c**] also had a similar effect. The monomer, **6.38** was similar to the *in*-*in*-bisbenzo[*a*]phenazines, with absorbance about half the intensity of the dimers at the same concentration. A much larger absorbance was observed for the *out*-*out*-bisbenzo[*a*]phenazine, (*S*)-**6.39**, compared to the *in*-*in*-bisbenzo[*a*]phenazines, suggesting that the conjugation is better in those systems.

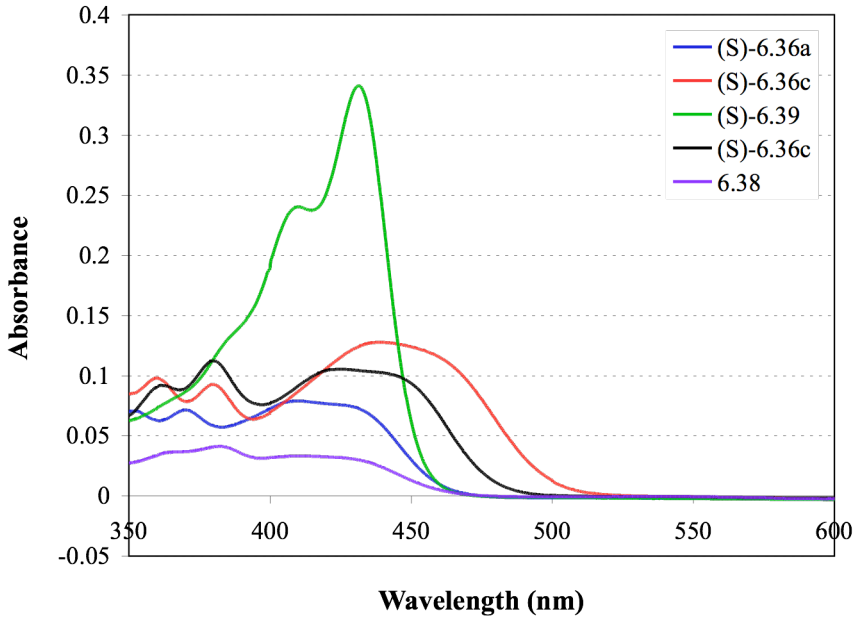

Figure 6.15 UV-Vis spectrum of benzo[*a*]phenazines in CH_2Cl_2 (0.01 mM).

Fluorescence of the bisbenzo[*a*]phenazines was also briefly examined. During the synthesis of *out*-*out*-tetrachloro phenazine, (*S*)-**6.39**, fluorescence was observed under normal light while handling the compound, prompting further evaluation. Compound (*S*)-**6.39** emits at 478 nm (excited at 431 nm, 2.5 μM in CH_2Cl_2). Based on preliminary qualitative examination of the fluorescence of (*S*)-**6.39** under 365 nm light, it appears that the compound is solvatochromic in its emission spectrum as the emission color is different between solvents. This tendency is most noticeable between CH_2Cl_2 and MeOH (Figure 6.16B and E). Other *out*-*out*-derivatives, including (*S*)-**6.40**, also fluoresce (Figure 6.16), as well as the non-chlorinated derivative **6.26**. The fluorescence properties are primarily a characteristic of the phenazine moiety, as seen by the fluorescence of the monomer (515 nm emission, 380 excitation). Notably, none of the *in*-*in*-phenazines fluoresce (Figure 6.16), which indicates a quenching pathway. Examination of the structure of the *in*-*in*-phenazine reveals potential interactions either between the oxygen functionality or pyrazine moiety of one half of the dimer and the pyrazine ring from the other half. Due to the close proximity of the two ring systems, it is possible that quenching is occurring via an intramolecular electron transfer, from an electron donor (one half of molecule) to an electronically excited acceptor (other half of molecule), forming a charge transfer complex, which can return to the ground state without emission.[130] For example, increasing fluorescence quenching has been observed with

(130) Lakowicz, J. R. *Principles of Fluorescence Spectroscopy*, 3rd ed.; Springer: New York, 2006.

shorter linkage units between donor-acceptor system containing methylviologen (acceptor) covalently linked to 1,8-naphthalimide (donor).[131]

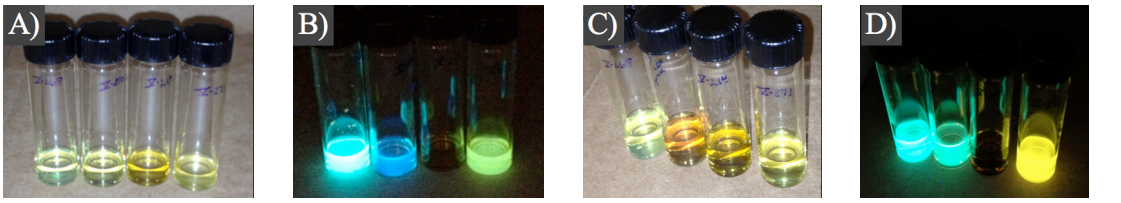

CH_2Cl_2, normal light CH_2Cl_2, 365 nm light Acetone, normal light Acetone, 365 nm light

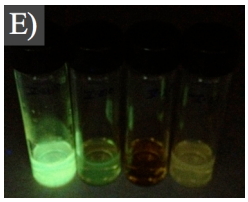

MeOH, 365 nm light

Figure 6.16 Fluorescence of phenazines in various solvents.
Compound order (left to right): (*S*)-**6.39**, (*S*)-**6.40**, (*S*)-**6.36c**, **6.38**

In summary, two different classes of bisbenzo[*a*]phenazines have been synthesized, the *in-in-* and *out-out*-bisbenzo[*a*]phenazines. The *in-in*-regioisomers were found to offer minor improvement over BINOL in some test reactions, however they were not better than the existing electron-deficient BINOLs. Exploration of derivatives with substitution at the 3,3'-positions, or the *out-out*-derivatives would likely improve selectivity and/or activity. Besides being electron-poor BINOL derivatives, the phenazine, like a quinone, also possesses redox properties and exploration of these compounds as potentially redox active ligands is indicated. In addition, many interesting properties were found for each set of regioisomers and/or for a specific compound within each set. At this point, the tetrachloro-compounds of both the *in-in-* and *out-out-*

(131) Le, T. P.; Rogers, J. E.; Kelly, L. A. "Photoinduced Electron Transfer in Covalently Linked 1,8-Naphthalimide/Viologen Systems" *J. Phys. Chem. A* **2000**, *104*, 6778–6785.

regioisomers have been found to be the most interesting and were the focus of most of these studies. The ability of the mechanochromic *in*-*in*-isomer, (*S*)-**6.36c**, to trap hexane or pentane and the associated color changes could be useful if they can produce a colorimetric response to other small molecules such as ethylene, by trapping it within the crystal.[132] In addition, the sensitivity of the compound to changes in solution or its immediate atmosphere may be useful as a sensor. The *out*-*out*-tetrachloro-compounds, also appear to be sensitive to their environment, displaying shifts in the emission depending on the solvent. Although not extensively studied, compound (*S*)-**6.39** shows solvatochromism. As seen in Figure 6.16A and Figure 6.16C, there is a distinct color change between methylene chloride and acetone as solvent. In addition, on two instances (*S*)-**6.39** appeared to form a gel-like solid with either benzene or methylene chloride. In the case of methylene chloride, 15 mg of the solid was dissolved completely in the 0.6 mL of solvent, but following a short time the solution had completely solidified. Further exploration of this aspect may also provide opportunities for application of these materials as organogelators.[96]

(132) Esser, B.; Swager, T. M. "Detection of Ethylene Gas by Fluorescence Turn-on of a Conjugated Polymer." *Angew. Chem. Int. Ed.* **2010**, *49*, 8872–8875.

CHAPTER 7: Experimental

7.1 General Considerations

All reactions were carried out under an atmosphere of dry nitrogen or argon, unless otherwise noted. When necessary, solvents and reagents were dried prior to use. Methylene chloride, 1,2-dichloroethane, and acetonitrile were distilled from CaH_2, THF was distilled from sodium/benzophenone ketyl, toluene was distilled from sodium, and DMF was distilled from $MgSO_4$. Freshly distilled TMSCl and diisopropylamine (both from CaH_2) were used in the preparation of dienes **4.17** and **4.37**. Dienes **4.17** and **4.37** were distilled under reduced pressure, and stored at –20 °C under argon. Diene **4.37** was used within two weeks of preparation and diene **4.17** was used within a month. Reactions were all monitored via analytical thin layer chromatography (TLC) using Silicycle glass backed TLC plates with 250 μm silica and F254 indicator. Visualization was accomplished with UV light and/or ceric ammonium molybdate stain. Column chromatography was performed with Silicycle SiliaFlash P60 silica gel (40-63 μm particle size).

NMR spectra were recorded on 300 MHz, 360 MHz, and 500 MHz spectrometers. Multiplicity for ^{1}H NMR data are reported as follows: s = singlet, d = doublet, t = triplet, br = broad, m = multiplet. ^{1}H NMR spectra were referenced to the residual solvent peaks: $CDCl_3$ (7.26 ppm), DMSO-*d*$_6$ (2.50 ppm), acetone-*d*$_6$ (2.05 ppm), THF-*d*$_8$ (3.58 ppm), CD_3OD (3.31 ppm), or C_6D_6 (7.16 ppm). ^{13}C NMR spectra were referenced to: $CDCl_3$ (77.16 ppm), DMSO-*d*$_6$ (39.52 ppm), acetone-*d*$_6$ (29.84 ppm), or THF-*d*$_8$ (67.57

ppm). Infrared spectra were recorded on either a Jasco FT/IR-480 Plus spectrometer[133] or an Applied Systems ReactIR 1000. UV spectra were measured on a JASCO FT/IR-480 Plus spectrometer.[133] High-resolution mass spectra were measured on a Waters LC-TOF mass spectrometer (model LCT-XE Premier) with ionization mode ESI+ or ESI–.[134] Enantiomeric excesses were determined using analytical HPLC on an Agilent 1100 Series HPLC with UV detection at 254 nm. An analytical Chiralpak IA column (4.6 mm x 250 mm, 5 μm) from Daicel was used. Compounds (*S*)-**4.34a**, (*S*)-**4.34b**, and (*S*)-**4.34c** were separated via semi-preparative normal-phase HPLC using a Waters 600 HPLC with UV detection at 276 nm and Dynamax column (Si 83-121-C, 21 mm).[76] Optical rotations were measured on a Jasco polarimeter with a sodium lamp.[135] CD spectra were obtained on a Jasco J-720 spectropolorimeter.[136]

7.2 Chapter 1 Experimental

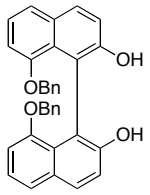

8,8'-Bis(benzyloxy)-[1,1'-binaphthalene]-2,2'-diol (**1.17a**). To a solution of commercially available naphthalene-1,7-diol (**1.15**, 1.00 g, 6.24 mmol) in acetone (25 mL) was added anhydrous K_2CO_3 (1.25 g, 9.05 mmol) and BnBr (0.89 mL, 7.5 mmol).

(133) The Smith group is thanked for use of their UV and IR spectrometers.

(134) Dr. Rakesh Kohli at the Mass Spectrometry Laboratory at the University of Pennsylvania is gratefully acknowledged for obtaining high resolution mass spectra.

(135) The Molander group is thanked for use of their polorimeter.

(136) Pawaret (Kla) Leowanawat of the Percec group is gratefully acknowledged for obtaining CD spectra.

After heating the reaction mixture to reflux for approximately 8 h, the solids were removed via vacuum filtration and washed with acetone. The filtrate was concentrated and the residue chromatographed (5% EtOAc/hexanes) to yield 8-(benzyloxy)naphthalen-2-ol (**1.16a)** as a light brown oil. ^{1}H NMR (500 MHz, $CDCl_3$) δ 7.73 (d, *J* = 6.7 Hz, 1H), 7.62 (d, *J* = 2.6 Hz, 1H), 7.53 (d, *J* = 7.3 Hz, 2H), 7.43 (t, *J* = 7.5 Hz, 2H), 7.40-7.36 (m, 2H), 7.23 (d, *J* = 7.9 Hz, 1H), 7.12 (dd, *J* = 8.8 Hz, 2.6 Hz, 1H), 6.88 (d, *J* = 7.6 Hz, 1H), 5.23 (s, 2H), 4.92 (s, 1H); ^{13}C NMR (125 MHz, $CDCl_3$) δ 153.6, 153.3, 137.3, 130.1, 129.7, 128.8, 128.1, 127.7, 127.0, 123.6, 120.6, 118.1, 105.9, 104.6, 70.3.

$VO(acac)_2$ (9 mol %, 8.0 mg) was added to a solution of **1.16a** (83 mg, 0.33 mmol) in CH_2Cl_2 (3.3 mL) and the reaction mixture stirred under an oxygen atmosphere. After 3 h, the mixture was concentrated. The residue was chromatographed (15% EtOAc/hexanes) to yield **1.17a** as an off-white solid (30 mg, 36%, 68% based on recovered starting material): mp 188-190 °C; ^{1}H NMR (500 MHz, $CDCl_3$) δ 7.47 (d, *J* = 8.9 Hz, 2H), 7.26 (d, *J* = 8.2 Hz, 2H), 7.15 (t, *J* = 7.7 Hz, 2H), 7.13 (d, *J* = 6.7 Hz, 2H), 7.04 (d, *J* = 8.9 Hz, 2H), 7.03 (t, *J* = 7.6 Hz, 4H), 6.73 (d, *J* = 7.2 Hz, 2H), 6.57 (d, *J* = 7.2 Hz, 4H), 5.00 (s, 2H), 4.55 (d, *J* = 11.4 Hz, 2H), 4.51 (d, *J* = 11.4 Hz, 2H); ^{13}C NMR (125 MHz, $CDCl_3$) δ 155.2, 151.5, 136.2, 131.3, 130.3, 128.2, 127.6, 127.4, 125.4, 123.3, 121.7, 117.2, 113.4, 107.3, 70.5; IR (film) 3483, 3059, 2920, 2873, 1583, 1514, 1452, 1259 cm^{-1}; HRMS (ESI) *m/z* 521.1711 $[M+Na]^+$ (calcd for $C_{34}H_{26}O_4Na$, 521.1729).

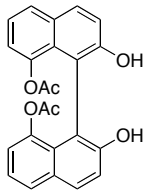

2,2'-Dihydroxy-[1,1'-binaphthalene]-8,8'-diyl diacetate (**1.17b**). A solution of naphthalene-1,7-diol (**1.15**, 500 mg, 3.12 mmol) in pyridine (3.1 mL) was cooled to 0 °C before adding Ac_2O (1.2 mL, 12.5 mmol). After stirring for 3 h, the reaction mixture was diluted with EtOAc and washed with 1 M HCl, followed by brine. The organic layer was dried over Na_2SO_4, filtered, and concentrated. The residue was chromatographed (10%–20% EtOAc/hexanes) to yield the diacetate as a white solid (652 mg, 86%): ^{1}H NMR (500 MHz, $CDCl_3$) δ 7.79 (d, *J* = 8.5 Hz, 1H), 7.74 (d, *J* = 8.2 Hz, 1H), 7.69 (d, *J* = 1.9 Hz, 1H), 7.46 (t, *J* = 7.9 Hz, 1H), 7.31-7.27 (m, 2H), 2.46 (s, 3H), 2.36 (s, 3H); ^{13}C NMR (125 MHz, $CDCl_3$) δ 169.6, 169.4, 149.1, 146.5, 132.8, 129.8, 127.4, 125.9, 125.4, 122.0, 118.9, 112.5, 21.3, 21.2.

To a solution of the diacetate (652 mg, 2.67 mmol) in CH_2Cl_2/MeOH (13 mL/13 mL) at 0 °C was added anhydrous K_2CO_3 (462 mg, 3.34 mmol). After stirring for an hour, the reaction was quenched with 1 M HCl and extracted with CH_2Cl_2. The organic layer was washed with brine and dried over Na_2SO_4, followed by filtration and concentration. The residue was chromatographed (10%–20% EtOAc/hexanes) to yield 7-hydroxynaphthalen-1-yl acetate (**1.16b**) as a yellow solid (226 mg, 42% yield): ^{1}H NMR (300 MHz, $CDCl_3$) δ 7.76 (d, *J* = 8.7 Hz, 1H), 7.66 (d, *J* = 8.1 Hz, 1H), 7.31 (t, *J* = 7.8 Hz, 1H), 7.21 (d, *J* = 7.5, 1H), 7.13 (d, *J* = 2.1 Hz, 1H), 7.08 (dd, *J* = 8.7 Hz, 2.4 Hz, 1H), 2.44 (s, 3H).

CuCl(OH)TMEDA (27 mg, 10 mol %) was added to a solution of the monoacetate, **1.16b**, (237 mg, 1.17 mmol) in $ClCH_2CH_2Cl$ (11.7 mL) and the reaction mixture stirred under an oxygen atmosphere. After 2 h, the mixture was concentrated and suspended in hexanes. Following sonication, the solids were collected via vacuum filtration and washed thoroughly with 1 M HCl, followed by water. Then the solid was washed carefully with cold EtOAc and a minimal amount of acetone to remove pinkish color, leaving **1.17b** as a white solid (140.5 mg, 59%): mp >200 ºC (decomp); ^{1}H NMR (500 MHz, acetone-d_6) δ 7.88 (d, J = 8.9 Hz, 2H), 7.78 (dd, J = 8.2, 1.1 Hz, 2H), 7.61 (bs, 2H), 7.29 (t, J = 7.8 Hz, 2H), 7.29 (d, J = 8.9, 2H), 6.99 (dd, J = 7.5, 1.2 Hz, 2H), 0.93 (s, 6H); ^{13}C NMR (125 MHz, acetone-d_6) δ 169.1, 154.4, 147.6, 132.3, 130.7, 129.0, 127.1, 123.1, 121.7, 119.9, 114.7, 19.6; IR (film) 3344, 1730, 1514, 1220 cm^{-1}; HRMS (ESI) *m/z* 425.1007 $[M+Na]^+$ (calcd for $C_{24}H_{18}O_6Na$, 425.1001).

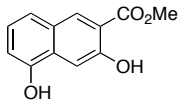

Methyl 3,5-dihydroxy-2-naphthoate (**1.19**). To a solution of 3,5-dihydroxy-2-naphthoic acid (33.3 g, 0.16 mol) in MeOH (715 mL) was carefully added concentrated H_2SO_4 (35 mL). After heating the solution at reflux for 1.5 d, the mixture was cooled and poured over ice. The precipitate was collected via vacuum filtration, washed with water, and dried to yield **1.19** as a yellow solid (35.4 g, 99%): mp 160-162 ºC; ^{1}H NMR (500 MHz, $CDCl_3$) δ 10.46 (s, 1H), 8.48 (s, 1H), 7.64 (s, 1H), 7.42 (d, J = 8.5 Hz, 1H), 7.17 (t, J = 7.9 Hz, 1H), 6.86 (d J = 7.5 Hz, 1H), 5.31 (s, 1H), 4.04 (s, 3H); ^{13}C NMR (125 MHz, $CDCl_3$) δ 170.5, 156.3, 150.3, 132.4, 129.4, 128.5, 124.0, 122.1, 114.8, 111.4, 106.5,

52.8; IR (film) 3510, 3276, 1670, 1523, 1458, 1276, 1181 cm^{-1}; HRMS (ES) calcd for $C_{12}H_9O_4$ (MH^-) 217.0501, found 217.0500.

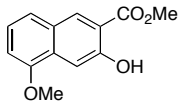

Methyl 3-hydroxy-5-methoxy-2-naphthoate (**1.20**). In a modified procedure,[137] anhydrous K_2CO_3 (4.59 g, 33.2 mmol) was added to a solution of **1.19** (5.00 g, 22.9 mmol) in acetone (78 mL). Following dropwise addition of Me_2SO_4 (2.4 mL, 25.4 mmol), the reaction was heated at reflux. After 4 h, water was added and the aqueous layer extracted with CH_2Cl_2. The organic extract was washed with brine and dried over Na_2SO_4. Following filtration and concentration, the crude solid was combined with crude solid from two 15.00 g scale reactions and recrystallized from MeOH to afford **11a** as a yellow solid (26.2 g, 70% yield): mp 145-148 ºC; ^{1}H NMR (500 MHz, $CDCl_3$) δ 10.38 (s, 1H), 8.44 (s, 1H), 7.72 (s, 1H), 7.39 (d, J = 8.3 Hz, 1H), 7.23 (t, J = 7.9 Hz, 1H), 6.83 (d, J = 7.6 Hz, 1H), 4.02 (s, 3H), 3.99 (s, 3H); ^{13}C NMR (125 MHz, $CDCl_3$) δ 170.5, 156.5, 154.4, 132.0, 130.7, 128.2, 124.0, 121.4, 114.6, 107.1, 106.4, 55.8, 52.7; IR (film) 3159, 3024, 2962, 1686, 1284, 1198 cm^{-1}; HRMS (ESI) *m/z* 233.0815 $[M+H]^+$ (calcd for $C_{13}H_{13}O_4$, 233.0814).

(137) Mercep, M.; Mesic, M., Hrvacic, B.; Elenkov, I. J.; Malnar, I.; Markovic, S.; Simicic, L.; Klonkay, A. C.; Filipovic, A.; PCI Int. Appl. WO2005010006-A1, Feb. 3, 2005.

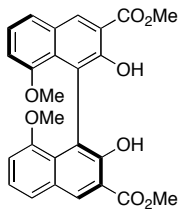

(*S*)-**Dimethyl-2,2'-dihydroxy-8,8'-dimethoxy-1,1'-binaphthyl-3,3'-dicarboxylate** [(*S*)-**1.21**]. To a solution of **1.20** (40 mg, 0.17 mmol) in $ClCH_2CH_2Cl$ (2 mL) was added (*R,R*)-**1.12** (6.3 mg, 10 mol %). Following sonication, the solution was placed under an oxygen atmosphere and heated in a 40 °C oil bath. After 20 h, the mixture was diluted with water and extracted with EtOAc. The organic layer was washed with brine, dried over $MgSO_4$, and concentrated. The residue was chromatographed (30% EtOAc/hexanes) to afford (*S*)-**1.21** as a yellow solid (47 mg, 59% yield, 88% ee): mp >250 °C, $[\alpha]_D^{26}$ –80 (*c* 0.061, 88% ee, CH_2Cl_2), ^{1}H NMR (500 MHz, $CDCl_3$) δ 10.51 (s, 2H), 8.50 (s, 2H), 7.47 (d, *J* = 8.2 Hz, 2H), 7.19 (t, *J* = 7.9 Hz, 2H), 6.70 (d, *J* = 7.2 Hz, 2H), 4.02 (s, 6H), 3.13 (s, 6H); ^{13}C NMR (125 MHz, $CDCl_3$) δ 170.8, 156.6, 152.9, 131.1, 129.8, 128.7, 123.4, 122.8, 120.9, 113.5, 108.9, 56.2, 52.7; IR (film) 3175, 3013, 2949, 1676, 1260, 1127 cm^{-1}; HRMS (ESI) *m/z* 463.1391 $[M+H]^+$ (calcd for $C_{26}H_{23}O_8$ 463.1393).

Racemate (*rac*-**1.21**). To a solution of **1.20** (5.00 g, 21.5 mmol) in 2:1 MeCN/$ClCH_2CH_2Cl$ (375 mL) was added CuCl(OH)TMEDA (0.500 g, 10 mol %). The reaction mixture was warmed in a 35 ºC oil bath and stirred under an oxygen atmosphere. After 10 h, the mixture was cooled and diluted with CH_2Cl_2. The organic layer was washed with 0.5 M HCl, followed by water and brine. After drying the organic layer over Na_2SO_4, the mixture was filtered and concentrated. The residue was triturated with

cold 1:1 EtOAc/hexanes to afford *rac*-**1.21** as a yellow solid (4.44 g, 87% yield): CSP HPLC (Chiralpak AD, 1.0 mL/min, 90:10 hexanes:*i*-PrOH): $t_R(S)$ = 12.0 min, $t_R(R)$ = 23.1 min.

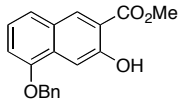

Methyl 5-(benzyloxy)-3-hydroxy-2-naphthoate (**1.22**). To a solution of **1.19** (500 mg, 2.29 mmol) in acetone (10 mL) was added anhydrous K_2CO_3 (458 mg, 3.31 mmol) and BnBr (0.30 mL, 2.52 mmol). After heating at reflux for 6.5 h, the reaction mixture was filtered through Celite™ and concentrated. Next, 0.5 M HCl was added and the aqueous layer extracted three times with EtOAc. The combined organic extracts were washed with brine, dried over Na_2SO_4, filtered, and concentrated. The residue was chromatographed (5% EtOAc/hexanes) to afford **1.22** as a yellow solid (515 mg, 73%): mp 88-90 ºC; ^{1}H NMR (500 MHz, $CDCl_3$) δ 10.42 (s, 1H), 8.45 (s, 1H), 7.82 (s, 1H), 7.52 (d, J = 7.3 Hz, 2H), 7.44 (m, 4H), 7.22 (t, J = 7.8 Hz, 1H), 6.90 (d, J = 7.5 Hz, 1H), 5.22 (s, 2H), 4.02 (s, 3H); ^{13}C NMR (125 MHz, $CDCl_3$) δ 170.4, 156.4, 153.3, 137.0, 132.0, 130.8, 128.8, 128.2, 128.1, 127.5, 123.9, 121.6, 114.6, 107.7, 107.2, 70.3, 52.7; IR (film) 3236, 3066, 2958, 1684, 1514, 1444 cm^{-1}; HRMS (ES) calcd for $C_{19}H_{17}O_4$ (MH^+) 309.1127, found 309.1140.

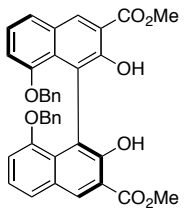

(*S*)-Dimethyl-8,8'-bis(benzyloxy)-2,2'-dihydroxy-1,1'-binaphthyl-3,3'-dicarboxylate [(*S*)-**1.23**]. To a solution of **1.22** (400 mg, 1.30 mmol) in dry $ClCH_2CH_2Cl$ (13 mL) was added crushed 4 Å MS (320 mg), followed by (*R,R*)-**1.12** (50 mg, 11 mol %). The reaction mixture was warmed in a 40 ºC oil bath and stirred under O_2 atmosphere. After 24 h, the mixture was cooled and diluted with CH_2Cl_2. It was then filtered through cotton and washed twice with 0.5 M HCl. The organic layer was washed with brine, dried over Na_2SO_4, filtered, and concentrated. The residues from two reactions on this scale were combined and chromatographed (CH_2Cl_2) to afford (*S*)-**1.23** as a yellow solid (489 mg, 61% yield). The product (1.70 g, 86–88% ee) was enantioenriched by dissolving in CH_2Cl_2 (40 mL), adding an equal volume 30% EtOAc/hexanes, cooling to –20 °C overnight, then decanting. Concentration of the solution provided the product (1.33 g, 78% recovery, >99% ee). (*S*)-**1.23**: mp 174-175 ºC, $[\alpha]_D^{25}$ –211.3 (*c* 0.05, >99% ee, CH_2Cl_2); (*R*)-**1.23**: $[\alpha]_D^{25}$ +188.0 (*c* 0.05, >99% ee, CH_2Cl_2).

Racemate (*rac*-**1.23**). To a solution of **1.22** (1.00 g, 3.24 mmol) in 2:1 MeCN/$ClCH_2CH_2Cl$ (30 mL) was added CuCl(OH)TMEDA (0.067 g, 0.29 mmol). The reaction mixture was warmed in a 37 ºC oil bath and stirred under O_2. After 4.5 h, the mixture was cooled and diluted with CH_2Cl_2. After washing with 0.5 M HCl, the layers were separated. The aqueous layer was extracted two times with CH_2Cl_2. The combined

organic extracts were washed with brine, dried over Na_2SO_4, filtered, and concentrated. The residue was triturated with cold 1:1 EtOAc/hexanes to afford *rac*-**1.23** as a yellow solid (0.912 g, 91%): mp 204-206 ºC; ^{1}H NMR (500 MHz, $CDCl_3$) δ 10.41 (s, 2H), 7.99 (s, 2H), 7.27 (d, J = 6.5 Hz, 2H), 7.18 (t, J = 7.5 Hz, 2H), 7.12 (t, J = 7.8 Hz, 2H), 7.03 (t, J = 7.8 Hz, 4H), 6.74 (d, J = 7.0 Hz, 2H), 6.58 (d, J = 7.5 Hz, 4H), 4.52 (overlapping d, 4H), 3.96 (2, 6H); ^{13}C NMR (125 MHz, $CDCl_3$) δ 170.6, 155.3, 152.8, 136.1, 131.3, 129.2, 128.7, 128.0, 127.9, 127.5, 123.1, 122.9, 120.5, 113.0, 108.4, 70.6, 52.4; IR (film) 3159, 2950, 1676, 1506, 1452, 1305, 1259 cm^{-1}; HRMS (ES) calcd for $C_{38}H_{31}O_8$ (MH^+) 615.2019, found 615.2015. CSP HPLC (Chiralpak IA, 1.0 mL/min, 80:20 hexanes:*i*-PrOH): t_R(*S*) = 7.2 min, t_R(*R*) = 9.5 min.

7.3 Chapter 2 Experimental

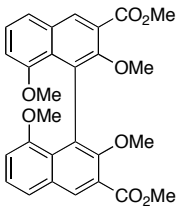

Dimethyl 2,2',8,8'-tetramethoxy-[1,1'-binaphthalene]-3,3'-dicarboxylate (2.1). A solution of *rac*-**1.21** (400 mg, 0.866 mmol) in dry DMF/THF (5 mL/3 mL) was cooled to 0 °C. To this solution was added NaH (60%, 295 mg, 7.32 mmol), followed by MeI (0.50 mL, 7.3 mmol). After stirring 5.5 h at room temperature, the mixture was cooled to 0 °C and quenched with water. The mixture was extracted with EtOAc (×2) and the combined organic extracts were washed thoroughly with 1 M HCl, followed by brine. The organic layer was dried over Na_2SO_4, filtered, and concentrated. The residue was

chromatographed (20% EtOAc/hexanes) to afford **2.1** as a white solid (390 mg, 92% yield): mp 168-168.5 °C; ^{1}H NMR (500 MHz, $CDCl_3$) δ 8.37 (s, 2H), 7.51 (d, J = 7.8 Hz, 2H), 7.30 (t, J = 7.9 Hz, 2H), 6.68 (d, J = 7.4 Hz, 2H), 3.95 (s, 6H), 3.37 (s, 6H), 3.09 (s, 6H); ^{13}C NMR (125 MHz, $CDCl_3$) δ 167.4, 156.5, 152.2, 131.9, 131.0, 129.9, 128.3, 125.1, 124.5, 121.9, 107.6, 61.7, 55.5, 52.4; IR (film) 2943, 2842, 1730, 1568, 1460, 1274, 1120 cm^{-1}; HRMS (ESI) *m/z* 491.1694 $[M+H]^+$ (calcd for $C_{28}H_{27}O_8$, 491.1706).

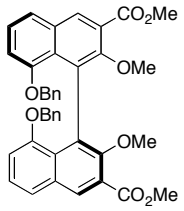

(*S*)-Dimethyl-8,8'-bis(benzyloxy)-2,2'-dimethoxy-1,1'-binaphthyl-3,3'-dicarboxylate [(*S*)-**2.2**]. A solution of (*S*)-**1.23** (700 mg, 1.14 mmol) in dry DMF (22 mL) was cooled to 0 ºC. To this solution was added, portion-wise, NaH (60%, 184 mg, 4.60 mmol). After stirring 5 min at 0 ºC, MeI (0.3 mL, 4.8 mmol) was added and the mixture stirred for an additional 5-10 min. The mixture was stirred at room temperature for 2 h, then cooled to 0 ºC and quenched slowly with cold water. This mixture was extracted with EtOAc (x2) and washed with 1M HCl (x2) followed by brine. The organic layer was dried over Na_2SO_4, filtered, and concentrated. The residue was chromatographed (10% EtOAc/hexanes to 20% EtOAc/hexanes) to afford (*S*)-**2.2** as colorless resin (725 mg, 99% yield): mp (*rac*-**2.2**) 153-155 ºC; $[\alpha]_D^{25}$ –9.5 (*c* 0.1, >99% ee, CH_2Cl_2); ^{1}H NMR (500 MHz, $CDCl_3$) δ 7.90 (s, 2H), 7.23 (d, J = 8.5 Hz, 2H), 7.19 (t, J = 7.8 Hz, 2H), 7.15 (t, J = 7.8 Hz, 2H), 7.01 (t, J = 7.5 Hz, 4H), 6.74 (d, J = 7.5 Hz, 2H), 6.49 (d, J = 7.5 Hz, 4H), 4.49 (d, J = 11.0, 2H), 4.41 (d, J = 10.5, 2H), 3.90 (s, 6H),

3.32 (s, 6H); ^{13}C NMR (125 MHz, $CDCl_3$) δ 167.1, 155.5, 152.1, 135.5, 132.1, 131.0, 129.6, 128.2, 127.92, 127.90, 127.6, 124.6, 123.9, 122.4, 107.6, 70.4, 61.6, 52.2; IR (film) 2943, 1722, 1568, 1452, 1267 cm^{-1}; HRMS (ES) calcd for $C_{40}H_{34}O_8Na$ (MNa^+) 665.2151, found 665.2136.

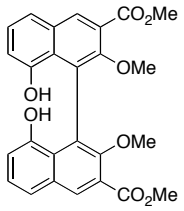

Dimethyl 8,8'-dihydroxy-2,2'-dimethoxy-1,1'-binaphthyl-3,3'-dicarboxylate (**2.3**). To a solution of **2.1** (396 mg, 0.616 mmol) in EtOH/EtOAc (9 mL/5 mL) was added 1 M HCl (120 μL). Following an evacuation and purge of the reaction mixture with N_2, Pd/C (10 wt%, 78 mg) was added and the flask evacuated and purged twice with H_2. After stirring under an H_2 atmosphere for 4 h, the mixture was filtered through Celite™ and concentrated. The residue was dissolved in EtOAc and washed with water, followed by brine. The organic layer was dried over Na_2SO_4. After filtration and concentration, the solid was triturated with 15% EtOAc/hexanes, or if necessary, chromatographed (20% acetone/hexanes) to afford **2.3** as a tan solid (284 mg, 99% yield): mp 206-208 ºC; ^{1}H NMR (500 MHz, acetone-d_6) δ 8.29 (s, 2H), 8.11 (s, 2H), 7.48 (d, J = 8.2 Hz, 2H), 7.24 (t, J = 7.7 Hz, 2H), 6.78 (d, J = 7.5 Hz, 2H), 3.90 (s, 6H), 3.41 (s, 6H); ^{13}C NMR (125 MHz, acetone-d_6) δ 167.6, 155.0, 153.1, 132.4, 132.2, 130.3, 128.0, 126.2, 125.7, 121.4, 112.3, 61.7, 52.4; IR (film) 3383, 2950, 1707, 1568, 1452, 1282, 1236 cm^{-1}; HRMS (ES) calcd for $C_{26}H_{22}O_8Na$ $(M+Na)^+$ 485.1212, found 485.1195.

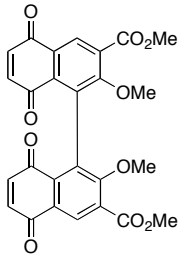

Dimethyl-2,2'-dimethoxy-5,5',8,8'-tetraoxo-5,5',8,8'-tetrahydro-1,1'-binaphthyl-3,3'-dicarboxylate (**2.4**). To a solution of **2.3** (22 mg, 0.048 mmol) in DMF (1 mL) was added Co-salen (3 mg, 0.009 mmol). After stirring under an O_2 for 3 h, the mixture was filtered through Celite™, diluted with water and extracted several times with EtOAc. The combined organic extracts were washed with water (×4), followed by brine. The organic layer was dried over Na_2SO_4, filtered, and concentrated. The residue was chromatographed (10% acetone/5% CH_2Cl_2/hexanes) to afford **2.4** as a yellow solid in 57% yield: mp 204-206 ºC; ^{1}H NMR (500 MHz, $CDCl_3$) δ 8.66 (s, 2H), 6.97 (d, J = 10.3 Hz, 2H), 6.75 (d, J = 10.3 Hz, 2H), 3.98 (s, 6H), 3.57 (s, 6H); ^{13}C NMR (125 MHz, $CDCl_3$) δ 185.1, 183.6, 165.2, 162.0, 139.9, 138.2, 132.9, 132.6, 131.0, 128.3, 128.2, 62.7, 53.0; IR (film) 2927, 2858, 1730, 1668, 1591, 1444 cm^{-1}; HRMS (ES) calcd for $C_{26}H_{18}O_{10}Na$ $(M+Na)^+$ 513.0798, found 513.0797.

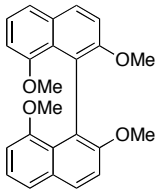

2,2',8,8'-Tetramethoxy-1,1'-binaphthalene (2.5). A solution of **2.1** (100 mg, 0.204 mmol) in toluene (10 mL) was cooled to 0 °C. To this solution was slowly added

DIBAL (1.6 mL, 1.60 mmol). After 30 min at 0 °C, the mixture was quenched with water, followed by 1 M HCl. The mixture was extracted with EtOAc (×2), then, washed with 1 M HCl and brine. The organic layer was dried over Na_2SO_4, filtered, and concentrated. The resin was used without further purification: ^{1}H NMR (500 MHz, $CDCl_3$) δ 7.82 (s, 2H), 7.44 (d, *J* = 8.0 Hz, 2H), 7.27 (t, *J* = 8.0 Hz, 2H), 6.61 (d, *J* = 8.0 Hz, 2H), 4.99 (d, *J* = 13.0 Hz, 2H), 4.83 (d, *J* = 13.5 Hz, 2H), 3.34 (s, 6H), 3.06 (s, 6H); ^{13}C NMR (125 MHz, $CDCl_3$) δ 156.9, 152.3, 133.8, 132.2, 128.2, 126.7, 126.6, 124.6, 121.1, 105.9, 62.3, 60.6, 55.3; IR (film) 3391, 2935, 1576, 1460, 1267, 1081 cm^{-1}; HRMS (ESI) *m/z* 457.1617 $[M+Na]^+$ (calcd for $C_{26}H_{26}O_6Na$, 457.1627).

To a solution of the alcohol (99.9 mg, 0.230 mmol) in EtOAc (15 mL) was added 2-iodoxybenzoic acid (178.4 mg, 0.637 mmol). The mixture was heated at reflux for 2.5 h. After cooling to room temperature, the reaction was diluted with EtOAc and filtered through Celite™. The filtrate was concentrated and filtered through an HPLC filter. The filtrate was concentrated to afford the bisaldehyde as a yellow solid that was used without purification: ^{1}H NMR (300 MHz, $CDCl_3$) δ 10.52 (s, 2H), 8.44 (s, 2H), 7.62 (d, *J* = 8.1 Hz, 2H), 7.36 (t, *J* = 8.0 Hz, 2H), 6.75 (d, *J* = 7.5 Hz, 2H), 3.44 (s, 3H), 3.07 (s, 3H); ^{13}C NMR (125 MHz, $CDCl_3$) δ 191.2, 156.5, 154.6, 131.4, 130.3, 129.5, 128.8, 128.3, 125.7, 123.2, 108.5, 63.1, 55.4; IR (film) 2935, 2858, 1692, 1591, 1460, 1267, 1081 cm^{-1}; HRMS (ESI) *m/z* 431.1498 $[M+H]^+$ (calcd for $C_{26}H_{23}O_6$, 431.1495).

Using oven-dried glassware, diglyme (8 mL) was actively purged with Ar for 30 min and transferred via cannula to a dry round bottom flask containing the bisaldehyde. This solution was actively purged with Ar for 30 min. and transferred dropwise via

cannula to a Schlenk flask containing $RhCl(PPH_3)_3$ (470 mg, 0.483 mmol). The resulting mixture was actively purged with Ar for 20 min before placing in a preheated oil bath at 90 °C. After 14 h, the mixture was diluted with EtOAc and filtered through Celite™. The filtrate was washed thoroughly with 1 M HCl, followed by brine. The organic layer was dried over Na_2SO_4, and concentrated. The residue was reconstituted in EtOAc with a small amount of hexanes, and refiltered through Celite™. The residue was chromatographed (10% EtOAc/hexanes) to afford **2.5** as a white solid (74.2 mg; 93% over three steps): mp 168-169°C; ^{1}H NMR (500 MHz, $CDCl_3$) δ 7.80 (d, *J* = 9.0 Hz, 2H), 7.44 (d, *J* = 7.5 Hz, 2H), 7.35 (d, *J* = 9.0 Hz, 2H), 7.19 (t, *J* = 8.0 Hz, 2H), 6.60 (d, *J* = 7.5 Hz, 2H), 3.68 (s, 6H), 3.07 (s, 6H); ^{13}C NMR (125 MHz, $CDCl_3$) δ 157.2, 153.9, 131.1, 127.8, 126.6, 123.8, 123.0, 121.3, 114.8, 106.5, 57.5, 56.0; IR (film) 2927, 2858, 1599, 1460, 1259, 1066 cm^{-1}; HRMS (ESI) *m/z* 375.1602 $[M+H]^+$ (calcd for $C_{24}H_{23}O_4$, 375.1596).

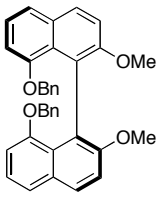

(*S*)-8,8'-Bis(benzyloxy)-2,2'-dimethoxy-1,1'-binaphthalene [(*S*)-**2.6**]. A solution of (*S*)-**2.2** (321 mg, 0.50 mmol) in toluene (20 mL) was cooled to 0 ºC. To this solution was slowly added DIBALH (5.0 mL, 5.0 mmol, 1M in hexanes). After 30 min at 0 °C, the mixture was quenched with cold water followed by 1 M HCl. The mixture was extracted with EtOAc (2x) and washed with 1 M HCl followed by brine. The organic layer was dried over Na_2SO_4, filtered, and concentrated. The resin was used

without further purification: ^{1}H NMR (500 MHz, $CDCl_3$) δ 7.38 (s, 2H), 7.27-7.19 (m, 6H), 7.08 (t, *J* = 7.6 Hz, 4H), 6.71 (d, *J* = 7.4 Hz, 2H), 6.49 (d, *J* = 7.2 Hz, 4H), 4.76 (d, *J* = 13.1 Hz, 2H), 4.61 (d, *J* = 13.1 Hz, 2H), 4.49 (d, *J* = 10.9 Hz, 2H), 4.41 (d, *J* = 10.8 Hz, 2H), 3.25 (s, 6H); ^{13}C NMR (125 MHz, $CDCl_3$) δ 155.8, 152.1, 136.0, 133.3, 132.4, 128.3, 128.1, 128.0, 127.5, 127.2, 126.1, 124.2, 121.6, 106.0, 70.3, 62.1, 60.5; IR (film) 3406, 3059, 2935, 1568, 1452, 1259 cm^{-1}; HRMS (ES) calcd for $C_{38}H_{34}O_6Na$ (MNa^+) 609.2253, found 609.2239.

To a solution of the alcohol (0.50 mmol) in EtOAc (30 mL) was added 2-iodoxybenzoic acid (430 mg, 1.54 mmol). The mixture was heated at reflux with stirring. Additional IBX was added to push the reaction to completion. When complete, as judged by TLC, the mixture was cooled to room temperature, diluted with EtOAc, filtered through Celite™, and concentrated to afford a yellow solid that was used without purification: ^{1}H NMR (300 MHz, $CDCl_3$) δ 10.31 (s, 2H), 7.93 (s, 2H), 7.35 (d, *J* = 8.1 Hz, 2H), 7.28 (t, *J* = 7.5 Hz, 2H), 7.21 (t, *J* = 7.5 Hz, 2H), 7.05 (t, *J* = 7.7 Hz, 4H), 6.84 (d, *J* = 7.8 Hz, 2H), 6.46 (d, *J* = 7.2 Hz, 4H), 4.51 (d, *J* = 10.5 Hz, 2H), 4.43 (d, *J* = 10.5 Hz, 2H), 3.38 (s, 6H).

Using oven-dried glassware, diglyme (8.3 mL) was actively purged with Ar for 30 min and transferred via cannula to a dry round bottom flask containing the bisaldehyde (166 mg, 0.29 mmol). After the bisaldehyde dissolved, the solution was actively purged with Ar for 30 min and transferred slowly via cannula to a Schlenk flask containing $RhCl(PPH_3)_3$ (551 mg, 0.596 mmol). This mixture was heated in a preheated oil bath at 90 °C for 18 h. After cooling to room temperature, the solution was diluted with EtOAc,

filtered through Celite™ and washed with 1M HCl (x3) followed by brine. The organic extract was dried over Na_2SO_4, filtered, and concentrated. The residue was chromatographed (5%-10% EtOAc/hexanes) to afford (*S*)-**2.6** as a resin (104 mg; 63% over three steps): $[\alpha]_D^{23}$ – 68.5 (*c* 0.106, >99% ee, CH_2Cl_2); ^{1}H NMR (500 MHz, $CDCl_3$) δ 7.47 (d, *J* = 8.9 Hz, 2H), 7.27 (d, *J* = 8.3 Hz, 2H), 7.11 (overlapping t, *J* = 7.5 Hz, 8.1 Hz, 4H), 7.07 (d, *J* = 8.9 Hz, 2H), 7.03 (t, *J* = 7.8 Hz, 4H), 6.64 (d, *J* = 7.1 Hz, 2H), 6.52 (d, *J* = 7.4 Hz, 4H), 4.50 (d, *J* = 11.8 Hz, 2H), 4.45 (d, *J* = 11.8 Hz, 2H), 3.59 (s, 6H); ^{13}C NMR (125 MHz, acetone-d_6) δ 156.6, 154.7, 137.7, 132.1, 128.64, 128.57, 127.8, 127.7, 127.2, 124.4, 123.4, 122.1, 115.0, 107.3, 70.7, 57.0; IR (film) 3059, 2927, 2858, 1599, 1460, 1259 cm^{-1}; HRMS (ES) calcd for $C_{36}H_{30}O_4Na$ (MNa^+) 549.2042, found 549.2020.

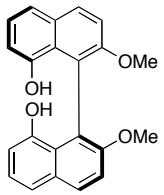

(*S*)-2,2'-Dimethoxy-[1,1'-binaphthalene]-8,8'-diol [(*S*)-**2.7**]. A solution of (*S*)-**2.6** (120 mg, 0.23 mmol) in MeOH/THF (6 mL) was evacuated and purged with Ar. To this solution was added Pd/C (10 wt%, 43 mg) and the flask was evacuated and purged three times with H_2. After stirring under hydrogen atmosphere for 15 h, the mixture was filtered through Celite™ with EtOAc and concentrated. The residue was passed through a short column of silica (15% EtOAc/hexanes) to afford (*S*)-**2.7** as a white solid in quantitative yield (79 mg, 100%, >99% ee): mp (*rac*-**2.7**) 218-219 ºC; mp (*S*-**2.7**) 226-227 ºC; $[\alpha]_D^{23}$ – 179.4 (*c* 0.096, >99% ee, CH_2Cl_2); ^{1}H NMR (500 MHz, $CDCl_3$) δ 8.01 (d, *J* = 9.1 Hz, 2H), 7.46 (dd, *J* = 8.2 Hz, 1.1 Hz, 2H), 7.37 (d, *J* = 9.1 Hz, 2H), 7.27 (t, *J*

= 7.8 Hz, 2H), 6.80 (dd, J = 7.6 Hz, 1.1 Hz, 2H), 5.86 (s, 2H), 3.75 (s, 6H); ^{13}C NMR (125 MHz, $CDCl_3$) δ 155.3, 153.1, 132.4, 131.3, 125.3, 123.4, 121.2, 114.5, 113.6, 112.6, 57.1; IR (film) 3460, 3059, 2943, 2842, 1599, 1444, 1259 cm^{-1}; HRMS (ES) calcd for $C_{22}H_{17}O_4$ (MH^-) 345.1127, found 345.1124. CSP HPLC (Chiralpak IA, 0.5 mL/min, 90:10 hexanes:*i*-PrOH): $t_R(S)$ = 65.6 min, $t_R(R)$ = 68.5 min.

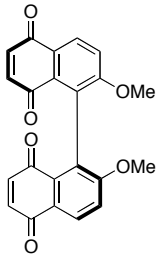

(*S*)-2,2'-Dimethoxy-[1,1'-binaphthalene]-5,5',8,8'-tetraone [(*S*)-**2.8**]. Oxygen was bubbled through a solution of (*S*)-**2.7** (61.5 mg, 0.178 mmol) in DMF (1.8 mL) for 5–10 min. Then, salcomine (3.5 mg, 6 mol %) was added, turning the mixture a red brown. After stirring under O_2 atmosphere for 1 h, an additional 6 mol % salcomine was added, followed by a further 6 mol % salcomine after an additional hour. After 4 h total reaction time, the mixture was diluted with water and extracted with EtOAc (2x). The combined organic extracts were washed several times with water and brine, dried over Na_2SO_4, filtered, and concentrated. The residue was chromatographed (60% EtOAc/hexanes) to afford (*S*)-**2.8** as a yellow solid (41.6 mg, 63%): mp >250 ºC; $[\alpha]_D^{23}$ – 341.2 (*c* 0.0255, >99% ee, CH_2Cl_2); ^{1}H NMR (500 MHz, $CDCl_3$) δ 8.25 (d, J = 8.7 Hz, 2H), 7.27 (d, J = 9.4 Hz, 2H), 6.87 (d, J = 10.2 Hz, 2H), 6.66 (d, J = 10.2 Hz, 2H), 3.75 (s, 6H); ^{13}C NMR (125 MHz, $CDCl_3$) δ 185.8, 184.6, 161.7, 139.7, 138.1, 130.6, 129.2,

127.3, 126.5, 114.6, 56.4; IR (film) 3082, 2927, 2850, 1661, 1576, 1274 cm^{-1}; HRMS (ES) calcd for $C_{22}H_{15}O_6$ (MH^+) 375.0869, found 375.0873.

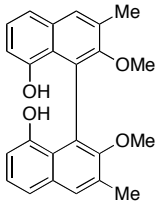

2,2'-Dimethoxy-3,3'-dimethyl-[1,1'-binaphthalene]-8,8'-diol (**2.9**). A solution of **2.2** (325 mg, 0.506 mmol) in toluene (24 mL) was cooled to 0 ºC. To this solution was slowly added DIBAL-H (4.0 mL, 4.0 mmol, 1 M in hexanes). After 30 min at 0 °C, the mixture was quenched with cold water and 1 M HCl. The mixture was extracted with EtOAc (×2) and the combined organic layers were washed with 1 M HCl, followed by brine. After drying over Na_2SO_4, the mixture was filtered, and concentrated. The colorless resin was used without further purification.

Under an argon atmosphere, the diol (0.506 mmol) was suspended in THF/MeOH (1:1, 10 mL). Pd/C (10 wt%, 100 mg) was added and the flask evacuated and purged with three times with H_2. The reaction mixture was stirred under an H_2 atmosphere overnight, then filtered through Celite™ with EtOAc. The residue was passed through a short column of silica (40% acetone/hexanes) to yield **2.9** as a white solid (188 mg, 99% yield over 2 steps): mp 221-224 ºC; ^{1}H NMR (500 MHz, acetone-d_6) δ 7.69 (s, 2H), 7.44 (s, 2H), 7.31 (dd, J = 8.2, 1.0 Hz, 2H), 7.15 (t, J = 7.8 Hz, 2H), 6.62 (dd, J = 7.4 Hz, 1.1 Hz 2H), 3.35 (s, 6H), 2.43 (s, 6H); ^{13}C NMR (125 MHz, acetone-d_6) δ 155.0, 154.8, 133.8, 131.6, 130.1, 127.5, 125.7, 124.9, 120.0, 110.1, 59.9, 17.2; IR (film) 3491,

2935,1707, 1568, 1452, 1282, 1236 cm^{-1}; HRMS (ES) calcd for $C_{24}H_{23}O_4$ $(M+H)^+$ 375.1596, found 375.1608.

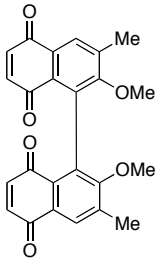

2,2'-Dimethoxy-3,3'-dimethyl-[1,1'-binaphthalene]-5,5',8,8'-tetraone (**2.10**). Co-salen (4.5 mg, 6 mol %) was added to a solution of **2.9** (87 mg, 0.23 mmol) in DMF (2.3 mL). After stirring under an O_2 atmosphere for 1 h, an additional 6 mol % Co-salen was added, followed by a further 6 mol % Co-salen after an additional hour. When the reaction was complete (3 h total reaction time), the mixture was filtered through Celite™ with EtOAc and washed with water. The organic layer was washed with 1 M HCl (×3) followed by brine, dried over Na_2SO_4, and concentrated. The residue was chromatographed (50% EtOAc/hexanes) to afford **2.10** as a yellow powder (58 mg, 62%): ^{1}H NMR (500 MHz, $CDCl_3$) δ 8.07 (s, 2H), 6.86 (d, J = 10.2 Hz, 2H), 6.66 (d, J = 10.2 Hz, 2H), 3.40 (s, 6H), 2.47 (s, 6H); ^{13}C NMR (125 MHz, $CDCl_3$) δ 185.7, 184.9, 160.6, 139.8, 138.0, 137.6, 132.4, 130.2, 129.1, 129.0, 60.2, 17.3; IR (film) 3059, 2950, 2858, 1661, 1614, 1460, 1321, 1282 cm^{-1}; HRMS (ES) calcd for $C_{24}H_{19}O_6$ $(M+H)^+$ 403.1182, found 403.1196.

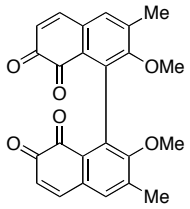

2,2'-Dimethoxy-3,3'-dimethyl-[1,1'-binaphthalene]-7,7',8,8'-tetraone (**2.11**). To a solution of **2.9** (20 mg, 0.053 mmol) in anhydrous DMF (1.3 mL) was added 4 Å MS (40 mg, powdered). After stirring the mixture 0.5 h, *o*-iodoxybenzoic acid (31.7 mg 0.113 mmol) was added. When the reaction was complete (after an additional 3 h), water was added and the mixture extracted with EtOAc. The organic layer was washed with 1 M HCl (×2) followed by brine, dried over Na_2SO_4, and concentrated. The residue was chromatographed (50% EtOAc/hexanes) to yield **2.11** as a red amorphous solid (10 mg, 74%): ^{1}H NMR (500 MHz, $CDCl_3$) δ 7.40 (d, J = 10.0 Hz, 2H), 7.26 (s, 2H), 6.31 (d, J = 10.1 Hz, 2H), 3.42 (s, 6H), 2.41 (s, 6H); ^{13}C NMR (125 MHz, $CDCl_3$) δ 180.8, 179.0, 158.1, 146.3, 140.2, 136.9, 133.6, 132.2, 128.5, 126.4, 60.5, 17.3; IR (film) 2944, 1663, 1579, 1468, 1260 cm^{-1}; HRMS (ES) calcd for $C_{24}H_{18}O_6Na$ $(M+Na)^+$ 425.1001, found 425.1011.

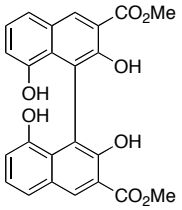

Dimethyl 2,2',8,8'-tetrahydroxy-1,1'-binaphthyl-3,3'-dicarboxylate (**2.12**). A solution of **2.2** (400 mg, 0.65 mmol) in THF/MeOH (21 mL/14 mL) was evacuated and purged with Ar. To this solution was added Pd/C (10 wt%, 100 mg) and the flask was

evacuated and purged three times with H_2. After stirring under an H_2 atmosphere for 15 h, the mixture was filtered through Celite™ with EtOAc and concentrated. The residue was passed through a short column of silica (CH_2Cl_2) to afford **2.12** as a yellow solid (264 mg, 93% yield): mp 278-280 ºC; ^{1}H NMR (500 MHz, $CDCl_3$) δ 10.84 (s, 2H), 8.68 (s, 2H), 7.53 (dd, J = 8.2 Hz, 0.9 Hz, 2H), 7.29 (t, J = 7.9 Hz, 2H), 6.94 (dd, J = 7.6 Hz, 1.1 Hz, 2H), 5.85 (s, 2H), 4.04 (s, 6H); ^{13}C NMR (125 MHz, $CDCl_3$) δ 170.2, 154.4, 152.6, 135.2, 129.1, 126.6, 125.4, 123.2, 115.4, 114.1, 112.7, 53.1; IR (film) 3468, 3221, 2958, 1676, 1514, 1444, 1328, 1274 cm^{-1}; HRMS (ES) calcd for $C_{24}H_{17}O_8$ $(M–H)^-$ 433.0923, found 433.0923.

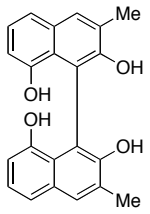

3,3'-Dimethyl-[1,1'-binaphthalene]-2,2',8,8'-tetraol (**2.13**). In a flame-dried flask, **2.2** (400 mg, 0.651 mmol) was partially dissolved in toluene (26.5 mL) and the mixture was cooled to 0 ºC. To this solution was slowly added DIBAL-H (6.0 mL, 6.0 mmol, 1 M in hexanes) over 15 min. After 15 min at 0 °C, the mixture was warmed to room temperature and stirred for an additional 2 h before quenching with 0.5 M HCl. The mixture was extracted several times with EtOAc. The combined organic layers were washed with 1 M HCl followed by brine. After drying over Na_2SO_4, the mixture was filtered, concentrated, and used without further purification.

Under an argon atmosphere, the tetraol (0.651 mmol) was dissolved in MeOH/THF (1:1, 20 mL). To this solution was added Pd/C (10 wt%, 135 mg) and the flask was evacuated and purged three times with H_2. After stirring under an H_2 atmosphere for 14 h, the mixture was filtered through Celite™ with EtOAc and concentrated. The residue was chromatographed (10-30% EtOAc/hexanes) to afford **2.13** as a white solid in 83% yield over 2 steps: mp >250 °C decomp; ^{1}H NMR (500 MHz, acetone-d_6) δ 7.67 (s, 2H), 7.28 (dd, J = 8.2, 0.9 Hz, 2H), 7.12 (bs, 4H), 7.08 (t, J = 7.8 Hz, 2H), 6.60 (dd, J = 7.5, 1.1 Hz, 2H), 2.39 (s, 6H); ^{13}C NMR (125 MHz, acetone-d_6) δ 154.3, 153.2, 132.3, 131.2, 128.0, 124.4, 124.2, 120.3, 112.5, 110.7, 17.4; IR (film) 3267, 3059, 2927, 2858, 1607, 1452, 1282, 1213 cm^{-1}; HRMS (ES) calcd for $C_{22}H_{17}O_4$ $(M–H)^-$ 345.1127, found 345.1131.

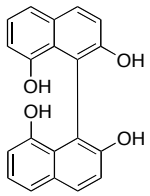

[1,1'-Binaphthalene]-2,2',8,8'-tetraol (**2.14**). A solution of **2.2** (25 mg, 0.047 mmol) in dry CH_2Cl_2 (3.0 mL) was cooled to 0 ºC. Then, BBr_3 (10 equiv) was added slowly. After stirring 6 h at room temperature, the reaction mixture was cooled to 0 ºC and quenched with water. Extraction with CH_2Cl_2 afforded an organic layer, which was washed with brine, dried over Na_2SO_4, and concentrated. The residue was chromatographed (30% EtOAc/hexanes) to afford **2.14** in 70% yield: mp 218-219 ºC; ^{1}H NMR (500 MHz, $CDCl_3$) δ 7.98 (d, J = 9.0 Hz, 2H), 7.49 (dd, J = 8.1 Hz, 1.0 Hz, 2H), 7.33 (d, J = 9.0 Hz, 2H), 7.30 (t, J = 7.9 Hz, 2H), 6.85 (dd, J = 7.6 Hz, 1.1 Hz 2H), 5.42

(bs, 2H), 5.13 (bs, 2H); ^{13}C NMR (125 MHz, acetone-d_6) δ 154.7, 153.8, 132.2, 131.2, 125.7, 124.3, 121.0, 119.0, 114.2, 111.4; IR (film) 3468, 3429, 3059, 1599, 1514, 1444, 1344, 1267, 1197 cm^{-1}; HRMS (ES) calcd for $C_{20}H_{13}O_4$ $(M–H)^-$ 317.0814, found 317.0811.

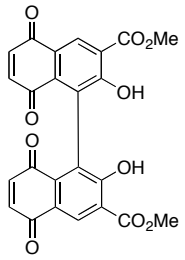

Dimethyl-2,2'-dihydroxy-5,5',8,8'-tetraoxo-5,5',8,8'-tetrahydro-1,1'-binaphthyl-3,3'-dicarboxylate (**2.15**). Co-salen (12 mg, 0.037 mmol) was added to a solution of **2.12** (143 mg, 0.329 mmol) in DMF (4 mL) and the reaction mixture stirred under an O_2 atmosphere. After 20 h, the mixture was filtered through Celite™, diluted with water, and extracted with EtOAc. The organic extract was washed with water (×4) followed by brine, dried over Na_2SO_4, and concentrated. The residue was chromatographed (20% acetone/5% CH_2Cl_2/hexanes) to afford **2.15** (84 mg) as a yellow/orange solid in 55% yield: mp 136-137 ºC; ^{1}H NMR (500 MHz, $CDCl_3$) δ 11.59 (s, 2H), 8.79 (s, 2H), 6.96 (d, J = 10.3 Hz, 2H), 6.75 (d, J = 10.3 Hz, 2H), 4.04 (s, 6H); ^{13}C NMR (125 MHz, $CDCl_3$) δ 185.1, 183.5, 170.0, 163.5, 139.7, 138.7, 134.1, 130.2, 126.2, 124.9, 115.7, 53.4; IR (film) 3321, 3074, 2958, 1668, 1614, 1568, 1444, 1359 cm^{-1}; HRMS (ES) calcd for $C_{24}H_{13}O_{10}$ $(M–H)^-$ 461.0509, found 461.0502.

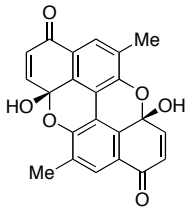

(±)-Bishemiketal (*HK*, *rac*-**2.16**). Co-salen (1.2 mg, 7 mol %) was added to a solution of **6a** (17 mg, 0.05 mmol) in 0.5 mL DMF. After stirring under an O_2 atmosphere for 1 h, an additional 7 mol % Co-salen was added. When the reaction was complete (2.5 h total reaction time), the reaction mixture was filtered through Celite™ with EtOAc. The organic layer was washed with water (×4) followed by brine, dried over Na_2SO_4, and concentrated. The residue was triturated with EtOAc, followed by acetone to afford **15a** as a mixture of *Q* and *HK*, plus a minor side product. ^{1}H NMR (500 MHz, DMSO-d_6), *HK*:*Q* = >20:1, δ 8.15 (bs, 2H), 7.82 (s, 2H), 7.41 (d, J = 10.3 Hz, 2H), 6.39 (d, J = 10.3 Hz, 2H), 2.38 (s, 6H); ^{13}C NMR (125 MHz, DMSO-d_6) δ 182.6, 150.0, 143.9, 129.1, 128.9, 128.8, 127.0, 121.2, 112.8, 90.2, 15.1; IR (film) 3337, 2927, 2858, 1668, 1591, 1305 cm^{-1}; HRMS (ES) calcd for $C_{22}H_{13}O_6$ $(M–H)^-$ 373.0712, found 373.0730.

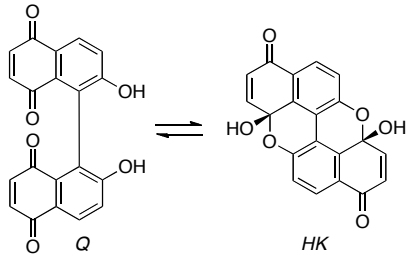

2,2'-Dihydroxy-[1,1'-binaphthalene]-5,5',8,8'-tetraone (*Q*) and **bishemiketal** (*HK*, **2.17**). After oxygen was bubbled through a solution of **2.14** (122 mg, 0.384 mmol)

in DMF (3.0 mL) for 5-10 min, Co-salen (7.5 mg, 6 mol %) was added. An additional 6 mol % Co-salen was added after stirring under an O_2 atmosphere for 1 h. Following two additional hours, 6 mol % Co-salen was added. When the reaction was complete (3.5 h total reaction time), the mixture was diluted with water and extracted with EtOAc (×2). The combined organic extracts were washed with water (×4) followed by brine, then dried over Na_2SO_4 and concentrated. The residue was absorbed onto silica and chromatographed (2.5–5% MeOH/CH_2Cl_2). This solid was triturated with CH_2Cl_2, followed by acetone to afford **2.17** as a mixture of *Q* and *HK* (75 mg, 57%): ^{1}H NMR (500 MHz, THF-d_8), *Q*:*HK* = 1:2.8, Quinone (*Q*): δ 7.99 (d, *J* = 8.5 Hz, 2H), 7.11 (d, *J* = 8.5 Hz, 2H), 6.79 (d, *J* = 10.2 Hz, 2H), 6.61 (d, *J* = 10.2 Hz, 2H); bishemiketal (*HK*): δ 7.99 (d, *J* = 8.5 Hz, 2H), 7.27 (d, *J* = 10.4 Hz, 2H), 7.25 (d, *J* = 8.5 Hz, 2H), 6.33 (d, *J* = 10.4 Hz, 2H); ^{13}C NMR (125 MHz, THF-d_8) bishemiketal (*HK*): δ 182.9, 153.2, 144.0, 130.4, 129.7, 128.7, 123.7, 118.2, 114.6, 91.6; Quinone (*Q*): δ 186.2, 184.8, 161.4, 140.1, 138.4, 132.6, 132.2, 126.9, 126.1, 119.1; IR (film) 3221, 2958, 2920, 1661, 1576, 1460, 1305 cm^{-1}; HRMS (ES) calcd for $C_{20}H_9O_6$ $(M–H)^-$ 345.0399, found 345.0388.

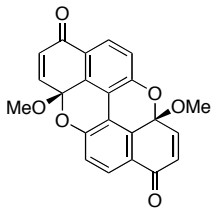

(±)-Bisketal (*rac*-**2.18**). A mixture of **2.17** (5 mg, 0.0145) was suspended in CH_2Cl_2 (1.0 mL). Ag_2O (10 mg, 3 equiv) and MeI (<0.05 mL, excess) were added and the mixture stirred overnight in the dark. After 14 h, the reaction mixture was diluted with CH_2Cl_2 and filtered through Celite™. The residue was chromatographed (30%

EtOAc/hexanes) to afford bisketal (1 mg, 19%) as a white solid: ^{1}H NMR (360 MHz, acetone-d_6) δ 8.08 (d, J = 8.5 Hz, 2H), 7.64 (d, J = 10.6 Hz, 2H), 7.48 (d, J = 8.5 Hz, 2H), 6.58 (d, J = 10.5 Hz, 2H), 3.45 (s, 6H); ^{13}C NMR (125 MHz, $CDCl_3$) δ 182.6, 151.7, 140.0, 132.6, 129.7, 129.6, 123.6, 117.9, 113.8, 93.3, 51.7; HRMS (ES) calcd for $C_{21}H_{11}O_5$ $(M–OMe)^+$ 343.0606, found 343.0616. X-ray quality crystals were obtained by slow evaporation of a solution of the bisketal in ethyl acetate. See Appendix B for crystallographic data.

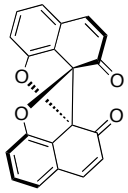

(±)-Naphtho[1,8-bc]naphtho[1',8':3,4,5]furo[2,3-d]furan-5,12-dione (*rac*-**2.19**). To a solution of **2.14** (20 mg, 0.063 mmol) in MeCN (1.5 mL) was added Co-salen (5 mg, 0.015 mmol). After stirring under an O_2 atmosphere for 15.5 h, the reaction mixture was filtered through Celite™ with EtOAc and concentrated. The residue was chromatographed (15–30% EtOAc/hexanes) to afford **2.19** as a yellow-orange solid (10 mg, 50%): mp 230-232 ºC decomp; ^{1}H NMR (300 MHz, acetone-d_6) δ 7.73 (d, J = 9.9 Hz, 2H), 7.52 (t, J = 7.8 Hz, 2H), 7.23 (d, J = 7.4 Hz, 2H), 7.04 (d, J = 8.3 Hz, 2H), 6.13 (d, J = 9.9 Hz, 2H); ^{13}C NMR (125 MHz, acetone-d_6) δ 190.9, 161.4, 143.0, 135.3, 131.5, 126.8, 124.6, 121.8, 114.0, 95.1; IR (film) 3059, 2935, 2866, 1684, 1630, 1552, 1460, 1236 cm^{-1}. X-ray quality crystals were obtained by dissolving *rac*-**2.19** in a minimal amount of acetone, then, layering this solution with hexanes and allowing for slow evaporation of solvent. See Appendix B for crystallographic data.

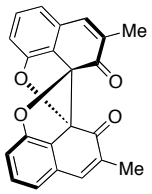

(±)-6,13-Dimethylnaphtho[1,8-*bc*]naphtho[1',8':3,4,5]furo[2,3-*d*]furan-5,12-dione (*rac*-**2.20**). A solution of *rac*-**2.13** (20 mg, 0.057 mmol) in dry MeCN (1 mL) was cooled to 0 °C. Phenyliododiacetate (55.8 mg, 0.173 mmol) was added. When complete, as judged by TLC, the reaction was quenched with water and extracted with EtOAc. The organic layer was washed with water followed by brine and concentrated. The residue was chromatographed (10% EtOAc/hexanes) to yield *rac*-**2.20** as a red-orange solid (14.7 mg, 75%): mp > 186 ºC decomp; ^{1}H NMR (500 MHz, $CDCl_3$) δ 7.31 (t, *J* = 7.9 Hz, 2H), 7.20 (d, *J* = 1.4, 2H), 6.90 (d, *J* = 7.4 Hz, 2H), 6.82 (d, *J* = 8.3, 2H), 2.02 (d, *J* = 1.4 Hz, 6H); ^{13}C NMR (125 MHz, $CDCl_3$) δ 191.3, 160.3, 137.6, 134.6, 134.0, 131.2, 123.5, 119.7, 112.4, 94.6, 16.2; IR (film) 2927, 1684, 1637, 1576, 1460, 1259 cm^{-1}; HRMS (ES) calcd for $C_{22}H_{15}O_4$ $(M+H)^+$ 343.0970, found 343.0959.

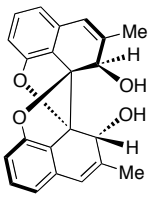

(±)-6,13-Dimethyl-5,12-dihydronaphtho[1,8-*bc*]naphtho[1',8':3,4,5]furo[2,3-*d*]furan-5,12-diol (*rac*-**2.21**). To *rac*-**2.20** (40 mg, 0.12 mmol) dissolved in dry THF (16 mL) was added EtOH (absolute, 12.5 mL) and the solution was cooled to 0 °C. A solution of $NaBH_4$ (43 mg, 1.1 mmol) in EtOH (3.5 mL) was added slowly. The mixture was stirred for 2 h, then concentrated without heating. EtOAc and water were added to

the residue and the layers separated. The organic layer was washed with brine, dried over Na_2SO_4, and concentrated without heating. The resulting fine powder was suspended in a small amount of cold EtOAc, sonicated, and transferred to a centrifuge tube. After centrifugation, the filtrate was removed and the process repeated to yield *rac*-**2.21** as a fine white powder (31 mg, 77%): ^{1}H NMR (300 MHz, DMSO-d_6) δ 7.20 (t, J = 7.8 Hz, 2H), 6.65 (d, J = 7.6 Hz, 2H), 6.62 (d, J = 8.2 Hz, 2H), 6.36 (m, 2H), 5.31 (d, J = 9.0 Hz, 2H), 4.85 (d, J = 9.0 Hz, 2H), 1.97 (s, 6H); ^{13}C NMR (125 MHz, DMSO-d_6) δ 158.8, 144.0, 132.4, 132.1, 121.8, 119.7, 115.3, 108.2, 97.2, 70.8, 19.4; IR (film) 3306, 3035, 2912, 1583, 1468, 1174, 1081 cm^{-1}; HRMS (ES) calcd for $C_{22}H_{17}O_4$ $(M–H)^-$ 345.1127, found 345.1118. X-ray quality crystals were obtained by slow evaporation from EtOAc/acetone. See Appendix B for crystallographic data.

7.4 Chapter 4 Experimental

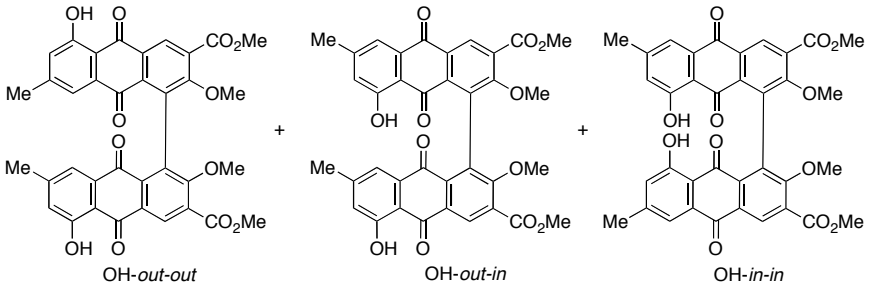

Bisanthraquinones [**4.23a**, **4.23b**, **4.23c** (major)]. To a suspension of **2.4** (30 mg, 0.062 mmol) in dry benzene (1.0 mL) was added diene **4.17** (46 μL, 4 equiv). Additional diene (4 equiv) was added after 6 h and 24 h. After a total of 32 h, the reaction mixture was diluted with CH_2Cl_2 and poured over silica (1200 mg). The solvent

was allowed to evaporate open to air. More silica was added as needed. When complete, the silica was loaded directly onto a column and chromatographed (CH_2Cl_2–2.5% EtOAc/CH_2Cl_2) to afford **4.23** as a mixture of regioisomers in a 4:22:74 ratio (**a**, **b**, **c**; 56%, 10% mono-*peri*-methyl ether also isolated): ^{1}H NMR (500 MHz, $CDCl_3$) **4.23a** (*out*-*out*-OH): δ 12.51 (s, 2H), 8.91 (s, 2H), 7.30 (s, 2H), 7.07 (s, 2H), 4.00 (s, 6H), 3.59 (s, 6H), 2.33 (s, 6H). **4.23b** (*out*-*in*-OH): δ 12.52 (s, 1H), 11.99 (s, 1H), 8.90 (s, 1H), 8.88 (s, 1H), 7.66 (d, J = 1.5 Hz, 1H), 7.32 (d, J = 1.5 Hz, 1H), 7.08 (s, 1H), 7.00 (s, 1H), 4.01 (s, 3H), 3.99 (s, 3H), 3.61 (s, 3H), 3.57 (s, 3H), 2.43 (s, 3H), 2.34 (s, 3H); **4.23c** (*in*-*in*-OH): δ 12.01 (s, 2H), 8.87 (s, 2H), 7.67 (d, J = 1.0 Hz, 2H), 7.01 (s, 2H), 4.00 (s, 6H), 3.59 (s, 6H), 2.44 (s, 6H). Major isomer **4.23c** (*in*-*in*-OH): ^{13}C NMR (125 MHz, $CDCl_3$) δ 188.2, 181.6, 165.4, 163.1, 161.8, 149.1, 134.7, 134.1, 132.8, 131.6, 129.9, 128.7, 124.4, 120.9, 114.8, 62.8, 53.0, 22.4; HRMS (ESI) *m/z* 673.1355 $[M+Na]^+$ (calcd for $C_{36}H_{26}O_{12}Na$, 673.1322).

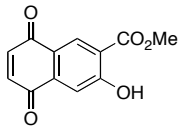

Methyl 3-hydroxy-5,8-dioxo-5,8-dihydronaphthalene-2-carboxylate (**4.25**). To a solution of **1.19** (100 mg, 0.458 mmol) in DMF (9 mL) was added Co-salen (30 mg, 20 mol %). After stirring under an oxygen atmosphere for 3 h, the mixture was diluted with Et_2O and washed with saturated aqueous NH_4Cl. The organic layer was dried over Na_2SO_4, filtered, and concentrated. The crude solid was chromatographed (30%–60% EtOAc/hexanes) to afford **4.25** as a yellow solid (55.3 mg, 52%): mp 218-220ºC (decomp.); ^{1}H NMR (500 MHz, $CDCl_3$) δ 11.37 (s, 1H), 8.64 (s, 1H), 7.62 (s, 1H), 6.99

(s, 2H), 4.04 (s, 3H); ^{13}C NMR (125 MHz, $CDCl_3$) δ 184.3, 183.3, 169.8, 165.8, 139.8, 138.9, 137.3, 130.7, 124.0, 116.5, 115.9, 53.3; IR (film) 3159, 3082, 2966, 2927, 1668, 1568, 1452, 1313, 1244 cm^{-1}; HRMS (ESI) *m/z* 233.0440 $[M+H]^+$ (calcd for $C_{12}H_9O_5$, 233.0450).

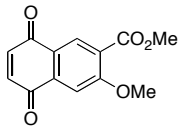

Methyl 3-methoxy-5,8-dioxo-5,8-dihydronaphthalene-2-carboxylate (**4.26**). To a suspension of **4.25** (35.7 mg, 0.154 mmol) in CH_2Cl_2 (1 mL) was added Ag_2O (30 mg, 0.8 equiv), followed by MeI (20 μL, 2 equiv). After stirring the mixture for 21.5 h in the dark, additional Ag_2O (30 mg, 0.8 equiv) and MeI (20 μL, 2 equiv) were added. When the reaction was complete, the mixture was filtered through Celite™ with CH_2Cl_2 and concentrated. The residue was chromatographed (15%–30% EtOAc/hexanes) to afford **4.26** as a yellow solid (30 mg, 79%): mp 163-164 ºC (decomp.); ^{1}H NMR (500 MHz, $CDCl_3$) δ 8.45 (s, 1H), 7.59 (s, 1H), 6.98 (s, 1H), 6.97 (s, 1H), 4.06 (s, 3H), 3.93 (s, 3H); ^{13}C NMR (125 MHz, $CDCl_3$) δ 184.6, 183.4, 165.2, 163.0, 139.5, 138.5, 135.7, 130.9, 125.6, 124.9, 109.0, 57.0, 52.7; IR (film) 3066, 2958, 2858, 1730, 1668, 1599, 1321, 1236 cm^{-1}; HRMS (ESI) *m/z* 247.0609 $[M+H]^+$ (calcd for $C_{13}H_{11}O_5$, 247.0606).

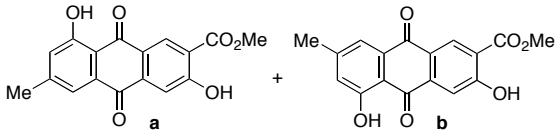

Anthraquinone monomers 4.24a and **4.24b**. Naphthoquinone **4.25** (20 mg, 0.081 mmol) was suspended in glacial acetic acid (0.2 mL), and a solution of Br_2 in

AcOH was added dropwise (1 equiv). When the reaction was complete as determined by TLC, it was diluted with cold water and quenched with $NaHSO_3$. The mixture was extracted with EtOAc, washed with brine, and dried over Na_2SO_4. The residue was chromatographed (15% EtOAc/hexanes) to remove any over brominated material and dissolved in AcOH (5 mL). Following the addition of NaOAc (100 mg), the solution was heated to reflux for 5 min. After cooling to room temperature, the reaction mixture was diluted with water and extracted with EtOAc. The organic layer was washed with water and brine, followed by drying over Na_2SO_4. The product was obtained as an inseparable mixture of bromoquinones **4.30a** and **4.30b** (25:75 ratio) and used without further purification: ^{1}H NMR (300 MHz, $CDCl_3$) **4.30a** (*anti*-Br): δ 11.42 (bs, 1H), 8.71 (s, 1H), 7.62 (s, 1H), 7.54 (s, 1H), 4.06 (s, 3H). **4.30b** (*syn*-Br): δ 11.42 (bs, 1H), 8.63 (s, 1H), 7.72 (s, 1H), 7.53 (s, 1H), 4.04 (s, 3H).

To a 0 ºC solution of a 25:75 mixture of bromoquinones **4.30a** and **4.30b** (5.4 mg, 0.016 mmol) in dry toluene (2 mL), was added diene **4.17** (8 μL, 2.6 equiv). After 1 h, the reaction mixture was concentrated, diluted with CH_2Cl_2 and poured over silica (50 mg). The solvent was allowed to evaporate open to air. After overnight, the silica was filtered to afford **4.24** as a 24:76 mixture of anthraquinones **4.24a** and **4.24b** (4.2 mg, 84%): ^{1}H NMR (300 MHz, $CDCl_3$) **4.24a** (*anti*-OH): δ 12.65 (s, 1H), 11.40 (s, 1H), 8.84 (s, 1H), 7.80 (s, 1H), 7.65 (s, 1H), 7.11 (s, 1H), 4.06 (s, 3H), 2.47 (s, 3H). **4.24b** (*syn*-OH): δ 12.43 (s, 1H), 11.38 (s, 1H), 8.83 (s, 1H), 7.83 (s, 1H), 7.67 (d, J = 1.3 Hz, 1H), 7.11 (d, J = 0.7 Hz, 1H), 4.06 (s, 3H), 2.47 (s, 3H).

Isomer **4.24b** (*syn*-OH) was purified via chromatography (8% EtOAc/hexanes): mp 224–226 ºC; ^{13}C NMR (500 MHz, $CDCl_3$) δ 187.1, 181.0, 169.8, 165.8, 163.2, 149.5,

139.0, 133.5, 131.6, 125.5, 124.1, 121.2, 117.0, 116.0, 114.7, 53.3, 22.5; IR (film) 3128, 3082, 2927, 2858, 1692, 1645, 1568, 1444, 1298, 1251 cm^{-1}; HRMS (ESI) *m/z* 313.0713 $[M+H]^+$ (calcd for $C_{17}H_{13}O_6$, 313.0712). X-ray quality crystals were obtained by suspending **4.24b** in 1:1 EtOAc/hexanes and adding a minimal amount of CH_2Cl_2 until fully dissolved, followed by slow evaporation. See Appendix B for crystallographic data.

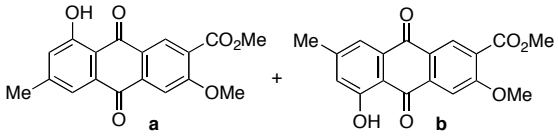

Anthraquinone monomers 4.27a and **4.27b**. A solution of **4.26** (20 mg, 0.081 mmol) in benzene (1 mL) was cooled to 5 °C before addition of diene **4.17** (2 equiv). When complete, as determined by TLC, the reaction mixture was poured over silica (200 mg) and allowed to evaporate open to air. After one day, the silica was filtered with CH_2Cl_2–2.5% MeOH/CH_2Cl_2 and the residue chromatographed (30–50% EtOAc/hexanes) to afford the anthraquinone as a 13:87 mixture of regioisomers **4.27a** (*anti*-OH) and **4.27b** (*syn*-OH). Isomers containing *peri*-methylethers instead of hydroxyls were also isolated (62% combined anthraquinone yield): ^{1}H NMR (500 MHz, $CDCl_3$) **4.27a** (*anti*-OH): δ 12.58 (s, 1H), 8.65 (s, 1H), 7.79 (s, 1H), 7.63 (d, *J* = 1.2 Hz, 1H), 7.12 (m, 1H), 4.10 (s, 3H), 3.96 (s, 3H), 2.47 (s, 3H). **4.27b** (*syn*-OH): δ 12.38 (s, 1H), 8.63 (s, 1H), 7.80 (s, 1H), 7.65 (d, *J* = 1.4 Hz, 1H), 7.10 (m, 1H), 4.10 (s, 3H), 3.96 (s, 3H), 2.47 (s, 3H). ^{13}C NMR (125 MHz, $CDCl_3$) **4.27b** (*syn*-OH): δ 187.3, 181.1, 165.2, 163.1, 149.5, 148.5, 137.3, 133.3, 131.8, 126.4, 125.8, 124.0, 121.2, 114.4, 109.0, 57.0, 52.7, 22.5; HRMS (ESI) *m/z* 327.0865 $[M+H^+]$ (calcd for $C_{18}H_{15}O_6$, 327.0869).

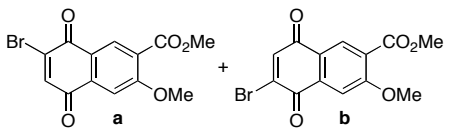

Bromoquinone monomers (**4.31a** and **4.31b**). Naphthoquinone **4.26** (5.0 mg, 0.020 mmol) was dissolved in propionic acid (1 mL) flushed with Ar, and cooled to –10 °C. The addition of HBr/AcOH (33% wt, 50 μL) turned the solution green. After 10 min, the reaction mixture was diluted with water, extracted with EtOAc, and washed several times with water and brine. The organic layer was dried over Na_2SO_4, filtered, and concentrated. The residue was reconstituted in THF (0.7 mL), followed by the addition of Na_2SO_4 (44 mg) and Ag_2O (7.7 mg, 0.033 mmol). After stirring the mixture in the dark for 12.5 h, it was filtered through Celite™ and chromatographed on a short column of silica (CH_2Cl_2) to afford **4.31** as an inseparable 93:7 mixture of bromoquinones **4.31a** and **4.31b** (3.7 mg, 56% yield): ^{1}H NMR (300 MHz, $CDCl_3$) **4.31a** (*anti*-Br): δ 8.53 (s, 1H), 7.60 (s, 1H), 7.53 (s, 1H), 4.07 (s, 3H), 3.95 (s, 3H). **4.31b** (*syn*-Br): δ 8.46 (s, 1H), 7.68 (s, 1H), 7.52 (s, 1H), 4.08 (s, 3H), 3.94 (s, 3H); major isomer **4.31a** (*anti*-Br): ^{13}C NMR (125 MHz, $CDCl_3$) δ 182.0, 176.3, 165.0, 163.3, 141.5, 140.2, 135.6, 132.2, 125.0, 123.6, 109.4, 57.1, 52.9; HRMS (ESI) *m/z* 324.9723 $[M+H]^+$ (calcd for $C_{13}H_{10}O_5Br$, 324.9712).

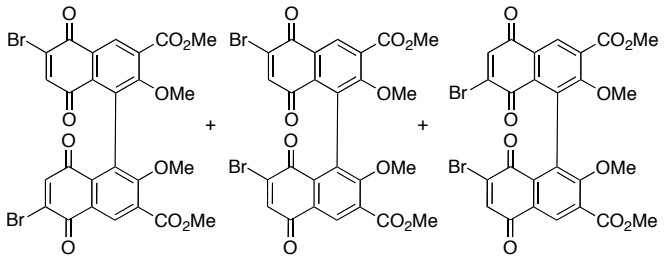

Bishaloquinones (**4.32a**, **4.32b**, **4.32c**). To a suspension of **2.4** (250 mg, 0.509 mmol) in glacial AcOH (2.5 mL) was added bromine (2 mL, 0.5 M in AcOH). After stirring 10 min, ice/water was added and the mixture extracted with EtOAc. The organic layer was washed with saturated aqueous sodium thiosulfate, followed by water and brine. After concentrating, the residue was reconstituted in AcOH (10 mL). Anhydrous NaOAc (417 mg, 5.09 mmol) was added and the mixture heated to reflux for 3 min. After cooling the mixture to 0 °C, the solid was collected via vacuum filtration and washed well with water. The crude solid was chromatographed (CH_2Cl_2–5% EtOAc/CH_2Cl_2) to afford a yellow solid as an inseparable 37:50:13 mixture of **4.32a**, **4.32b**, and **4.32c** (287 mg, 87%): ^{1}H NMR (500 MHz, C_6D_6) **4.32a** (*out*-*out*-Br): δ 8.78 (s, 2H), 6.68 (s, 2H), 3.41 (s, 6H), 3.35 (s, 6H). **4.32b** (*out*-*in*-Br): δ 8.80 (s, 1H), 8.78 (s, 1H), 6.83 (s, 1H), 6.61 (s, 1H), 3.41 (s, 3H), 3.40 (s, 3H), 3.35 (s, 3H), 3.34 (s, 3H). **4.32c** (*in*-*in*-Br): δ 8.81 (s, 2H), 6.79 (s, 2H), 3.39 (s, 6H), 3.35 (s, 6H); ^{13}C NMR (500 MHz, acetone-d_6) **4.32a** (*out*-*out*-Br): δ 183.1, 177.5, 165.8 (overlap with b and c), 162.8, 142.2, 140.0, 133.8, 133.2, 131.9, 129.1, 127.9, 63.1 (overlap with b and c), 53.3 (overlap with b and c). **4.32b** (*out*-*in*-Br): δ 183.2, 181.7, 178.6, 177.4, 165.8 (2 peaks, overlap with a and c), 162.7, 162.4, 142.2, 141.1, 140.9, 140.1, 134.6, 133.9, 133.2, 132.3, 131.9, 130.9, 129.6, 129.1, 128.8, 128.0, 63.1 (2 peaks, overlap with a and c), 53.3 (2 peaks,

overlap with a and c). **4.32c** (*in-in*-Br): δ 181.7, 178.6, 165.8 (overlap with a and b), 162.4, 141.2, 140.8, 134.6, 132.3, 131.0, 129.5, 128.9, 63.1 (overlap with a and b), 53.3 (overlap with a and b); HRMS (ESI) *m/z* 646.9209 $[M+H]^+$ (calcd for $C_{26}H_{17}O_{10}Br_2$, 646.9188).

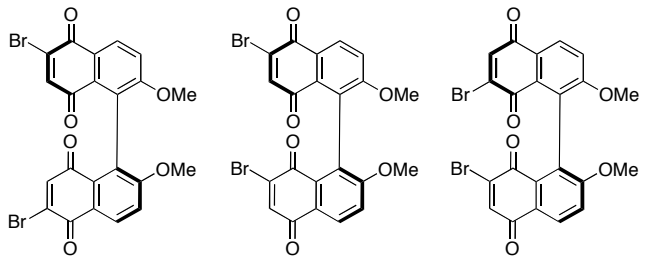

(*S*)-6,6' and **6,7'** and **7,7'-dibromo-2,2'-dimethoxy-[1,1'-binaphthalene]-5,5',8,8'-tetraone** [(*S*)-**4.34a**, (*S*)-**4.34b**, (*S*)-**4.34c**]**.** To a suspension of (*S*)-**2.8** (46.5 mg, 0.124 mmol) in glacial AcOH (0.65 mL), was added Br_2 (0.50 mL, 0.5 M in AcOH) dropwise. After stirring 20 min, the mixture was diluted with water. EtOAc was added and the organic layer washed with saturated aqueous sodium thiosulfate. The organic layer was washed with water and brine, dried over Na_2SO_4, and concentrated. The residue was reconstituted in AcOH (8 mL) and anhydrous NaOAc (305 mg) added. After heating to reflux for 5 min, the solution was cooled to room temperature and cold water was added. This mixture was extracted with EtOAc (x2), washed with water (2x) and brine, dried over Na_2SO_4, and concentrated to give a mixture of bromoquinones [43% (*S*)-**4.34a**, 47% (*S*)-**4.34b**, 10% (*S*)-**4.34c**]. The mixture was chromatographed to yield the bromoquinone mixture (62.7 mg, 95%). Regioisomers were separated via semi-preparative HPLC (Dynamax column Si 83-121-C, 21 mm, 20 mL/min DCM): t_R(**4.34a**) = 38.3 min, t_R(**4.34b**) = 59.7 min, t_R(**4.34c**) = 98.0 min. Compounds (*S*)-**4.34a**, (*S*)-

4.34b, (*S*)-**4.34c** were obtained as yellow-orange amorphous solids [38% (*S*)-**4.34a**, 28% (*S*)-**4.34b**, 9% (*S*)-**4.34c**; all >99% ee]. CSP HPLC (Chiralpak IA, 0.75 mL/min, 60:40 hexanes:*i*-PrOH): **4.34a**: $t_R(R)$ = 36.9 min, $t_R(S)$ = 86.7 min; **4.34b**: $t_R(R)$ = 24.8 min, $t_R(S)$ = 29.6 min; **4.34c**: $t_R(S)$ = 13.1 min, $t_R(R)$ = 23.9 min.

(*S*)-**4.34a**: ^{1}H NMR (500 MHz, C_6D_6) δ 8.22 (d, *J* = 8.6 Hz, 2H), 6.74 (s, 2H), 6.48 (d, *J* = 8.7 Hz, 2H), 2.96 (s, 6H); ^{13}C NMR (125 MHz, $CDCl_3$) δ 183.0, 177.3, 162.1, 141.1, 139.8, 130.8, 130.4, 127.5, 125.3, 114.7, 56.5; IR (film) 2918, 1668, 1569, 1276, 1246 cm^{-1}; HRMS (ES) calcd for $C_{22}H_{13}O_6Br_2$ (MH^+) 530.9079, found 530.9091. CD in $ClCH_2CH_2Cl$, 0.19 mM, 23 °C [nm ([θ])]: 289 (+ 58797), 278 (0), 266 (– 90011).

(*S*)-**4.34b**: ^{1}H NMR (500 MHz, C_6D_6) δ 8.23 (d, *J* = 8.7 Hz, 1H), 8.21 (d, *J* = 8.7 Hz, 1H), 6.87 (s, 1H), 6.68 (s, 1H), 6.53 (d, *J* = 8.7 Hz, 1H), 6.47 (d, *J* = 8.7 Hz, 1H), 2.96 (s, 3H), 2.92 (s, 3H); ^{13}C NMR (125 MHz, $CDCl_3$) δ 183.0, 181.8, 178.3, 177.3, 162.0, 161.7, 141.1, 140.5, 140.2, 139.8, 130.9, 130.4, 129.7, 129.5, 128.5, 127.6, 126.2, 125.3, 115.1, 114.8, 56.54, 56.53; IR (film) 2919, 1672, 1659, 1273 cm^{-1}; HRMS (ES) calcd for $C_{22}H_{13}O_6Br_2$ (MH^+) 530.9079, found 530.9101.

(*S*)-**4.34c**: ^{1}H NMR (500 MHz, C_6D_6) δ 8.22 (d, *J* = 8.6 Hz, 2H), 6.85 (s, 2H), 6.52 (d, *J* = 8.7 Hz, 2H), 2.91 (s, 6H); ^{13}C NMR (125 MHz, $CDCl_3$) δ 181.9, 178.4, 161.6, 140.4, 140.2, 129.7, 129.4, 128.6, 126.3, 115.3, 56.6; IR (film) 2918, 1681, 1651, 1570, 1270 cm^{-1}; HRMS (ES) calcd for $C_{22}H_{13}O_6Br_2$ (MH^+) 530.9079, found 530.9088.

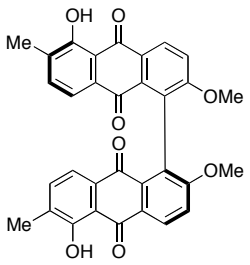

(*S*)-5,5'-dihydroxy-2,2'-dimethoxy-6,6'-dimethyl-[1,1'-bianthracene]-9,9',10,10'-tetraone [(*S*)-**4.38a**]. In a microwave vial, (*S*)-**4.34a** (32.4 mg, 0.061 mmol) was partially dissolved in toluene (1.0 mL). Then, 4 equiv compound **4.37** (45 μL) was added and the sealed vial was heated in a 55-60 °C oil bath. Up to 20 equiv additional diene was added periodically over 52 h (cooling to rt with each addition). After 52 h the reaction was complete as judged by TLC and the mixture was cooled to room temperature. The solution was diluted with 10 mL CH_2Cl_2 and poured over 1000 mg silica (silica scraped from TLC plate) and the solvent left to evaporate. More silica was added as needed (up to 1000 mg), as indicated by monitoring via TLC. When the aromatization was complete, after 2.5 d, the mixture was filtered with CH_2Cl_2 through a short column of silica. The resulting solid was triturated with hexanes, followed by a small amount of CH_2Cl_2 to yield (*S*)-**4.38a** as a yellow amorphous solid (26.0 mg, 80%, >99% ee): ^{1}H NMR (500 MHz, $CDCl_3$) δ 13.15 (s, 2H), 8.51 (d, J = 8.7 Hz, 2H), 7.41 (d, J = 7.7 Hz, 2H), 7.37 (d, J = 7.8 Hz, 2H), 7.35 (d, J = 8.8 Hz, 2H), 3.77 (s, 6H), 2.33 (s, 6H); ^{13}C NMR (500 MHz, $CDCl_3$) δ 188.6, 183.1, 162.2, 160.8, 136.8, 134.3, 132.5, 132.4, 129.6, 129.1, 127.6, 119.1, 115.3, 114.8, 56.5, 16.2; IR (film) 2927, 2858, 1668, 1630, 1576, 1460, 1274 cm^{-1}; HRMS (ES) calcd for $C_{32}H_{22}O_8$ (MNa^+) 557.1212, found 557.1191.

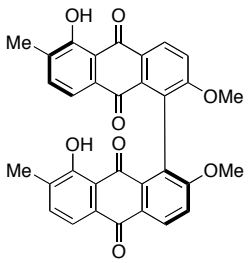

(*S*)-5,8'-dihydroxy-2,2'-dimethoxy-6,7'-dimethyl-[1,1'-bianthracene]-9,9',10,10'-tetraone [(*S*)-**4.38b**]. In a microwave vial, (*S*)-**4.34b** (11.2 mg, 0.021 mmol) was partially dissolved in toluene (0.38 mL). Then, 4 equiv compound **4.37** (16 μL) was added and the sealed vial was heated in a 50-55 °C oil bath. Up to 20 equiv diene was added periodically over 52 h, followed by an additional 4-8 equiv over the remaining time for a total of 5 d 23 h (cooling to rt with each addition). After this time, the reaction was complete as judged by TLC, and the mixture was cooled to rt. The solution was diluted with 5 mL CH_2Cl_2 and poured over 600 mg silica (silica scraped from TLC plate) and the solvent left to evaporate. More silica was added as needed (up to 300 mg), as indicated by monitoring via TLC. When the aromatization was complete (after 2.5 days), it was filtered with CH_2Cl_2 through a short column of silica. The resulting solid was triturated with CH_2Cl_2/hexanes to yield (*S*)-**4.38b** as an amorphous yellow solid (8.0 mg, 71%, >99% ee): ^{1}H NMR (500 MHz, $CDCl_3$) δ 13.16 (s, 1H), 12.59 (s, 1H), 8.51 (d, J = 8.7 Hz, 1H), 8.48 (d, J = 8.7 Hz, 1H), 7.73 (d, J = 7.7 Hz, 1H), 7.46 (d, J = 7.7 Hz, 1H), 7.43 (d, J = 7.7 Hz, 1H), 7.39 (d, J = 7.9 Hz, 1H), 7.34 (overlapping d, J = 8.7, 8.8 Hz, 2H), 3.77 (s, 3H), 3.74 (s, 3H), 2.34 (s, 3H), 2.26 (s, 3H); ^{13}C NMR (125 MHz, $CDCl_3$) δ 190.0, 188.6, 183.2, 183.1, 162.2, 161.6, 161.0, 160.8, 136.9, 136.8, 134.3 (2 overlapping peaks), 132.5, 132.4, 131.9, 131.6, 129.9, 129.5, 129.2, 128.9, 128.2, 127.6, 119.1, 118.6, 116.2, 115.5, 115.3, 114.9, 56.53, 56.48, 16.3, 16.2; IR (film) 3443, 3432, 2924, 2851,

1662, 1629, 1571, 1427, 1324, 1272, 1254 cm^{-1}; HRMS (ES) calcd for $C_{32}H_{22}O_8Na$ (MNa^+) 557.1212, found 557.1204. CD in MeOH, 0.24 mM, 23 °C [nm ([θ])]: 258 (+ 164309), 235 (+86951), 230 (0), 222 (– 204798).

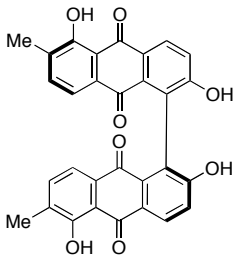

(*S*)-Bisoranjidiol [(*S*)-**4.39a**]. A solution of (*S*)-**4.38a** (13.2 mg, 0.0247mmol) in CH_2Cl_2 (1.6 mL) was cooled to 0 °C. BBr_3 (12 equiv, 0.3 mL, 1 M in CH_2Cl_2) was added with stirring. The reaction mixture was allowed to warm to room temperature and over time turns from red to dark purple with a precipitate. After 4 h, the reaction mixture was sonicated to break up solids and stirred an additional 2 h. After 6 h total, it was cooled to 0 °C and quenched with cold water. The mixture was extracted with EtOAc (using a small amount of MeOH and sonication to break up solids), washed with water and brine, dried over Na_2SO_4, filtered, and concentrated. The residue was chromatographed (CH_2Cl_2 to 0.5% MeOH to 1% MeOH/CH_2Cl_2) to afford (*S*)-**4.39a** as an orange powder (10.0 mg, 80%, >99% ee): mp >150 °C decomposition; $[\alpha]_D^{25}$ +306.9 (*c* 0.036, >99% ee, CH_2Cl_2); ^{1}H NMR (300 MHz, acetone-d_6) δ 13.20 (s, 2H), 9.44 (br s, 2H), 8.36 (d, *J* = 8.4 Hz, 2H), 7.52 (d, *J* = 7.8 Hz, 2H), 7.43 (d, *J* = 8.4 Hz, 2H), 7.37 (d, *J* = 7.8 Hz, 2H), 2.31 (s, 6H); ^{1}H NMR (500 MHz, DMSO-d_6) δ 13.15 (s, 2H), 10.79 (br s, 2H), 8.25 (d, *J* = 8.6 Hz, 2H), 7.54 (d, *J* = 7.7 Hz, 2H), 7.34 (d, *J* = 8.6 Hz, 2H), 7.31 (d, *J* = 7.7 Hz, 2H), 2.26 (s, 6H); ^{13}C NMR (125 MHz, DMSO-d_6) δ 187.8, 182.3, 161.5, 159.6, 136.9, 133.4,

132.5, 131.6, 128.6, 127.2, 125.2, 120.1, 118.4, 114.4, 15.6; IR (film) 3437, 3198, 2927, 2858, 1668, 1630, 1576, 1460, 1305, 1267 cm^{-1}; HRMS (ES) calcd for $C_{30}H_{17}O_8$ (MH^-) 505.0923, found 505.0928. CSP HPLC (Chiralpak IA, 1.0 mL/min, 80:20 hexanes:*i*-PrOH): $t_R(S)$ = 10.1 min, $t_R(R)$ = 26.0 min. CD in MeOH, 0.18 mM, 23 °C [nm ([θ])]: 256 (+ 281646), 232 (0), 219 (– 238322).

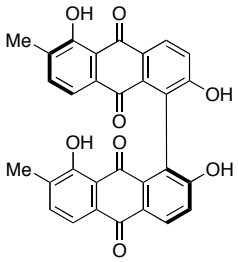

(*S*)-2,2',5,8'-tetrahydroxy-6,7'-dimethyl-[1,1'-bianthracene]-9,9',10,10'-tetraone [(*S*)-**4.39b**]. A solution of (*S*)-**4.38b** (8.0 mg, 0.015 mmol) in CH_2Cl_2 (1.0 mL) was cooled to 0 °C. BBr_3 (12 equiv, 0.18 mL, 1 M in CH_2Cl_2) was added with stirring. The reaction mixture was allowed to warm to room temperature and becomes dark purple with a precipitate. An additional 12 equiv BBr_3 was added after 4.5h. The reaction mixture was sonicated several times to break up solids over a total reaction time of 7h. Then, it was cooled to 0 °C and quenched with cold water. The mixture was extracted with EtOAc, washed with water and brine, dried over Na_2SO_4, filtered, and concentrated. The residue was chromatographed (1% MeOH/CH_2Cl_2, flush with acetone) and further purified by chromatography (5% MeOH/CH_2Cl_2) to afford (*S*)-**4.39b** as a red-brown resin (3 mg, 39%, >99% ee): ^{1}H NMR (500 MHz, acetone-d_6) δ 13.20 (s, 1H), 12.70 (s, 1H), 8.37 (d, J = 8.6 Hz, 1H), 8.29 (d, J = 8.5 Hz, 1H), 7.69 (dd, J = 7.7 Hz, 1.6 Hz, 1H), 7.62 (d, J = 7.6 Hz, 1H), 7.54 (d, J = 7.7 Hz, 1H), 7.45 (d, J = 8.6 Hz, 1H), 7.43 (d, J = 8.5 Hz,

1H), 7.39 (dd, J = 7.7 Hz, 1.9Hz, 1H), 2.32 (s, 3H), 2.25 (s, 2.25); ^{13}C NMR (125 MHz, DMSO-d_6) δ 189.9, 187.8, 182.5, 180.9, 161.4, 160.6, 159.8, 159.7, 137.4, 137.0, 133.6, 133.5, 132.4, 132.0, 131.6, 130.8, 128.8, 128.7, 127.2, 127.2, 126.1, 125.3, 120.8, 120.2, 118.5, 118.2, 115.2, 114.5, 15.73, 15.65; IR (film) 3276, 2924, 1628, 1570, 1425, 1300, 1248 cm^{-1}; HRMS (ES) calcd for $C_{30}H_{17}O_8$ (MH^-) 505.0923, found 505.0922.

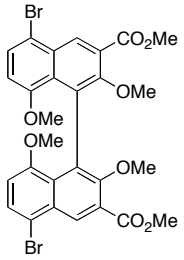

Dimethyl-5,5'-dibromo-2,2',8,8'-tetramethoxy-[1,1'-binaphthalene]-3,3'-dicarboxylate (4.44a). To a solution of **2.1** (300 mg, 0.612 mmol) in glacial acetic acid (9 mL) was added slowly two equivalents of Br_2 in 4.5 mL AcOH. After 20 min, the solution was quenched with aqueous $NaHSO_3$. The mixture was diluted with water and extracted with EtOAc. The organic layer was washed several times with water and brine and dried over Na_2SO_4. Concentration of the organic layer afforded **4.44a** as a yellow solid (379 mg, 96%): mp 208-209 ºC; ^{1}H NMR (300 MHz, $CDCl_3$) δ 8.77 (s, 2H), 7.60 (d, J = 8.4 Hz, 2H), 6.55 (d, J = 8.4 Hz, 2H), 3.97 (s, 6H), 3.37 (s, 6H), 3.10 (s, 6H); ^{13}C NMR (75 MHz, $CDCl_3$) δ 167.0, 156.2, 152.9, 131.2, 130.2, 129.2, 128.91, 128.85, 125.7, 114.5, 108.1, 61.9, 55.7, 52.7; IR (film) 2950, 2842, 1730, 1591, 1452, 1244 cm^{-1}; HRMS (ESI) m/z 668.9766 $[M+Na]^+$ (calcd for $C_{28}H_{24}Br_2O_8Na$, 668.9736).

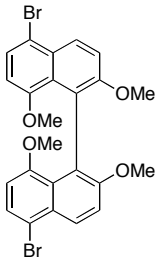

5,5'-Dibromo-2,2',8,8'-tetramethoxy-1,1'-binaphthalene (4.44b). Compound **2.5** (62.3 mg, 0.180 mmol) was suspended in dry DMF (0.3 mL). A solution of NBS (67.9 mg, 0.381 mmol) in DMF (1.6 mL) was transferred to this solution via cannula (turns dark). After 5.5 h, the reaction mixture was diluted with water, extracted with EtOAc, and washed several times with water and brine. The organic layer was dried over Na_2SO_4, and concentrated. The residue was chromatographed (5 to 15% EtOAc/hexanes) to afford **4.44b** as a white solid (76.5 mg, 80%): mp 188-190 ºC; ^{1}H NMR (500 MHz, $CDCl_3$) δ 8.24 (d, J = 9.5 Hz, 2H), 7.48 (d, J = 8.5 Hz, 2H), 7.42 (d, J = 9.5 Hz, 2H), 6.45 (d, J = 8.0 Hz, 2H), 3.69 (s, 6H), 3.06 (s, 6H); ^{13}C NMR (125 MHz, $CDCl_3$) δ 156.9, 154.5, 128.5, 127.6, 127.4, 127.0, 123.7, 115.2, 114.1, 106.8, 57.2, 56.0; IR (film) 2935, 2842, 1591, 1460, 1251, 1058 cm^{-1}; HRMS (ESI) *m/z* 530.9803 $[M+H]^+$ (calcd for $C_{24}H_{21}Br_2O_4$, 530.9807).

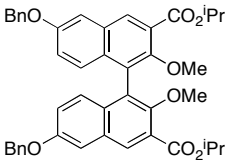

Diisopropyl-6,6'-bis(benzyloxy)-2,2'-dimethoxy-[1,1'-binaphthalene]-3,3'-dicarboxylate (**4.46**). Biaryl **6.23** (817 mg, 1.271 mmol) was suspended in 2-propanol (10 mL), followed by the addition of Ti(O*i*-Pr)$_4$ (0.8 mL). After heating the mixture at 90

°C for 6 h, additional Ti(O*i*-Pr)$_4$ (0.8 mL) was added. When the reaction was complete, it was quenched with 1 M HCl and extracted several times with EtOAc. After concentrating the organic layer, the residue was chromatographed (10-20% EtOAc/hexanes) to afford **4.46** as a white foam (771 mg, 87%): ^{1}H NMR (500 MHz, $CDCl_3$) δ 8.33 (s, 2H), 7.47 (d, *J* = 7.4 Hz, 4H), 7.40 (t, *J* = 7.6 Hz, 4H), 7.34 (m, 2H), 7.33 (d, *J* = 2.1 Hz, 2H), 7.09 (dd, *J* = 9.2 Hz, 2.3 Hz, 2H), 7.06 (d, *J* = 9.2 Hz, 2H), 5.33 (septet, *J* = 6.2 Hz, 2H), 5.18 (s, 4H), 3.45 (s, 6H), 1.43 (d, *J* = 5.9 Hz, 6H), 1.42 (d, *J* = 5.5 Hz, 6H); ^{13}C NMR (125 MHz, $CDCl_3$) δ 166.4, 156.6, 153.0, 136.8, 131.6, 131.3, 130.8, 128.8, 128.3, 127.7, 127.4, 126.6 (overlapping peaks), 121.7, 108.2, 70.3, 68.9, 62.2, 22.12, 22.11; IR (film) 2979, 2938, 1721, 1595, 1498, 1237, 1109 cm^{-1}; HRMS (ESI) *m/z* 699.2955 $[M+H]^+$ (calcd for $C_{44}H_{43}O_8$, 699.2958).

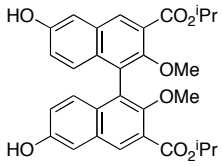

Diisopropyl-6,6'-dihydroxy-2,2'-dimethoxy-[1,1'-binaphthalene]-3,3'-dicarboxylate (**4.47**). Compound **4.46** (61 mg, 0.087 mmol) was dissolved in THF (1.5mL). Following the addition of MeOH (1.5 mL) and Pd/C (10 wt%, 15 mg), the reaction vessel was evacuated and purged with H_2 (×3). After stirring overnight, the reaction mixture was filtered through Celite™ and concentrated. The residue was chromatographed (30% EtOAc/hexanes) to afford **4.47** (quantitative yield): mp 114-116 °C; ^{1}H NMR (500 MHz, $CDCl_3$) δ 8.73 (bs, 2H), 8.26 (s, 2H), 7.38 (d, *J* = 2.4 Hz, 2H), 7.06 (dd, *J* =9.1 Hz, 2.5 Hz, 2H), 7.00 (d, *J* = 9.2 Hz, 2H), 5.28 (septet, *J* = 6.3 Hz, 2H),

3.44 (s, 6H), 1.40 (d, J = 6.2 Hz, 12H); ^{13}C NMR (125 MHz, $CDCl_3$) δ 166.8, 156.0, 152.8, 132.1, 131.2, 131.0, 128.1, 127.8, 127.3, 121.6, 110.8, 69.2, 62.1, 22.12, 22.11; IR (film) 3382, 2981, 2938, 1700, 1597, 1503, 1267, 1108 cm^{-1}; HRMS (ESI) *m/z* 541.1837 $[M+Na]^+$ (calcd for $C_{30}H_{30}O_8Na$, 541.1838).

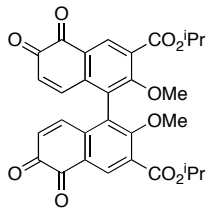

Diisopropyl-2,2'-dimethoxy-5,5',6,6'-tetraoxo-5,5',6,6'-tetrahydro-[1,1'-binaphthalene]-3,3'-dicarboxylate (**4.48**). To a solution of compound **4.47** (112 mg, 0.216 mmol) in DMF (4.0 mL) was added 2-iodoxybenzoic acid (124.8 mg, 0.443 mmol). After 4 h, the reaction mixture was diluted with water and extracted with EtOAc. The organic layer was washed with water, 25% aq $NaHCO_3$, and brine. After drying the organic layer over Na_2SO_4 and concentrating, the residue was chromatographed (CH_2Cl_2 to 0.5-1% MeOH/CH_2Cl_2) to afford **4.48** as an orange solid (116 mg, 98%): mp >140 ºC (decomp); ^{1}H NMR (500 MHz, $CDCl_3$) δ 8.60 (s, 2H), 7.00 (d, J = 10.5 Hz, 2H), 6.45 (d, J = 10.5 Hz, 2H), 5.31 (septet, J = 6.3, 2H), 3.75 (s, 6H), 1.43 (d, J = 6.3 Hz, 12H); ^{13}C NMR (125 MHz, $CDCl_3$) δ 180.1, 177.2, 164.2, 163.4, 140.3, 137.5, 134.7, 130.6, 128.7, 127.0, 126.2, 70.4, 62.6, 22.0; IR (film) 2981, 1676, 1583, 1468, 1267 cm^{-1}; HRMS (ESI) *m/z* 547.1624 $[M+H]^+$ (calcd for $C_{30}H_{27}O_{10}$, 547.1604).

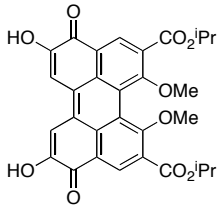

Diisopropyl-5,8-dihydroxy-1,12-dimethoxy-4,9-dioxo-4,9-dihydroperylene-2,11-dicarboxylate (**4.49**). In a separatory funnel, orthoquinone **4.48** (30 mg, 0.0549 mmol) was dissolved in CH_2Cl_2 (3 mL). Following the addition of Et_2O (6 mL), a freshly prepared aqueous solution of $Na_2S_2O_4$ (100 mg/8 mL) was added. The mixture was shaken until the color changed from red to yellow. The layers were separated and washed with brine. The organic layer was dried over Na_2SO_4 while under a stream of argon. After filtration, the solution was concentrated and reconstituted in dry *t*-BuOH (1 mL). The solution of the tetrol was then added to a flask containing a solution of *t*-BuOK (22.2 mg, 0.198) in *t*-BuOH (1.1 mL), which had O_2 bubbling through for at least 5 min prior. The reaction immediately turns dark green and after 3-4 min, it was quenched with cold 1 M HCl, which turned the solution dark purple. The reaction mixture was diluted with EtOAc and washed with 1 M HCl, followed by brine. The organic layer was dried over Na_2SO_4 and concentrated. The residue was triturated with acetone, followed by hexanes to afford perylenequinone **4.49** as a dark purple amorphous solid (21.9 mg, 73%): ^{1}H NMR (500 MHz, DMSO-d_6) δ 10.56 (s, 2H), 8.62 (s, 2H), 7.70 (s, 2H), 5.26 (septet, J = 6.3, 2H), 3.68 (s, 6H), 1.40 (d, J = 6.5 Hz, 12H); ^{13}C NMR (125 MHz, DMSO-d_6) δ 178.2, 165.0, 162.4, 152.0, 130.3, 129.4, 128.3, 124.2, 122.2, 119.1, 109.9, 69.3, 62.6, 21.6; IR (film) 3280, 2980, 1725, 1699, 1614, 1573, 1470, 1370, 1305, 1255, 1299 cm^{-1}; HRMS (ESI) *m/z* 547.1605 $[M+H]^+$ (calcd for $C_{30}H_{27}O_{10}$, 547.1604).

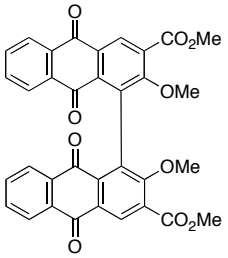

Dimethyl-2,2'-dimethoxy-9,9',10,10'-tetraoxo-9,9',10,10'-tetrahydro-[1,1'-bianthracene]-3,3'-dicarboxylate (**4.53**). Compound **4.32a-c** (20.0 mg, 0.0309) was partially dissolved in toluene (0.5 mL). After the addition of 1-(trimethylsiloxy)-1,3-butadiene (22 μL, 0.123 mmol), the mixture was heated to 50 °C. Additional diene was added as necessary in three portions (12 equiv total) over 2 d. After 2 d, the reaction mixture was concentrated and reconstituted in CH_2Cl_2. Once the mixture was cooled to 0 °C, NEt_3 (10 equiv) was added while exposed to air. After 40 min, the mixture was washed with 1 M HCl and passed through Na_2SO_4. The residue was chromatographed (CH_2Cl_2–5% EtOAc/CH_2Cl_2) to afford **4.53** as a yellow solid (11.8 mg, 65%): mp >250 °C; ^{1}H NMR (500 MHz, $CDCl_3$) δ 8.93 (s, 2H), 8.32 (d, J = 7.6 Hz, 2H), 7.96 (d, J = 7.6 Hz, 2H), 7.77 (t, J = 7.5 Hz, 2H), 7.68 (t, J = 7.5 Hz, 2H), 4.00 (s, 6H), 3.59 (s, 6H); ^{13}C NMR (125 MHz, $CDCl_3$) δ 183.3, 182.0, 165.5, 161.9, 134.7, 134.4, 134.3 (overlapped peaks), 134.2, 133.2, 131.7, 129.9, 128.7, 127.6, 127.3, 62.7, 53.0; IR (film) 1729, 1676, 1267, 1240 cm^{-1}; HRMS (ESI) *m/z* 591.1292 $[M+H]^+$ (calcd for $C_{34}H_{23}O_{10}$, 591.1291).

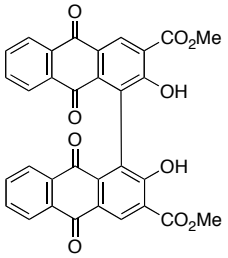

Dimethyl-2,2'-dihydroxy-9,9',10,10'-tetraoxo-9,9',10,10'-tetrahydro-[1,1'-bianthracene]-3,3'-dicarboxylate (**4.54**). A solution of **4.53** (9.1 mg, 0.016 mmol) in CH_2Cl_2 (1.5 mL) was cooled to 0 °C, followed by the dropwise addition of BCl_3 (1 M in hexanes, 3.2 equiv). After 15 min, the reaction was quenched with cold water and the layers separated. The organic layer was washed with brine, dried over Na_2SO_4, and concentrated. The residue was chromatographed (CH_2Cl_2) to afford **4.54** as a yellow solid (6.9 mg, 80%): mp >250 °C; ^{1}H NMR (500 MHz, $CDCl_3$) δ 11.59 (s, 2H), 9.08 (s, 2H), 8.33 (dd, *J* = 7.8 Hz, 0.9 Hz, 2H), 7.99 (dd, *J* = 7.5 Hz, 0.9 Hz, 2H), 7.76 (dt, *J* = 7.5 Hz, 1.3 Hz, 2H), 7.67 (dt, *J* = 7.5 Hz, 1.3 Hz 2H), 4.07 (s, 6H); ^{13}C NMR (125 MHz, $CDCl_3$) δ 183.4, 181.8, 170.2, 163.4, 135.7, 134.3 (overlapped peaks), 134.0, 133.5, 131.0, 127.8, 127.5, 127.3, 126.5, 116.0, 53.3; IR (film) 2918, 1663, 1283, 1252 cm^{-1}; HRMS (ESI) *m/z* 563.0979 $[M+H]^+$ (calcd for $C_{32}H_{19}O_{10}$, 563.0978).

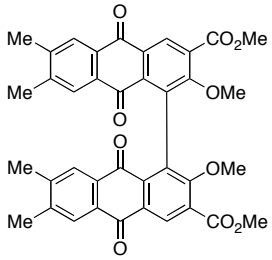

Dimethyl-2,2'-dimethoxy-6,6',7,7'-tetramethyl-9,9',10,10'-tetraoxo-9,9',10,10'-tetrahydro-[1,1'-bianthracene]-3,3'-dicarboxylate (**4.56**). To a suspension of **4.32a-c** (20 mg, 0.031 mmol) in toluene (0.5 mL) was added 2,3-dimethyl-1,3-

butadiene (4 equiv). The reaction mixture was heated to 50 °C. Additional diene was added as needed, in three portions (12 equiv total) over 44 h. After 44 h, the solution was cooled to 0 °C and NEt_3 (> 20 equiv) was added while exposed to air. When the reaction was complete, the mixture was concentrated and chromatographed (30% EtOAc/hexanes) to yield **4.56** as a yellow solid (14 mg, 71%): mp >250 °C; ^{1}H NMR (500 MHz, $CDCl_3$) δ 8.89 (s, 2H), 8.05 (s, 2H), 7.71 (s, 2H), 3.99 (s, 6H), 3.57 (s, 6H), 2.40 (s, 6H), 2.30 (s, 6H); ^{13}C NMR (125 MHz, $CDCl_3$) δ 183.5, 182.2, 165.6, 161.8, 144.4, 144.2, 134.7, 134.5, 132.2, 131.4, 131.2, 130.1, 128.5, 128.4, 128.1, 62.7, 52.9, 20.31, 20.26; IR (film) 2950, 1733, 1673, 1602, 1585, 1281, 1251 cm^{-1}; HRMS (ESI) *m/z* 647.1932 $[M+H]^+$ (calcd for $C_{38}H_{31}O_{10}$, 647.1917).

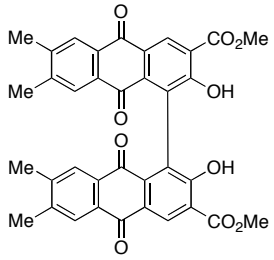

Dimethyl 2,2'-dihydroxy-6,6',7,7'-tetramethyl-9,9',10,10'-tetraoxo-9,9',10,10'-tetrahydro-[1,1'-bianthracene]-3,3'-dicarboxylate (**4.57**). BCl_3 (1M in hexanes, 3.2 equiv) was added dropwise to a solution of **4.56** (10 mg, 0.016 mmol) in CH_2Cl_2 (1.5 mL) at 0 °C. After 15 min, the reaction was quenched with cold water and the layers separated. The organic layer was washed with brine, dried over Na_2SO_4, filtered and concentrated. The residue was chromatographed ($CHCl_3$) on a short column to afford **4.57** as a yellow solid (8.4 mg, 88%): mp >250 °C; ^{1}H NMR (500 MHz, $CDCl_3$) δ 11.55 (s, 2H), 9.03 (s, 2H), 8.06 (s, 2H), 7.74 (s, 2H), 4.05 (s, 6H), 2.41 (s, 6H), 2.30 (s, 6H); ^{13}C NMR (125 MHz, $CDCl_3$) δ 183.6, 182.0, 170.3, 163.3, 144.4, 143.9, 135.8, 132.3,

131.5, 130.7, 128.5, 128.1, 127.8, 126.6, 115.7, 53.2, 20.3, 20.2; IR (film) 3418, 1669, 1291 cm^{-1}; HRMS (ESI) *m/z* 619.1594 $[M+H]^+$ (calcd for $C_{36}H_{27}O_{10}$, 619.1604).

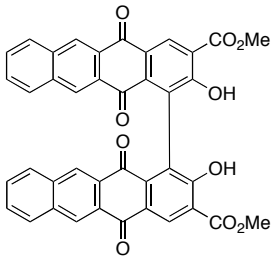

Dimethyl-2,2'-dihydroxy-5,5',12,12'-tetraoxo-5,5',12,12'-tetrahydro-[1,1'-bitetracene]-3,3'-dicarboxylate (**4.60**). A solution of **31a-c** (20 mg, 0.0309 mmol) and sultine **4.58**[138] (15 mg, 0.089 mmol) in toluene (0.5 mL) was heated to 85–90 °C. Additional **4.58** (30 mg, 0.178 mmol) was added after 16 h. After 25 h total, the reaction mixture was concentrated, reconstituted in toluene, and NEt_3 (200 μL) was added with the flask open to air. When the reaction was complete as judged by TLC, the mixture was diluted with CH_2Cl_2 and washed with 1 M HCl. The organic layer was passed through Na_2SO_4 and used without further purification: ^{1}H NMR (300 MHz, $CDCl_3$) δ 9.06 (s, 2H), 8.90 (s, 2H), 8.54 (s, 2H), 8.11 (d, *J* = 8.1 Hz, 2H), 7.93 (d, *J* = 8.1 Hz, 2H), 7.72–7.61 (m, 4H), 4.04 (s, 6H), 3.65 (s, 6H); HRMS (ESI) *m/z* 713.1420 $[M+Na]^+$ (calcd for $C_{42}H_{26}O_{10}Na$, 713.1424).

The crude anthraquinone was dissolved in CH_2Cl_2 (3 mL) and cooled to 0 °C, followed by the dropwise addition of BCl_3 (1 M in hexanes, 90 μL). After 40 min the reaction was quenched with cold water and extracted with CH_2Cl_2. The organic layer was washed with brine, dried over Na_2SO_4 and concentrated. The residue was

(138) Hoey, M. D.; Dittmer, D. C. "A Convenient Synthesis of 1,4-Dihydro-2,3-benzoxathiin 3-oxide, a Useful Precursor of *o*-Quinodimethane" *J. Org. Chem.* **1991**, *56*, 1947–1940.

chromatographed (30% EtOAc/hexanes) to yield **4.60** as a yellow solid (9.3 mg, 45%, 2 steps): mp >250 °C; ^{1}H NMR (500 MHz, $CDCl_3$) δ 11.63 (s, 2H), 9.18 (s, 2H), 8.88 (s, 2H), 8.56 (s, 2H), 8.09 (d, *J* = 8.3 Hz, 2H), 7.91 (d, *J* = 8.1 Hz, 2H), 7.68-7.65 (m, 2H), 7.63-7.59 (m, 2H), 4.09 (s, 6H); ^{13}C NMR (125 MHz, $CDCl_3$) δ 183.4, 181.8, 170.3, 163.4, 136.6, 135.4, 135.2, 131.2, 130.5, 130.2 (overlapped peaks), 130.1, 129.71, 129.68, 129.5, 129.4, 128.2, 127.5, 116.2, 53.3; IR (film) 2923, 2852, 1725, 1676, 1444, 1287, 1252 cm^{-1}; HRMS (ESI) *m/z* 661.1119 [M–H$^-$] (calcd for $C_{40}H_{21}O_{10}$, 661.1135).

7.5 Chapter 5 Experimental

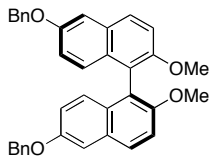

(*S*)-6,6'-Bis(benzyloxy)-2,2'-dimethoxy-1,1'-binaphthalene [(*S*)-**5.6**]. To a solution of (*S*)-**5.5**[15,16] (143 mg, 0.29 mmol, 98% ee) at 0 °C, was added NaH (60%, 62.5 mg, 1.56 mmol), followed by MeI (7 μL, 1.1 mmol) after 10 min. After stirring 2 h at room temperature, the mixture was cooled to 0 °C and quenched with H_2O. This mixture was extracted with EtOAc (× 2) and washed several times with H_2O, followed by brine. The organic layer was dried over Na_2SO_4, filtered, and concentrated. The residue was chromatographed (20% EtOAc/hexanes) to afford (*S*)-**5.6** as a white solid (119 mg, 73%, 98% ee): mp 78–81 ºC; IR (film) ν_{max} 2933, 1596, 1504, 1253 cm^{-1}; ^{1}H NMR (500 MHz, $CDCl_3$) δ 7.85 (2H, d, *J* = 9.0 Hz), 7.48 (4H, d, *J* = 7.4 Hz), 7.42 (2H, d, *J* = 9.1 Hz), 7.40 (4H, t, *J* = 7.5 Hz), 7.34 (2H, t, *J* = 7.3 Hz), 7.27 (2H, d, *J* = 2.5 Hz), 7.05 (2H, d, *J* = 9.3

Hz), 7.0 (2H, dd, J = 9.2 Hz, 2.5 Hz), 5.16 (4H, s), 3.74 (6H, s); ^{13}C NMR (125 MHz, $CDCl_3$) δ 155.4 (C–O ×2), 153.8 (C–O ×2), 137.3 (C ×2), 130.2 (C ×2), 129.7 (C ×2), 128.7 (CH ×4), 128.2 (CH ×2), 128.1 (CH ×2), 127.7 (CH ×4), 127.1 (CH ×2), 120.3 (C ×2), 119.7 (CH ×2), 115.2 (CH ×2), 107.4 (CH ×2), 70.2 (CH_2 ×2), 57.3 (OCH_3 ×2); HRMS *m/z* 527.2219 $[M+H]^+$ (calcd for $C_{36}H_{30}O_4$, 527.2222).

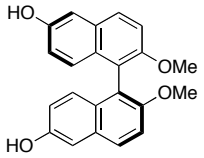

(*S*)-2,2'-Dimethoxy-[1,1'-binaphthalene]-6,6'-diol [(*S*)-**5.3**]. A solution of (*S*)-**5.6** (279 mg, 0.529 mmol) in MeOH/THF (11.2 mL) was evacuated and purged with Ar. To this solution was added Pd/C (10 wt%, 104 mg) and the mixture evacuated and purged three times with H_2. After stirring under hydrogen atmosphere overnight, the mixture was filtered through Celite with EtOAc and concentrated. The residue was passed through a short column of silica (30% EtOAc/hexanes) to afford (*S*)-**5.3** as a white solid (182 mg, 99%): mp >240 ºC decomp; IR (film) ν_{max} 3366, 1598, 1511, 1256 cm^{-1}; ^{1}H NMR (500 MHz, acetone-d_6) δ 8.33 (2H, s), 7.81 (2H, d, J = 9.0 Hz), 7.46 (2H, d, J = 9.0 Hz), 7.23 (2H, d, J = 2.3 Hz), 6.93 (2H, d, J = 9.1 Hz), 6.89 (2H, dd, J = 9.1 Hz, 2.4 Hz), 3.68 (6H, s); ^{13}C NMR (125 MHz, acetone-d_6) δ 154.3 (C–O ×2), 154.0 (C–O ×2), 131.6 (C ×2), 129.7 (C ×2), 128.1 (CH ×2), 127.6 (CH ×2), 121.0, 119.5, 115.9, 109.8, 57.0 (OCH_3 ×2); HRMS *m/z* 347.1284 $[M+H]^+$ (calcd for $C_{22}H_{18}O_4$, 347.1283).

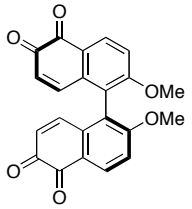

(*S*)-2,2'-Dimethoxy-[1,1'-binaphthalene]-5,5',6,6'-tetraone [(*S*)-**5.2**]. To a solution of (*S*)-**5.3** (15.4 mg, 0.044 mmol) in 0.8 mL DMF was added 2-iodoxybenzoic acid (25.0 mg, 0.089 mmol). The mixture was stirred for 3 h in the dark. Following this time, the mixture was diluted with H_2O and extracted with EtOAc. The organic layer was washed with 25% aqueous $NaHCO_3$, dried over Na_2SO_4, filtered, and concentrated. The residue was chromatographed (5%–10% EtOAc/CH_2Cl_2) to afford (*S*)-**5.2** as an orange solid (16.2 mg, 97%): mp 190 ºC decomp; $[\alpha]_D^{25}$ –42.1 (c 0.054, 98% ee, CH_2Cl_2); UV (CH_2Cl_2) λ_{max} (log ε) 388 (6.91), 270 (6.88); IR (film) ν_{max} 2927, 2850, 1661, 1568, 1468, 1274 cm^{-1}; ^1H NMR (500 MHz, $CDCl_3$) δ 8.29 (2H, d, *J* = 8.7 Hz), 7.10 (2H, d, *J* = 8.7 Hz), 6.97 (2H, d, *J* = 10.4 Hz), 6.34 (2H, d, *J* = 10.4 Hz), 3.86 (6H, s); ^{13}C NMR (125 MHz, $CDCl_3$) δ 181.2 (C=O ×2), 177.7 (C=O ×2), 163.2 (C–O ×2), 141.5 (CH ×2), 135.6 (C ×2), 133.7 (CH ×2), 129.2 (CH ×2), 125.5 (C ×2), 123.3 (C ×2), 112.0 (CH ×2), 56.7 (OCH_3); HRMS *m/z* 375.0877 $[M+H]^+$ (calcd for $C_{22}H_{14}O_6$, 375.0869). X-ray quality crystals of a racemic sample of **5.2** were obtained by slow evaporation from CH_2Cl_2. See Appendix B for crystallographic data. The crystallographic data for *rac*-**5.2** have been deposited at the Cambridge Crystallographic Data Centre with the deposition number 883203. Copies of the data can be obtained, free of charge, on application to the Director, CCDC, 12 Union Road, Cambridge CB21EZ, UK [fax: +44(0)-1233-336033 or e-mail: deposit@ccdc.cam.ac.uk].

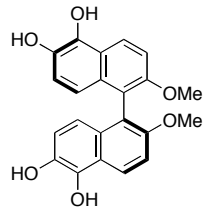

(*S*)-2,2'-Dimethoxy-[1,1'-binaphthalene]-5,5',6,6'-tetraol [(*S*)-**5.1**]. In a separatory funnel, (*S*)-**5.2** (16 mg, 0.043) was dissolved in CH_2Cl_2 (2 mL) and diluted with Et_2O (4 mL). Then, an aqueous solution of $Na_2S_2O_4$ (40 mg/6 mL) was added. The mixture was shaken and additional $Na_2S_2O_4$ (50 mg) was added, followed by shaking until a loss of orange color was observed in the organic layer. After separating the layers, the organic layer was washed with brine, dried over Na_2SO_4, filtered, and concentrated to afford (*S*)-**5.1** as an air-sensitive, off-white solid (98% ee): IR (film) ν_{max} 3375, 2925, 1600, 1518, 1367, 1259, 1095 cm^{-1}; ^1H NMR (300 MHz, acetone-d_6) see Table 5.1; ^{13}C NMR (125 MHz, acetone-d_6) Table 5.1; compound partially oxidized during ionization: HRMS *m/z* 375.0863 $[M–H]^-$ (calcd for $C_{22}H_{15}O_6$, 375.0869).

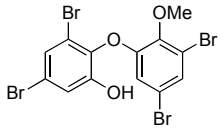

Natural Product Isolate (Tetrabrominated diphenyl ether 5.7). IR (film) ν_{max} 3366, 2930, 1569, 1469, 1393, 1255, 1216, 914 cm^{-1}; ^1H NMR (500 MHz, $CDCl_3$ and CD_3OD) see Table 5.2; ^{13}C NMR (125 MHz, $CDCl_3$) see Table 5.2; HRMS *m/z* 526.7119 $[M–H]^-$ (calcd for $C_{13}H_7Br_4O_3$, 526.7129).

7.7 Chapter 6 Experimental

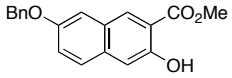

Methyl 7-(benzyloxy)-3-hydroxy-2-naphthoate (6.21). To a solution of commercially available 3,7-dihydroxy-2-naphthoic acid (**6.20**, 12.0 g, 58.8 mmol) in MeOH (264 mL) was added concentrated H_2SO_4 (10.6 mL). After heating at reflux for 3.5 h, the reaction mixture was cooled and poured over ice. The precipitate was filtered, washed with water, and dried to afford methyl 3,7-dihydroxy-2-naphthoate as a yellow solid (11.6 g, 90%). If necessary, the solid was chromatographed (10-20% EtOAc/hexanes). The ^{1}H NMR matched that of the reported compound.[139]

To a solution of methyl 3,7-dihydroxy-2-naphthoate (11.6 g, 53.4 mmol) in acetone (235 mL) was added anhydrous K_2CO_3 (10.7 g) and BnBr (6.3 mL, 53.0 mmol). After heating at reflux 6 h, the reaction mixture was cooled to room temperature and concentrated. Then, water was added to dissolve the K_2CO_3 and the mixture was filtered. The solid was washed with 1 M HCl and water, followed by a minimal amount of cold acetone and EtOAc to afford **6.21** as a yellow solid (9.1 g, 55% yield). The ^{1}H NMR matched that of the reported compound[140]: ^{1}H NMR (500 MHz, $CDCl_3$) δ 10.27 (s, 1H), 8.34 (s, 1H), 7.60 (d, J = 9.1 Hz, 1H), 7.47 (m, 2H), 7.40 (m, 2H), 7.34 (m, 1H), 7.27 (dd, J = 9.0 Hz, 2.6 Hz, 1H) 7.26 (s, 1H), 7.14 (d, J = 2.5 Hz, 1H); ^{13}C NMR (125 MHz,

(139) West, K. R.; Ludlow, R. F.; Corbett, P. T.; Besenius, P.; Mansfeld, F. M.; Cormack, P. A. G.; Sherrington, D. C.; Goodman, J. M.; Stuart, M. C. A.; Otto, S. "Dynamic Combinatorial Discovery of a [2]-Catenane and its Guest-Induced Conversion into a Molecular Square Host" *J. Am. Chem. Soc.*, **2008**, *130*, 10834–10835).

(140) Mercep, M.; Mesic, M., Hrvacic, B.; Elenkov, I. J.; Malnar, I.; Markovic, S.;; Klonkay, A. C.; Filipovic, A., Simicic, L.; "Substituted Furochromene Compounds of Antiinflammatory Action" PCI Int. Appl. WO2005/10006-A1, Feb. 3, 2005.

$CDCl_3$) δ 170.5, 155.4, 155.2, 136.9, 133.9, 130.8, 128.8, 128.2, 128.0, 127.9, 127.7, 123.2, 114.5, 112.0, 107.9, 70.3, 52.7; IR (film) 3167, 3066, 2958, 1676, 1522, 1437, 1290, 1220 cm^{-1}.

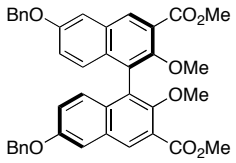

(*R*)-Dimethyl-6,6'-bis(benzyloxy)-2,2'-dimethoxy-[1,1'-binaphthalene]-3,3'-dicarboxylate [(*R*)-**6.23**]. To a solution of **6.21** (200 mg, 0.649 mmol) in $ClCH_2CH_2Cl$ (6.5 mL) was added 4 Å MS and (*S,S*)-**1.12** (22.6 mg, 10 mol %). The reaction mixture was stirred at room temperature under an O_2 atmosphere. After 25 h, the mixture was diluted with CH_2Cl_2 and washed twice with 1 M HCl. The layer organic was washed with brine, dried over Na_2SO_4, and concentrated. The residue was chromatographed (20% hexanes/CH_2Cl_2 to CH_2Cl_2) to afford (*R*)-**6.22** as a yellow powder (120 mg, 60%).

Racemate (*rac*-**6.23**). To a solution of **6.21** (50.0 mg, 0.162 mmol) in $ClCH_2CH_2Cl$ (1.6 mL) was added CuCl(OH)TMEDA (3.8 mg, 10 mol %). The reaction mixture was warmed in a 40 ºC oil bath and stirred under O_2. After 4.5 h, the mixture was cooled and diluted with CH_2Cl_2. Following the addition of 50% 1 M HCl, the layers were separated. The organic layer was washed with brine, dried over Na_2SO_4, and concentrated. The residue was chromatographed (CH_2Cl_2) to afford *rac*-**6.22** as a yellow powder (43.5 mg, 87%): mp 203-204 ºC; ^{1}H NMR (500 MHz, $CDCl_3$) δ 10.55 (s, 2H), 8.54 (s, 2H), 7.47 (m, *J* = 7.8 Hz 4H), 7.40 (m, *J* = 7.5 Hz, 0.8 Hz, 4H), 7.34 (m, *J* = 7.3 Hz, 0.8 Hz, 2H), 7.27 (d, *J* = 2.4 Hz, 2H), 7.13 (dd, *J* = 9.3 Hz, 2.5 Hz, 2H), 7.09 (d, *J* =

9.3 Hz, 2H), 5.16 (s, 4H), 4.04 (s, 6H); ^{13}C NMR (125 MHz, $CDCl_3$) δ 170.7, 155.5, 152.9, 136.9, 133.1, 131.3, 128.8, 128.2, 128.1, 127.7, 126.5, 123.2, 117.5, 114.5, 108.5, 70.3, 52.8; IR (film) 3213, 2958, 1684, 1506, 1444, 1220 cm^{-1}; HRMS (ESI) *m/z* 637.1851 $[M+Na]^+$ (calcd for $C_{38}H_{30}O_8Na$, 637.1838).

A suspension of (*R*)-**6.22** or *rac*-**6.22** (120 mg, 0.195 mmol) in DMF (5.4 mL) was cooled to 0 ºC. To this suspension was added NaH (60%, 39.1 mg, 0.978 mmol) and MeI (60 μL, 0.96 mmol). After 3.5 h at room temperature, the mixture was cooled to 0 ºC and quenched with cold water. Then, the mixture was extracted with EtOAc and washed with 1 M HCl, followed by water and brine. The organic layer was dried over Na_2SO_4, filtered, and concentrated. The residue was chromatographed (20-30% EtOAc/hexanes) to afford (*R*)-**6.23** or *rac*-**6.23** as a white foam (120 mg, 96%, 83% ee): $[\alpha]_D^{25}$ +22.0 (*c* 0.10, 83% ee, CH_2Cl_2). ^{1}H NMR (500 MHz, $CDCl_3$) δ 8.41 (s, 2H), 7.48 (d, *J* = 7.2 Hz, 4H), 7.41 (t, *J* = 7.2, 4H), 7.35 (t, *J* = 7.3 Hz, 2H), 7.33 (d, *J* = 2.2 Hz, 2H), 7.11 (dd, *J* = 9.2 Hz, 2.4 Hz, 2H), 7.07 (d, *J* = 9.3 Hz, 2H), 5.18 (s, 4H), 3.99 (s, 6H), 3.47 (s, 6H); ^{13}C NMR (125 MHz, $CDCl_3$) δ 167.2, 156.6, 152.9, 136.7, 132.0, 131.3, 130.8, 128.8, 128.3, 127.7, 127.3, 126.6, 125.4, 121.9, 108.2, 70.3, 62.2, 52.5; IR (film) 2950, 1730, 1591, 1498, 1228, 1004 cm^{-1}; HRMS (ESI) *m/z* 665.2183 $[M+Na]^+$ (calcd for $C_{40}H_{34}O_8Na$, 665.2151).

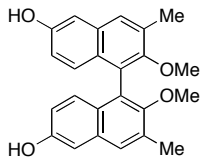

2,2'-Dimethoxy-3,3'-dimethyl-[1,1'-binaphthalene]-6,6'-diol (**6.24**). A solution of **6.23** (500 mg, 0.778 mmol) in toluene (39 mL) was cooled to 0 ºC. To this solution was slowly added DIBALH (6.2 mL, 6.2 mmol, 1 M in hexanes). After 50 min at 0 °C, the mixture was quenched with cold water. Then, 1 M HCl was added, and the mixture extracted with EtOAc (×3). The organic layer was washed with 1 M HCl, followed by brine and dried over Na_2SO_4. After concentration, the diol was obtained as a white solid and used without further purification.

The diol (0.778 mmol) was suspended in THF (10 mL). Then, 10 mL of MeOH was added, followed by Pd/C (10 wt%, 100 mg), and the flask evacuated and backfilled with H_2 (×3). The reaction was stirred under H_2 atmosphere until complete by TLC. The reaction was not complete after 23 h, so it was filtered through Celite™ and resubjected to the same conditions. When complete by TLC, the reaction mixture was filtered through Celite™ with EtOAc and chromatographed (30% EtOAc) to afford **6.24** (272 mg, 93% over 2 steps): mp >136 ºC; ^{1}H NMR (500 MHz, $CDCl_3$) δ 7.60 (s, 2H), 7.09 (d, *J* = 2.5 Hz, 2H), 7.01 (d, *J* = 9.0, 2H), 6.77 (dd, *J* = 9.0, 2.5 Hz, 2H), 3.32 (s, 6H), 2.51 (s, 6H); ^{13}C NMR (125 MHz, $CDCl_3$) δ 153.9, 152.7, 132.5, 132.0, 128.5, 128.2, 127.9, 125.0, 117.2, 109.1, 60.3, 17.4; IR (film) 3381, 2924, 2850, 1232, 1107 cm^{-1}; HRMS (ESI) *m/z* 397.1411 $[M+Na]^+$ (calcd for $C_{24}H_{22}O_4Na$, 397.1416).

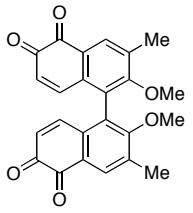

2,2'-Dimethoxy-3,3'-dimethyl-[1,1'-binaphthalene]-5,5',6,6'-tetraone (**6.25**). Compound **6.24** (100 mg, 0.267 mmol) was dissolved in DMF (4.8 mL). Then, 2-iodoxybenzoic acid (153 mg 0.547 mmol) was added. After 2.5 h, the mixture was diluted with water and extracted with EtOAc. The organic layer was washed with 25% aq $NaHCO_3$, followed by brine and drying over Na_2SO_4. After concentration, the residue was chromatographed (CH_2Cl_2 to 5% CH_2Cl_2/EtOAc to afford **6.25** (90 mg, 83%): mp >180 ºC (decomp); ^{1}H NMR (500 MHz, $CDCl_3$) δ 8.13 (s, 2H), 7.00 (d, J = 10.5 Hz, 2H), 6.32 (d, J = 10.4 Hz, 2H), 3.57 (s, 6H), 2.44 (s, 6H); ^{13}C NMR (125 MHz, $CDCl_3$) δ 180.6, 178.2, 162.8, 141.6, 134.9, 134.8, 133.3, 128.5, 128.3, 128.0, 60.6, 17.0; IR (film) 3059, 2950, 1661, 1583, 1468, 1282 cm^{-1}; HRMS (ESI) *m/z* 403.1176 $[M+H]^+$ (calcd for $C_{24}H_{19}O_6$, 403.1182).

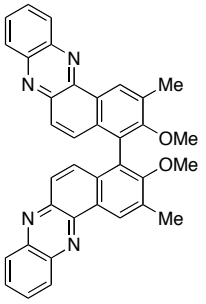

3,3'-Dimethoxy-2,2'-dimethyl-4,4'-bibenzo[*a*]phenazine (**6.27**). A suspension of **6.25** (112.2 mg, 0.276 mmol) and *o*-phenylenediamine (60.2 mg, 0.557 mmol) in EtOH (7.5 mL) and CH_2Cl_2 (3.7 mL) was stirred at room temperature. When the reaction

was complete by TLC, the solution was concentrated and the residue chromatographed (30% EtOAc/hexanes) to afford **6.27** as a yellow solid (138.7 mg, 96%): mp > 186 ºC (decomp); ^{1}H NMR (500 MHz, $CDCl_3$) δ 9.49 (s, 2H), 8.42 (dd, *J* = 8.7, 1.5 Hz, 2H), 8.26 (dd, *J* = 8.1, 1.0 Hz, 2H), 7.91-7.84 (m, 4H), 7.76 (d, *J* = 9.6 Hz, 2H), 7.47 (d, *J* = 9.6 Hz, 2H), 3.48 (s, 6H), 2.75 (s, 6H); ^{13}C NMR (125 MHz, $CDCl_3$) δ 159.0, 143.3, 142.9, 142.7, 142.4, 133.1, 132.6, 130.8, 130.1, 130.0, 129.8, 129.4, 128.4, 127.8, 127.3, 126.7, 60.5, 17.5; IR (film) 3060, 2925, 2850, 1489, 1444, 1348, 1255, 1127 cm^{-1}; HRMS (ESI) *m/z* 547.2134 $[M+H]^+$ (calcd for $C_{36}H_{27}N_4O_2$, 547.2134).

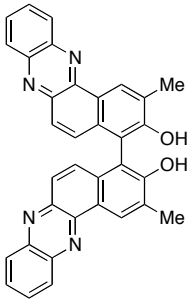

2,2'-Dimethyl-[4,4'-bibenzo[*a*]phenazine]-3,3'-diol (**6.28**). A solution of **6.27** (12.9 mg, 0.0247 mmol) in 0.5 mL CH_2Cl_2 was cooled to –70 °C. Then, a solution of BBr_3 (0.15 mL, 1 M in CH_2Cl_2, 6 equiv) was added. After warming to room temperature, the reaction was stirred until complete by TLC. When complete, cold water was added and the mixture extracted with CH_2Cl_2. The organic layer was washed with satd aq $NaHCO_3$, followed by brine and drying over Na_2SO_4. After concentration, the resultant solid was washed with CH_2Cl_2 to afford **6.28** as an amorphous yellow powder (10.3 mg, 81%): ^{1}H NMR (360 MHz, DMSO-d_6) δ 9.27 (s, 2H), 9.06 (bs, 2H), 8.40 (d, *J* = 8.1, 2H), 8.24 (d, *J* = 8.7 Hz, 2H), 8.01-7.91 (m, 4H), 7.73 (d, *J* = 9.6 Hz, 2H), 7.30 (d, *J* = 9.6 Hz, 2H), 2.62 (s, 6H); ^{13}C NMR (125 MHz, DMSO-d_6) δ 156.4, 142.2, 142.1, 141.7,

141.3, 132.5, 130.8, 130.3, 129.7, 129.0, 128.9, 127.6, 126.9, 126.3, 123.4, 118.2, 17.7; IR (film) 3300-2800, 3061, 2922, 1595, 1490, 1443, 1358, 1129 cm^{-1}; HRMS (ESI) *m/z* 519.1843 $[M+H]^+$ (calcd for $C_{34}H_{23}N_4O_2$, 519.1821).

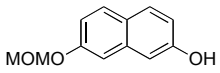

7-(Methoxymethoxy)naphthalen-2-ol (**6.30**). To a cooled solution (0 °C) of naphthalene-2,7-diol (10.00 g, 62.4 mmol) in DMF (50 mL) was added NaH (60%, 3 g, 1.2 equiv). After stiring for 0.5 h at room temperature, the mixture was cooled to 0 °C and MOMCl (5.1 mL, 1.1 equiv) was added slowly. Following 1 h, the reaction mixture was quenched with satd aq NH_4Cl and extracted with EtOAc. The organic layer was washed with satd aq NH_4Cl and brine, followed by drying over Na_2SO_4. After concentrating, the residue was chromatographed (15% EtOAc/hexanes) to yield **6.30** as a white solid (4.24 g, 33% yield). ^1H NMR matches that of the reported compound.[141] mp 62-64 °C; ^{13}C NMR (125 MHz, $CDCl_3$) δ 155.8, 154.1, 135.9, 129.7, 129.5, 125.1, 116.7, 116.0, 109.1, 108.8, 94.6, 56.2.

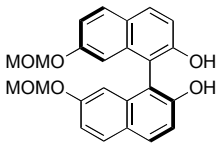

(*S*)-**7,7'-bis(methoxymethoxy)-[1,1'-binaphthalene]-2,2'-diol** [(*S*)-**6.31**]. In a modified procedure,[15,16] oxygen was bubbled through a solution of **6.30** (50.0 mg, 0.245

(141) Ballart, B.; Martí, J.; Velasco, D.; López-Calahorra, F.; Pascual, J.; García, M. L.; Cabré, F.; Mauleón, D. "Synthesis and Pharmacological Evaluation of New 4-[2-(7-Heterocycle-methoxynaphtalen-2-ylmethoxy)ethyl]benzoic Acids as LTD4-Antagonists" *Eur. J. Med. Chem*. **2000**, *35*, 439–447.

mmol) and **V1** catalyst (13.5 mg, 0.0184 mmol) in CH_2Cl_2 (1.2 mL). After 1 d, the solution was concentrated and the residue chromatographed (20-30% EtOAc/hexanes) to afford (*S*)-**6.31** (40.5 mg, 81%, 75% ee). This sample was combined with other samples (2.087 g, 75% ee) and dissolved in a minimum CH_2Cl_2, followed by addition of an equal volume of 30% EtOAc/hexanes and the solution cooled to –20 °C. After overnight, the liquid was decanted to afford (*S*)-**6.31** (929.3 mg, 99% ee): $[\alpha]_D^{25}$ +194 (*c* 0.10, 97% ee, CH_2Cl_2); ^{1}H NMR (500 MHz, $CDCl_3$) δ 7.85 (d, *J* = 8.9 Hz, 2H), 7.79 (d, *J* = 8.9 Hz, 2H), 7.21 (d, *J* = 8.9 Hz, 2H), 7.15 (dd, *J* = 8.9 Hz, 2.4 Hz, 2H), 6.66 (d, *J* = 2.4 Hz, 2H), 5.14 (s, 2H), 4.99 (d, *J* = 6.5 Hz, 2H), 4.98 (d, *J* = 6.6 Hz, 2H), 3.32 (s, 6H); ^{13}C NMR (125 MHz, $CDCl_3$) δ 156.6, 153.4, 134.8, 131.2, 130.2, 125.6, 116.0, 115.9, 110.2, 108.2, 94.6, 56.1; IR (film) 3419, 2956, 2827, 1621, 1513, 1151 cm^{-1}; HRMS (ESI) *m/z* 407.1480 $[M+H]^+$ (calcd for $C_{24}H_{23}O_6$, 407.1495). CSP HPLC (Chiralpak IA, 1.0 mL/min, 85:15 hexanes:*i*-PrOH): $t_R(S)$ = 26.9 min, $t_R(R)$ = 40.3 min.

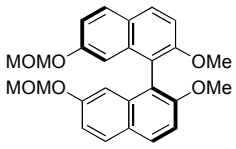

(*S*)-**2,2'-dimethoxy-7,7'-bis(methoxymethoxy)-1,1'-binaphthalene** [(*S*)-**6.32**]. Biaryl (*S*)-**6.31** (4.54 g, 11.2 mmol) was dissolved in DMF (127 mL) and cooled to 0 °C, before adding NaH (60%, 1.34 g, 3 equiv). After 10 min, MeI (2.1 mL, 3 equiv) was added and the mixture was warmed to room temperature. When the reaction was complete, it was cooled to 0 °C and quenched with cold water. The mixture was extracted with EtOAc, then washed with water and brine. The organic layer was dried over Na_2SO_4, filtered and concentrated. The residue was chromatographed (20%

hexanes/CH_2Cl_2 to CH_2Cl_2) to afford (*S*)-**6.32** as a white resin (4.23 g, 87%): $[\alpha]_D^{25}$ +44.4 (*c* 0.075, 99% ee, CH_2Cl_2); ^{1}H NMR (500 MHz, $CDCl_3$) δ 7.90 (d, *J* = 9.0 Hz, 2H), 7.79 (d, *J* = 8.9 Hz, 2H), 7.33 (d, *J* = 9.0 Hz, 2H), 7.11 (dd, *J* = 8.9 Hz, 2.5 Hz, 2H), 6.66 (s, *J* = 2.4 Hz), 5.00 (d, *J* = 6.4 Hz, 2H), 4.95 (d, *J* = 6.4 Hz, 2H) 3.77 (s, 6H), 3.32 (s, 6H); ^{13}C NMR (125 MHz, acetone-d_6) δ 156.6, 156.5, 136.1, 130.5, 130.0, 126.4, 119.4, 116.8, 112.9, 109.1, 95.0, 56.6, 55.9; IR (film) 2935, 1623, 1509, 1258, 1150, 1003 cm^{-1}; HRMS (ESI) *m/z* 435.1810 $[M+H]^+$ (calcd for $C_{26}H_{27}O_6$, 435.1808).

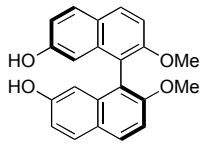

(*S*)-**2,2'-dimethoxy-[1,1'-binaphthalene]-7,7'-diol** [(*S*)-**6.33**]. Biaryl (*S*)-**6.32** (330.6 mg, 0.761 mmol) was dissolved in THF (33.6 mL) and actively purged with Ar for 10 min. After cooling the solution to 0 °C, conc. HCl (8.9 mL) was added slowly. After 6 h at 0 °C, the reaction mixture was poured over ice and extracted with EtOAc. The organic layer was washed with satd aq $NaHCO_3$, followed by brine. After drying over Na_2SO_4, the organic solution was concentrated and a white solid was precipitated upon addition of hexanes. This mixture was concentrated to afford (*S*)-**6.33** as an off-white solid (252.0 mg, 96%). ^{1}H NMR matches that of the reported structure.[142]

(142) Reeder, J.; Castro, P. P.; Knobler, C. B. "Chiral Recognition of Cinchona Alkaloids at the Minor and Major Grooves of 1,l'-Binaphthyl Receptors." *J. Org. Chem*. **1994**, *59*, 3151–3160.

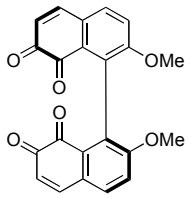

(*S*)-**2,2'-dimethoxy-[1,1'-binaphthalene]-7,7',8,8'-tetraone** [(*S*)-**6.34**]. To a solution of biaryl (*S*)-**6.33** (506 mg, 1.460 mmol) in DMF (13.2 mL) was added 2-iodoxybenzoic acid (839 mg, 2.05 equiv). After 7 h, the reaction mixture was diluted with water and the suspension vacuum filtered. The solid was washed well with water to afford (*S*)-**6.34** as a red solid (511 mg, 93%): mp >250 °C; $[\alpha]_D^{25}$ +3337 (*c* 0.020, 99% ee, CH_2Cl_2); ^{1}H NMR (500 MHz, $CDCl_3$) δ 7.43 (d, *J* = 10.1 Hz, 2H), 7.38 (d, *J* = 8.4 Hz, 2H), 7.12 (d, *J* = 8.4 Hz, 2H), 6.26 (d, *J* = 10.1 Hz, 2H), 3.71 (s, 6H); ^{13}C NMR (125 MHz, $CDCl_3$) δ 180.9, 179.5, 159.6, 147.0, 132.2, 131.8, 130.0, 128.6, 124.7, 115.9, 56.4; IR (film) 2927, 2858, 1661, 1568, 1475, 1267 cm^{-1}; HRMS (ESI) *m/z* 375.0868 $[M+H]^+$ (calcd for $C_{22}H_{15}O_6$, 375.0869).

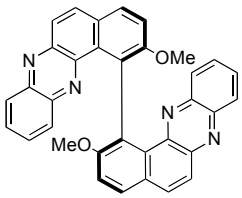

(*S*)-**2,2'-dimethoxy-1,1'-bibenzo[*a*]phenazine** [(*S*)-**6.35a**]. A suspension of **6.34** (50.0 mg, 0.134 mmol) and *o*-phenylenediamine (36.0 mg, 0.333 mmol) in glacial AcOH (1.4 mL) was stirred at room temperature until the reaction was complete as judged by TLC (3 h –6.5 h). When complete, the reaction mixture was diluted with water and extracted with EtOAc. The organic layer was washed with satd aq $NaHCO_3$, followed by

water and brine. After drying over Na_2SO_4, the solution was concentrated and the residue chromatographed (30-50% EtOAc/hexanes) to afford (*S*)-**6.35a** as a yellow solid (54.6 mg, 79%, 99% ee). X-ray quality crystals from the racemate were obtained by passing *rac*-**6.35a** through a short column of silica (30-50% EtOAc/hexanes) and allowing a concentrated fraction to evaporate slowly: mp >230 ºC (decomp); $[\alpha]_D^{25}$ +1033 (*c* 0.050, 99% ee, CH_2Cl_2); ^{1}H NMR (500 MHz, $CDCl_3$) δ 8.18 (d, *J* = 8.6 Hz, 2H), 8.13 (d, *J* = 9.3 Hz, 2H), 7.96 (dd, *J* = 8.5, 0.5 Hz, 2H), 7.72 (d, *J* = 9.3 Hz, 2H), 7.61 (d, *J* = 8.6 Hz, 2H), 7.56 (m, *J* = 8.3, 1.4 Hz, 2H), 7.43 (m, *J* = 8.3, 1.4 Hz, 2H), 6.88 (dd, *J* = 8.5, 0.8 Hz, 2H), 3.68 (s, 6H); ^{13}C NMR (125 MHz, $CDCl_3$) δ 158.1, 144.4, 144.2, 141.3, 140.2, 134.7, 130.3, 130.0, 129.8, 129.6, 128.9, 128.7, 128.6, 128.5, 124.4, 114.2, 56.9; IR (film) 2931, 2833, 1495, 1266, 1024 cm^{-1}; HRMS (ESI) *m/z* 519.1838 $[M+H]^+$ (calcd for $C_{34}H_{23}N_4O_2$, 519.1821). CSP HPLC (Chiralpak IA, 1.0 mL/min, 80:20 hexanes:*i*-PrOH): $t_R(R)$ = 6.5 min, $t_R(S)$ = 8.2 min.

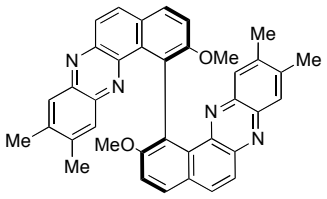

(*S*)-**2,2'-dimethoxy-9,9',10,10'-tetramethyl-1,1'-bibenzo[*a*]phenazine** [(*S*)-**6.35b**]. Quinone (*S*)-**6.34** (30 mg, 0.0801 mmol) and 4,5-dimethylbenzene-1,2-diamine (27.3 mg, 0.200 mmol) were suspended in AcOH (0.8 mL). After 3 h, the mixture was diluted with water and extracted with CH_2Cl_2. The organic layer was washed with satd aq $NaHCO_3$, dried over Na_2SO_4 and concentrated. The residue was chromatographed (3% EtOAc/CH_2Cl_2 to 5% EtOAc/CH_2Cl_2) to afford (*S*)-**6.35b** as a yellow solid (37 mg,

80%): mp >250 °C; $[\alpha]_D^{25}$ +1407 (*c* 0.051, 99% ee, CH_2Cl_2); ^1H NMR (500 MHz, $CDCl_3$) δ 8.15 (d, *J* = 8.6 Hz, 2H), 8.09 (d, *J* = 9.3 Hz, 2H), 7.69 (d, *J* = 9.1 Hz, 2H), 7.68 (s, 2H), 7.58 (d, *J* = 8.6 Hz, 2H), 6.60 (s, 2H), 3.66 (s, 6H), 2.35 (s, 6H), 2.29 (s, 6H); ^{13}C NMR (125 MHz, $CDCl_3$) δ 157.9, 143.8, 143.6, 140.5, 140.4, 139.5, 139.2, 133.7, 130.5, 129.8, 128.9, 128.6, 128.4, 127.1, 124.5, 114.1, 57.0, 20.6 (two peaks); IR (film) 2938, 1594, 1494, 1267, 1026 cm^{-1}; HRMS (ESI) *m/z* 575.2451 $[M+H]^+$ (calcd for $C_{38}H_{31}N_4O_2$, 575.2447).

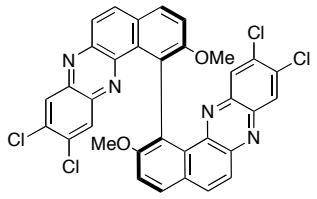

(*S*)-**9,9',10,10'-tetrachloro-2,2'-dimethoxy-1,1'-bibenzo[*a*]phenazine** [(*S*)-**6.35c**]. Quinone (*S*)-**6.34** (300 mg, 0.801 mmol) and 4,5-dichlorobenzene-1,2-diamine (312 mg, 1.763 mmol) were suspended in AcOH (4 mL). After 5 h, the mixture was diluted with water and extracted with EtOAc. The organic layer was washed with satd aq $NaHCO_3$ and brine. Following drying over Na_2SO_4 and concentration, the residue was chromatographed (CH_2Cl_2 to 5% EtOAc/CH_2Cl_2) to afford (*S*)-**6.35c** as a yellow solid (446 mg, 85%): mp >250°C; $[\alpha]_D^{25}$ +1837 (*c* 0.066, 99% ee, CH_2Cl_2); ^1H NMR (500 MHz, $CDCl_3$) δ 8.19 (d, *J* = 8.6 Hz, 2H), 8.17 (d, *J* = 9.3 Hz, 2H), 8.10 (s, 2H), 7.68 (d, *J* = 9.3 Hz, 2H), 7.62 (d, *J* = 8.6 Hz, 2H), 6.93 (s, 2H), 3.69 (s, 6H); ^{13}C NMR (125 MHz, $CDCl_3$) δ 158.2, 145.1, 144.7, 140.1, 138.7, 135.7, 134.2, 133.1, 129.9, 129.8, 129.7, 129.1, 129.04, 128.97, 124.1, 114.5, 56.8; IR (film) 2926, 2835, 1594, 1531, 1487, 1439,

1266, 1100, 1026 cm^{-1}; HRMS (ESI) *m/z* 655.0237 $[M+H]^+$ (calcd for $C_{34}H_{19}N_4O_2Cl_4$, 655.0262).

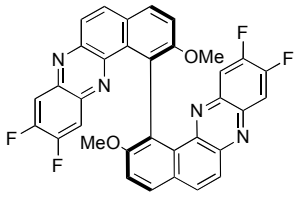

(*S*)-**9,9',10,10'-tetrafluoro-2,2'-dimethoxy-1,1'-bibenzo[*a*]phenazine** [(*S*)-**6.35d**]. A suspension of quinone (*S*)-**6.34** (50.8 mg, 0.136 mmol) and 4,5-difluorobenzene-1,2-diamine (42.4 mg, 0.294 mmol) in AcOH (0.7 mL) was stirred. After 3 h, the mixture was diluted with water and extracted with EtOAc. The organic layer was washed with satd aq $NaHCO_3$, dried over Na_2SO_4, and concentrated. The residue was chromatographed (10-20% EtOAc/hexanes) to afford (*S*)-**6.35d** as a yellow solid (70.9 mg, 89%): mp 162-165 °C; $[\alpha]_D^{25}$ +1333 (*c* 0.023, 99% ee, CH_2Cl_2); ^1H NMR (500 MHz, $CDCl_3$) δ 8.19 (d, *J* = 8.6 Hz, 2H), 8.16 (d, *J* = 9.3 Hz, 2H), 7.69-7.66 (m, 4H), 7.62 (d, *J* = 8.6 Hz, 2H), 6.53 (dd, $^2J_{FH}$ = 8.5 Hz, $^3J_{FH}$ = 8.5 Hz, 2H), 3.70 (s, 6H); ^{13}C NMR (125 MHz, $CDCl_3$) δ 158.1, 153.4 (dd, $^1J_{FC}$ = 94.6 Hz, $^2J_{FC}$ = 17.1 Hz), 151.3 (dd, $^1J_{FC}$ = 94.1 Hz, $^2J_{FC}$ = 16.8 Hz), 144.4, 144.0, 138.8 (d, $^3J_{FC}$ = 11.0 Hz), 137.3 (d, $^3J_{FC}$ = 11.0 Hz), 135.0, 129.74, 129.69, 128.92, 128.89, 124.0, 114.4, 114.3 (d, $^2J_{FC}$ = 12.8 Hz), 113.4 (d, $^2J_{FC}$ = 16.0 Hz), 56.9; IR (film) 3059, 2935, 2835, 1489, 1309, 1268, 1022 cm^{-1}; HRMS (ESI) *m/z* 591.1451 $[M+H]^+$ (calcd for $C_{34}H_{19}N_4O_2F_4$, 591.1444).

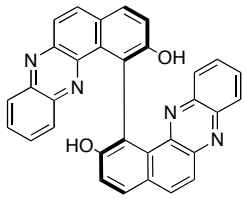

(*S*)-**[1,1'-bibenzo[*a*]phenazine]-2,2'-diol** [(*S*)-**6.36a**]. A solution of phenazine (*S*)-**6.35a** (266 mg, 0.514 mmol) in CH_2Cl_2 (20 mL) was cooled to 0 °C, followed by addition of BBr_3 (4 mL, 1M in CH_2Cl_2, 8 equiv). The mixture was stirred at room temperature, with occasional sonication. When the reaction was complete, it was quenched with water and extracted with CH_2Cl_2. The organic layer was washed with 25% aq $NaHCO_3$ and brine, followed by drying over Na_2SO_4. After concentration, the residue was chromatographed (0.5% MeOH/CH_2Cl_2 to 1% MeOH/ CH_2Cl_2) to afford (*S*)-**6.36a** as a yellow-orange solid (215 mg, 85%, 99% ee): mp 198-200 ºC; $[\alpha]_D^{25}$ + 1408 (*c* 0.050, 99% ee, CH_2Cl_2); ^{1}H NMR (500 MHz, acetone-d_6) δ 8.25 (d, J = 9.3 Hz, 2H), 8.19 (d, J = 8.5 Hz, 2H), 7.93 (d, J = 8.5 Hz, 2H), 7.69 (d, J = 9.2 Hz, 2H), 7.62 (m, 2H), 7.60 (d, J = 8.4 Hz, 2H), 7.50 (m, 2H), 6.93 (d, J = 8.1, 2H); ^{13}C NMR (125 MHz, acetone-d_6) δ 157.1, 144.9, 144.8, 141.8, 140.8, 135.9, 131.9, 130.7, 130.4, 130.3, 129.7, 129.4, 129.1, 126.4, 124.0, 120.0; IR (film) 3500-2500, 2916, 1592, 1495, 1293 cm^{-1}; HRMS (ESI) *m/z* 491.1492 $[M+H]^+$ (calcd for $C_{32}H_{19}N_4O_2$, 491.1508). CSP HPLC (Chiralpak IA, 1.0 mL/min, 80:20 hexanes:*i*-PrOH): t_R(*R*) = 15.9 min, t_R(*S*) = 27.2 min.

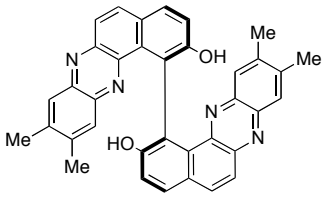

(*S*)-**9,9',10,10'-tetramethyl-[1,1'-bibenzo[*a*]phenazine]-2,2'-diol** [(*S*)-**6.36b**]. A solution of phenazine (*S*)-**6.35b** (40 mg, 0.070 mmol) in CH_2Cl_2 (2 mL) was cooled to 0 °C. To this solution was slowly added BBr_3 (1 M CH_2Cl_2, 0.42 mL, 6 equiv). The mixture was stirred at room temperature with occasional sonication. When the reaction was complete, it was quenched with cold water and extracted with CH_2Cl_2. The organic layer was washed with 25% aq $NaHCO_3$, and brine, followed by drying over Na_2SO_4. The concentrated sample was chromatographed (20-30% acetone/hexanes) to afford (*S*)-**6.36b** as a yellow-orange solid (24.2 mg, 64%): mp >170 °C (decomp); $[\alpha]_D^{25}$ +2551 (*c* 0.080, 99% ee, CH_2Cl_2); ^{1}H NMR (500 MHz, $CDCl_3$) δ 8.08 (d, *J* = 8.6 Hz, 2H), 7.99 (d, *J* = 9.3 Hz, 2H), 7.69 (d, *J* = 9.2 Hz, 2H), 7.63 (s, 2H), 7.58 (d, *J* = 8.5 Hz, 2H), 6.57 (s, 2H), 5.98 (bs, 2H), 2.29 (s, 6H), 2.26 (s, 6H); ^{13}C NMR (125 MHz, $CDCl_3$) δ 154.8, 143.2, 142.5, 141.2, 140.7, 139.9, 139.7, 133.0, 130.9, 130.4, 129.1, 128.4, 127.0, 124.8, 121.0, 118.7, 20.6 (two peaks); IR (film) 3500-2300, 2921, 2845, 1595, 1495, 1310, 1287 cm^{-1}; HRMS (ESI) *m/z* 545.1969 $[M–H]^-$ (calcd for $C_{36}H_{25}N_4O_2$, 545.1978).

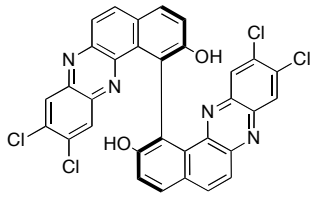

(*S*)-**9,9',10,10'-tetrachloro-[1,1'-bibenzo[*a*]phenazine]-2,2'-diol** [(*S*)-**6.36c**]. A solution of phenazine (*S*)-**6.35c** (50 mg, 0.076 mmol) was dissolved in CH_2Cl_2 (2 mL) and cooled to 0 °C. To this solution was slowly added BBr_3 (1 M CH_2Cl_2, 0.46 mL, 6 equiv). The mixture was stirred at room temperature, with occasional sonication. When the reaction was complete, it was quenched with cold water and extracted with CH_2Cl_2. The organic layer was washed with 25% aq $NaHCO_3$, and brine. Following drying over Na_2SO_4 and concentration, the residue was chromatographed (20% acetone/hexanes). The solid was concentrated from MeOH to afford (*S*)-**6.36c** as an amorphous orange powder (38.6 mg, 81%). X-ray quality crystals were obtained by slow vapor diffusion of hexanes into a solution of (*S*)-**6.36c** in THF: $[\alpha]_D^{25}$ +1854 (*c* 0.062, 99% ee, CH_2Cl_2); ^{1}H NMR (500 MHz, acetone-d_6) δ 8.29 (d, J = 9.3 Hz, 2H), 8.23 (d, J = 8.5 Hz, 2H), 7.93 (s, 2H), 7.64 (d, J = 8.5 Hz, 2H), 7.55 (d, J = 9.2 Hz), 6.98 (s, 2H); ^{13}C NMR (125 MHz, acetone-d_6) δ 157.4, 145.8, 145.4, 140.7, 139.2, 136.7, 133.9, 133.0, 131.3, 130.5, 130.4, 130.0, 129.5, 126.7, 123.9, 120.5; IR (film) 3400-2500, 2923, 1486, 1441, 1305, 1102 cm^{-1}; HRMS (ESI) *m/z* 626.9950 $[M+H]^+$ (calcd for $C_{32}H_{15}N_4O_2Cl_4$, 626.9949).

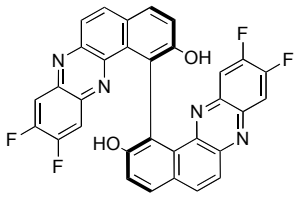

(*S*)-**9,9',10,10'-tetrafluoro-[1,1'-bibenzo[*a*]phenazine]-2,2'-diol** [(*S*)-**6.36d**]. A solution of phenazine (*S*)-**6.35d** (50.0 mg, 0.0847 mmol) in CH_2Cl_2 (8.0 mL) was cooled to 0 °C. To this solution was slowly added BBr_3 (1 M CH_2Cl_2, 0.51 mL, 6 equiv). After 3 h stirring at room temperature, the mixture was sonicated and additional BBr_3 (1 M CH_2Cl_2, 0.25 mL) was added. After a total of 7 h the reaction was quenched with satd aq $NaHCO_3$ and extracted with EtOAc. The organic layer was washed brine, dried over Na_2SO_4 and concentrated. If necessary the residue was resubjected to the reaction conditions. The residue was chromatographed (30% EtOAc/hexanes) to afford (*S*)-**6.36d** as a yellow-orange powder (38.9 mg, 80%): mp >168 °C (decomp); $[\alpha]_D^{25}$ +977 (*c* 0.05, 99% ee, CH_2Cl_2); ^{1}H NMR (500 MHz, $CDCl_3$) δ 8.14 (d, J = 8.6 Hz, 2H), 8.07 (d, J = 9.3 Hz, 2H), 7.67 (d, J = 9.3 Hz, 2H), 7.63 (d, J = 8.6 Hz, 2H), 7.60 (dd, $^2J_{FH}$ = 8.5 Hz, $^3J_{FH}$ = 8.5 Hz, 2H), 6.49 (dd, $^2J_{FH}$ = 8.5 Hz, $^3J_{FH}$ = 8.5 Hz, 2H), 5.93 (bs, 2H); ^{13}C NMR (125 MHz, $CDCl_3$) δ 155.1, 153.7 (dd, $^1J_{FC}$ = 95.0 Hz, $^2J_{FC}$ = 17.5 Hz), 151.6 (dd, $^1J_{FC}$ = 93.8 Hz, $^2J_{FC}$ = 17.5 Hz), 143.7, 142.8, 139.0 (d, $^3J_{FC}$ = 11.3 Hz), 137.6 (d, $^3J_{FC}$ = 11.3 Hz), 134.3, 130.9, 130.2, 129.3, 124.5, 121.0, 119.5, 114.3 (d, $^2J_{FC}$ = 16.3 Hz), 113.4 (d, $^2J_{FC}$ = 17.5 Hz); IR (film) 3400-2800, 3058, 1595, 1490, 1319, 1228, 1206 cm^{-1}; HRMS (ESI) *m/z* 563.1130 $[M+H]^+$ (calcd for $C_{32}H_{15}N_4O_2F_4$, 563.113.

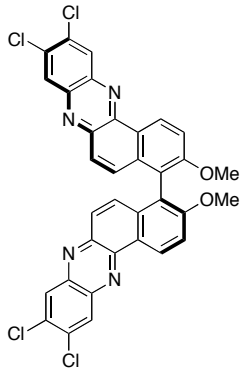

(*S*)-**9,9',10,10'-tetrachloro-3,3'-dimethoxy-4,4'-bibenzo[*a*]phenazine** [(*S*)-**6.39**]. A suspension of quinone (*S*)-**5.2** (20 mg, 0.053 mmol, 99% ee) and 4,5-dichlorobenzene-1,2-diamine (18.9 mg, 0.107 mmol) in AcOH (0.3 mL) was stirred at room temperature. After 1 h, the mixture was diluted with water and extracted with CH_2Cl_2. The organic layer was washed with brine, passed through Na_2SO_4, and concentrated. The residue was chromatographed (CH_2Cl_2 to 5% EtOAc/ CH_2Cl_2) to afford phenazine (*S*)-**6.39** as a yellow resin (35 mg, quantitative): $[\alpha]_D^{25}$ –482 (*c* 0.066, 99% ee, CH_2Cl_2); ^{1}H NMR (500 MHz, $CDCl_3$) δ 9.51 (d, *J* = 9.1 Hz, 2H), 8.49 (s, 2H), 8.34 (s, 2H), 7.68 (d, *J* = 9.7 Hz, 2H), 7.63 (d, *J* = 9.2 Hz, 2H), 7.43 (d, *J* = 9.7 Hz, 2H), 3.9 (s, 6H); ^{13}C NMR (125 MHz, $CDCl_3$) δ 159.4, 143.8, 143.8, 141.1, 140.8, 134.6, 134.4, 134.2, 131.9, 130.0, 129.7, 127.9, 127.9, 124.9, 121.2, 112.8, 56.5; IR (film) 2924, 1471, 1272 cm^{-1}; HRMS (ESI) *m/z* 655.0262 $[M+H]^+$ (calcd for $C_{34}H_{19}N_4O_2$, 655.0262).

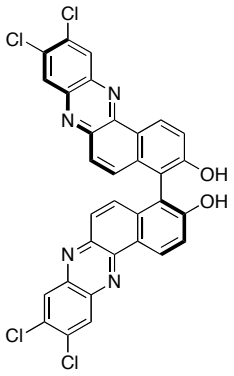

(*S*)-**9,9',10,10'-tetrachloro-[4,4'-bibenzo[*a*]phenazine]-3,3'-diol** [(*S*)-**6.40**]. A solution of phenazine (*S*)-**6.39** (15 mg, 0.0229 mmol) in CH_2Cl_2 (2.6 mL) was cooled to 0 °C, before adding BBr_3 (1 M in CH_2Cl_2 CH_2Cl_2, 0.14 mL, 6 equiv). After 7 h, the reaction was quenched satd aq $NaHCO_3$ and extracted with CH_2Cl_2. The organic layer was washed with brine and concentrated. It was necessary to resubject the residue to the same reaction conditions. The residue was chromatographed on a short column of silica (30% EtOAc/hexanes) to afford (*S*)-**6.40** as a yellow amorphous solid (13.3 mg, 92%): ^{1}H NMR (500 MHz, DMSO-d_6) δ 10.34 (bs, 2H), 9.26 (d, J = 9.0 Hz, 2H), 8.64 (s, 2H), 8.55 (s, 2H), 7.74 (d, J = 9.7 Hz, 2H), 7.62 (d, J = 8.9 Hz, 2H), 7.45 (d, J = 9.6 Hz, 2H); ^{13}C NMR (125 MHz, DMSO-d_6) δ 158.1, 143.0, 142.8, 140.3, 140.0, 134.2, 133.0, 132.3, 132.1, 129.6, 129.5, 126.8, 126.6, 122.6, 118.8, 117.9; IR (film) 3150, 2921, 1578, 1471, 1341, 1168, 1103 cm^{-1}; HRMS (ESI) *m/z* 626.9974 $[M+H]^+$ (calcd for $C_{32}H_{15}N_4O_2Cl_4$, 626.9949).

APPENDIX A: Spectroscopic Data

7.1 Chapter 1

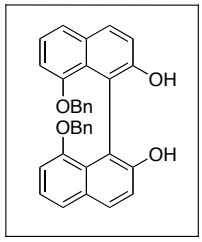

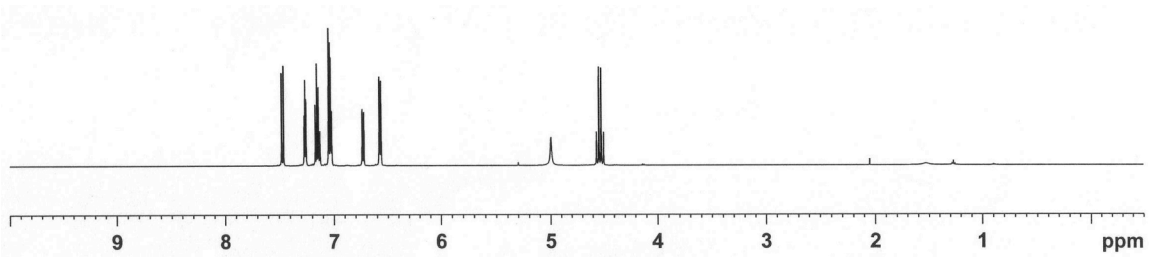

Figure A1.17a_1 ^{1}H NMR Spectrum of Compound **1.17a** (500 MHz, $CDCl_3$).

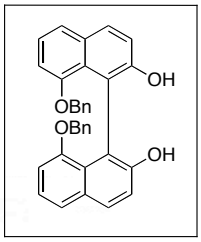

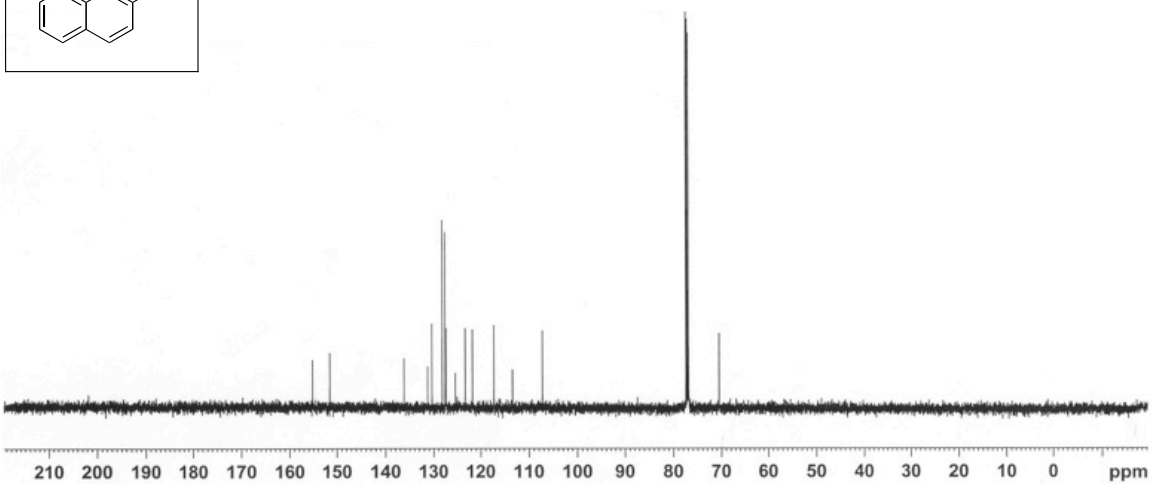

Figure A1.17a_2 ^{13}C NMR Spectrum of Compound **1.17a** (125 MHz, $CDCl_3$).

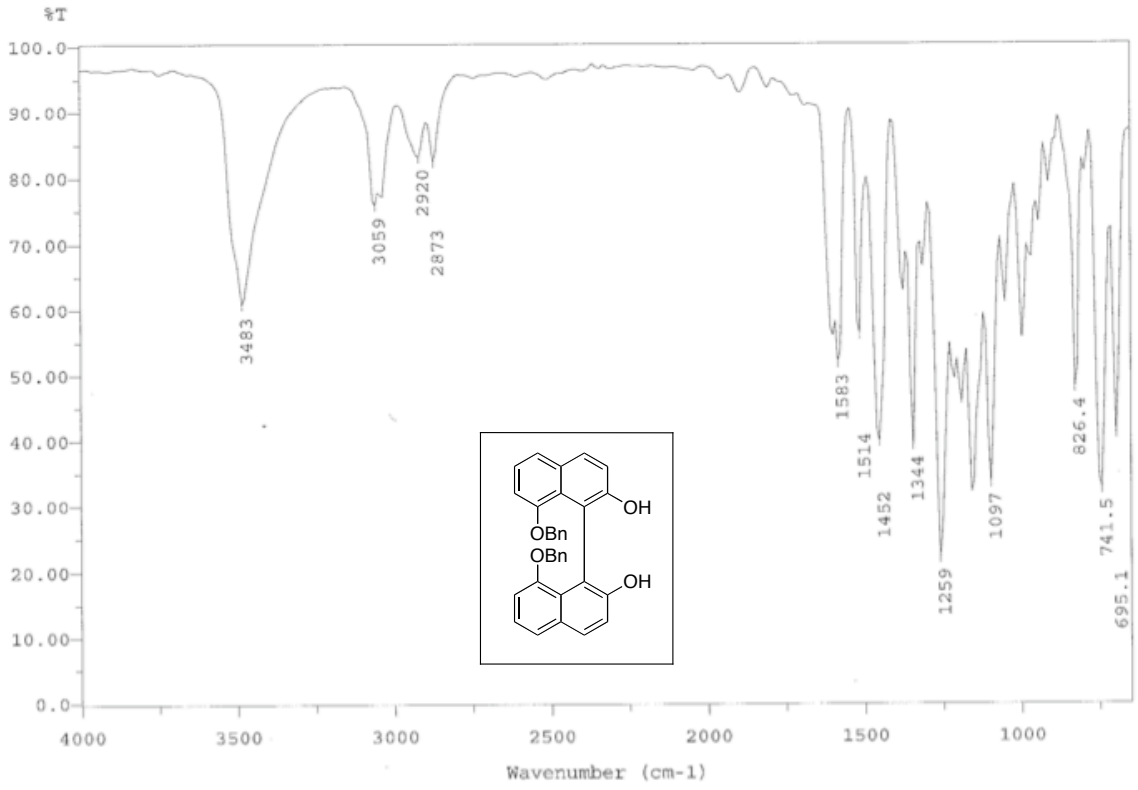

Figure A1.17a_3 IR Spectrum of Compound **1.17a** (film).

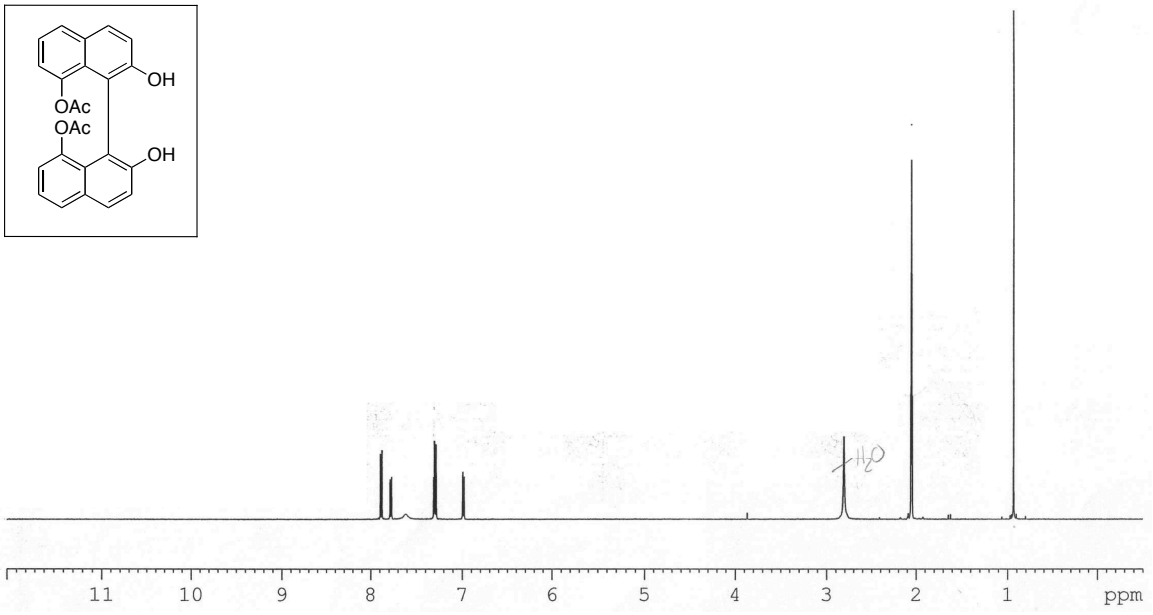

Figure A 1.17b_1 ^{1}H NMR Spectrum of Compound **1.17b** (500 MHz, acetone-d_6).

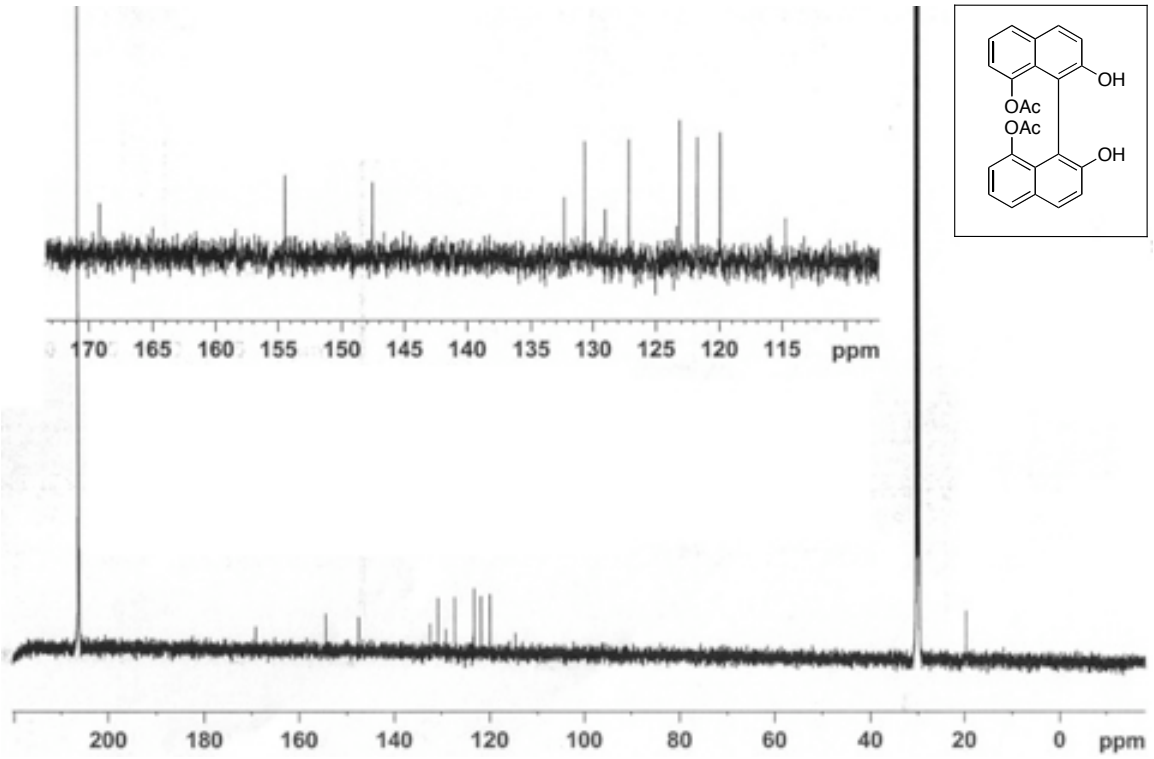

Figure A1.17b_2 ^{13}C NMR Spectrum of Compound **1.17b** (125 MHz, acetone-d_6).

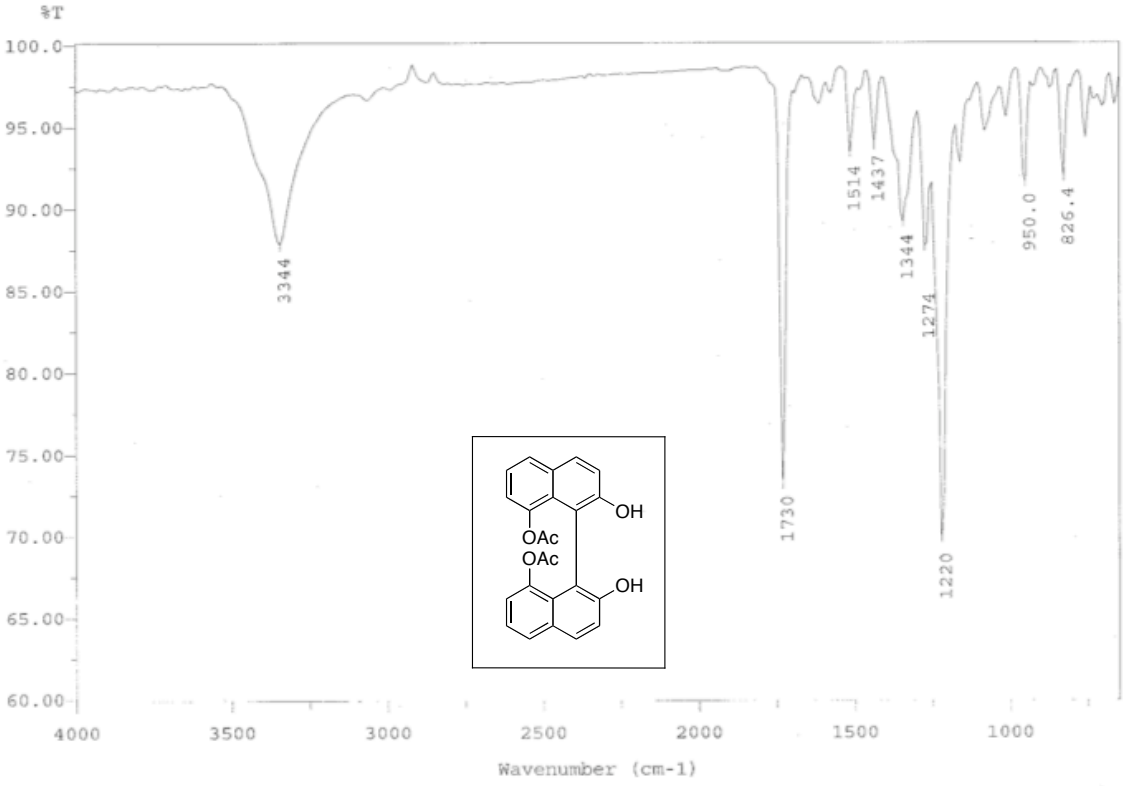

Figure A1.17b_3 IR Spectrum of Compound **1.17b** (film).

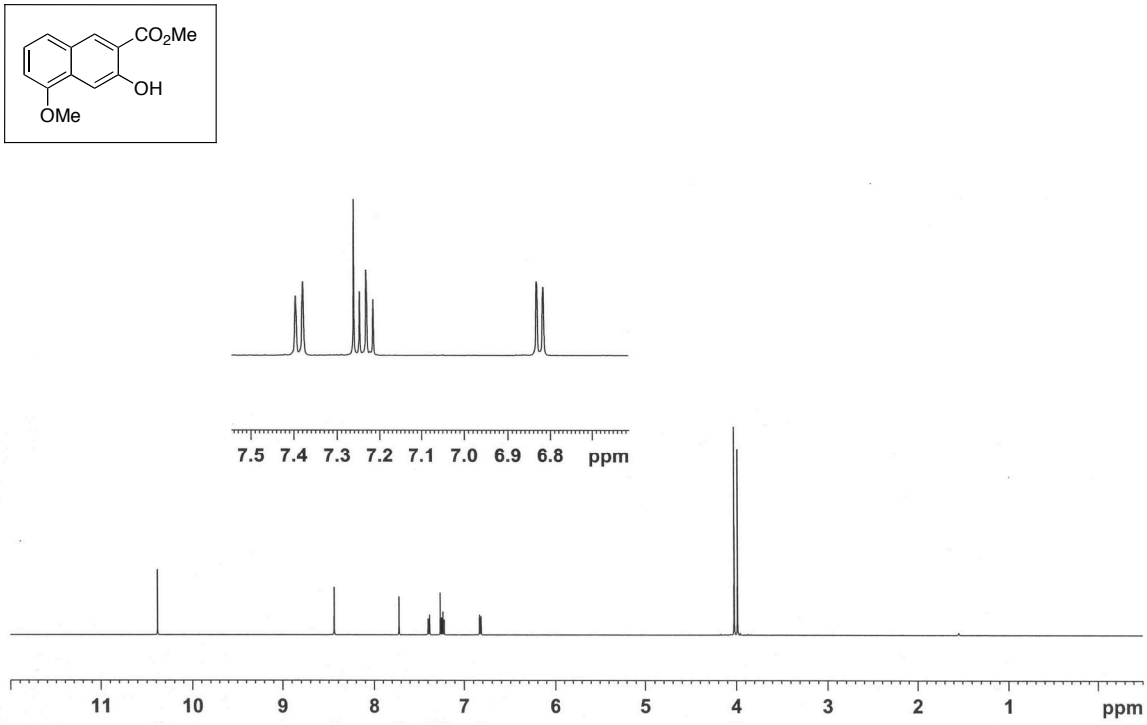

Figure A1.20_1 ^{1}H NMR Spectrum of Compound **1.20** (500 MHz, $CDCl_3$).

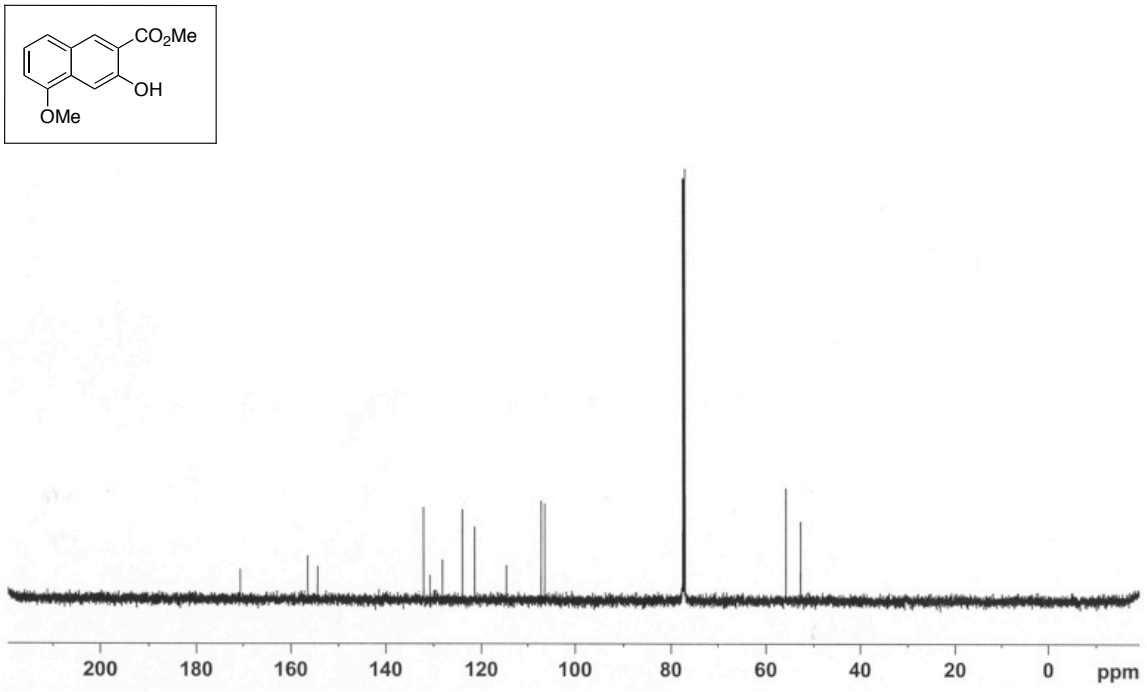

Figure A1.20_2 ^{13}C NMR Spectrum of Compound **1.20** (125 MHz, $CDCl_3$).

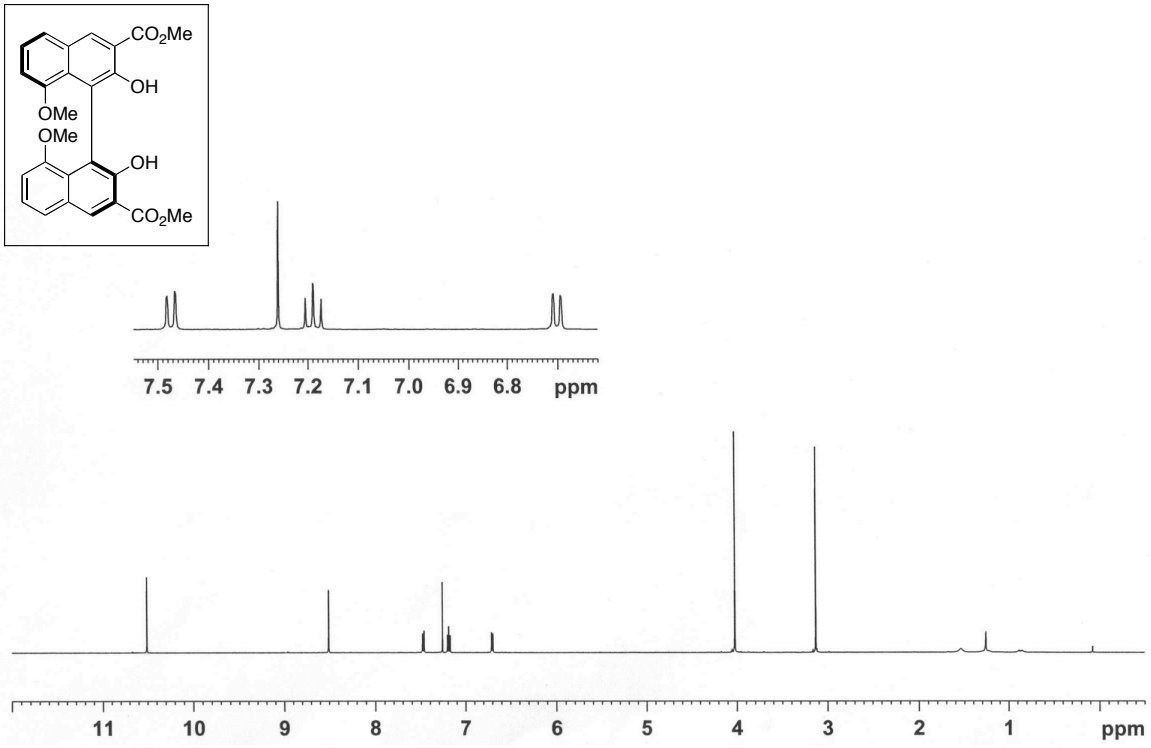

Figure A1.21_1 ^{1}H NMR Spectrum of Compound (*S*)-**1.21** (500 MHz, $CDCl_3$).

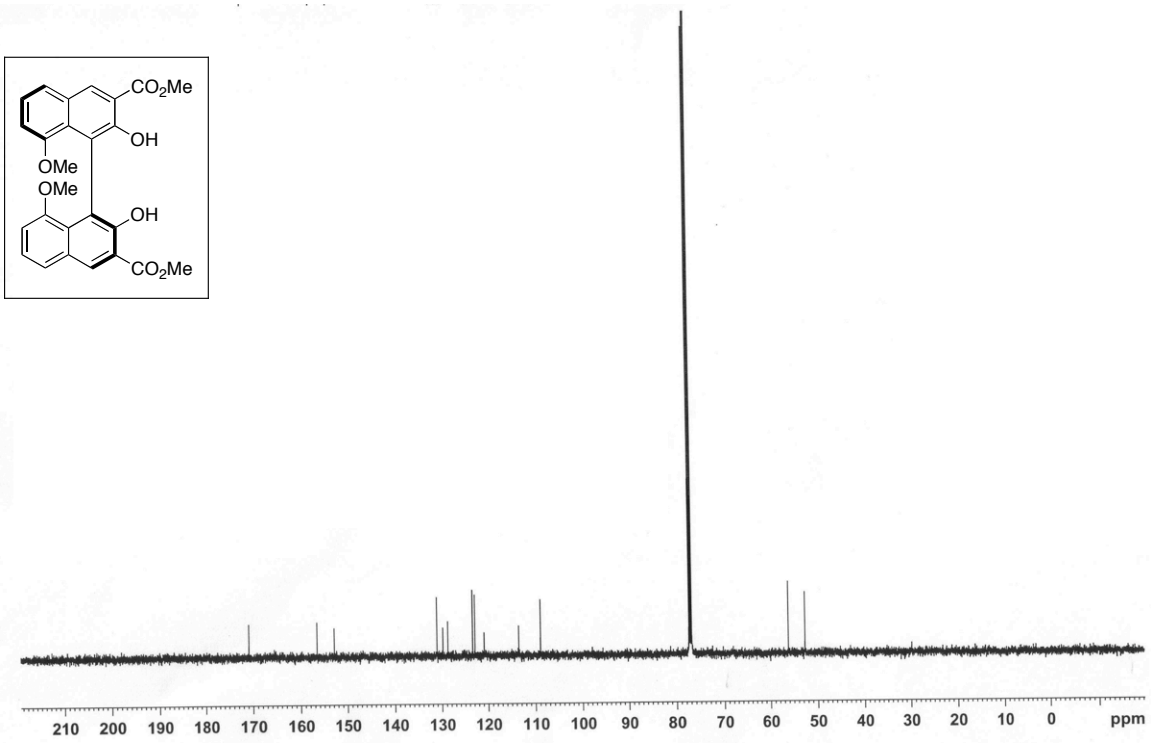

Figure A1.21_2 ^{13}C NMR Spectrum of Compound (*S*)-**1.21** (125 MHz, $CDCl_3$).

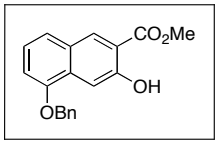

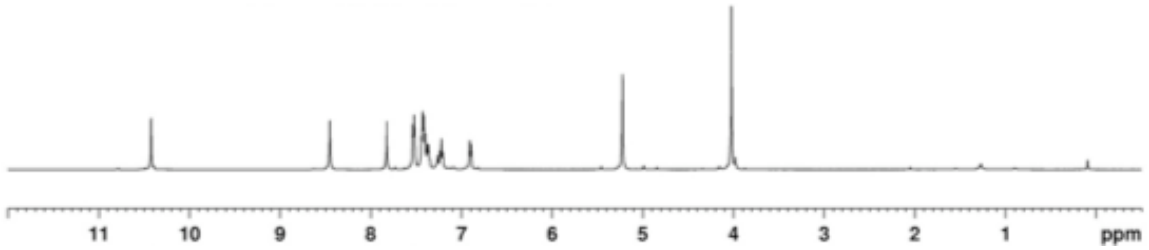

Figure A1.22_1 ^{1}H NMR Spectrum of Compound **1.22** (500 MHz, $CDCl_3$).

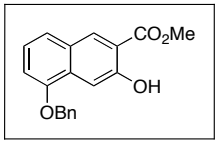

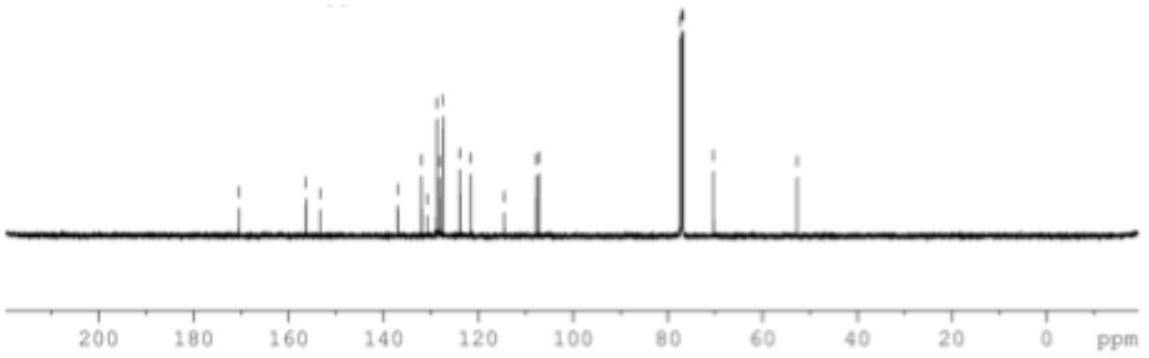

Figure A1.22_2 ^{13}C NMR Spectrum of Compound **1.22** (125 MHz, $CDCl_3$).

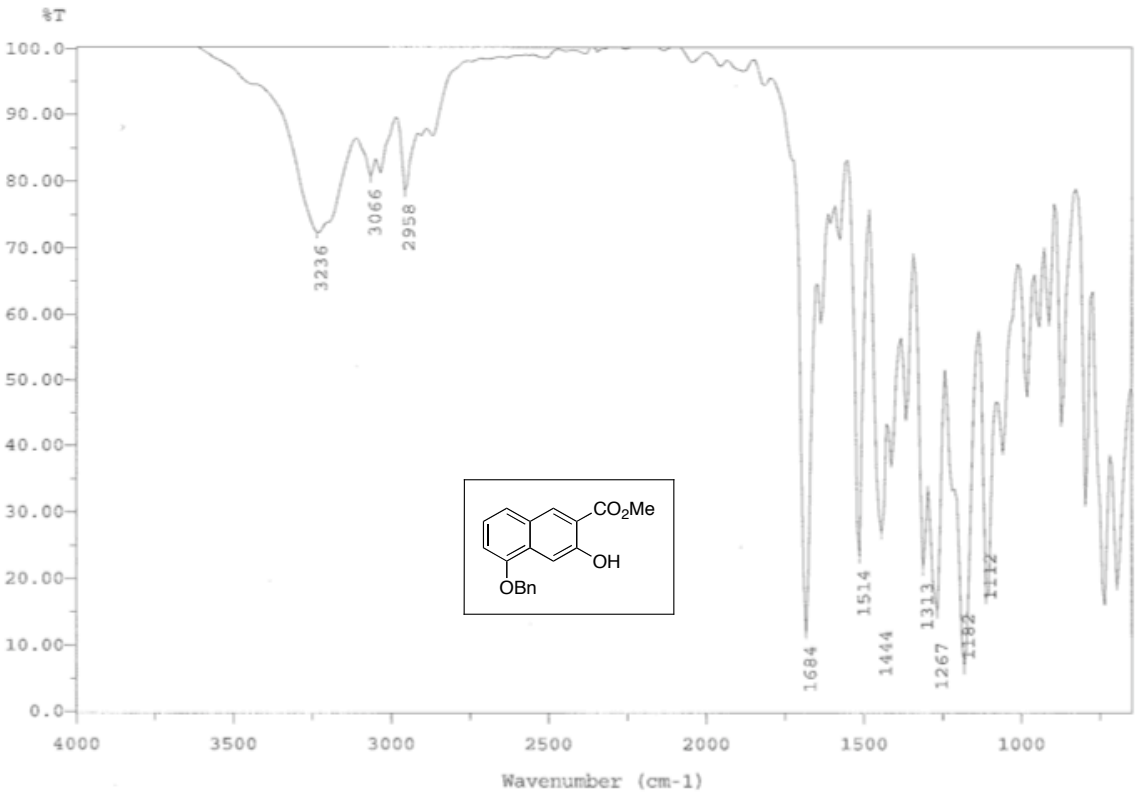

Figure A1.22_3 IR Spectrum of Compound **1.22** (film).

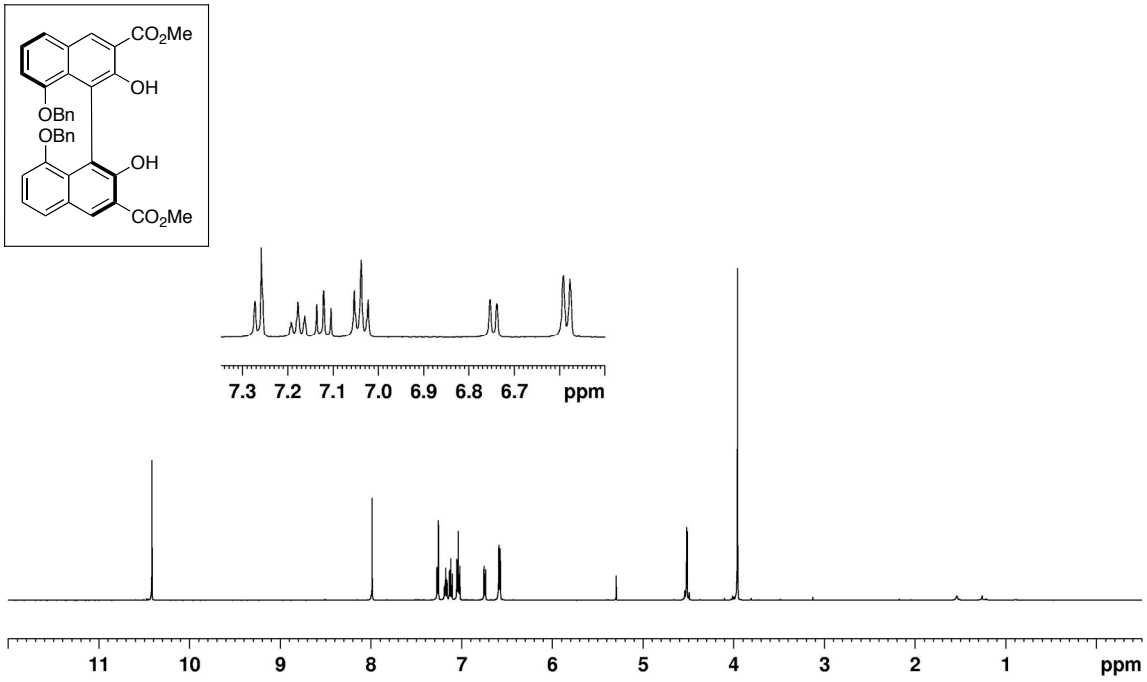

Figure A1.23_1 ^{1}H NMR Spectrum of Compound (*S*)-**1.23** (500 MHz, $CDCl_3$).

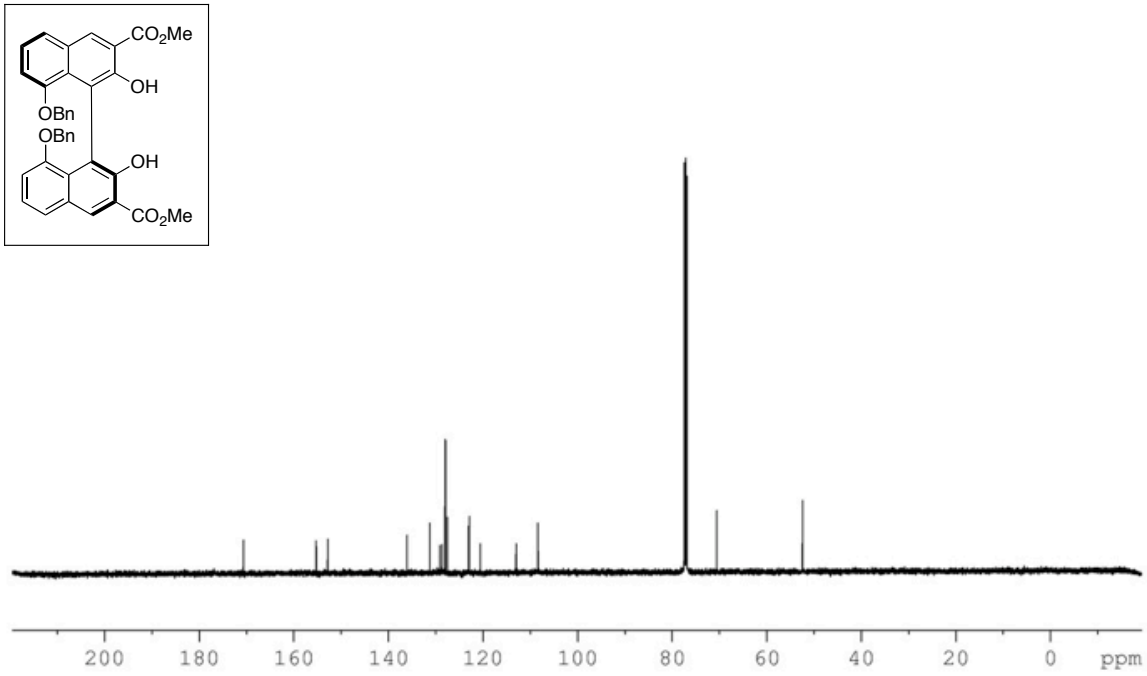

Figure A1.23_2 ^{13}C NMR Spectrum of Compound (*S*)-**1.23** (125 MHz, $CDCl_3$).

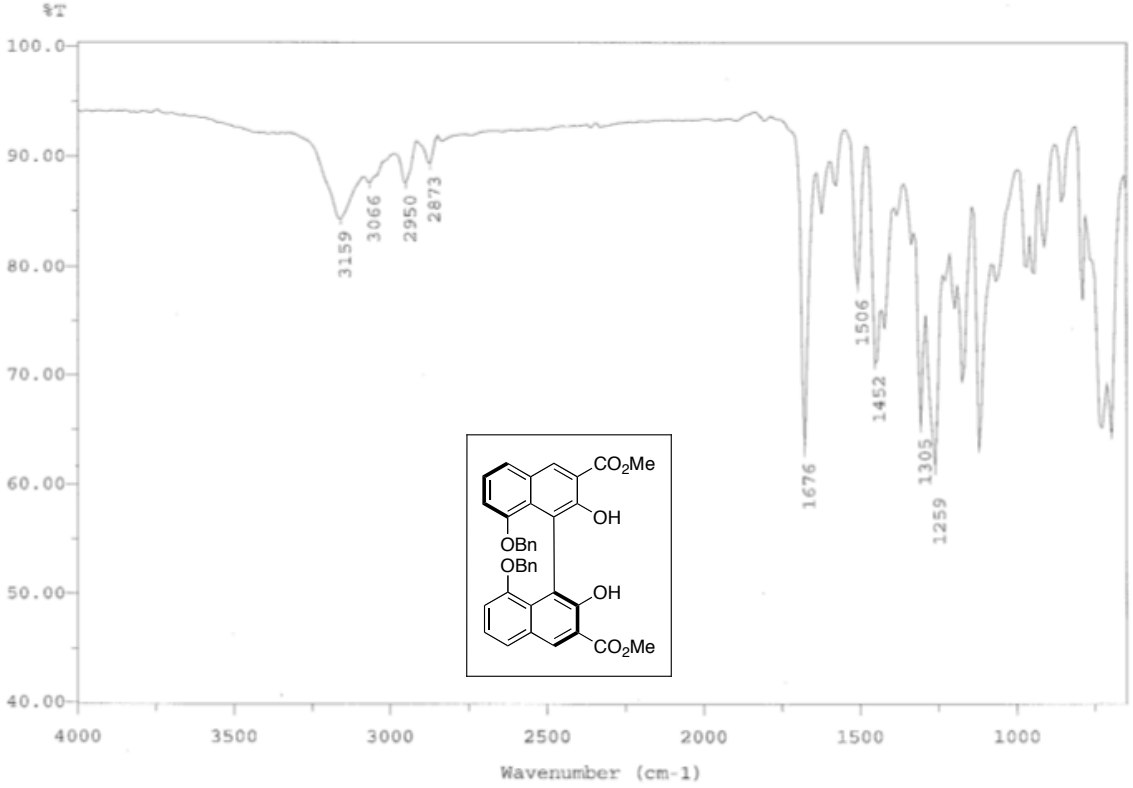

Figure A1.23_3 IR Spectrum of Compound (*S*)-**1.23** (film).

7.2 Chapter 2

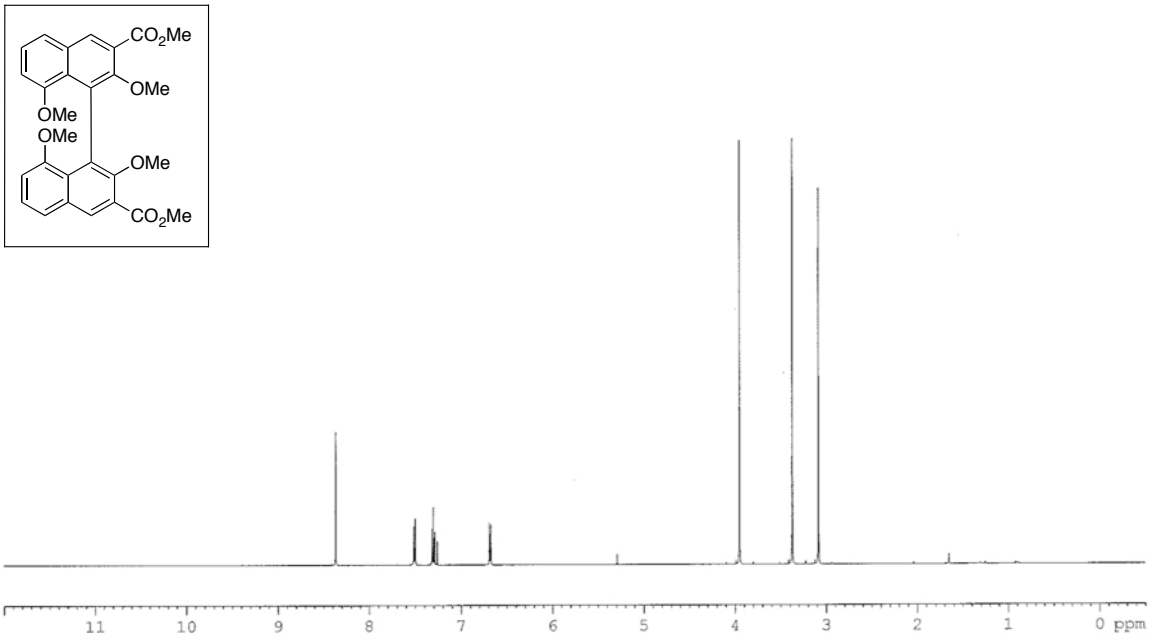

Figure A2.1_1 ^{1}H NMR Spectrum of Compound **2.1** (500 MHz, $CDCl_3$).

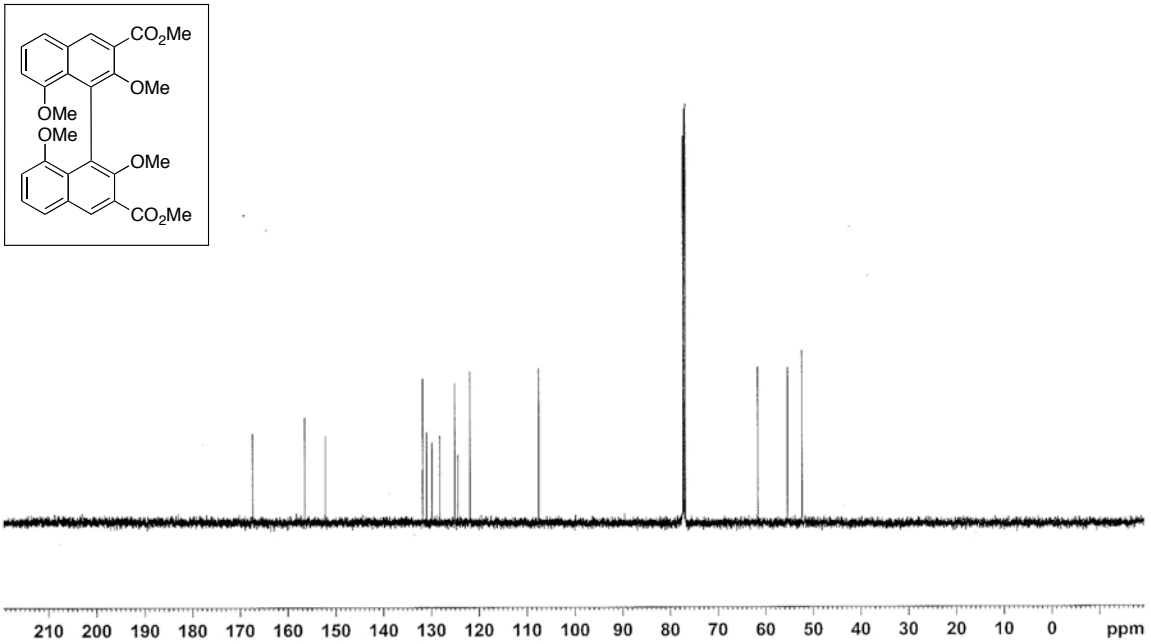

Figure A2.1_2 ^{13}C NMR Spectrum of Compound **2.1** (125 MHz, $CDCl_3$).

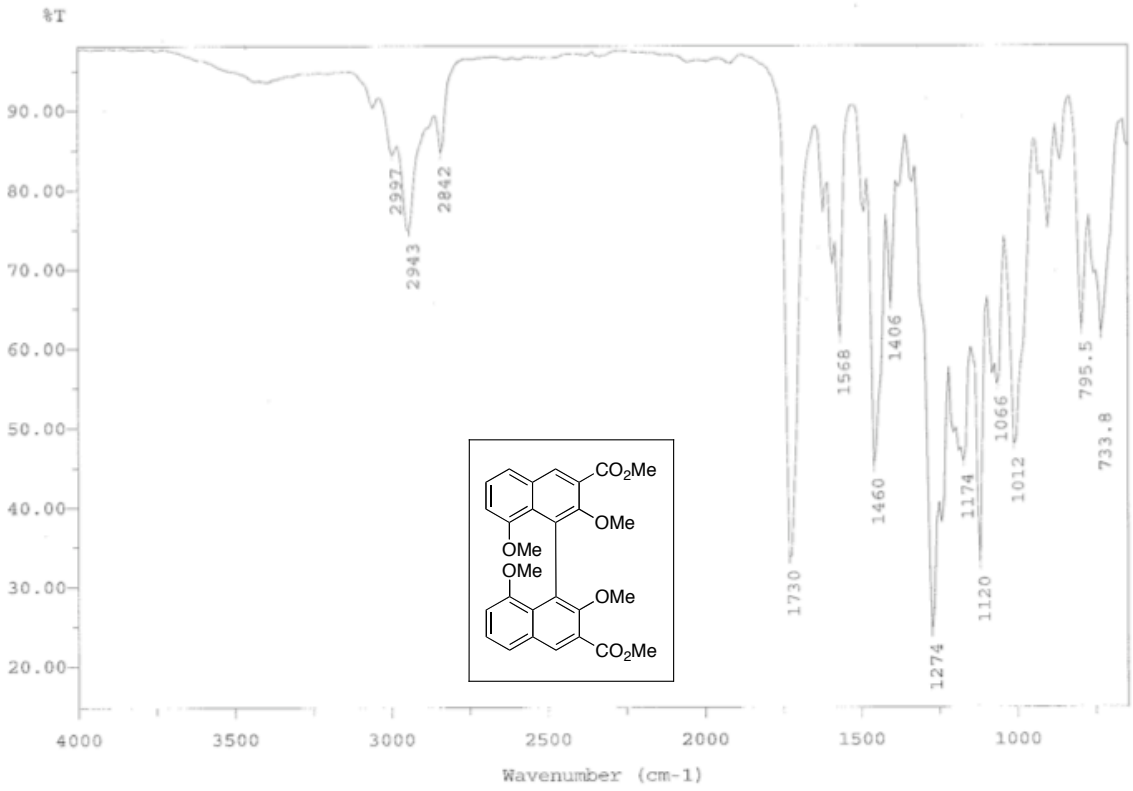

Figure A2.1_3 IR Spectrum of Compound **2.1** (film).

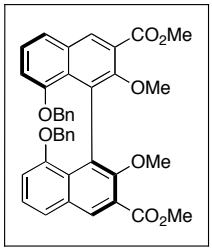

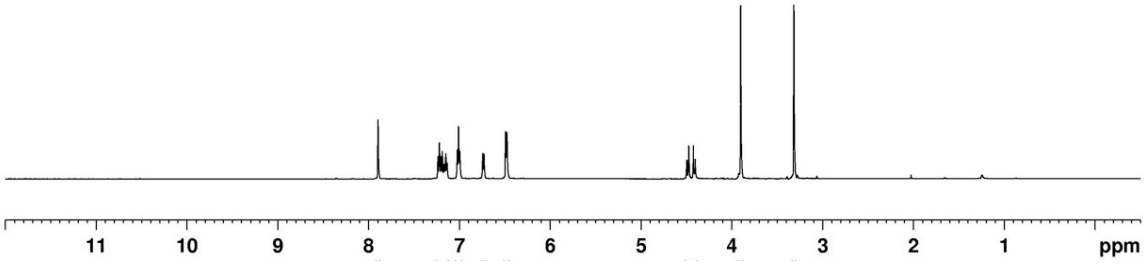

Figure A2.2_1 ^{1}H NMR Spectrum of Compound (*S*)-**2.2** (500 MHz, $CDCl_3$).

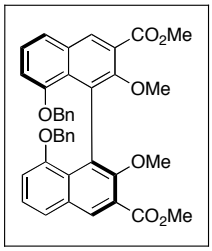

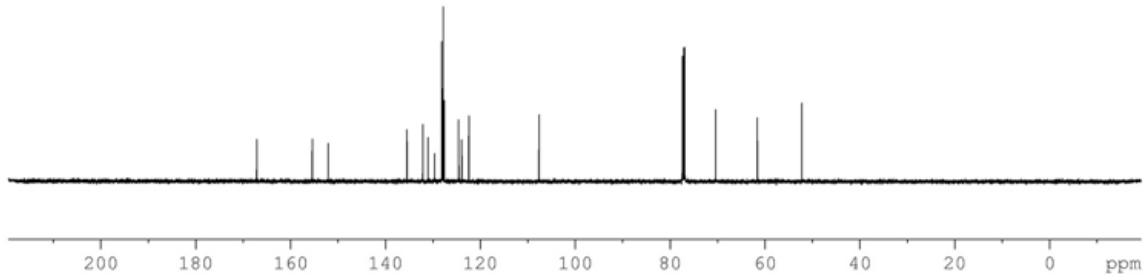

Figure A2.2_2 ^{13}C NMR Spectrum of Compound (*S*)-**2.2** (125 MHz, $CDCl_3$).

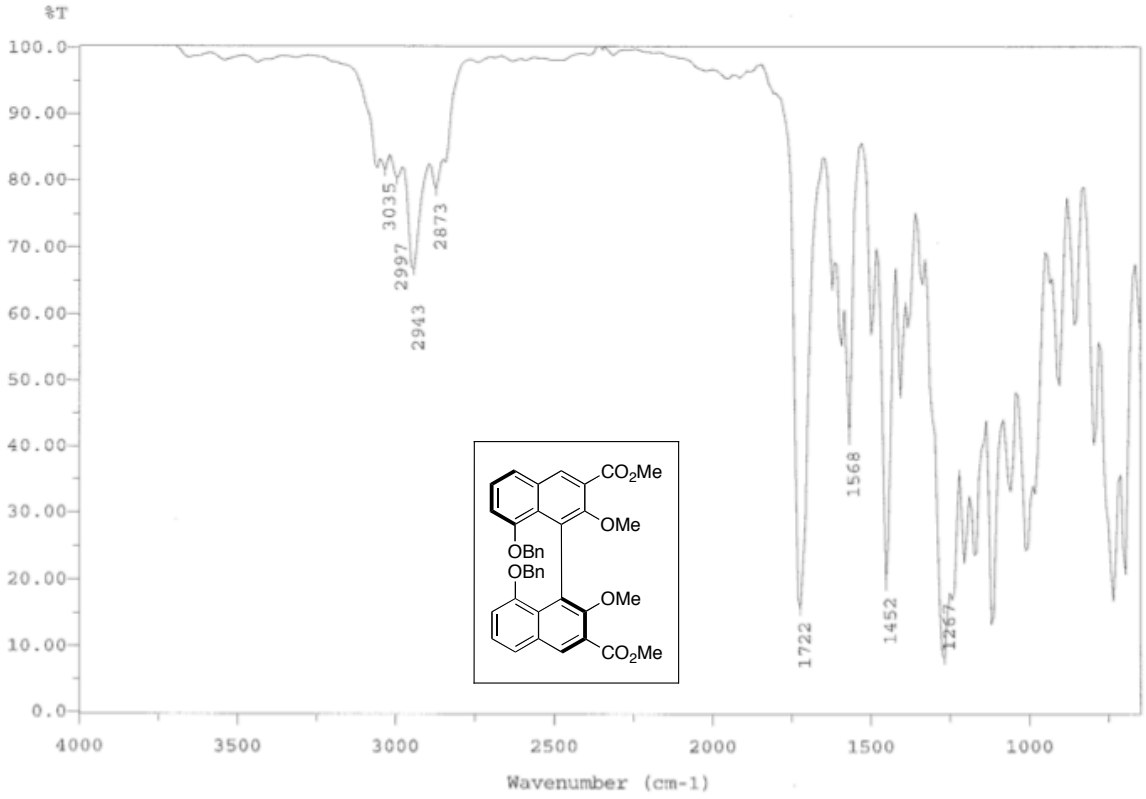

Figure A2.2_3 IR Spectrum of Compound (*S*)-**2.2** (film).

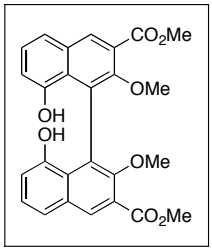

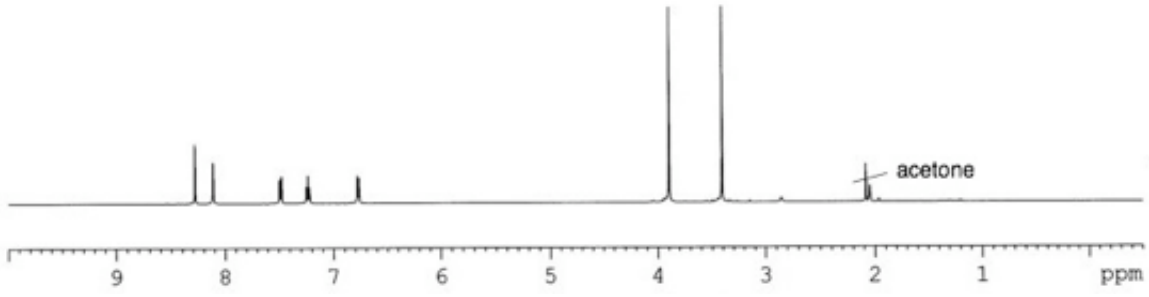

Figure A2.3_1 ^{1}H NMR Spectrum of Compound **2.3** (500 MHz, acetone-d_6).

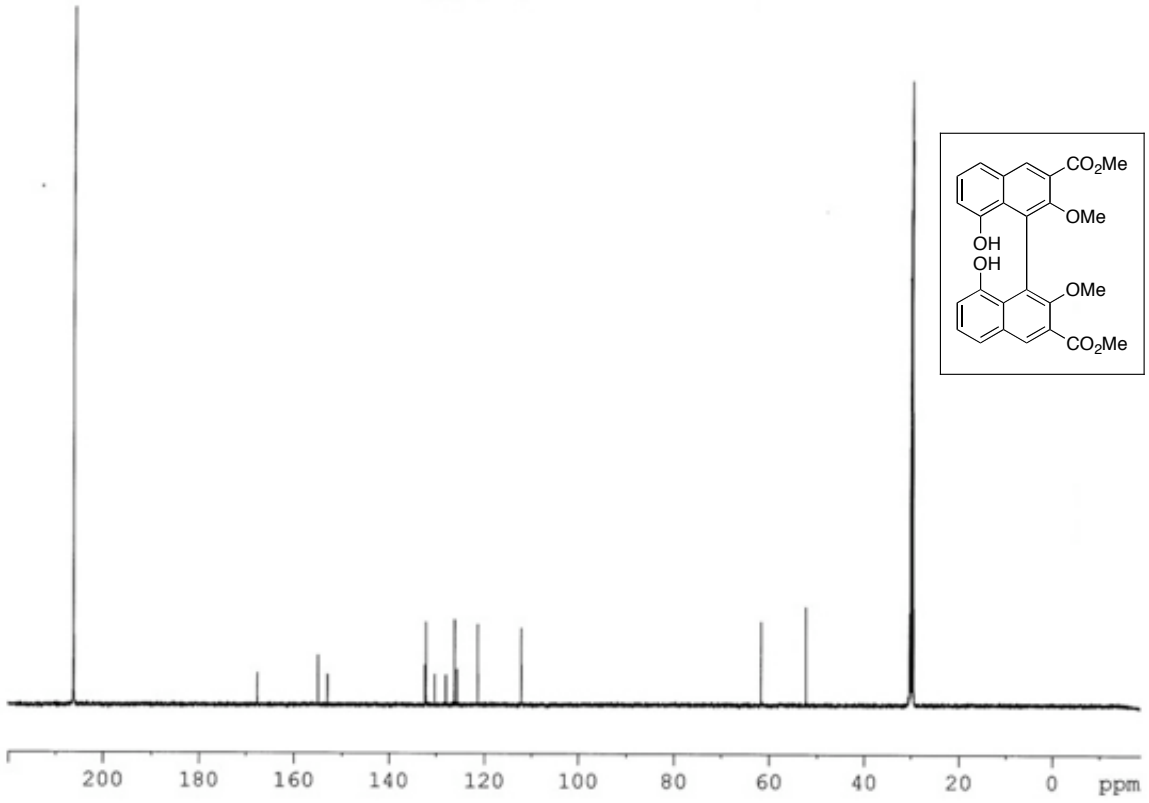

Figure A2.3_2 ^{13}C NMR Spectrum of Compound **2.3** (125 MHz, acetone-d_6).

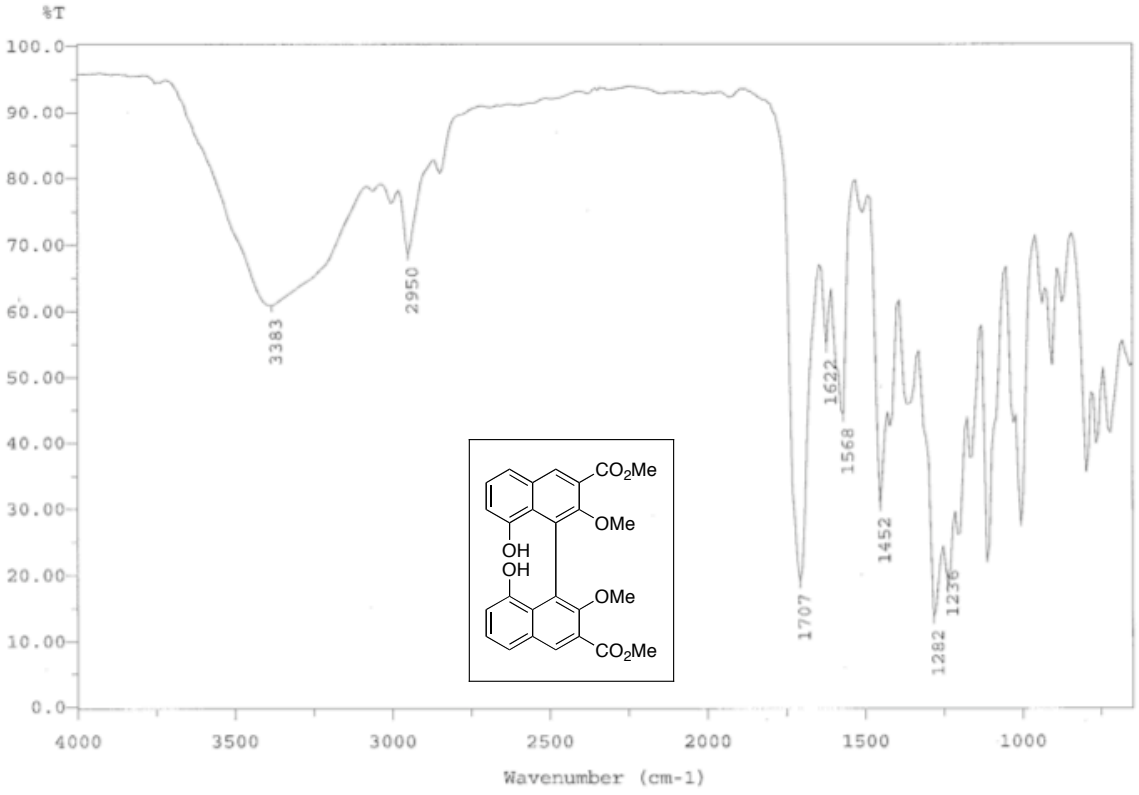

Figure A2.3_3 IR Spectrum of Compound **2.3** (film).

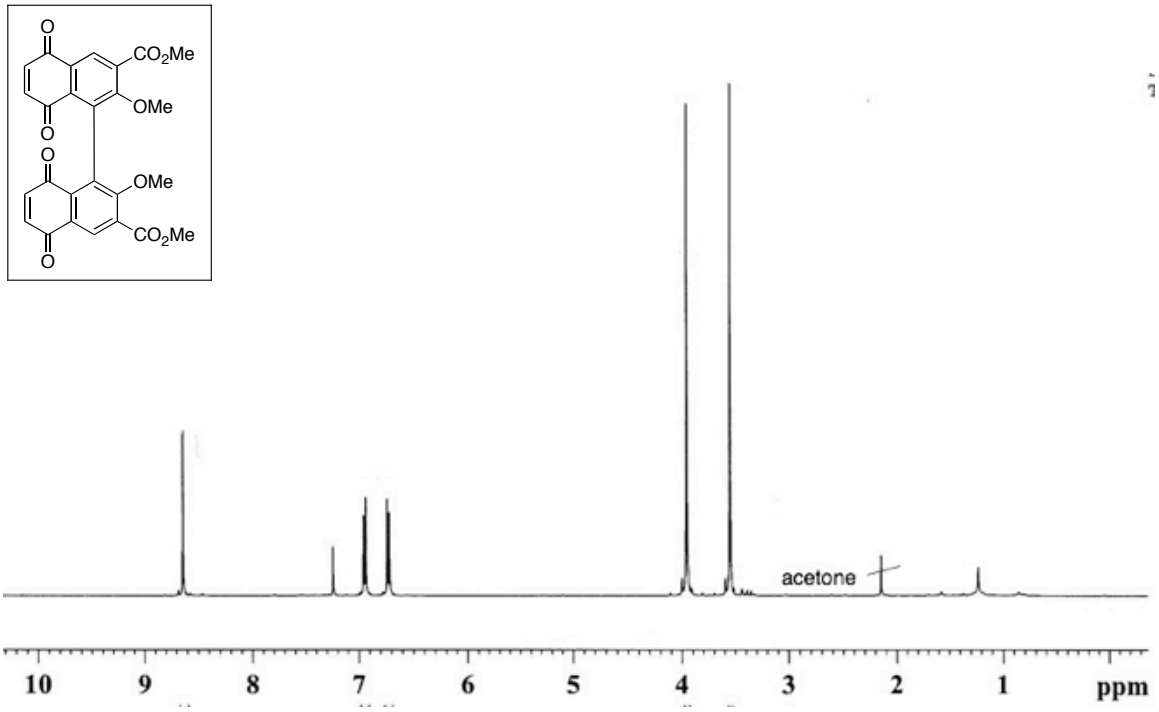

Figure A2.4_1 ^{1}H NMR Spectrum of Compound **2.4** (500 MHz, $CDCl_3$).

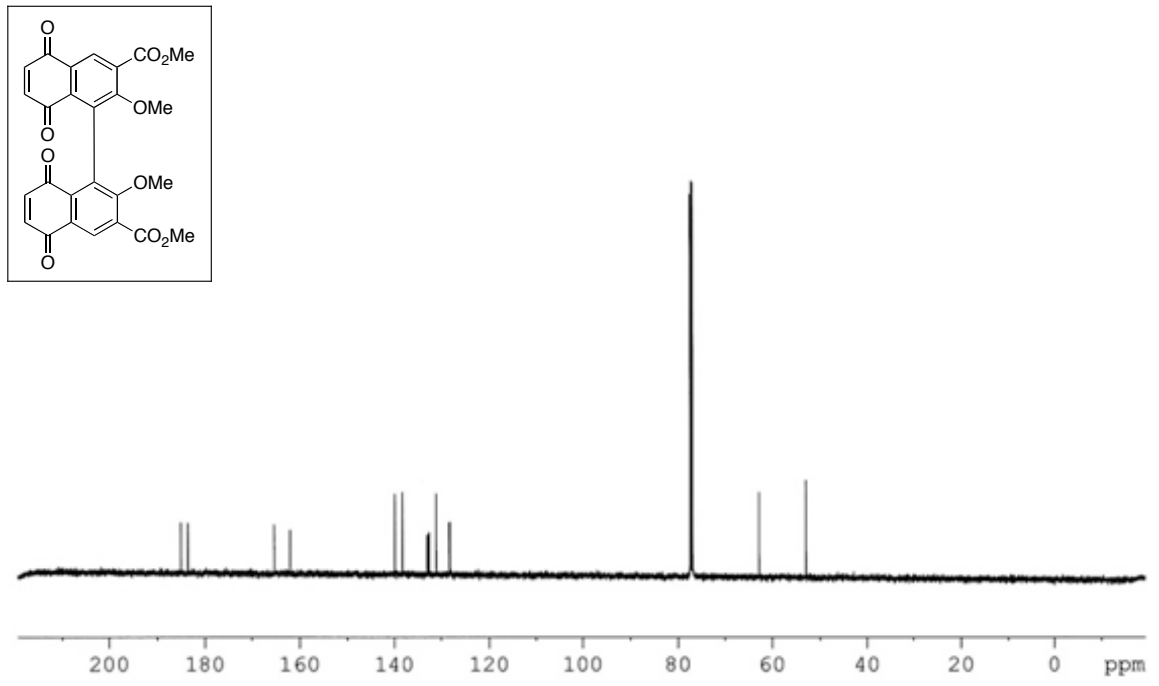

Figure A2.4_2 ^{13}C NMR Spectrum of Compound **2.4** (125 MHz, $CDCl_3$).

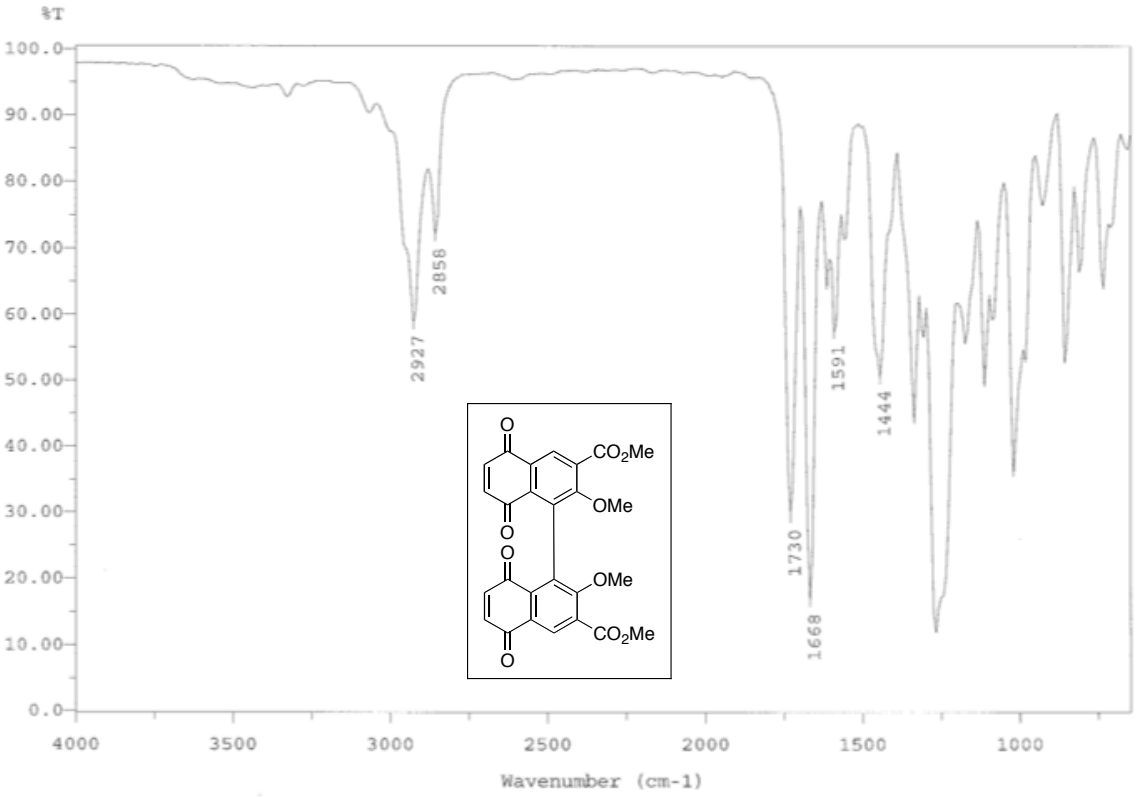

Figure A2.4_3 IR Spectrum of Compound **2.4** (film).

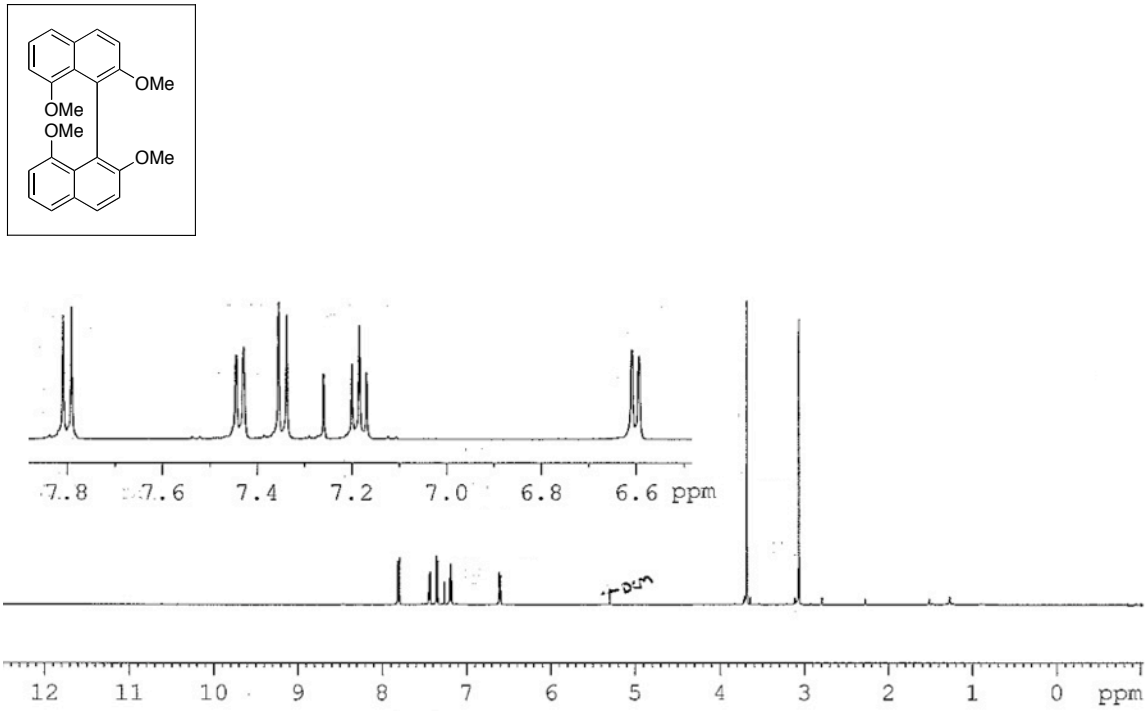

Figure A2.5_1 ^{1}H NMR Spectrum of Compound **2.5** (500 MHz, $CDCl_3$).

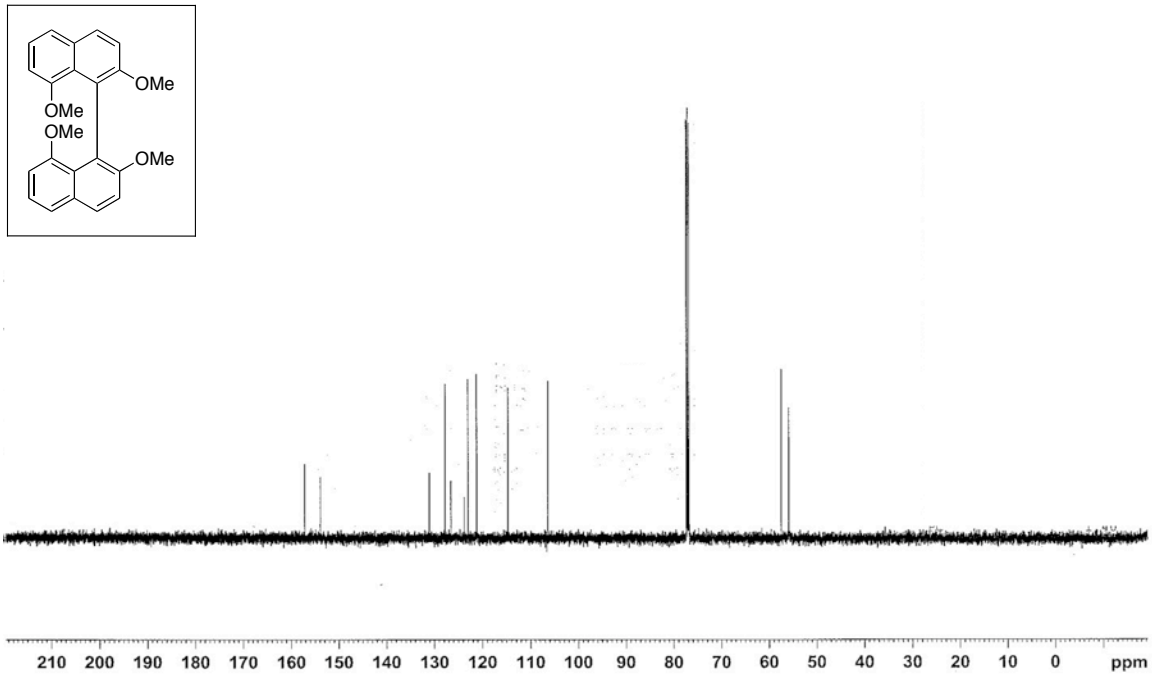

Figure A2.5_2 ^{13}C NMR Spectrum of Compound **2.5** (125 MHz, $CDCl_3$).

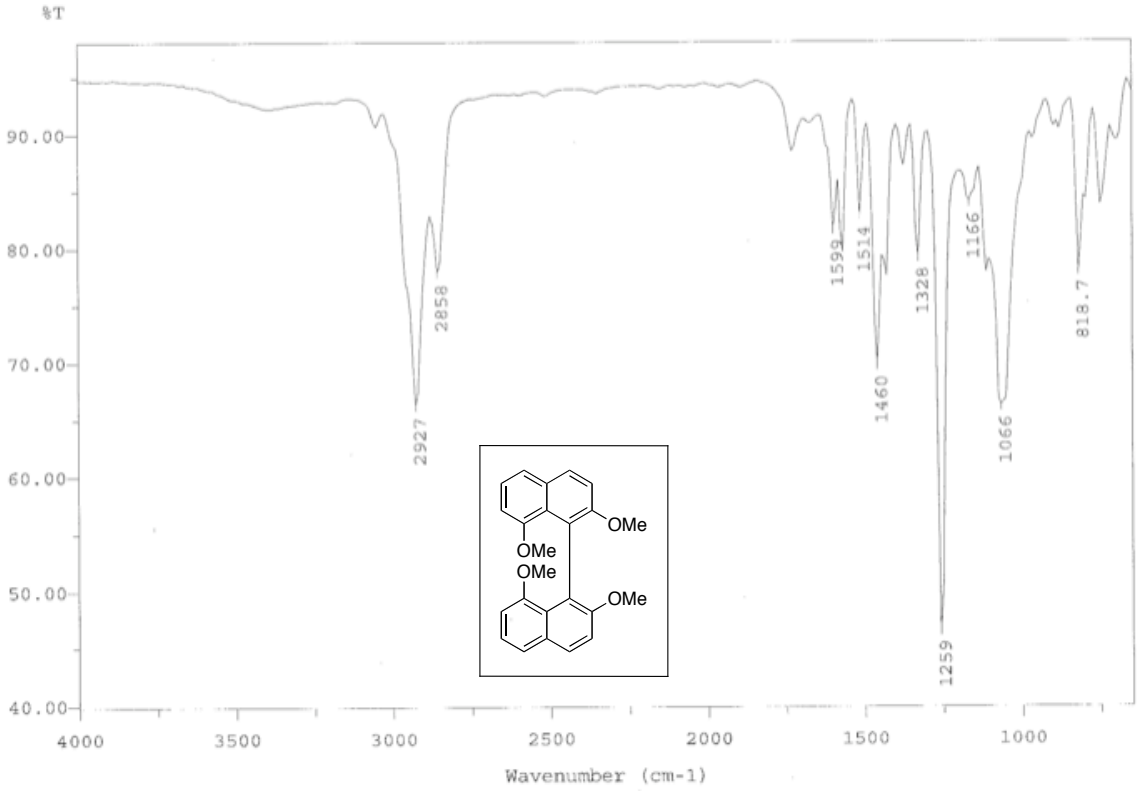

Figure A2.5_3 IR Spectrum of Compound **2.5** (film).

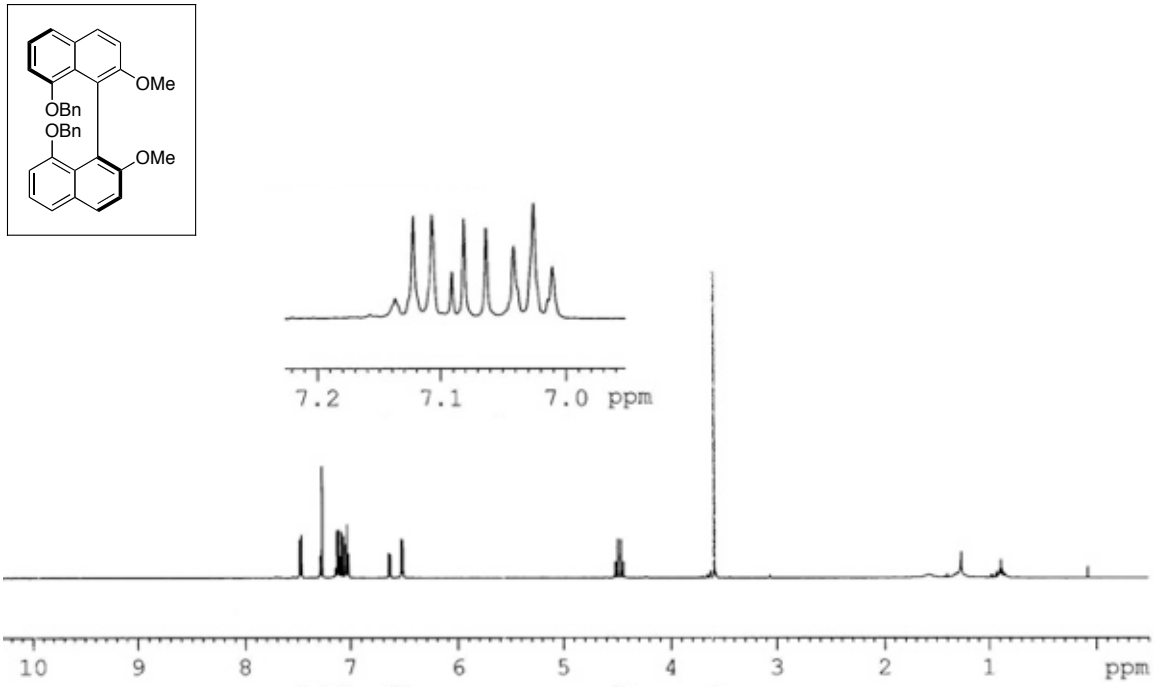

Figure A2.6_1 ^{1}H NMR Spectrum of Compound (*S*)-**2.6** (500 MHz, $CDCl_3$).

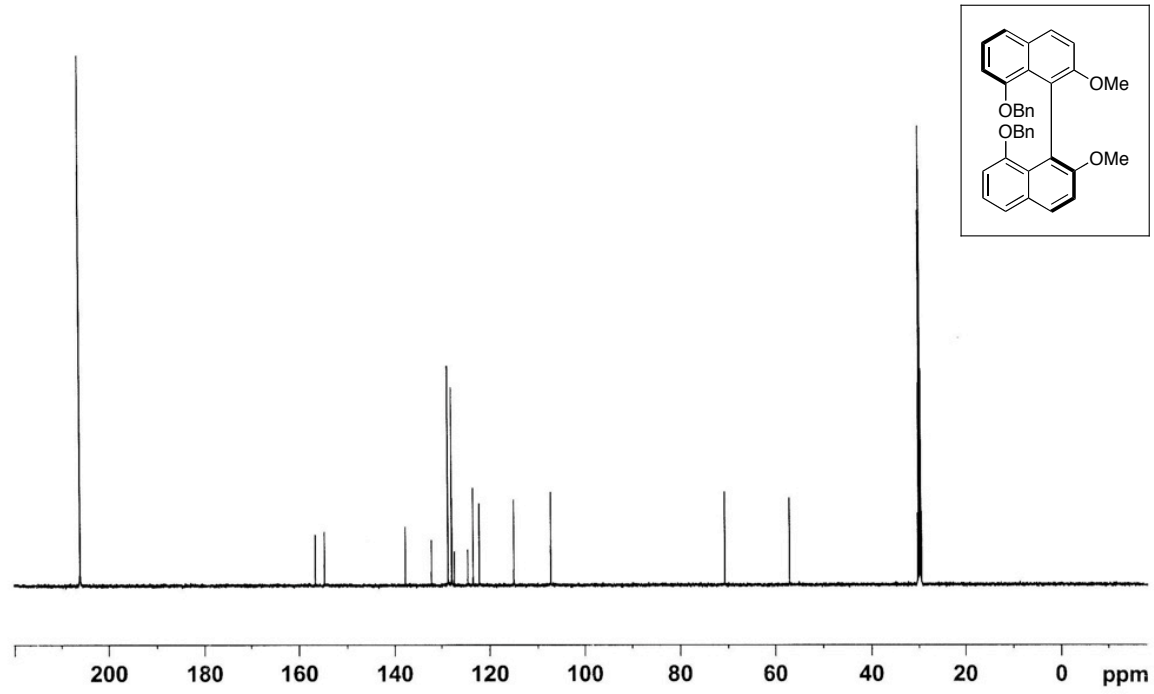

Figure A2.6_2 ^{13}C NMR Spectrum of Compound (*S*)-**2.6** (125 MHz, $CDCl_3$).

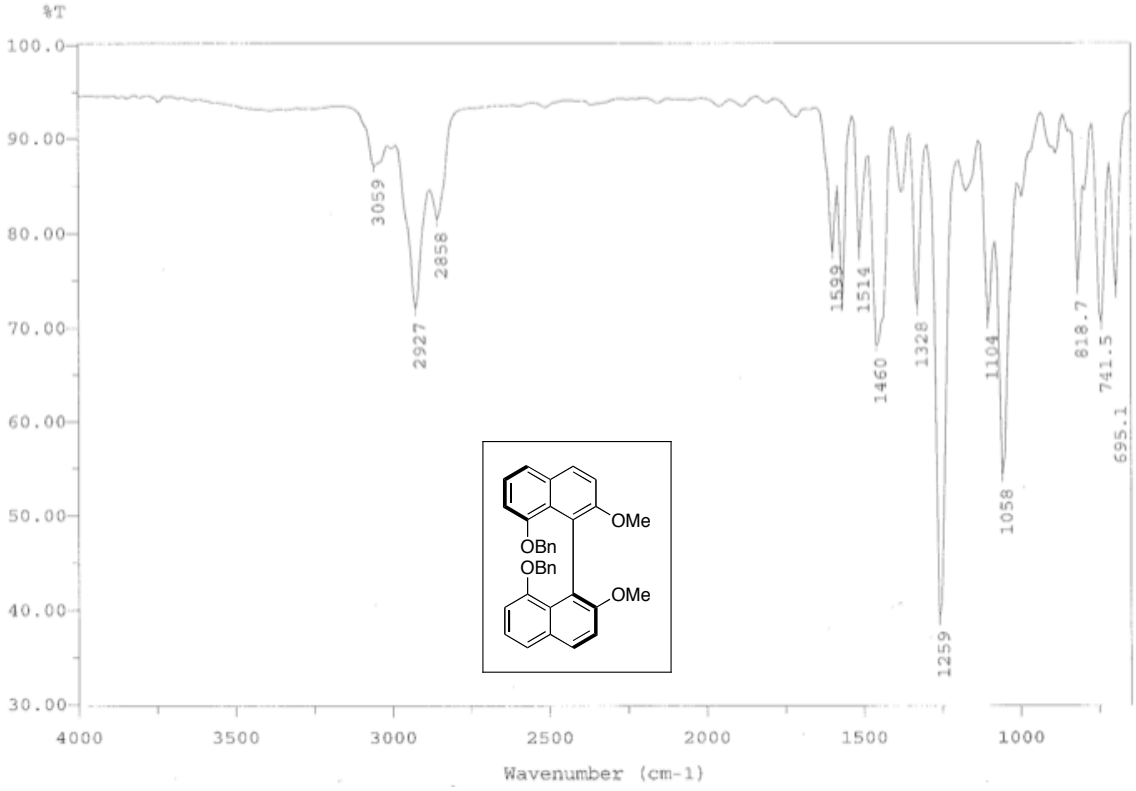

Figure A2.6_3 IR Spectrum of Compound (*S*)-**2.6** (film).

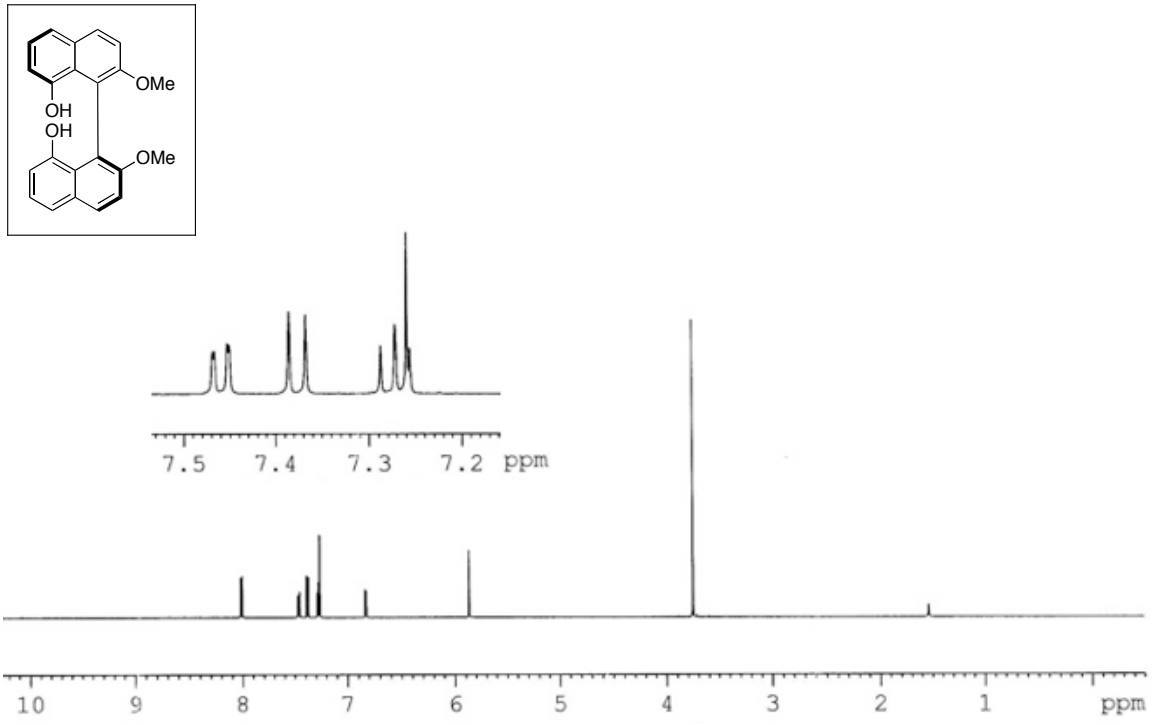

Figure A2.7_1 ^{1}H NMR Spectrum of Compound (*S*)-**2.7** (500 MHz, $CDCl_3$).

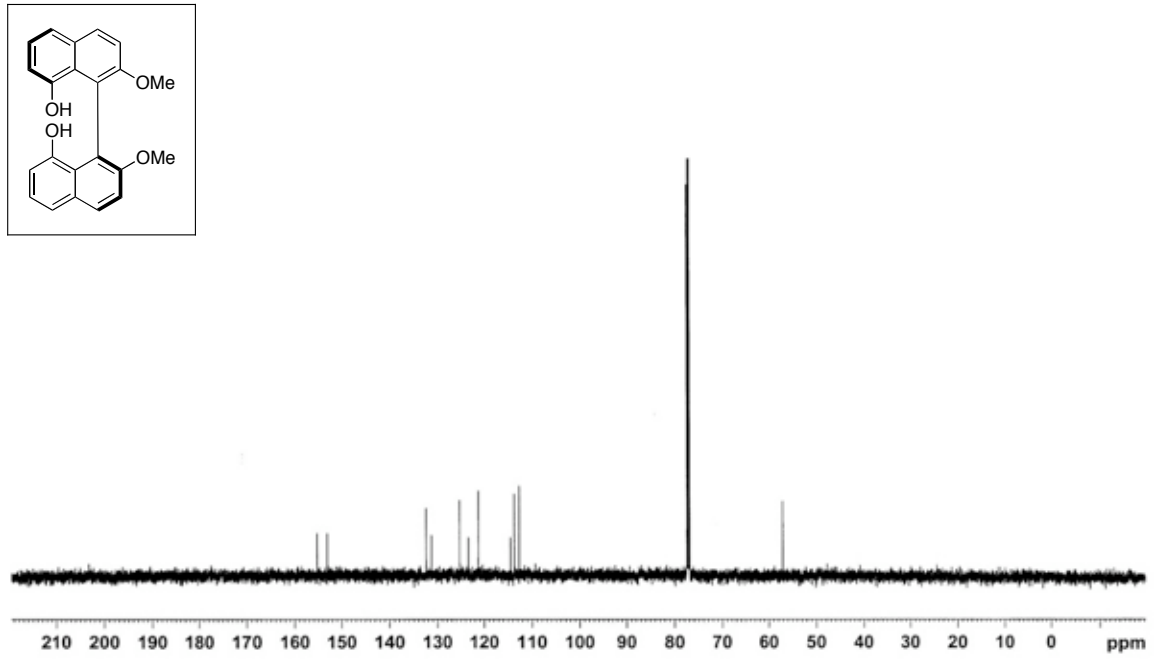

Figure A2.7_2 ^{13}C NMR Spectrum of Compound (*S*)-**2.7** (125 MHz, $CDCl_3$).

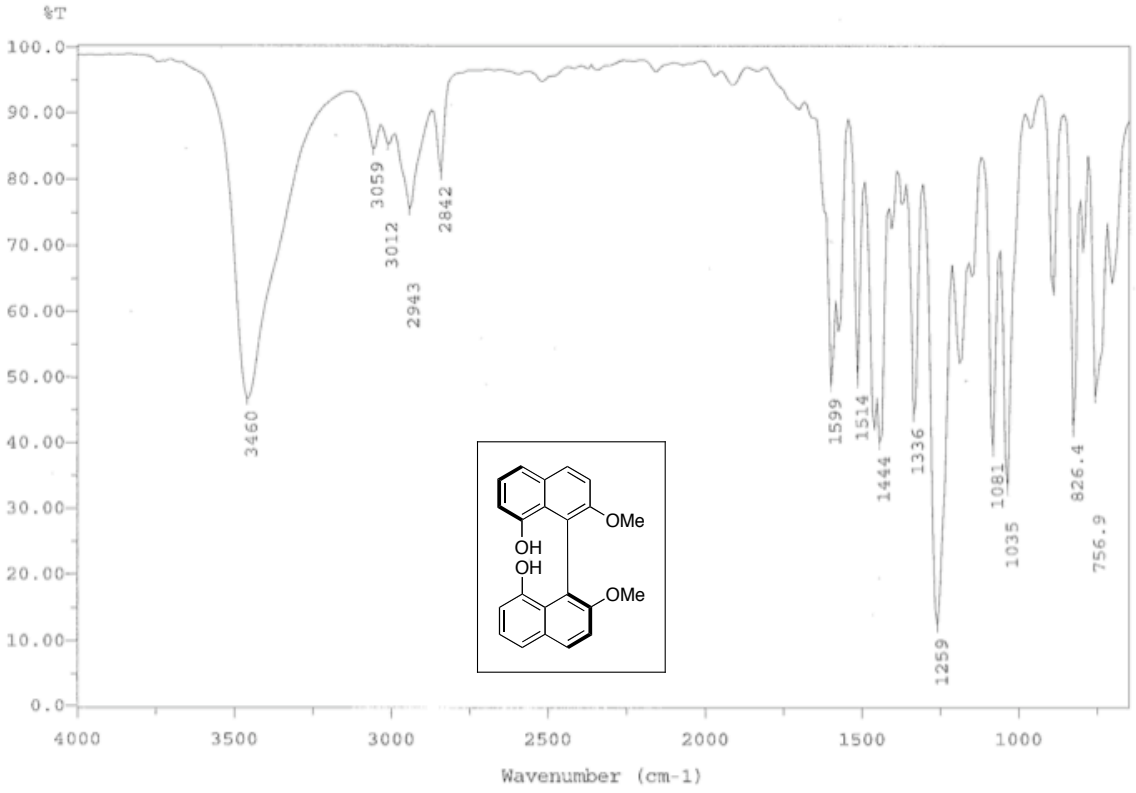

Figure A2.7_3 IR Spectrum of Compound (*S*)-**2.7** (film).

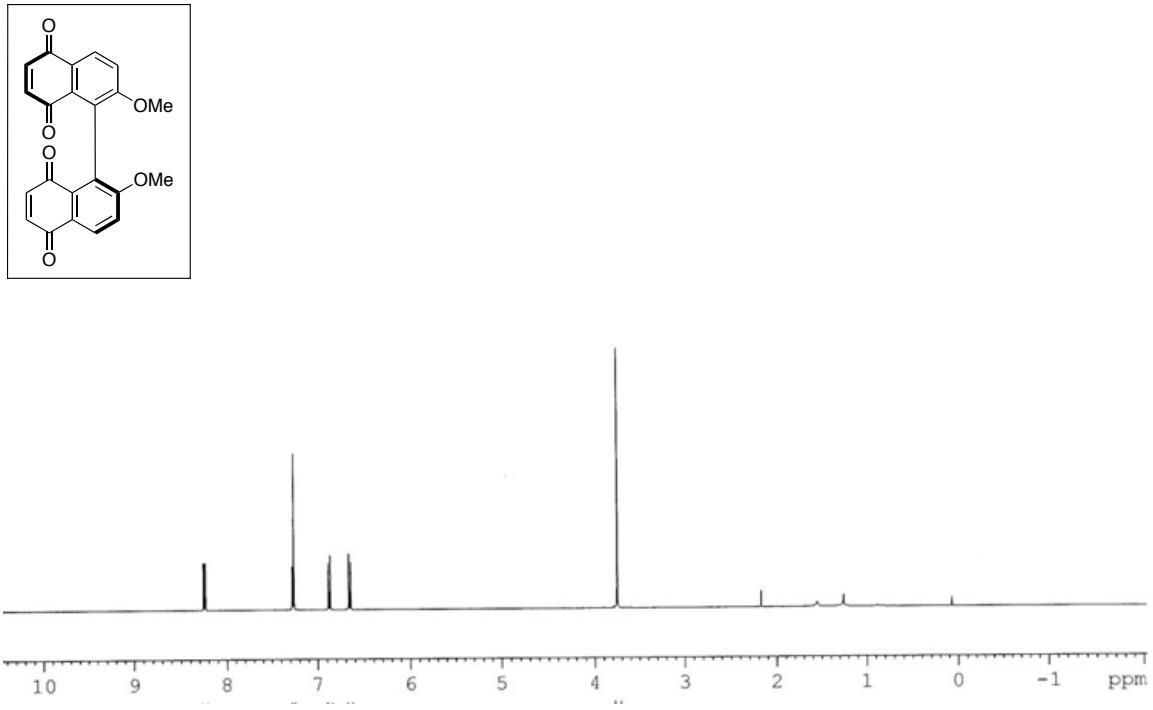

Figure A2.8_1 ^{1}H NMR Spectrum of Compound (*S*)-**2.8** (500 MHz, $CDCl_3$).

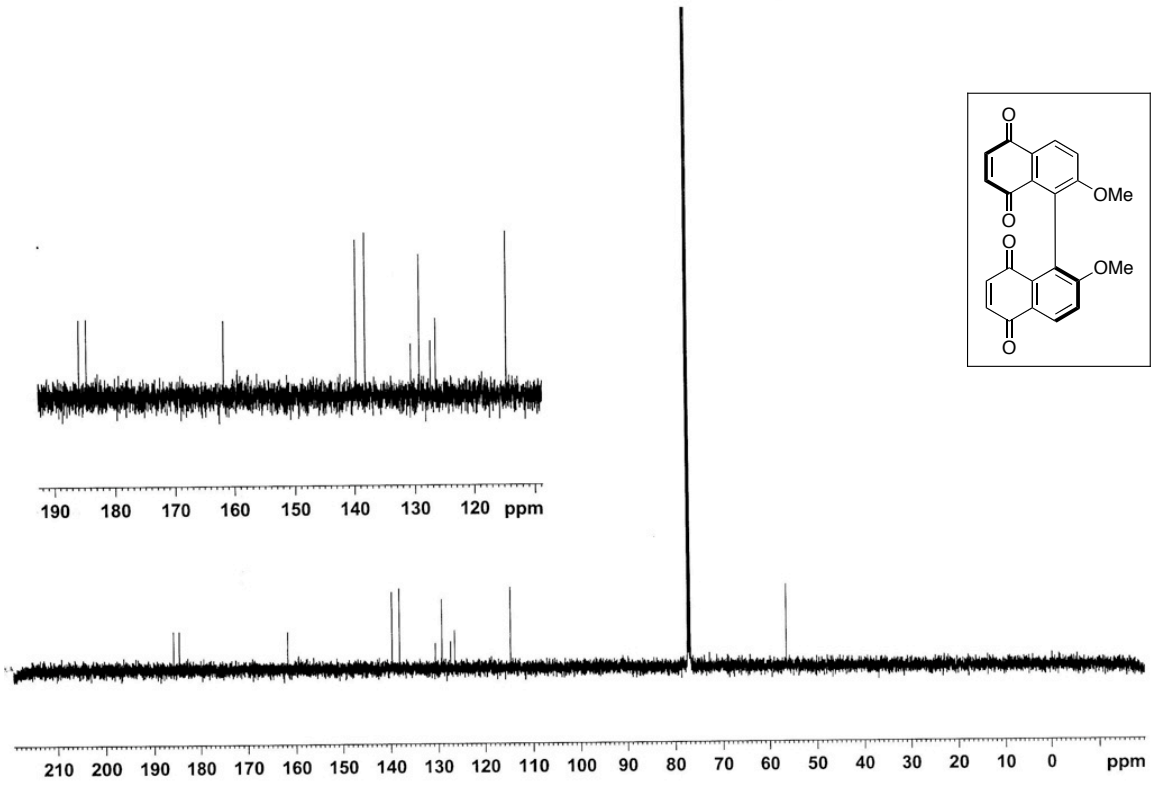

Figure A2.8_2 ^{13}C NMR Spectrum of Compound (*S*)-**2.8** (125 MHz, $CDCl_3$).

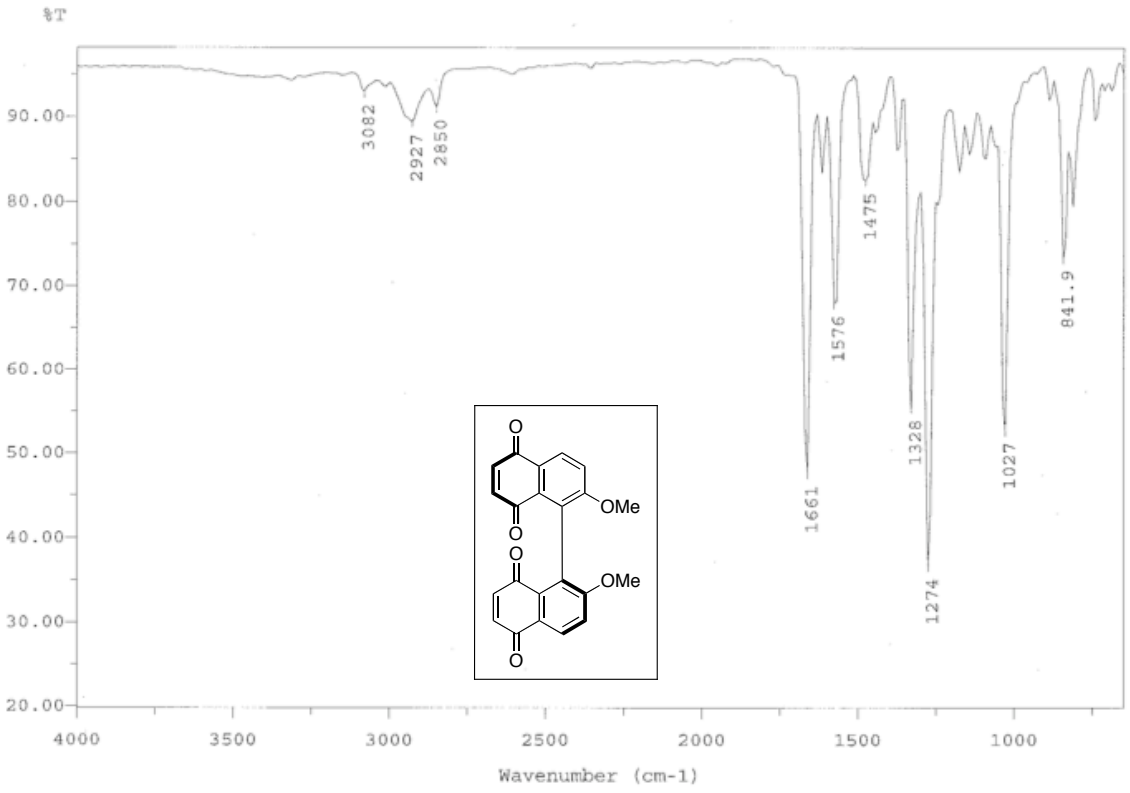

Figure A2.8_3 IR Spectrum of Compound (*S*)-**2.8** (film).

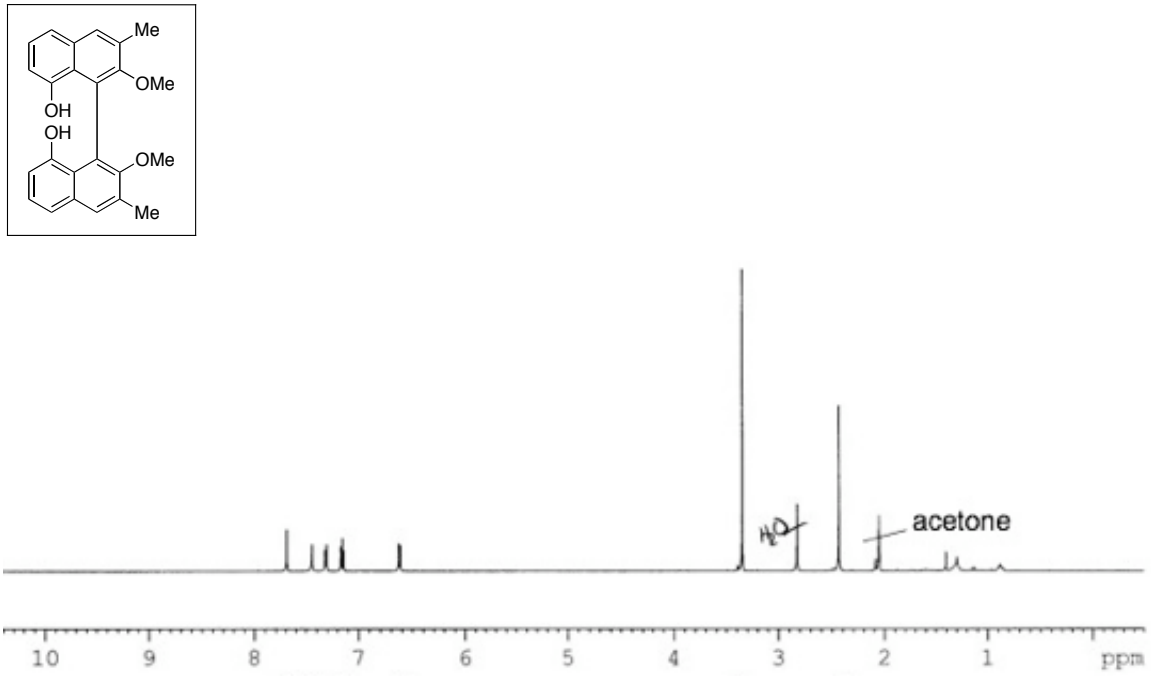

Figure A2.9_1 ^{1}H NMR Spectrum of Compound **2.9** (500 MHz, acetone-d_6).

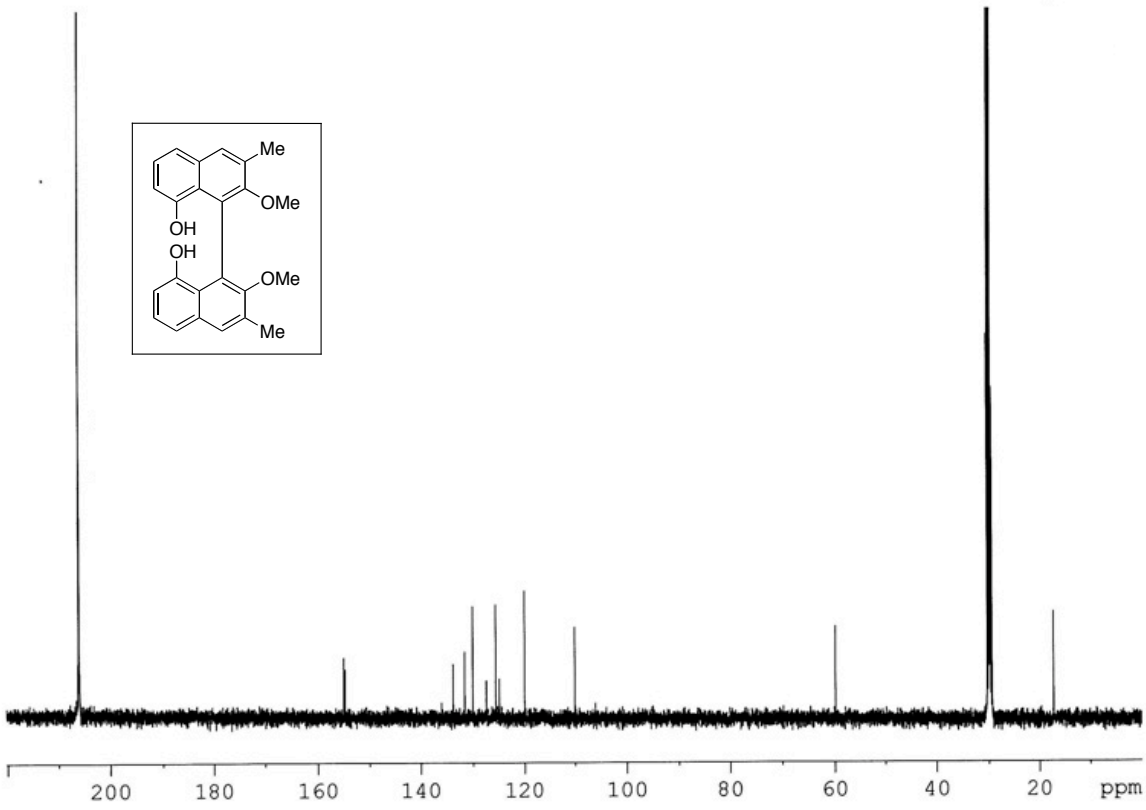

Figure A2.9_2 ^{13}C NMR Spectrum of Compound **2.9** (125 MHz, acetone-d_6).

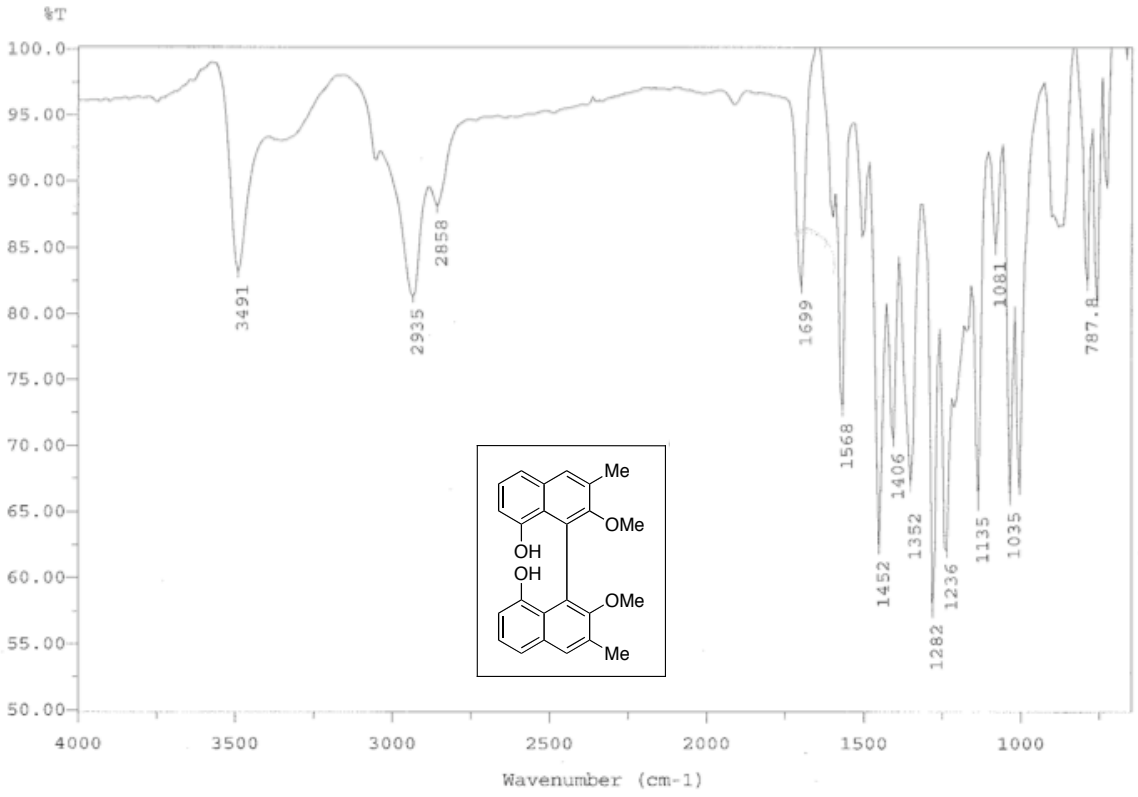

Figure A2.9_3 IR Spectrum of Compound **2.9** (film).

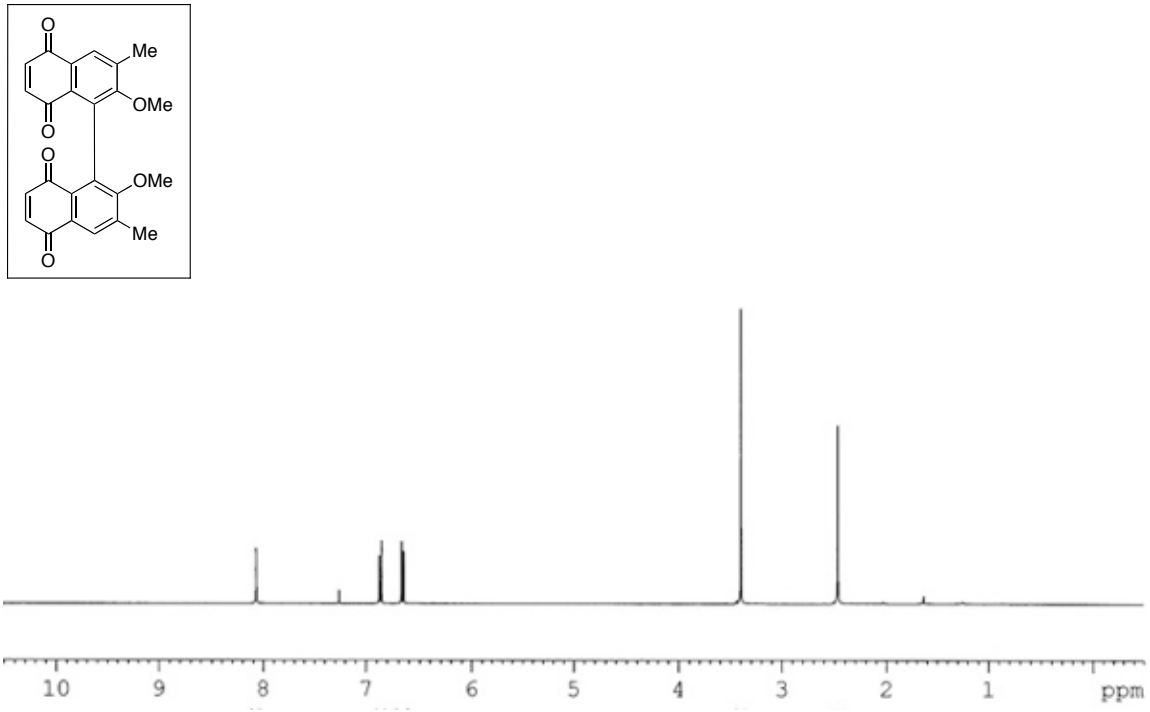

Figure A2.10_1 ^{1}H NMR Spectrum of Compound **2.10** (500 MHz, $CDCl_3$).

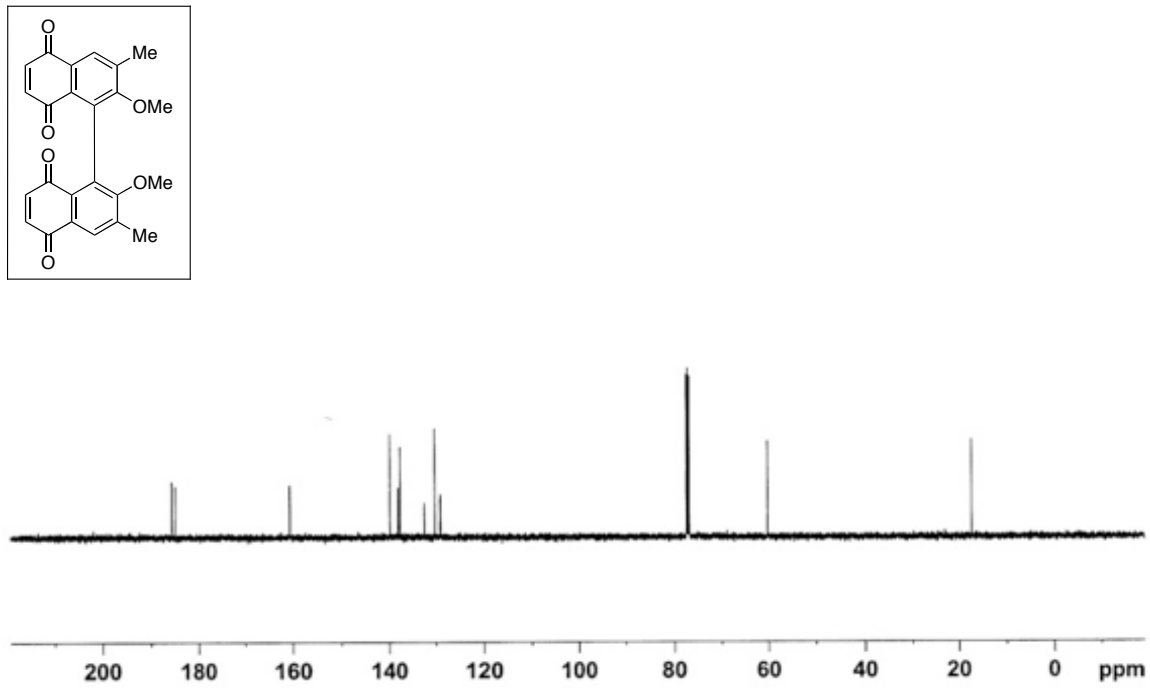

Figure A2.10_2 ^{13}C NMR Spectrum of Compound **2.10** (125 MHz, $CDCl_3$).

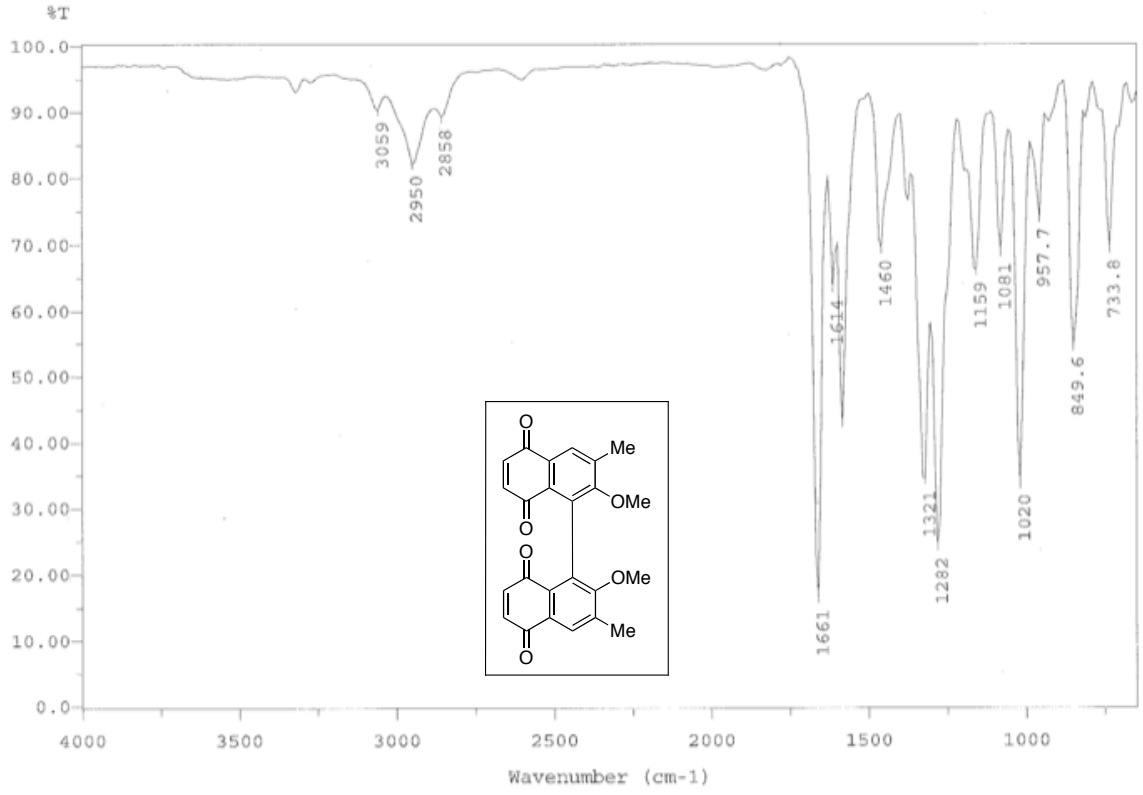

Figure A2.10_3 IR Spectrum of Compound **2.10** (film).

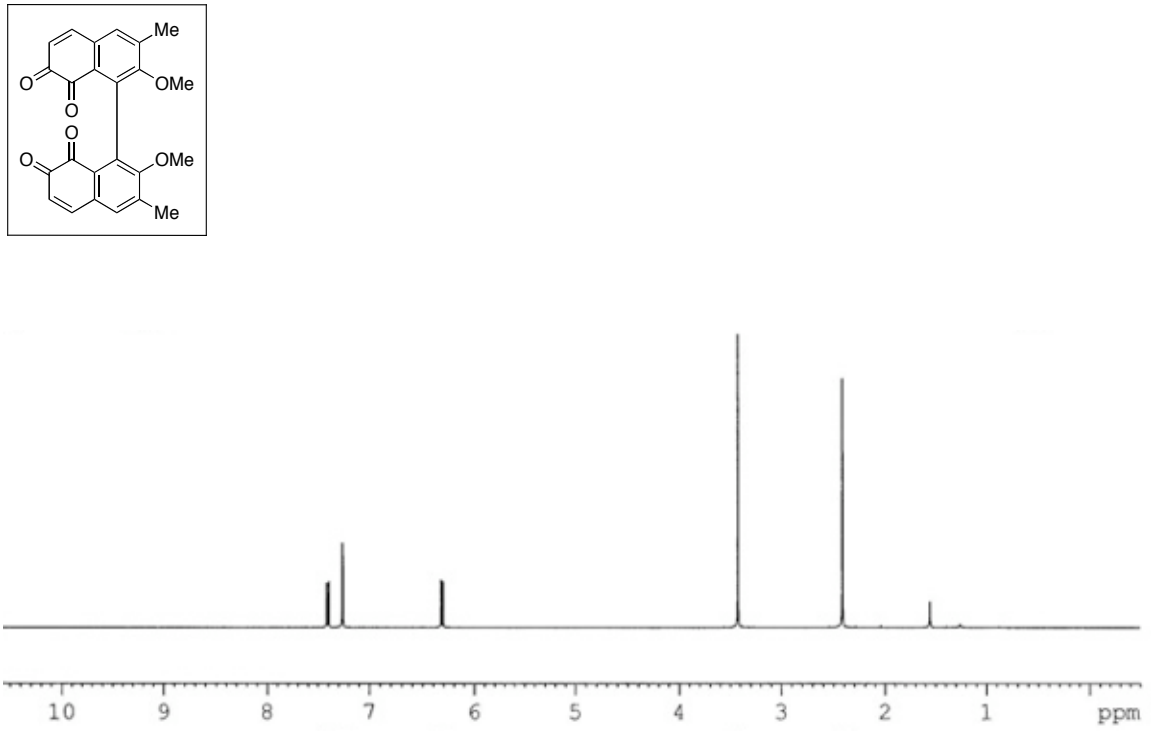

Figure A2.11_1 ^{1}H NMR Spectrum of Compound **2.11** (500 MHz, $CDCl_3$).

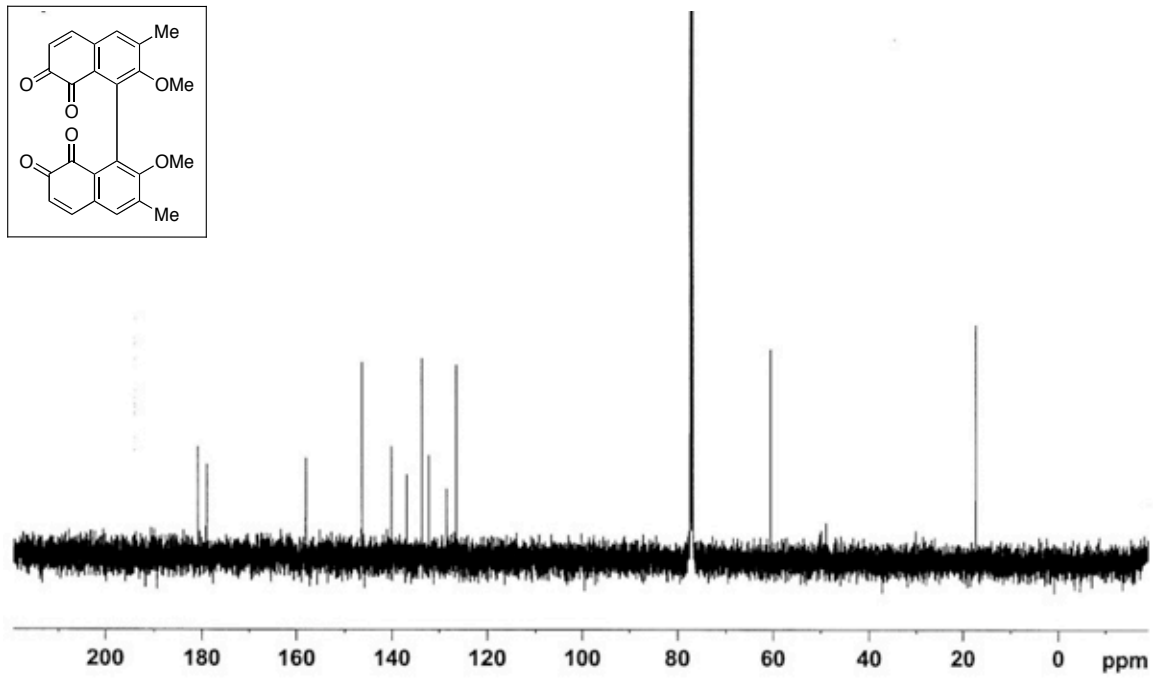

Figure A2.11_2 ^{13}C NMR Spectrum of Compound **2.11** (125 MHz, $CDCl_3$).

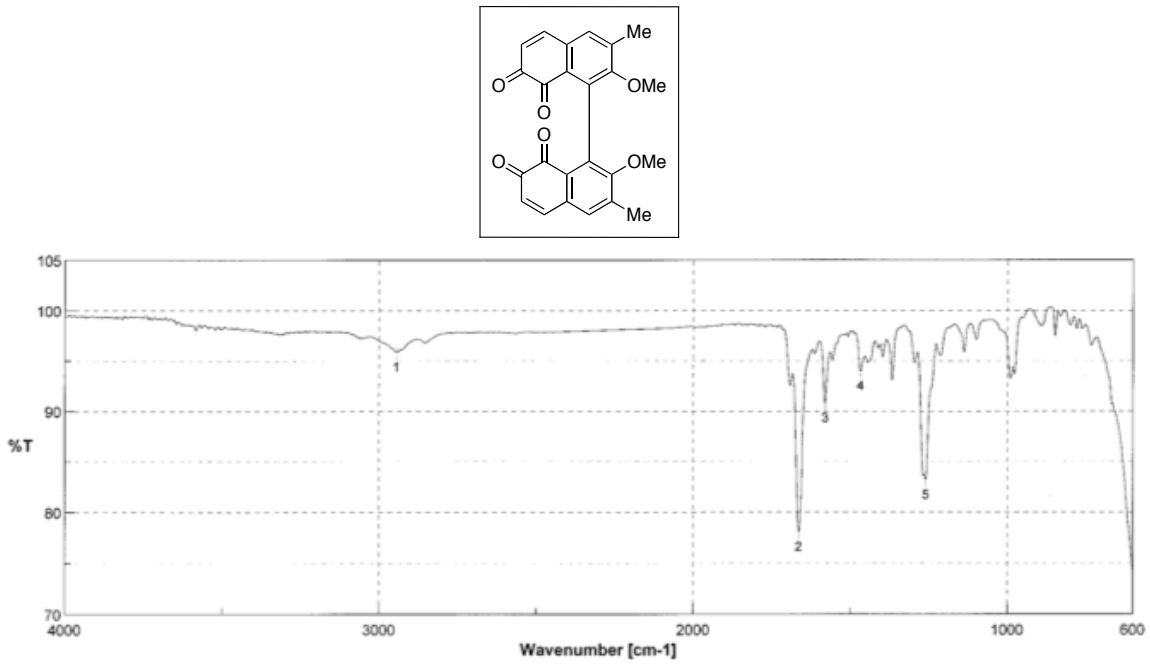

Figure A2.11_3 IR Spectrum of Compound **2.11** (film).

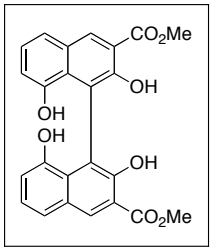

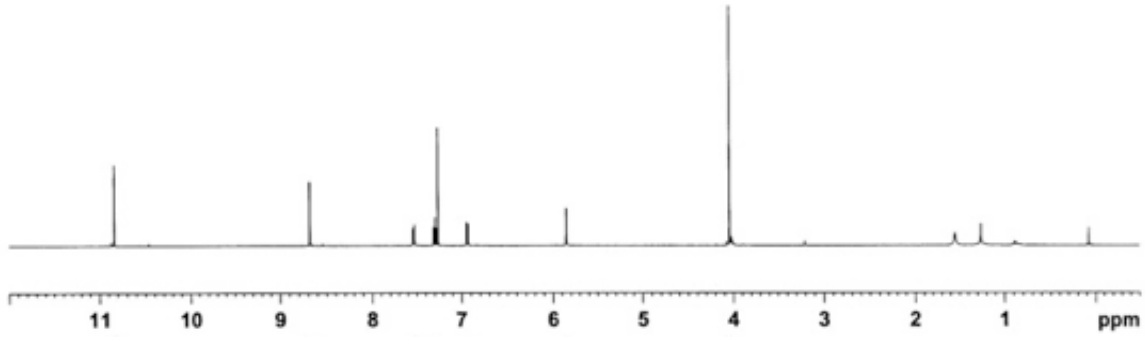

Figure A2.12_1 ^{1}H NMR Spectrum of Compound **2.12** (500 MHz, $CDCl_3$).

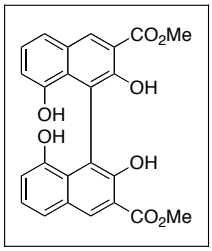

Figure A2.12_2 ^{13}C NMR Spectrum of Compound **2.12** (125 MHz, $CDCl_3$).

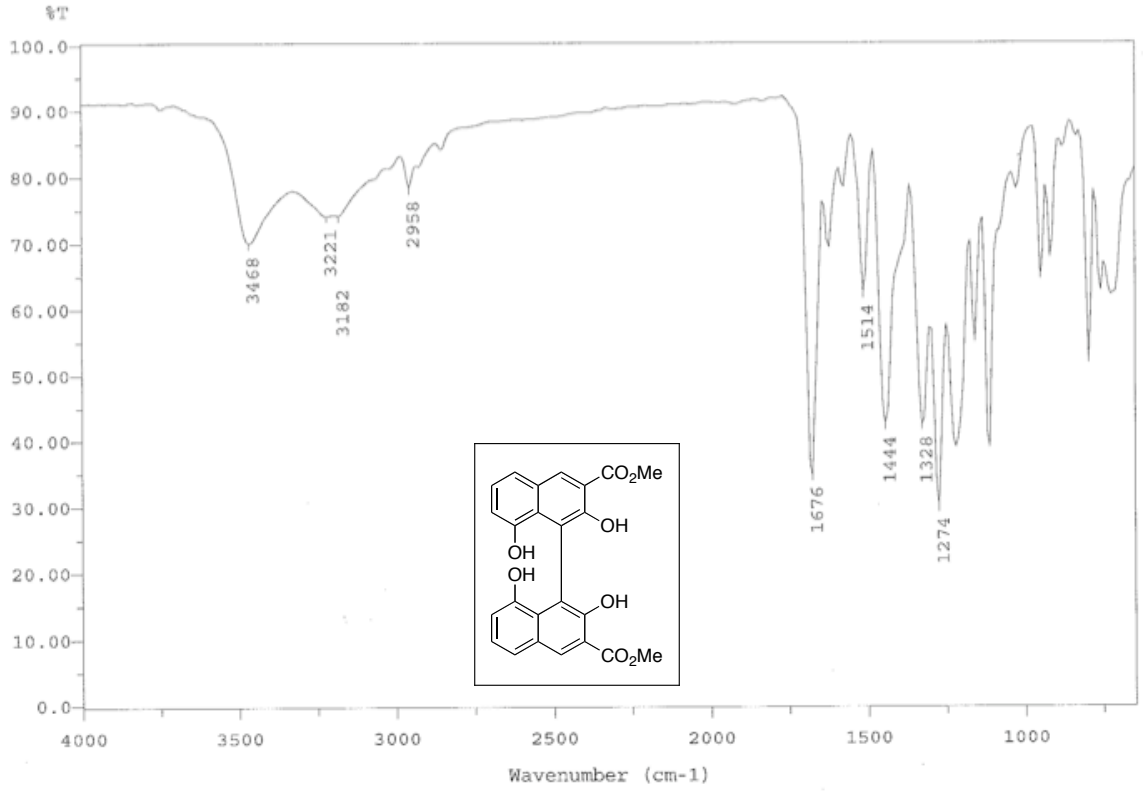

Figure A2.12_3 IR Spectrum of Compound **2.12** (film).

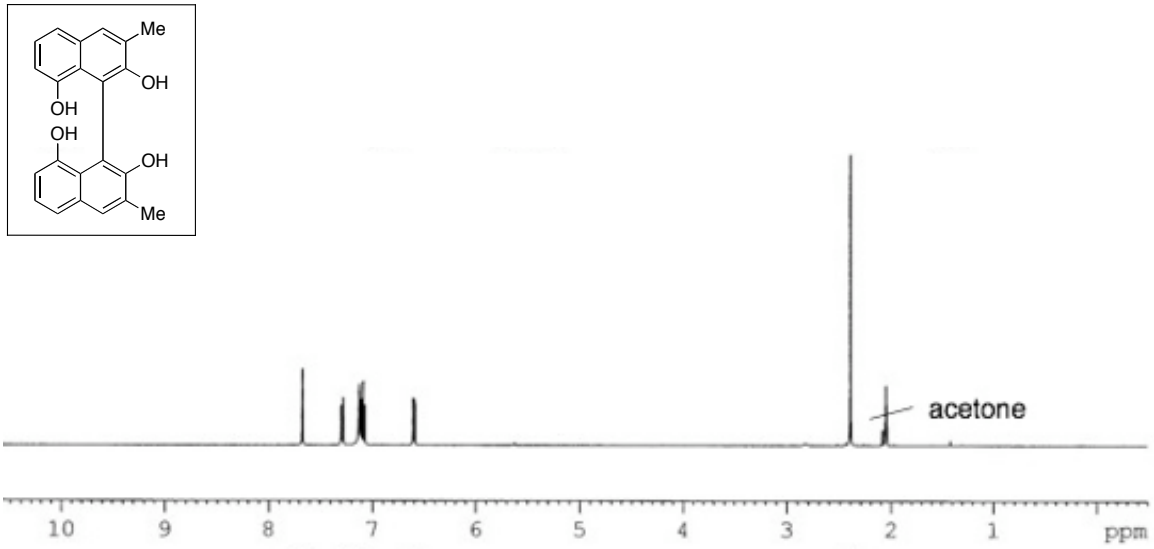

Figure A2.13_1 ^{1}H NMR Spectrum of Compound **2.13** (500 MHz, acetone-d_6).

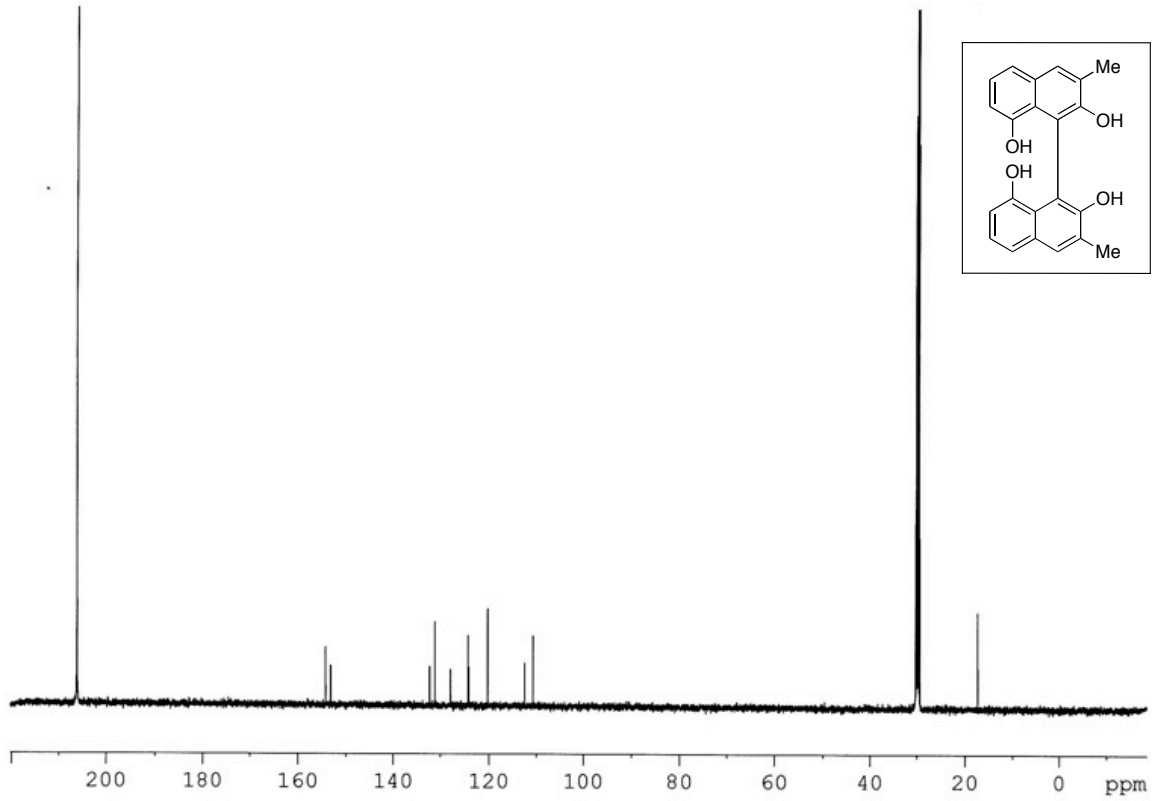

Figure A2.13_2 ^{13}C NMR Spectrum of Compound **2.13** (125 MHz, acetone-d_6).

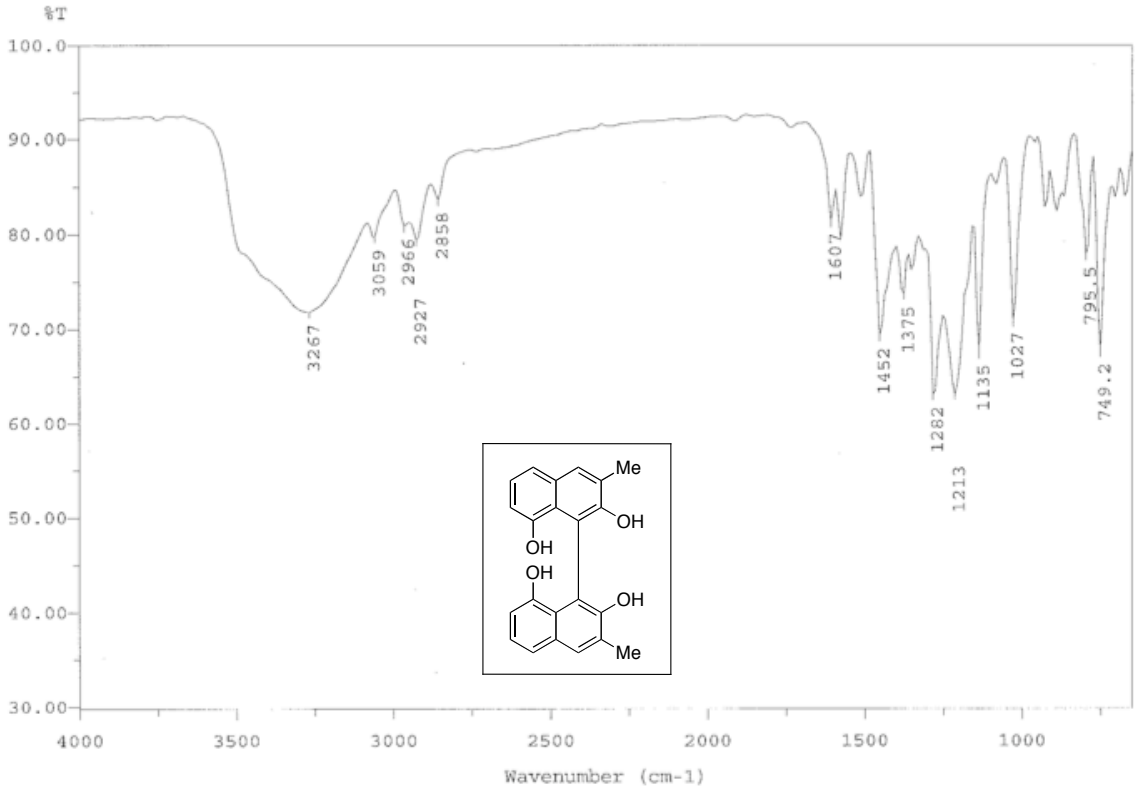

Figure A2.13_3 IR Spectrum of Compound **2.13** (film).

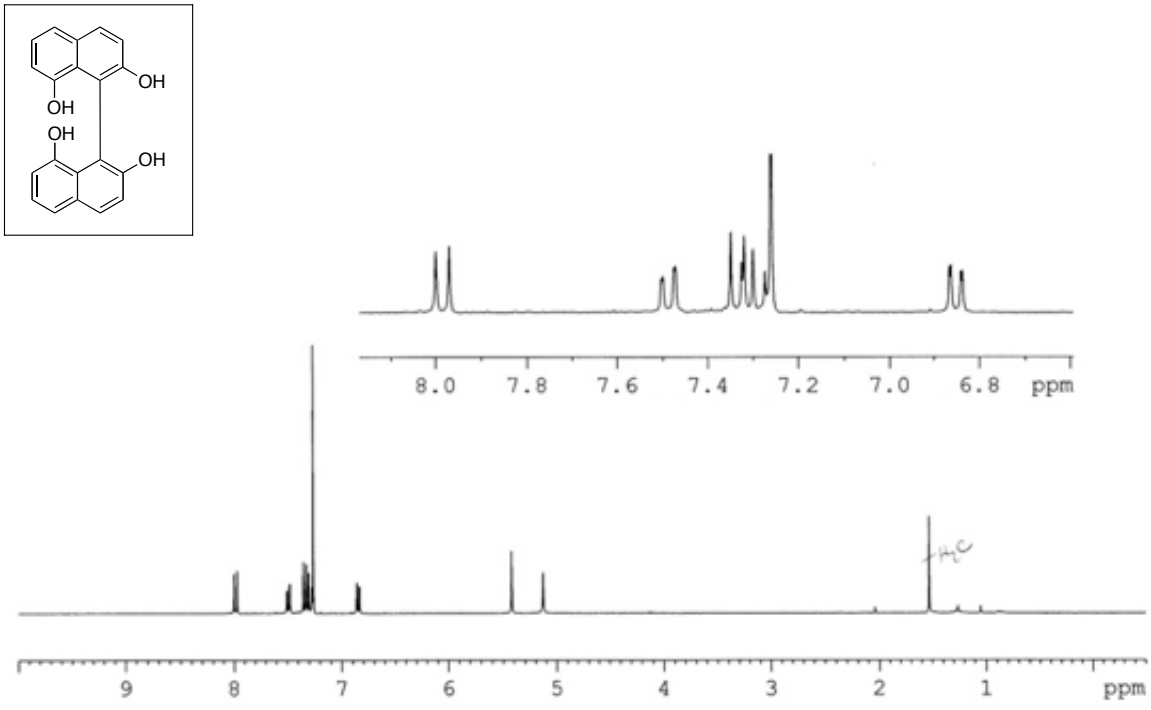

Figure A2.14_1 ^{1}H NMR Spectrum of Compound **2.14** (500 MHz, $CDCl_3$).

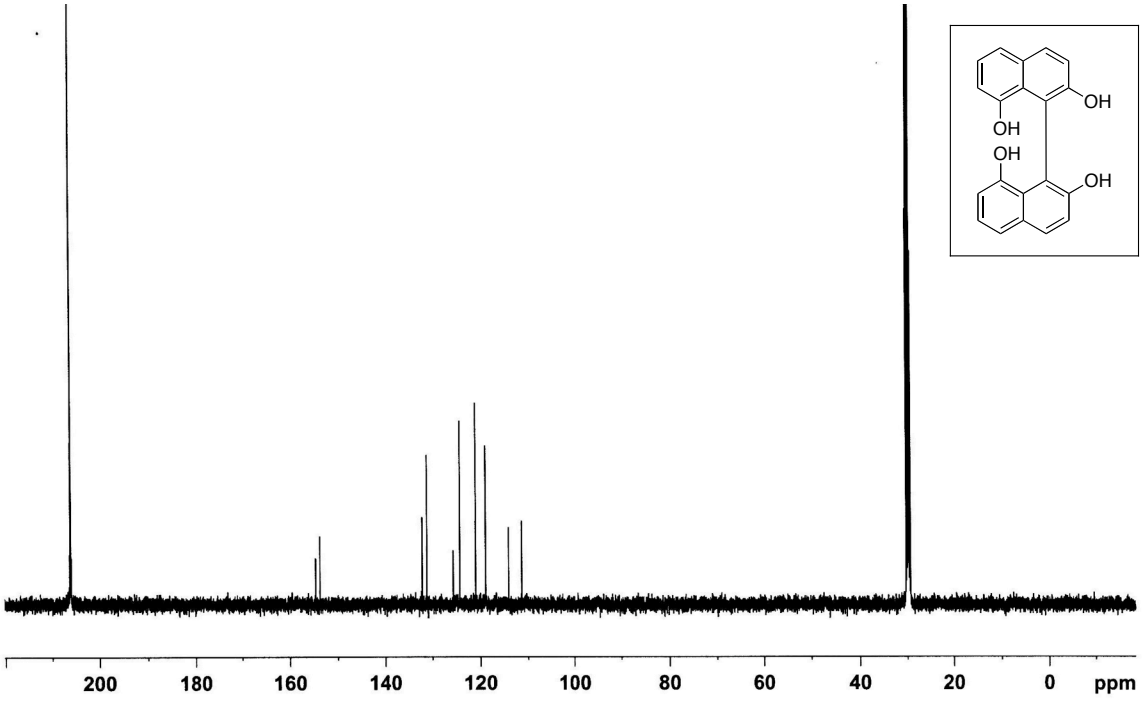

Figure A2.14_2 ^{13}C NMR Spectrum of Compound **2.14** (125 MHz, acetone-d_6).

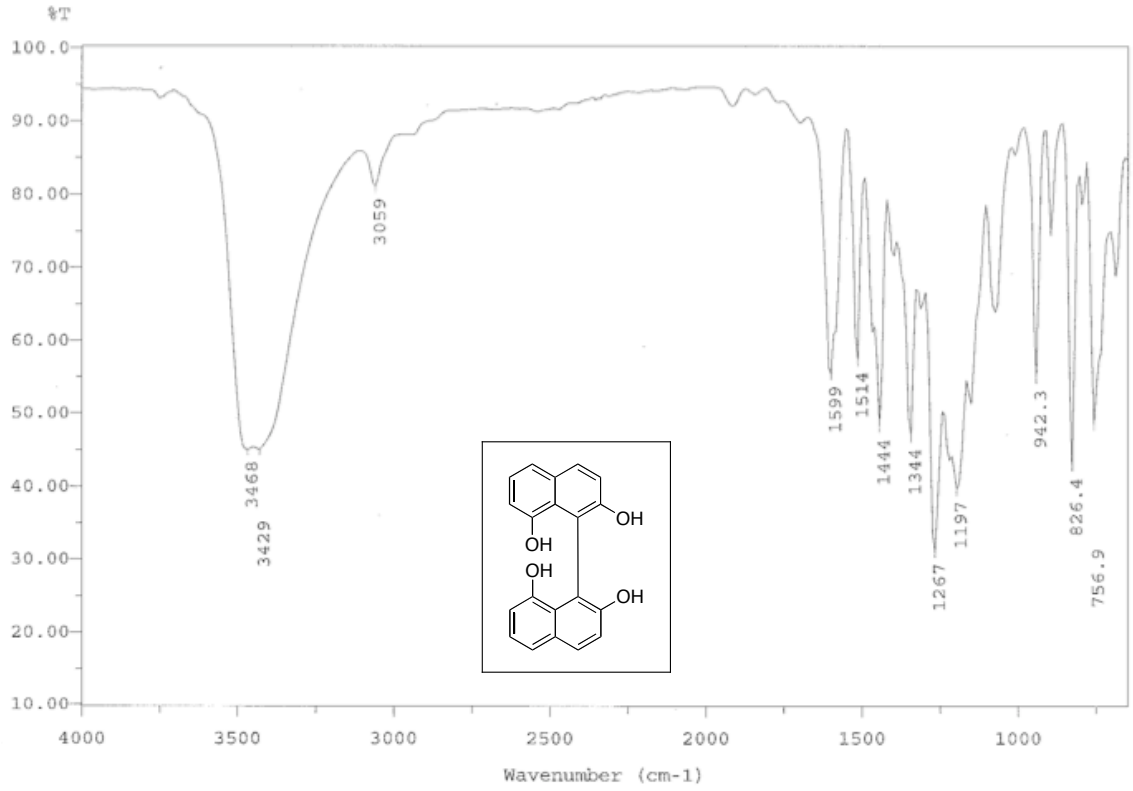

Figure A#.#_3 IR Spectrum of Compound **2.14** (film).

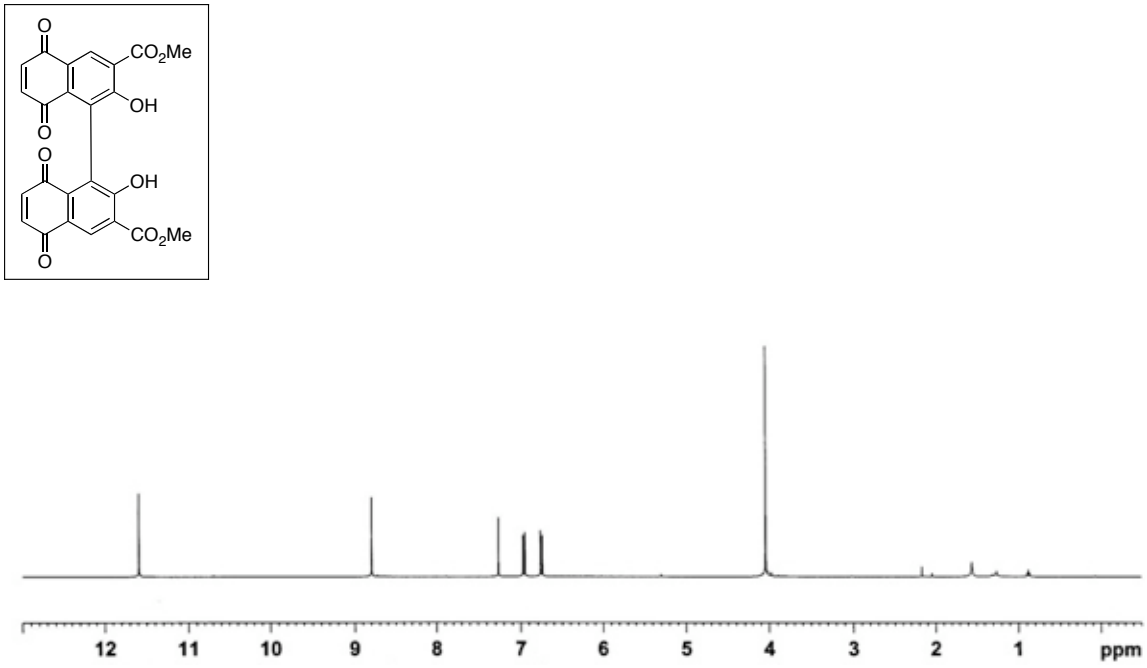

Figure A2.15_1 ^{1}H NMR Spectrum of Compound **2.15** (500 MHz, $CDCl_3$).

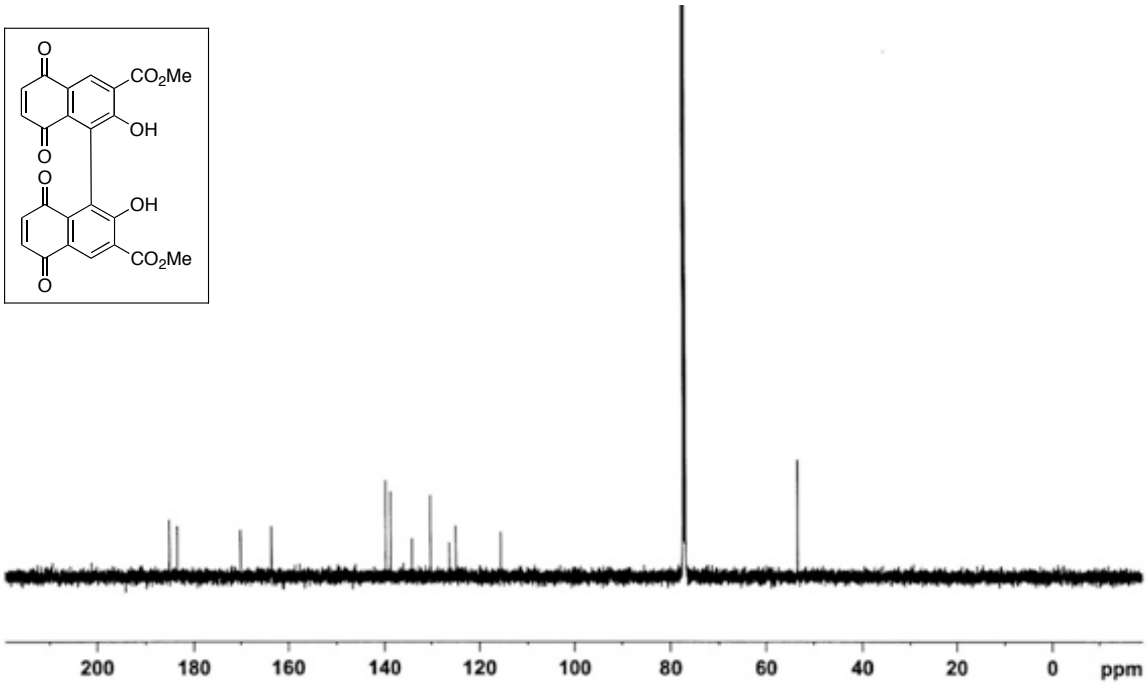

Figure A2.15_2 ^{13}C NMR Spectrum of Compound **2.15** (125 MHz, $CDCl_3$).

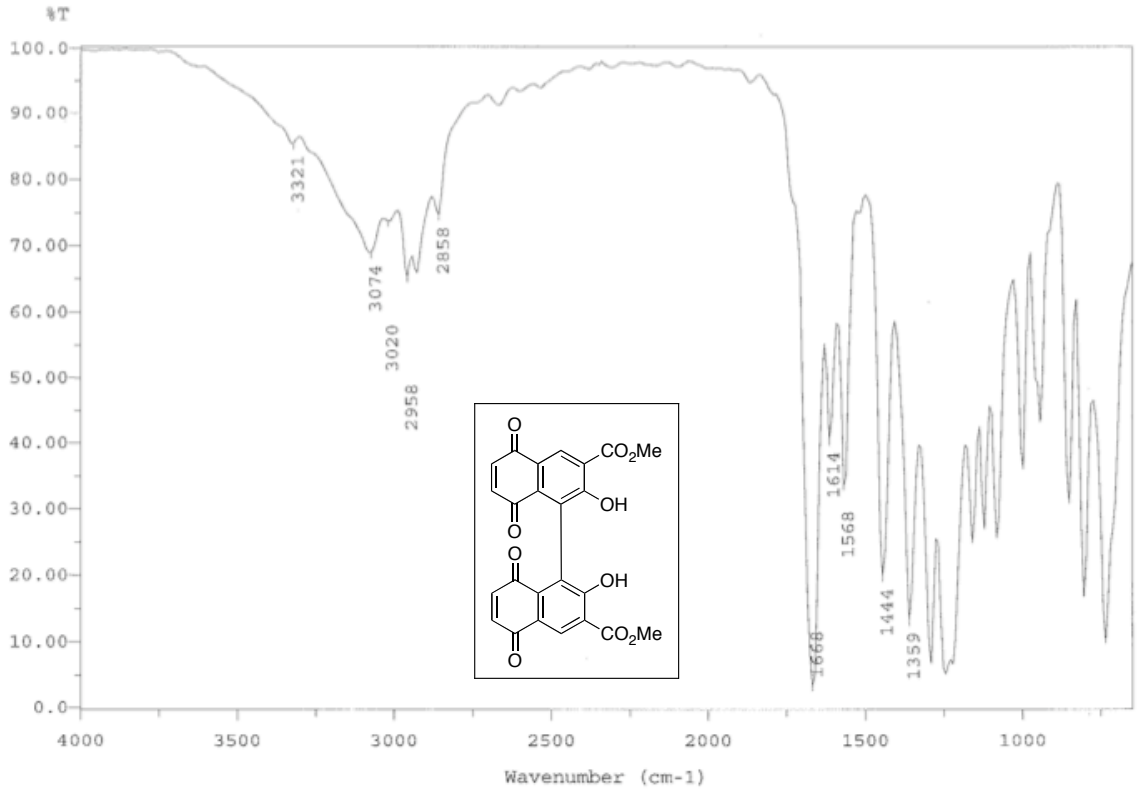

Figure A2.15_3 IR Spectrum of Compound **2.15** (film).

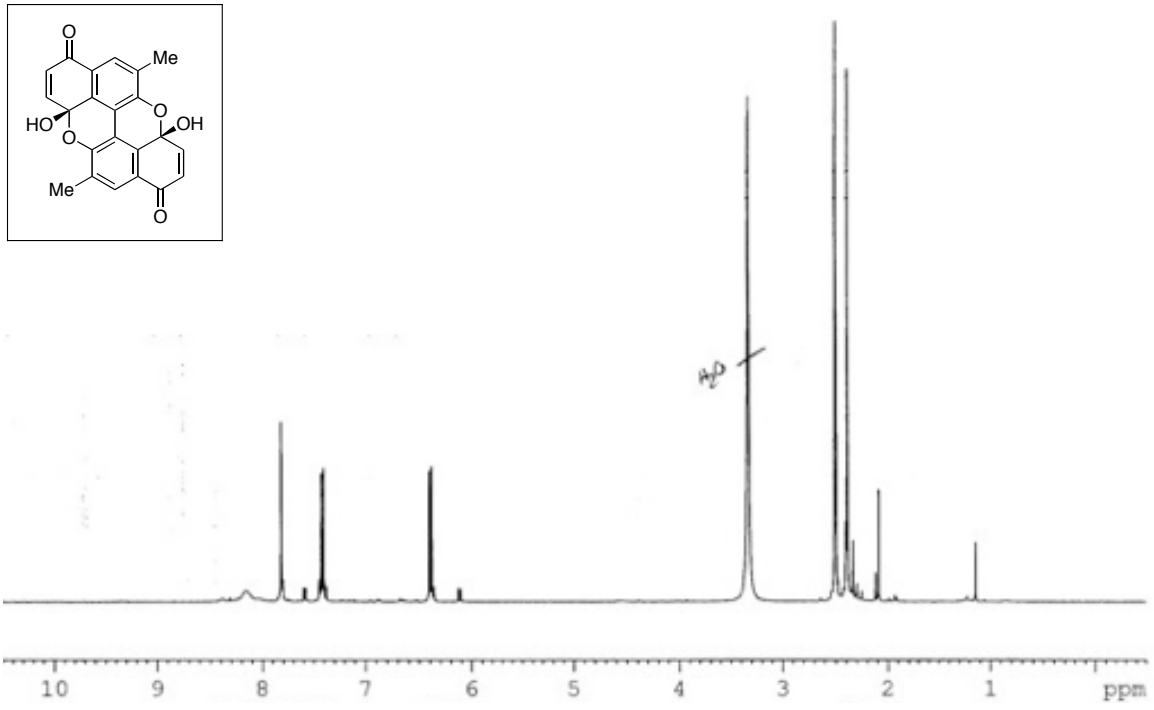

Figure A2.16_1 ^{1}H NMR Spectrum of Compound **2.16** (500 MHz, DMSO-d_6).

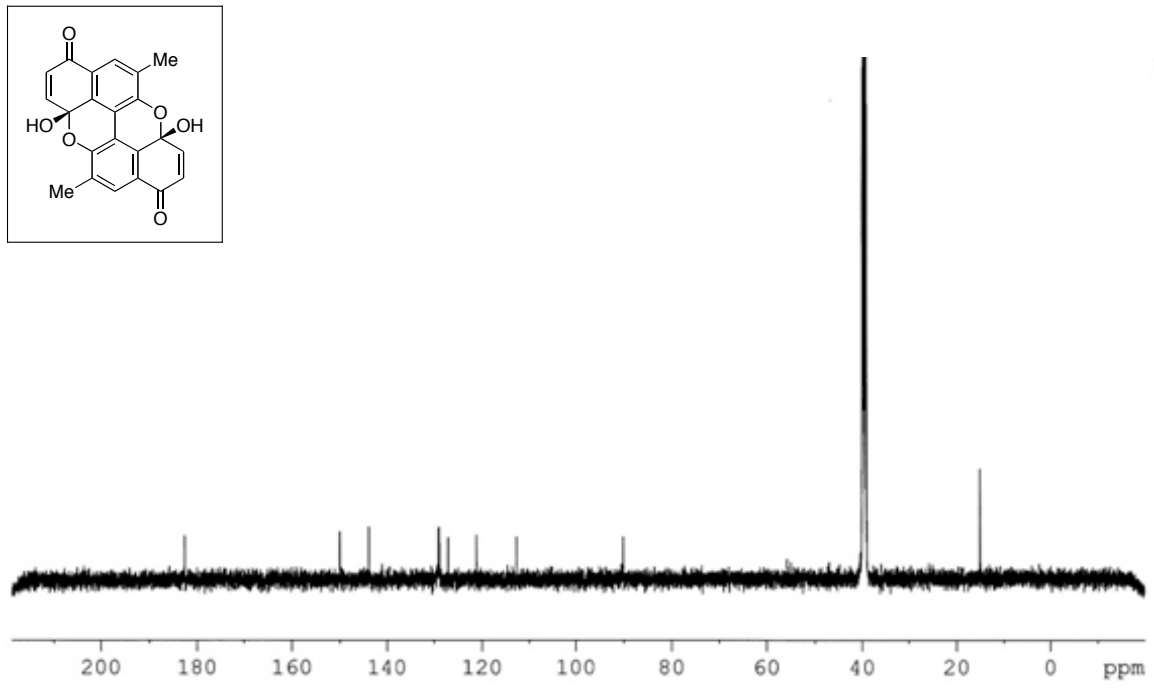

Figure A2.16_2 ^{13}C NMR Spectrum of Compound **2.16** (125 MHz, DMSO-d_6).

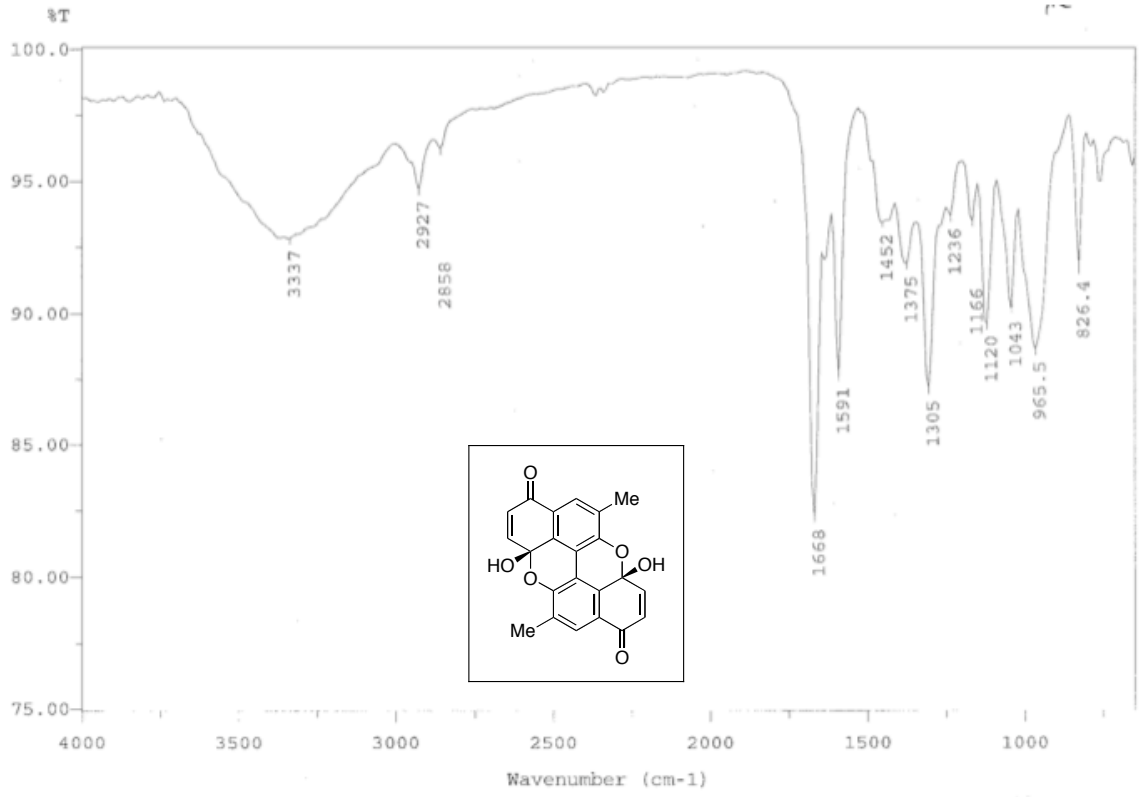

Figure A2.16_3 IR Spectrum of Compound **2.16** (film).

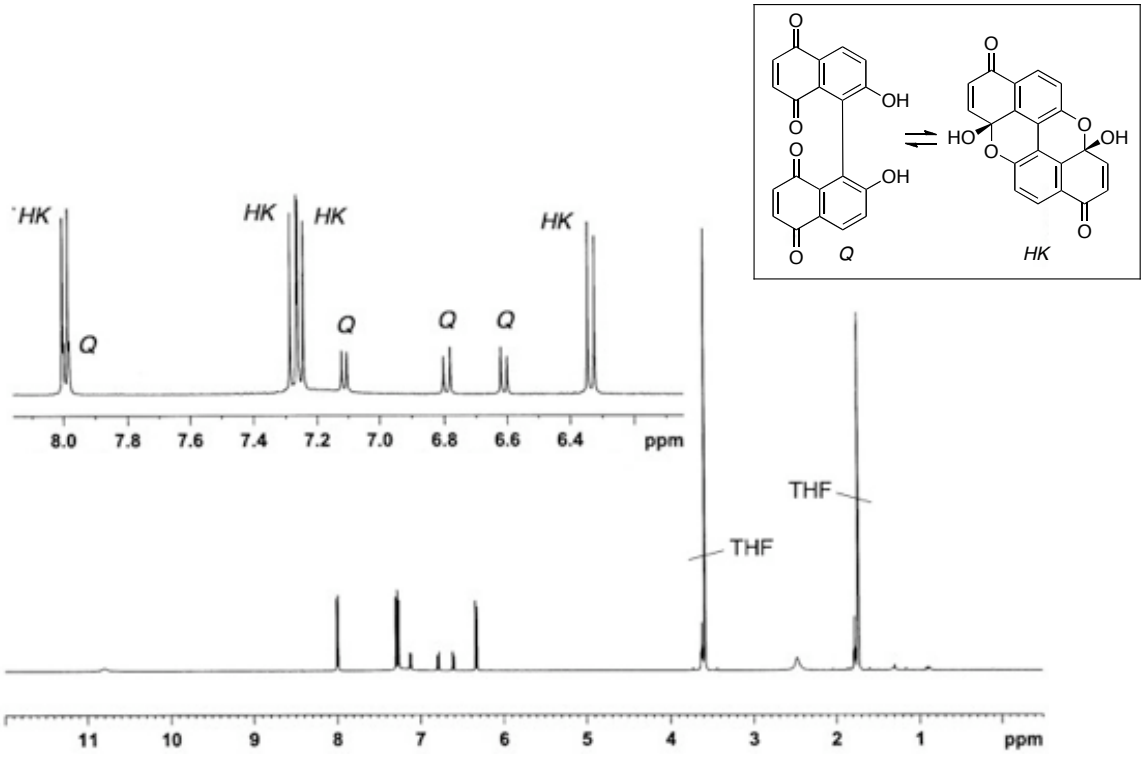

Figure A2.17_1 ^{1}H NMR Spectrum of Compound **2.17** (500 MHz, THF-d_8).

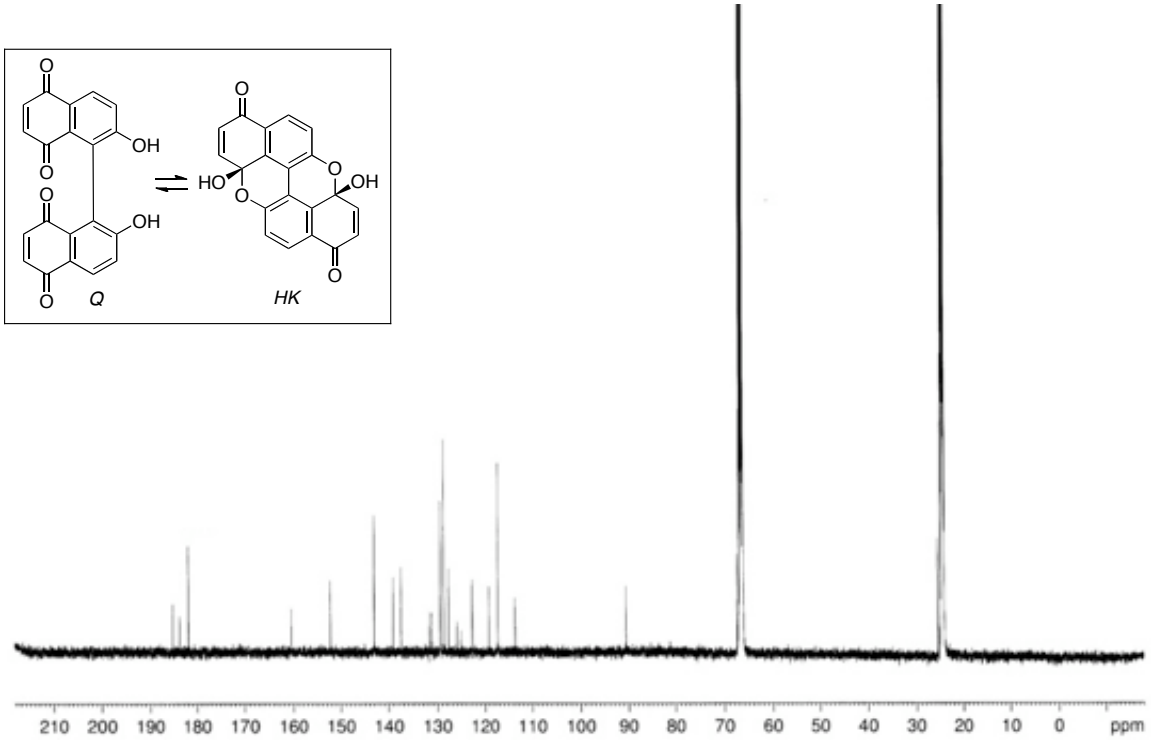

Figure A2.17_2 ^{13}C NMR Spectrum of Compound **2.17** (125 MHz, THF-d_8).

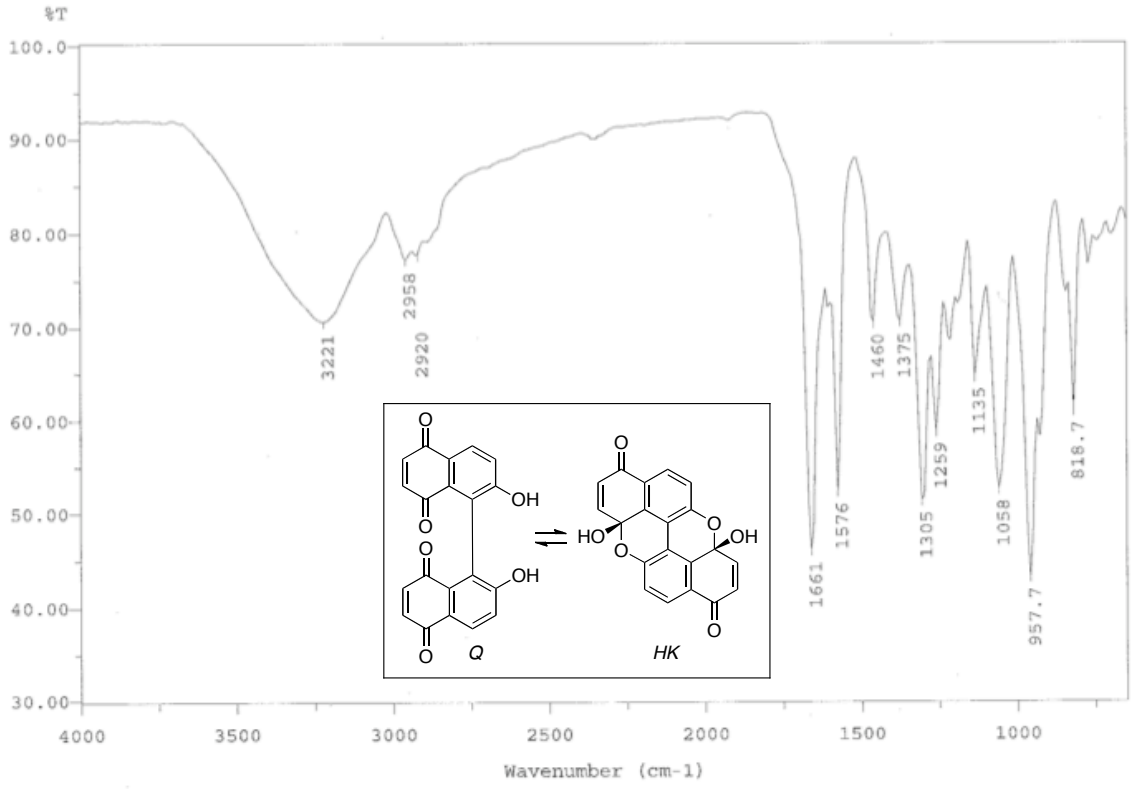

Figure A2.17_3 IR Spectrum of Compound **2.17** (film).

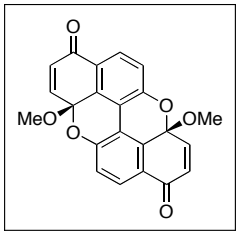

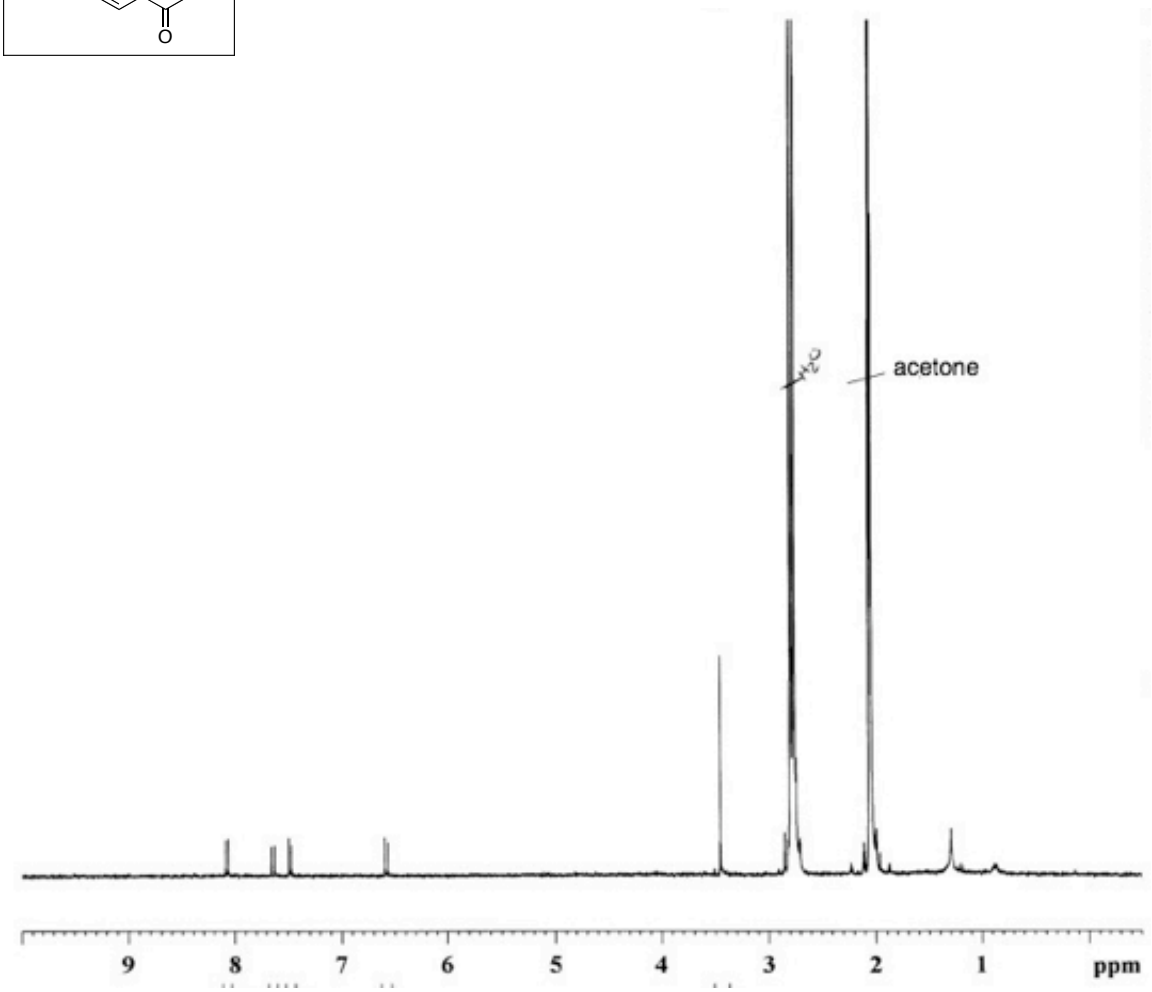

Figure A2.18_1 ^{1}H NMR Spectrum of Compound *rac*-**2.18** (360 MHz, acetone-d_6).

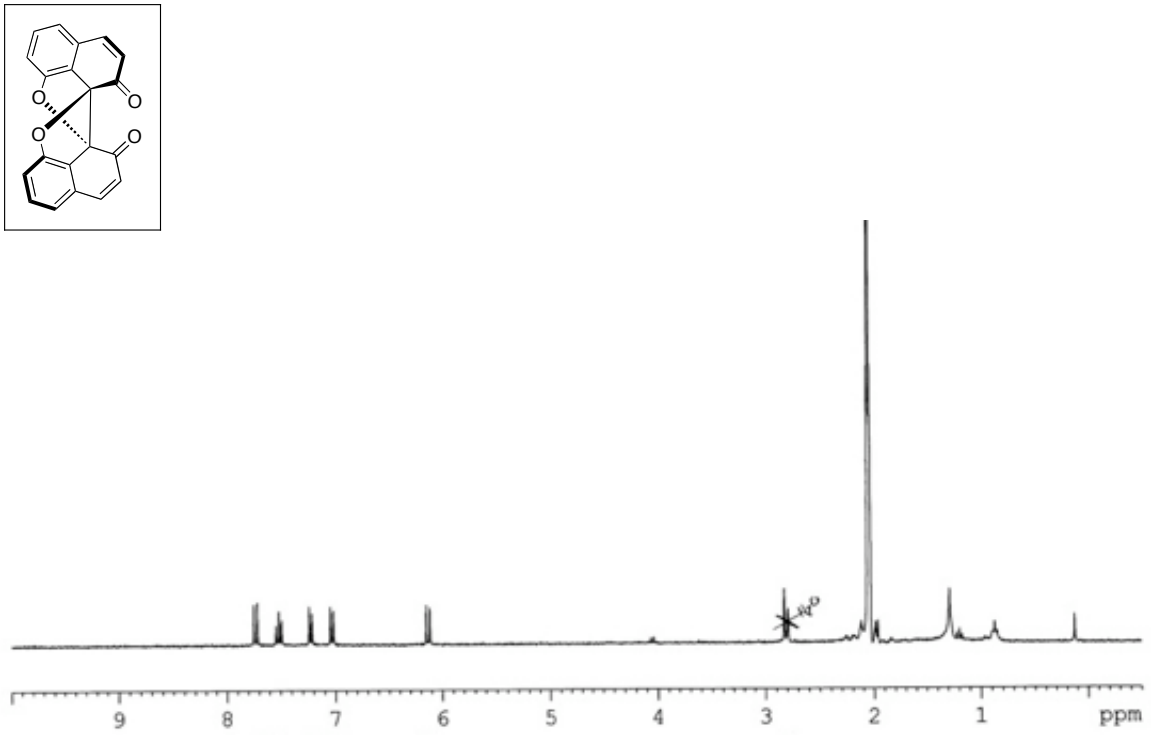

Figure A2.19_1 ^{1}H NMR Spectrum of Compound *rac*-**2.19** (300 MHz, acetone-d_6).

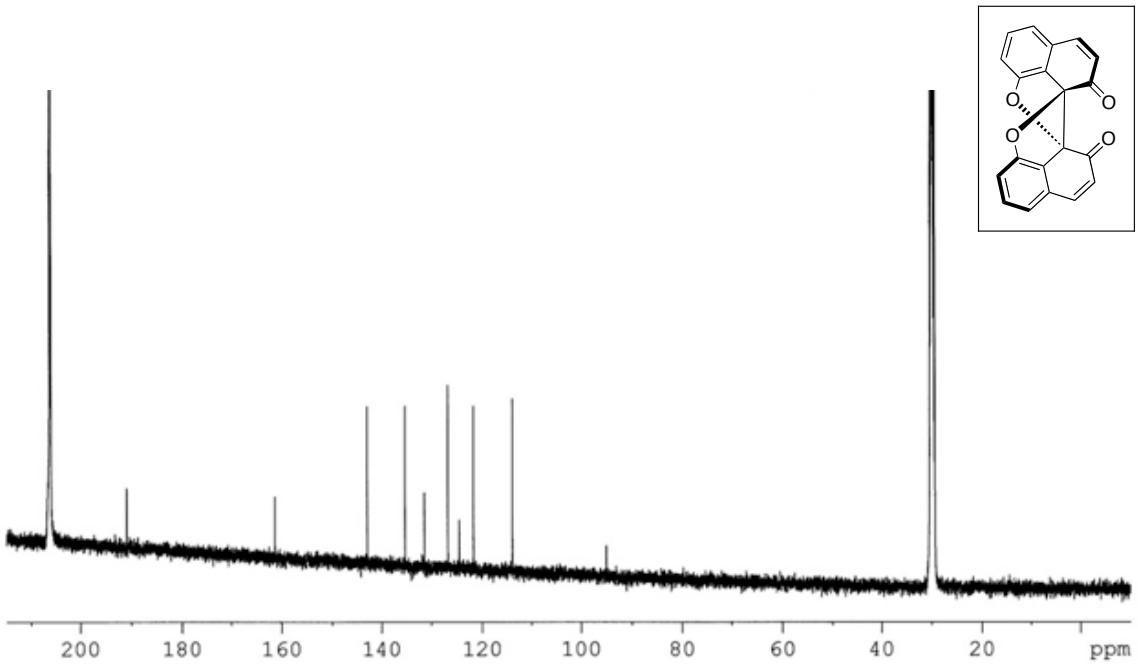

Figure A2.19_2 ^{13}C NMR Spectrum of Compound *rac*-**2.19** (125 MHz, acetone-d_6).

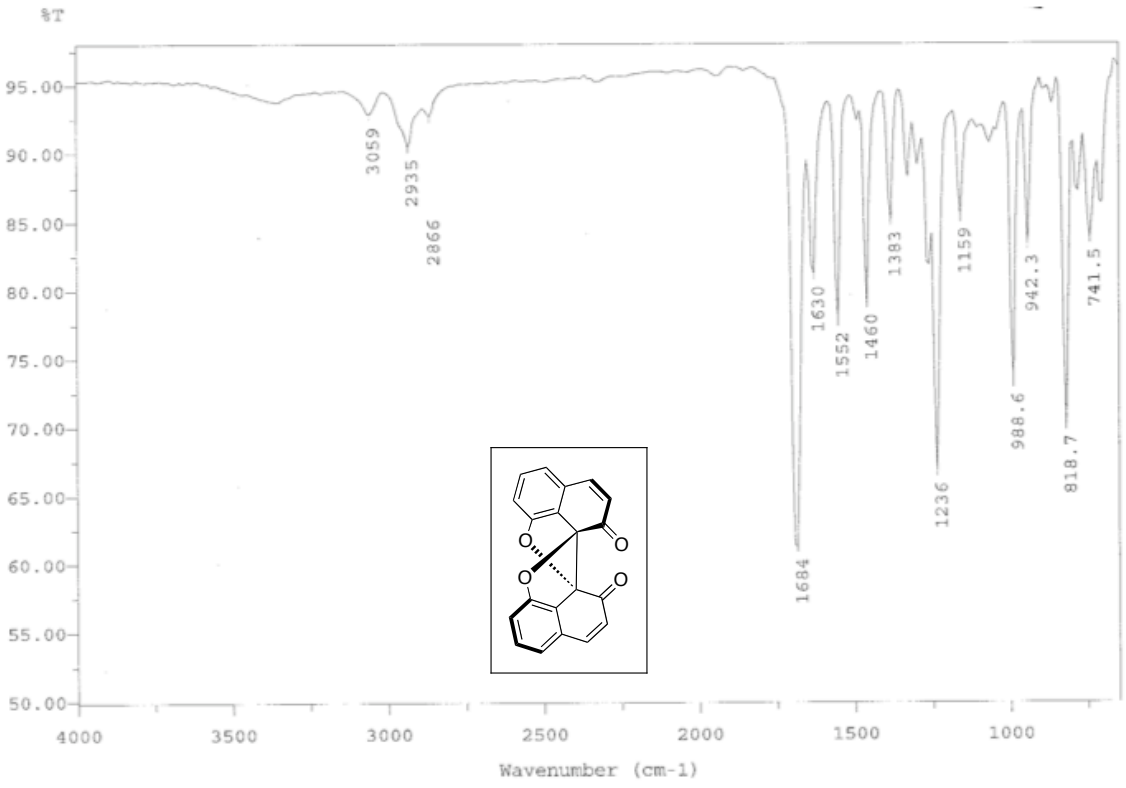

Figure A2.19_3 IR Spectrum of Compound *rac*-**2.19** (film).

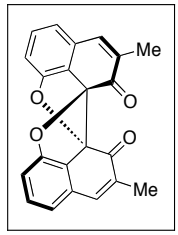

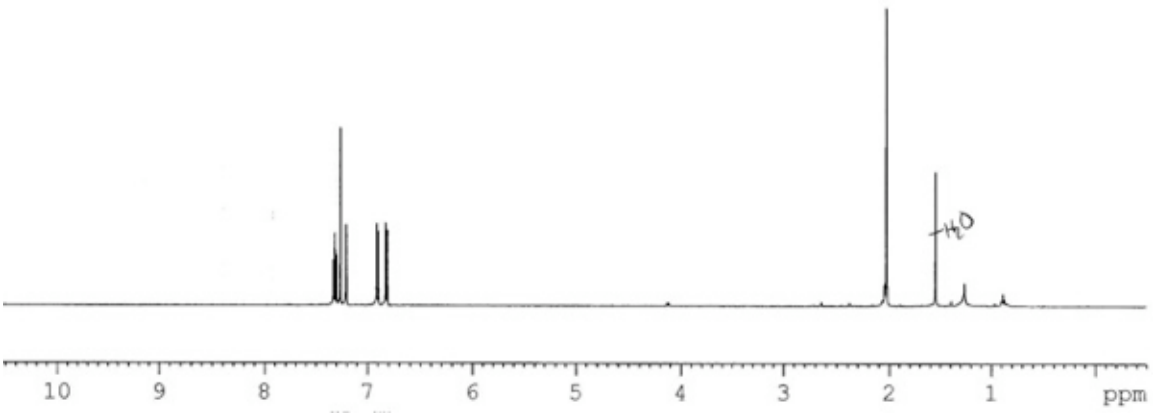

Figure A2.20_1 ^{1}H NMR Spectrum of Compound *rac*-**2.20** (500 MHz, $CDCl_3$).

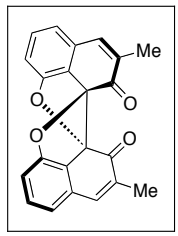

Figure A2.20_2 ^{13}C NMR Spectrum of Compound *rac*-**2.20** (125 MHz, $CDCl_3$).

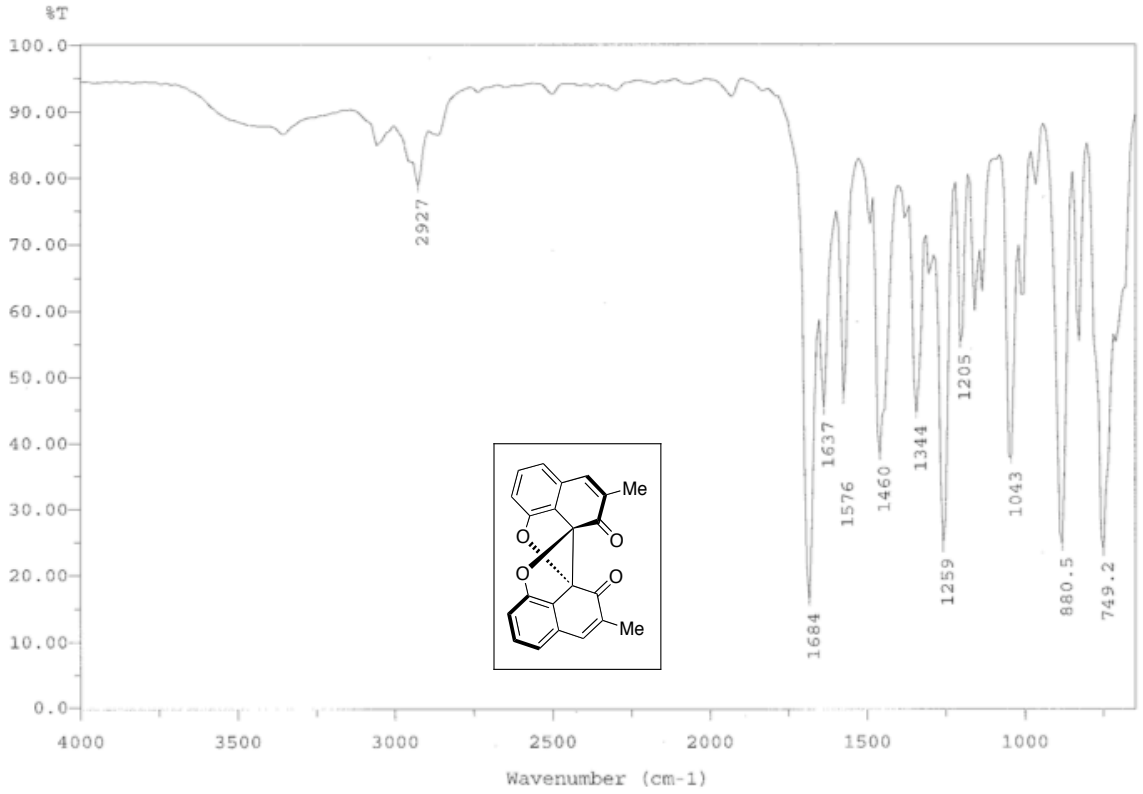

Figure A2.20_3 IR Spectrum of Compound *rac*-**2.20** (film).

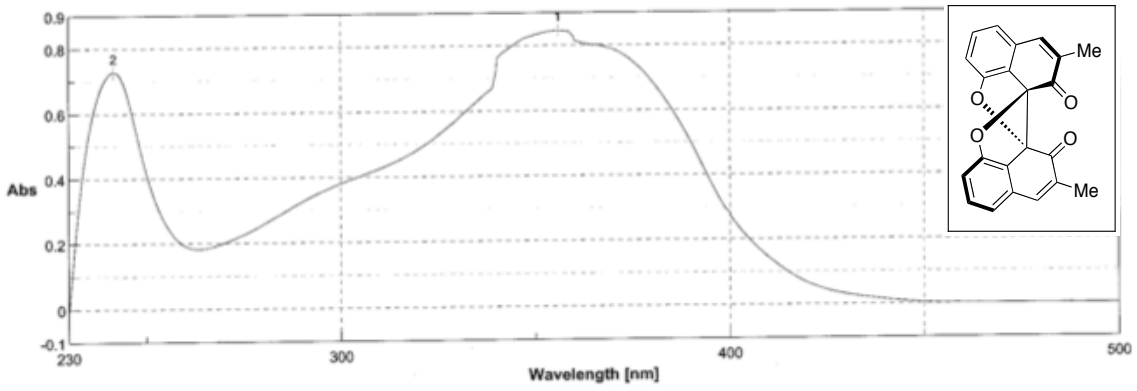

Figure A2.20_3 UV Spectrum of Compound *rac*-**2.20** (CH_2Cl_2).

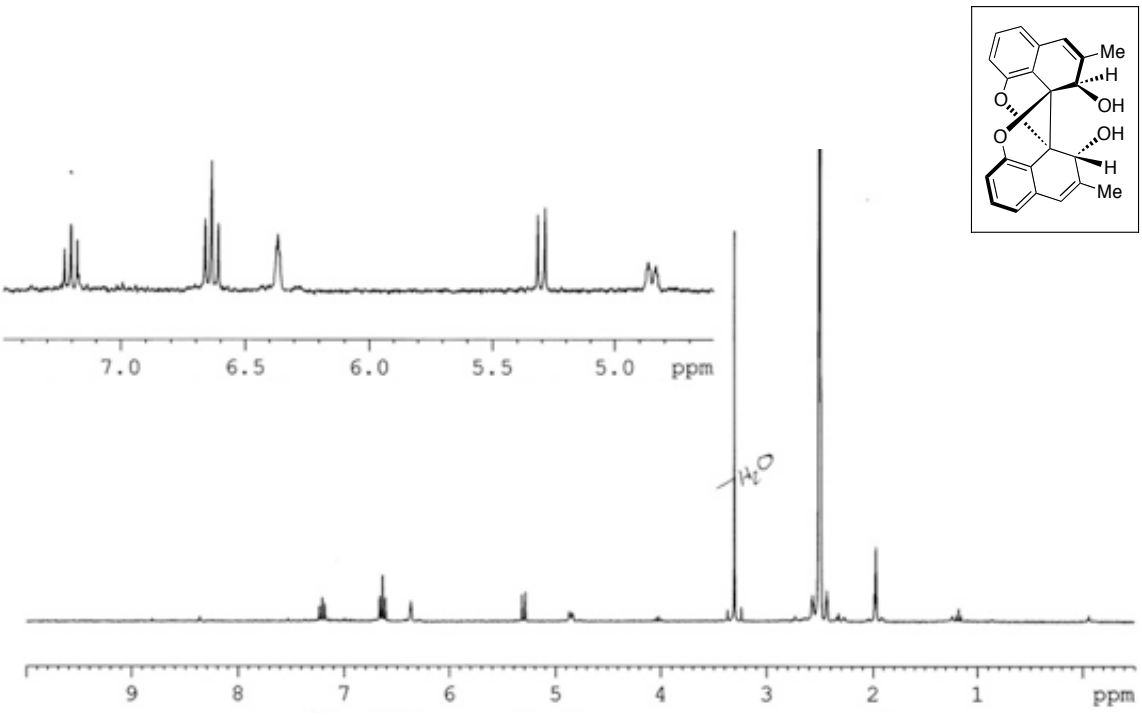

Figure A2.21_1 ^{1}H NMR Spectrum of Compound *rac*-**2.21** (300 MHz, DMSO-d_6).

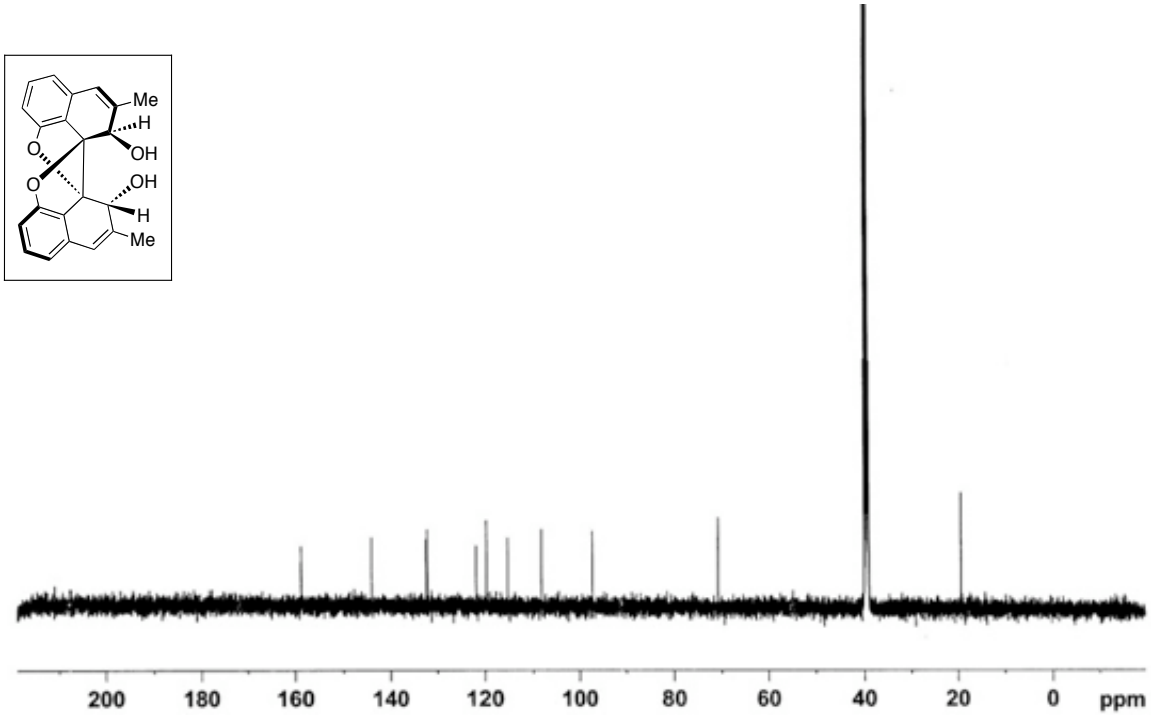

Figure A2.21_2 ^{13}C NMR Spectrum of Compound *rac*-**2.21** (125 MHz, DMSO-d_6).

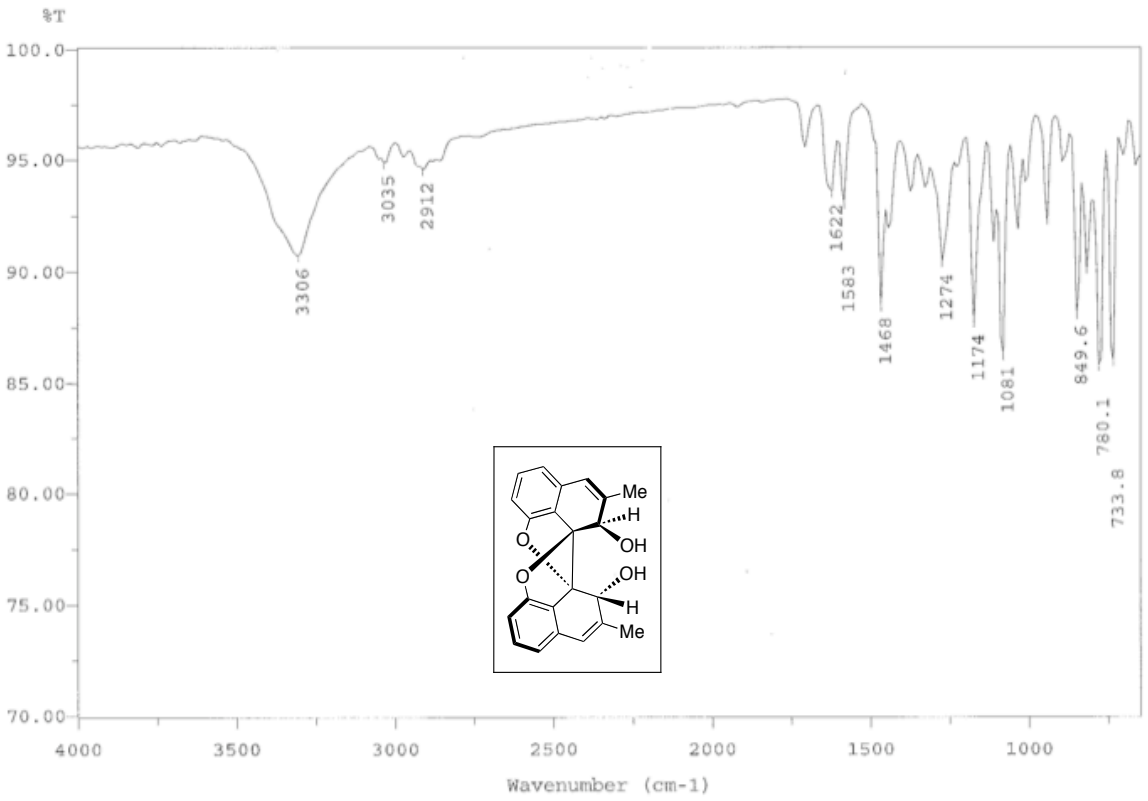

Figure A2.21_3 IR Spectrum of Compound *rac*-**2.21** (film).

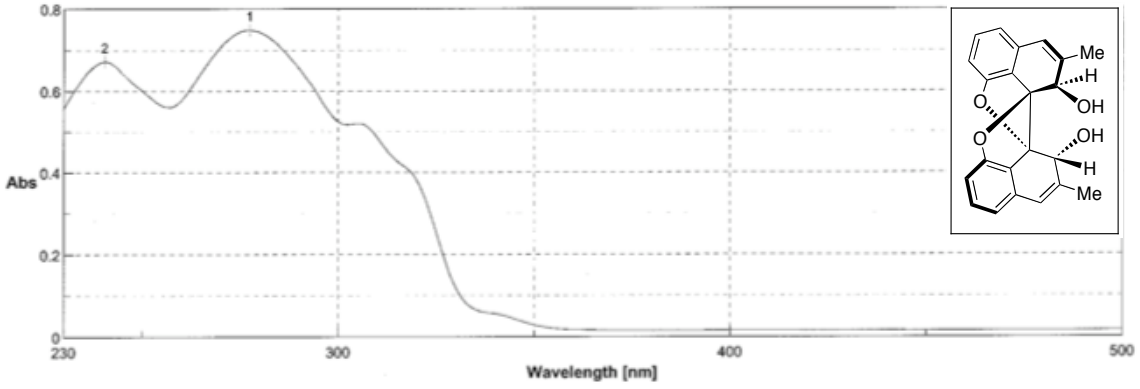

Figure A2.21_3 UV Spectrum of Compound *rac*-**2.21** (EtOH).

7.3 Chapter 4

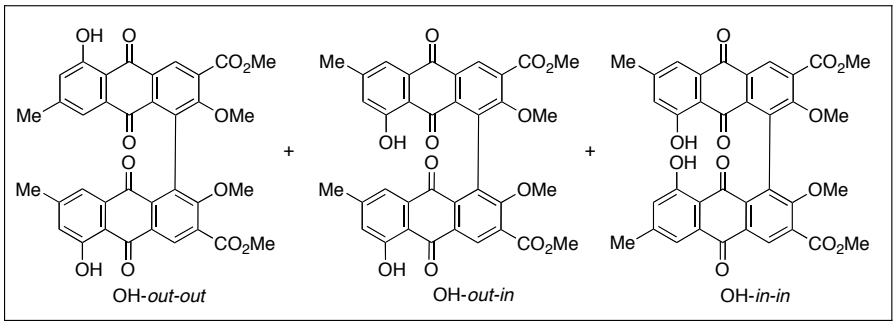

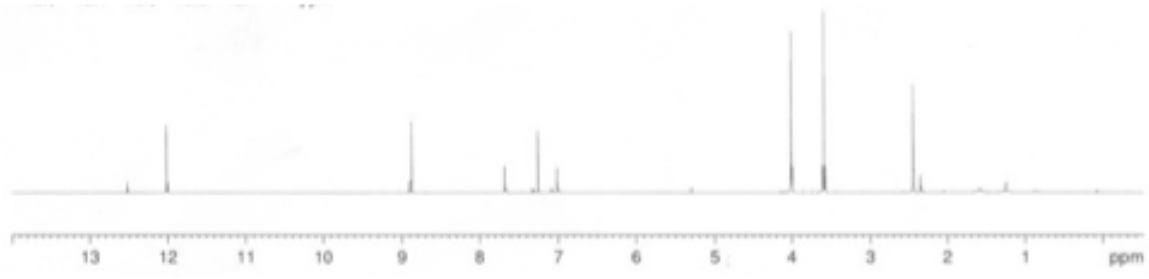

Figure A4.23_1 ^{1}H NMR Spectrum of Compound **4.23a-c** (500 MHz, $CDCl_3$).

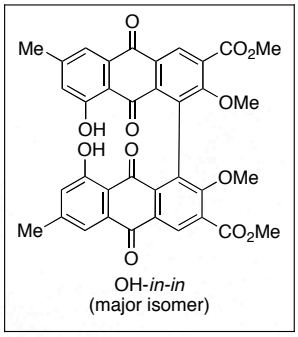

Figure A4.23_2 ^{13}C NMR Spectrum of Compound **4.23c** (125 MHz, $CDCl_3$).

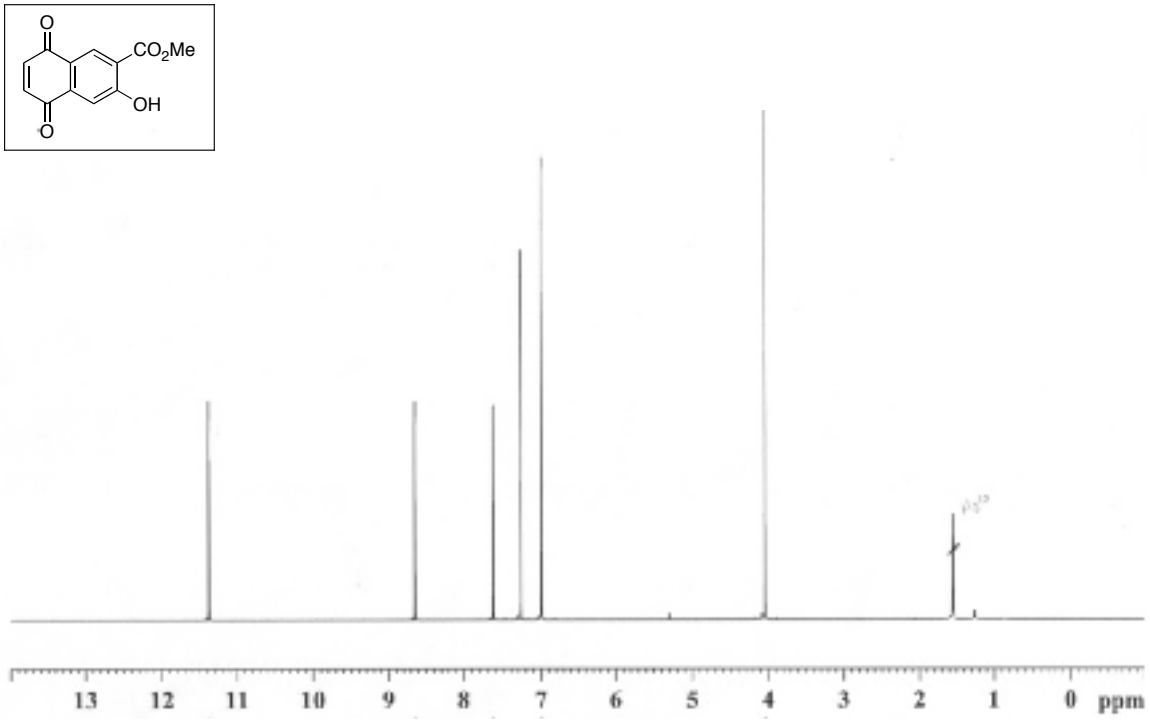

Figure A4.25_1 ^{1}H NMR Spectrum of Compound **4.25** (500 MHz, $CDCl_3$).

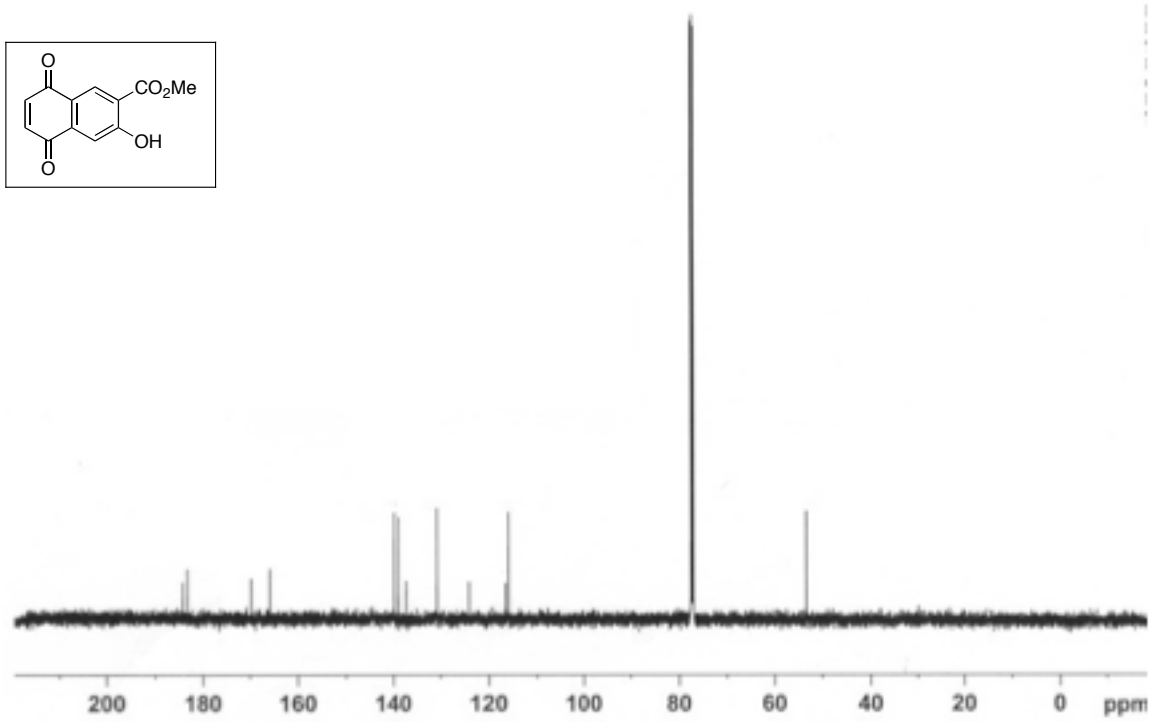

Figure A4.25_2 ^{13}C NMR Spectrum of Compound **4.25** (125 MHz, $CDCl_3$).

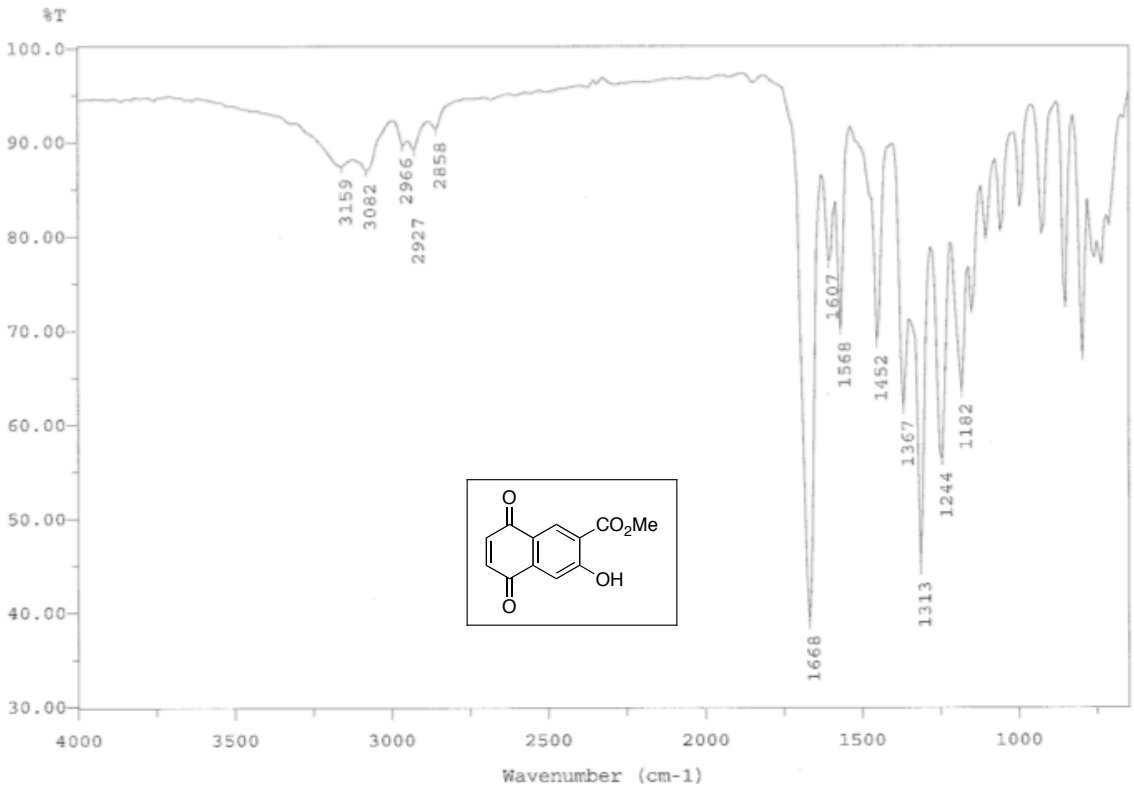

Figure A4.25_3 IR Spectrum of Compound **4.25** (film).

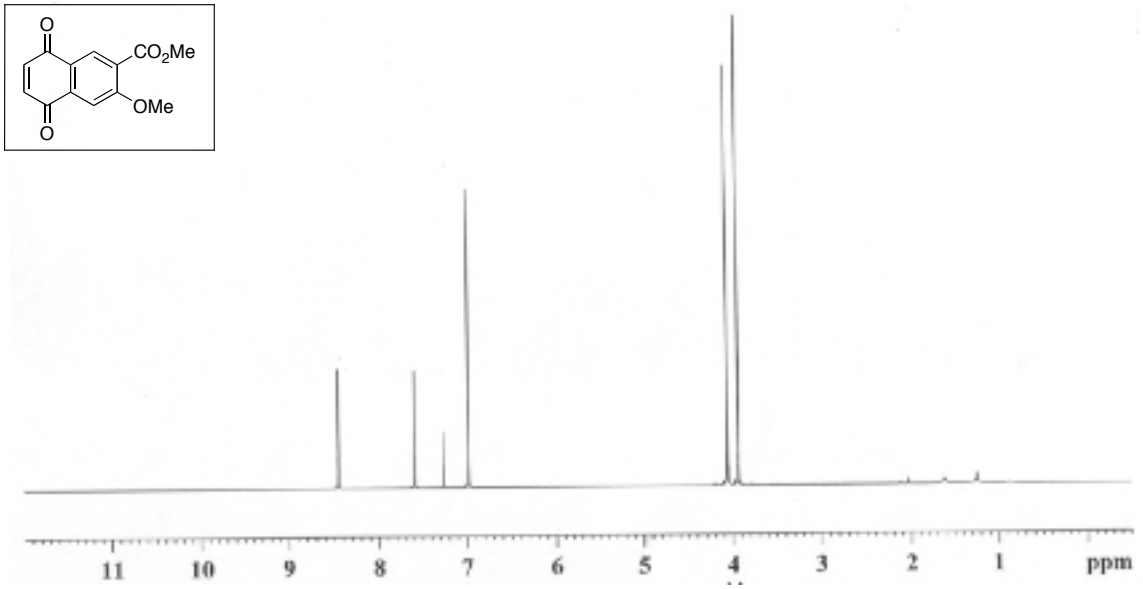

Figure A4.26_1 ^{1}H NMR Spectrum of Compound **4.26** (500 MHz, $CDCl_3$).

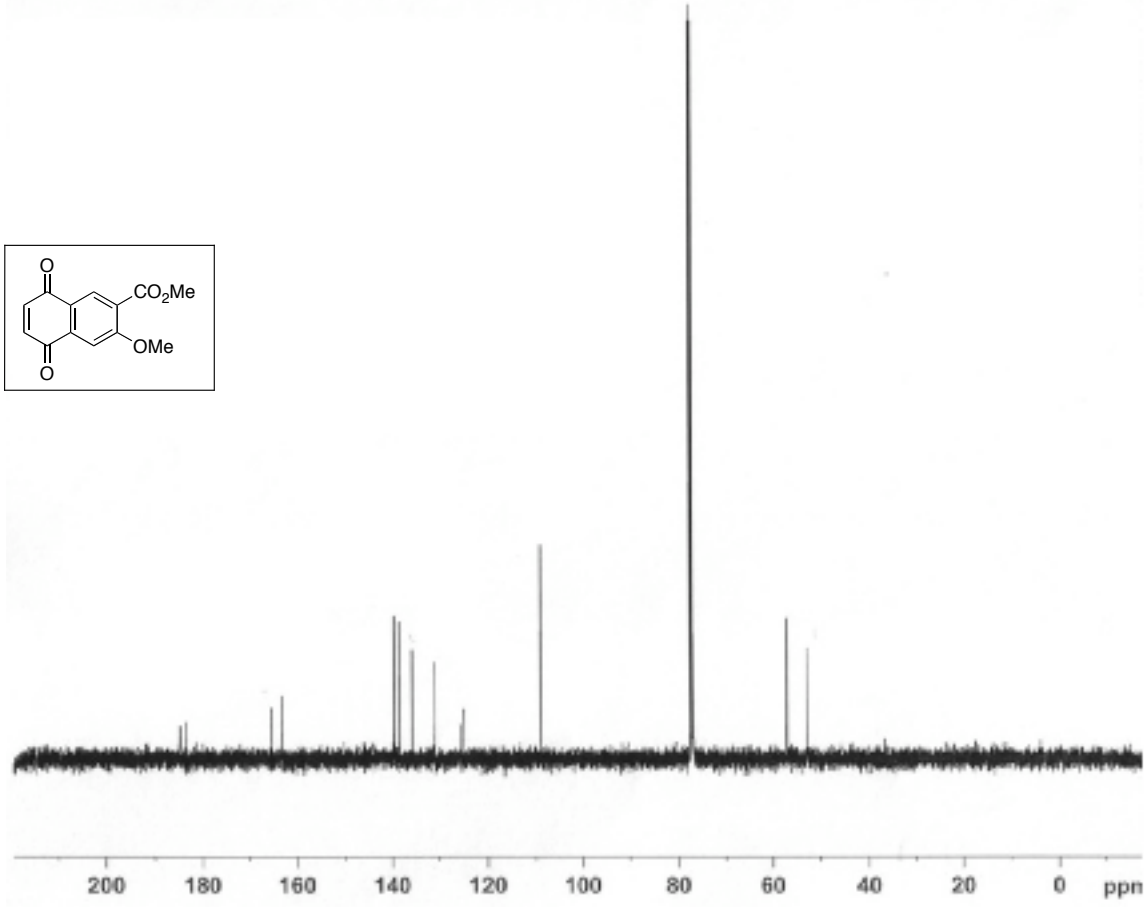

Figure A4.26_2 ^{13}C NMR Spectrum of Compound **4.26** (125 MHz, $CDCl_3$).

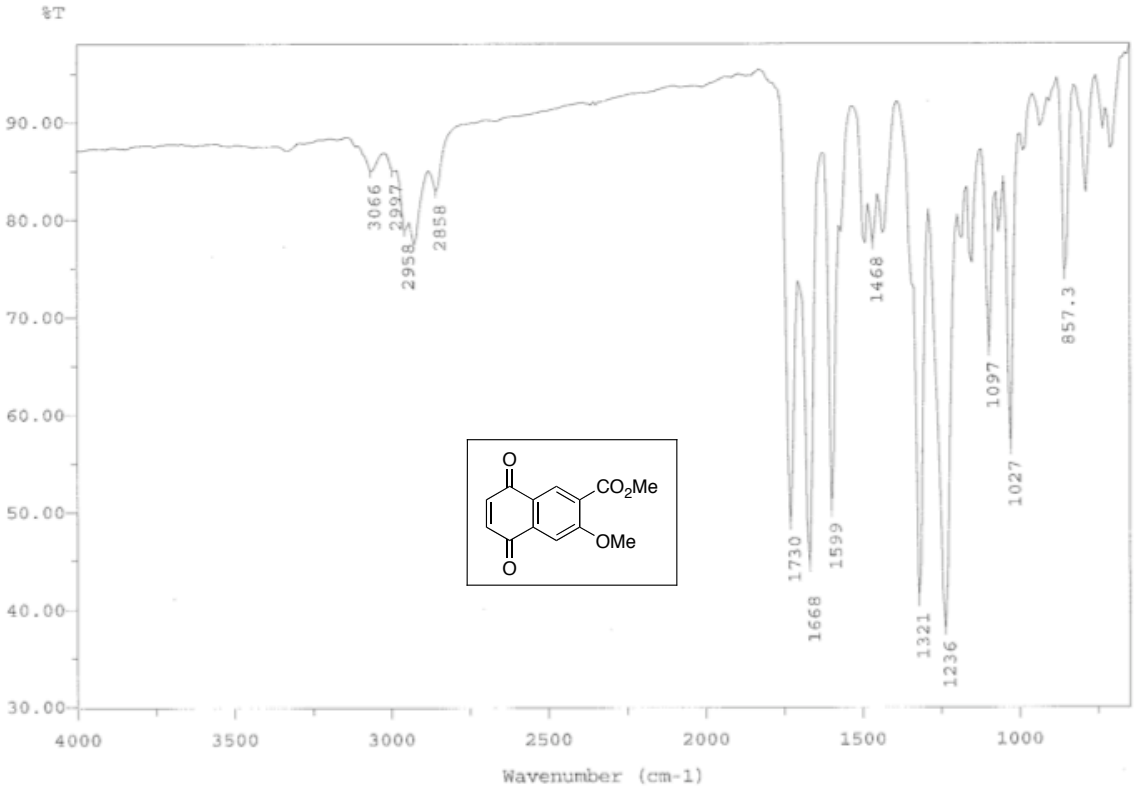

Figure A4.26_3 IR Spectrum of Compound **4.26** (film).

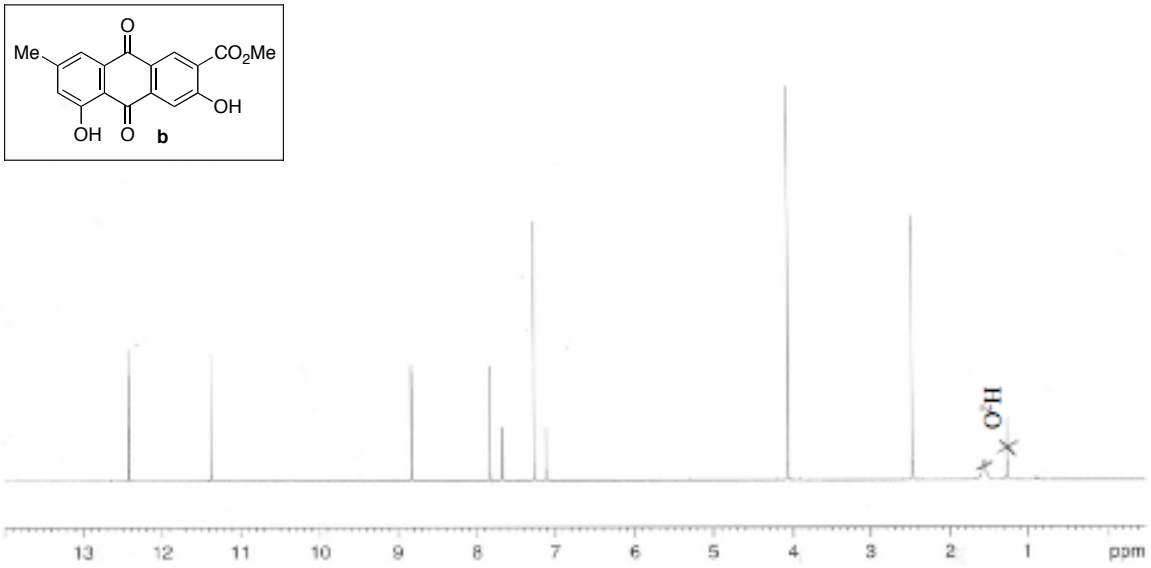

Figure A4.24_1 ^{1}H NMR Spectrum of Compound **4.24b** (500 MHz, $CDCl_3$).

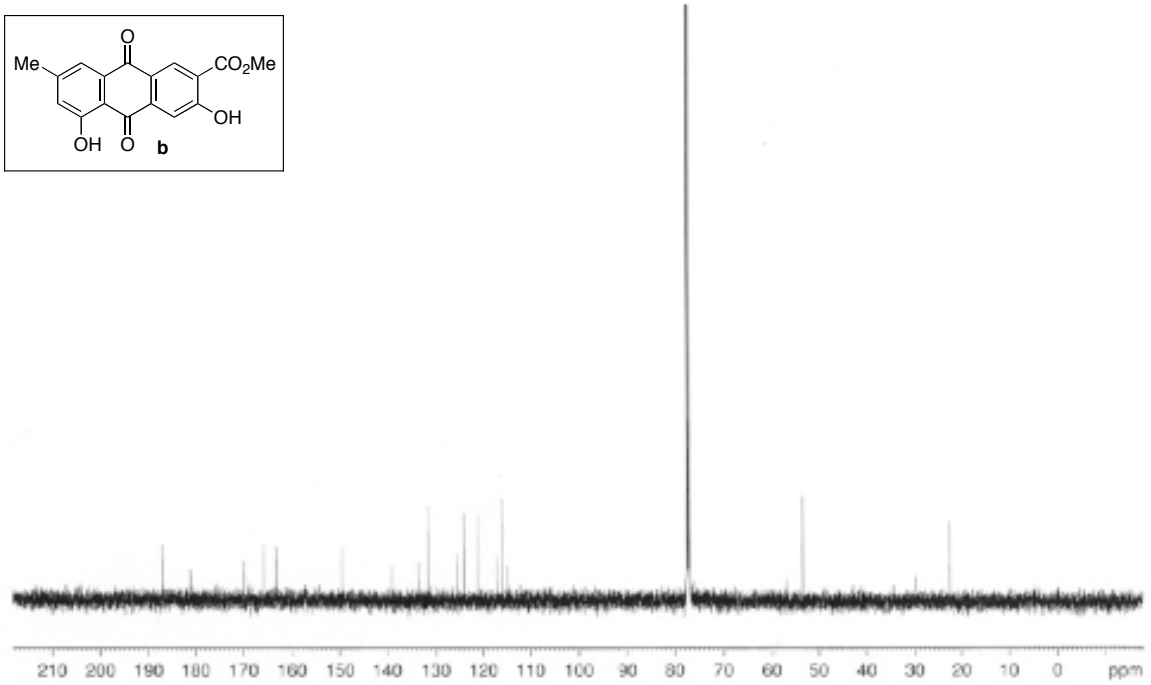

Figure A4.24_2 ^{13}C NMR Spectrum of Compound **4.24b** (125 MHz, $CDCl_3$).

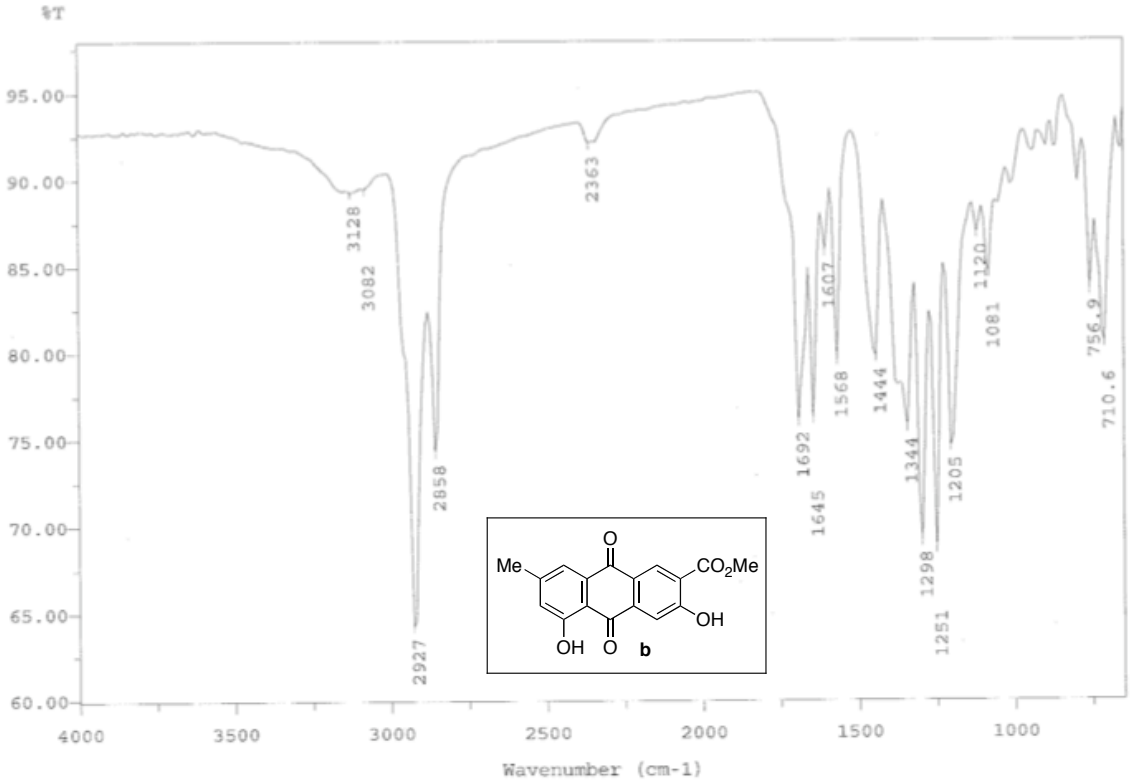

Figure A4.24_3 IR Spectrum of Compound **4.24b** (film).

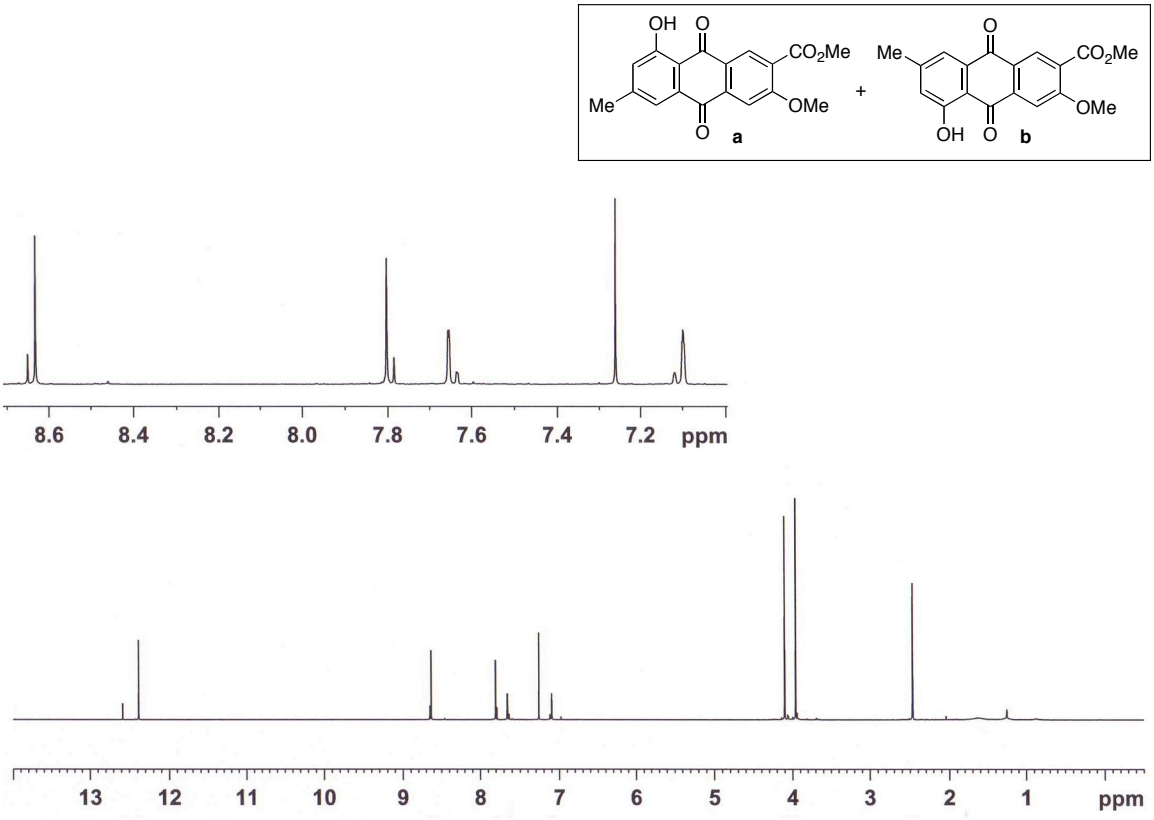

Figure A4.27_1 ^{1}H NMR Spectrum of Compound **4.27a-b** (500 MHz, $CDCl_3$).

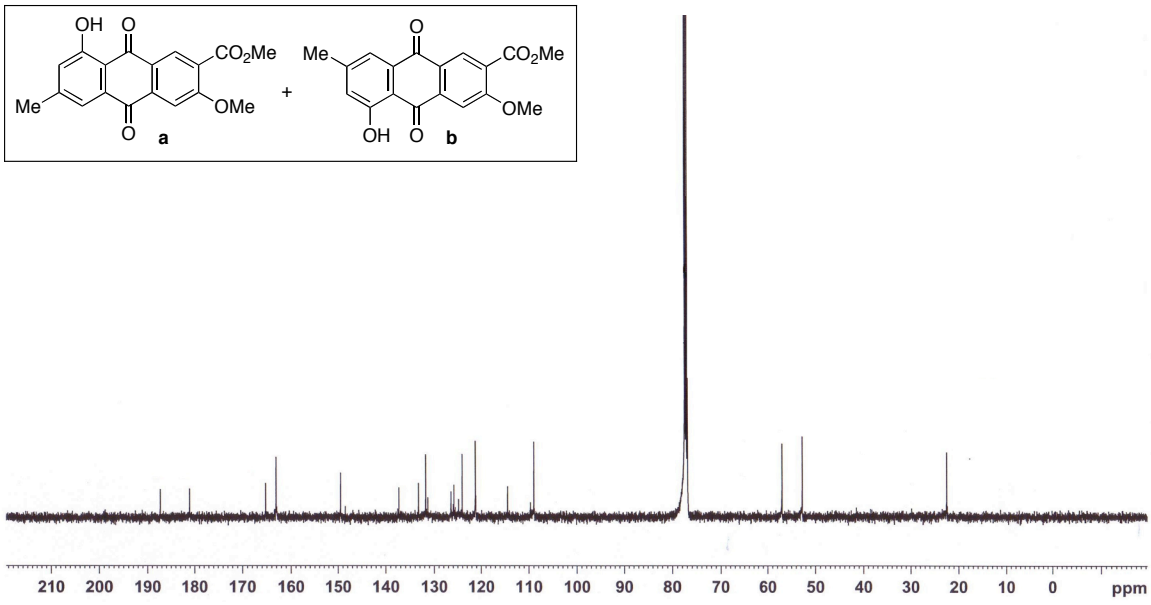

Figure A4.27_2 ^{13}C NMR Spectrum of Compound **4.27a-b** (125 MHz, $CDCl_3$).

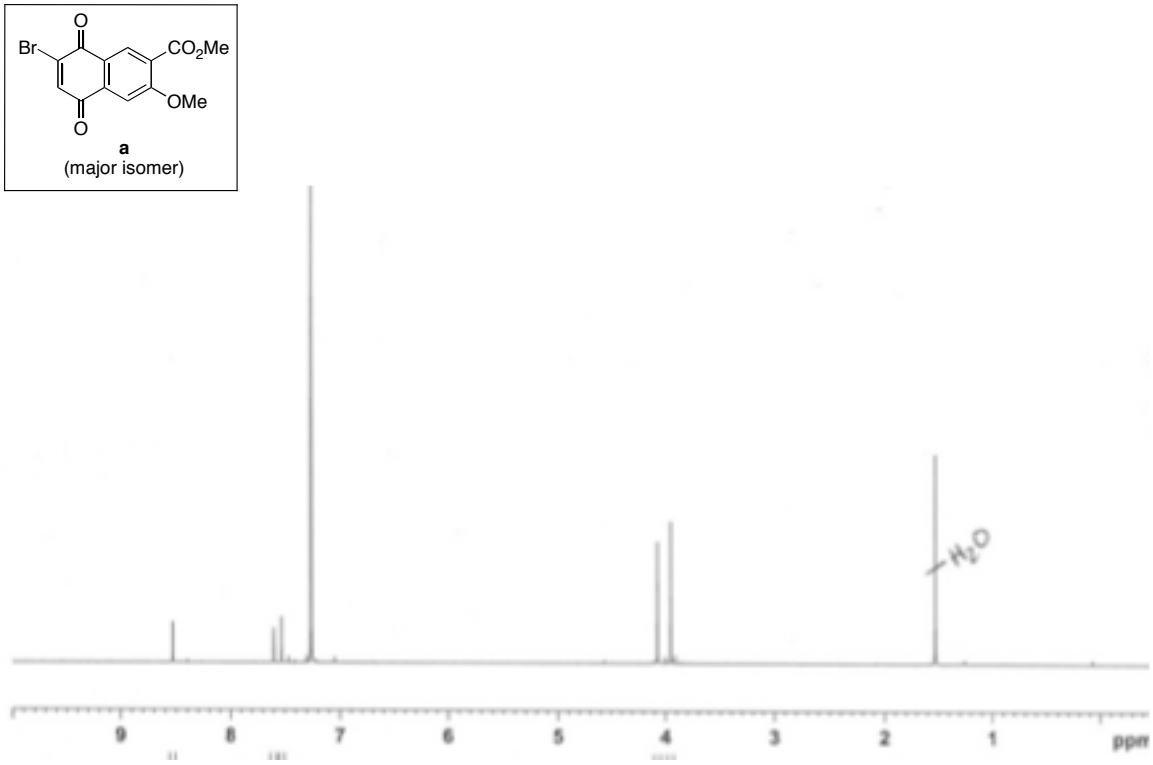

Figure A4.31_1 ^{1}H NMR Spectrum of Compound **4.31a** (500 MHz, $CDCl_3$).

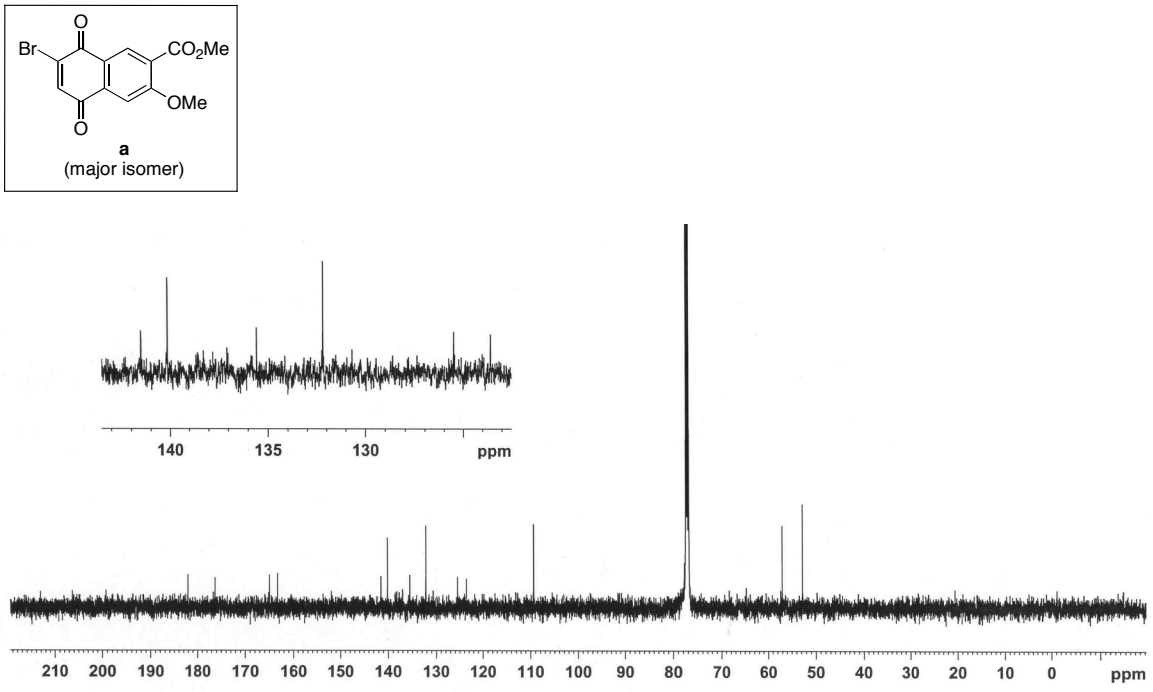

Figure A4.31_2 ^{13}C NMR Spectrum of Compound **4.31a** (125 MHz, $CDCl_3$).

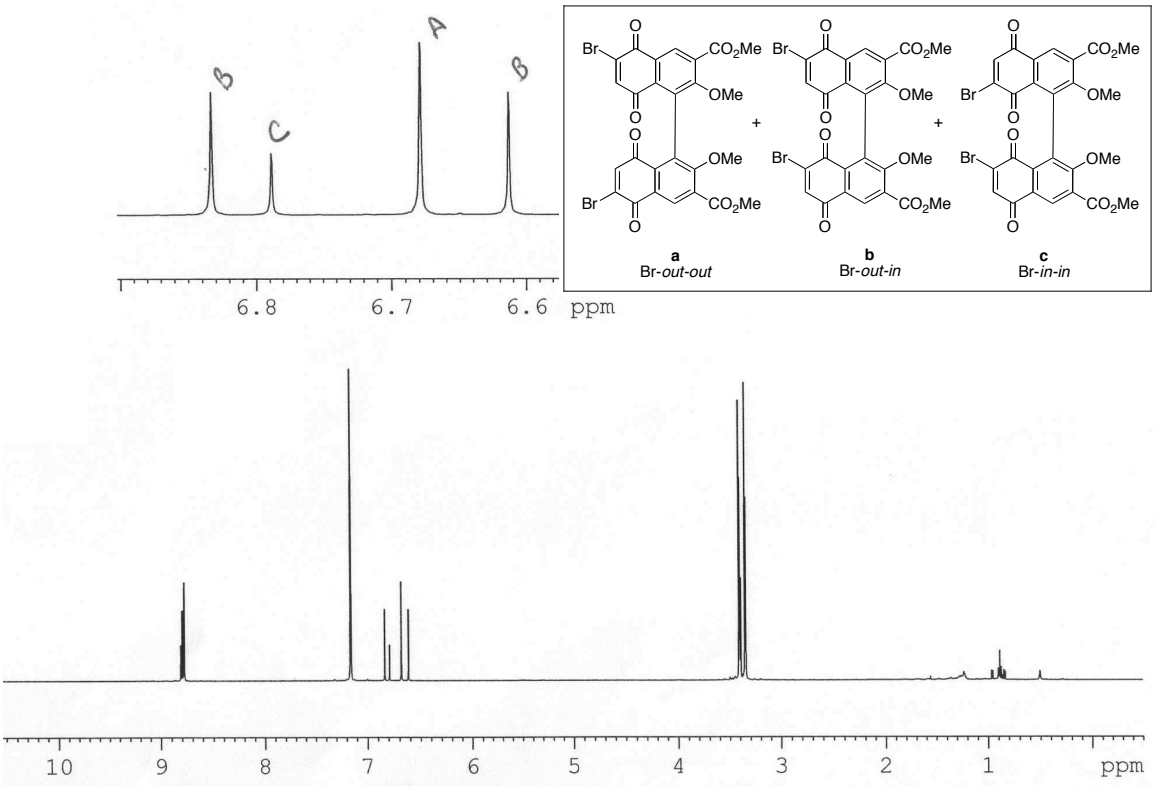

Figure A4.32_1 ^{1}H NMR Spectrum of Compound **4.32a-c** (500 MHz, C_6D_6).

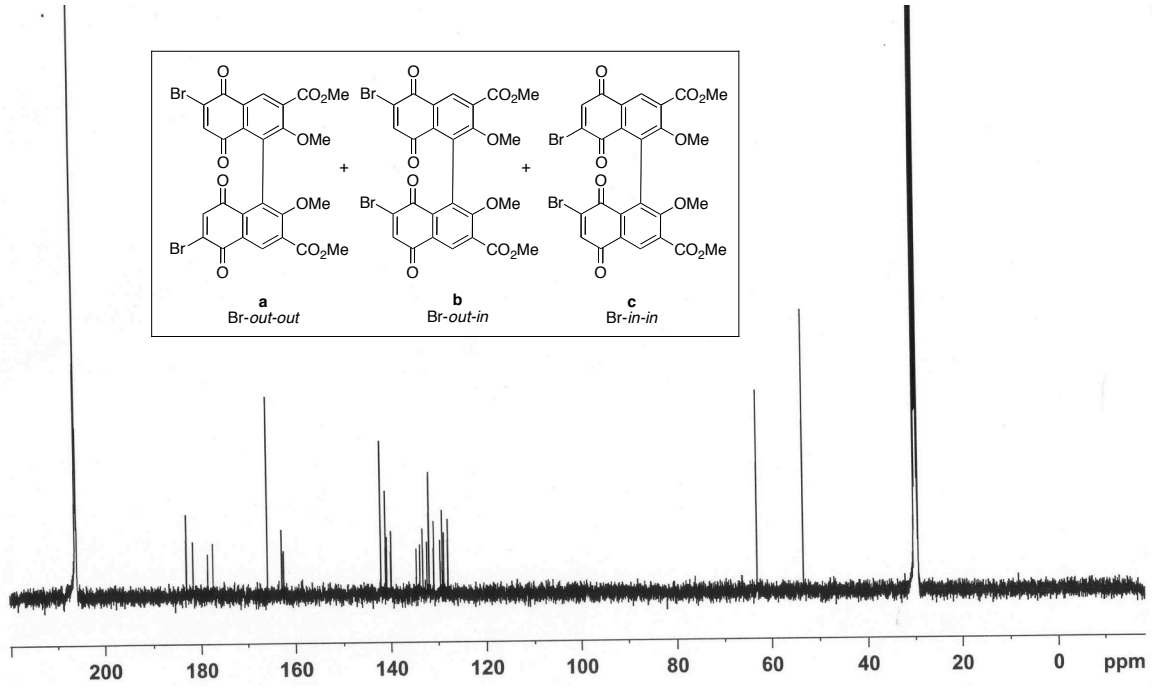

Figure A4.32_2 ^{13}C NMR Spectrum of Compound **4.32a-c** (125 MHz, acetone-d_6).

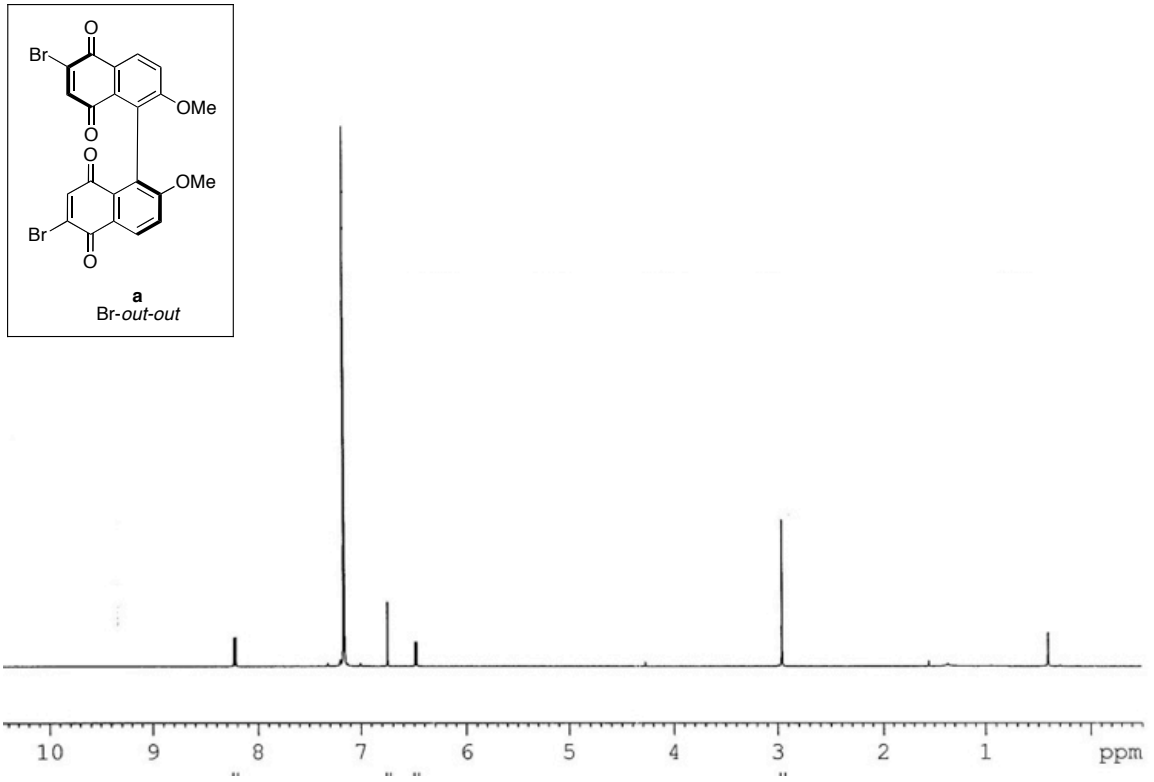

Figure A4.34a_1 ^{1}H NMR Spectrum of Compound (*S*)-**4.34a** (500 MHz, C_6D_6).

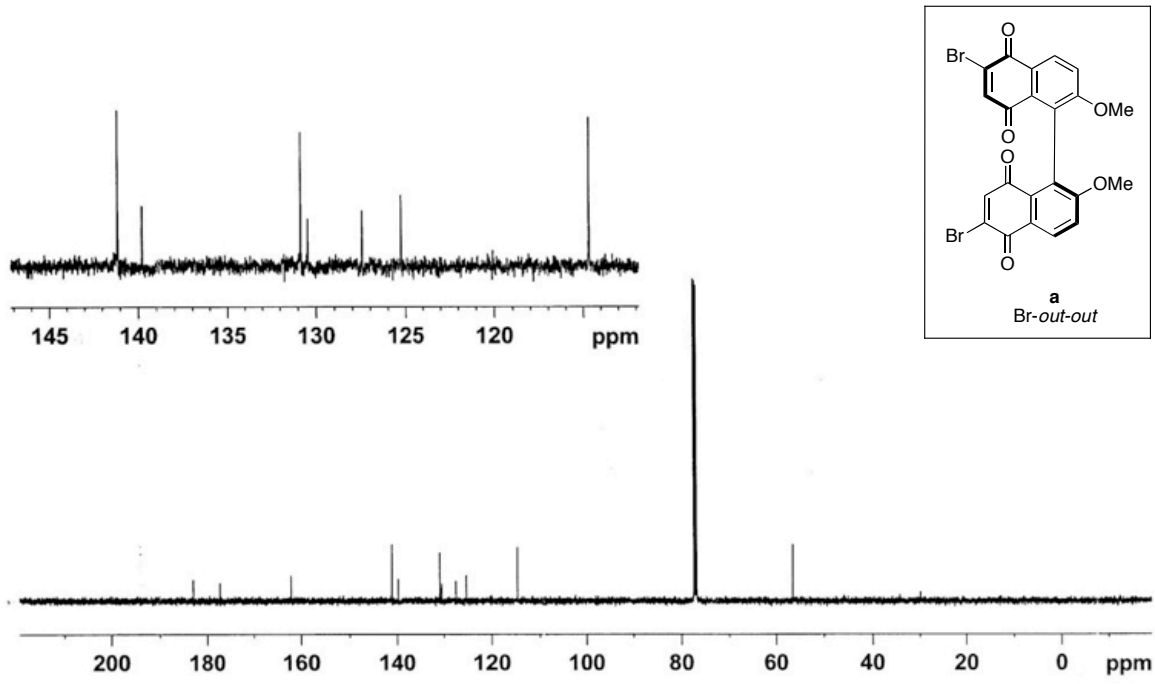

Figure A4.34a_2 ^{13}C NMR Spectrum of Compound (*S*)-**4.34a** (125 MHz, $CDCl_3$).

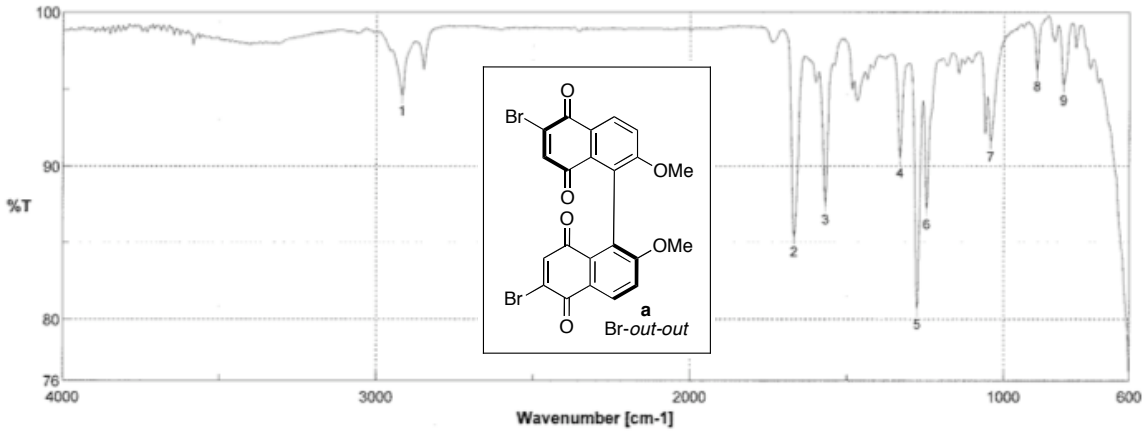

Figure A4.34a_3 IR Spectrum of Compound (*S*)-**4.34a** (film).

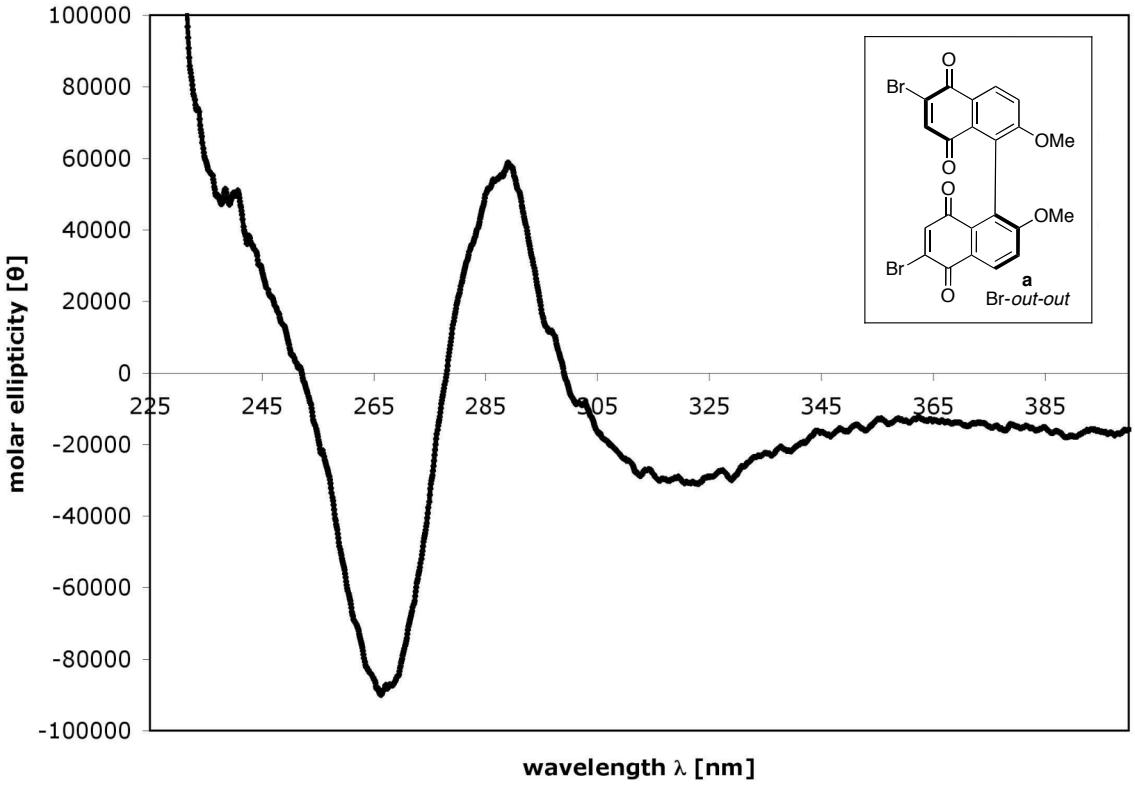

Figure A4.34a_4 CD Spectrum of Compound (*S*)-**4.34a**
(0.19 mM, $ClCH_2CH_2Cl$, 23 °C).

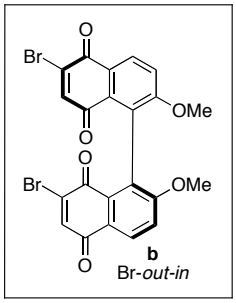

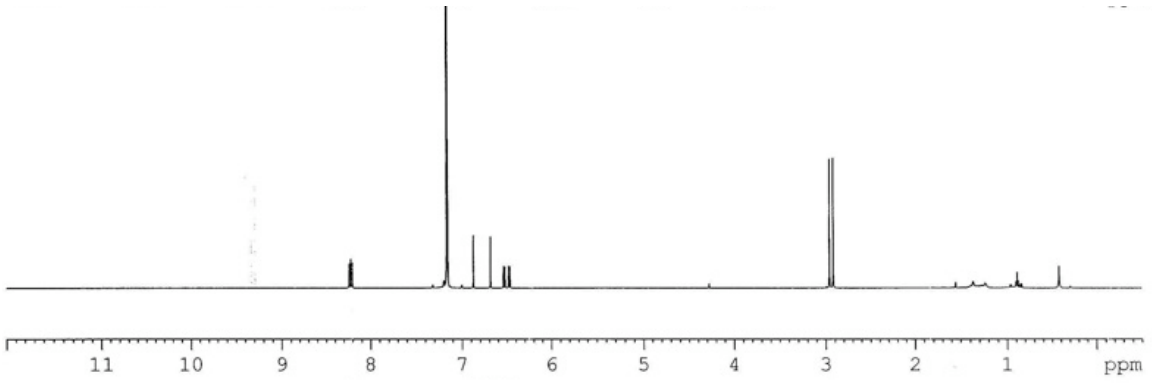

Figure A4.34b_1 ^{1}H NMR Spectrum of Compound (*S*)-**4.34b** (500 MHz, C_6D_6).

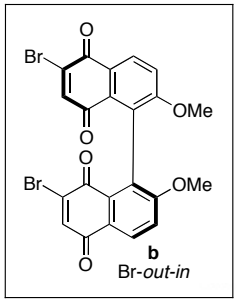

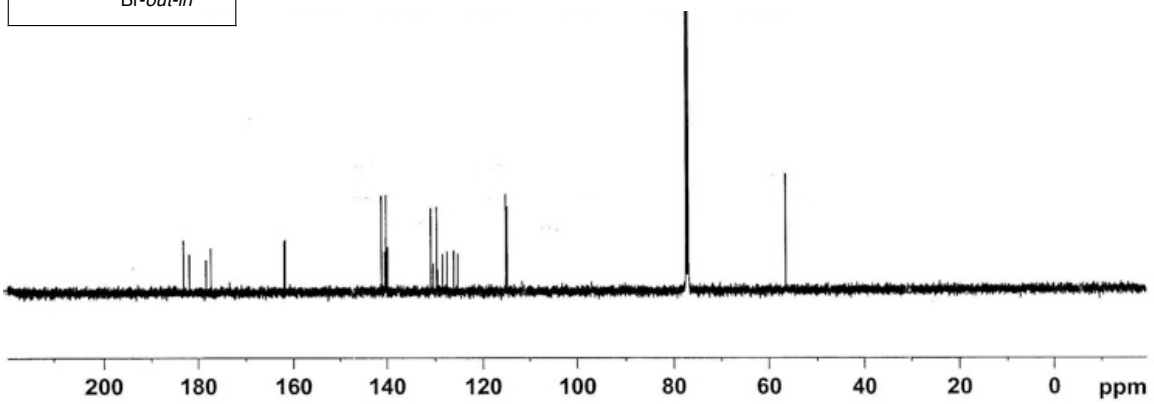

Figure A4.34b_2 ^{13}C NMR Spectrum of Compound (*S*)-**4.34b** (125 MHz, $CDCl_3$).

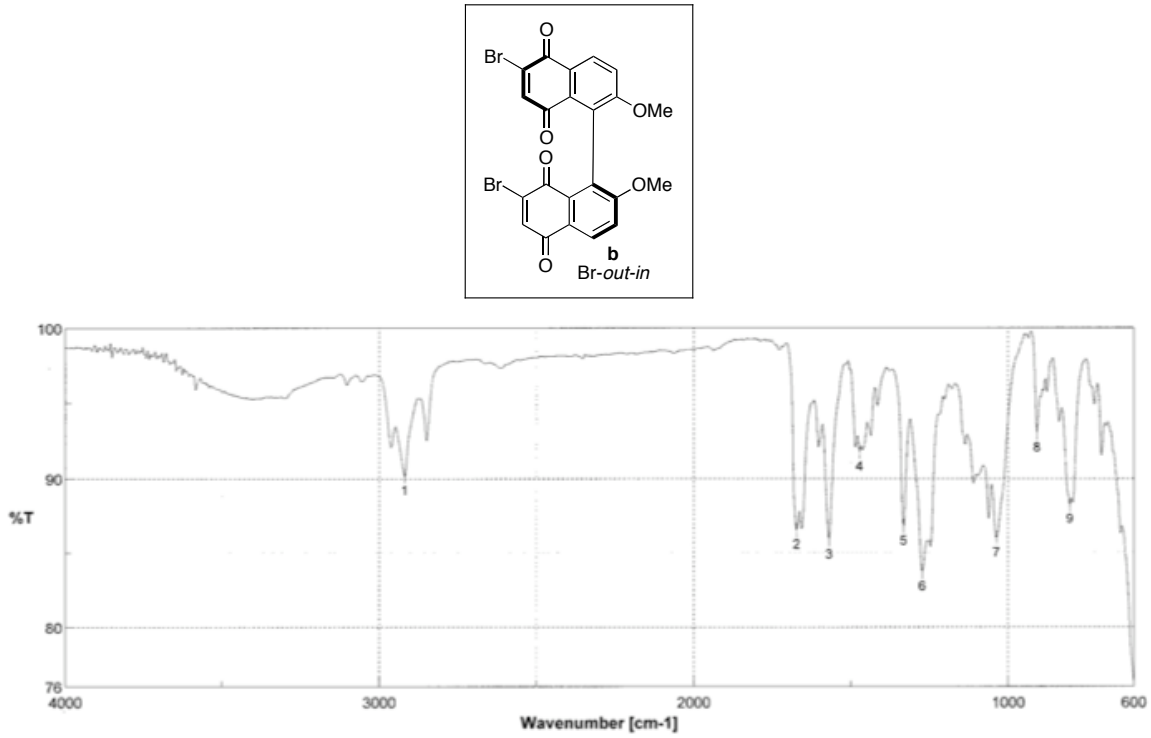

Figure A4.34b_3 IR Spectrum of Compound (*S*)-**4.34b** (film).

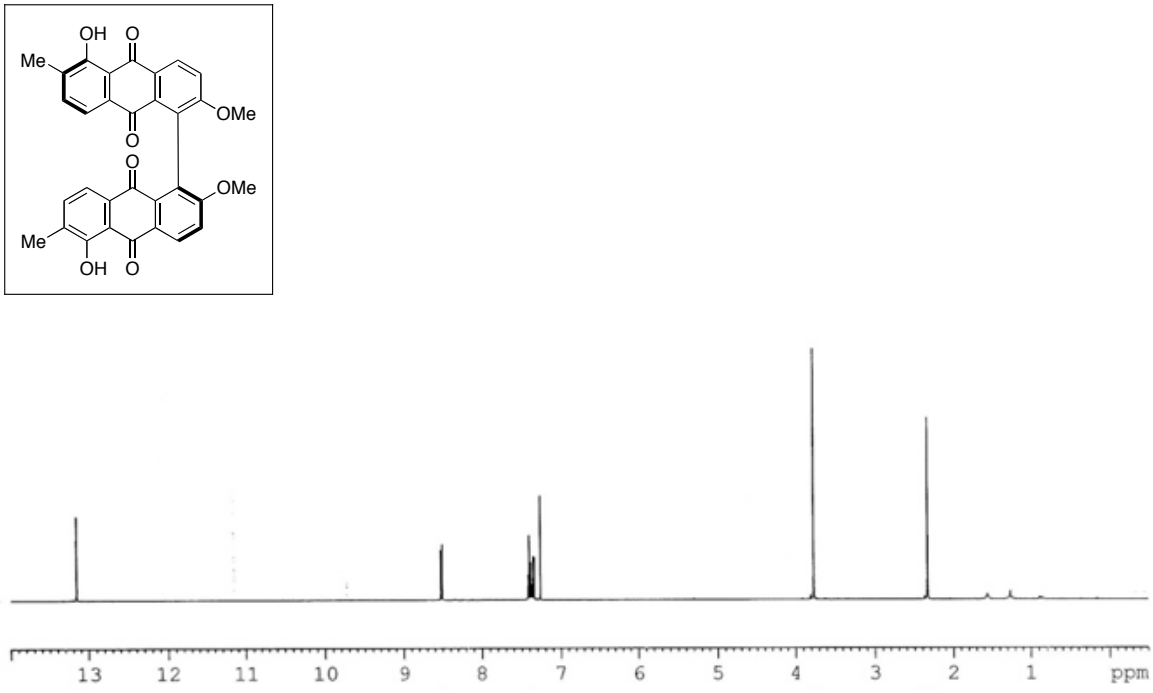

Figure A4.38a_1 ^{1}H NMR Spectrum of Compound (*S*)-**4.38a** (500 MHz, $CDCl_3$).

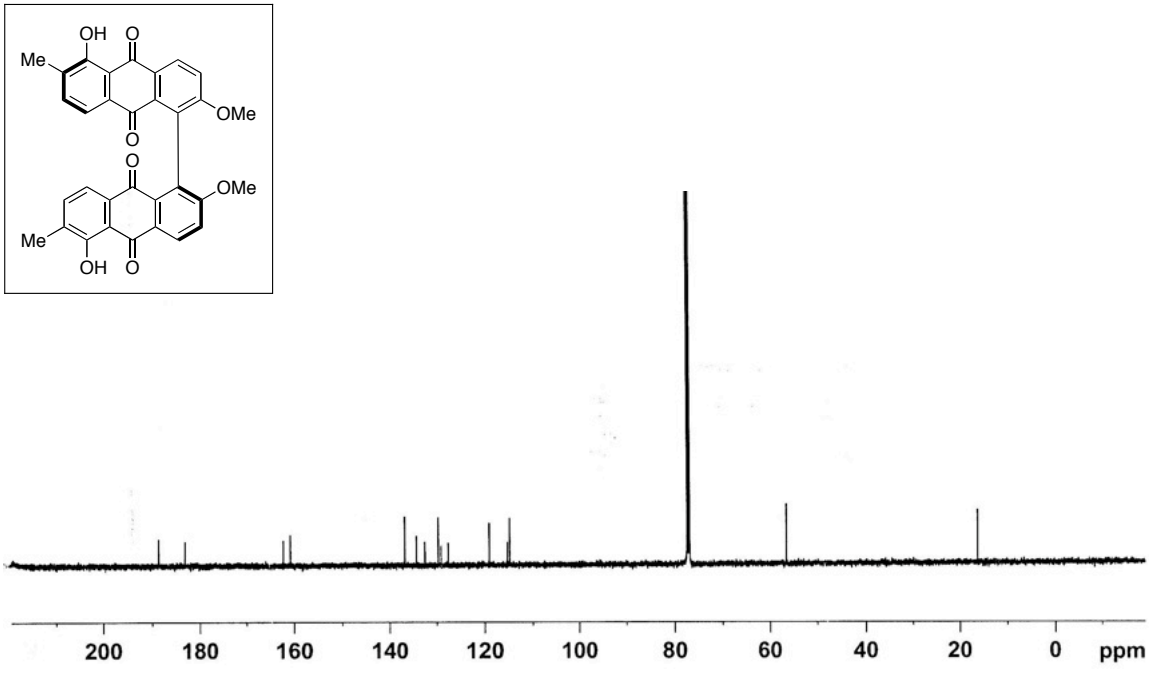

Figure A4.38a_2 ^{13}C NMR Spectrum of Compound (*S*)-**4.38a** (125 MHz, $CDCl_3$).

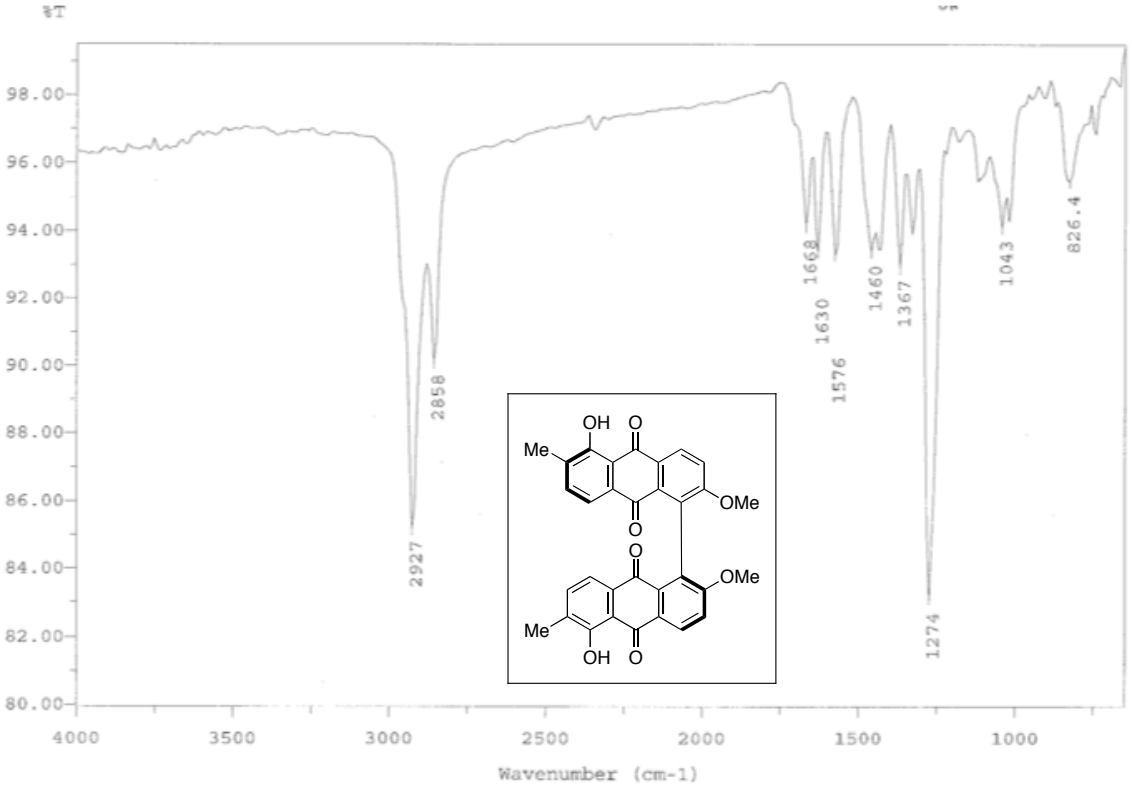

Figure A4.38a_3 IR Spectrum of Compound (*S*)-**4.38a** (film).

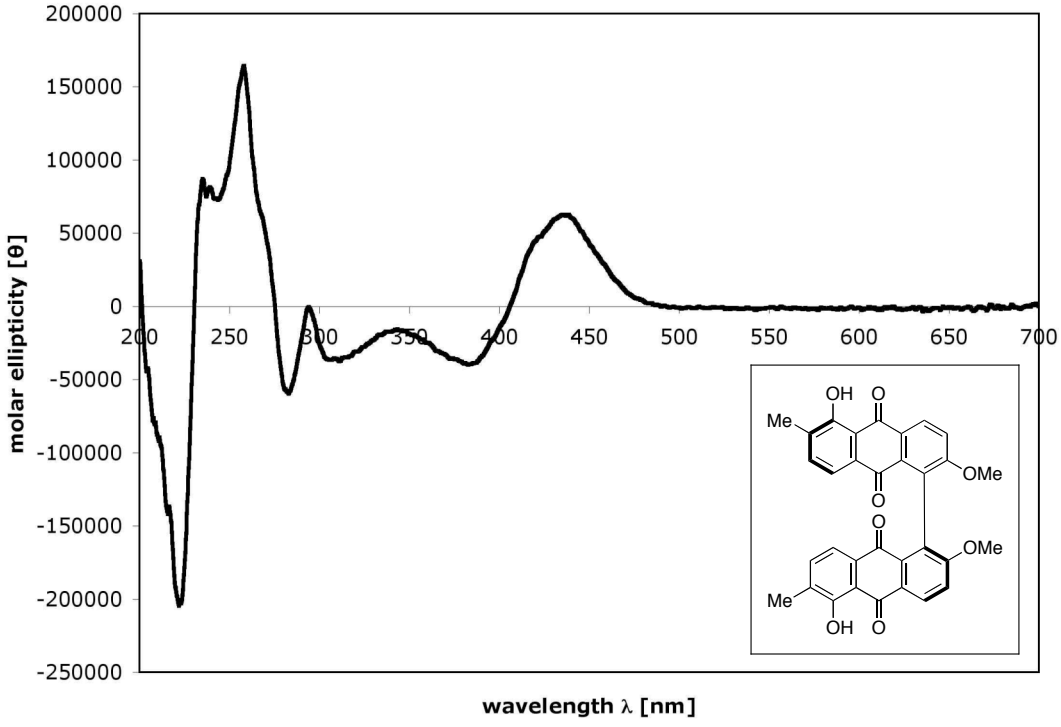

Figure A4.38a_4 CD Spectrum of Compound (*S*)-**4.38a** (0.24 mM, MeOH, 23 °C).

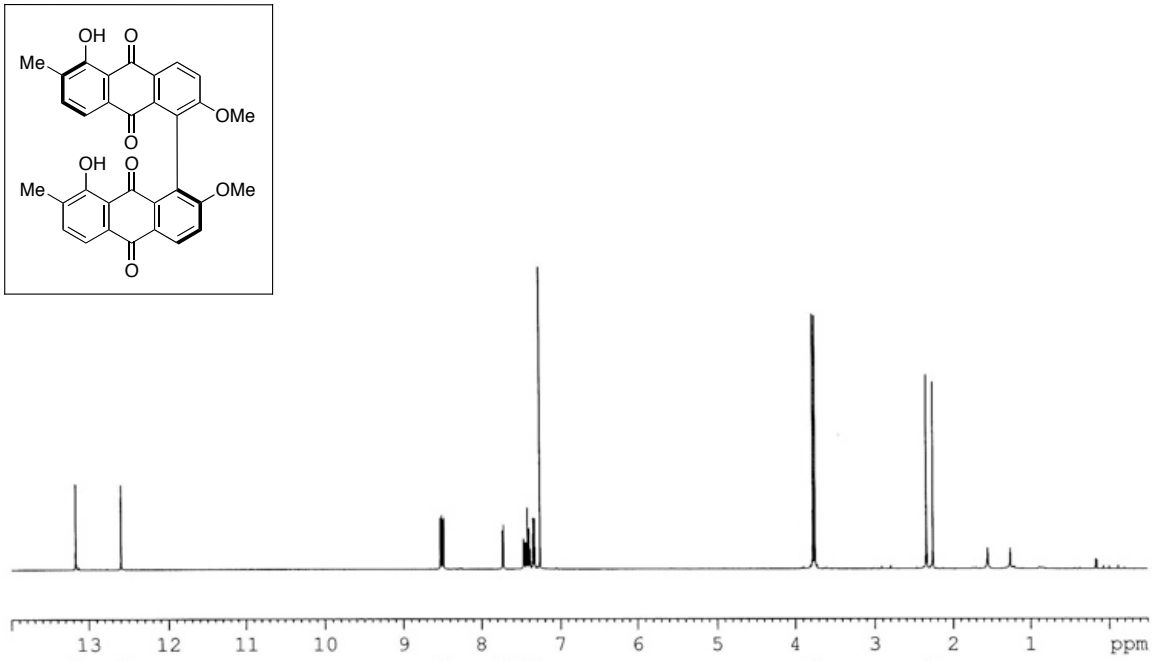

Figure A4.38b_1 ^{1}H NMR Spectrum of Compound (*S*)-**4.38b** (500 MHz, $CDCl_3$).

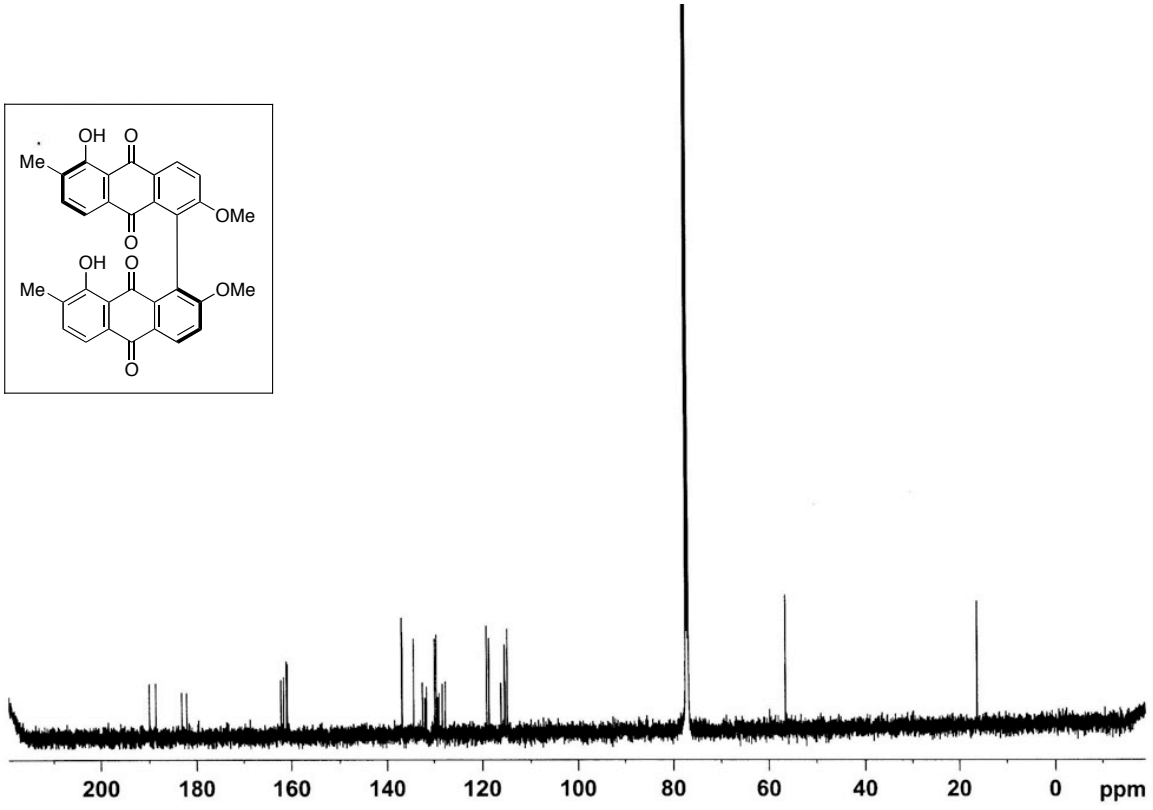

Figure A4.38b_2 ^{13}C NMR Spectrum of Compound (*S*)-**4.38b** (125 MHz, $CDCl_3$).

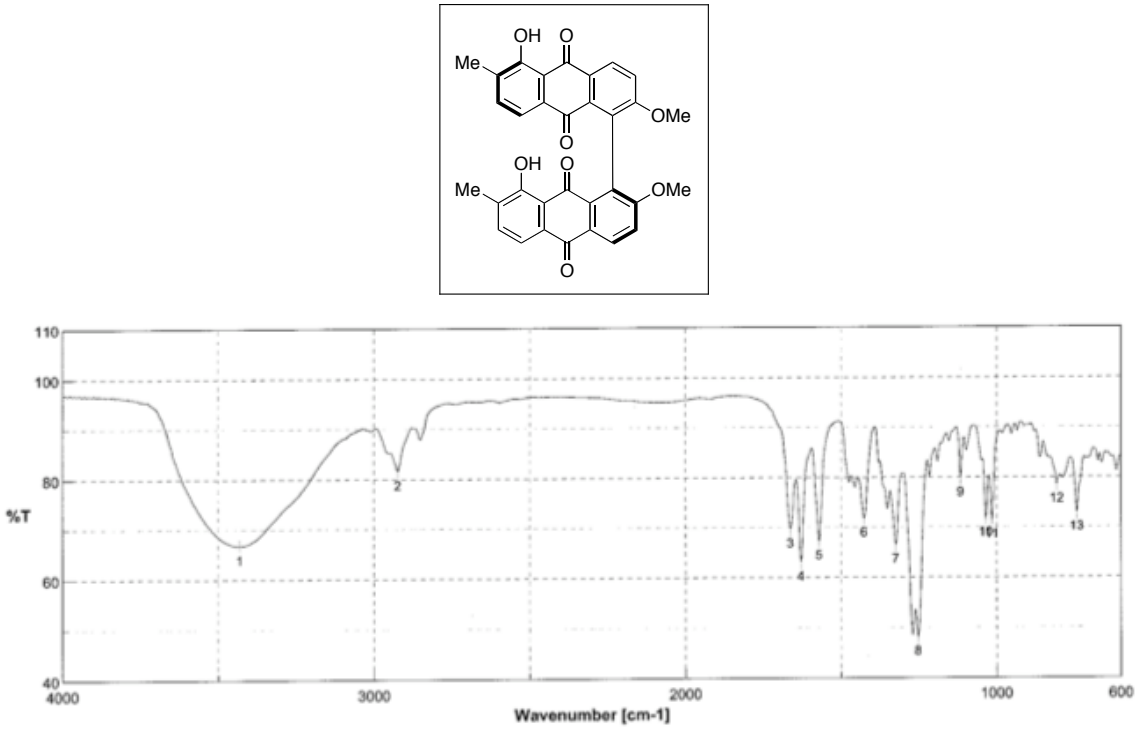

Figure A4.38b_3 IR Spectrum of Compound (*S*)-**4.38b** (film).

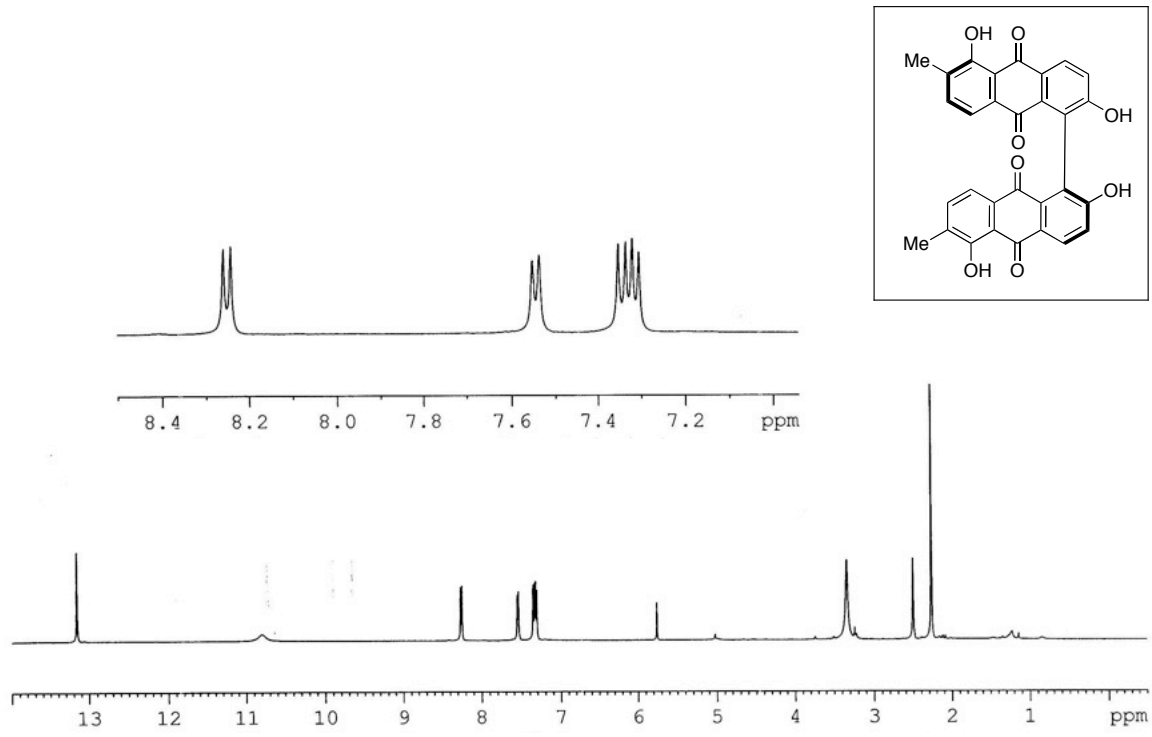

Figure A4.39a_1 ^{1}H NMR Spectrum of Compound (*S*)-**4.39a** (500 MHz, DMSO-d_6).

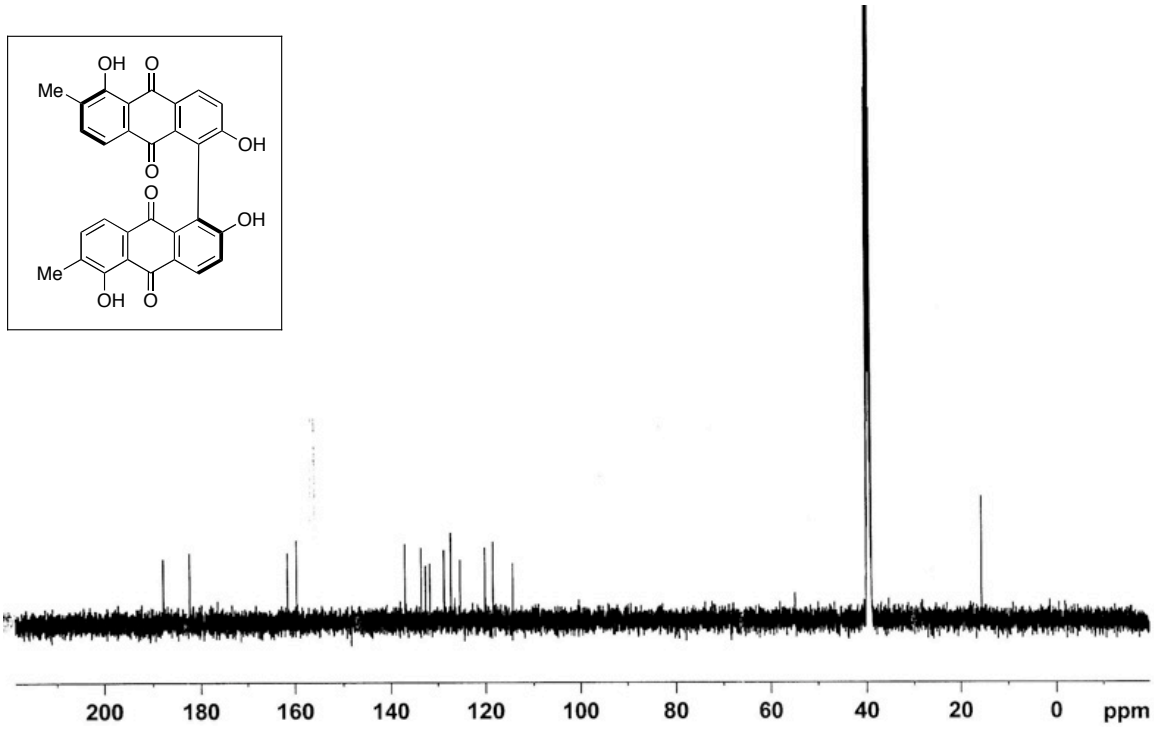

Figure A4.39a_2 ^{13}C NMR Spectrum of Compound (*S*)-**4.39a** (125 MHz, DMSO-d_6).

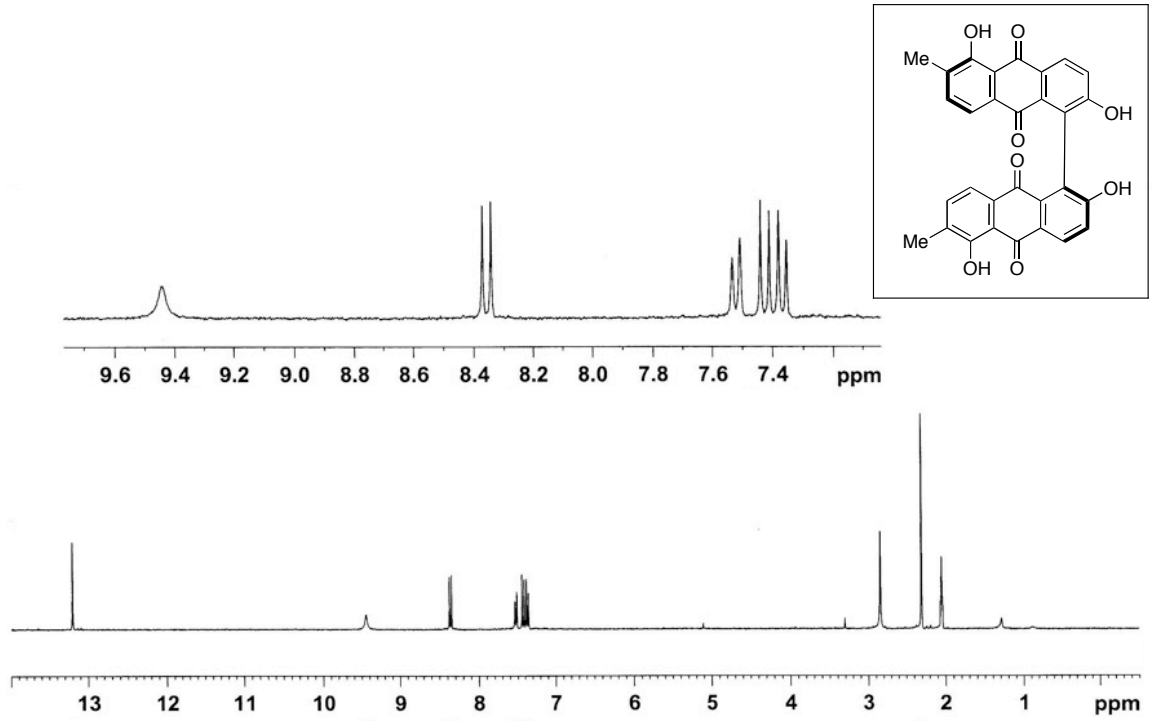

Figure A4.39a_3 ^{1}H NMR Spectrum of Compound (*S*)-**4.39a** (300 MHz, acetone-d_6).

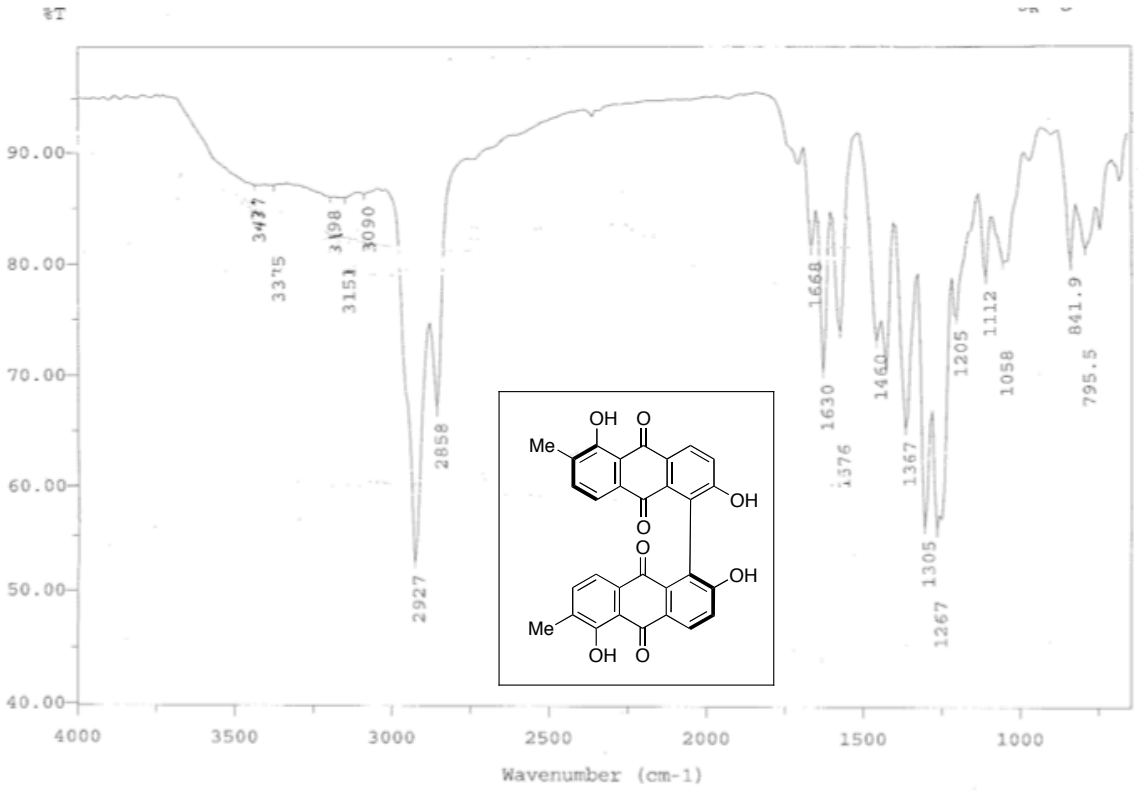

Figure A4.39a_4 IR Spectrum of Compound (*S*)-**4.39a** (film).

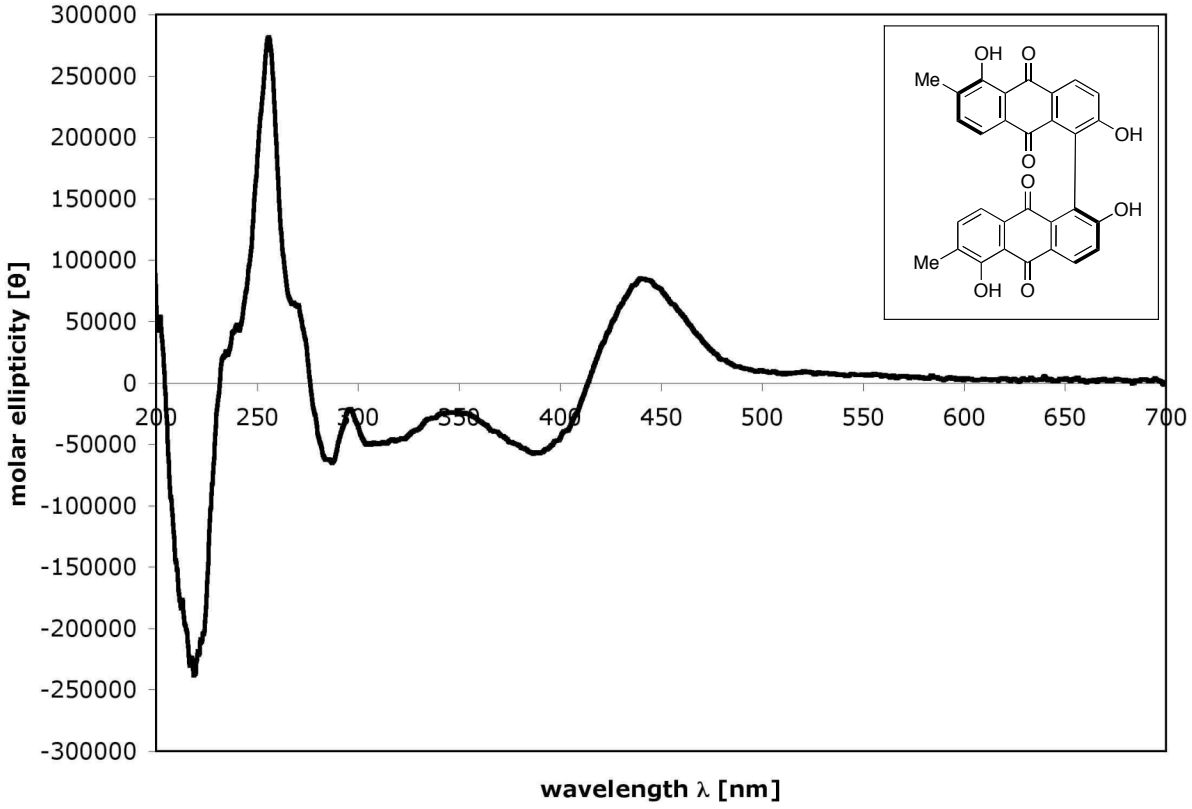

Figure A4.39a_5 CD Spectrum of Compound (*S*)-**4.39a** (0.18 mM, MeOH, 23 °C).

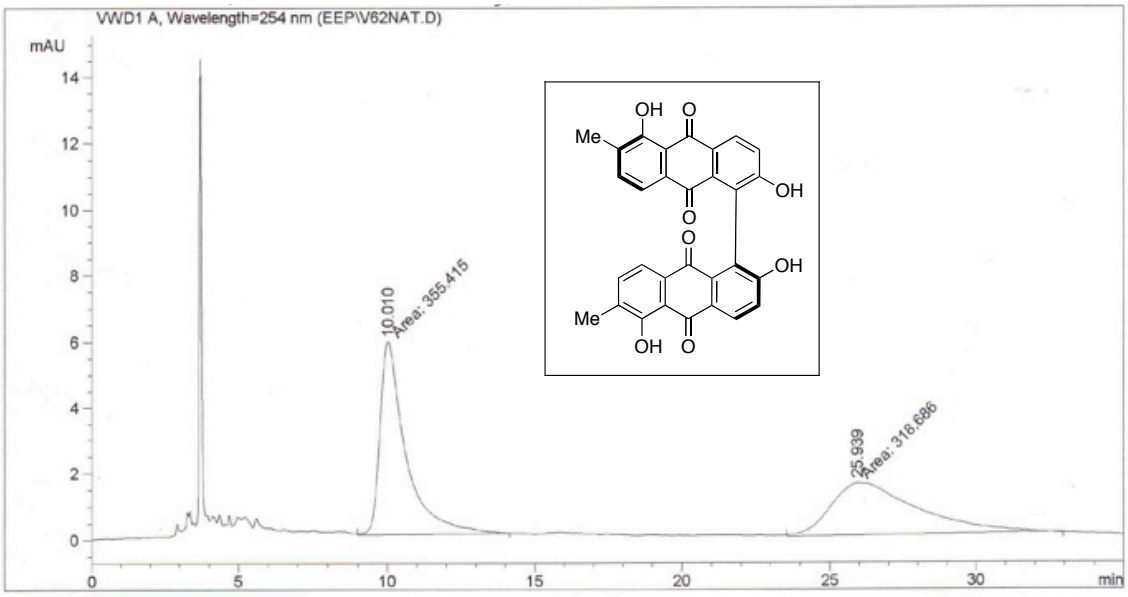

Figure A4.39a_6 HPLC Trace of (S)-Bisoranjidiol [(*S*)-**4.39a**], Authentic Sample (5% ee, IA column, 20% IPA/hexanes).

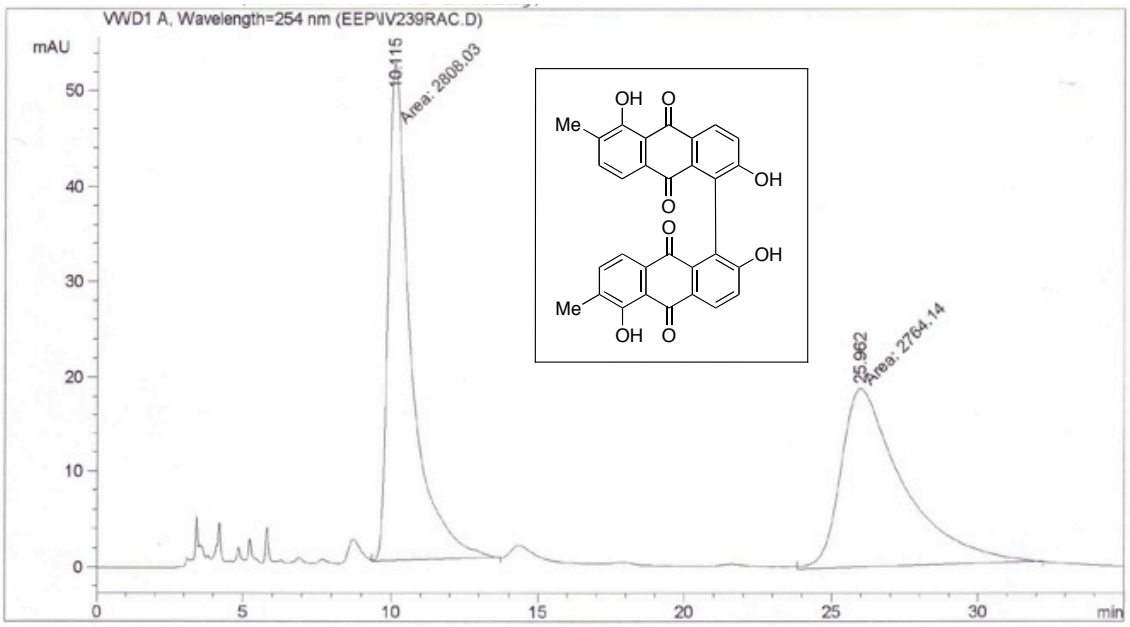

Figure A4.39a_7 HPLC Trace of *rac*-Bisoranjidiol [*rac*-**4.39a**], Synthetic Racemic Sample (IA column, 20% IPA/hexanes).

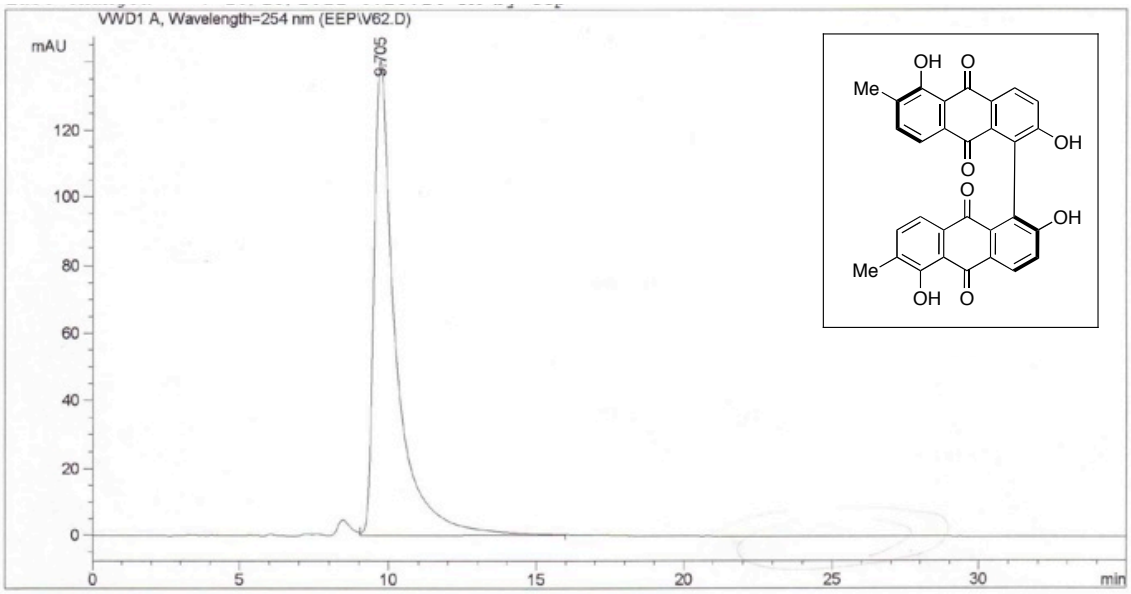

Figure A4.39a_8 HPLC Trace of (*S*)-Bisoranjidiol [(*S*)-**4.39a**], Synthetic Enantiopure Sample (>99% ee, IA column, 20% IPA/hexanes).

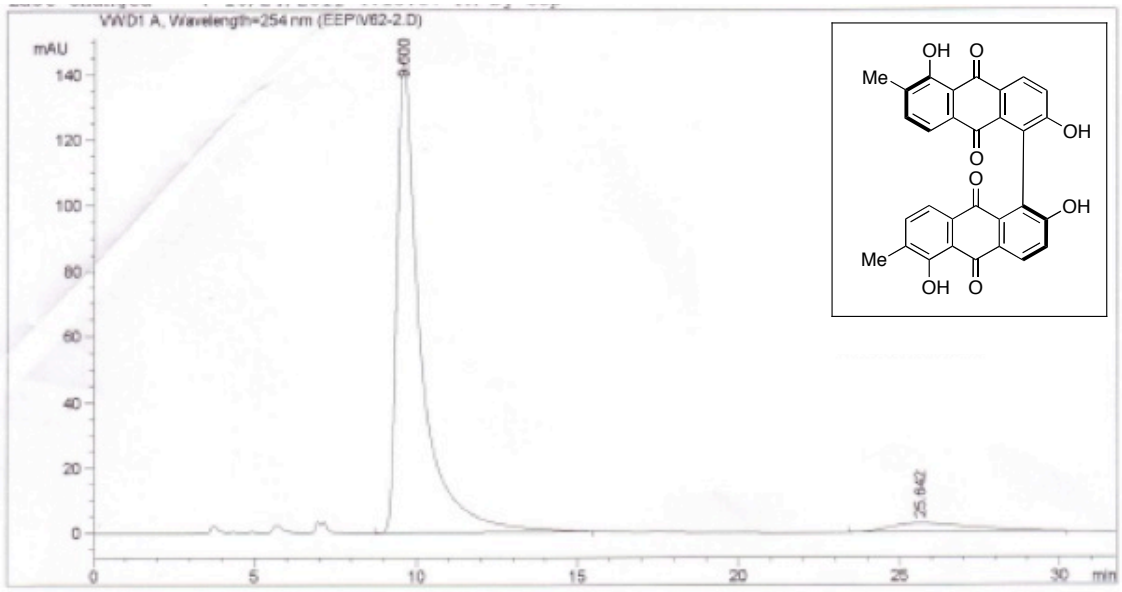

Figure A4.39a_9 HPLC Trace of (*S*)-Bisoranjidiol [(*S*)-**4.39a**], Synthetic Enantiopure Sample After 10 days in MeOH at Room Temperature (87% ee, IA column, 20% IPA/hexanes).

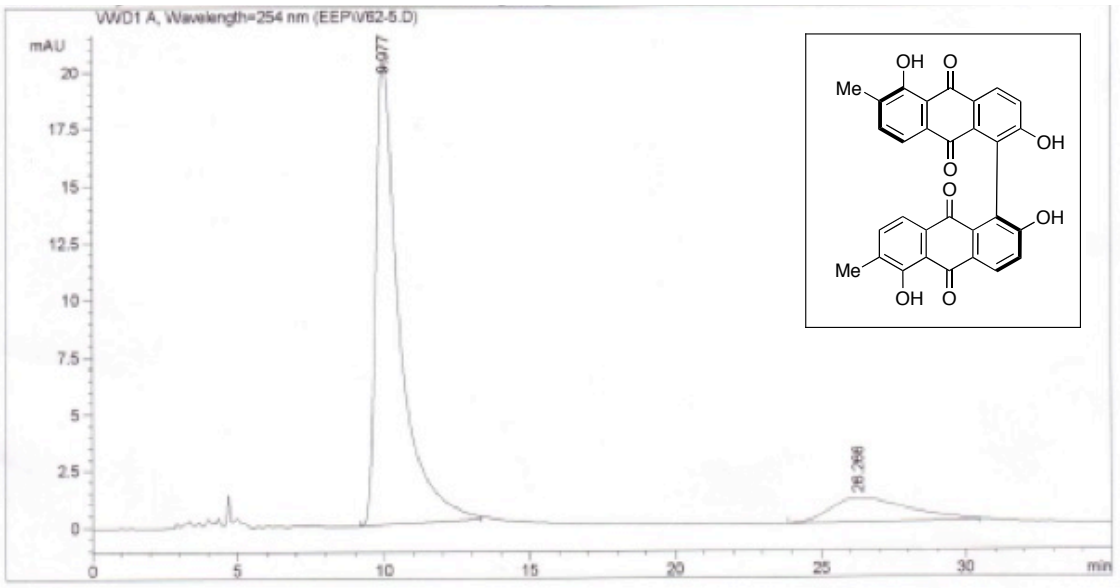

Figure A4.39a_10 HPLC Trace of (*S*)-Bisoranjidiol [(*S*)-**4.39a**], Synthetic Enantiopure Sample After 26 days in MeOH at Room Temperature (71% ee, IA column, 20% IPA/hexanes).

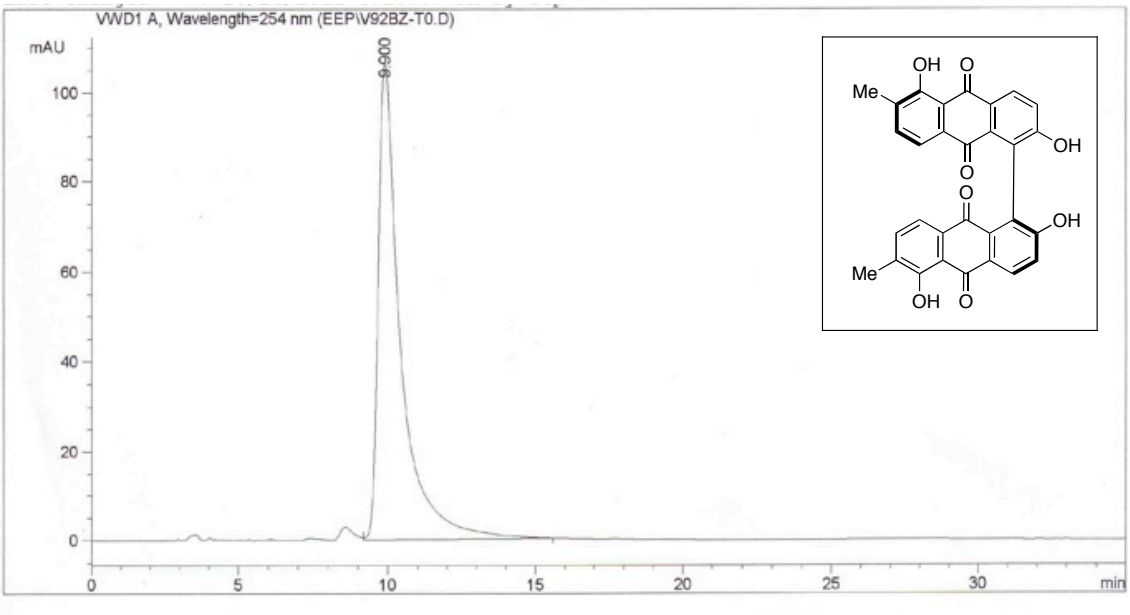

Figure A4.39a_11 HPLC Trace of (*S*)-Bisoranjidiol [(*S*)-**4.39a**], Synthetic Enantiopure Sample After 30 days as solid in fridge (>99% ee, IA column, 20% IPA/hexanes).

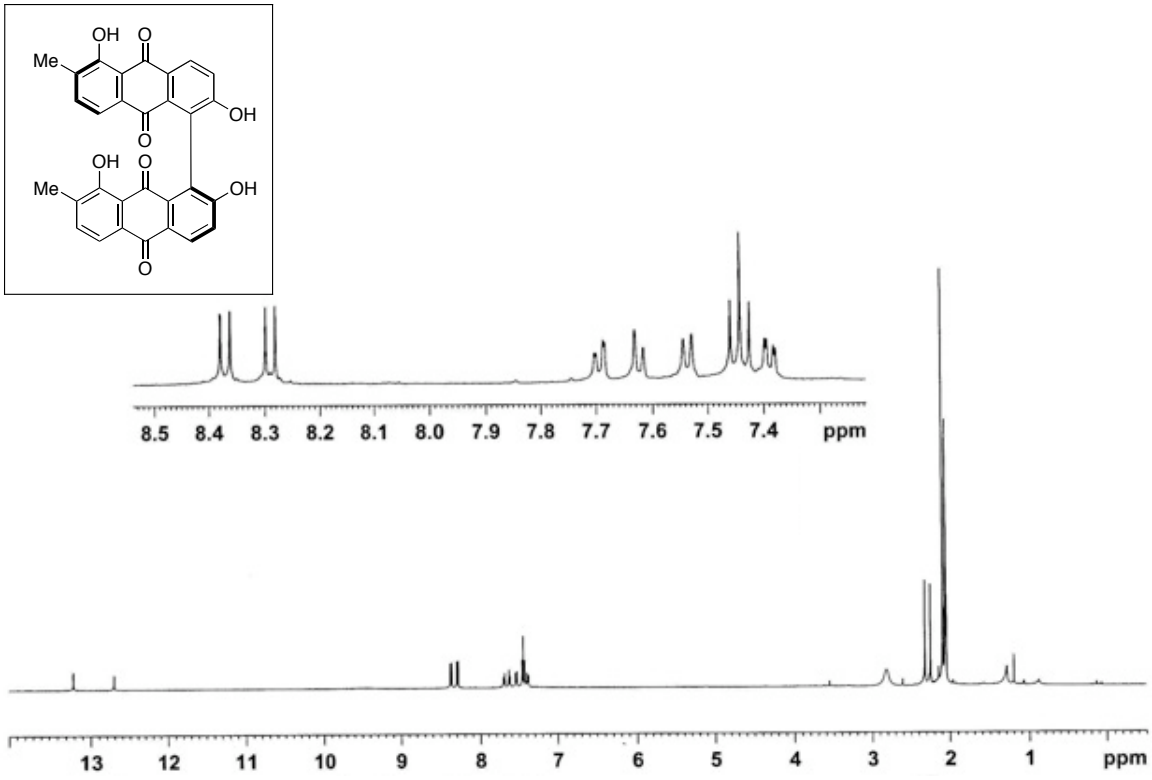

Figure A4.39b_1 ^{1}H NMR Spectrum of Compound (*S*)-**4.39b** (500 MHz, acetone-d_6).

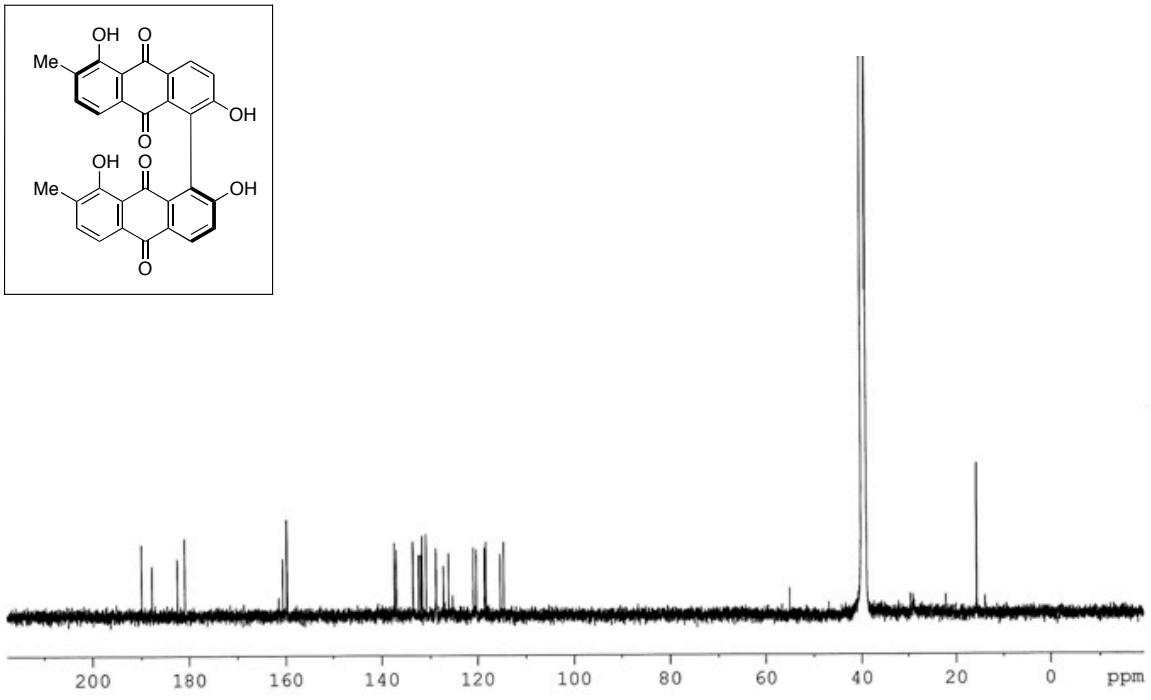

Figure A4.39b_2 ^{13}C NMR Spectrum of Compound (*S*)-**4.39b** (125 MHz, DMSO-d_6).

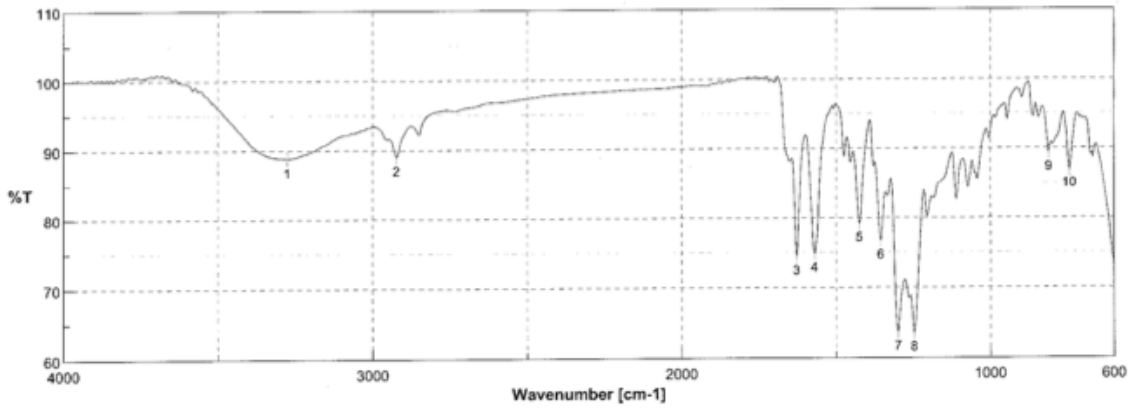

Figure A4.39b_3 IR Spectrum of Compound (*S*)-**4.39b** (film).

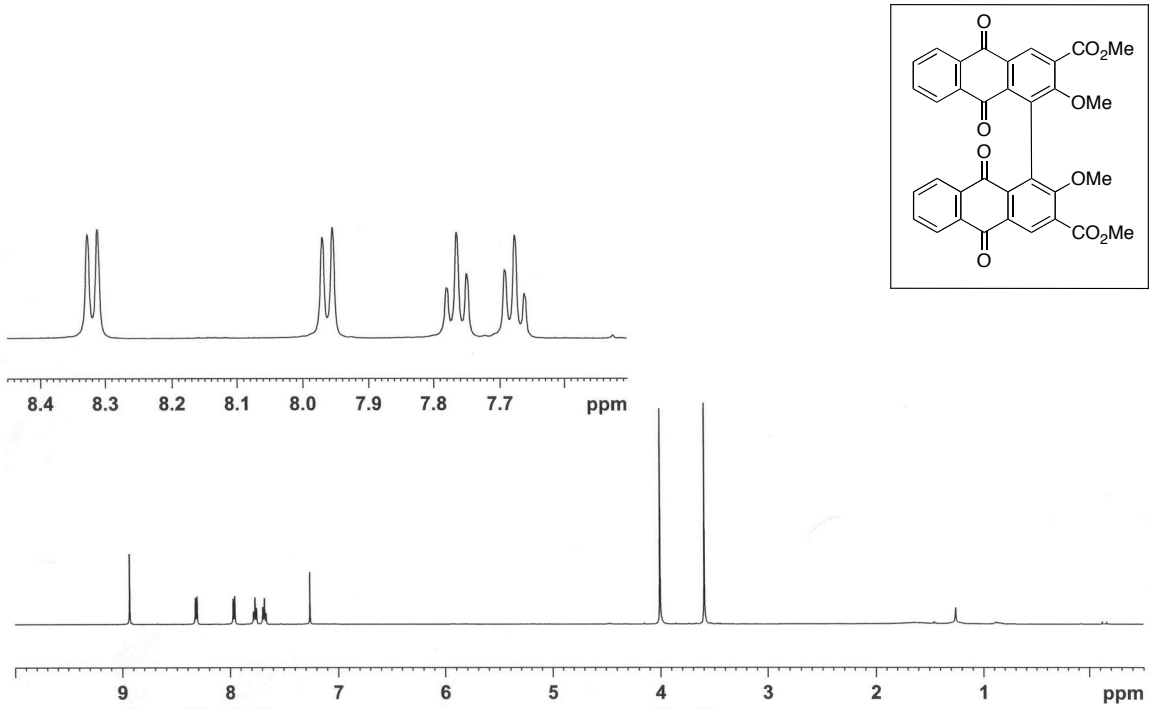

Figure A4.53_1 ^{1}H NMR Spectrum of Compound **4.53** (500 MHz, $CDCl_3$).

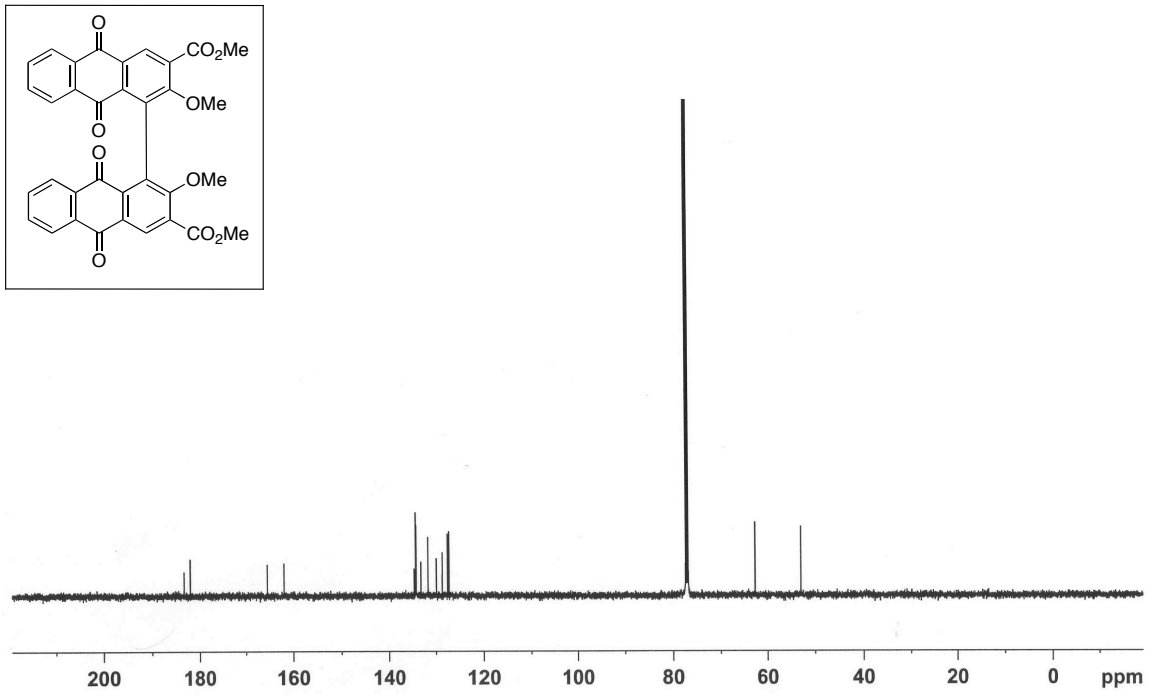

Figure A4.53_2 ^{13}C NMR Spectrum of Compound **4.53** (125 MHz, $CDCl_3$).

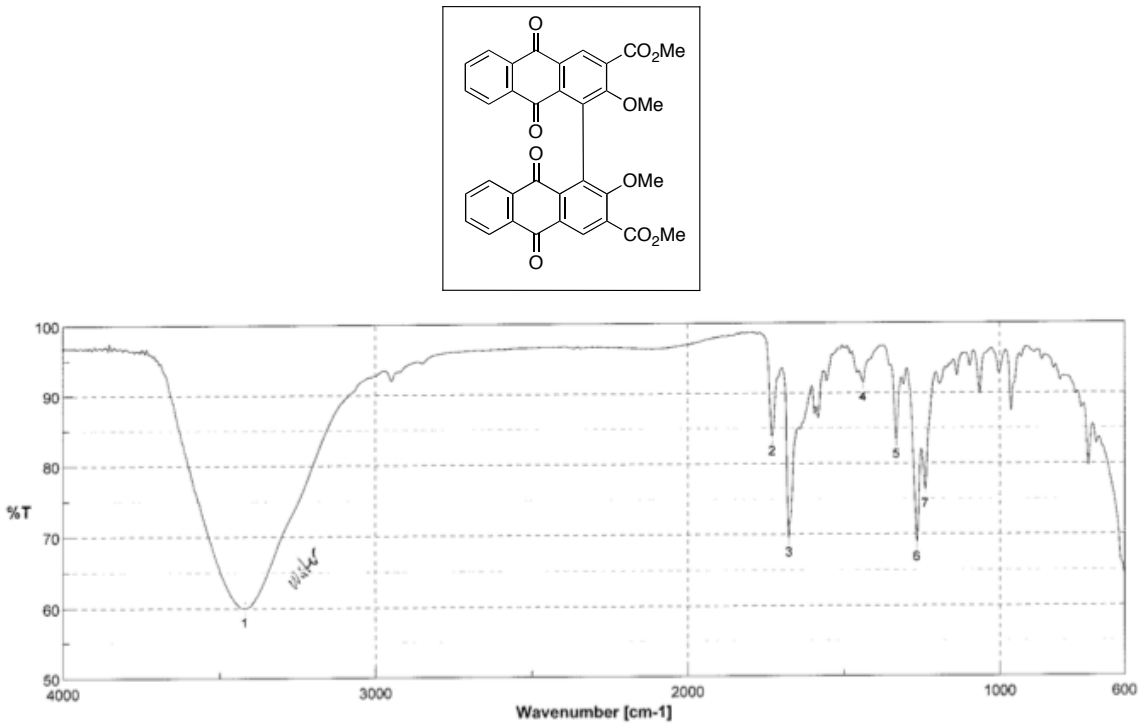

Figure A4.53_3 IR Spectrum of Compound **4.53** (film).

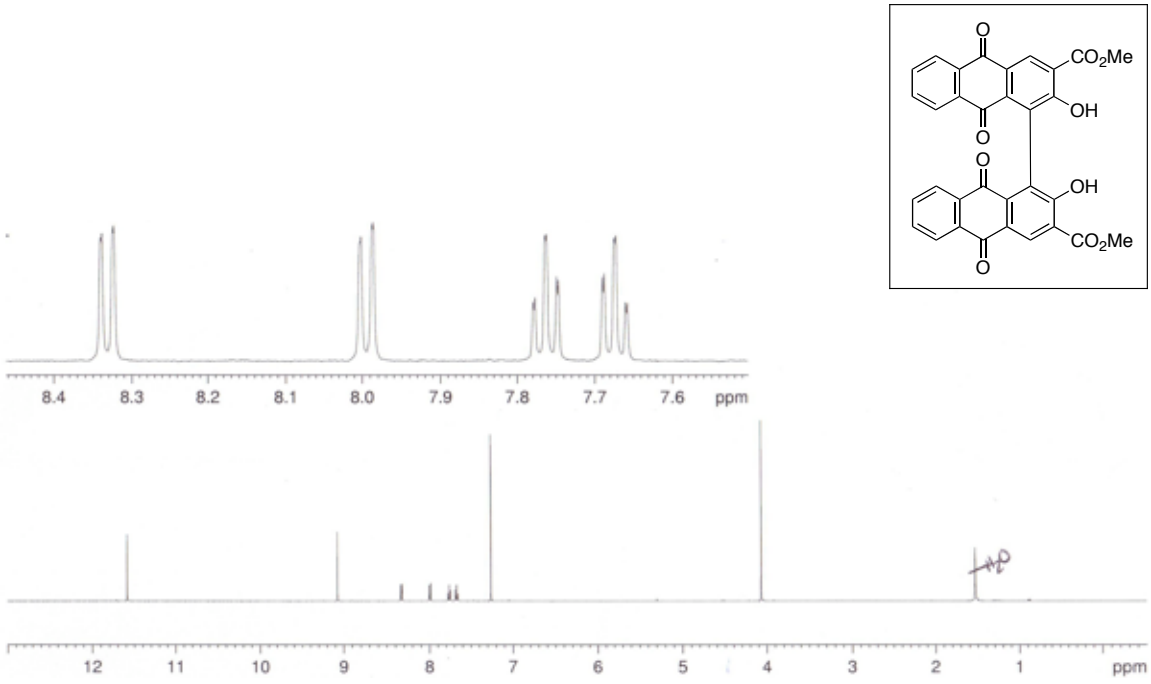

Figure A4.54_1 ^{1}H NMR Spectrum of Compound **4.54** (500 MHz, $CDCl_3$).

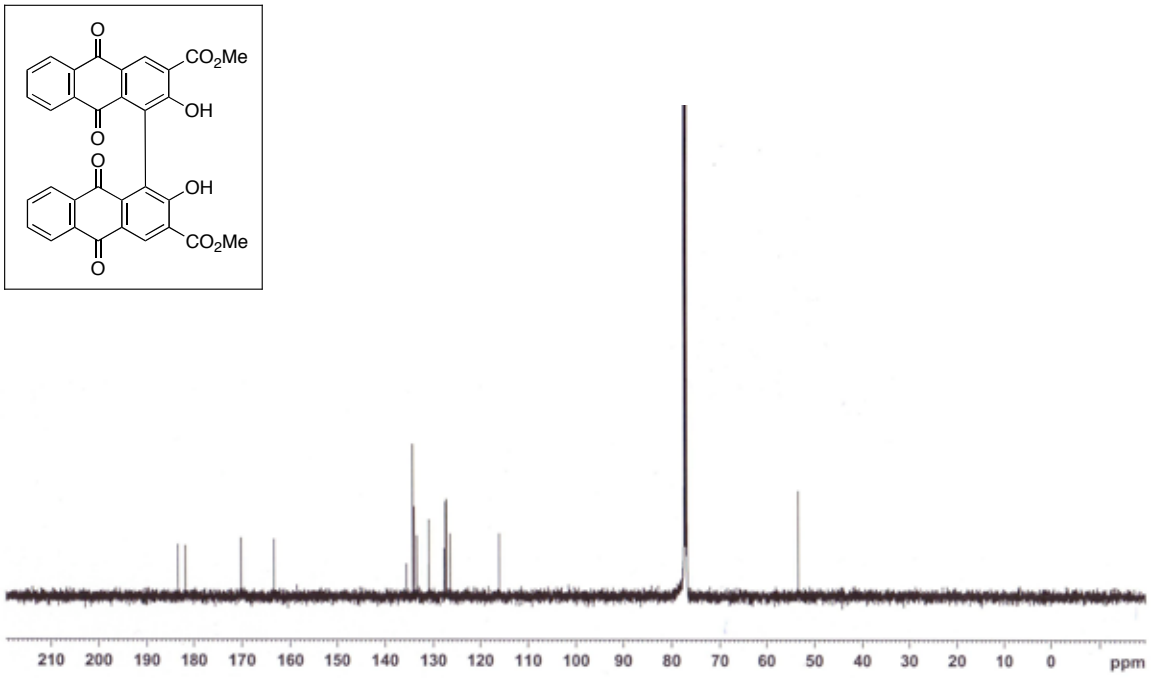

Figure A4.54_2 ^{13}C NMR Spectrum of Compound **4.54** (125 MHz, $CDCl_3$).

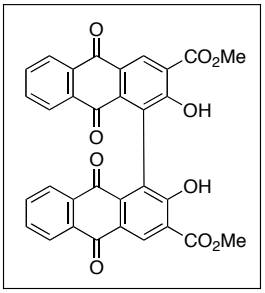

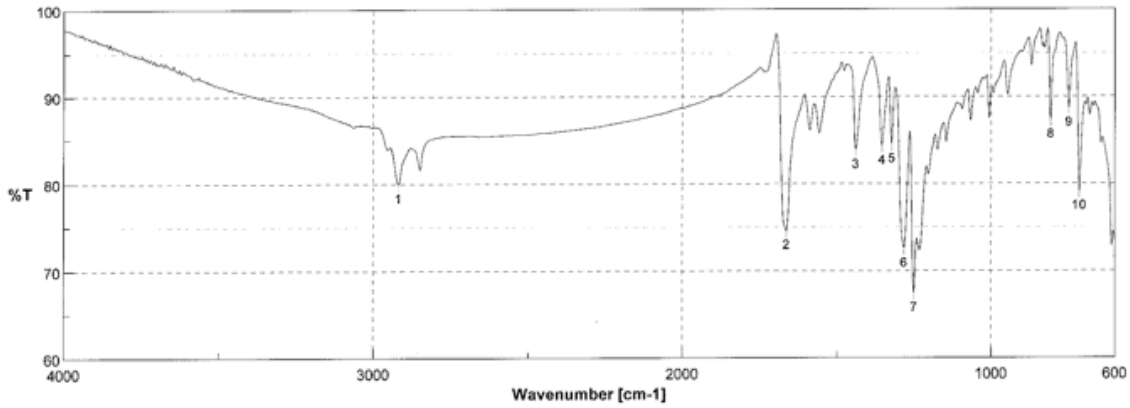

Figure A4.54_3 IR Spectrum of Compound **4.54** (film).

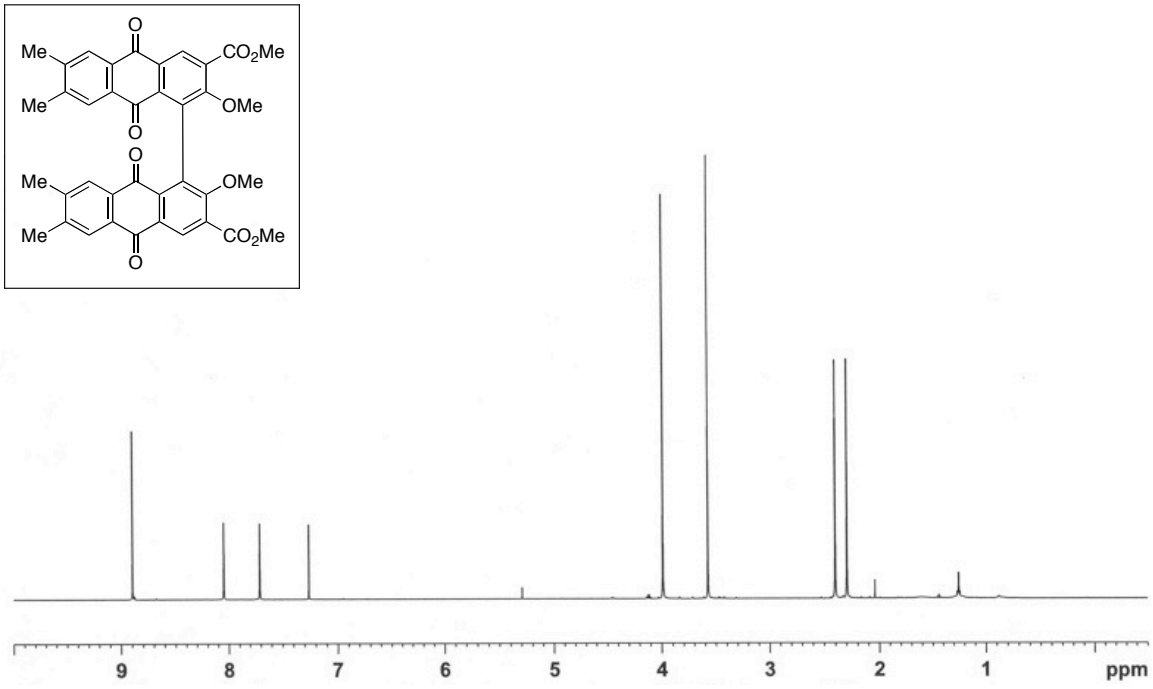

Figure A4.56_1 ^{1}H NMR Spectrum of Compound **4.56** (500 MHz, $CDCl_3$).

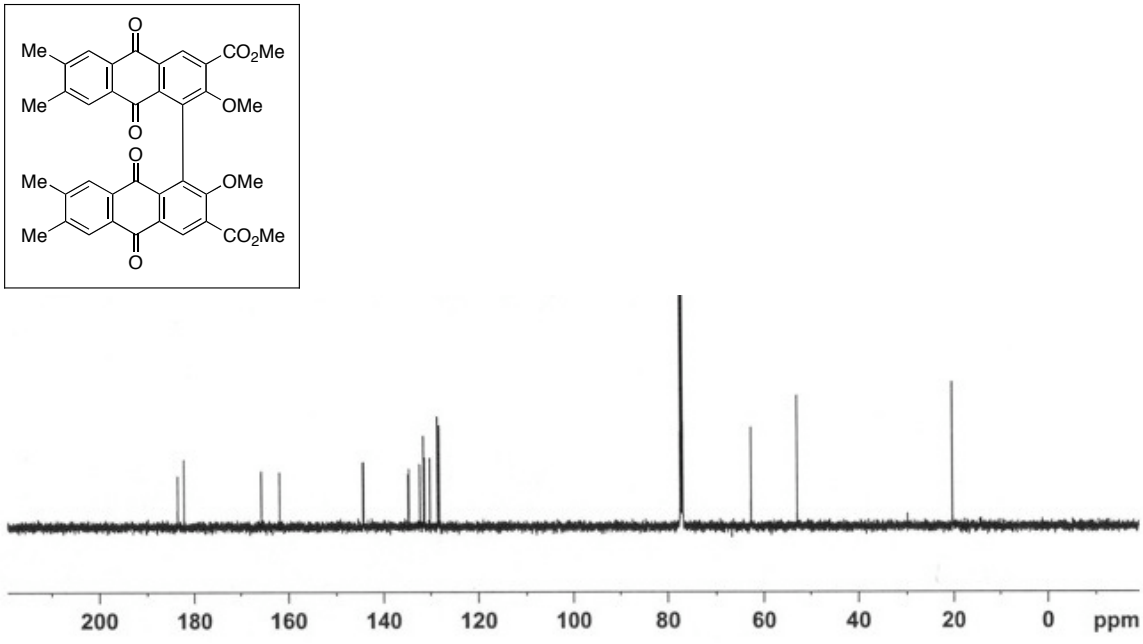

Figure A4.56_2 ^{13}C NMR Spectrum of Compound **4.56** (125 MHz, $CDCl_3$).

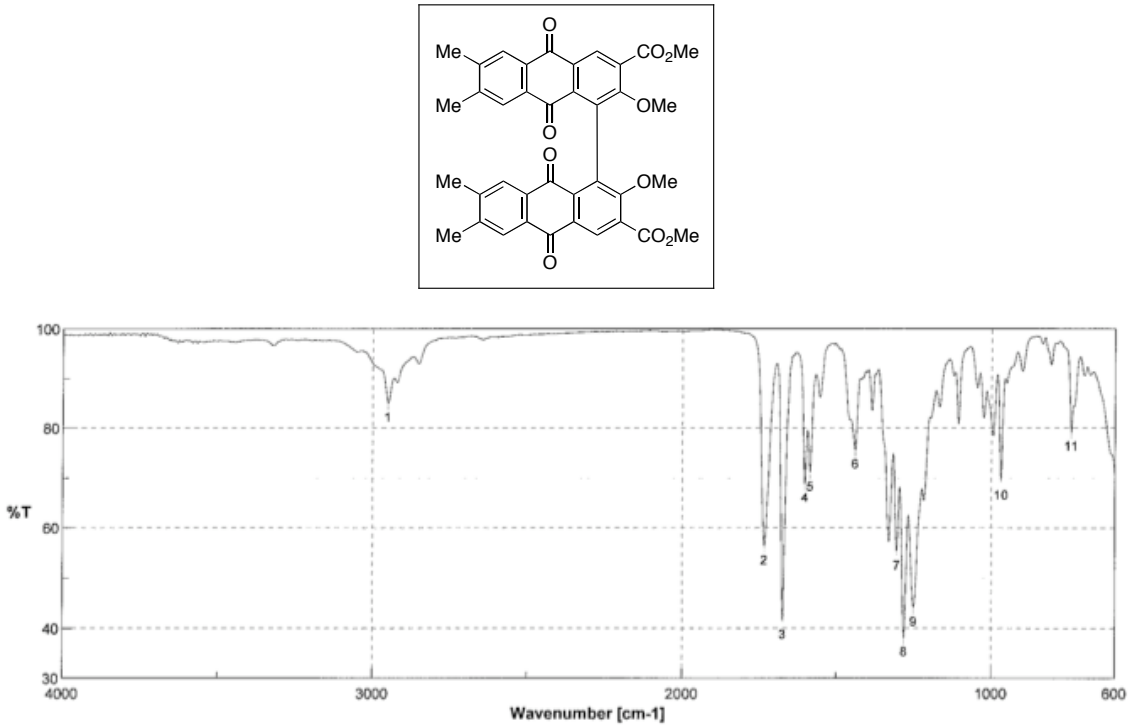

Figure A4.56_3 IR Spectrum of Compound **4.56** (film).

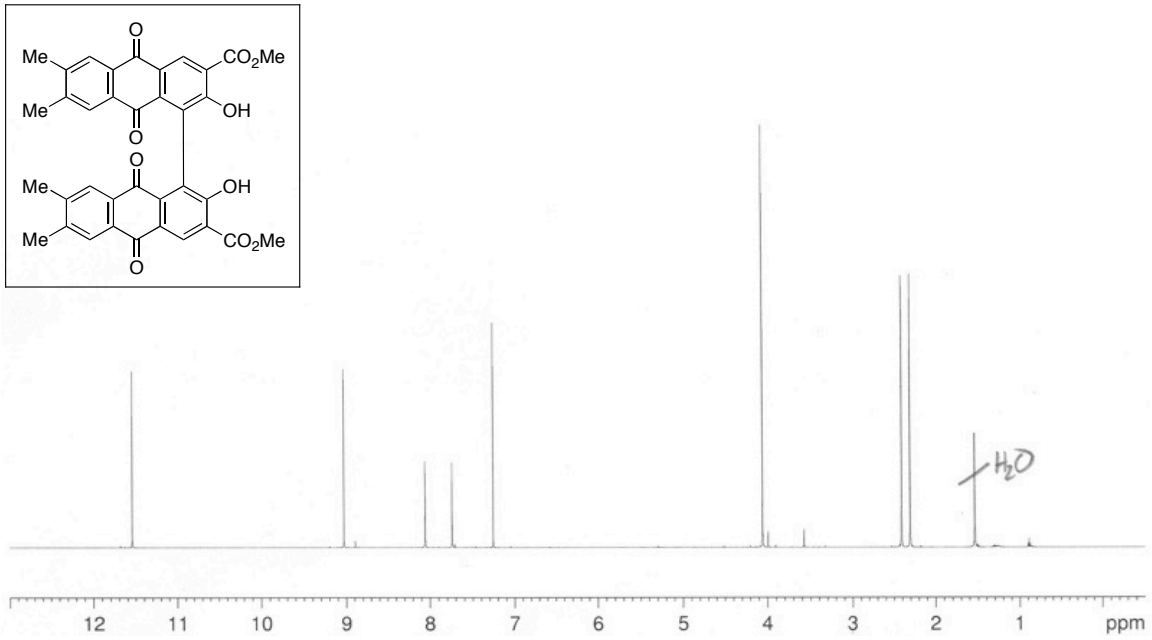

Figure A4.57_1 ^{1}H NMR Spectrum of Compound **4.57** (500 MHz, $CDCl_3$).

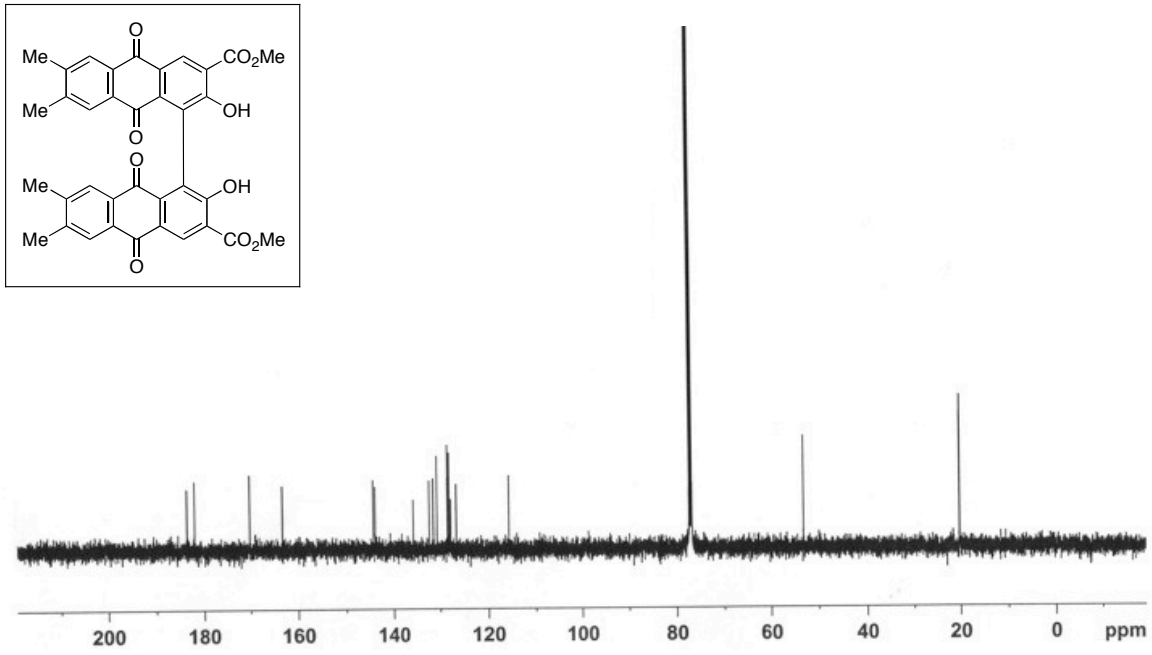

Figure A4.57_2 ^{13}C NMR Spectrum of Compound **4.57** (125 MHz, $CDCl_3$).

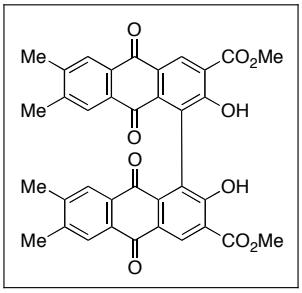

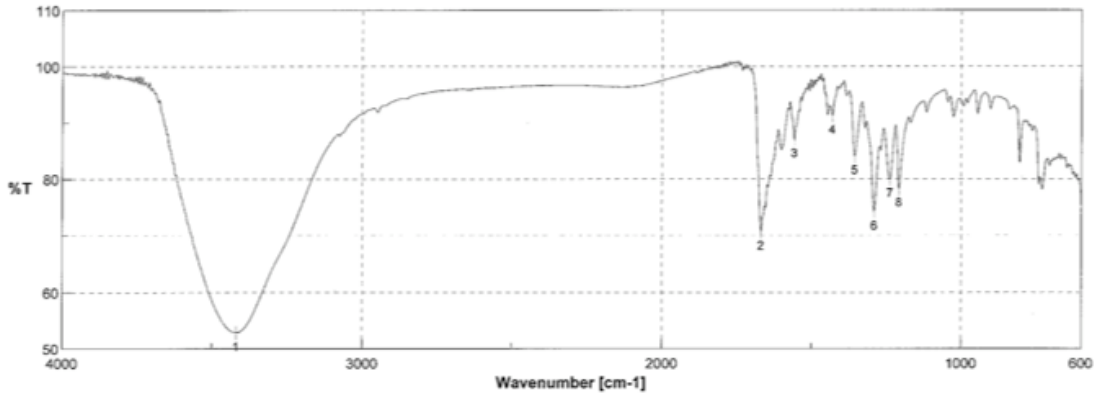

Figure A4.57_3 IR Spectrum of Compound **4.57** (film).

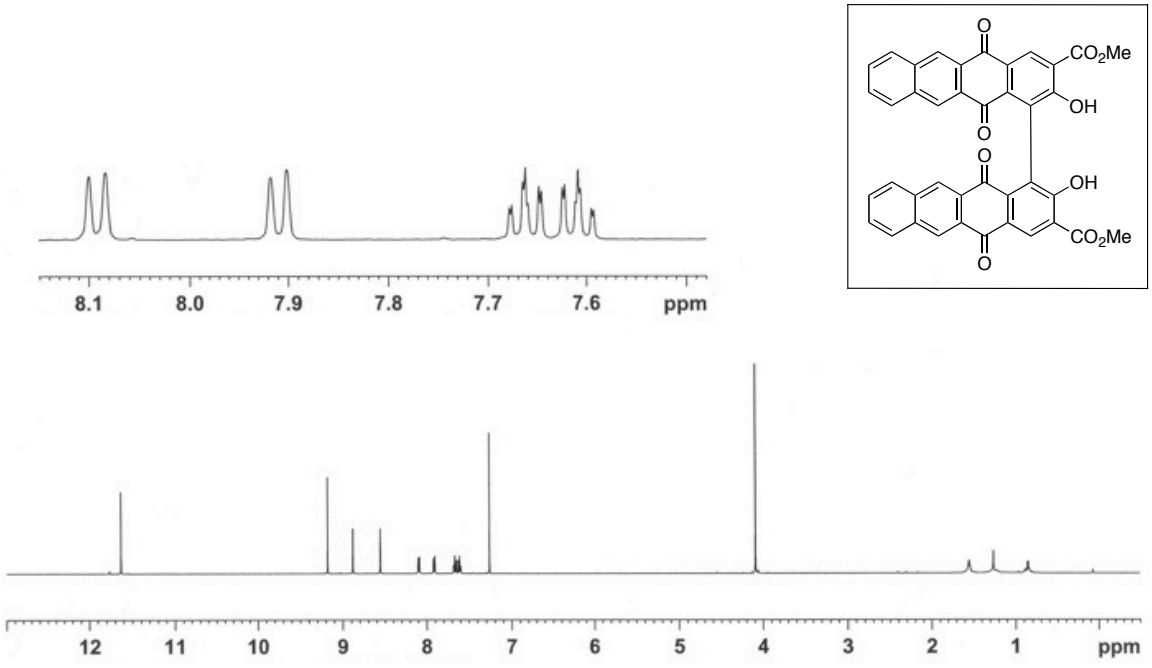

Figure A4.60_1 ^{1}H NMR Spectrum of Compound **4.60** (500 MHz, $CDCl_3$).

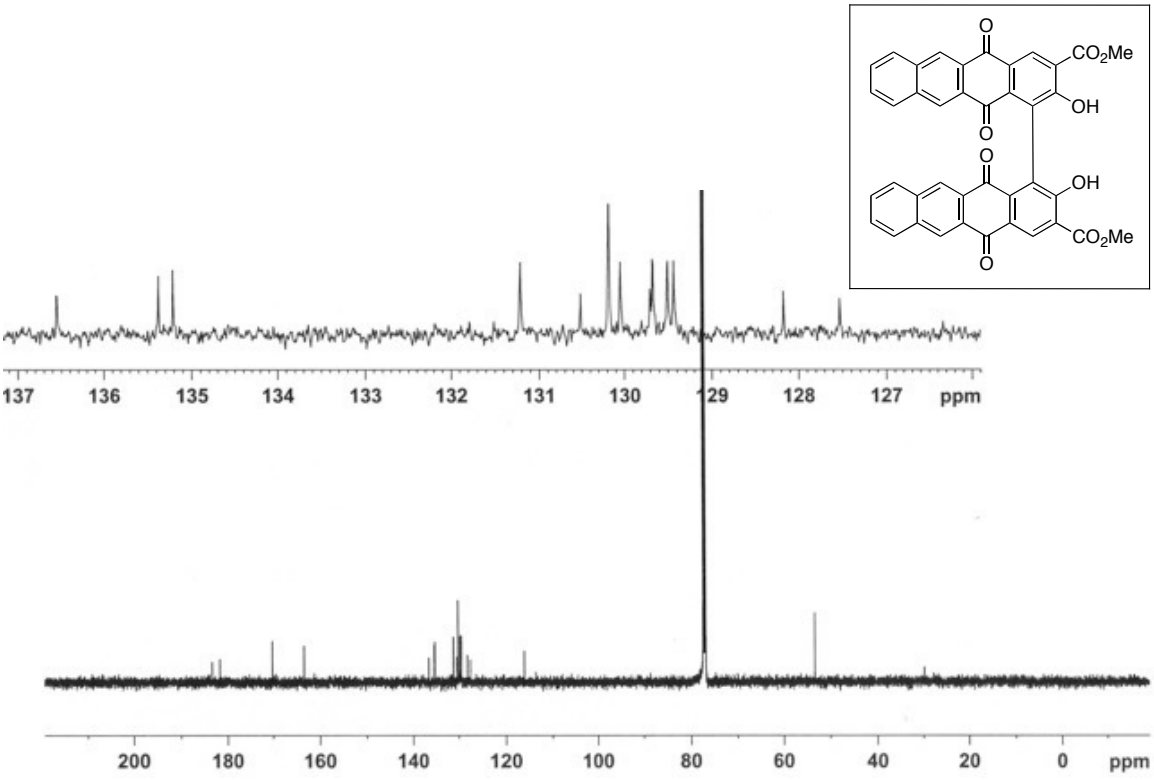

Figure A4.60_2 ^{13}C NMR Spectrum of Compound **4.60** (125 MHz, $CDCl_3$).

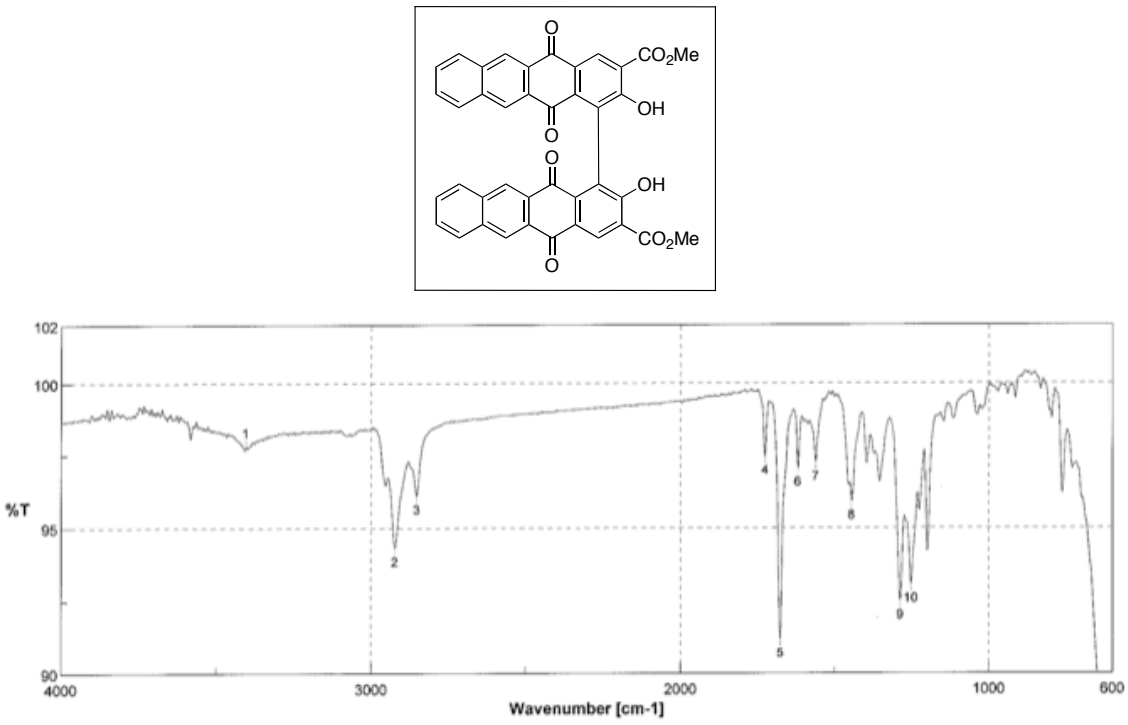

Figure A4.60_3 IR Spectrum of Compound **4.60** (film).

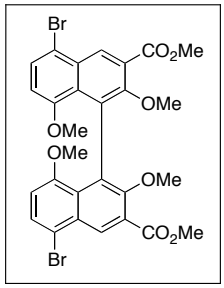

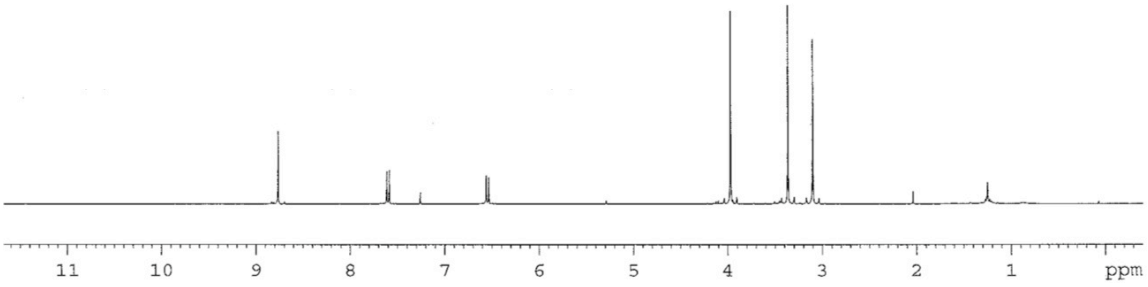

Figure A4.44a_1 ^{1}H NMR Spectrum of Compound **4.44a** (300 MHz, $CDCl_3$).

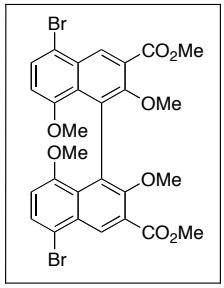

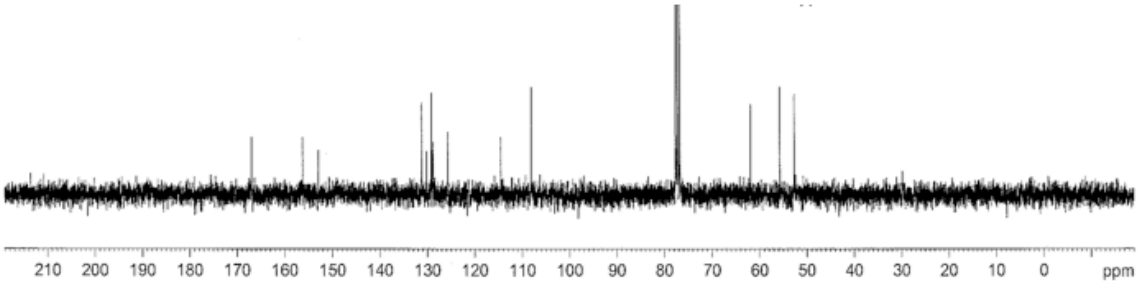

Figure A4.44a_2 ^{13}C NMR Spectrum of Compound **4.44a** (75 MHz, $CDCl_3$).

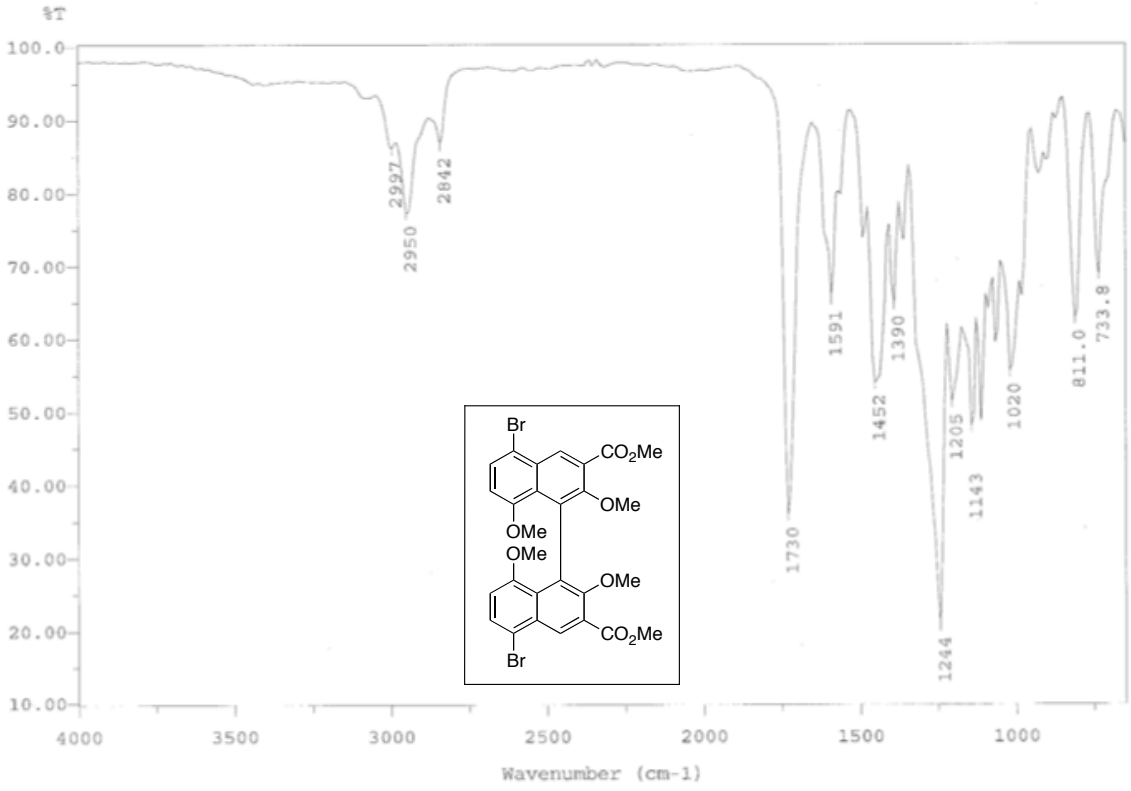

Figure A4.44a_3 IR Spectrum of Compound **4.44a** (film).

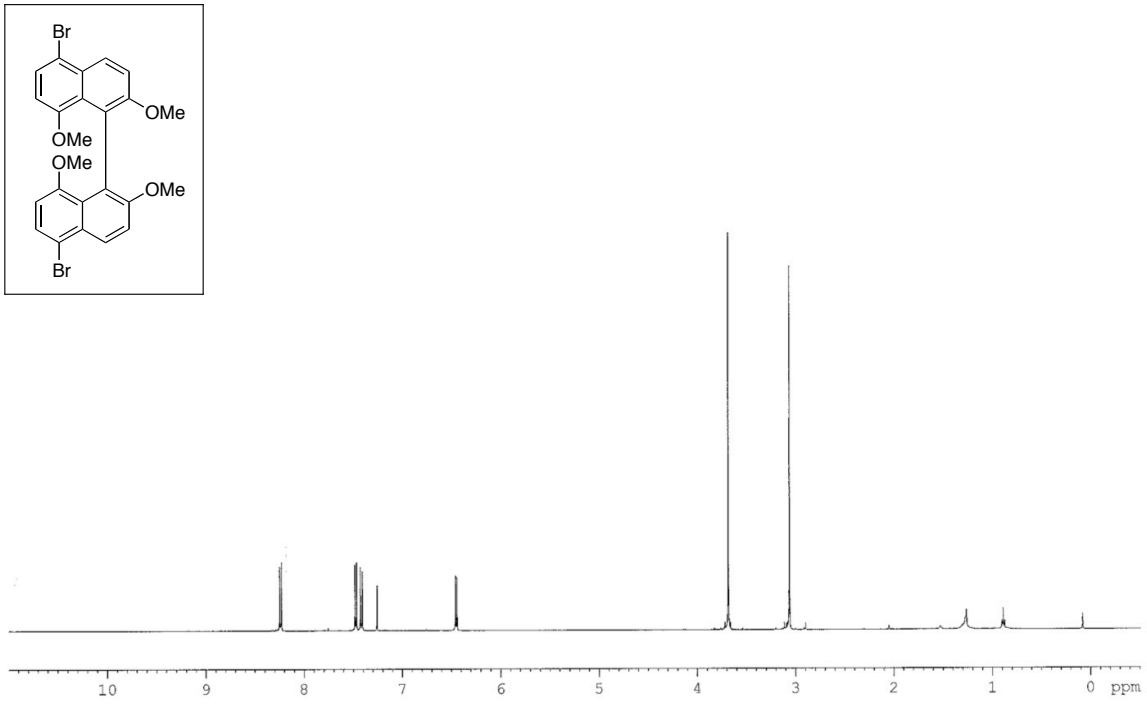

Figure A4.44b_1 ^{1}H NMR Spectrum of Compound **4.44b** (500 MHz, $CDCl_3$).

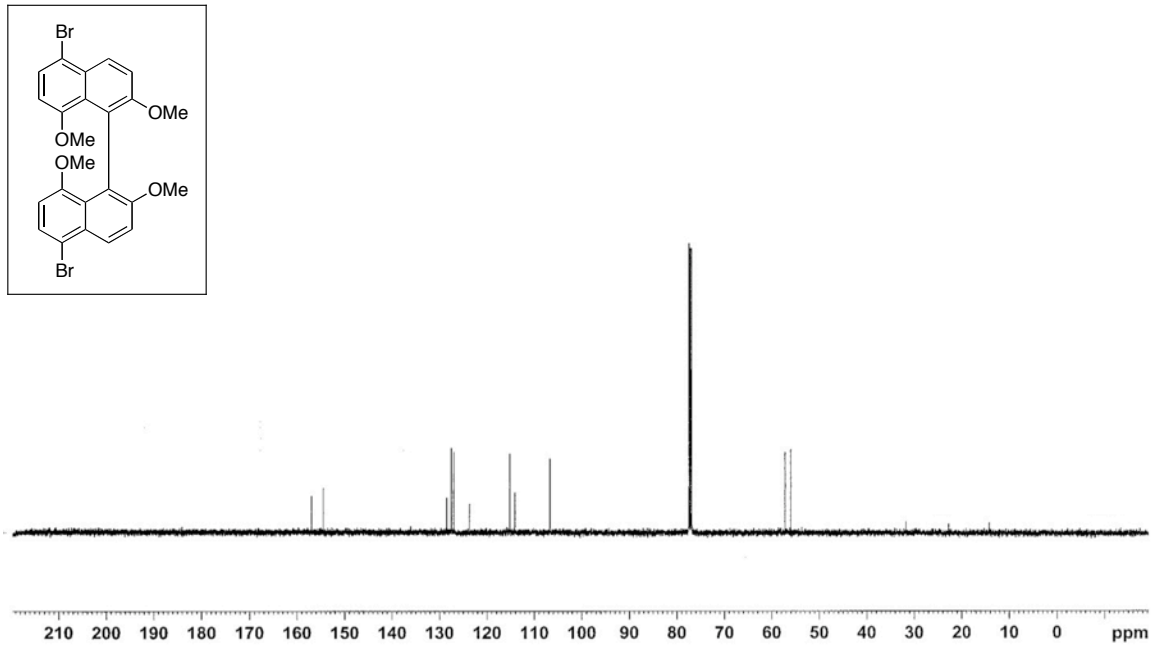

Figure A4.44b_2 ^{13}C NMR Spectrum of Compound **4.44b** (125 MHz, $CDCl_3$).

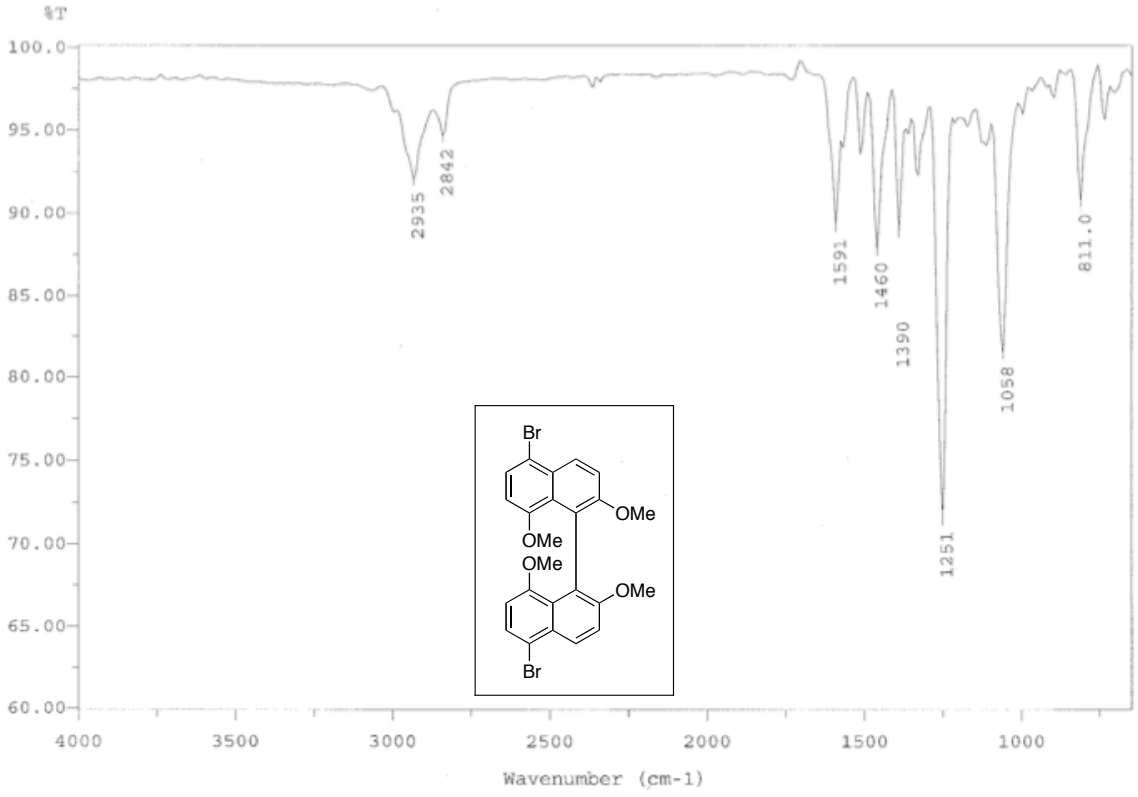

Figure A4.44b_3 IR Spectrum of Compound **4.44b** (film).

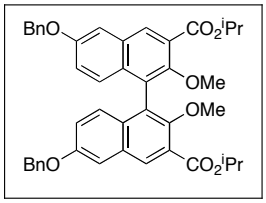

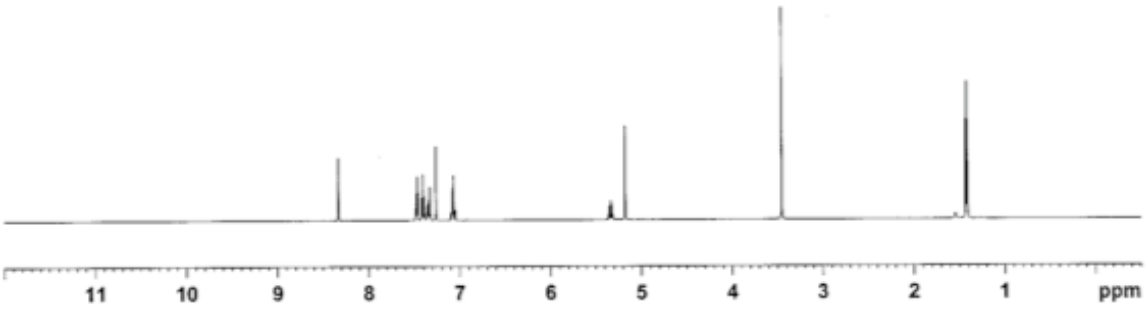

Figure A4.46_1 ^{1}H NMR Spectrum of Compound **4.46** (500 MHz, $CDCl_3$).

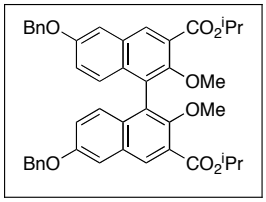

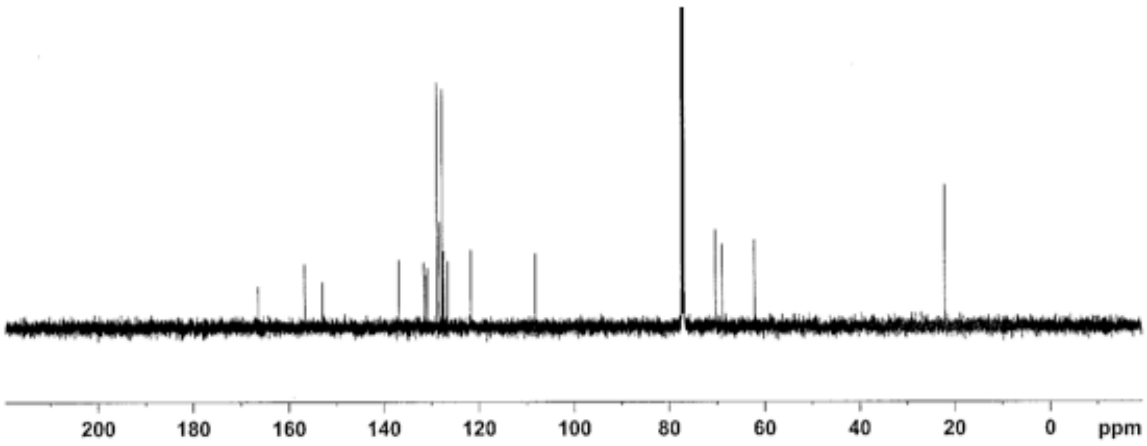

Figure A4.46_2 ^{13}C NMR Spectrum of Compound **4.46** (125 MHz, $CDCl_3$).

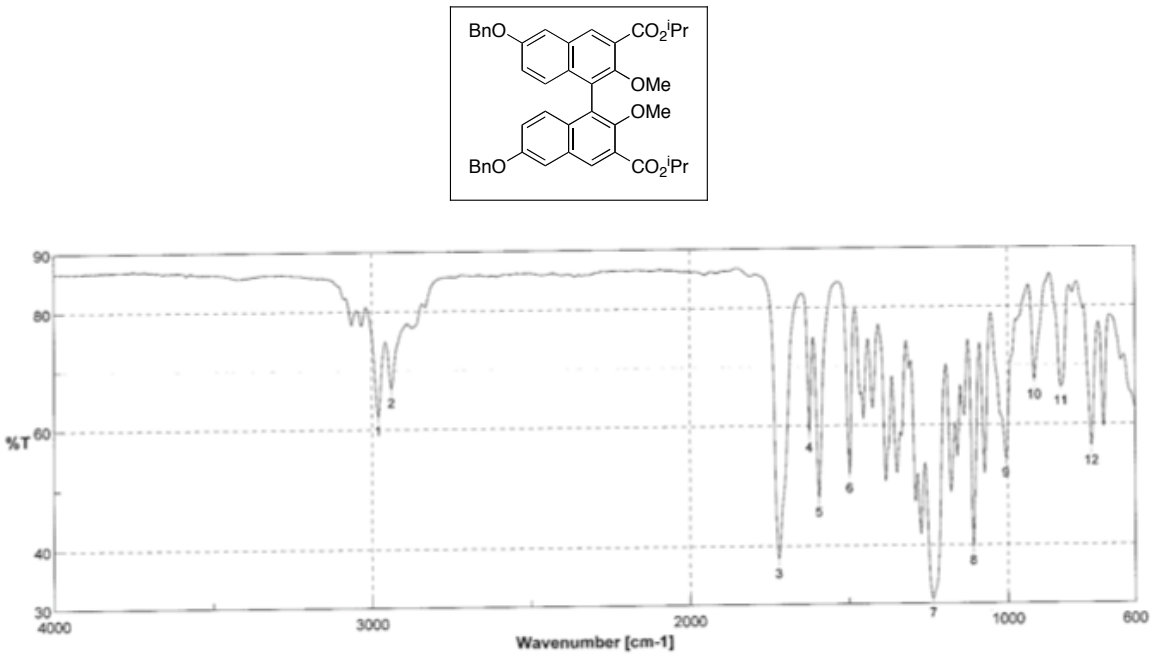

Figure A4.46_3 IR Spectrum of Compound **4.46** (film).

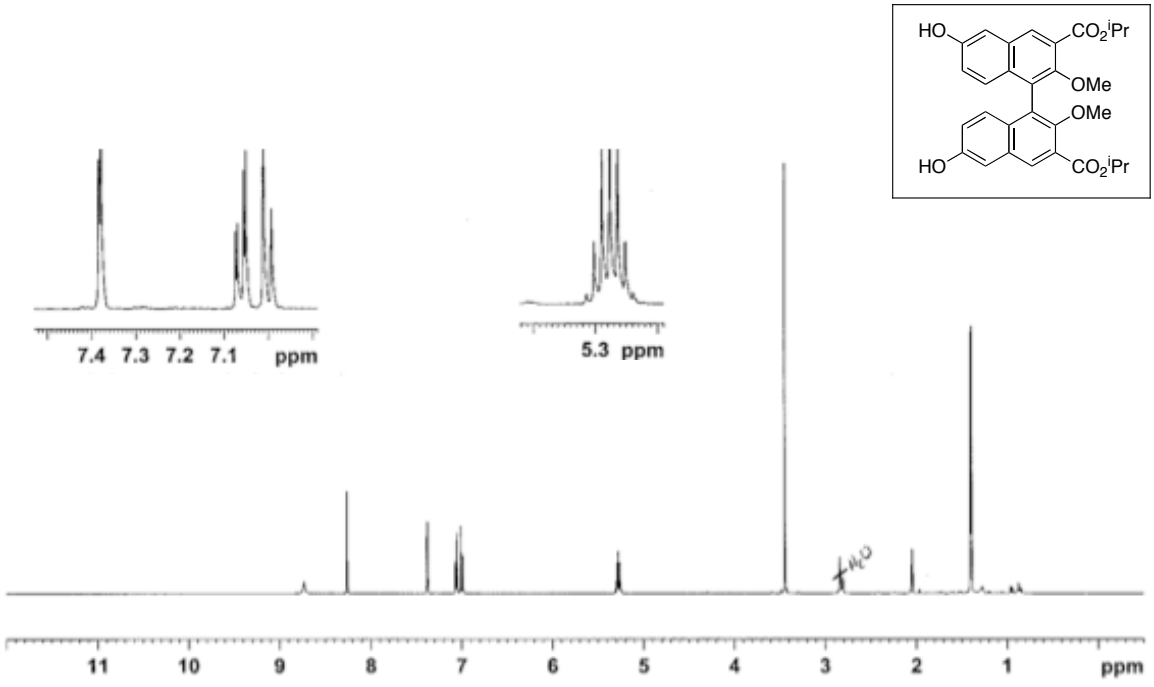

Figure A4.47_1 ^{1}H NMR Spectrum of Compound **4.47** (500 MHz, $CDCl_3$).

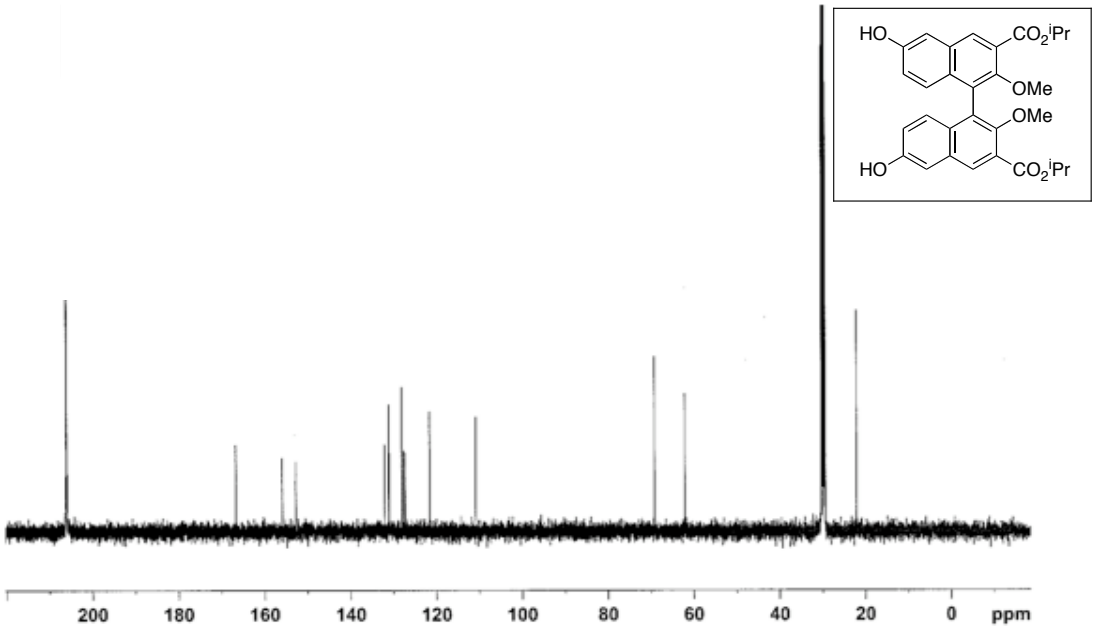

Figure A4.47_2 ^{13}C NMR Spectrum of Compound **4.47** (125 MHz, $CDCl_3$).

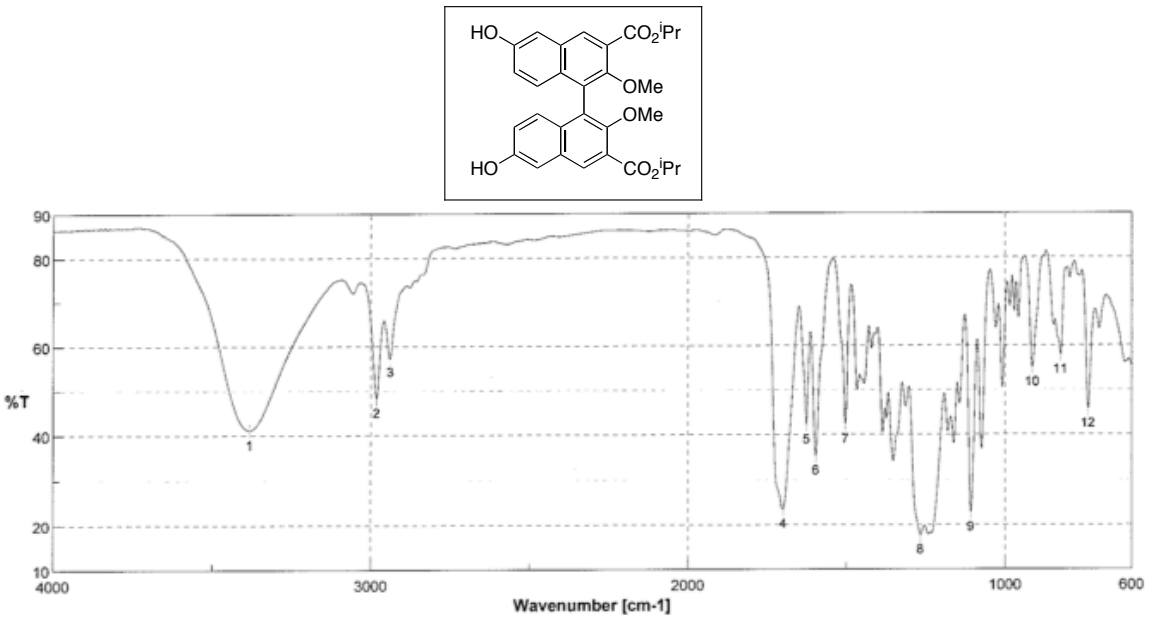

Figure A4.47_3 IR Spectrum of Compound **4.47** (film).

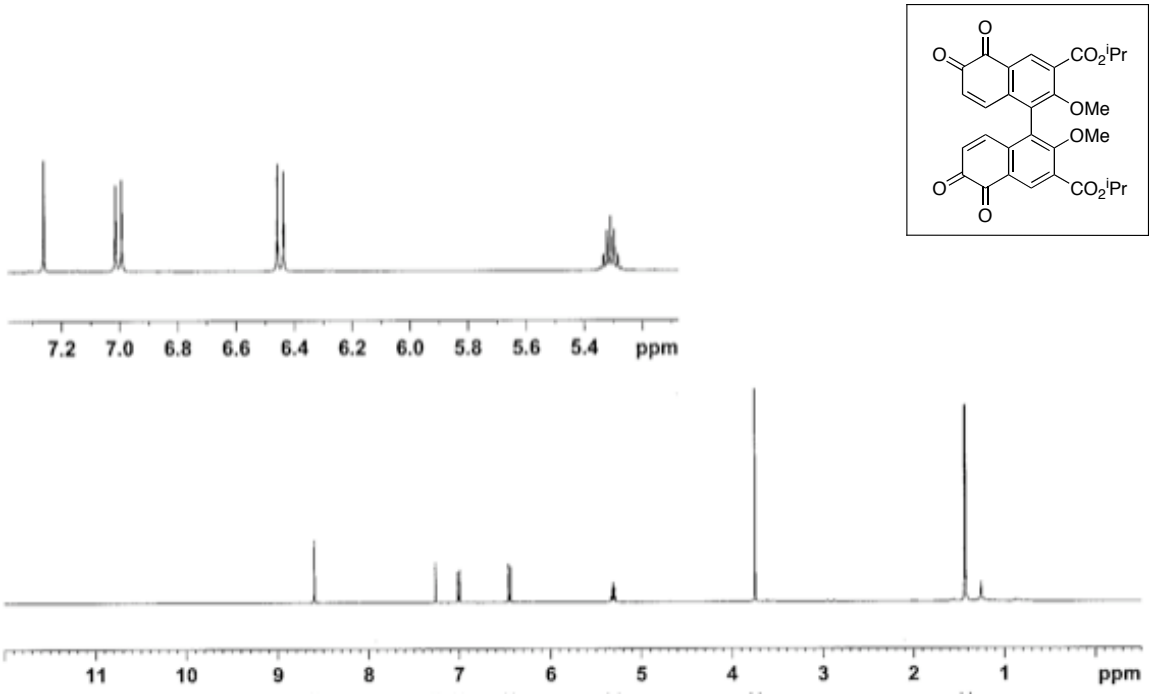

Figure A4.48_1 ^{1}H NMR Spectrum of Compound **4.48** (500 MHz, $CDCl_3$).

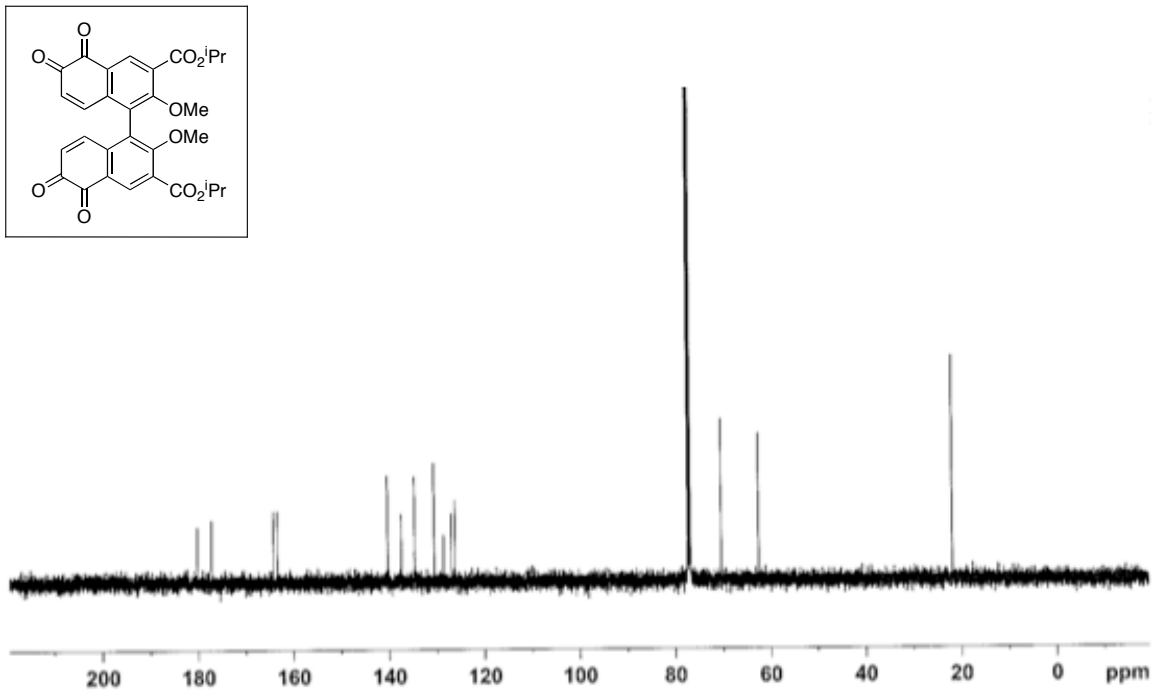

Figure A4.48_2 ^{13}C NMR Spectrum of Compound **4.48** (125 MHz, $CDCl_3$).

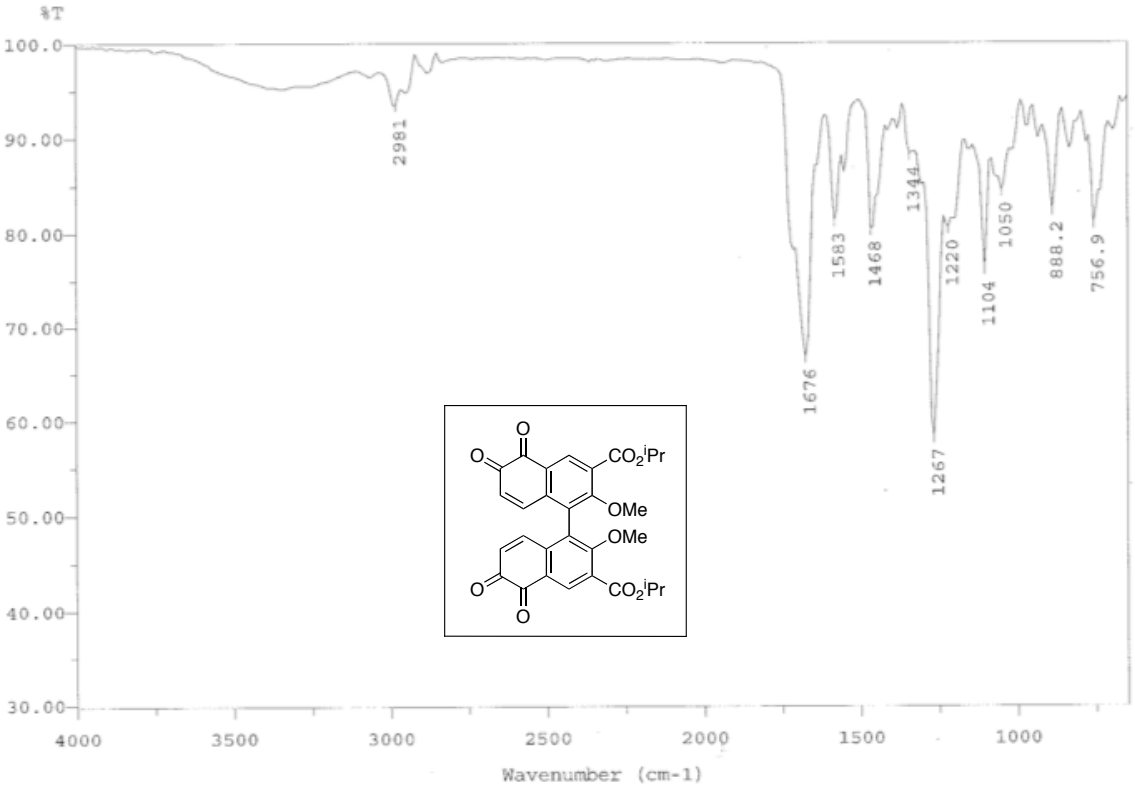

Figure A4.48_3 IR Spectrum of Compound **4.48** (film).

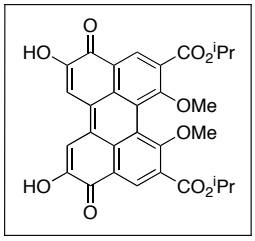

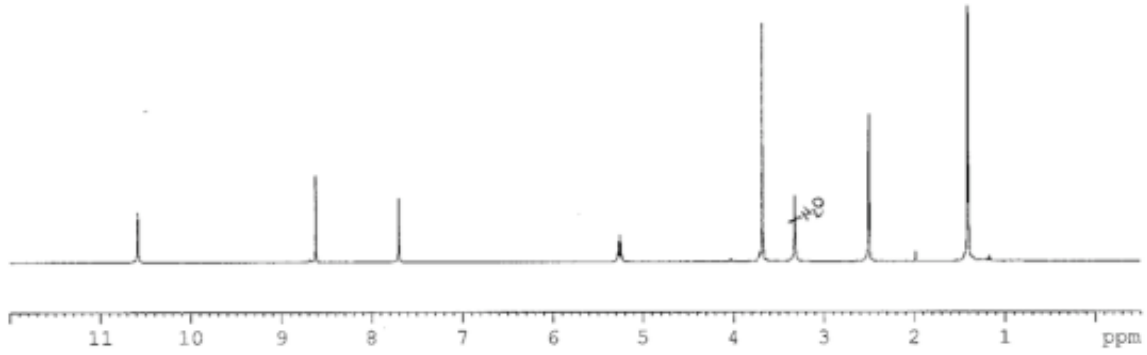

Figure A4.49 _1 ^{1}H NMR Spectrum of Compound **4.49** (500 MHz, DMSO-d_6).

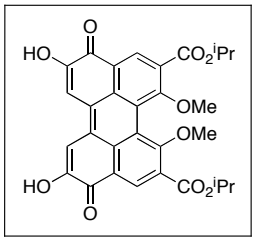

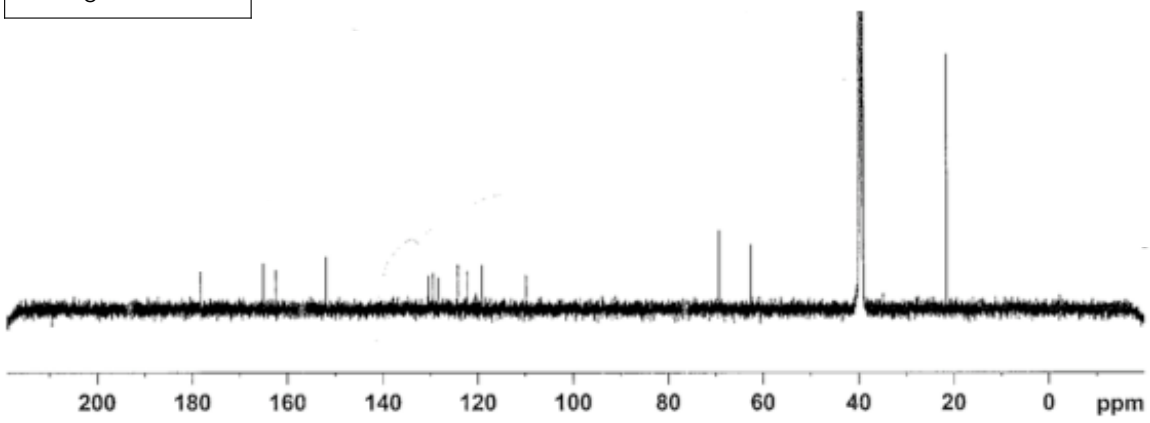

Figure A4.49_2 ^{13}C NMR Spectrum of Compound **4.49** (125 MHz, DMSO-d_6).

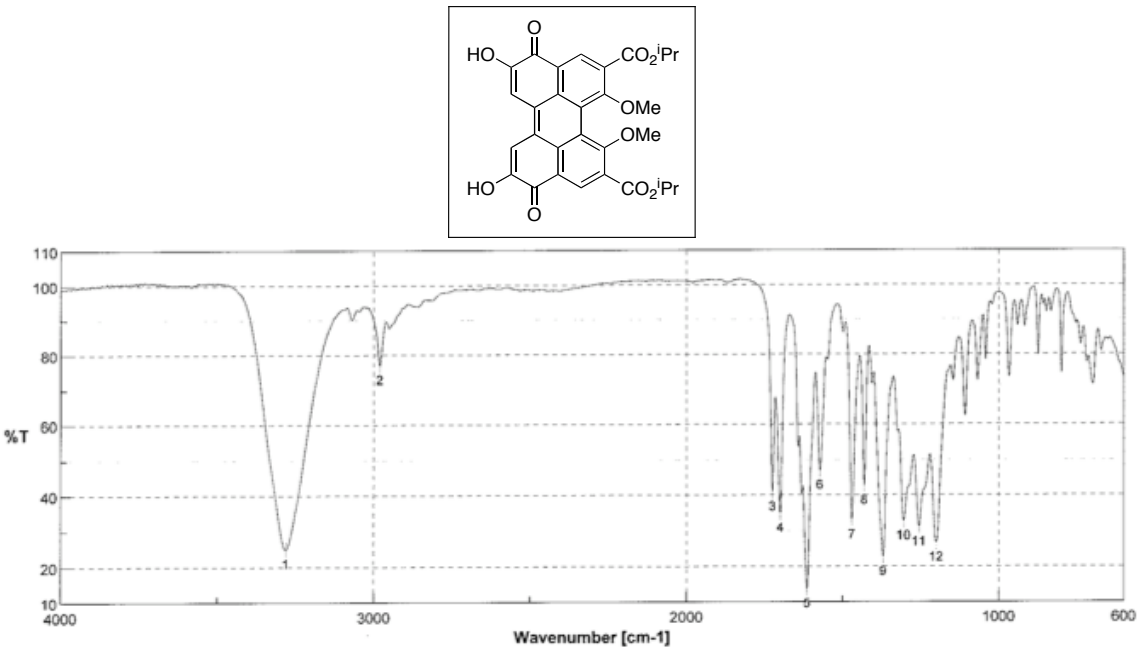

Figure A4.49_3 IR Spectrum of Compound **4.49** (film).

7.4 Chapter 5

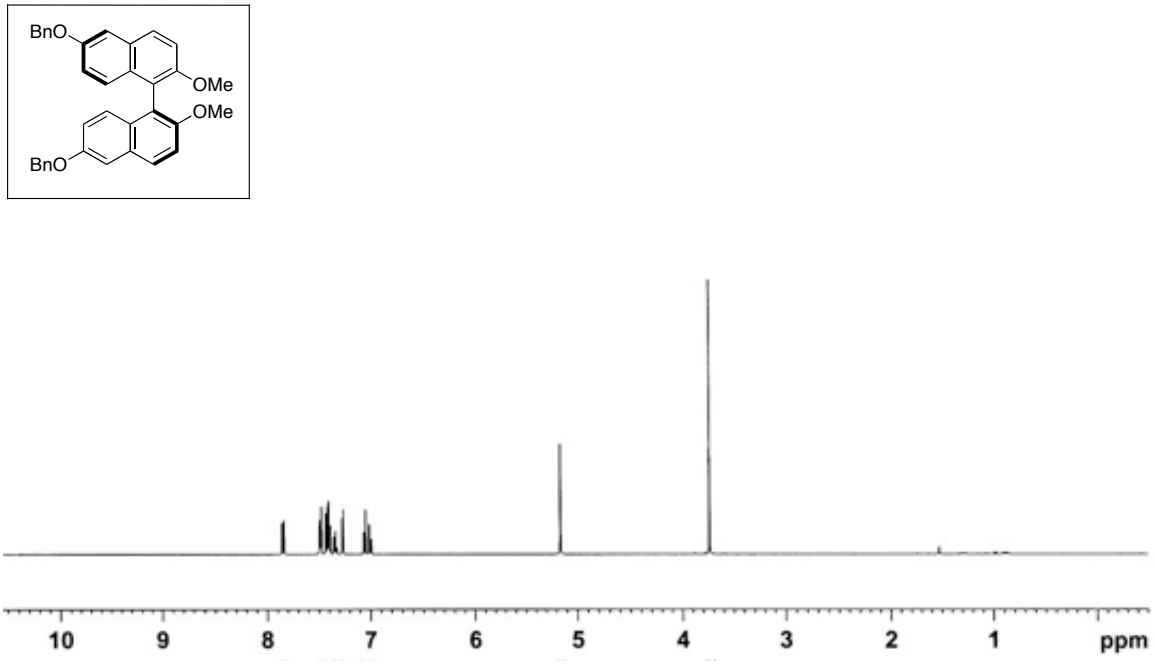

Figure A5.6_1 ^{1}H NMR Spectrum of Compound (*S*)-**5.6** (500 MHz, $CDCl_3$).

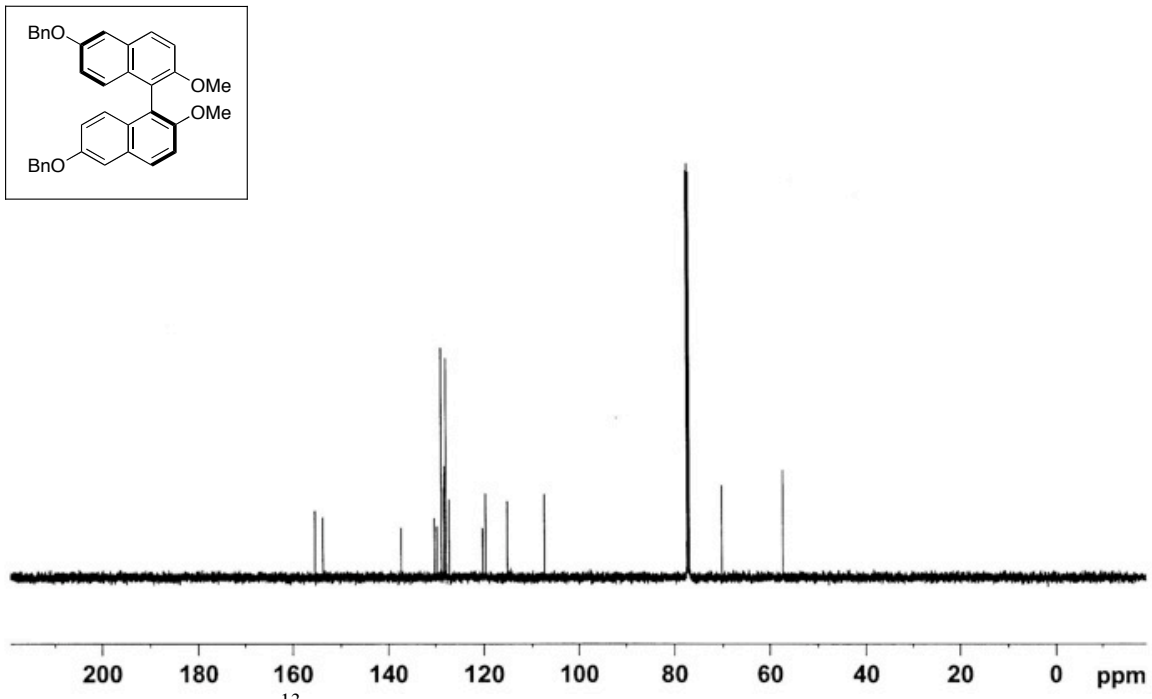

Figure A5.6_2 ^{13}C NMR Spectrum of Compound (*S*)-**5.6** (125 MHz, $CDCl_3$).

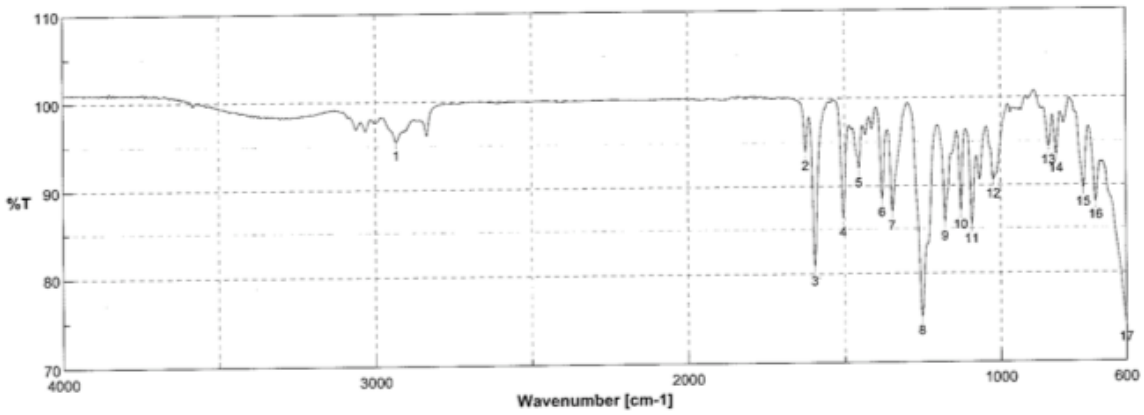

Figure A_3 IR Spectrum of Compound (*S*)-**5.6** (film).

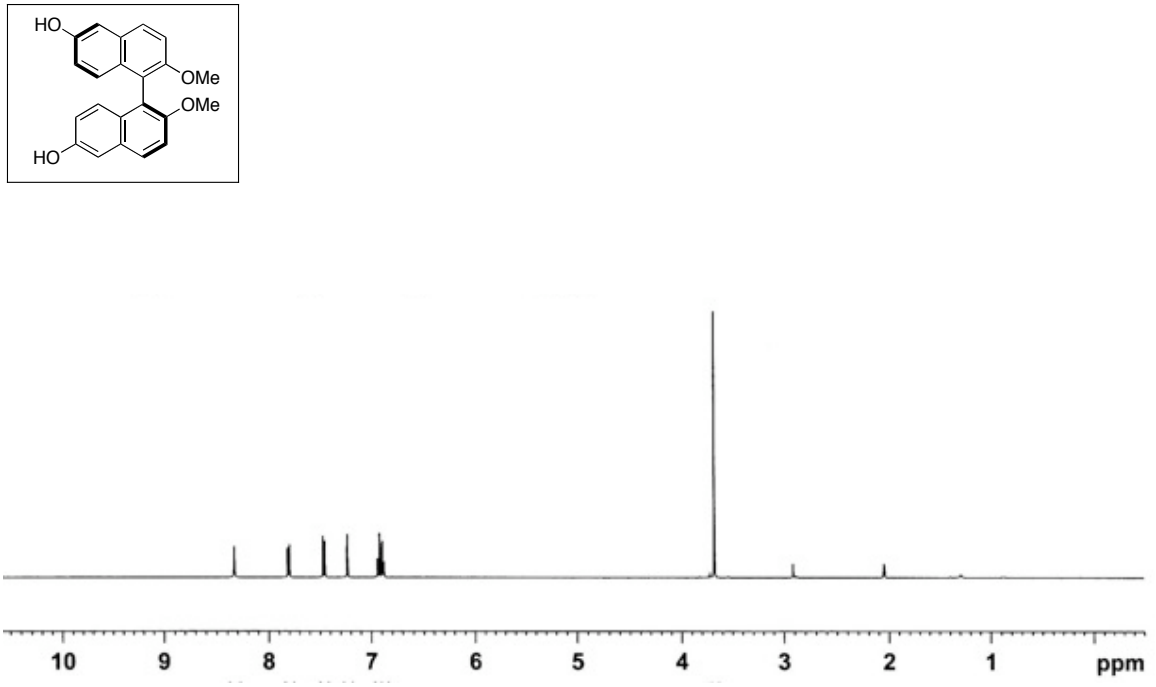

Figure A5.3_1 ^{1}H NMR Spectrum of Compound (*S*)-**5.3** (500 MHz, acetone-d_6).

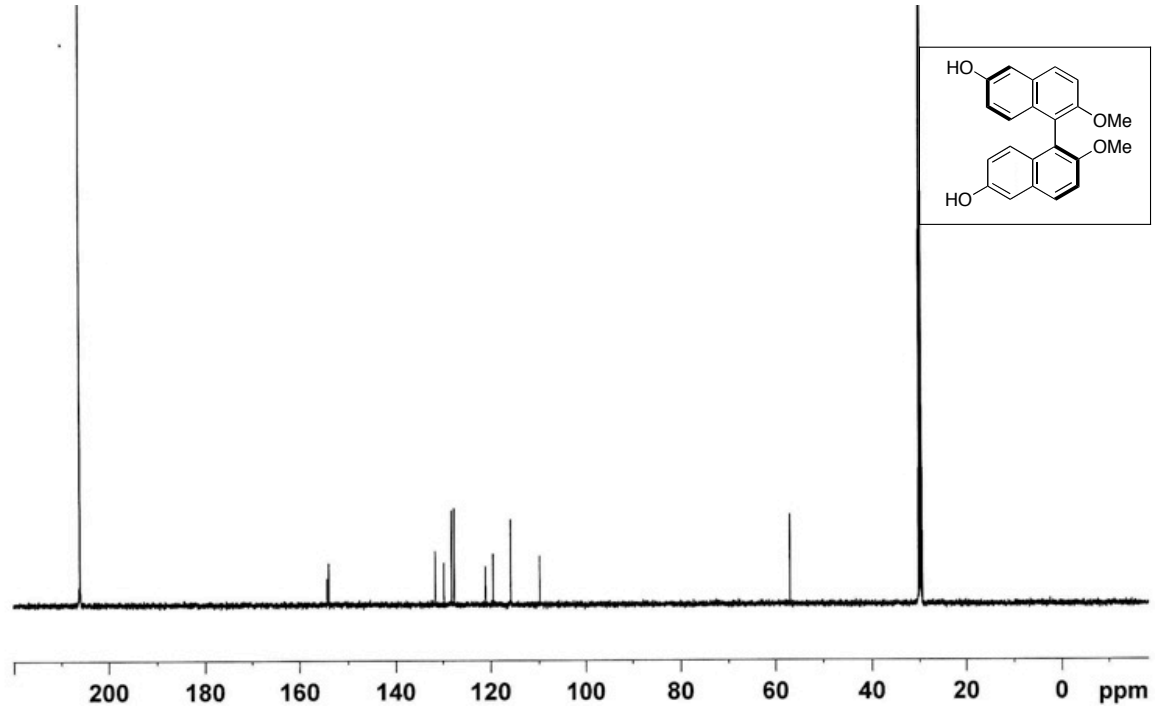

Figure A5.3_2 ^{13}C NMR Spectrum of Compound (*S*)-**5.3** (125 MHz, acetone-d_6).

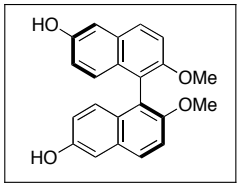

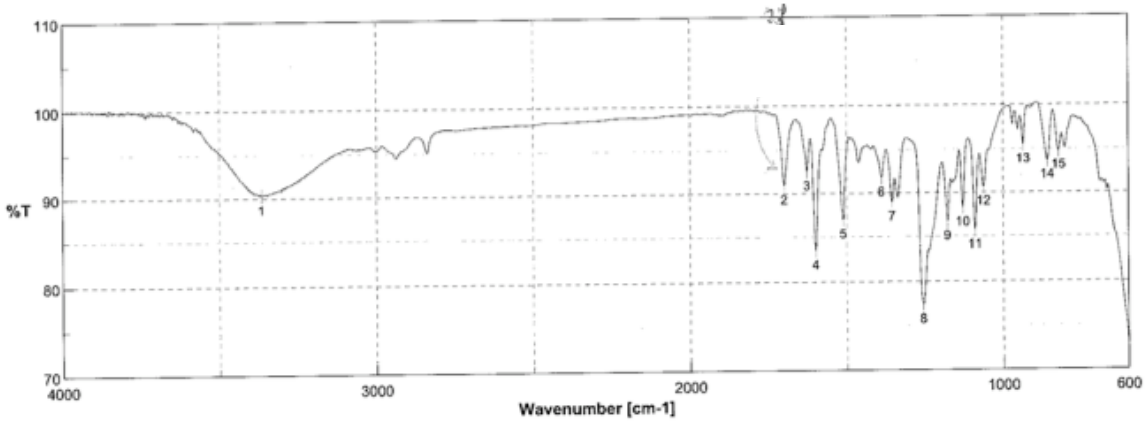

Figure A5.3_3 IR Spectrum of Compound (*S*)-**5.3** (film).

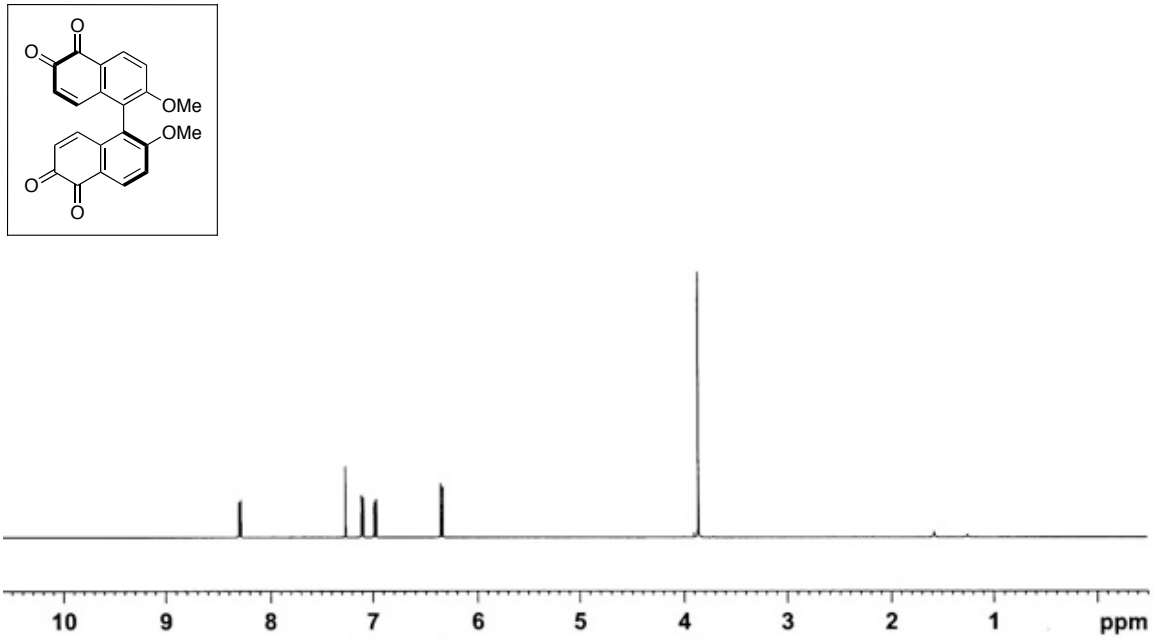

Figure A5.2_1 ^{1}H NMR Spectrum of Compound (*S*)-**5.2** (500 MHz, $CDCl_3$).

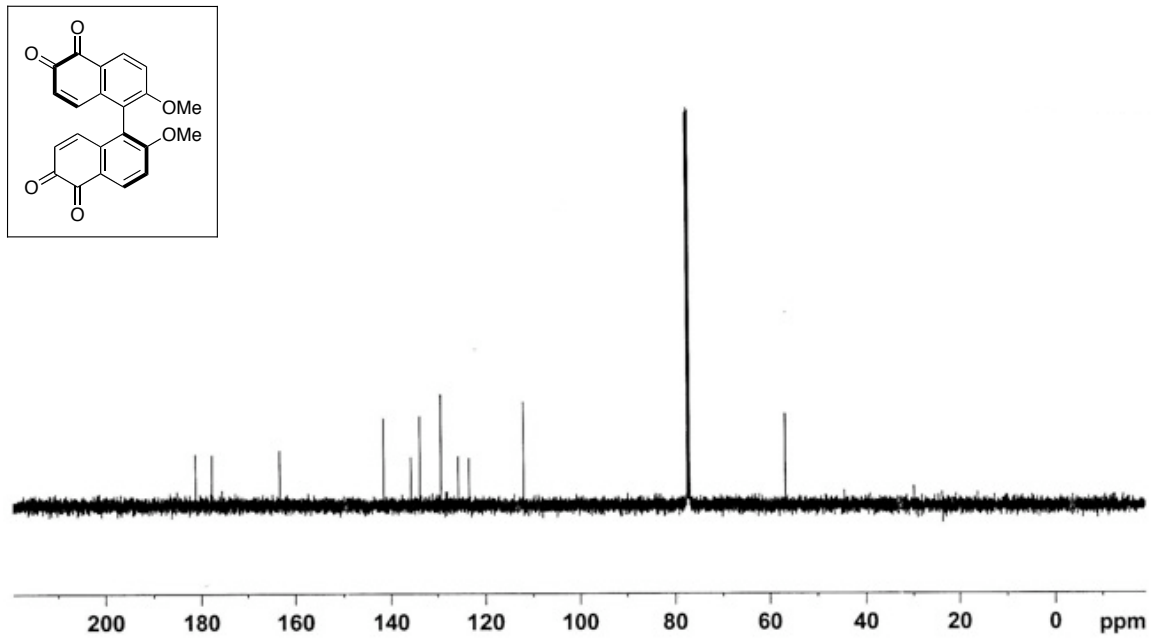

Figure A5.2_2 ^{13}C NMR Spectrum of Compound (*S*)-**5.2** (125 MHz, $CDCl_3$).

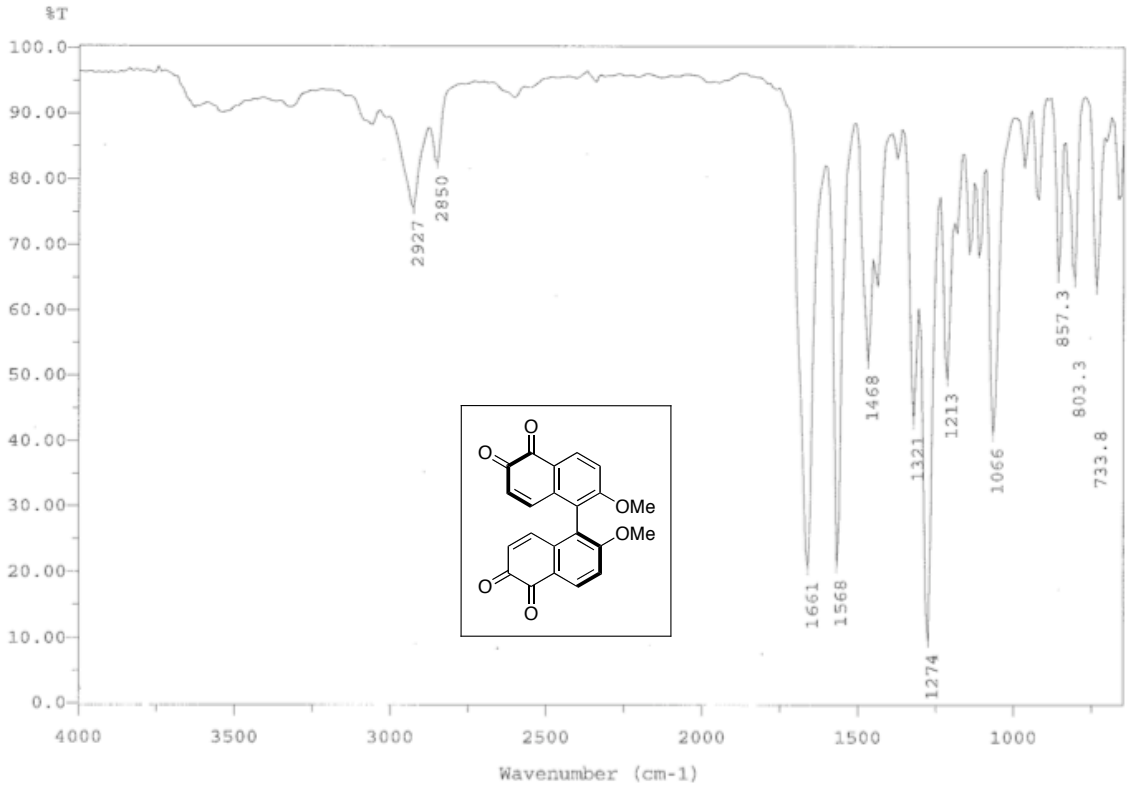

Figure A5.2_3 IR Spectrum of Compound (*S*)-**5.2** (film).

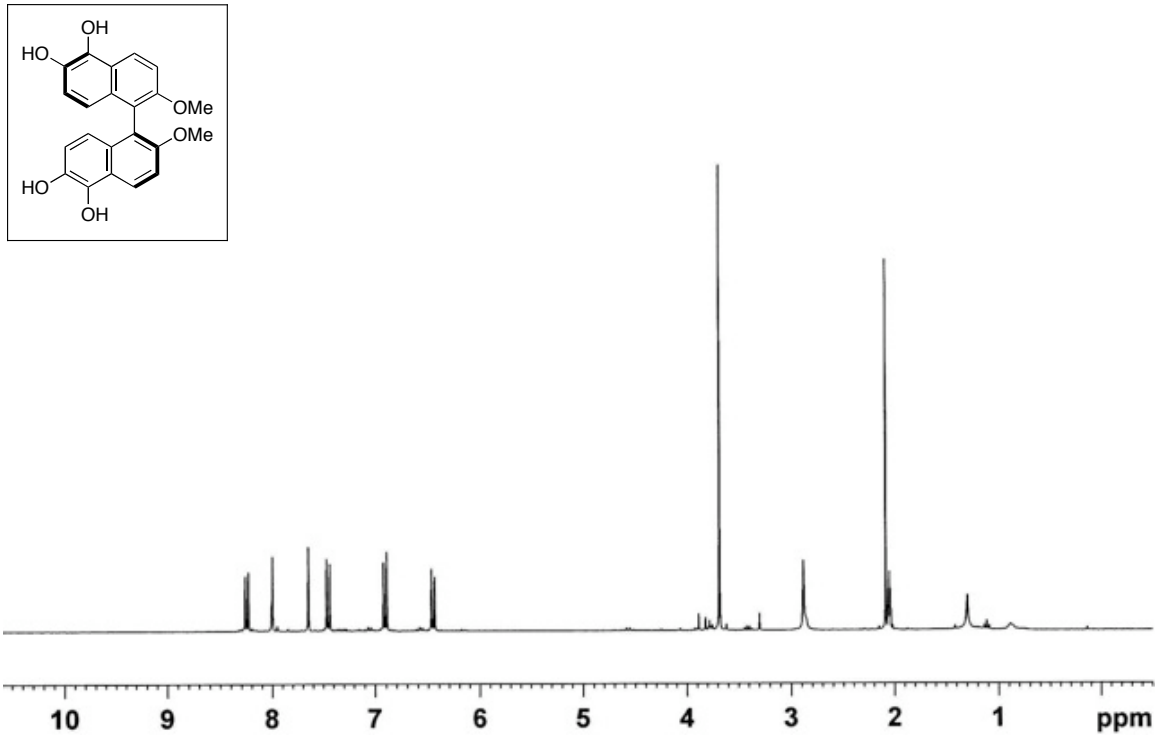

Figure A5.1_1 ^{1}H NMR Spectrum of Compound (*S*)-**5.1** (300 MHz, acetone-d_6).

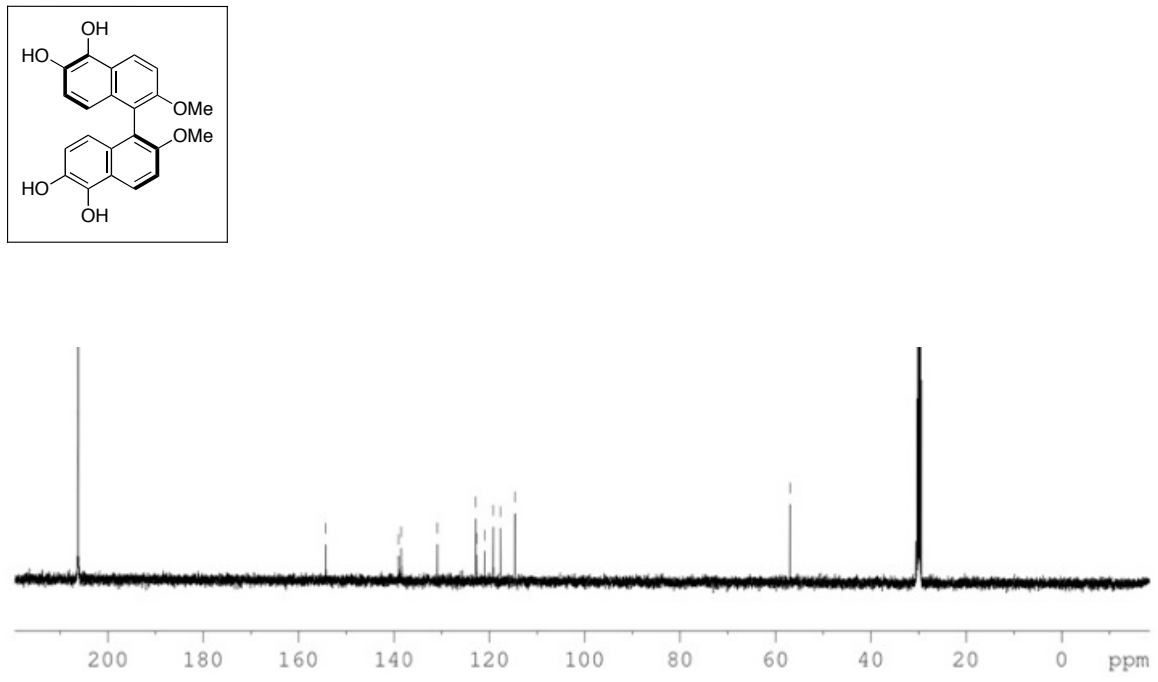

Figure A5.1_2 ^{13}C NMR Spectrum of Compound (*S*)-**5.1** (125 MHz, acetone-d_6).

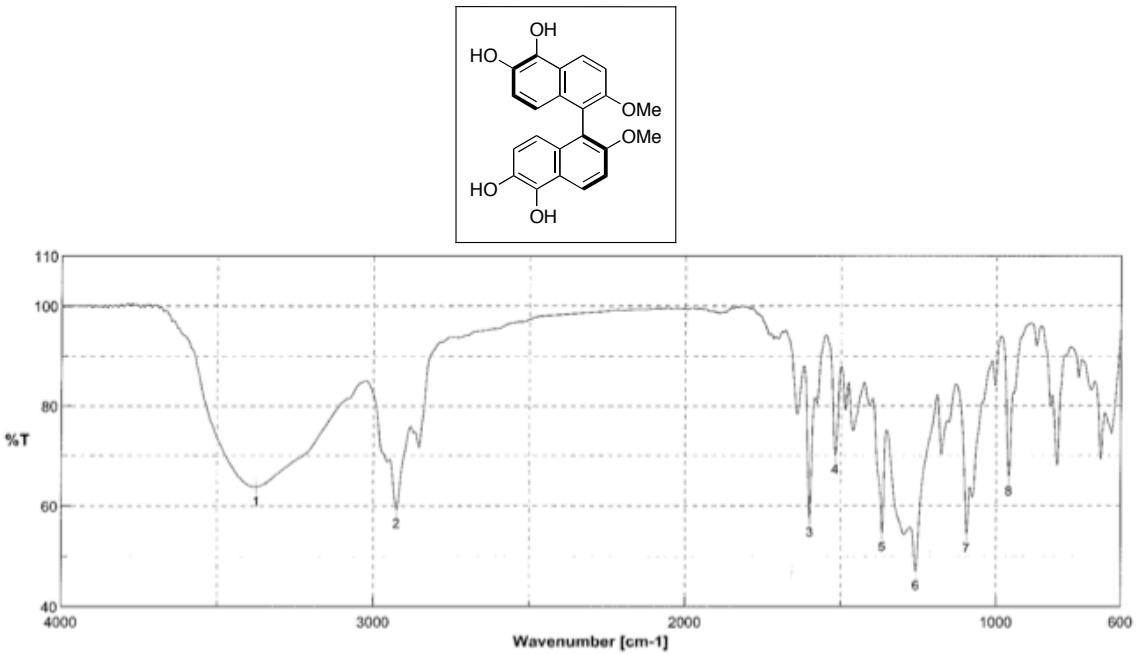

Figure A5.1_3 IR Spectrum of Compound (*S*)-**5.1** (film).

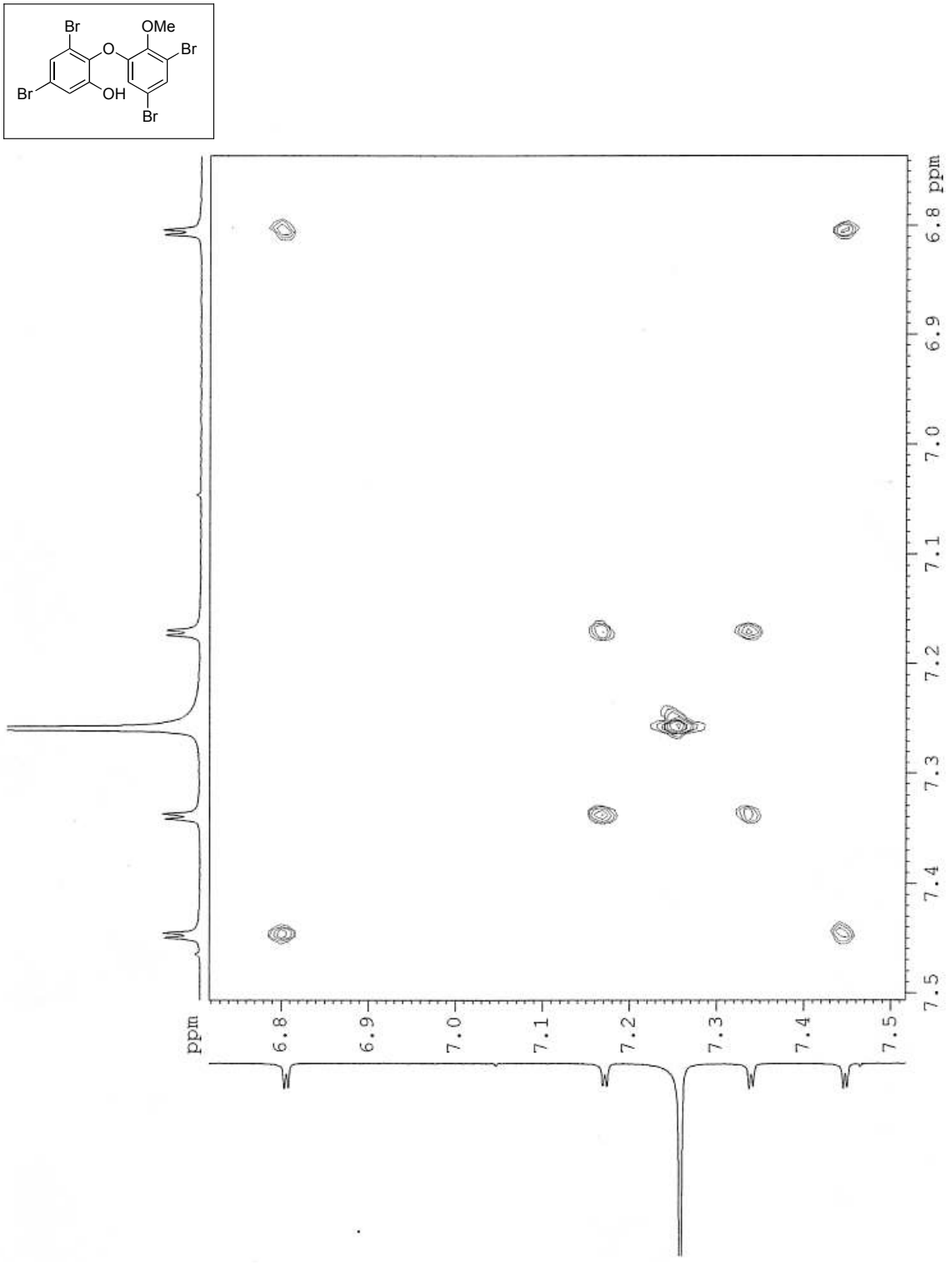

Figure A5.7_1 COSY NMR Spectrum of Compound **5.7** ($CDCl_3$).

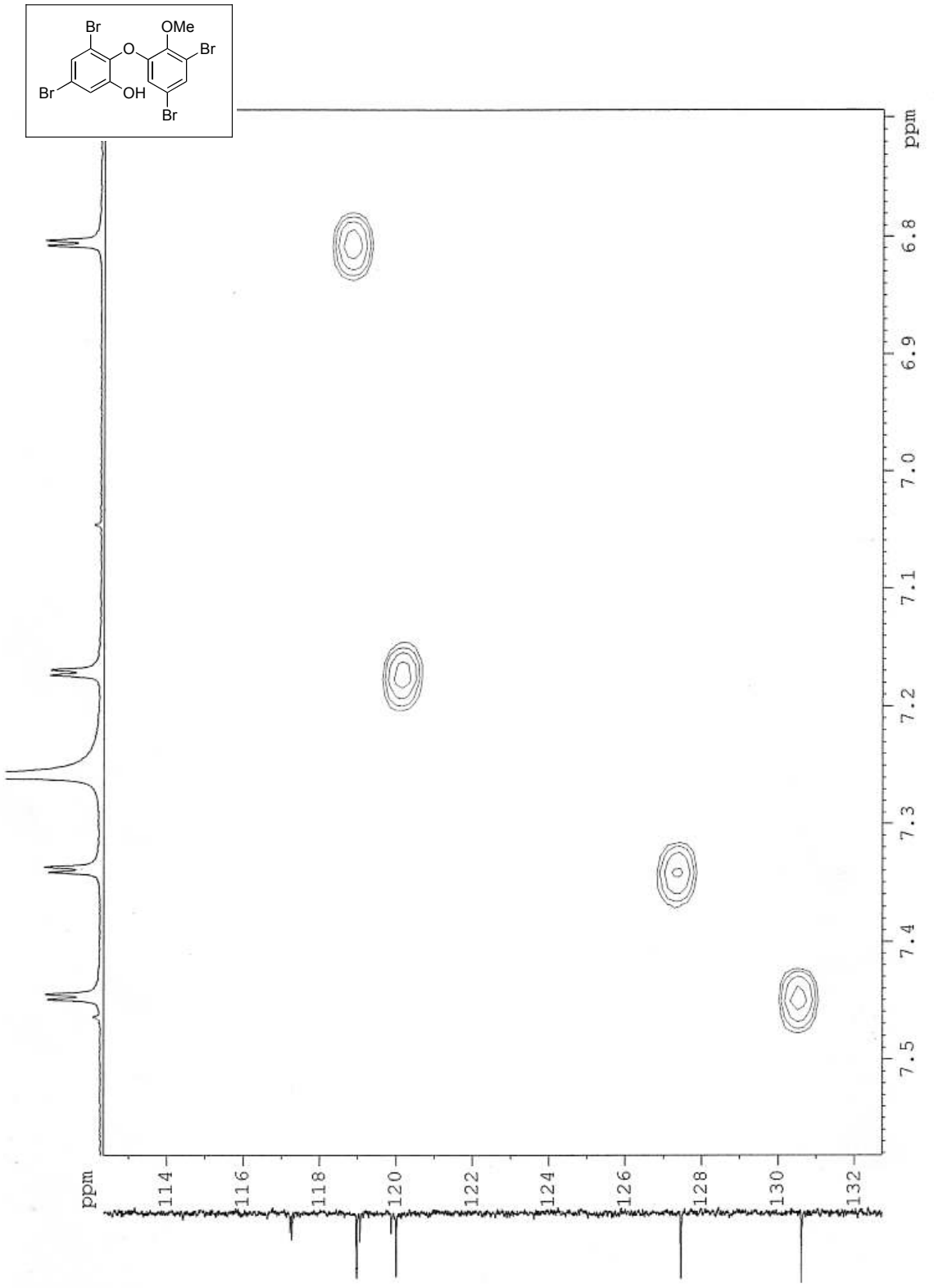

Figure A5.7_2 HSQC Spectrum of Compound **5.7** ($CDCl_3$).

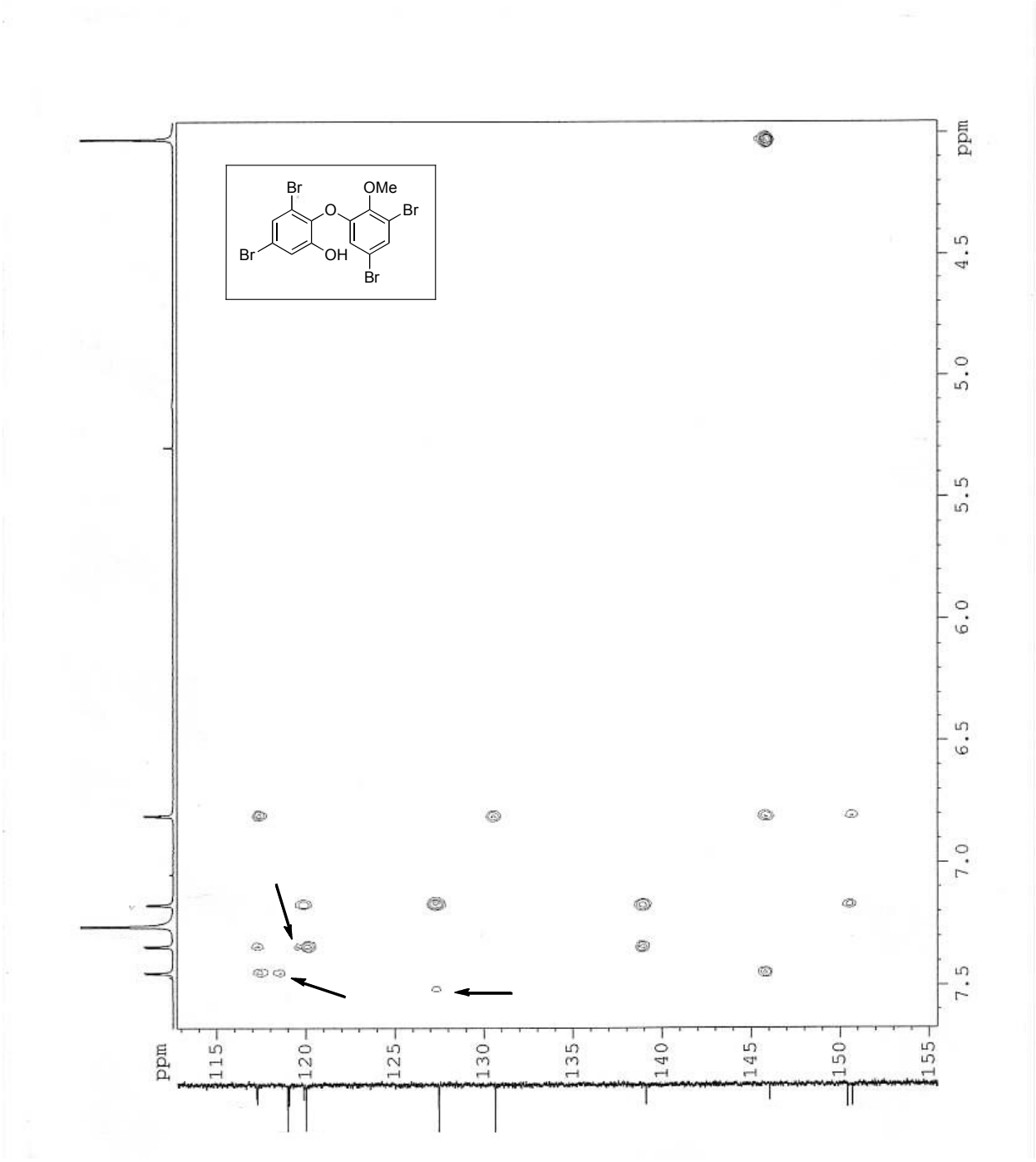

Figure A5.7_2 HMBC Spectrum of Compound **5.7** ($CDCl_3$).
Arrows indicate peaks which did not correlate to either a carbon or proton and were considered impurities

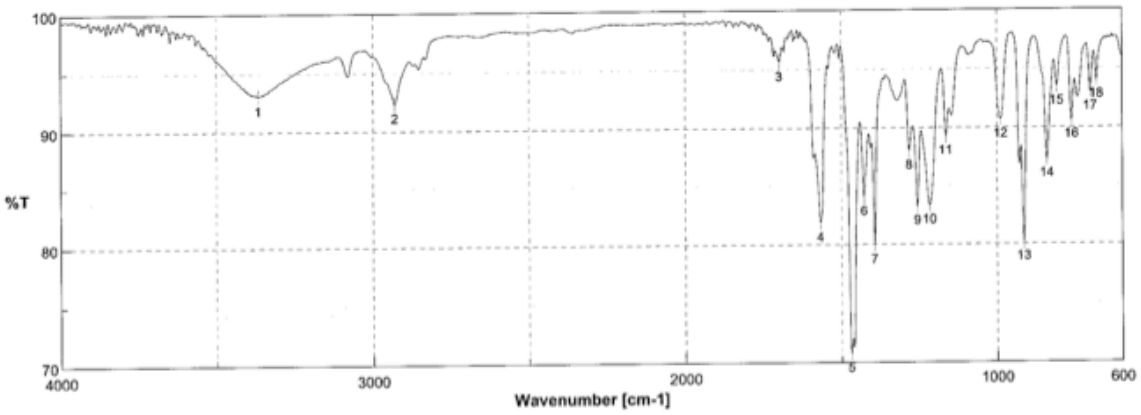

Figure A5.7_3 IR Spectrum of Compound **5.7** (film).

7.5 Chapter 6

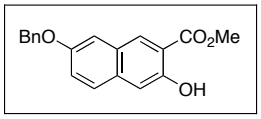

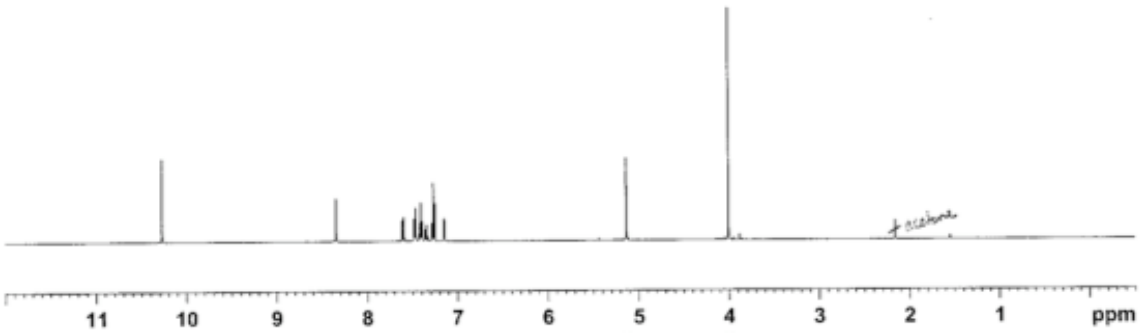

Figure A6.21_1 ^{1}H NMR Spectrum of Compound **6.21** (500 MHz, $CDCl_3$).

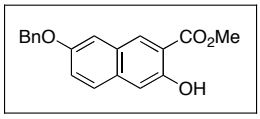

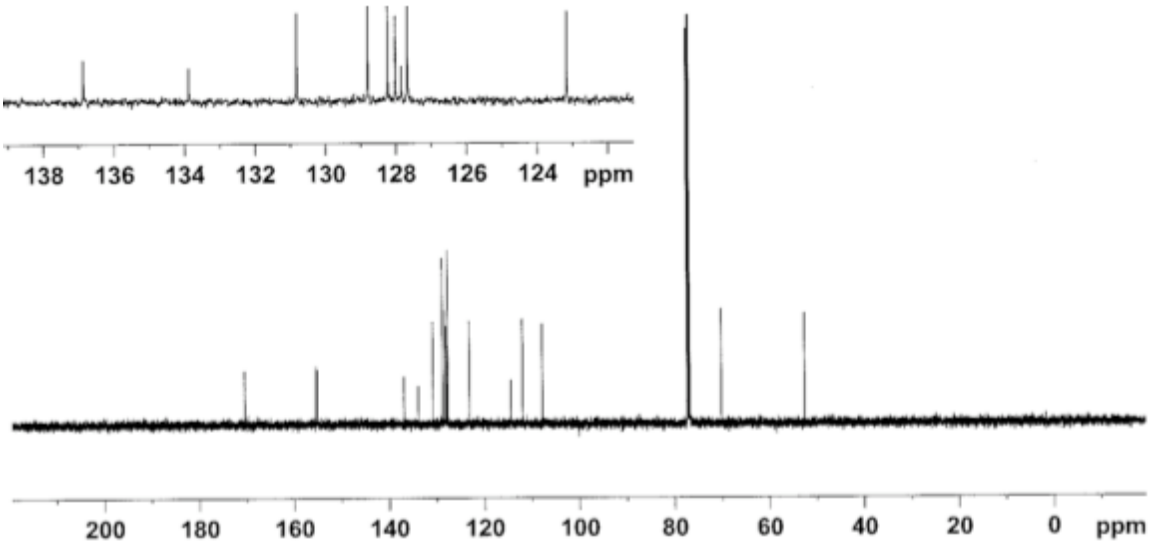

Figure A6.21_2 ^{13}C NMR Spectrum of Compound **6.21** (125 MHz, $CDCl_3$).

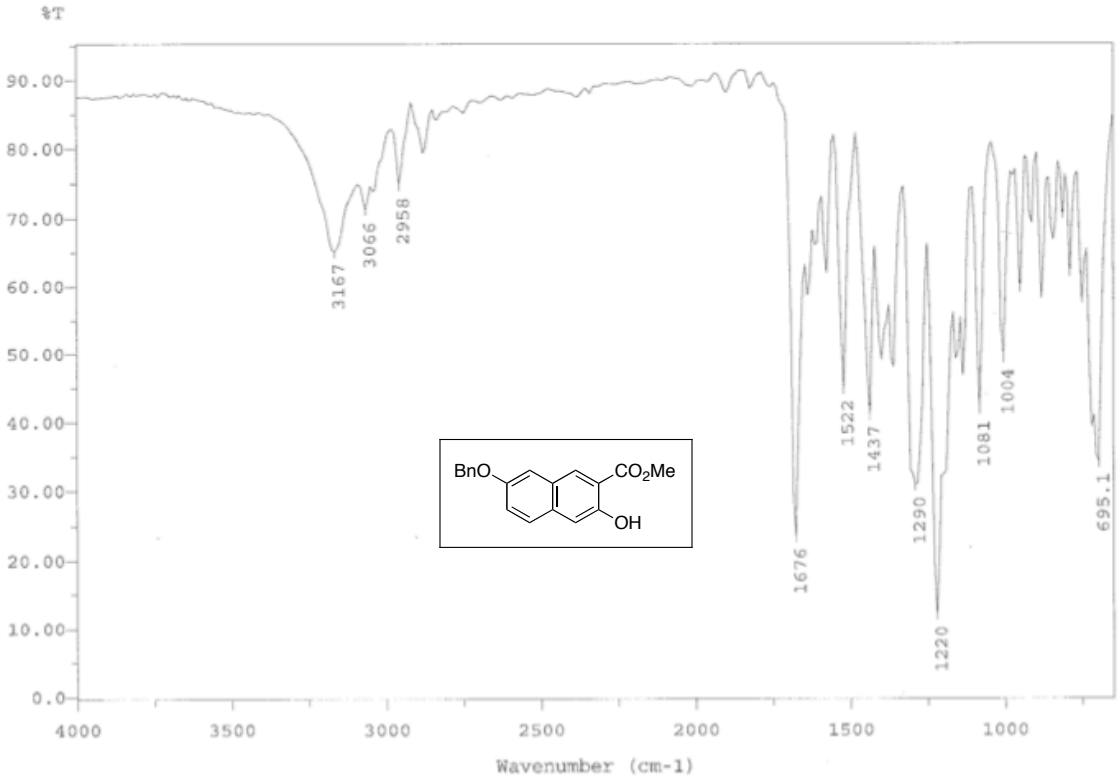

Figure A6.21_3 IR Spectrum of Compound **6.21** (film).

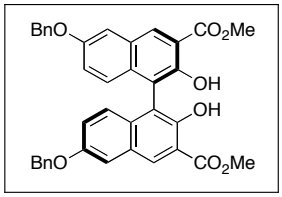

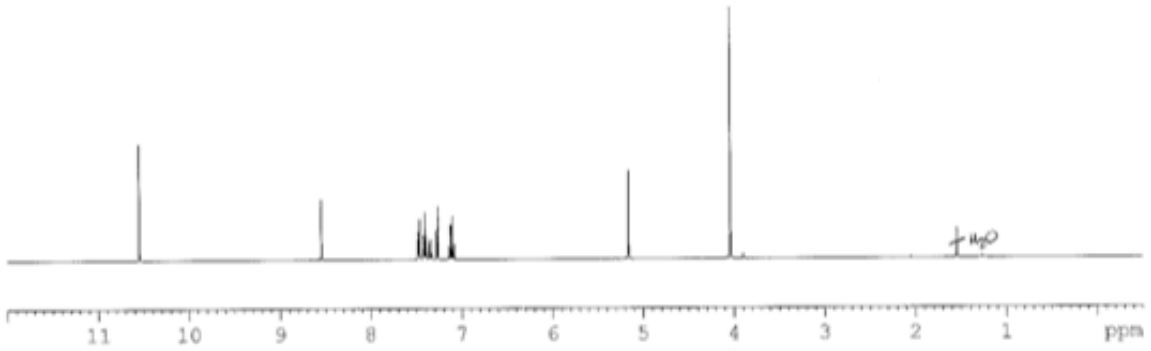

Figure A6.22_1 ^{1}H NMR Spectrum of Compound (*R*)-**6.22** (500 MHz, $CDCl_3$).

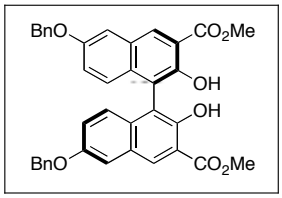

Figure A6.22_2 ^{13}C NMR Spectrum of Compound (*R*)-**6.22** (125 MHz, $CDCl_3$).

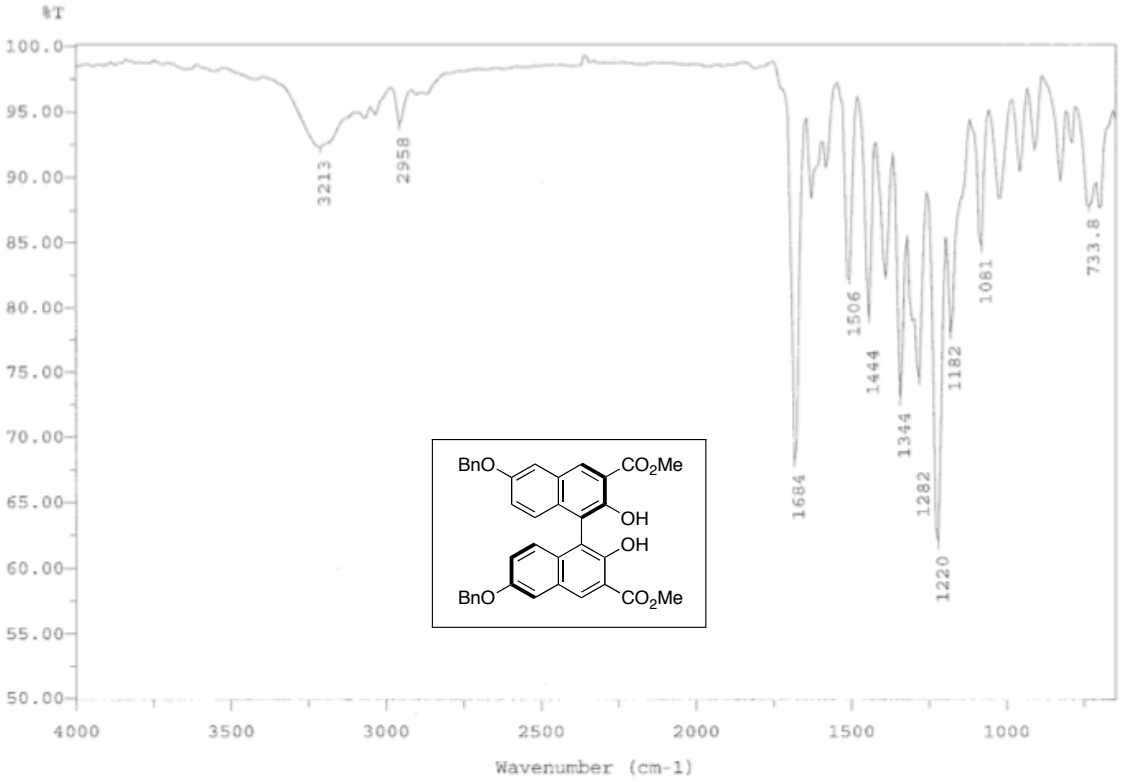

Figure A6.22_3 IR Spectrum of Compound (*R*)-**6.22** (film).

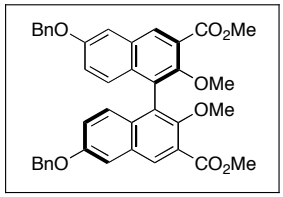

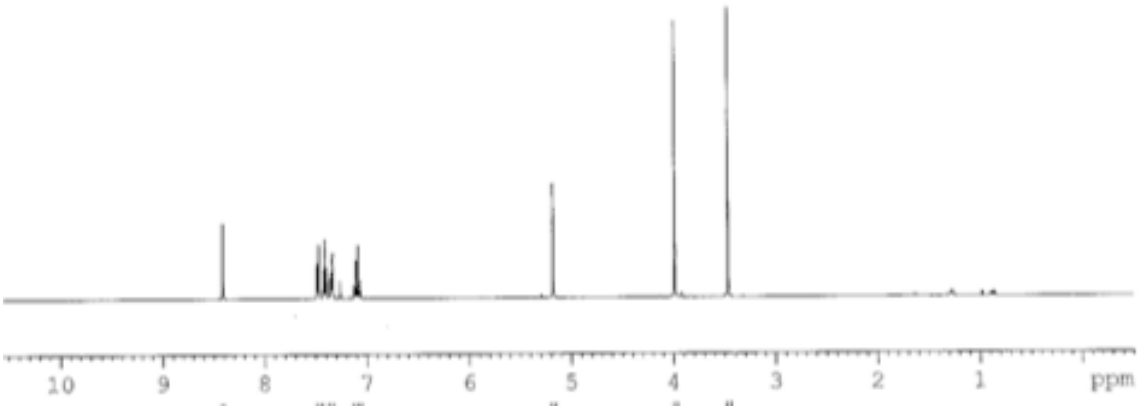

Figure A6.23_1 ^{1}H NMR Spectrum of Compound (*R*)-**6.23** (500 MHz, $CDCl_3$).

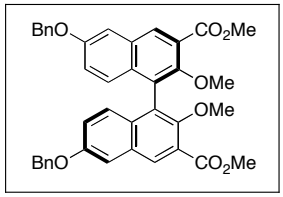

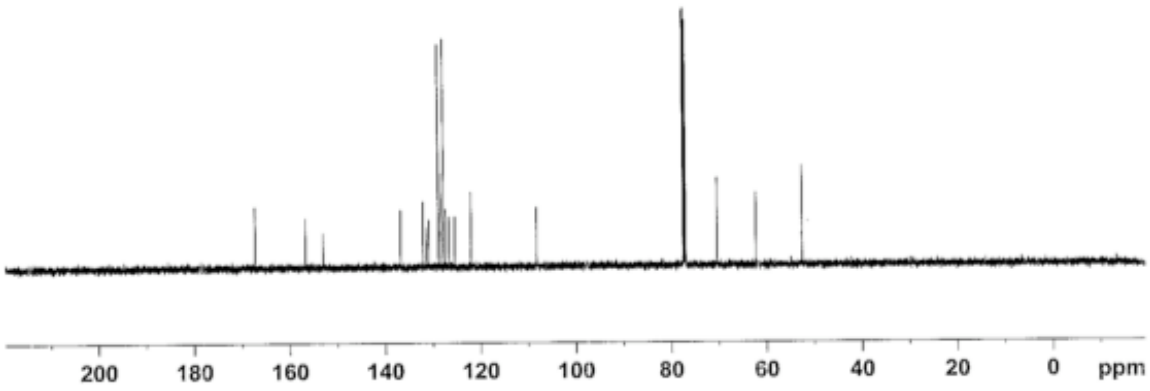

Figure A6.23_2 ^{13}C NMR Spectrum of Compound (*R*)-**6.23** (125 MHz, $CDCl_3$).

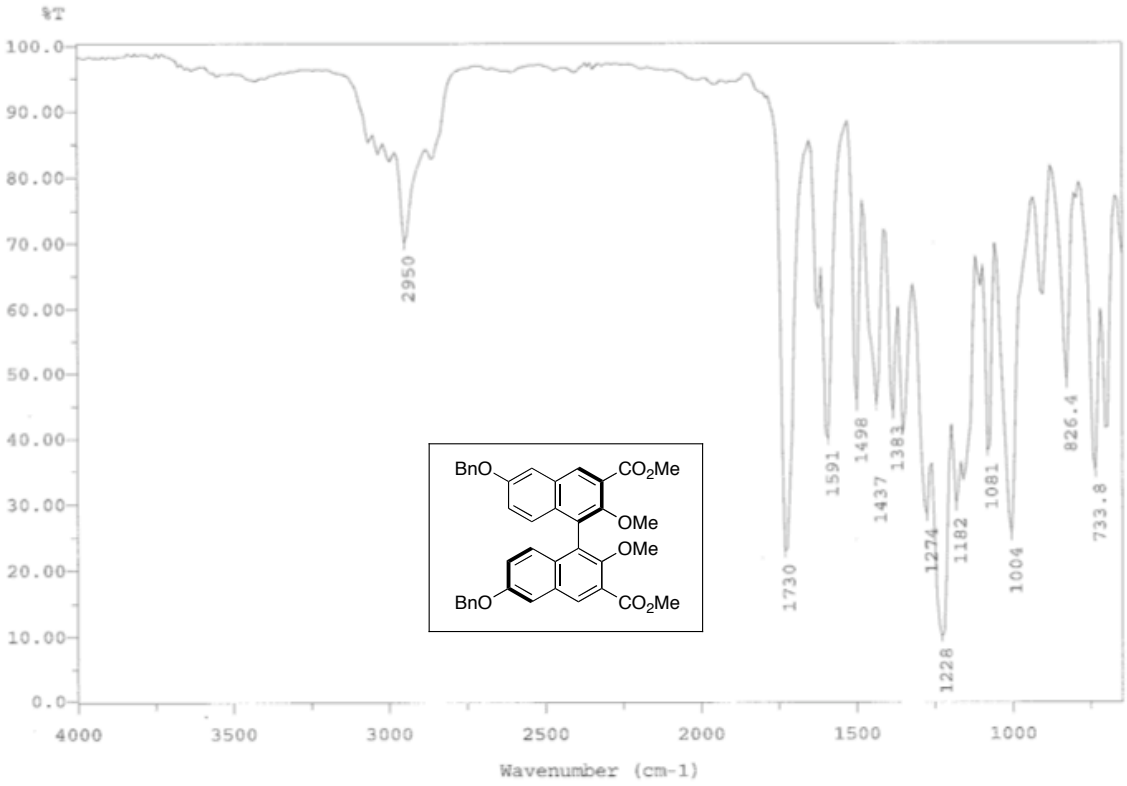

Figure A6.23_3 IR Spectrum of Compound (*R*)-**6.23** (film).

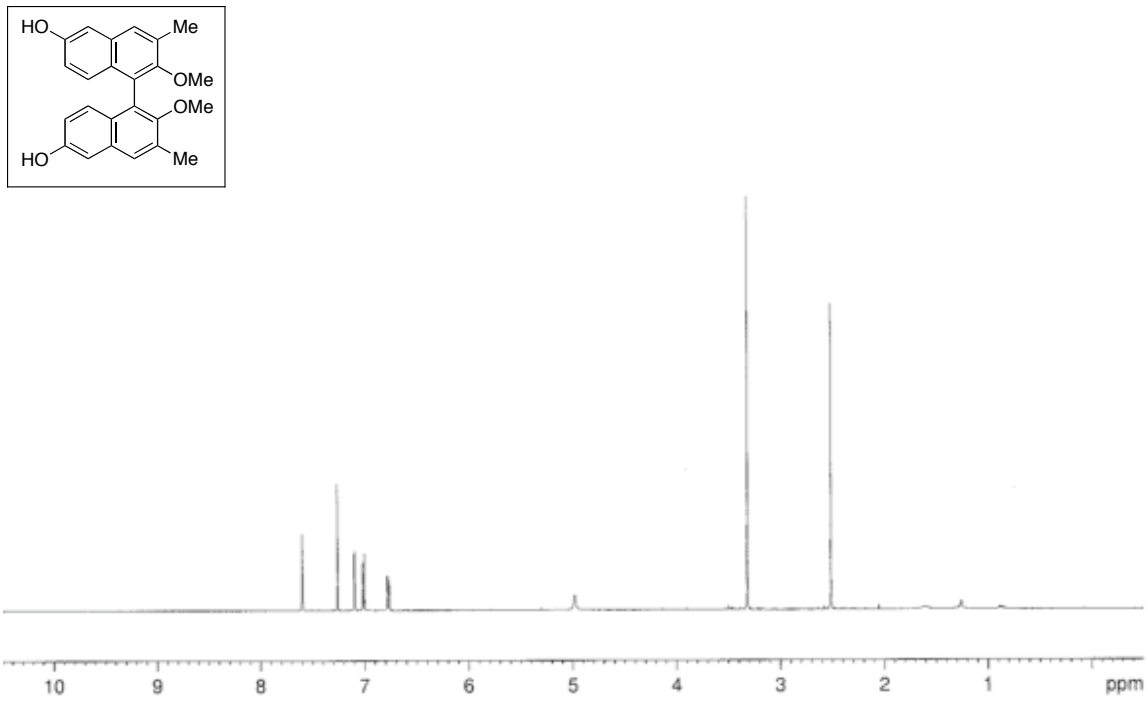

Figure A6.24_1 ^{1}H NMR Spectrum of Compound **6.24** (500 MHz, $CDCl_3$).

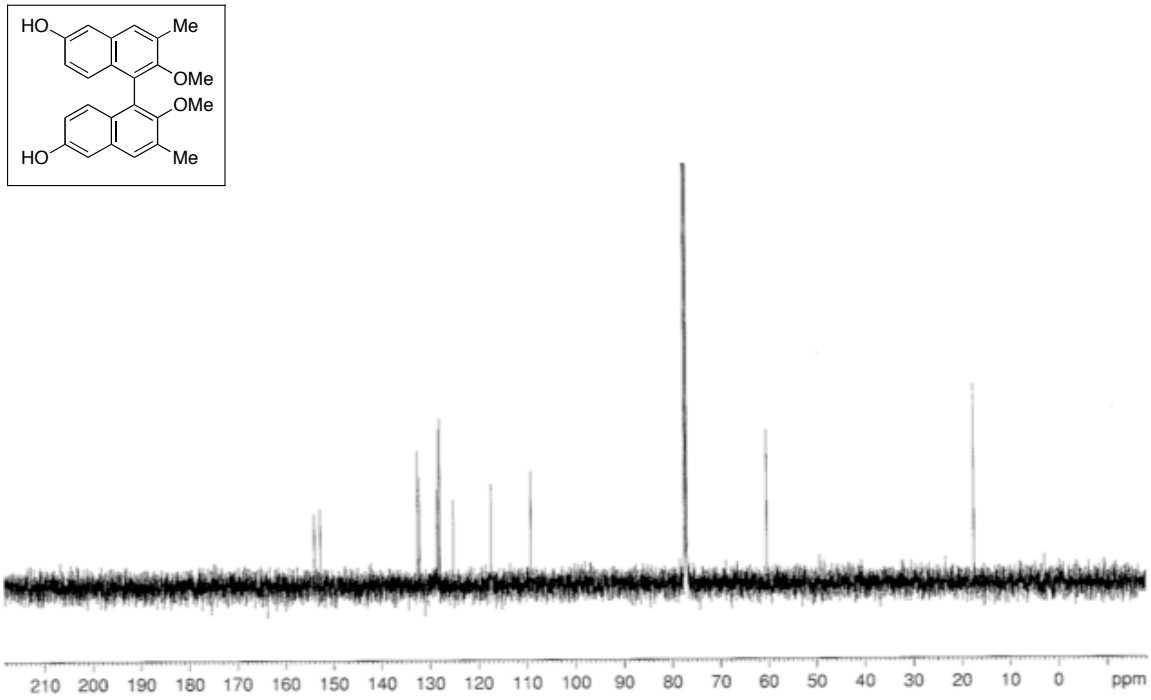

Figure A6.24_2 ^{13}C NMR Spectrum of Compound **6.24** (125 MHz, $CDCl_3$).

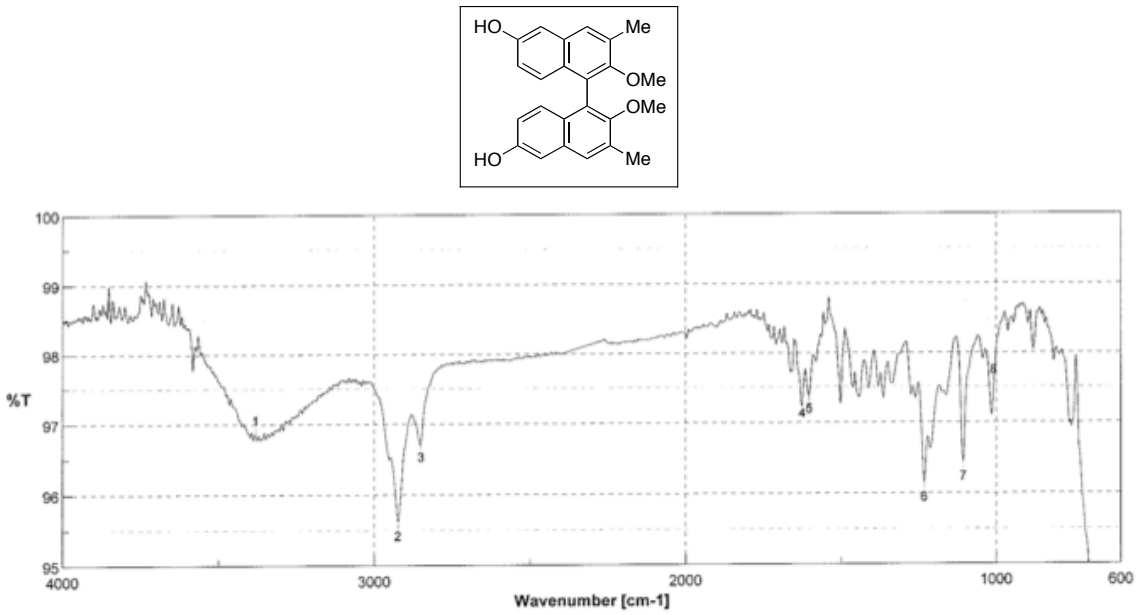

Figure A6.24_3 IR Spectrum of Compound **6.24** (film).

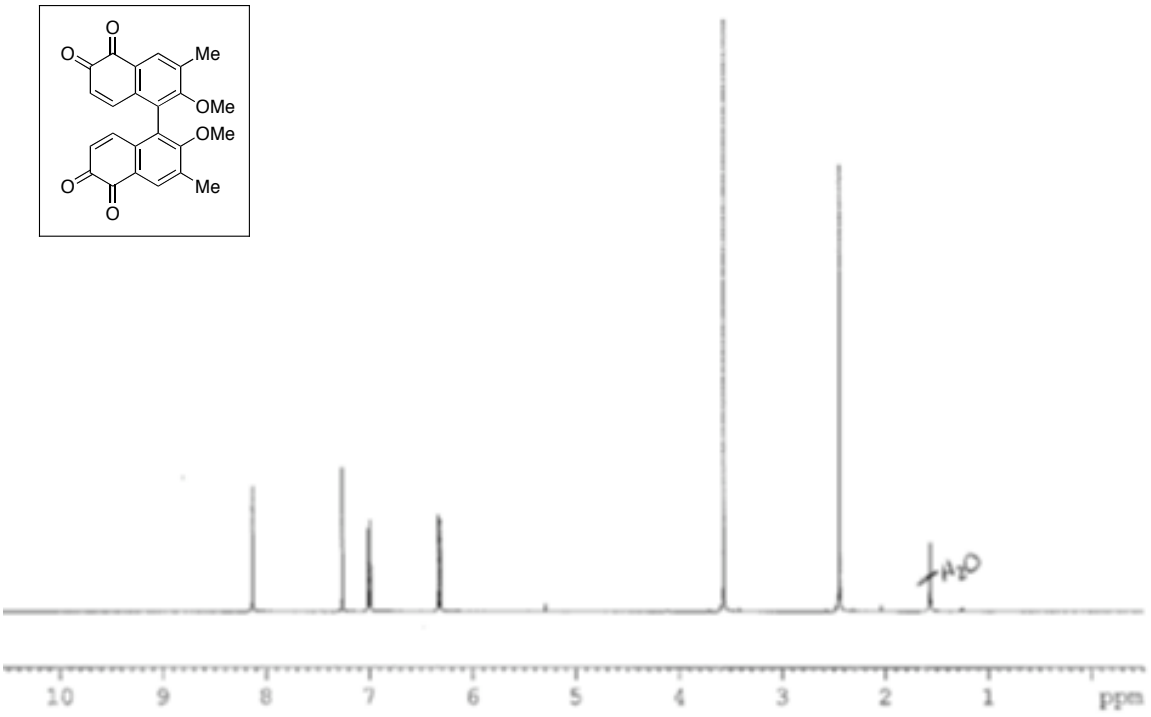

Figure A6.25_1 ^{1}H NMR Spectrum of Compound **6.25** (500 MHz, $CDCl_3$).

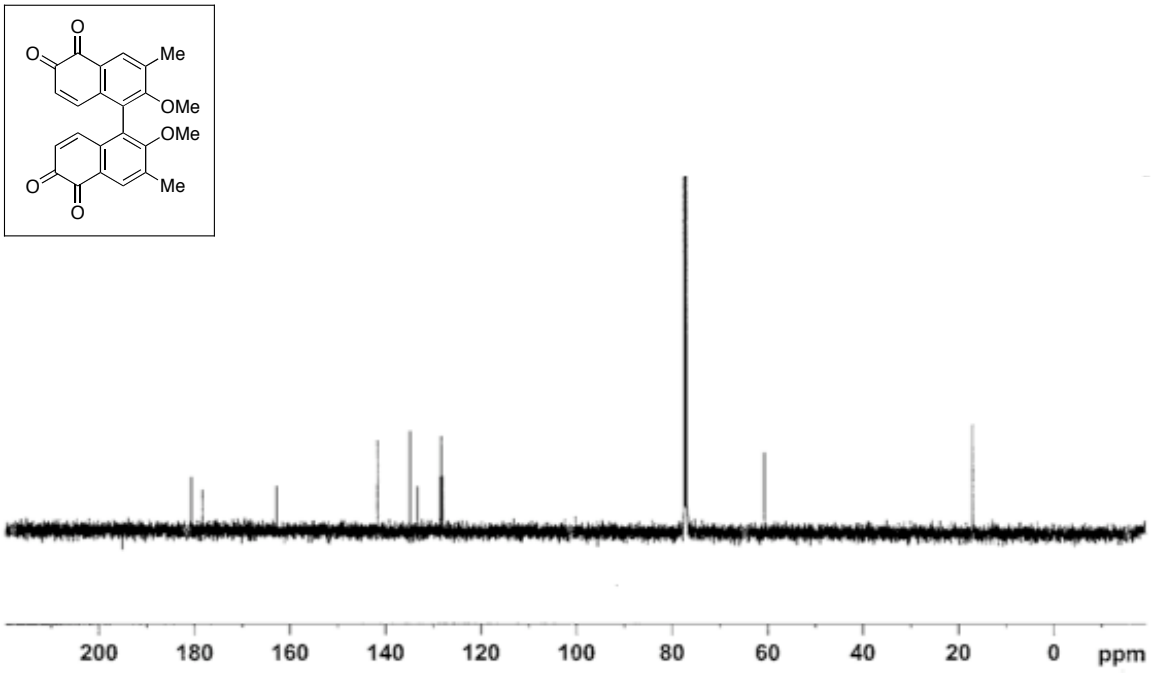

Figure A6.25_2 ^{13}C NMR Spectrum of Compound **6.25** (125 MHz, $CDCl_3$).

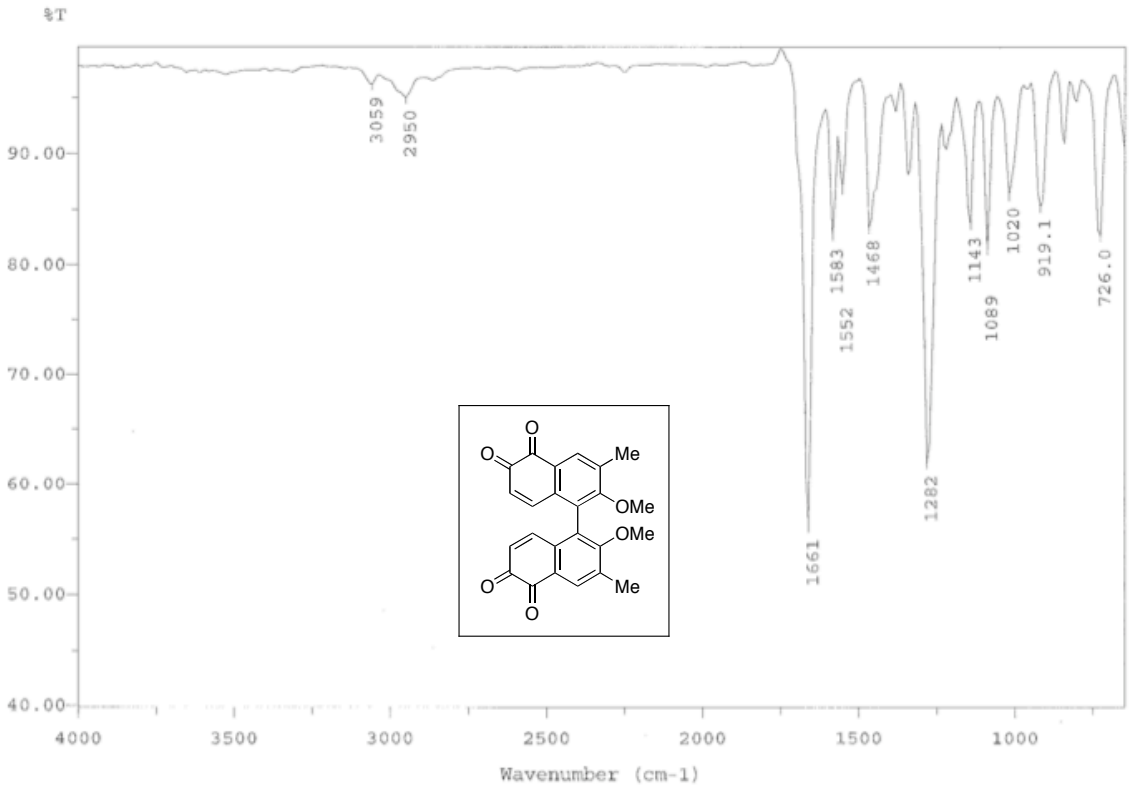

Figure A6.25_3 IR Spectrum of Compound **6.25** (film).

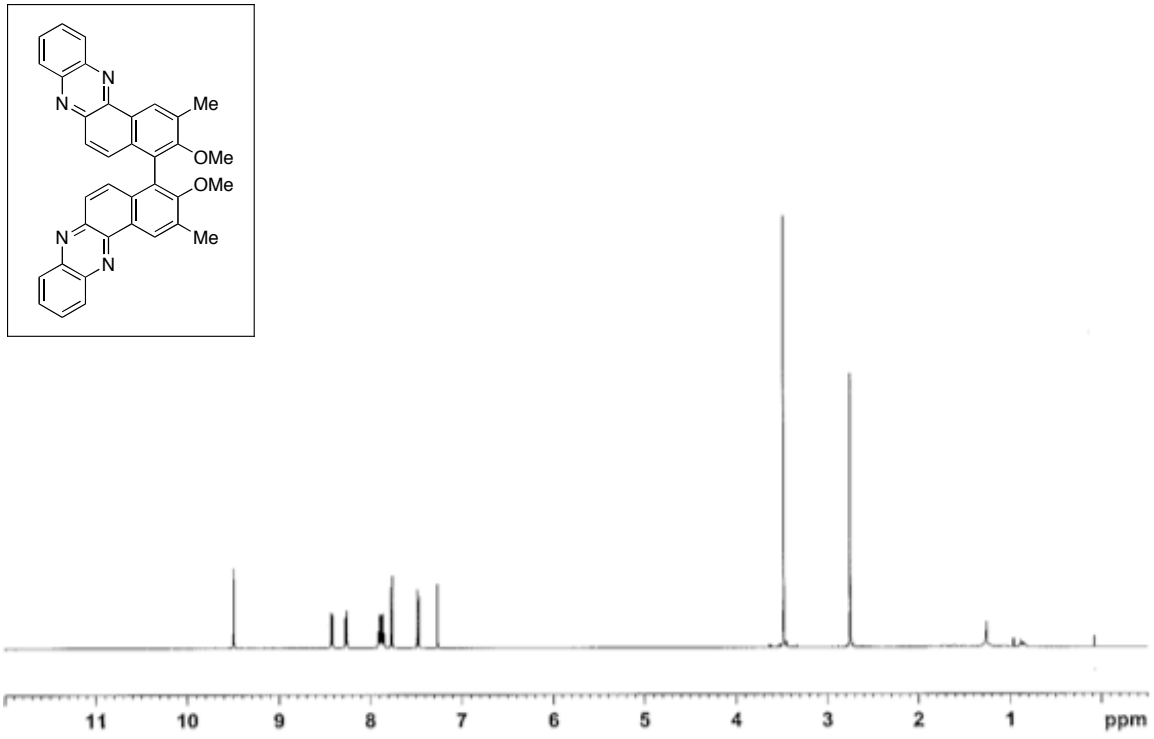

Figure A6.27_1 ^{1}H NMR Spectrum of Compound **6.27** (500 MHz, $CDCl_3$).

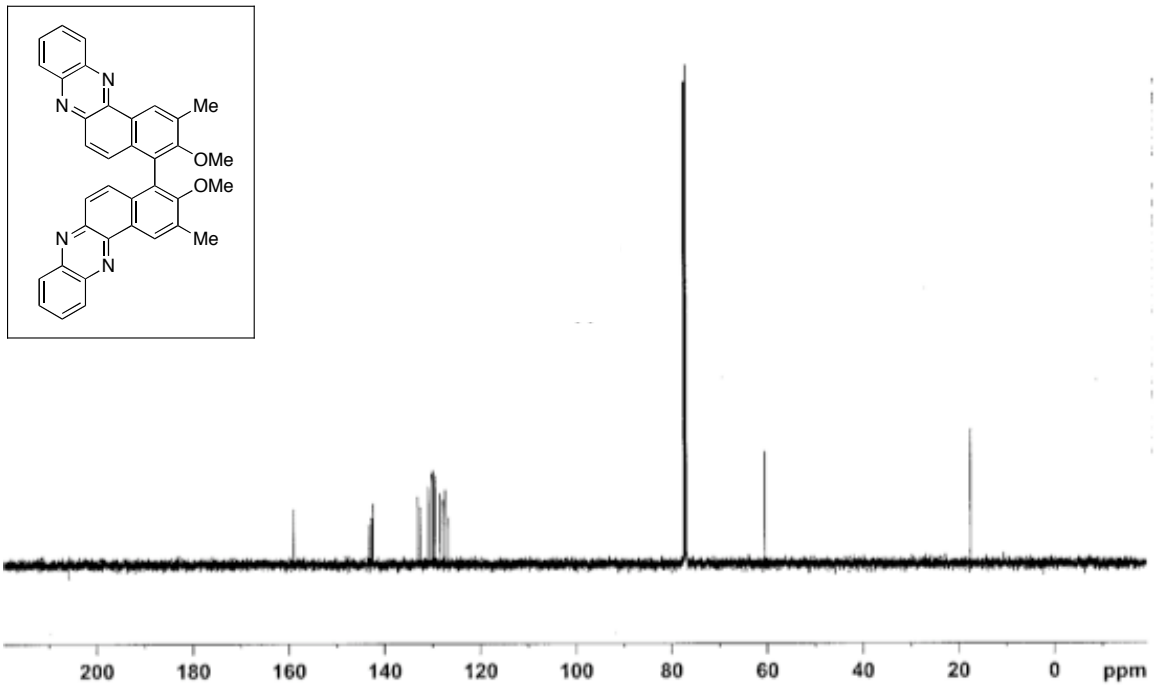

Figure A6.27_2 ^{13}C NMR Spectrum of Compound **6.27** (125 MHz, $CDCl_3$).

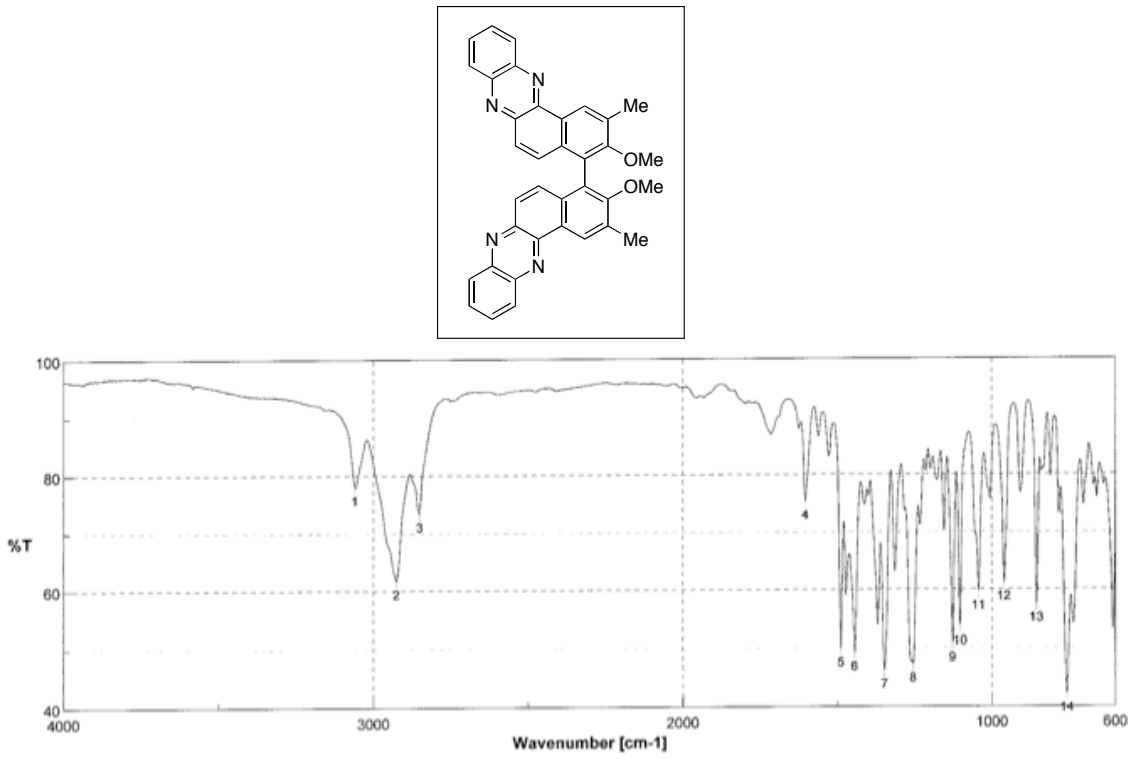

Figure A6.27_3 IR Spectrum of Compound **6.27** (film).

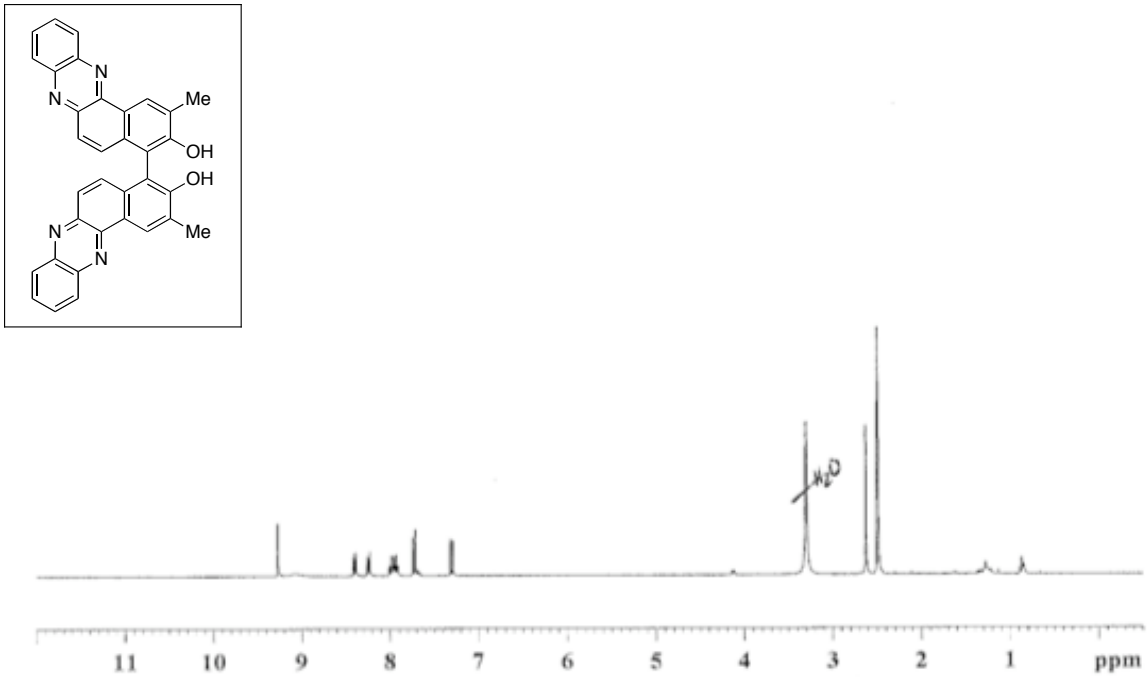

Figure A6.28_1 ^{1}H NMR Spectrum of Compound **6.28** (360 MHz, DMSO-d_6).

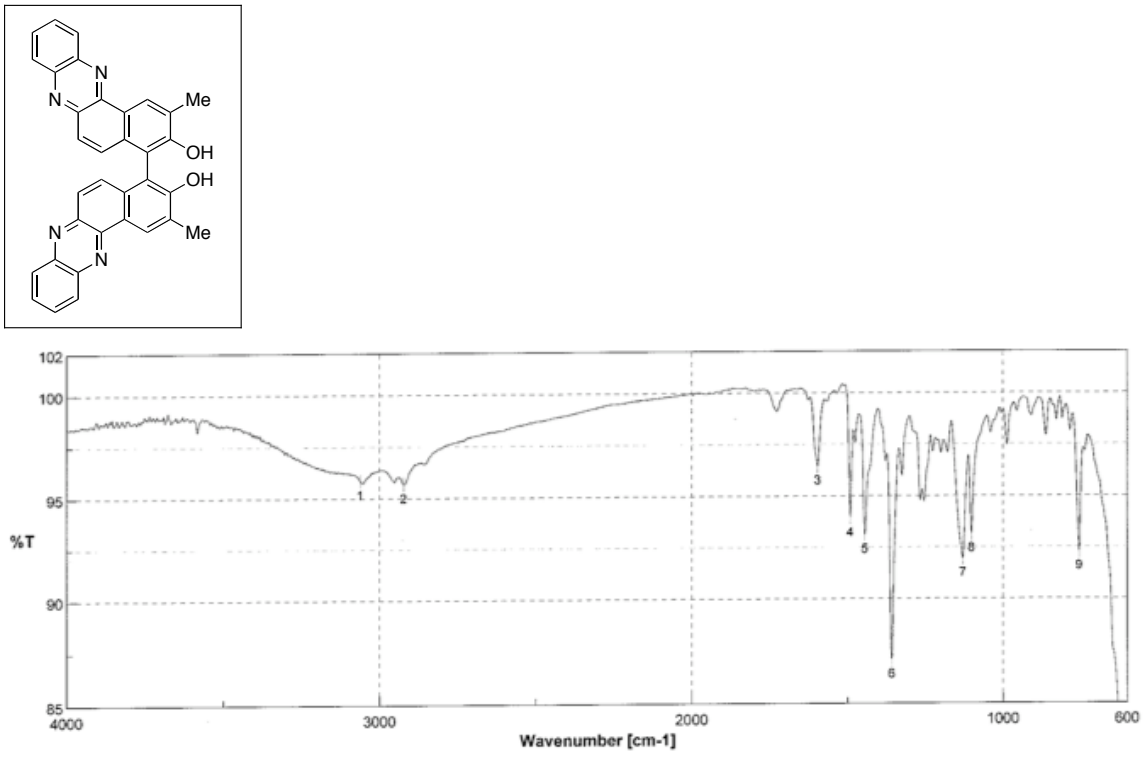

Figure A6.28_3 IR Spectrum of Compound **6.28** (film).

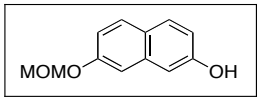

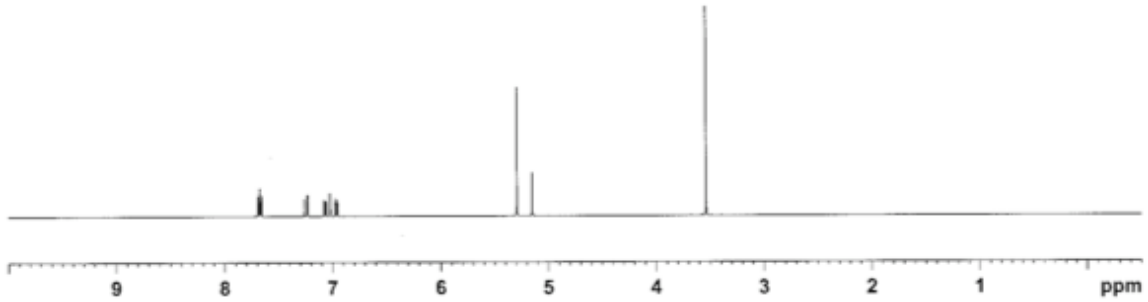

Figure A6.30_1 ^{1}H NMR Spectrum of Compound **6.30** (500 MHz, $CDCl_3$).

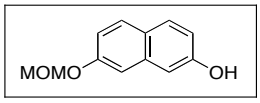

Figure A6.30_2 ^{13}C NMR Spectrum of Compound **6.30** (125 MHz, $CDCl_3$).

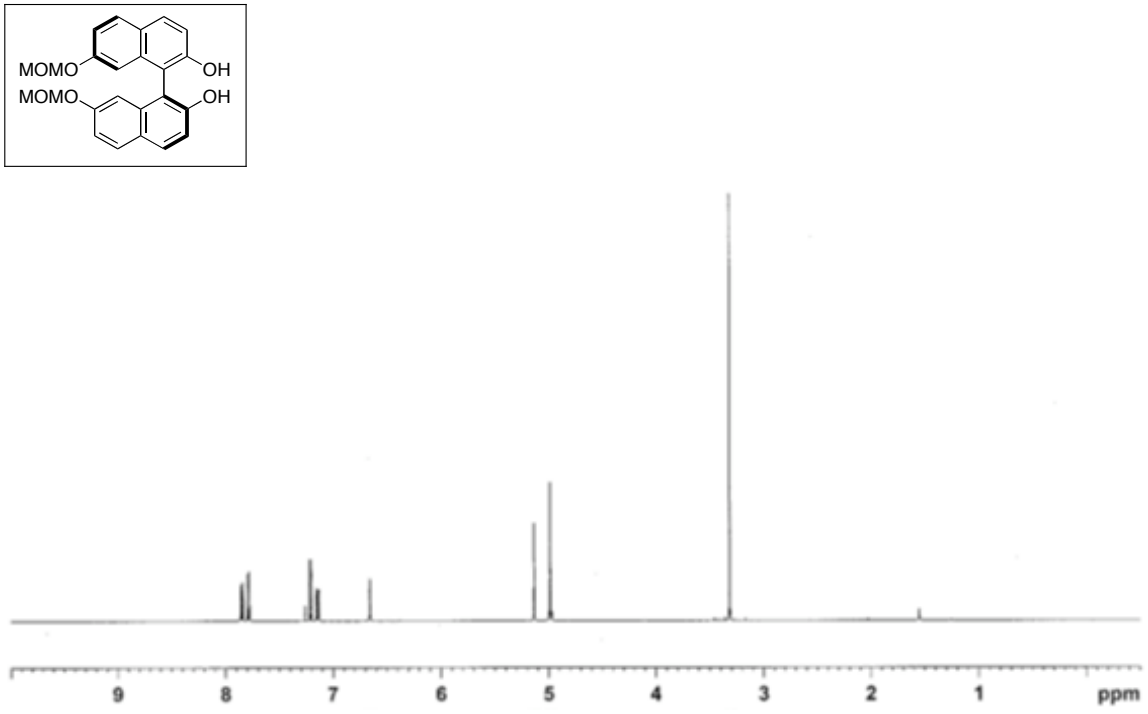

Figure A6.31_1 ^{1}H NMR Spectrum of Compound (*S*)-**6.31** (500 MHz, $CDCl_3$).

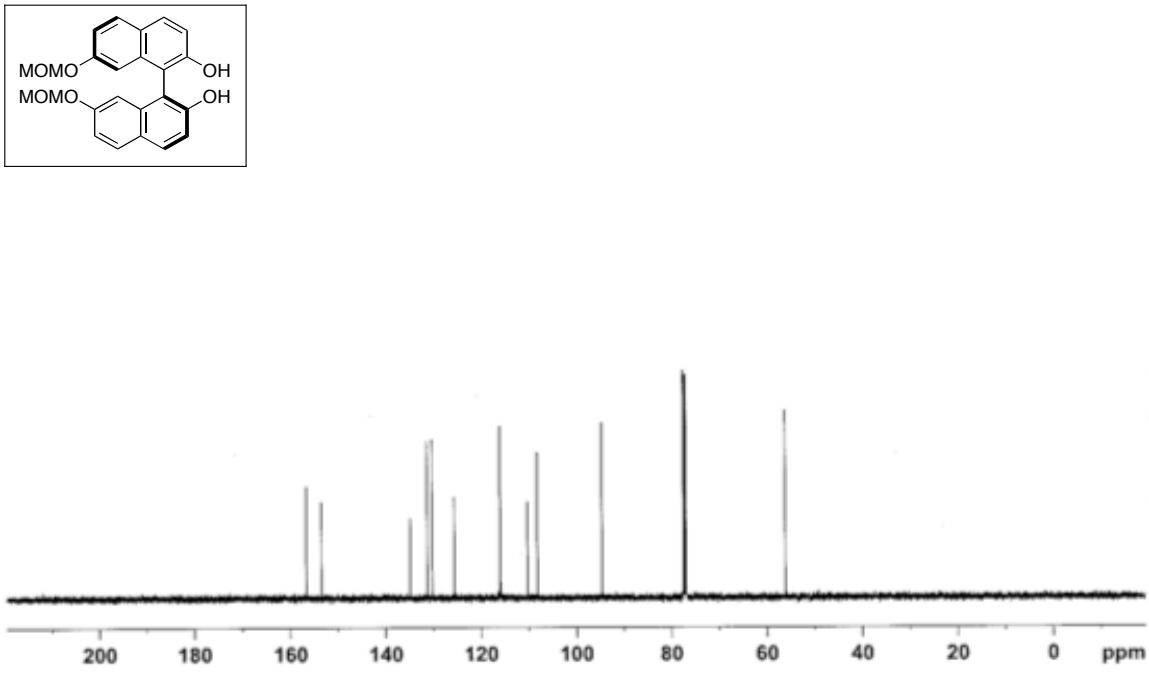

Figure A6.31_2 ^{13}C NMR Spectrum of Compound (*S*)-**6.31** (125 MHz, $CDCl_3$).

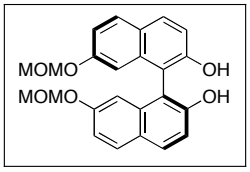

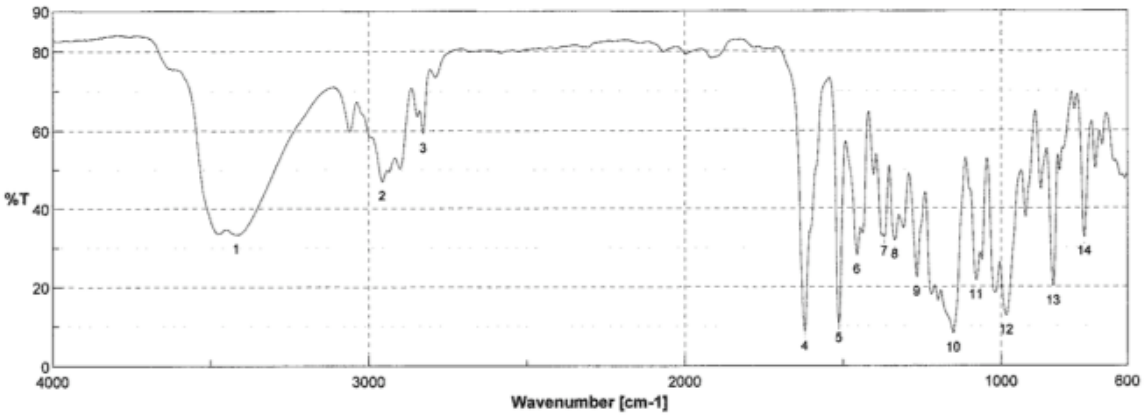

Figure A6.31_3 IR Spectrum of Compound (*S*)-**6.31** (film).

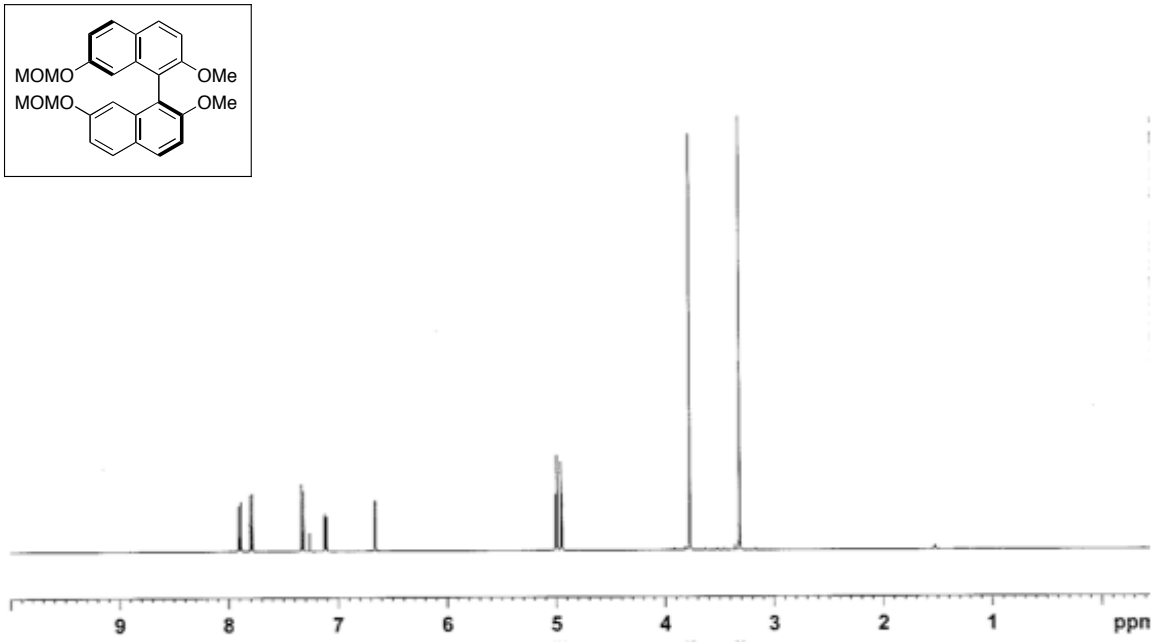

Figure A6.32_1 ^{1}H NMR Spectrum of Compound (*S*)-**6.32** (500 MHz, $CDCl_3$).

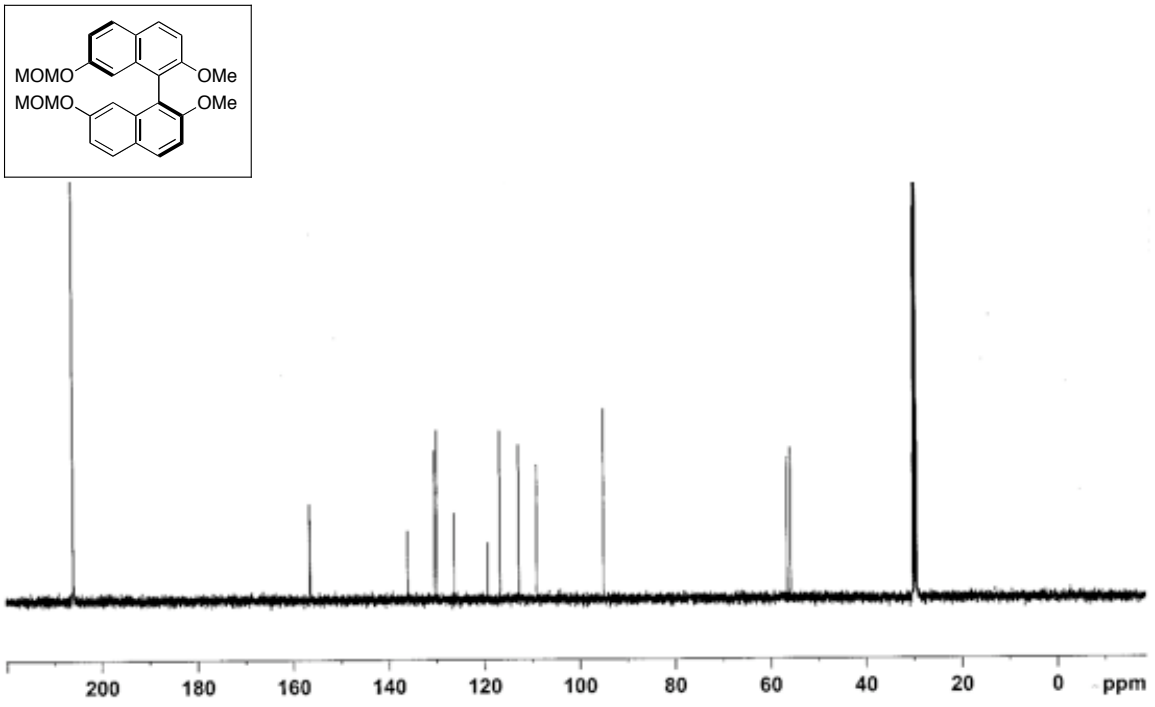

Figure A6.32_2 ^{13}C NMR Spectrum of Compound (*S*)-**6.32** (125 MHz, acetone-d_6).

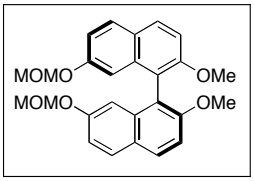

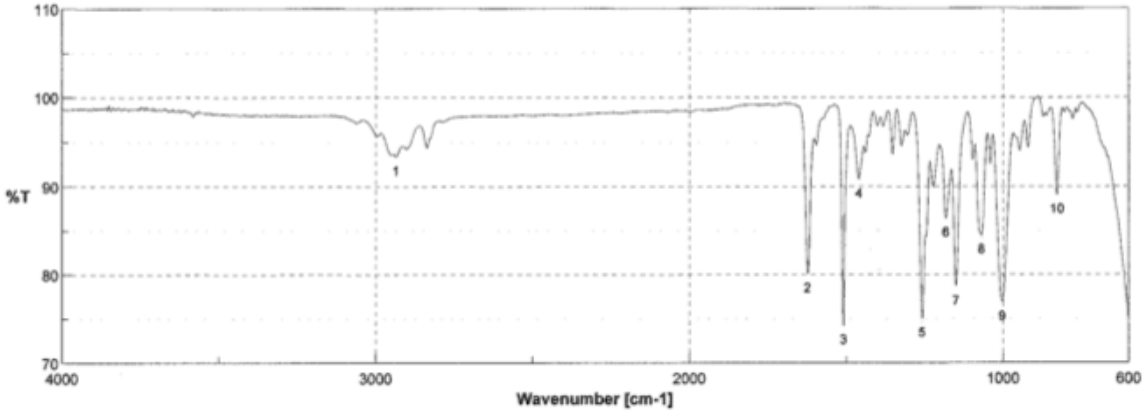

Figure A6.32_3 IR Spectrum of Compound (*S*)-**6.32** (film).

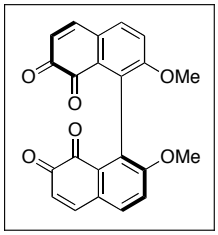

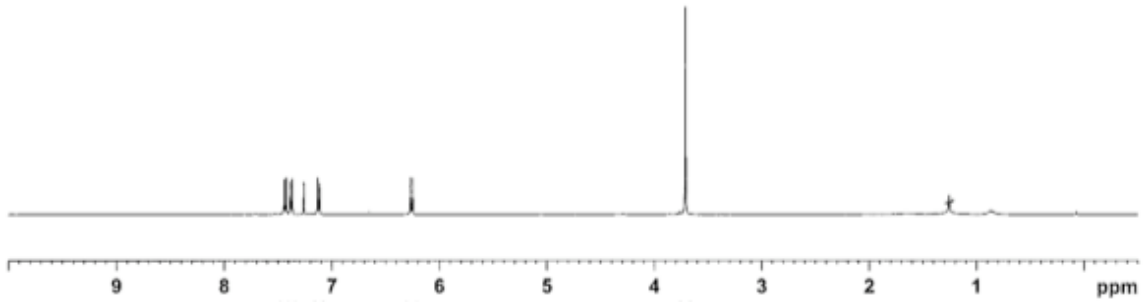

Figure A6.34_1 ^{1}H NMR Spectrum of Compound (*S*)-**6.34** (500 MHz, $CDCl_3$).

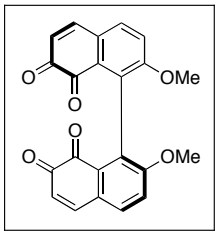

Figure A6.34_2 ^{13}C NMR Spectrum of Compound (*S*)-**6.34** (125 MHz, $CDCl_3$).

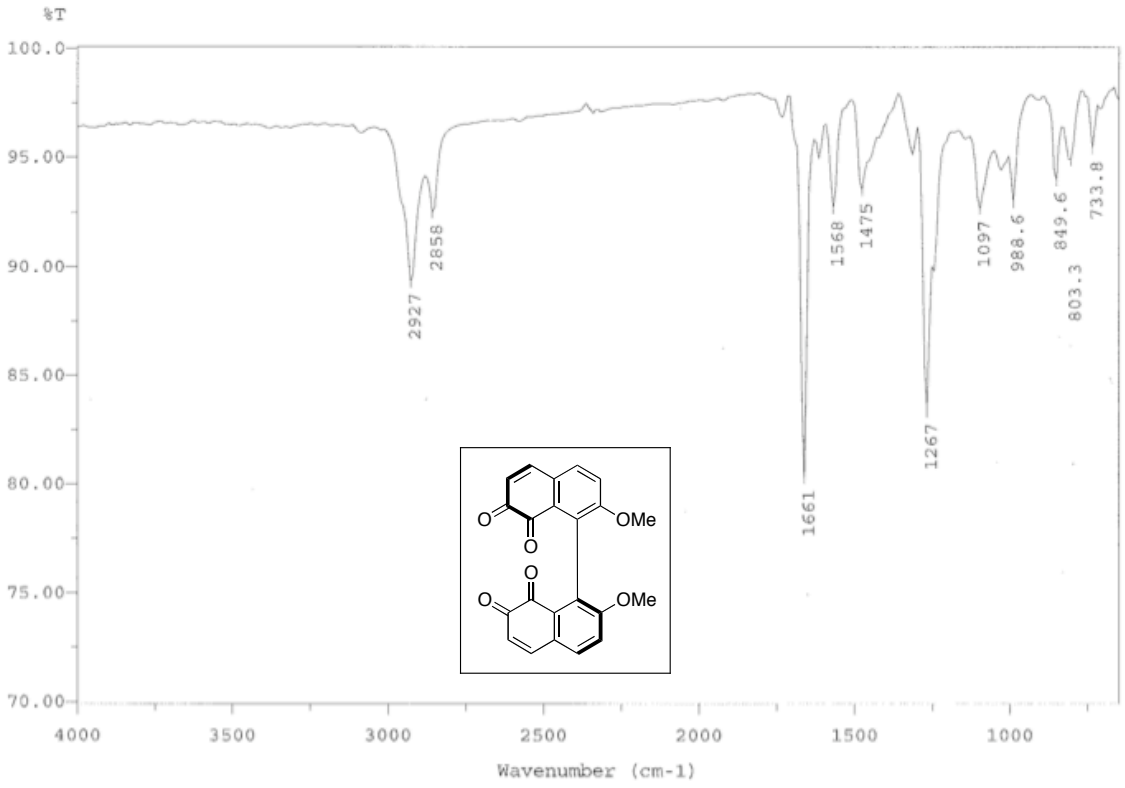

Figure A6.34_3 IR Spectrum of Compound (*S*)-**6.34** (film).

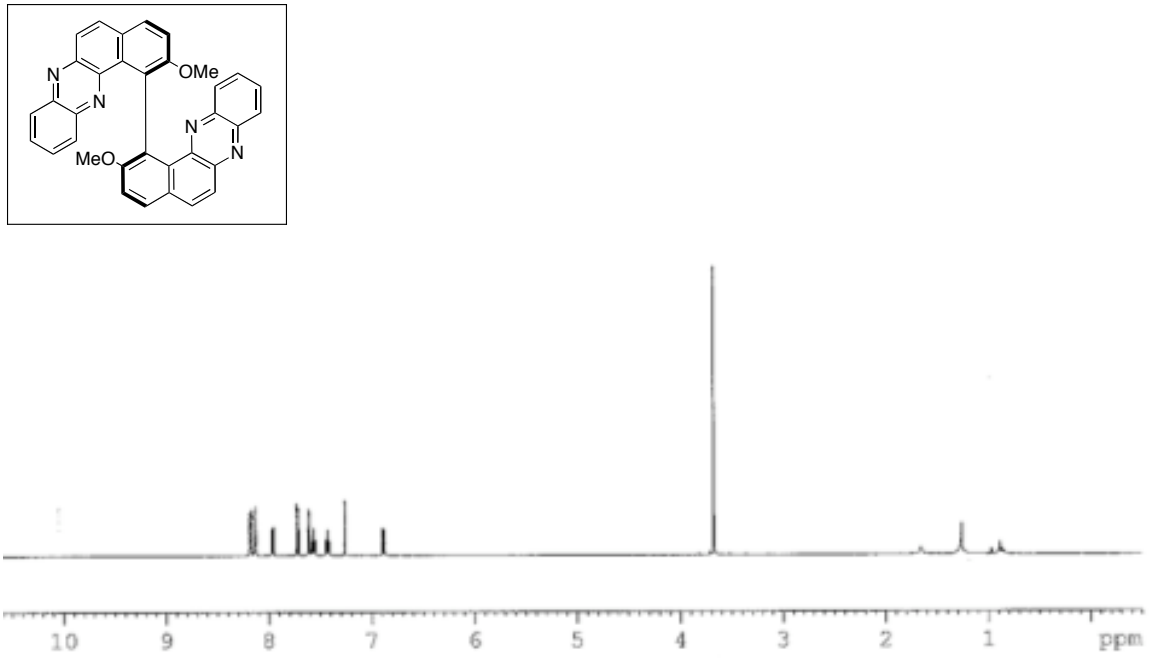

Figure A6.35a_1 ^{1}H NMR Spectrum of Compound (*S*)-**6.35a** (500 MHz, $CDCl_3$).

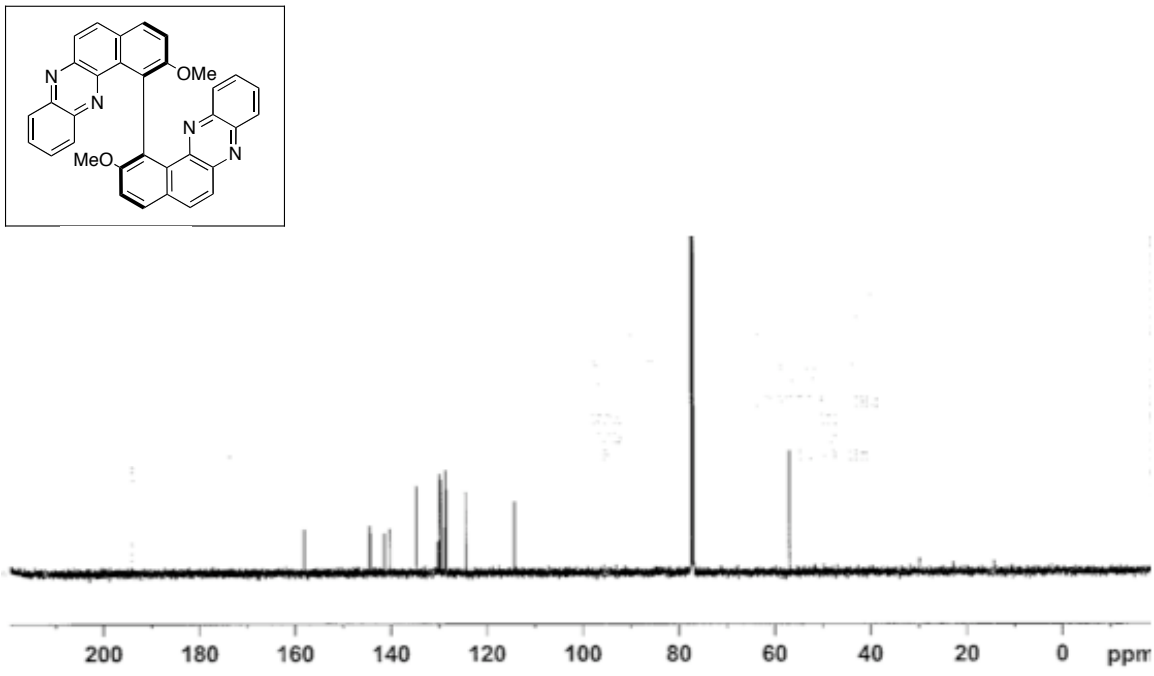

Figure A6.35a_2 ^{13}C NMR Spectrum of Compound (*S*)-**6.35a** (125 MHz, $CDCl_3$).

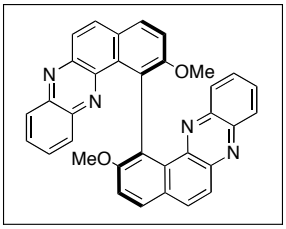

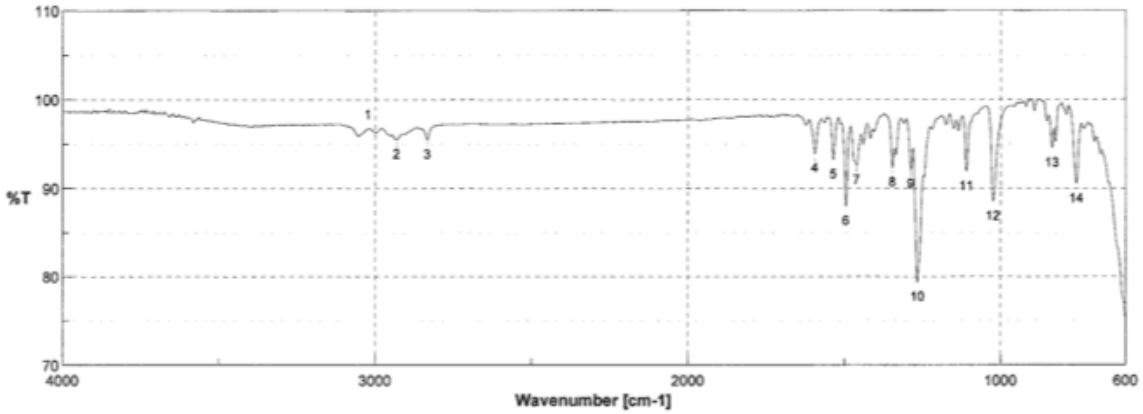

Figure A6.35_3 IR Spectrum of Compound (*S*)-**6.35a** (film).

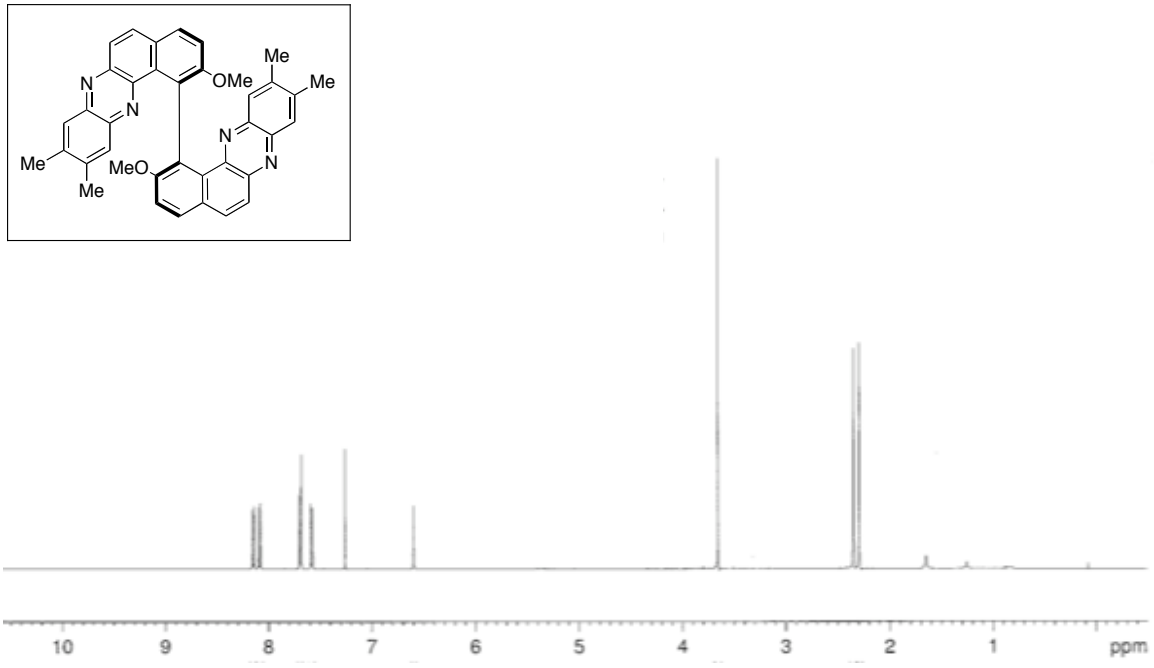

Figure A6.35b_1 ^{1}H NMR Spectrum of Compound (*S*)-**6.35b** (500 MHz, $CDCl_3$).

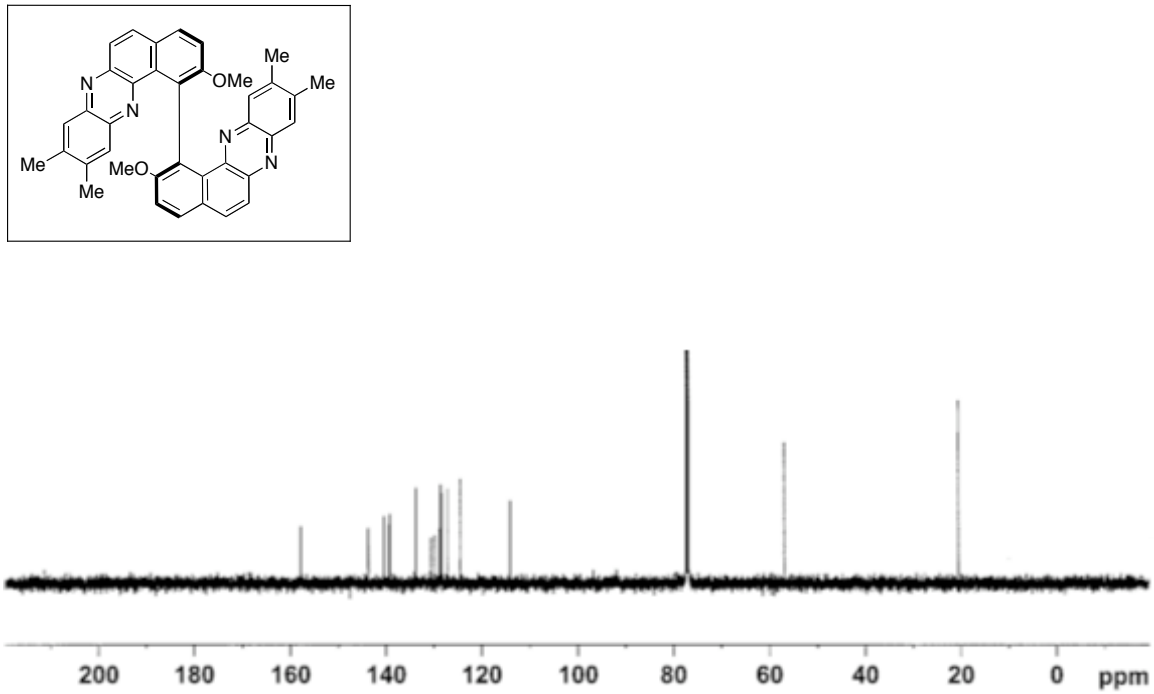

Figure A6.35b_2 ^{13}C NMR Spectrum of Compound (*S*)-**6.35b** (125 MHz, $CDCl_3$).

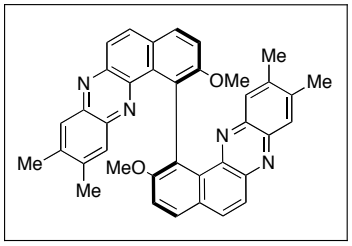

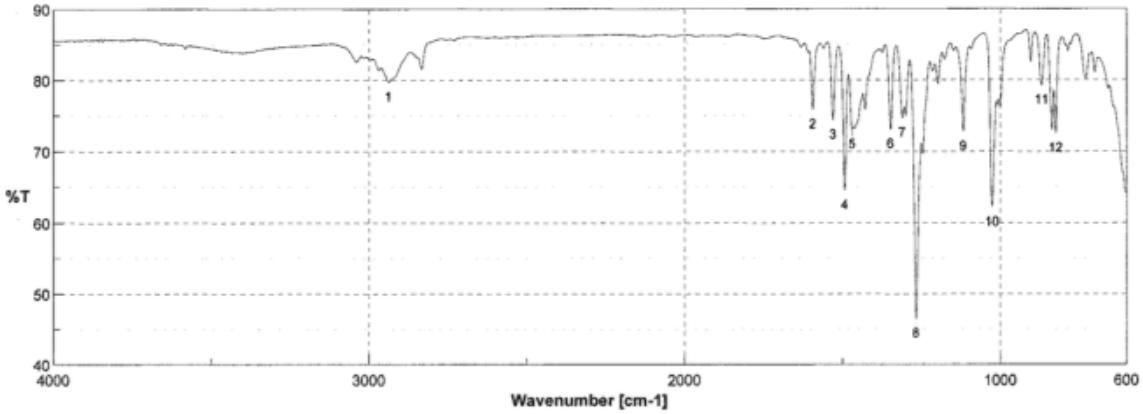

Figure A6.35b_3 IR Spectrum of Compound (*S*)-**6.35b** (film).

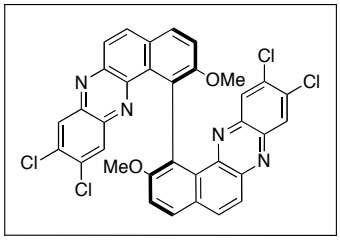

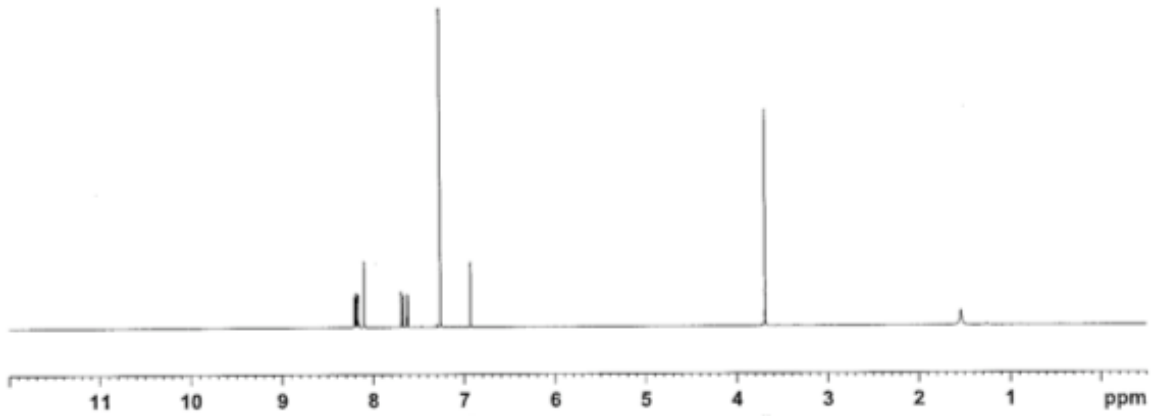

Figure A6.35c_1 ^{1}H NMR Spectrum of Compound (*S*)-**6.35c** (500 MHz, $CDCl_3$).

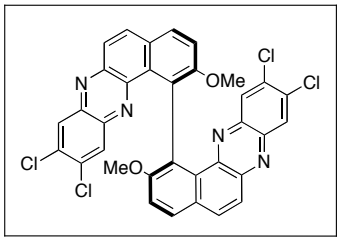

Figure A6.35c_2 ^{13}C NMR Spectrum of Compound (*S*)-**6.35c** (125 MHz, $CDCl_3$).

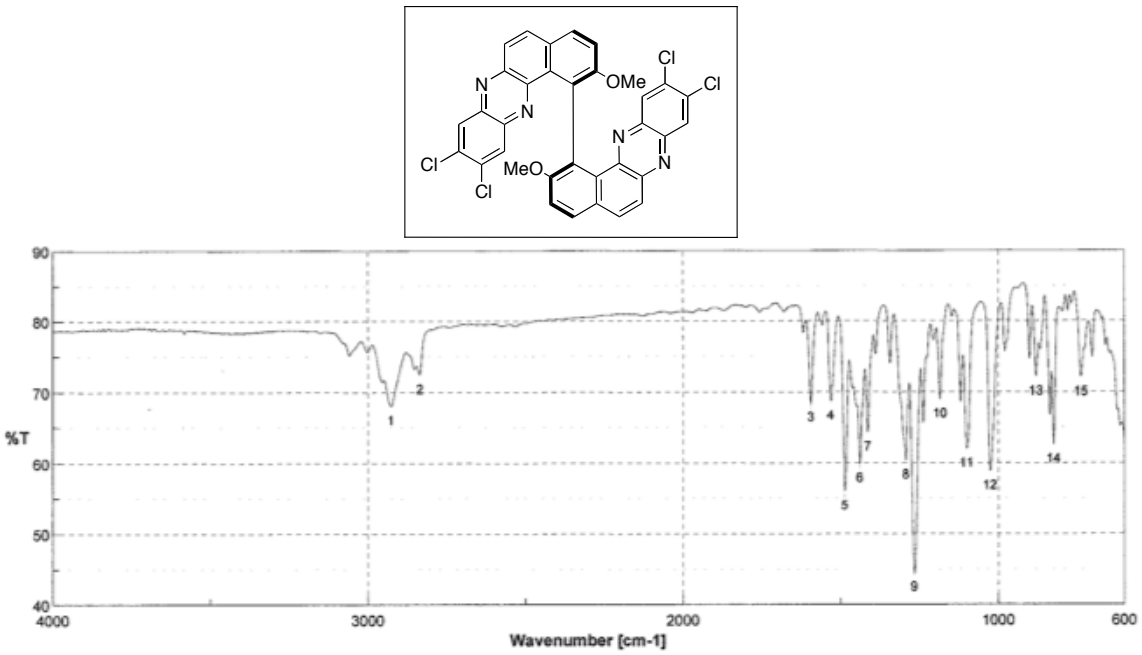

Figure A6.35c_3 IR Spectrum of Compound (*S*)-**6.35c** (film).

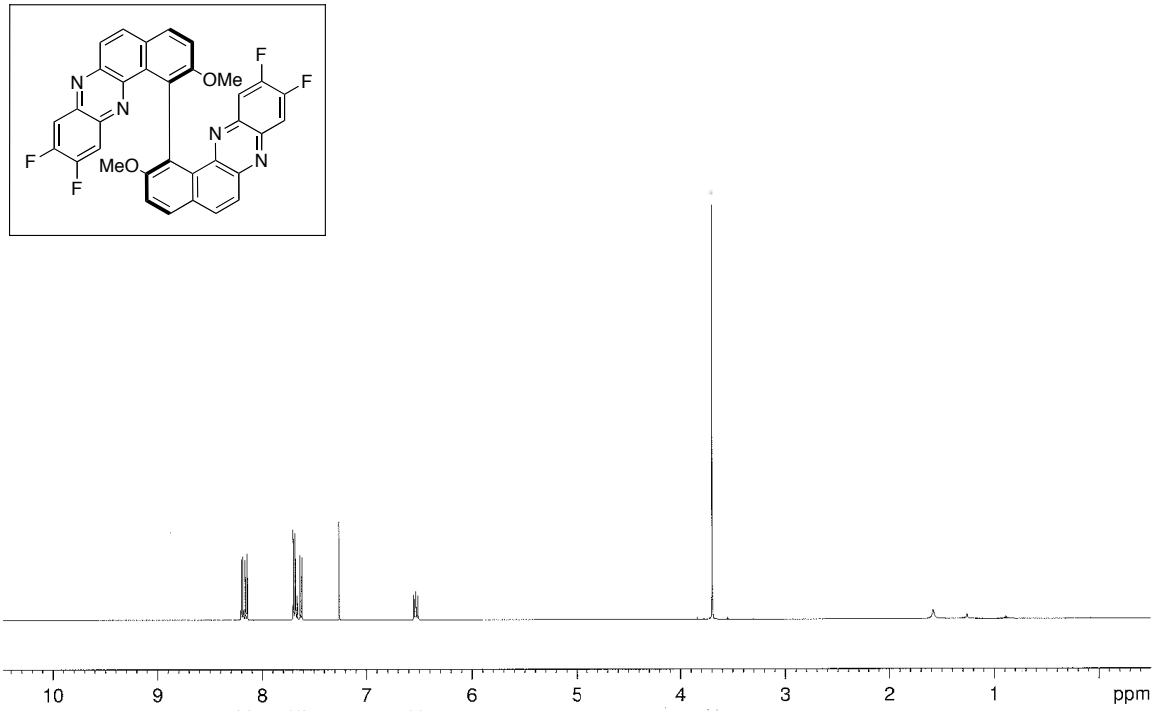

Figure A6.35d_1 ^{1}H NMR Spectrum of Compound (*S*)-**6.35d** (500 MHz, $CDCl_3$).

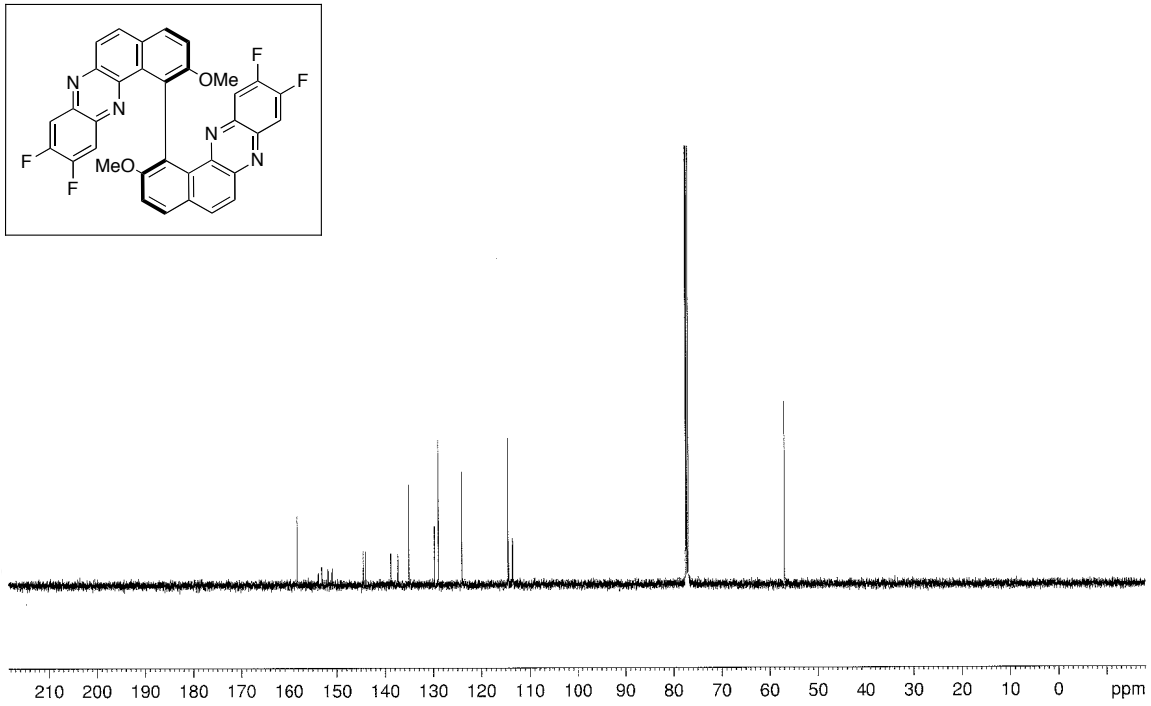

Figure A6.35_2 ^{13}C NMR Spectrum of Compound (*S*)-**6.35d** (125 MHz, $CDCl_3$).

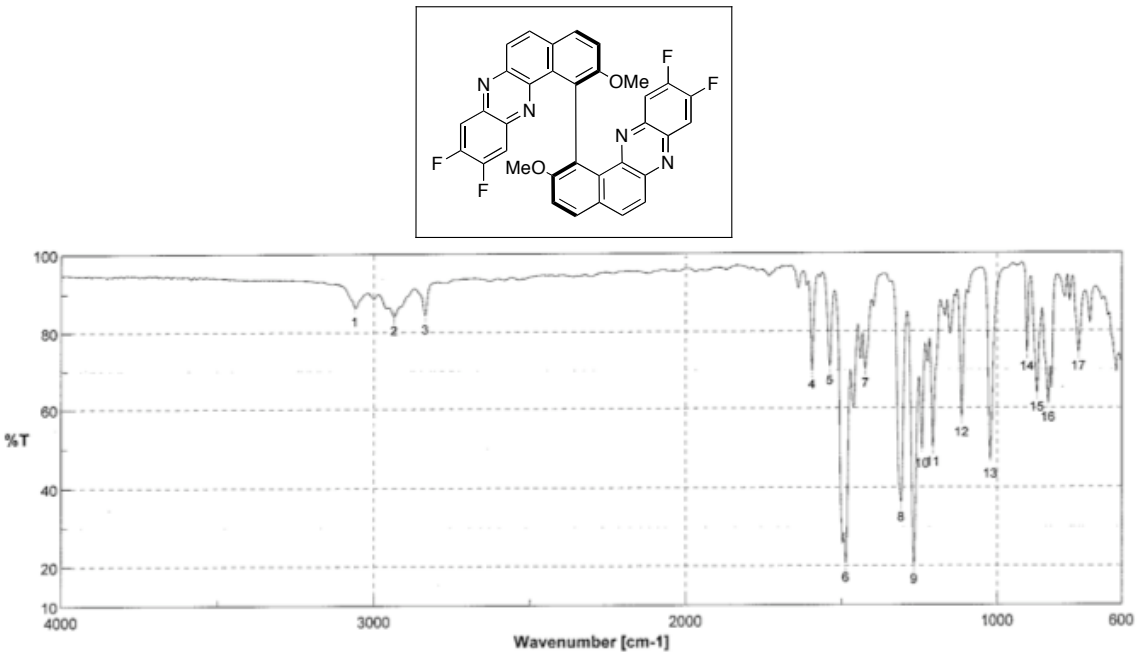

Figure A6.35_3 IR Spectrum of Compound (*S*)-**6.35d** (film).

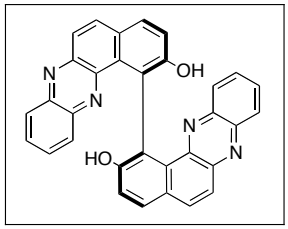

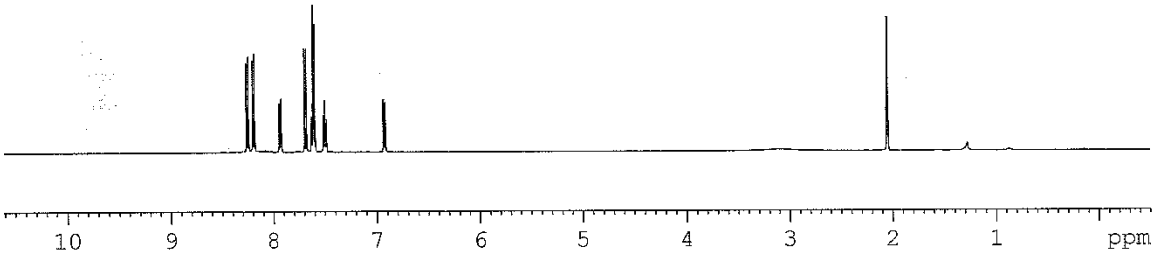

Figure A6.36a_1 ^{1}H NMR Spectrum of Compound (*S*)-**6.36a** (500 MHz, acetone-d_6).

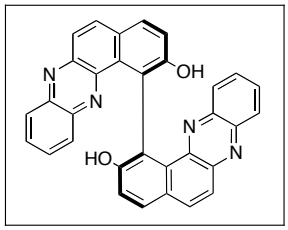

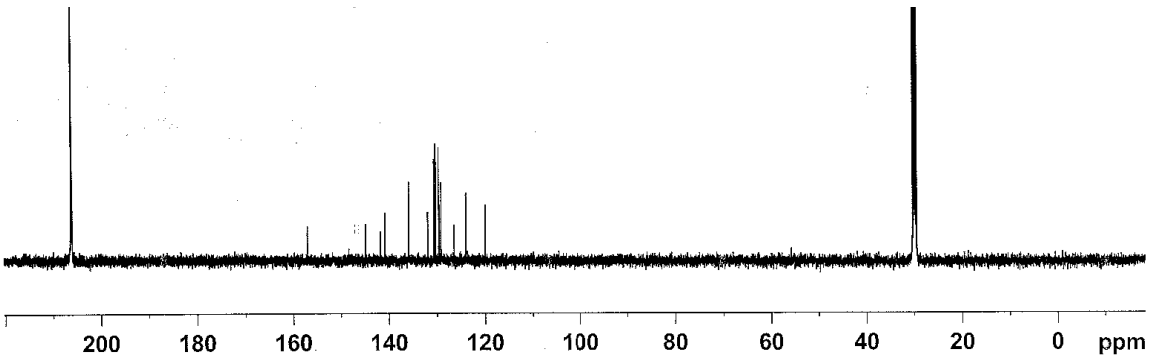

Figure A6.36a_2 ^{13}C NMR Spectrum of Compound (*S*)-**6.36a** (125 MHz, acetone-d_6).

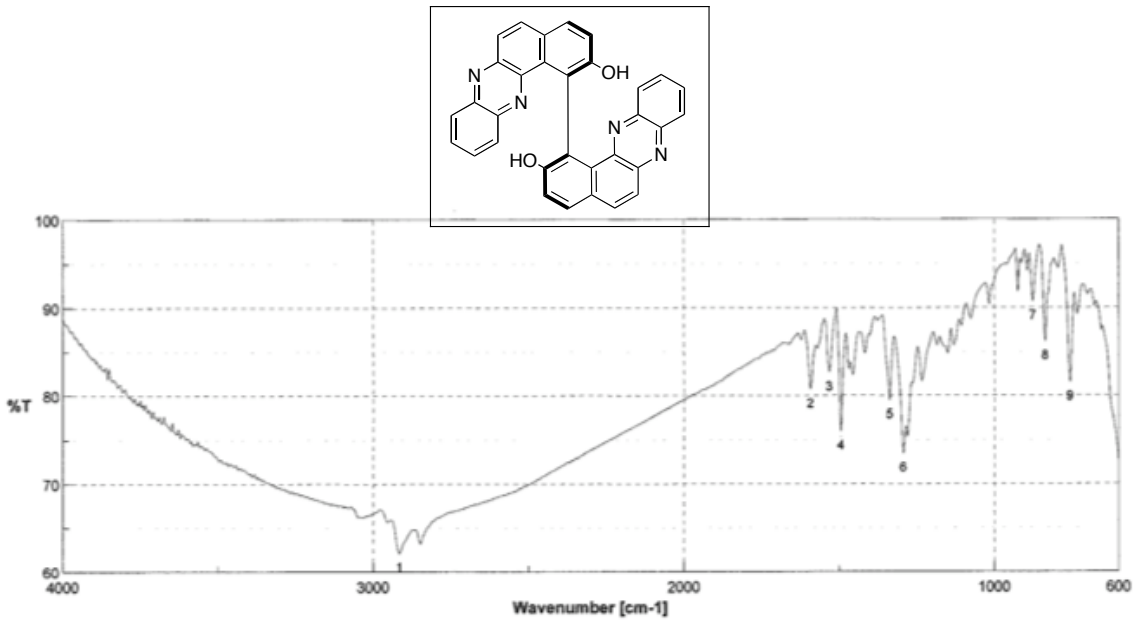

Figure A6.36a_3 IR Spectrum of Compound (*S*)-**6.36a** (film).

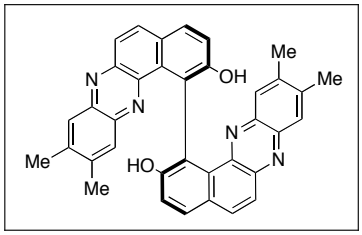

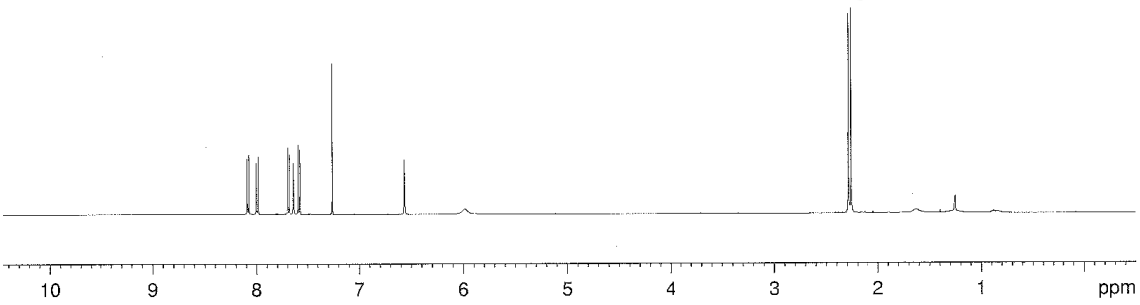

Figure A6.36b_1 ^{1}H NMR Spectrum of Compound (*S*)-**6.36b** (500 MHz, $CDCl_3$).

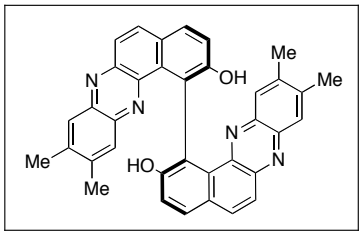

Figure A6.36b_2 ^{13}C NMR Spectrum of Compound (*S*)-**6.36b** (125 MHz, $CDCl_3$).

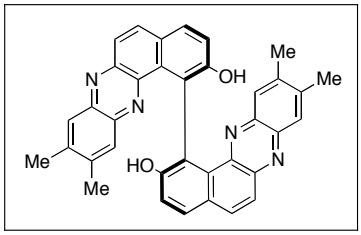

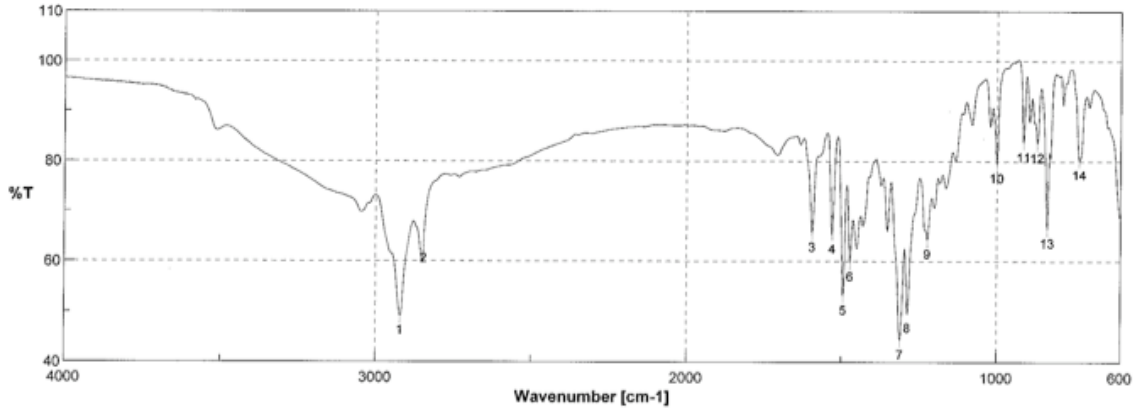

Figure A6.36b_3 IR Spectrum of Compound (*S*)-**6.36b** (film).

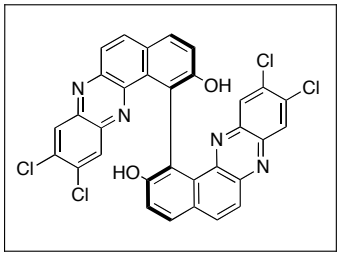

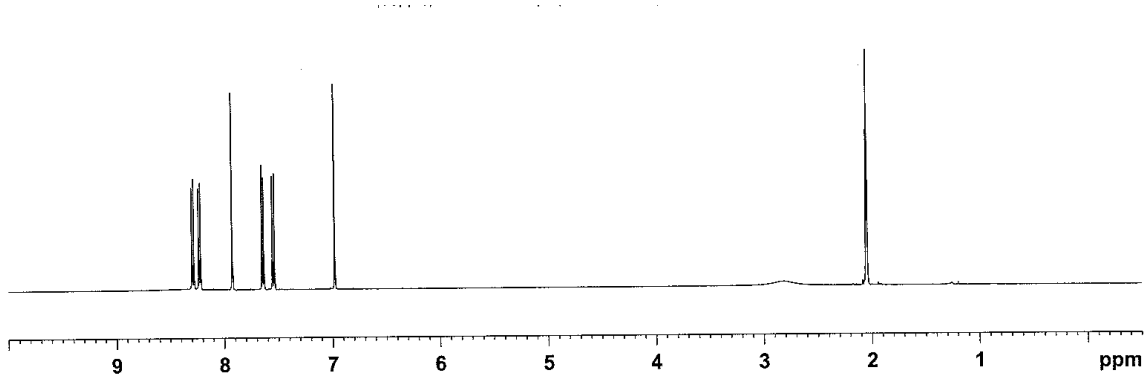

Figure A6.36c_1 ^{1}H NMR Spectrum of Compound (*S*)-**6.36c** (500 MHz, acetone-d_6).

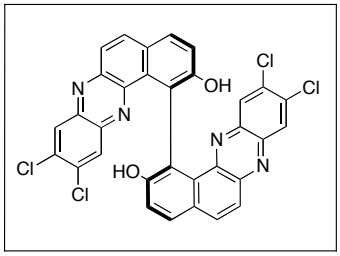

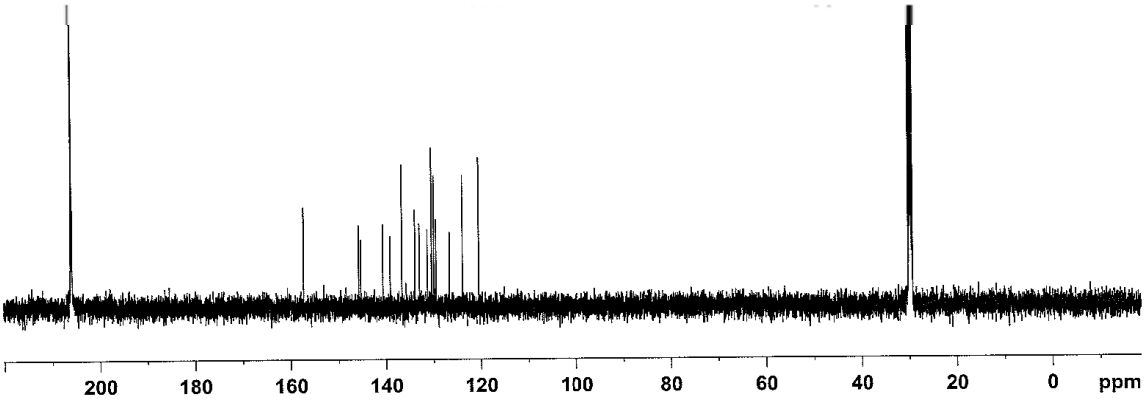

Figure A6.36c_2 ^{13}C NMR Spectrum of Compound (*S*)-**6.36c** (125 MHz, acetone-d_6).

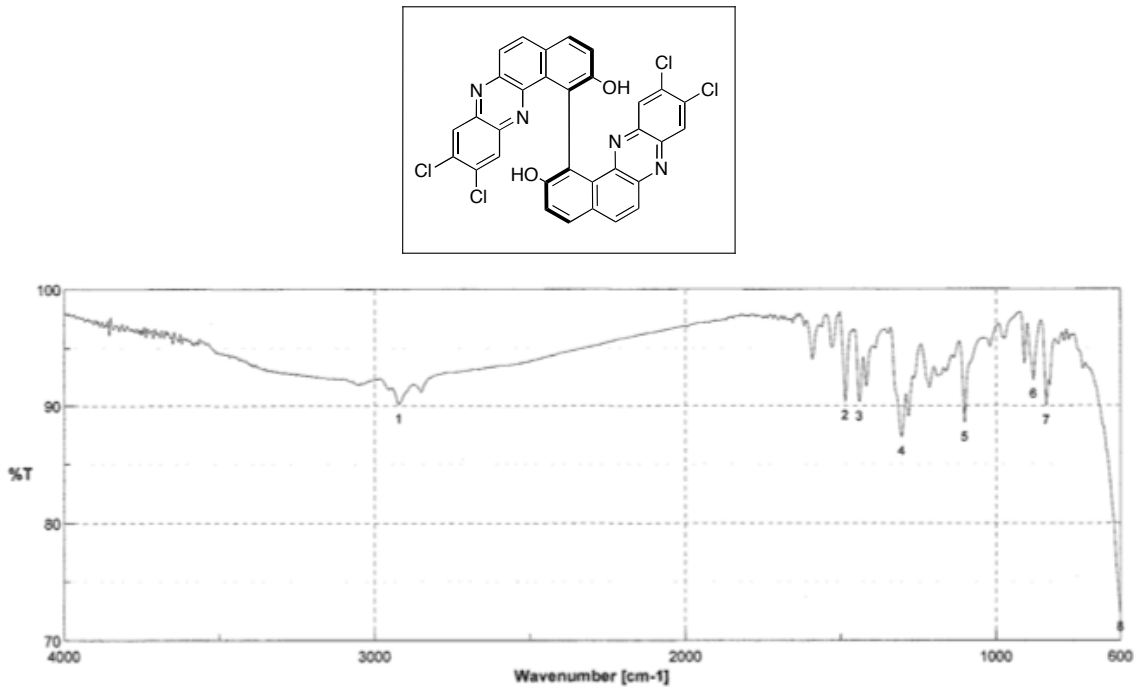

Figure A6.36c_3 IR Spectrum of Compound (*S*)-**6.36c** (film).

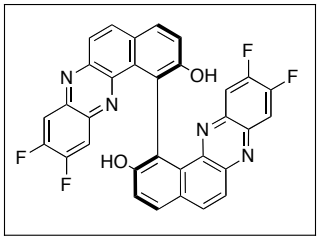

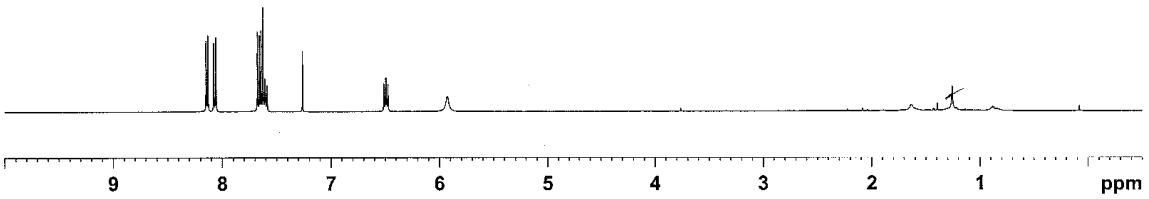

Figure A6.36d_1 ^{1}H NMR Spectrum of Compound (*S*)-**6.36d** (500 MHz, $CDCl_3$).

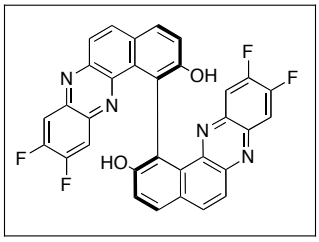

Figure A6.36d_2 ^{13}C NMR Spectrum of Compound (*S*)-**6.36d** (125 MHz, $CDCl_3$).

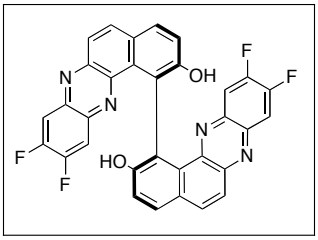

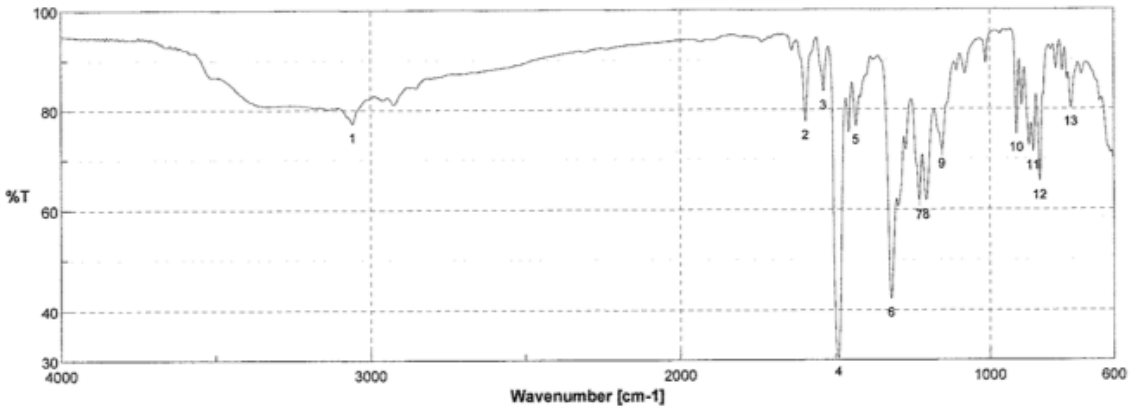

Figure A6.36d_3 IR Spectrum of Compound (*S*)-**6.36d** (film).

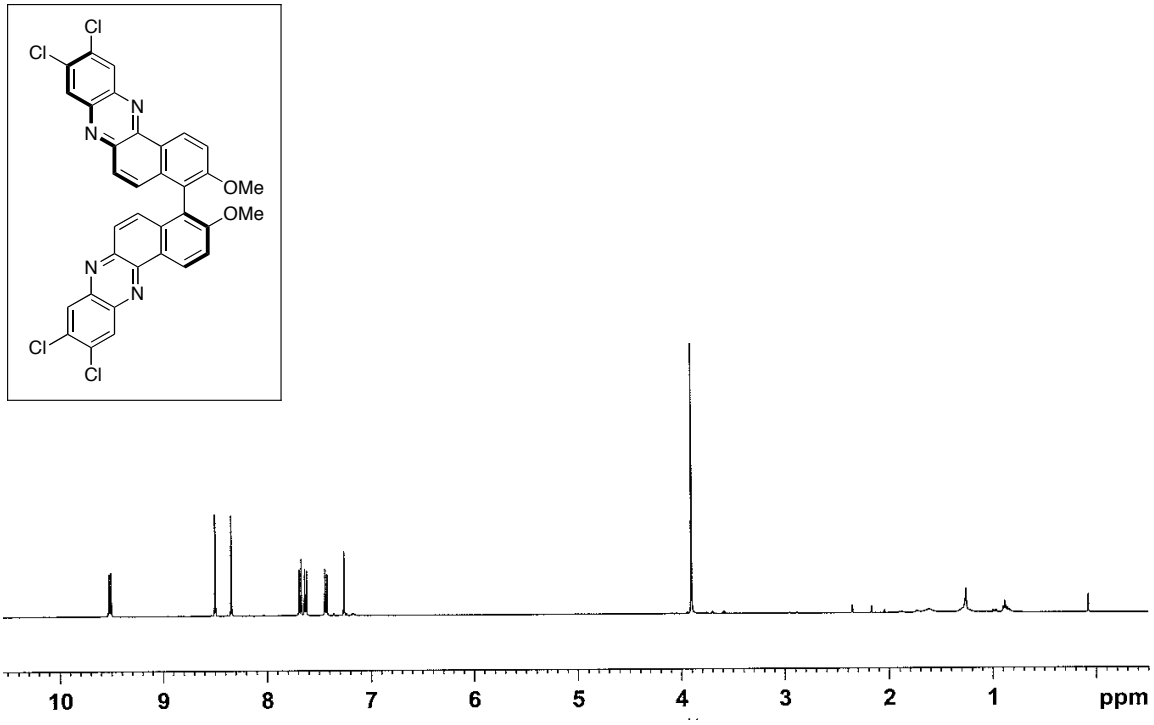

Figure A6.39_1 ^{1}H NMR Spectrum of Compound (*S*)-**6.39** (500 MHz, $CDCl_3$).

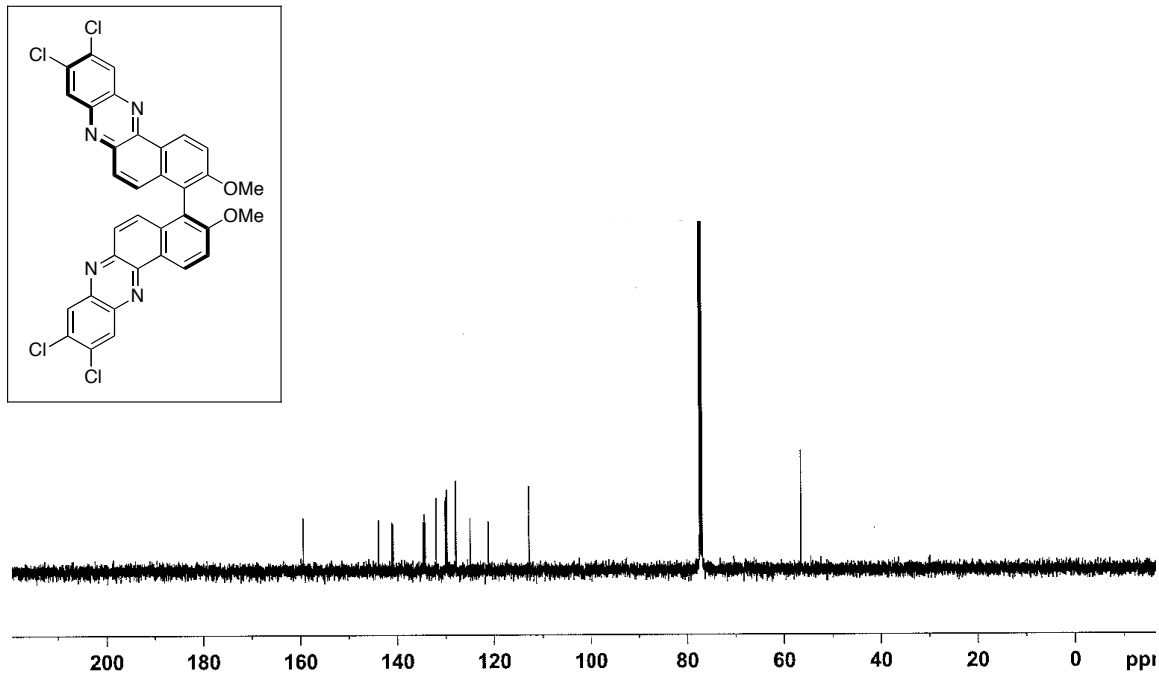

Figure A6.39_2 ^{13}C NMR Spectrum of Compound (*S*)-**6.39** (125 MHz, $CDCl_3$).

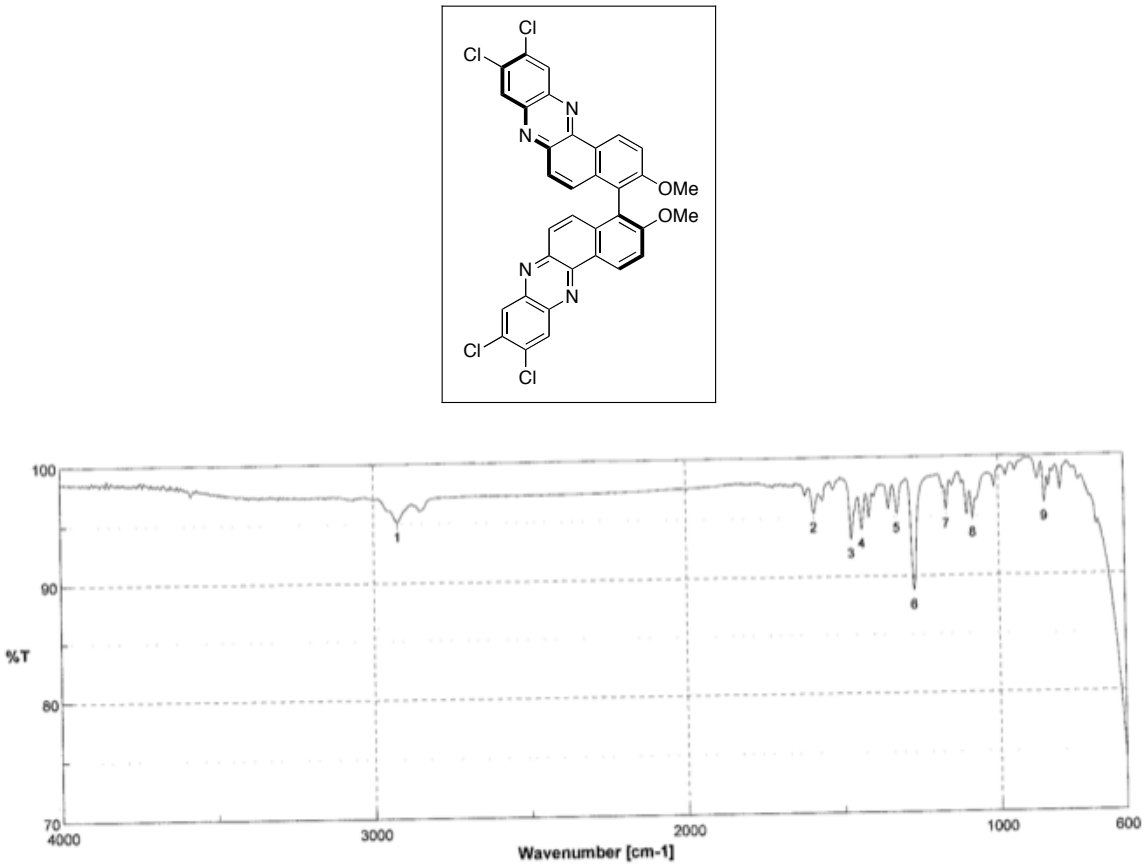

Figure A6.39_3 IR Spectrum of Compound (*S*)-**6.39** (film).

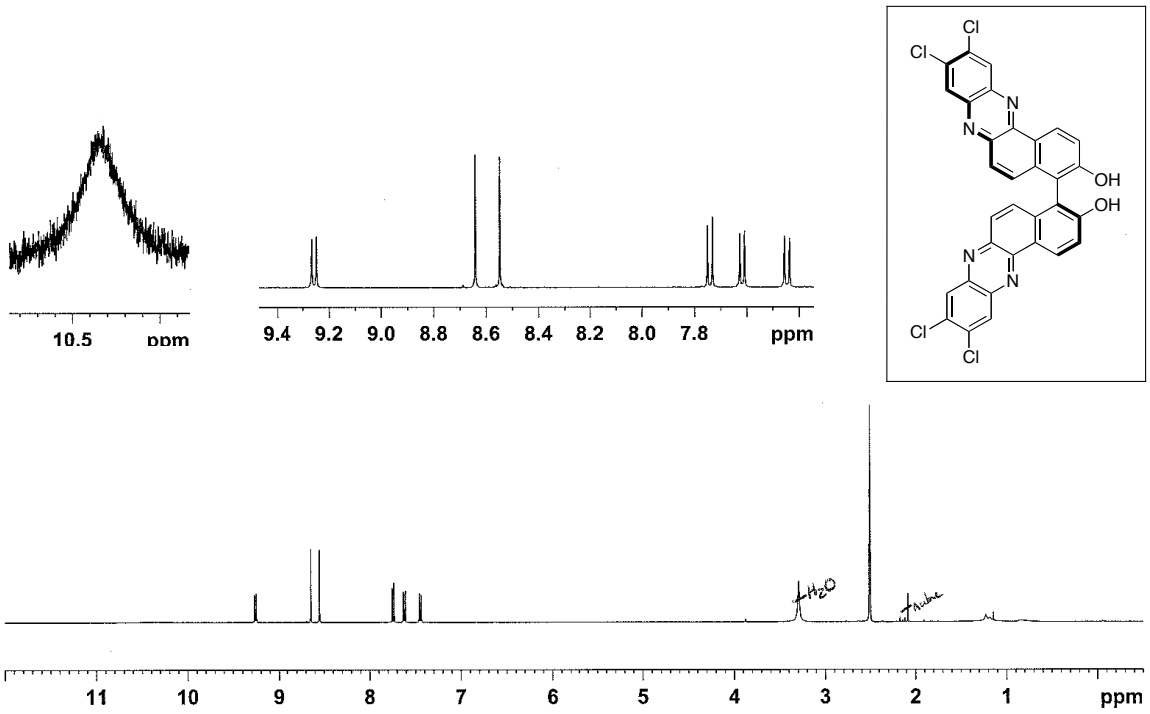

Figure A6.40_1 ^{1}H NMR Spectrum of Compound (*S*)-**6.40** (500 MHz, DMSO-d_6).

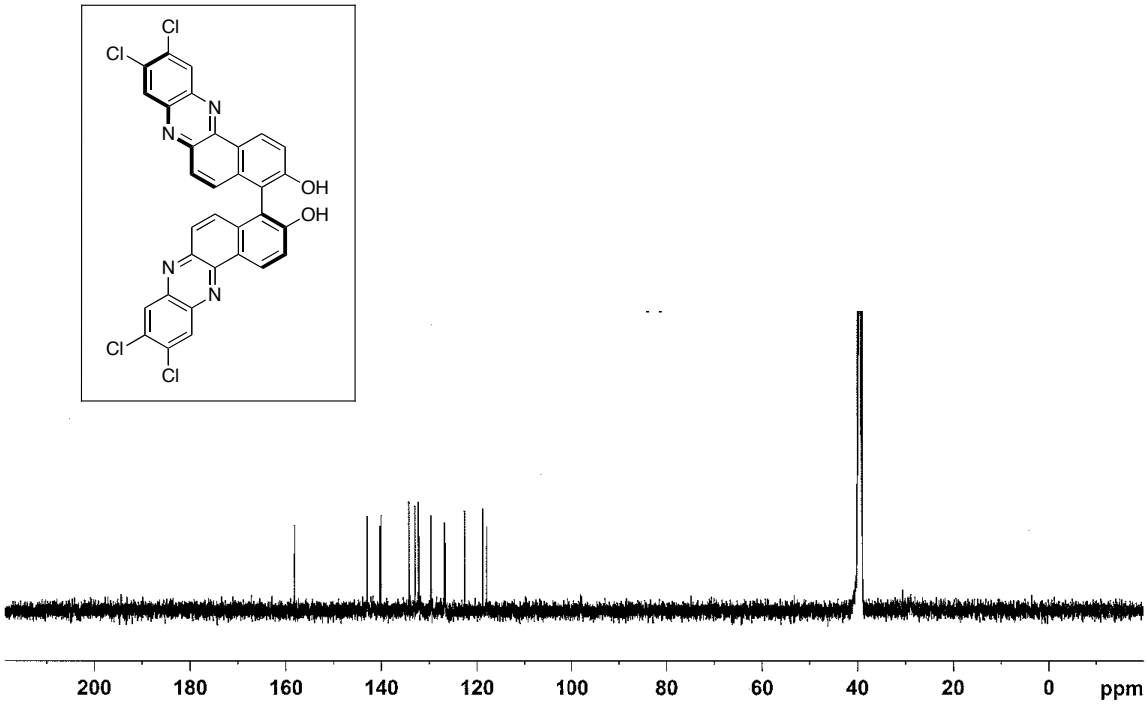

Figure A6.40_2 ^{13}C NMR Spectrum of Compound (*S*)-**6.40** (125 MHz, DMSO-d_6).

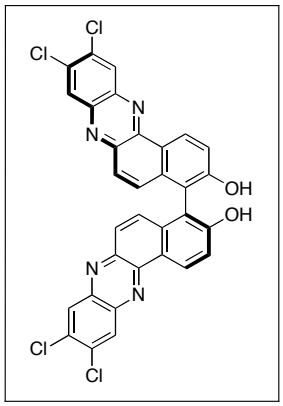

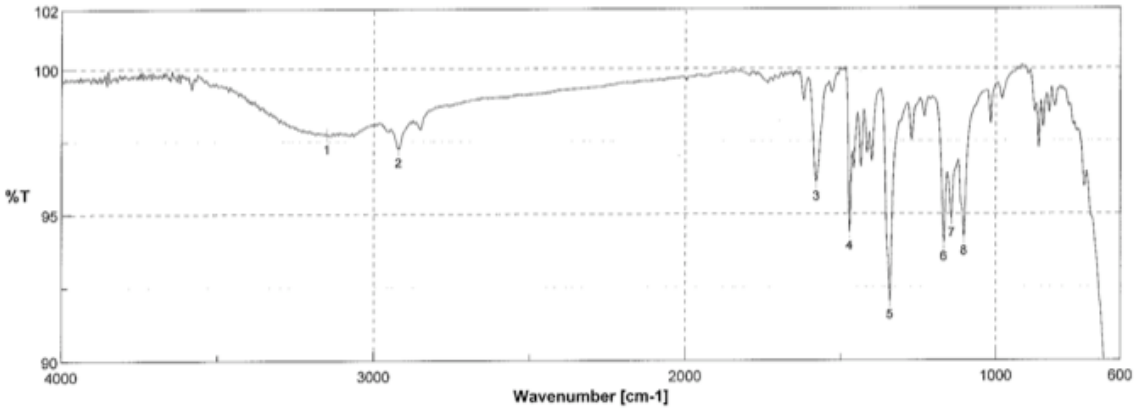

Figure A6.40_3 IR Spectrum of Compound (*S*)-**6.40** (film).

APPENDIX B: X-RAY CRYSTALLOGRAPHIC DATA[143]

B.1 X-Ray Structure Determination of Compound *rac*-2.18

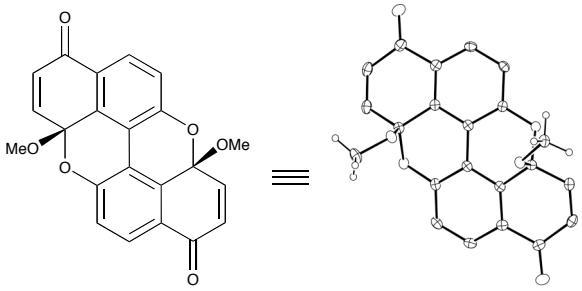

Compound *rac*-**2.18**, $C_{22}H_{14}O_6$, crystallizes in the monoclinic space group $P2_1/c$ (systematic absences 0k0: k=odd and h0l: l=odd) with a=11.3087(6)Å, b=13.2371(8)Å, c=11.2330(7)Å, α=90°, β=102.401(2)°, γ=90°, V=1642.28(17)Å^3, Z=4, and d_{calc}=1.514 g/cm^3. X-ray intensity data were collected on a Bruker APEXII CCD area detector employing graphite-monochromated Mo-Kα radiation (λ=0.71073 Å) at a temperature of 100(1)K. Preliminary indexing was performed from a series of thirty-six 0.5° rotation frames with exposures of 5 seconds. A total of 1892 frames were collected with a crystal to detector distance of 37.488 mm, rotation widths of 0.5° and exposures of 5 seconds:

scan type	2θ	ω	ϕ	χ	frames
ϕ	19.50	59.55	-11.29	-26.26	739
ω	-15.50	-117.02	18.69	41.79	212
ω	14.50	-77.44	54.11	21.36	202
ϕ	-20.50	-17.45	-38.45	-73.06	739

Rotation frames were integrated using SAINT[144], producing a listing of unaveraged F^2 and $\sigma(F^2)$ values which were then passed to the SHELXTL[145] program

(143) Dr. Patrick J. Carroll is gratefully acknowledged for solving the crystal structures of several compounds.

(144) Bruker (2009) SAINT. Bruker AXS Inc., Madison, Wisconsin, USA.

(145) Bruker (2009) SHELXTL. Bruker AXS Inc., Madison, Wisconsin, USA.

package for further processing and structure solution on a Dell Pentium 4 computer. A total of 26239 reflections were measured over the ranges $2.40 \leq \theta \leq 25.09°$, $-13 \leq h \leq 13$, $-15 \leq k \leq 15$, $-13 \leq l \leq 13$ yielding 2882 unique reflections (Rint = 0.0255). The intensity data were corrected for Lorentz and polarization effects and for absorption using SADABS[146] (minimum and maximum transmission 0.6852, 0.7452).

The structure was solved by direct methods (SHELXS-97[147]). Refinement was by full-matrix least squares based on F^2 using SHELXL-97.[147] All reflections were used during refinement. The weighting scheme used was $w=1/[\sigma^2(F_o^2)+ (0.0101P)^2 + 0.3457P]$ where $P = (F_o^2 + 2F_c^2)/3$. Non-hydrogen atoms were refined anisotropically and hydrogen atoms were refined using a riding model. Refinement converged to R1=0.0361 and wR2=0.1186 for 2664 observed reflections for which $F > 4\sigma(F)$ and R1=0.0559 and wR2=0.1630 and GOF =1.320 for all 2882 unique, non-zero reflections and 256 variables.[148] The maximum Δ/σ in the final cycle of least squares was 0.000 and the two most prominent peaks in the final difference Fourier were +1.109 and -0.858 e/Å^3.

Table B.1 lists cell information, data collection parameters, and refinement data. Final positional and equivalent isotropic thermal parameters are given in Table B.2 and Table B.3. Anisotropic thermal parameters are in Table B.4. Table B.5 and Table B.6 list bond distances and bond angles. Figure B.1 is an ORTEP[149] representation of the molecule with 30% probability thermal ellipsoids displayed.

---

(146) Sheldrick, G.M. (2007) SADABS. University of Gottingen, Germany.

(147) Sheldrick, G.M. (2008) Acta Cryst. A64,112-122.

(148) $R1 = \Sigma||F_o| - |F_c|| / \Sigma |F_o|$; $wR2 = [\Sigma w(F_o^2 - F_c^2)^2/\Sigma w(F_o^2)^2]^{½}$; $GOF = [\Sigma w(F_o^2 - F_c^2)^2/(n - p)]^{½}$ where n = the number of reflections and p = the number of parameters refined.

(149) "ORTEP-II: A Fortran Thermal Ellipsoid Plot Program for Crystal Structure Illustrations". C.K. Johnson (1976) ORNL-5138.

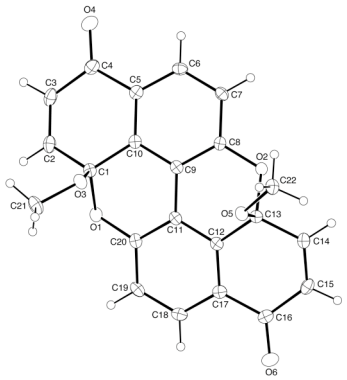

Figure B.1 ORTEP drawing of *rac*-**2.18** with 30% probability thermal ellipsoids.

Table B.1 Summary of structure determination of *rac*-**2.18**.

Empirical formula	$C_{22}H_{14}O_6$
Formula weight	374.33
Temperature	100(1) K
Wavelength	0.71073 Å
Crystal system	monoclinic
Space group	$P2_1/c$
Cell constants:	
a	11.3087(6) Å
b	13.2371(8) Å
c	11.2330(7) Å
b	102.401(2)°
Volume	1642.28(17) $Å^3$
Z	4
Density (calculated)	1.514 Mg/m^3
Absorption coefficient	0.111 mm^{-1}
F(000)	776
Crystal size	0.40 x 0.25 x 0.22 mm^3
Theta range for data collection	2.40 to 25.09°
Index ranges	$-13 \le h \le 13$, $-15 \le k \le 15$, $-13 \le l \le 13$
Reflections collected	26239
Independent reflections	2882 [R(int) = 0.0255]
Completeness to theta = 25.10°	98.4 %
Absorption correction	Semi-empirical from equivalents
Max. and min. transmission	0.7452 and 0.6852
Refinement method	Full-matrix least-squares on F^2
Data / restraints / parameters	2882 / 0 / 256
Goodness-of-fit on F^2	1.320

Final R indices [I>2sigma(I)]	R1 = 0.0361, wR2 = 0.1186
R indices (all data)	R1 = 0.0559, wR2 = 0.1630
Largest diff. peak and hole	1.109 and -0.858 e.Å^{-3}

Table B.2 Refined positional parameters for compound *rac*-**2.18**.

Atom	x	Y	z	U_{eq}, Å^2
C1	0.74562(14)	0.38931(12)	0.77668(15)	0.0172(4)
C2	0.73839(15)	0.38129(13)	0.90838(15)	0.0219(4)
C3	0.79048(16)	0.44959(13)	0.98932(15)	0.0242(4)
C4	0.84946(16)	0.54269(13)	0.95724(15)	0.0221(4)
C5	0.83351(14)	0.56527(12)	0.82575(14)	0.0184(4)
C6	0.86665(15)	0.65793(12)	0.78295(15)	0.0198(4)
C7	0.84325(14)	0.68009(12)	0.65925(14)	0.0178(4)
C8	0.78341(14)	0.60870(12)	0.57697(14)	0.0151(4)
C9	0.75029(13)	0.51607(12)	0.61847(14)	0.0152(4)
C10	0.77734(14)	0.49397(12)	0.74200(14)	0.0156(4)
C11	0.67294(13)	0.44856(11)	0.53693(14)	0.0155(4)
C12	0.64896(13)	0.46933(12)	0.41344(14)	0.0153(4)
C13	0.72914(13)	0.54714(12)	0.37269(14)	0.0155(4)
C14	0.67556(14)	0.58881(12)	0.24854(14)	0.0187(4)
C15	0.58748(15)	0.54091(13)	0.17150(14)	0.0208(4)
C16	0.52905(14)	0.44751(12)	0.20394(14)	0.0191(4)
C17	0.55888(14)	0.41697(12)	0.33345(14)	0.0169(4)
C18	0.49652(14)	0.34040(12)	0.38007(15)	0.0192(4)
C19	0.52088(14)	0.31769(12)	0.50350(15)	0.0191(4)
C20	0.60882(14)	0.37323(12)	0.58272(14)	0.0167(4)
C21	0.83063(16)	0.22283(13)	0.78276(17)	0.0269(4)
C22	0.93587(14)	0.55528(12)	0.34693(15)	0.0201(4)
O1	0.62773(10)	0.35772(8)	0.70620(10)	0.0181(3)
O2	0.75092(9)	0.63257(8)	0.45518(9)	0.0159(3)
O3	0.83540(9)	0.32659(8)	0.74664(10)	0.0188(3)
O4	0.90419(13)	0.59923(10)	1.03624(11)	0.0311(4)
O5	0.83913(9)	0.49585(8)	0.37582(10)	0.0168(3)
O6	0.45690(11)	0.40058(9)	0.12670(11)	0.0265(3)

$U_{eq}={}^1/_3[U_{11}(aa^*)^2+U_{22}(bb^*)^2+U_{33}(cc^*)^2+2U_{12}aa^*bb^*\cos\gamma+2U_{13}aa^*cc^*\cos\beta+2U_{23}bb^*cc^*\cos\alpha]$

Table B.3 Positional parameters for hydrogens in compound *rac*-**2.18**.

Atom	x	Y	z	U_{iso}, Å^2
H2	0.6967	0.3276	0.9336	0.029
H3	0.7899	0.4384	1.0709	0.032
H6	0.9052	0.7058	0.8385	0.026
H7	0.8672	0.7415	0.6319	0.024
H14	0.7046	0.6496	0.2248	0.025
H15	0.5613	0.5673	0.0936	0.028
H18	0.4373	0.3039	0.3271	0.026
H19	0.4791	0.2661	0.5329	0.025
H21a	0.8554	0.2178	0.8698	0.040
H21b	0.8840	0.1833	0.7455	0.040
H21c	0.7494	0.1981	0.7571	0.040
H22a	0.9108	0.5824	0.2662	0.030
H22b	1.0059	0.5134	0.3509	0.030
H22c	0.9554	0.6096	0.4044	0.030

Table B.4 Refined thermal parameters (U's) for compound *rac*-**2.18**.

Atom	U_{11}	U_{22}	U_{33}	U_{23}	U_{13}	U_{12}
C1	0.0137(8)	0.0179(8)	0.0203(8)	0.0019(6)	0.0045(6)	0.0008(6)
C2	0.0203(8)	0.0252(9)	0.0220(9)	0.0072(7)	0.0083(7)	0.0028(7)
C3	0.0296(9)	0.0272(9)	0.0175(8)	0.0044(7)	0.0090(7)	0.0079(7)
C4	0.0251(9)	0.0228(9)	0.0185(8)	-0.0020(7)	0.0047(7)	0.0065(7)
C5	0.0181(8)	0.0193(8)	0.0185(8)	-0.0007(6)	0.0052(6)	0.0039(6)
C6	0.0198(8)	0.0178(8)	0.0215(8)	-0.0053(6)	0.0036(6)	0.0009(6)
C7	0.0180(8)	0.0135(8)	0.0228(8)	-0.0005(6)	0.0063(6)	0.0009(6)
C8	0.0132(7)	0.0165(8)	0.0164(8)	0.0013(6)	0.0051(6)	0.0038(6)
C9	0.0121(7)	0.0155(8)	0.0191(8)	-0.0001(6)	0.0058(6)	0.0023(6)
C10	0.0133(7)	0.0169(8)	0.0179(8)	0.0009(6)	0.0058(6)	0.0028(6)
C11	0.0119(7)	0.0144(8)	0.0207(8)	0.0008(6)	0.0049(6)	0.0022(6)
C12	0.0130(7)	0.0141(8)	0.0195(8)	-0.0008(6)	0.0050(6)	0.0043(6)
C13	0.0136(7)	0.0155(8)	0.0175(8)	-0.0012(6)	0.0036(6)	0.0021(6)
C14	0.0184(8)	0.0187(8)	0.0202(8)	0.0029(6)	0.0071(7)	0.0041(6)
C15	0.0202(8)	0.0257(9)	0.0164(8)	0.0024(6)	0.0036(6)	0.0069(7)
C16	0.0156(8)	0.0218(9)	0.0192(8)	-0.0040(6)	0.0026(6)	0.0054(6)

C17	0.0141(8)	0.0171(8)	0.0199(8)	-0.0029(6)	0.0046(6)	0.0041(6)
C18	0.0134(7)	0.0177(8)	0.0258(8)	-0.0046(6)	0.0025(6)	0.0012(6)
C19	0.0143(7)	0.0149(8)	0.0294(9)	0.0008(6)	0.0078(6)	0.0002(6)
C20	0.0139(7)	0.0170(8)	0.0206(8)	0.0022(6)	0.0070(6)	0.0036(6)
C21	0.0267(9)	0.0156(8)	0.0397(10)	0.0052(7)	0.0101(8)	0.0036(6)
C22	0.0161(8)	0.0228(8)	0.0226(8)	0.0034(6)	0.0068(6)	0.0007(6)
O1	0.0146(6)	0.0207(6)	0.0196(6)	0.0037(4)	0.0052(4)	-0.0012(4)
O2	0.0181(6)	0.0143(6)	0.0155(6)	0.0005(4)	0.0042(4)	0.0011(4)
O3	0.0165(6)	0.0155(6)	0.0255(6)	0.0023(4)	0.0069(4)	0.0016(4)
O4	0.0442(8)	0.0283(7)	0.0188(6)	-0.0047(5)	0.0026(6)	0.0010(6)
O5	0.0136(6)	0.0167(6)	0.0211(6)	0.0017(4)	0.0060(5)	0.0019(4)
O6	0.0267(7)	0.0280(7)	0.0224(6)	-0.0051(5)	-0.0004(5)	-0.0007(5)

The form of the anisotropic displacement parameter is:
$\exp[-2\pi^2(a^{*2}U_{11}h^2+b^{*2}U_{22}k^2+c^{*2}U_{33}l^2+2b^*c^*U_{23}kl+2a^*c^*U_{13}hl+2a^*b^*U_{12}hk)]$

Table B.5 Bond distances in compound *rac*-**2.18**, Å.

C1-O3	1.4075(19)	C1-O1	1.4580(19)	C1-C2	1.503(2)
C1-C10	1.503(2)	C2-C3	1.327(3)	C3-C4	1.482(3)
C4-O4	1.223(2)	C4-C5	1.480(2)	C5-C10	1.387(2)
C5-C6	1.398(2)	C6-C7	1.389(2)	C7-C8	1.392(2)
C8-O2	1.3750(18)	C8-C9	1.391(2)	C9-C10	1.387(2)
C9-C11	1.435(2)	C11-C12	1.383(2)	C11-C20	1.395(2)
C12-C17	1.390(2)	C12-C13	1.507(2)	C13-O5	1.4108(18)
C13-O2	1.4492(18)	C13-C14	1.501(2)	C14-C15	1.331(2)
C15-C16	1.484(2)	C16-O6	1.225(2)	C16-C17	1.477(2)
C17-C18	1.399(2)	C18-C19	1.387(2)	C19-C20	1.393(2)
C20-O1	1.3728(19)	C21-O3	1.437(2)	C22-O5	1.4400(18)

Table B.6 Bond angles in compound *rac*-**2.18**, °

O3-C1-O1	108.86(12)	O3-C1-C2	112.88(13)	O1-C1-C2	106.11(12)
O3-C1-C10	104.89(12)	O1-C1-C10	111.40(12)	C2-C1-C10	112.75(14)
C3-C2-C1	121.09(16)	C2-C3-C4	123.82(15)	O4-C4-C5	122.35(16)
O4-C4-C3	121.11(15)	C5-C4-C3	116.49(14)	C10-C5-C6	118.79(14)
C10-C5-C4	118.66(15)	C6-C5-C4	122.44(15)	C7-C6-C5	121.46(15)
C6-C7-C8	118.82(15)	O2-C8-C9	120.15(14)	O2-C8-C7	119.51(14)
C9-C8-C7	120.23(14)	C10-C9-C8	120.26(15)	C10-C9-C11	118.73(14)
C8-C9-C11	120.40(14)	C9-C10-C5	120.39(15)	C9-C10-C1	116.12(14)
C5-C10-C1	123.47(14)	C12-C11-C20	120.44(15)	C12-C11-C9	118.55(14)
C20-C11-C9	120.26(14)	C11-C12-C17	120.53(15)	C11-C12-C13	116.07(14)
C17-C12-C13	123.35(14)	O5-C13-O2	109.37(12)	O5-C13-C14	112.19(12)
O2-C13-C14	106.65(12)	O5-C13-C12	104.37(12)	O2-C13-C12	111.71(12)
C14-C13-C12	112.59(13)	C15-C14-C13	121.68(15)	C14-C15-C16	123.21(15)
O6-C16-C17	122.35(15)	O6-C16-C15	120.85(15)	C17-C16-C15	116.76(14)
C12-C17-C18	118.53(14)	C12-C17-C16	118.73(14)	C18-C17-C16	122.68(15)
C19-C18-C17	121.55(15)	C18-C19-C20	119.03(15)	O1-C20-C19	120.09(14)
O1-C20-C11	119.94(14)	C19-C20-C11	119.87(14)	C20-O1-C1	115.57(11)
C8-O2-C13	115.42(11)	C1-O3-C21	115.05(12)	C13-O5-C22	116.10(12)

B.2 X-Ray Structure Determination of Compound *rac*-2.19.

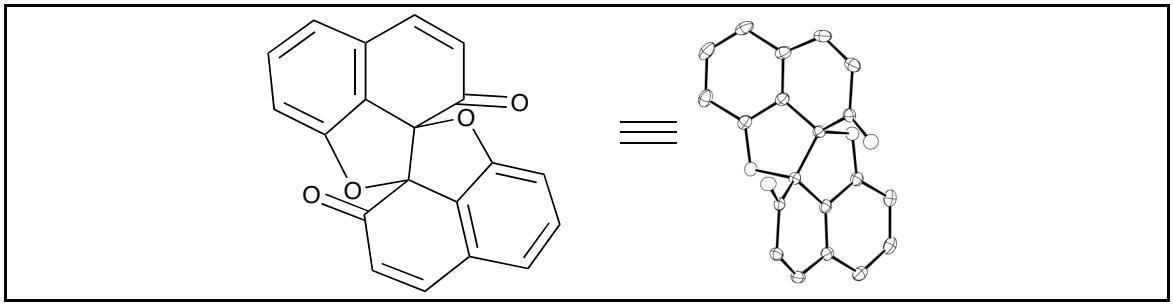

Compound *rac*-**2.19**, $C_{20}H_{10}O_4$, crystallizes in the triclinic space group $P\bar{1}$ with a=7.8712(2)Å, b=8.5353(2)Å, c=11.5772(3)Å, α=80.3130(10)°, β=79.3660(10)°, γ=68.6380(10)°, V=707.56(3)Å^3, Z=2, and d_{calc}=1.475 g/cm^3. X-ray intensity data were collected on a Bruker APEXII CCD area detector employing graphite-monochromated Mo-Kα radiation (λ=0.71073 Å) at a temperature of 157(1)K. Preliminary indexing was performed from a series of thirty-six 0.5° rotation frames with exposures of 10 seconds. A total of 3739 frames were collected with a crystal to detector distance of 49.918 mm, rotation widths of 0.5° and exposures of 10 seconds:

scan type	2θ	ω	ϕ	χ	frames
ϕ	27.00	19.86	-324.71	69.08	739
ϕ	-23.00	268.36	-338.26	47.18	730
ϕ	24.50	68.74	59.23	-42.87	363
ω	27.00	-11.01	59.97	48.96	75
ω	29.50	-7.40	-176.20	85.83	81
ω	-28.00	-67.83	-210.37	61.00	105
ω	24.50	-70.10	12.44	23.24	198
ϕ	-13.00	293.74	-320.91	61.00	709
ϕ	24.50	168.13	-56.89	-89.87	739

Rotation frames were integrated using SAINT[144], producing a listing of unaveraged F^2 and $\sigma(F^2)$ values which were then passed to the SHELXTL[145] program package for further processing and structure solution on a Dell Pentium 4 computer. A total of 13591 reflections were measured over the ranges $1.80 \leq \theta \leq 25.19°$, $-9 \leq h \leq 9$, -

$10 \leq k \leq 9$, $-13 \leq l \leq 13$ yielding 2542 unique reflections (Rint = 0.0165). The intensity data were corrected for Lorentz and polarization effects and for absorption using SADABS[146] (minimum and maximum transmission 0.6884, 0.7452).

The structure was solved by direct methods (SHELXS-97[147]). Refinement was by full-matrix least squares based on F^2 using SHELXL-97.[147] All reflections were used during refinement. The weighting scheme used was $w=1/[\sigma^2(F_o^2)+ (0.0445P)^2 + 0.2221P]$ where $P = (F_o^2 + 2F_c^2)/3$. Non-hydrogen atoms were refined anisotropically and hydrogen atoms were refined using a riding model. Refinement converged to R1=0.0334 and wR2=0.0853 for 2329 observed reflections for which $F > 4\sigma(F)$ and R1=0.0363 and wR2=0.0880 and GOF =1.071 for all 2542 unique, non-zero reflections and 218 variables.[148] The maximum Δ/σ in the final cycle of least squares was 0.000 and the two most prominent peaks in the final difference Fourier were +0.190 and -0.203 e/Å^3.

Table B.7 lists cell information, data collection parameters, and refinement data. Final positional and equivalent isotropic thermal parameters are given in Table B.8 and Table B.9. Anisotropic thermal parameters are in Table B.10. Table B.11 and Table B.12 list bond distances and bond angles. Figure B.2 is an ORTEP[149] representation of the molecule with 30% probability thermal ellipsoids displayed.

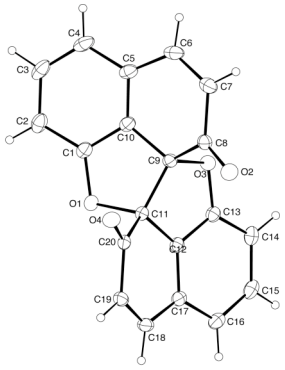

Figure B.2 ORTEP drawing of *rac*-**2.19** with 30% probability thermal ellipsoids.

Table B.7 Summary of structure determination of compound *rac*-**2.19**.

Empirical formula	$C_{20}H_{10}O_4$
Formula weight	314.28
Temperature	157(1) K
Wavelength	0.71073 Å
Crystal system	triclinic
Space group	$P\bar{1}$
Cell constants:	
a	7.8712(2) Å
b	8.5353(2) Å
c	11.5772(3) Å
a	80.3130(10)°
b	79.3660(10)°
g	68.6380(10)°
Volume	707.56(3) $Å^3$
Z	2
Density (calculated)	1.475 Mg/m^3
Absorption coefficient	0.104 mm^{-1}
F(000)	324
Crystal size	0.22 x 0.20 x 0.12 mm^3
Theta range for data collection	1.80 to 25.19°
Index ranges	$-9 \le h \le 9$, $-10 \le k \le 9$, $-13 \le l \le 13$
Reflections collected	13591
Independent reflections	2542 [R(int) = 0.0165]
Completeness to theta = 25.19°	99.8 %
Absorption correction	Semi-empirical from equivalents
Max. and min. transmission	0.7452 and 0.6884
Refinement method	Full-matrix least-squares on F^2
Data / restraints / parameters	2542 / 0 / 218
Goodness-of-fit on F^2	1.071
Final R indices [I>2sigma(I)]	R1 = 0.0334, wR2 = 0.0853
R indices (all data)	R1 = 0.0363, wR2 = 0.0880
Largest diff. peak and hole	0.190 and -0.203 $e.Å^{-3}$

Table B.8 Refined positional parameters for compound *rac*-**2.19**.

Atom	x	y	z	U_{eq}, Å^2
C1	-0.03804(17)	0.88304(16)	0.31170(11)	0.0281(3)
C2	-0.20654(19)	0.99111(18)	0.36052(13)	0.0356(3)
C3	-0.2457(2)	0.97148(19)	0.48289(14)	0.0406(4)
C4	-0.1299(2)	0.8469(2)	0.55498(13)	0.0386(4)
C5	0.03734(19)	0.73829(18)	0.50450(11)	0.0315(3)
C6	0.1633(2)	0.58613(19)	0.56243(11)	0.0359(3)
C7	0.29550(19)	0.46954(18)	0.49989(12)	0.0338(3)
C8	0.33016(17)	0.48784(16)	0.36968(11)	0.0271(3)
C9	0.24849(16)	0.66916(16)	0.31219(10)	0.0243(3)
C10	0.08003(17)	0.76790(16)	0.38341(11)	0.0269(3)
C11	0.19503(16)	0.71556(15)	0.18590(10)	0.0233(3)
C12	0.35504(16)	0.75261(15)	0.11641(11)	0.0246(3)
C13	0.46543(17)	0.76552(15)	0.19012(11)	0.0259(3)
C14	0.62744(17)	0.79676(16)	0.14421(12)	0.0307(3)
C15	0.67127(18)	0.80839(16)	0.02179(12)	0.0324(3)
C16	0.56546(18)	0.78290(16)	-0.05257(12)	0.0308(3)
C17	0.40439(17)	0.75055(15)	-0.00458(11)	0.0261(3)
C18	0.29296(18)	0.69430(16)	-0.06506(11)	0.0288(3)
C19	0.17000(17)	0.62479(16)	-0.00525(11)	0.0276(3)
C20	0.13382(16)	0.60316(15)	0.12493(11)	0.0241(3)
O1	0.02726(12)	0.87262(11)	0.19341(8)	0.0283(2)
O2	0.42451(13)	0.37215(12)	0.31241(8)	0.0355(2)
O3	0.40050(12)	0.73767(11)	0.30759(7)	0.0282(2)
O4	0.05332(13)	0.51119(12)	0.18048(8)	0.0321(2)

$U_{eq}={}^1/_3[U_{11}(aa^*)^2+U_{22}(bb^*)^2+U_{33}(cc^*)^2+2U_{12}aa^*bb^*\cos\gamma+2U_{13}aa^*cc^*\cos\beta+2U_{23}bb^*cc^*\cos\alpha]$

Table B.9 Positional parameters for hydrogens in compound *rac*-**2.19**.

Atom	x	y	z	U_{iso}, Å^2
H2	-0.2884	1.0720	0.3137	0.047
H3	-0.3547	1.0452	0.5184	0.054
H4	-0.1639	0.8362	0.6364	0.051
H6	0.1518	0.5695	0.6446	0.048
H7	0.3688	0.3724	0.5409	0.045
H14	0.7026	0.8092	0.1927	0.041
H15	0.7759	0.8343	-0.0120	0.043

H16	0.6023	0.7875	-0.1338	0.041
H18	0.3077	0.7070	-0.1473	0.038
H19	0.1046	0.5886	-0.0479	0.037

Table B.10 Refined thermal parameters (U's) for compound *rac*-**2.19**.

Atom	U_{11}	U_{22}	U_{33}	U_{23}	U_{13}	U_{12}
C1	0.0262(6)	0.0299(7)	0.0316(7)	-0.0115(5)	-0.0003(5)	-0.0118(5)
C2	0.0273(7)	0.0330(7)	0.0480(8)	-0.0173(6)	-0.0009(6)	-0.0087(6)
C3	0.0299(7)	0.0455(9)	0.0513(9)	-0.0292(7)	0.0106(6)	-0.0160(6)
C4	0.0393(8)	0.0535(9)	0.0328(7)	-0.0230(7)	0.0102(6)	-0.0268(7)
C5	0.0332(7)	0.0440(8)	0.0267(7)	-0.0138(6)	0.0025(5)	-0.0230(6)
C6	0.0439(8)	0.0522(9)	0.0211(6)	-0.0047(6)	-0.0014(6)	-0.0288(7)
C7	0.0387(8)	0.0408(8)	0.0265(7)	0.0022(6)	-0.0086(6)	-0.0197(6)
C8	0.0237(6)	0.0336(7)	0.0264(6)	-0.0028(5)	-0.0047(5)	-0.0124(5)
C9	0.0232(6)	0.0308(7)	0.0222(6)	-0.0062(5)	-0.0023(5)	-0.0120(5)
C10	0.0255(6)	0.0325(7)	0.0274(6)	-0.0113(5)	-0.0001(5)	-0.0137(5)
C11	0.0209(6)	0.0239(6)	0.0230(6)	-0.0038(5)	-0.0025(5)	-0.0048(5)
C12	0.0230(6)	0.0216(6)	0.0274(6)	-0.0021(5)	-0.0027(5)	-0.0060(5)
C13	0.0243(6)	0.0229(6)	0.0286(6)	-0.0035(5)	-0.0022(5)	-0.0062(5)
C14	0.0238(6)	0.0262(6)	0.0423(8)	-0.0044(5)	-0.0050(5)	-0.0085(5)
C15	0.0243(6)	0.0247(7)	0.0434(8)	-0.0012(6)	0.0037(6)	-0.0079(5)
C16	0.0306(7)	0.0237(6)	0.0304(7)	0.0004(5)	0.0037(5)	-0.0057(5)
C17	0.0270(6)	0.0206(6)	0.0251(6)	0.0004(5)	-0.0013(5)	-0.0038(5)
C18	0.0331(7)	0.0275(6)	0.0207(6)	-0.0021(5)	-0.0034(5)	-0.0048(5)
C19	0.0290(7)	0.0289(7)	0.0241(6)	-0.0054(5)	-0.0062(5)	-0.0066(5)
C20	0.0190(6)	0.0258(6)	0.0254(6)	-0.0050(5)	-0.0032(5)	-0.0041(5)
O1	0.0240(5)	0.0279(5)	0.0290(5)	-0.0066(4)	-0.0034(4)	-0.0028(4)
O2	0.0358(5)	0.0321(5)	0.0330(5)	-0.0047(4)	-0.0037(4)	-0.0050(4)
O3	0.0262(5)	0.0364(5)	0.0262(5)	-0.0058(4)	-0.0039(4)	-0.0145(4)
O4	0.0334(5)	0.0398(5)	0.0283(5)	-0.0055(4)	-0.0005(4)	-0.0198(4)

The form of the anisotropic displacement parameter is:
$\exp[-2\pi^2(a^{*2}U_{11}h^2+b^{*2}U_{22}k^2+c^{*2}U_{33}l^2+2b^*c^*U_{23}kl+2a^*c^*U_{13}hl+2a^*b^*U_{12}hk)]$

Table B.11 Bond distances in compound *rac*-**2.19**, Å.

C1-C10	1.3651(19)	C1-O1	1.3768(15)	C1-C2	1.3917(18)
C2-C3	1.388(2)	C3-C4	1.390(2)	C4-C5	1.394(2)
C5-C10	1.3824(18)	C5-C6	1.461(2)	C6-C7	1.344(2)
C7-C8	1.4736(17)	C8-O2	1.2126(16)	C8-C9	1.5290(18)
C9-C10	1.4712(17)	C9-O3	1.5007(14)	C9-C11	1.5436(16)
C11-C12	1.4711(17)	C11-O1	1.5019(14)	C11-C20	1.5300(17)
C12-C13	1.3676(18)	C12-C17	1.3841(17)	C13-O3	1.3749(15)
C13-C14	1.3891(18)	C14-C15	1.3910(19)	C15-C16	1.393(2)
C16-C17	1.3913(18)	C17-C18	1.4618(18)	C18-C19	1.3420(18)
C19-C20	1.4741(17)	C20-O4	1.2138(15)		

Table B.12 Bond angles in compound *rac*-**2.19**, °

C10-C1-O1	112.79(11)	C10-C1-C2	120.14(12)	O1-C1-C2	127.04(12)
C3-C2-C1	116.34(14)	C2-C3-C4	123.22(13)	C3-C4-C5	119.65(13)
C10-C5-C4	116.24(13)	C10-C5-C6	115.93(12)	C4-C5-C6	127.48(13)
C7-C6-C5	121.61(12)	C6-C7-C8	123.30(13)	O2-C8-C7	123.45(12)
O2-C8-C9	122.24(11)	C7-C8-C9	114.16(11)	C10-C9-O3	110.80(9)
C10-C9-C8	112.16(10)	O3-C9-C8	102.30(9)	C10-C9-C11	102.53(10)
O3-C9-C11	104.43(9)	C8-C9-C11	124.20(10)	C1-C10-C5	124.04(12)
C1-C10-C9	110.29(11)	C5-C10-C9	125.36(12)	C12-C11-O1	111.42(9)
C12-C11-C20	111.87(10)	O1-C11-C20	102.41(9)	C12-C11-C9	102.61(9)
O1-C11-C9	104.72(9)	C20-C11-C9	123.58(10)	C13-C12-C17	123.39(12)
C13-C12-C11	110.15(11)	C17-C12-C11	125.83(11)	C12-C13-O3	112.62(11)
C12-C13-C14	120.47(12)	O3-C13-C14	126.86(12)	C13-C14-C15	116.41(12)
C14-C15-C16	122.95(12)	C17-C16-C15	119.60(12)	C12-C17-C16	116.72(12)
C12-C17-C18	115.72(11)	C16-C17-C18	127.10(12)	C19-C18-C17	121.83(11)
C18-C19-C20	123.02(12)	O4-C20-C19	123.58(11)	O4-C20-C11	121.80(11)
C19-C20-C11	114.51(10)	C1-O1-C11	106.62(9)	C13-O3-C9	106.74(9)

B.3 X-Ray Structure Determination of Compound *rac*-2.21

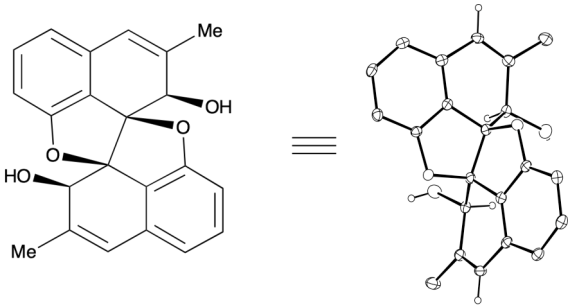

Compound *rac*-**2.21**, $C_{22}H_{18}O_4$, crystallizes in the monoclinic space group $P2_1/c$ (systematic absences 0k0: k=odd and h0l: l=odd) with a=12.1645(13)Å, b=6.6205(6)Å, c=20.4873(17)Å, α=90°, β=102.566(5)°, γ=90°, V=1610.4(3)Å^3, Z=4, and d_{calc}=1.429 g/cm^3. X-ray intensity data were collected on a Bruker APEXII CCD area detector employing graphite-monochromated Mo-Kα radiation (λ=0.71073 Å) at a temperature of 143(1)K. Preliminary indexing was performed from a series of thirty-six 0.5° rotation frames with exposures of 30 seconds. A total of 1942 frames were collected with a crystal to detector distance of 37.600 mm, rotation widths of 0.5° and exposures of 30 seconds:

scan type	2θ	ω	ϕ	χ	frames
ϕ	19.50	59.55	-11.29	-26.26	739
ω	-15.50	-14.20	-18.89	-63.64	89
ω	12.00	-37.72	-69.79	72.15	90
ω	-10.50	-14.33	80.80	-60.33	122
ω	14.50	-77.44	54.11	21.36	202
ϕ	-20.50	-17.45	19.14	-73.06	620
ω	-10.50	-53.05	-87.93	99.72	80

Rotation frames were integrated using SAINT[144], producing a listing of unaveraged F^2 and $\sigma(F^2)$ values which were then passed to the SHELXTL[145] program package for further processing and structure solution. A total of 2861 reflections were measured over the ranges $1.72 \le \theta \le 25.09°$, $-14 \le h \le 14$, $0 \le k \le 7$, $0 \le l \le 24$ yielding 2861 unique reflections (Rint = 0.0499). The intensity data were corrected for Lorentz

and polarization effects and for absorption using TWINABS[150] (minimum and maximum transmission 0.6490, 0.7452).

The structure was solved by direct methods (SHELXS-97[147]). Least squares refinement proceeded to a final R1 of only 14%. At this point, the program CELL_NOW[151] revealed that the crystal was a non-merohedral twin with two components related by a rotation of 180° about the 100 direct axis. Refinement was by full-matrix least squares based on F^2 using SHELXL-97.[147] All reflections were used during refinement. The weighting scheme used was $w=1/[\sigma^2(F_o^2)+ (0.0414P)^2 + 0.7044P]$ where $P = (F_o^2 + 2F_c^2)/3$. Non-hydrogen atoms were refined anisotropically and hydrogen atoms were refined using a riding model. Refinement converged to R1=0.0392 and wR2=0.0884 for 2499 observed reflections for which $F > 4\sigma(F)$ and R1=0.0504 and wR2=0.0929 and GOF =1.065 for all 2861 unique, non-zero reflections and 241 variables.[148] The maximum Δ/σ in the final cycle of least squares was 0.005 and the two most prominent peaks in the final difference Fourier were +0.179 and -0.283 e/Å^3.

Table B.13 lists cell information, data collection parameters, and refinement data. Final positional and equivalent isotropic thermal parameters are given in Table B.14 and Table B.15. Anisotropic thermal parameters are in Table B.16. Table B.17 and Table B.18 list bond distances and bond angles. Figure B.3 is an ORTEP[149] representation of the molecule with 30% probability thermal ellipsoids displayed.

(150) Sheldrick, G.M. (2008) TWINABS. University of Gottingen, Germany.

(151) Sheldrick, G.M. (2008) CELL_NOW. University of Gottingen, Germany.

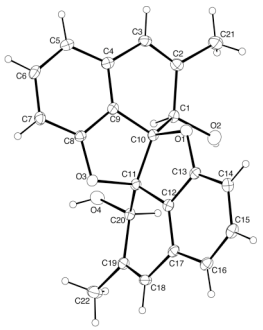

Figure B.3 ORTEP drawing of *rac*-**2.21** with 30% probability thermal ellipsoids.

Table B.13 Summary of Structure Determination of Compound *rac*-**2.21.**

Empirical formula	$C_{22}H_{18}O_4$
Formula weight	346.36
Temperature	143(1) K
Wavelength	0.71073 Å
Crystal system	monoclinic
Space group	$P2_1/c$
Cell constants:	
a	12.1645(13) Å
b	6.6205(6) Å
c	20.4873(17) Å
b	102.566(5)°
Volume	1610.4(3) $Å^3$
Z	4
Density (calculated)	1.429 Mg/m^3
Absorption coefficient	0.098 mm^{-1}
F(000)	728
Crystal size	0.18 x 0.13 x 0.07 mm^3
Theta range for data collection	1.72 to 25.09°
Index ranges	$-14 \le h \le 14, 0 \le k \le 7, 0 \le l \le 24$
Reflections collected	2861
Independent reflections	2861 [R(int) = 0.0000]
Completeness to theta = 25.09°	99.6 %
Absorption correction	Semi-empirical from equivalents
Max. and min. transmission	0.7452 and 0.6490
Refinement method	Full-matrix least-squares on F^2
Data / restraints / parameters	2861 / 0 / 241
Goodness-of-fit on F^2	1.065
Final R indices [I>2sigma(I)]	R1 = 0.0392, wR2 = 0.0884
R indices (all data)	R1 = 0.0504, wR2 = 0.0929
Largest diff. peak and hole	0.179 and -0.283 e.$Å^{-3}$\

Table B.14 Refined Positional Parameters for Compound *rac*-**2.21.**

Atom	x	y	z	U_{eq}, Å^2
C1	0.87876(18)	0.0796(4)	0.56807(11)	0.0212(5)
C2	0.89212(18)	-0.0114(4)	0.63841(11)	0.0238(5)
C3	0.84453(18)	0.0789(4)	0.68369(11)	0.0243(5)
C4	0.77393(18)	0.2590(3)	0.66666(11)	0.0221(5)
C5	0.74163(19)	0.3996(4)	0.70959(11)	0.0255(5)
C6	0.6783(2)	0.5676(4)	0.68356(11)	0.0262(5)
C7	0.64753(19)	0.6083(4)	0.61545(11)	0.0241(5)
C8	0.68156(18)	0.4683(3)	0.57344(11)	0.0201(5)
C9	0.73737(18)	0.2969(3)	0.59901(11)	0.0194(5)
C10	0.76226(17)	0.1694(3)	0.54454(10)	0.0188(5)
C11	0.73194(18)	0.3145(3)	0.48288(10)	0.0191(5)
C12	0.65763(17)	0.1864(3)	0.43306(11)	0.0192(5)
C13	0.63032(18)	0.0125(3)	0.46205(11)	0.0198(5)
C14	0.55910(18)	-0.1291(4)	0.42443(11)	0.0238(5)
C15	0.52261(19)	-0.0860(4)	0.35672(11)	0.0254(5)
C16	0.55637(19)	0.0855(4)	0.32665(11)	0.0250(5)
C17	0.62763(18)	0.2267(3)	0.36531(11)	0.0210(5)
C18	0.67814(19)	0.4084(4)	0.34307(11)	0.0235(5)
C19	0.76642(19)	0.4995(3)	0.38275(11)	0.0221(5)
C20	0.82062(17)	0.4088(3)	0.45110(10)	0.0204(5)
C21	0.9651(2)	-0.1957(4)	0.65447(12)	0.0373(7)
C22	0.8213(2)	0.6838(4)	0.36137(12)	0.0334(6)
O1	0.68178(12)	-0.0024(2)	0.52849(7)	0.0214(4)
O2	0.90591(14)	-0.0581(3)	0.52063(8)	0.0308(4)
O3	0.66713(13)	0.4820(2)	0.50533(7)	0.0228(4)
O4	0.89166(14)	0.5431(3)	0.49468(9)	0.0320(4)

$U_{eq}={}^1/_3[U_{11}(aa^*)^2+U_{22}(bb^*)^2+U_{33}(cc^*)^2+2U_{12}aa^*bb^*\cos\gamma+2U_{13}aa^*cc^*\cos\beta+2U_{23}bb^*cc^*\cos\alpha]$

Table B.15 Positional Parameters for Hydrogens in Compound *rac*-**2.21**.

Atom	x	y	z	U_{iso}, Å^2
H1	0.9325	0.1916	0.5719	0.028
H3	0.8564	0.0266	0.7268	0.032
H5	0.7624	0.3811	0.7556	0.034
H6	0.6555	0.6568	0.7131	0.035
H7	0.6065	0.7228	0.5990	0.032
H14	0.5372	-0.2458	0.4434	0.032
H15	0.4734	-0.1758	0.3302	0.034
H16	0.5314	0.1059	0.2809	0.033
H18	0.6485	0.4612	0.3008	0.031
H20	0.8687	0.2978	0.4423	0.027
H21a	0.9730	-0.2295	0.7008	0.056
H21b	1.0380	-0.1686	0.6456	0.056
H21c	0.9310	-0.3066	0.6273	0.056
H22a	0.7844	0.7194	0.3165	0.050
H22b	0.8994	0.6561	0.3630	0.050
H22c	0.8153	0.7939	0.3909	0.050
H2	0.9708	-0.0383	0.5168	0.046
H4	0.8595	0.6517	0.4953	0.048

Table B.16 Refined Thermal Parameters (U's) for Compound *rac*-**2.21**.

Atom	U_{11}	U_{22}	U_{33}	U_{23}	U_{13}	U_{12}
C1	0.0207(11)	0.0206(12)	0.0221(12)	-0.0037(9)	0.0042(9)	0.0003(9)
C2	0.0197(11)	0.0256(12)	0.0234(12)	0.0019(10)	-0.0014(9)	-0.0010(10)
C3	0.0254(12)	0.0272(13)	0.0182(11)	0.0035(10)	0.0006(10)	0.0001(10)
C4	0.0199(11)	0.0254(12)	0.0208(12)	-0.0006(9)	0.0040(9)	-0.0068(10)
C5	0.0257(12)	0.0324(14)	0.0185(12)	-0.0005(11)	0.0051(9)	-0.0034(11)
C6	0.0298(12)	0.0268(13)	0.0242(12)	-0.0076(10)	0.0106(10)	-0.0009(10)
C7	0.0248(12)	0.0216(12)	0.0273(13)	-0.0012(10)	0.0085(10)	0.0016(10)
C8	0.0206(11)	0.0221(12)	0.0178(11)	0.0000(9)	0.0047(9)	-0.0029(9)
C9	0.0185(11)	0.0206(12)	0.0201(11)	-0.0023(9)	0.0064(9)	-0.0034(9)
C10	0.0171(11)	0.0191(11)	0.0197(12)	-0.0012(9)	0.0031(9)	-0.0035(9)
C11	0.0186(11)	0.0195(12)	0.0194(11)	-0.0013(9)	0.0045(9)	0.0038(9)
C12	0.0151(11)	0.0211(12)	0.0219(11)	-0.0022(10)	0.0048(9)	0.0009(9)
C13	0.0164(10)	0.0234(12)	0.0204(12)	-0.0025(10)	0.0058(9)	0.0020(9)
C14	0.0188(11)	0.0228(13)	0.0296(13)	-0.0021(10)	0.0045(10)	-0.0013(10)
C15	0.0178(11)	0.0297(13)	0.0271(12)	-0.0079(10)	0.0013(9)	-0.0029(10)
C16	0.0208(11)	0.0314(14)	0.0215(12)	-0.0044(11)	0.0017(9)	0.0031(10)
C17	0.0183(11)	0.0251(12)	0.0197(12)	-0.0029(9)	0.0047(9)	0.0027(9)
C18	0.0275(12)	0.0258(12)	0.0177(11)	0.0036(10)	0.0057(10)	0.0038(10)
C19	0.0236(11)	0.0216(12)	0.0219(12)	0.0002(10)	0.0068(9)	0.0016(10)
C20	0.0203(11)	0.0193(12)	0.0218(12)	-0.0031(10)	0.0053(9)	-0.0014(9)
C21	0.0436(15)	0.0372(16)	0.0280(14)	0.0050(12)	0.0012(12)	0.0143(12)
C22	0.0389(14)	0.0332(15)	0.0266(13)	0.0071(11)	0.0035(11)	-0.0058(12)
O1	0.0216(8)	0.0210(9)	0.0205(8)	0.0015(7)	0.0023(6)	-0.0042(7)
O2	0.0298(9)	0.0343(10)	0.0312(10)	-0.0015(8)	0.0127(8)	0.0092(8)
O3	0.0280(8)	0.0220(9)	0.0185(8)	-0.0008(7)	0.0052(6)	0.0060(7)
O4	0.0350(10)	0.0278(10)	0.0288(9)	0.0009(8)	-0.0024(8)	-0.0124(8)

The form of the anisotropic displacement parameter is:
$\exp[-2\pi^2(a^{*2}U_{11}h^2+b^{*2}U_{22}k^2+c^{*2}U_{33}l^2+2b^*c^*U_{23}kl+2a^*c^*U_{13}hl+2a^*b^*U_{12}hk)]$

Table B.17 Bond Distances in Compound *rac*-**2.21**, Å.

C1-O2	1.423(3)	C1-C10	1.516(3)	C1-C2	1.538(3)
C2-C3	1.337(3)	C2-C21	1.502(3)	C3-C4	1.467(3)
C4-C9	1.383(3)	C4-C5	1.394(3)	C5-C6	1.391(3)
C6-C7	1.390(3)	C7-C8	1.388(3)	C8-C9	1.367(3)
C8-O3	1.371(3)	C9-C10	1.482(3)	C10-O1	1.490(3)
C10-C11	1.566(3)	C11-C12	1.475(3)	C11-O3	1.490(3)
C11-C20	1.511(3)	C12-C13	1.369(3)	C12-C17	1.382(3)
C13-O1	1.372(3)	C13-C14	1.390(3)	C14-C15	1.391(3)
C15-C16	1.396(3)	C16-C17	1.398(3)	C17-C18	1.468(3)
C18-C19	1.341(3)	C19-C22	1.502(3)	C19-C20	1.534(3)
C20-O4	1.414(3)				

Table B.18 Bond Angles in Compound *rac*-**2.21**, °

O2-C1-C10	111.96(17)	O2-C1-C2	113.33(19)	C10-C1-C2	110.66(18)
C3-C2-C21	122.4(2)	C3-C2-C1	120.1(2)	C21-C2-C1	117.4(2)
C2-C3-C4	121.2(2)	C9-C4-C5	116.0(2)	C9-C4-C3	115.4(2)
C5-C4-C3	128.6(2)	C6-C5-C4	120.0(2)	C7-C6-C5	123.1(2)
C8-C7-C6	116.2(2)	C9-C8-O3	112.82(19)	C9-C8-C7	120.5(2)
O3-C8-C7	126.7(2)	C8-C9-C4	124.0(2)	C8-C9-C10	110.50(19)
C4-C9-C10	125.3(2)	C9-C10-O1	111.64(17)	C9-C10-C1	108.29(17)
O1-C10-C1	107.15(17)	C9-C10-C11	101.96(18)	O1-C10-C11	105.20(15)
C1-C10-C11	122.49(19)	C12-C11-O3	110.83(17)	C12-C11-C20	109.07(17)
O3-C11-C20	107.52(17)	C12-C11-C10	101.93(17)	O3-C11-C10	104.79(16)
C20-C11-C10	122.41(18)	C13-C12-C17	124.2(2)	C13-C12-C11	110.69(19)
C17-C12-C11	124.9(2)	C12-C13-O1	112.91(19)	C12-C13-C14	120.5(2)
O1-C13-C14	126.6(2)	C13-C14-C15	116.1(2)	C14-C15-C16	123.1(2)
C15-C16-C17	120.0(2)	C12-C17-C16	115.8(2)	C12-C17-C18	115.65(19)
C16-C17-C18	128.5(2)	C19-C18-C17	121.0(2)	C18-C19-C22	122.5(2)
C18-C19-C20	120.4(2)	C22-C19-C20	117.01(19)	O4-C20-C11	112.53(18)
O4-C20-C19	114.35(18)	C11-C20-C19	110.46(17)	C13-O1-C10	107.45(16)
C8-O3-C11	107.80(16)				

B.4 X-ray Structure Determination of Compound 4.24b

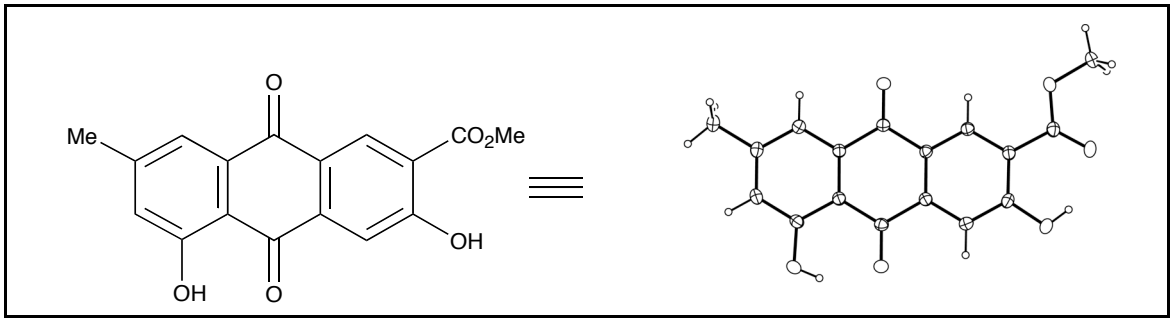

Compound **4.24b**, $C_{17}H_{12}O_6$, crystallizes in the monoclinic space group $P2_1/c$ (systematic absences 0k0: k=odd and h0l: l=odd) with a=5.7281(9)Å, b=26.834(4)Å, c=8.6983(14)Å, β=97.977(4)°, V=1324.1(4)Å^3, Z=4, and d_{calc}=1.566 g/cm^3. X-ray intensity data were collected on a Rigaku Mercury CCD area detector employing graphite-monochromated Mo-Kα radiation (λ=0.71073 Å) at a temperature of 143(1)K. Preliminary indexing was performed from a series of twelve 0.5° rotation images with exposures of 30 seconds. A total of 860 rotation images were collected with a crystal to detector distance of 35 mm, a 2θ swing angle of -12°, rotation widths of 0.5° and exposures of 30 seconds:

scan no.	scan type	ω	χ	ϕ
1	ϕ	10.0	20.0	45.0 — 315.0
2	ω	-20.0 — +20.0	-90.0	0.0
3	ω	-20.0 — +20.0	-90.0	45.0
4	ω	-20.0 — +20.0	-90.0	225.0
5	ω	-20.0 — +20.0	-90.0	315.0

Rotation images were processed using CrystalClear[152], producing a listing of unaveraged F^2 and $\sigma(F^2)$ values which were then passed to the CrystalStructure[153] program package for further processing and structure solution on a Dell Pentium 4

(152) CrystalClear: Rigaku Corporation, 1999.

(153) CrystalStructure: Crystal Structure Analysis Package, Rigaku Corp. Rigaku/MSC (2002).

computer. A total of 14179 reflections were measured over the ranges $2.81 \leq \theta \leq 25.01°$, $-6 \leq h \leq 5$, $-31 \leq k \leq 31$, $-10 \leq l \leq 10$ yielding 2327 unique reflections (Rint = 0.0266). The intensity data were corrected for Lorentz and polarization effects and for absorption using REQAB[154] (minimum and maximum transmission 0.8845, 1.0000).

The structure was solved by direct methods (SIR97[155]). Refinement was by full-matrix least squares based on F^2 using SHELXL-97.[147] All reflections were used during refinement. The weighting scheme used was $w=1/[\sigma^2(F_o^2)+ (0.0831P)^2 + 0.3930P]$ where $P = (F_o^2 + 2F_c^2)/3$. Non-hydrogen atoms were refined anisotropically and hydrogen atoms were refined using a riding model. Refinement converged to R1=0.0478 and wR2=0.1310 for 2022 observed reflections for which $F > 4\sigma(F)$ and R1=0.0529 and wR2=0.1363 and GOF =1.068 for all 2327 unique, non-zero reflections and 213 variables.[148] The maximum Δ/σ in the final cycle of least squares was 0.008 and the two most prominent peaks in the final difference Fourier were +0.325 and -0.220 e/Å^3.

Table B.19 lists cell information, data collection parameters, and refinement data. Final positional and equivalent isotropic thermal parameters are given in Table B.20 and Table B.21. Anisotropic thermal parameters are in Table B.22. Table B.23 and Table B.24 list bond distances and bond angles. Figure B.4 is an ORTEP[149] representation of the molecule with 30% probability thermal ellipsoids displayed.

(154) REQAB4: R.A. Jacobsen, (1994). Private Communication.

(155) SIR97: Altomare, A., M. Burla, M. Camalli, G. Cascarano, C. Giacovazzo, A. Guagliardi, A. Moliterni, G. Polidori & R. Spagna (1999). J. Appl. Cryst., 32, 115-119.

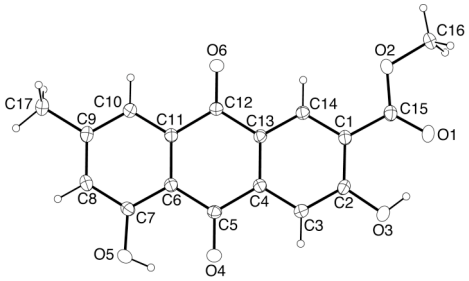

Figure B.4 ORTEP drawing of compound **4.24b** with 30% probability thermal ellipsoids.

Table B.19 Summary of Structure Determination of Compound **4.24b**

Empirical formula	$C_{17}H_{12}O_6$
Formula weight	312.27
Temperature	143(1) K
Wavelength	0.71073 Å
Crystal system	monoclinic
Space group	$P2_1/c$
Cell constants:	
a	5.7281(9) Å
b	26.834(4) Å
c	8.6983(14) Å
b	97.977(4)°
Volume	1324.1(4) $Å^3$
Z	4
Density (calculated)	1.566 Mg/m^3
Absorption coefficient	0.120 mm^{-1}
F(000)	648
Crystal size	0.32 x 0.18 x 0.08 mm^3
Theta range for data collection	2.81 to 25.01°
Index ranges	$-6 \le h \le 5$, $-31 \le k \le 31$, $-10 \le l \le 10$
Reflections collected	14179
Independent reflections	2327 [R(int) = 0.0266]
Completeness to theta = 25.01°	99.8 %
Absorption correction	Semi-empirical from equivalents
Max. and min. transmission	1.0000 and 0.8845
Refinement method	Full-matrix least-squares on F^2
Data / restraints / parameters	2327 / 0 / 213
Goodness-of-fit on F^2	1.068
Final R indices [I>2sigma(I)]	R1 = 0.0478, wR2 = 0.1310
R indices (all data)	R1 = 0.0529, wR2 = 0.1363
Largest diff. peak and hole	0.325 and -0.220 $e.Å^{-3}$

Table B.20 Refined Positional Parameters for Compound **4.24b**.

Atom	x	y	z	U_{eq}, Å^2
C1	0.4721(3)	0.35044(6)	0.18491(19)	0.0270(4)
C2	0.2826(3)	0.34122(6)	0.26880(19)	0.0284(4)
C3	0.2120(3)	0.29260(6)	0.29387(18)	0.0283(4)
C4	0.3311(3)	0.25302(6)	0.23825(18)	0.0253(4)
C5	0.2626(3)	0.20117(6)	0.27457(18)	0.0263(4)
C6	0.3981(3)	0.15980(6)	0.22189(17)	0.0254(4)
C7	0.3447(3)	0.11054(6)	0.25951(18)	0.0281(4)
C8	0.4734(3)	0.07100(6)	0.20833(19)	0.0304(4)
C9	0.6542(3)	0.07944(6)	0.12193(19)	0.0293(4)
C10	0.7094(3)	0.12854(6)	0.08501(19)	0.0286(4)
C11	0.5840(3)	0.16799(6)	0.13468(17)	0.0250(4)
C12	0.6514(3)	0.21972(6)	0.09585(18)	0.0266(4)
C13	0.5210(3)	0.26145(6)	0.15466(18)	0.0249(4)
C14	0.5889(3)	0.30997(6)	0.12875(18)	0.0265(4)
C15	0.5473(3)	0.40211(6)	0.16207(19)	0.0296(4)
C16	0.8159(3)	0.45534(6)	0.0615(2)	0.0386(4)
C17	0.7959(3)	0.03690(6)	0.0705(2)	0.0369(4)
O1	0.4571(2)	0.43846(4)	0.21487(15)	0.0398(4)
O2	0.7240(2)	0.40579(4)	0.07922(14)	0.0337(3)
O3	0.1654(2)	0.37838(5)	0.32953(15)	0.0380(3)
O4	0.0982(2)	0.19378(4)	0.34974(14)	0.0345(3)
O5	0.1754(2)	0.09968(5)	0.34731(15)	0.0365(3)
O6	0.8100(2)	0.22713(5)	0.01845(15)	0.0388(4)

$U_{eq}={}^1/_3[U_{11}(aa^*)^2+U_{22}(bb^*)^2+U_{33}(cc^*)^2+2U_{12}aa^*bb^*\cos\gamma+2U_{13}aa^*cc^*\cos\beta+2U_{23}bb^*cc^*\cos\alpha]$

Table B.21 Positional Parameters for Hydrogens in Compound **4.24b.**

Atom	x	y	z	U_{iso}, Å^2
H3	0.0854	0.2867	0.3477	0.038
H8	0.4365	0.0385	0.2330	0.040
H10	0.8310	0.1346	0.0269	0.038
H14	0.7139	0.3157	0.0733	0.035
H16a	0.6945	0.4760	0.0072	0.058

H16b	0.9465	0.4536	0.0034	0.058
H16c	0.8678	0.4693	0.1620	0.058
H17a	0.7376	0.0060	0.1058	0.055
H17b	0.9584	0.0409	0.1135	0.055
H17c	0.7822	0.0366	-0.0408	0.055
H3A	0.2225	0.4053	0.3098	0.057
H5	0.1077	0.1254	0.3667	0.055

Table B.22 Refined Thermal Parameters (U's) for Compound **4.24b**.

Atom	U_{11}	U_{22}	U_{33}	U_{23}	U_{13}	U_{12}
C1	0.0315(8)	0.0236(9)	0.0256(8)	0.0000(6)	0.0029(6)	0.0004(6)
C2	0.0326(8)	0.0255(9)	0.0272(8)	-0.0033(7)	0.0045(6)	0.0048(6)
C3	0.0278(8)	0.0301(9)	0.0277(9)	-0.0009(7)	0.0065(6)	0.0007(6)
C4	0.0271(8)	0.0249(9)	0.0236(8)	-0.0003(6)	0.0027(6)	-0.0007(6)
C5	0.0272(8)	0.0286(9)	0.0232(8)	0.0003(6)	0.0047(6)	-0.0012(6)
C6	0.0291(8)	0.0246(8)	0.0223(8)	-0.0004(6)	0.0031(6)	-0.0007(6)
C7	0.0312(8)	0.0275(9)	0.0258(8)	0.0013(7)	0.0049(6)	-0.0042(6)
C8	0.0361(9)	0.0225(8)	0.0319(9)	0.0016(7)	0.0024(7)	-0.0019(6)
C9	0.0339(9)	0.0249(9)	0.0283(9)	-0.0023(7)	0.0012(6)	0.0023(6)
C10	0.0308(8)	0.0267(9)	0.0290(8)	-0.0011(7)	0.0062(6)	0.0006(6)
C11	0.0279(8)	0.0246(9)	0.0224(8)	0.0003(6)	0.0026(6)	0.0002(6)
C12	0.0291(8)	0.0261(9)	0.0253(8)	0.0006(6)	0.0067(6)	0.0004(6)
C13	0.0279(8)	0.0241(9)	0.0231(8)	-0.0002(6)	0.0042(6)	0.0013(6)
C14	0.0293(8)	0.0264(9)	0.0243(8)	-0.0003(6)	0.0050(6)	0.0005(6)
C15	0.0359(9)	0.0249(9)	0.0275(9)	-0.0013(7)	0.0026(7)	0.0005(7)
C16	0.0462(10)	0.0231(9)	0.0487(11)	0.0005(8)	0.0142(8)	-0.0051(7)
C17	0.0427(10)	0.0255(9)	0.0429(10)	-0.0022(8)	0.0070(8)	0.0037(7)
O1	0.0514(8)	0.0226(7)	0.0480(8)	-0.0048(5)	0.0159(6)	0.0020(5)
O2	0.0412(7)	0.0212(6)	0.0407(7)	0.0000(5)	0.0133(5)	-0.0024(5)
O3	0.0427(7)	0.0258(7)	0.0487(8)	-0.0054(6)	0.0179(6)	0.0040(5)
O4	0.0356(7)	0.0313(7)	0.0400(7)	-0.0004(5)	0.0170(5)	-0.0019(5)
O5	0.0412(7)	0.0287(7)	0.0430(8)	0.0038(5)	0.0180(5)	-0.0036(5)
O6	0.0443(7)	0.0287(7)	0.0494(8)	0.0027(6)	0.0273(6)	0.0012(5)

The form of the anisotropic displacement parameter is:
$\exp[-2\pi^2(a^{*2}U_{11}h^2+b^{*2}U_{22}k^2+c^{*2}U_{33}l^2+2b^*c^*U_{23}kl+2a^*c^*U_{13}hl+2a^*b^*U_{12}hk)]$

Table B.23 Bond Distances in Compound **4.24b**, Å

C1-C14	1.399(2)	C1-C2	1.411(2)	C1-C15	1.474(2)
C2-O3	1.3499(19)	C2-C3	1.392(2)	C3-C4	1.385(2)
C4-C13	1.408(2)	C4-C5	1.491(2)	C5-O4	1.2346(19)
C5-C6	1.464(2)	C6-C7	1.405(2)	C6-C11	1.408(2)
C7-O5	1.3468(19)	C7-C8	1.400(2)	C8-C9	1.380(2)
C9-C10	1.403(2)	C9-C17	1.504(2)	C10-C11	1.382(2)
C11-C12	1.492(2)	C12-O6	1.2198(19)	C12-C13	1.476(2)
C13-C14	1.386(2)	C15-O1	1.223(2)	C15-O2	1.325(2)
C16-O2	1.446(2)				

Table B.24 Bond Angles in Compound **4.24b**, °

C14-C1-C2	118.95(15)	C14-C1-C15	121.36(15)	C2-C1-C15	119.67(14)
O3-C2-C3	117.39(15)	O3-C2-C1	122.18(15)	C3-C2-C1	120.42(14)
C4-C3-C2	119.74(15)	C3-C4-C13	120.68(15)	C3-C4-C5	118.98(14)
C13-C4-C5	120.28(14)	O4-C5-C6	121.36(15)	O4-C5-C4	120.29(14)
C6-C5-C4	118.33(13)	C7-C6-C11	118.53(14)	C7-C6-C5	119.89(14)
C11-C6-C5	121.58(14)	O5-C7-C8	117.95(15)	O5-C7-C6	122.18(15)
C8-C7-C6	119.85(15)	C9-C8-C7	121.13(15)	C8-C9-C10	119.28(15)
C8-C9-C17	120.95(15)	C10-C9-C17	119.75(15)	C11-C10-C9	120.28(15)
C10-C11-C6	120.92(15)	C10-C11-C12	118.66(14)	C6-C11-C12	120.41(14)
O6-C12-C13	121.26(15)	O6-C12-C11	120.84(14)	C13-C12-C11	117.89(13)
C14-C13-C4	119.30(15)	C14-C13-C12	119.28(14)	C4-C13-C12	121.42(14)
C13-C14-C1	120.91(15)	O1-C15-O2	122.65(15)	O1-C15-C1	123.58(15)
O2-C15-C1	113.77(14)	C15-O2-C16	116.32(13)		

B.5 X-ray Structure Determination of Compound *rac*-5.2

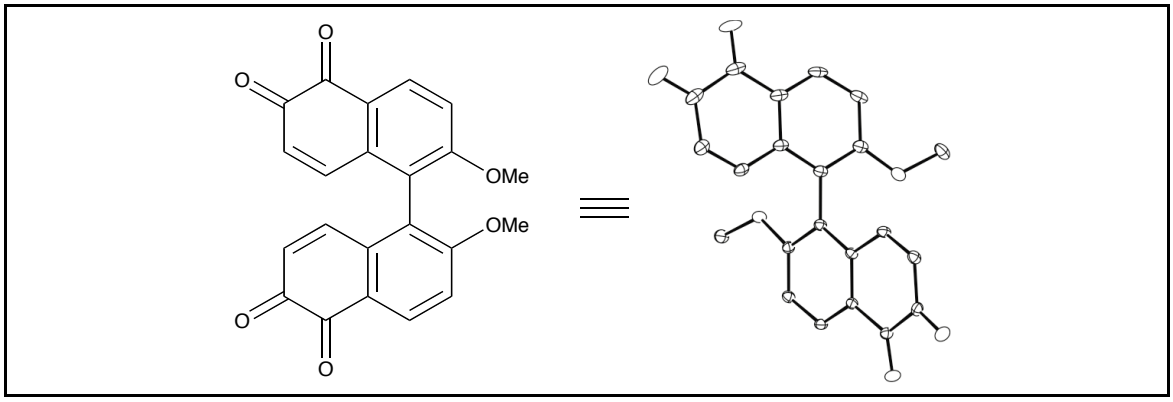

Compound *rac*-**5.2**, $C_{23}H_{16}O_6Cl_2$, crystallizes in the triclinic space group PT with a=8.8157(3)Å, b=10.5756(3)Å, c=12.1409(4)Å, α=70.4850(10)°, β=73.3250(10)°, γ=86.9450(10)°, V=1020.89(6)Å^3, Z=2, and d_{calc}=1.494 g/cm^3. X-ray intensity data were collected on a Bruker APEXII CCD area detector employing graphite-monochromated Mo-Kα radiation (λ=0.71073 Å) at a temperature of 143(1)K. Preliminary indexing was performed from a series of thirty-six 0.5° rotation frames with exposures of 10 seconds. A total of 2348 frames were collected with a crystal to detector distance of 37.628 mm, rotation widths of 0.5° and exposures of 20 seconds:

scan type	2θ	ω	ϕ	χ	frames
ϕ	-23.00	315.83	-347.52	28.88	739
ϕ	-15.50	258.48	-287.21	19.46	600
ϕ	9.50	319.15	14.56	27.01	645
ϕ	19.50	59.55	-11.29	-26.26	739
ϕ	-13.00	-24.58	-328.16	64.29	739
ω	-15.50	-19.20	-18.89	-63.64	91

Rotation frames were integrated using SAINT[144], producing a listing of unaveraged F^2 and $\sigma(F^2)$ values which were then passed to the SHELXTL[145] program package for further processing and structure solution. A total of 33038 reflections were measured over the ranges $1.86 \le \theta \le 25.38°$, $-10 \le h \le 10$, $-12 \le k \le 12$, $-14 \le l \le 14$ yielding 3722 unique reflections (Rint = 0.0205). The intensity data were corrected for

Lorentz and polarization effects and for absorption using SADABS[146] (minimum and maximum transmission 0.7006, 0.7452).

The structure was solved by direct methods (SHELXS-97[147]). There was a region of disordered solvent for which a reliable disorder model could not be devised; the X-ray data were corrected for the presence of disordered solvent using SQUEEZE[156]. Refinement was by full-matrix least squares based on F^2 using SHELXL-97.[147] All reflections were used during refinement. The weighting scheme used was $w=1/[\sigma^2(F_o^2)+(0.0753P)^2 + 1.4779P]$ where $P = (F_o^2 + 2F_c^2)/3$. Non-hydrogen atoms were refined anisotropically and hydrogen atoms were refined using a riding model. Refinement converged to R1=0.0611 and wR2=0.1673 for 3347 observed reflections for which $F > 4\sigma(F)$ and R1=0.0650 and wR2=0.1699 and GOF =1.051 for all 3722 unique, non-zero reflections and 256 variables.[148] The maximum Δ/σ in the final cycle of least squares was 0.000 and the two most prominent peaks in the final difference Fourier were +0.852 and -0.285 e/Å^3.

Table B.25 lists cell information, data collection parameters, and refinement data. Final positional and equivalent isotropic thermal parameters are given in Table B.26 and Table B.27. Anisotropic thermal parameters are in Table B.28. Table B.29 and Table B.30 list bond distances and bond angles. Figure B.5 is an ORTEP[149] representation of the molecule with 30% probability thermal ellipsoids displayed.

(156) v.d. Sluis, P. & A.L. Spek (1990). *Acta. Cryst.*, **A46**, 194.

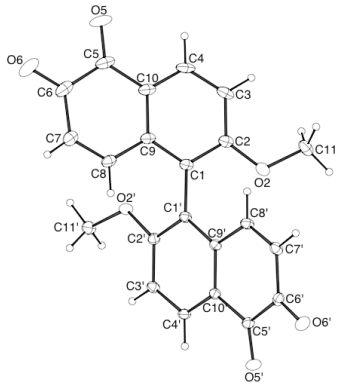

Figure B.5 ORTEP drawing of *rac*-**5.2** with 30% probability thermal ellipsoids.

Table B.25 Summary of Structure Determination of Compound *rac*-**5.2.**

Empirical formula	$C_{23}H_{16}O_6Cl_2$
Formula weight	459.26
Temperature	143(1) K
Wavelength	0.71073 Å
Crystal system	triclinic
Space group	$P\bar{1}$
Cell constants:	
a	8.8157(3) Å
b	10.5756(3) Å
c	12.1409(4) Å
a	70.4850(10)°
b	73.3250(10)°
g	86.9450(10)°
Volume	1020.89(6) $Å^3$
Z	2
Density (calculated)	1.494 Mg/m^3
Absorption coefficient	0.358 mm^{-1}
F(000)	472
Crystal size	0.38 x 0.30 x 0.20 mm^3
Theta range for data collection	1.86 to 25.38°
Index ranges	$-10 \le h \le 10$, $-12 \le k \le 12$, $-14 \le l \le 14$
Reflections collected	33038
Independent reflections	3722 [R(int) = 0.0205]
Completeness to theta = 25.38°	99.1 %
Absorption correction	Semi-empirical from equivalents
Max. and min. transmission	0.7452 and 0.7006
Refinement method	Full-matrix least-squares on F^2

Data / restraints / parameters	3722 / 0 / 256
Goodness-of-fit on F^2	1.051
Final R indices [I>2sigma(I)]	R1 = 0.0611, wR2 = 0.1673
R indices (all data)	R1 = 0.0650, wR2 = 0.1699
Largest diff. peak and hole	0.852 and -0.285 e.$Å^{-3}$

Table B.26 Refined Positional Parameters for Compound *rac*-**5.2.**

Atom	x	Y	z	U_{eq}, $Å^2$
C1	0.6666(3)	0.3539(2)	0.1573(2)	0.0214(5)
C2	0.6557(3)	0.3859(2)	0.0375(2)	0.0242(5)
C3	0.7311(3)	0.5038(2)	-0.0542(2)	0.0288(5)
C4	0.8180(3)	0.5874(2)	-0.0258(2)	0.0317(6)
C5	0.9302(3)	0.6437(2)	0.1186(3)	0.0340(6)
C6	0.9519(3)	0.5978(3)	0.2485(3)	0.0363(6)
C7	0.8801(3)	0.4682(2)	0.3325(2)	0.0304(5)
C8	0.7897(3)	0.3953(2)	0.3016(2)	0.0255(5)
C9	0.7629(3)	0.4351(2)	0.1818(2)	0.0239(5)
C10	0.8366(3)	0.5545(2)	0.0898(2)	0.0288(6)
C11	0.5636(3)	0.3152(3)	-0.1011(2)	0.0323(6)
O2	0.5676(2)	0.29758(16)	0.02042(14)	0.0270(4)
O5	0.9911(2)	0.75176(17)	0.0461(2)	0.0448(6)
O6	1.0271(2)	0.6706(2)	0.2750(2)	0.0519(6)
C1'	0.5617(2)	0.2411(2)	0.25711(19)	0.0195(4)
C2'	0.4378(3)	0.2748(2)	0.3446(2)	0.0197(4)
C3'	0.3274(3)	0.1776(2)	0.4346(2)	0.0207(5)
C4'	0.3398(3)	0.0458(2)	0.43662(19)	0.0208(5)
C5'	0.4702(3)	-0.1310(2)	0.3565(2)	0.0217(5)
C6'	0.6160(3)	-0.1685(2)	0.2693(2)	0.0218(5)
C7'	0.7252(3)	-0.0597(2)	0.1793(2)	0.0233(5)
C8'	0.7046(3)	0.0675(2)	0.1772(2)	0.0220(5)
C9'	0.5749(2)	0.1071(2)	0.26326(19)	0.0184(4)
C10'	0.4615(3)	0.0092(2)	0.35352(19)	0.0190(4)
C11'	0.3271(3)	0.4491(2)	0.4254(2)	0.0277(5)
O2'	0.43474(19)	0.40704(15)	0.33207(14)	0.0249(4)
O5'	0.3681(2)	-0.21824(16)	0.42276(16)	0.0320(4)
O6'	0.6348(2)	-0.28652(16)	0.27901(16)	0.0302(4)

$U_{eq}={}^1/_3[U_{11}(aa^*)^2+U_{22}(bb^*)^2+U_{33}(cc^*)^2+2U_{12}aa^*bb^*\cos\gamma+2U_{13}aa^*cc^*\cos\beta+2U_{23}bb^*cc^*\cos\alpha]$

Table B.27 Positional Parameters for Hydrogens in Compound *rac*-**5.2.**

Atom	x	y	z	U_{iso}, Å^2
H3	0.7227	0.5253	-0.1329	0.038
H4	0.8648	0.6672	-0.0856	0.042
H7	0.8971	0.4352	0.4090	0.040
H8	0.7416	0.3151	0.3598	0.034
H11a	0.5179	0.3991	-0.1330	0.048
H11b	0.5007	0.2430	-0.0997	0.048
H11c	0.6695	0.3154	-0.1520	0.048
H3'	0.2468	0.2009	0.4921	0.028
H4'	0.2650	-0.0193	0.4949	0.028
H7'	0.8106	-0.0787	0.1223	0.031
H8'	0.7768	0.1340	0.1178	0.029
H11a'	0.2200	0.4330	0.4273	0.042
H11b'	0.3461	0.5432	0.4083	0.042
H11c'	0.3429	0.3992	0.5030	0.042

Table B.28 Refined Thermal Parameters (U's) for Compound *rac*-**5.2.**

Atom	U_{11}	U_{22}	U_{33}	U_{23}	U_{13}	U_{12}
C1	0.0225(11)	0.0139(10)	0.0216(11)	-0.0043(9)	0.0005(9)	0.0046(8)
C2	0.0246(11)	0.0167(10)	0.0241(11)	-0.0045(9)	-0.0001(9)	0.0065(8)
C3	0.0315(12)	0.0207(11)	0.0204(11)	-0.0003(9)	0.0039(9)	0.0106(9)
C4	0.0275(12)	0.0152(11)	0.0325(13)	0.0008(10)	0.0107(10)	0.0036(9)
C5	0.0199(11)	0.0168(11)	0.0526(16)	-0.0117(11)	0.0088(11)	0.0015(9)
C6	0.0204(12)	0.0269(13)	0.0609(18)	-0.0240(13)	0.0006(11)	0.0004(10)
C7	0.0235(12)	0.0272(12)	0.0407(14)	-0.0167(11)	-0.0036(10)	0.0029(9)
C8	0.0213(11)	0.0174(11)	0.0337(13)	-0.0101(9)	-0.0001(9)	0.0010(8)
C9	0.0210(11)	0.0140(10)	0.0285(12)	-0.0064(9)	0.0038(9)	0.0028(8)
C10	0.0218(11)	0.0158(11)	0.0364(14)	-0.0064(10)	0.0074(10)	0.0021(9)
C11	0.0428(14)	0.0316(13)	0.0192(11)	-0.0064(10)	-0.0081(10)	0.0108(11)
O2	0.0354(9)	0.0224(8)	0.0190(8)	-0.0038(7)	-0.0057(7)	0.0047(7)
O5	0.0305(10)	0.0176(9)	0.0650(14)	-0.0098(9)	0.0152(9)	-0.0061(7)
O6	0.0390(11)	0.0382(11)	0.0840(17)	-0.0308(11)	-0.0113(11)	-0.0096(9)
C1'	0.0209(10)	0.0172(10)	0.0179(10)	-0.0036(8)	-0.0042(8)	0.0010(8)
C2'	0.0227(11)	0.0156(10)	0.0204(10)	-0.0051(8)	-0.0071(8)	0.0022(8)

C3'	0.0191(10)	0.0220(11)	0.0186(10)	-0.0064(9)	-0.0021(8)	0.0016(8)
C4'	0.0202(10)	0.0201(11)	0.0182(10)	-0.0027(8)	-0.0030(8)	-0.0039(8)
C5'	0.0263(11)	0.0172(11)	0.0202(11)	-0.0034(9)	-0.0074(9)	-0.0012(9)
C6'	0.0284(12)	0.0181(11)	0.0231(11)	-0.0073(9)	-0.0133(9)	0.0032(9)
C7'	0.0262(11)	0.0216(11)	0.0198(11)	-0.0069(9)	-0.0040(9)	0.0053(9)
C8'	0.0239(11)	0.0176(10)	0.0195(10)	-0.0018(9)	-0.0037(9)	0.0005(8)
C9'	0.0205(10)	0.0171(10)	0.0159(10)	-0.0026(8)	-0.0062(8)	0.0018(8)
C10'	0.0241(11)	0.0168(10)	0.0155(10)	-0.0030(8)	-0.0075(8)	0.0005(8)
C11'	0.0316(13)	0.0201(11)	0.0266(12)	-0.0097(10)	0.0006(10)	0.0038(9)
O2'	0.0305(9)	0.0141(7)	0.0233(8)	-0.0058(6)	0.0020(7)	0.0022(6)
O5'	0.0397(10)	0.0178(8)	0.0300(9)	-0.0045(7)	0.0001(8)	-0.0068(7)
O6'	0.0369(10)	0.0161(8)	0.0374(10)	-0.0098(7)	-0.0097(8)	0.0034(7)

The form of the anisotropic displacement parameter is:
$\exp[-2\pi^2(a^{*2}U_{11}h^2+b^{*2}U_{22}k^2+c^{*2}U_{33}l^2+2b^*c^*U_{23}kl+2a^*c^*U_{13}hl+2a^*b^*U_{12}hk)]$

Table B.29 Bond Distances in Compound *rac*-**5.2**, Å.

C1-C9	1.392(3)	C1-C2	1.410(3)	C1-C1'	1.502(3)
C2-O2	1.348(3)	C2-C3	1.404(3)	C3-C4	1.383(4)
C4-C10	1.385(4)	C5-O5	1.221(3)	C5-C10	1.471(4)
C5-C6	1.552(4)	C6-O6	1.216(3)	C6-C7	1.451(4)
C7-C8	1.342(3)	C8-C9	1.459(3)	C9-C10	1.412(3)
C11-O2	1.435(3)	C1'-C9'	1.395(3)	C1'-C2'	1.412(3)
C2'-O2'	1.355(3)	C2'-C3'	1.394(3)	C3'-C4'	1.385(3)
C4'-C10'	1.384(3)	C5'-O5'	1.219(3)	C5'-C10'	1.469(3)
C5'-C6'	1.541(3)	C6'-O6'	1.221(3)	C6'-C7'	1.456(3)
C7'-C8'	1.340(3)	C8'-C9'	1.460(3)	C9'-C10'	1.413(3)
C11'-O2'	1.434(3)				

Table B.30 Bond Angles in Compound *rac*-**5.2**, °

C9-C1-C2	119.2(2)	C9-C1-C1'	121.8(2)	C2-C1-C1'	118.7(2)
O2-C2-C3	124.2(2)	O2-C2-C1	115.28(19)	C3-C2-C1	120.5(2)
C4-C3-C2	119.2(2)	C3-C4-C10	121.3(2)	O5-C5-C10	123.5(3)
O5-C5-C6	118.5(2)	C10-C5-C6	118.0(2)	O6-C6-C7	123.3(3)
O6-C6-C5	119.2(3)	C7-C6-C5	117.5(2)	C8-C7-C6	121.1(3)
C7-C8-C9	123.5(2)	C1-C9-C10	119.9(2)	C1-C9-C8	119.9(2)
C10-C9-C8	120.2(2)	C4-C10-C9	119.7(2)	C4-C10-C5	120.8(2)
C9-C10-C5	119.5(2)	C2-O2-C11	118.80(18)	C9'-C1'-C2'	118.84(19)
C9'-C1'-C1	123.42(19)	C2'-C1'-C1	117.63(18)	O2'-C2'-C3'	123.86(19)
O2'-C2'-C1'	114.76(18)	C3'-C2'-C1'	121.37(19)	C4'-C3'-C2'	118.8(2)
C10'-C4'-C3'	121.2(2)	O5'-C5'-C10'	123.7(2)	O5'-C5'-C6'	118.51(19)
C10'-C5'-C6'	117.75(18)	O6'-C6'-C7'	123.4(2)	O6'-C6'-C5'	119.0(2)
C7'-C6'-C5'	117.58(18)	C8'-C7'-C6'	121.1(2)	C7'-C8'-C9'	123.4(2)
C1'-C9'-C10'	119.58(19)	C1'-C9'-C8'	120.51(19)	C10'-C9'-C8'	119.91(19)
C4'-C10'-C9'	120.16(19)	C4'-C10'-C5'	120.03(19)	C9'-C10'-C5'	119.78(19)
C2'-O2'-C11'	119.02(17)				

B.6 X-ray Structure Determination of Compound *rac*-6.35a

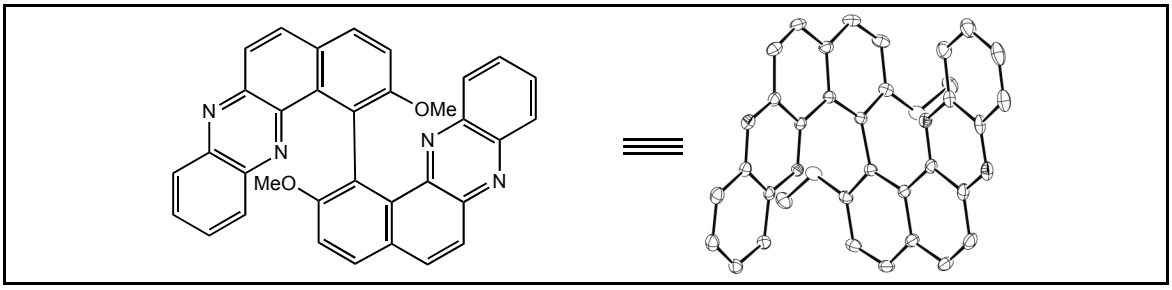

Compound *rac*-**6.35a**, $C_{34}H_{22}N_4O_2$, crystallizes in the orthorhombic space group Pbca (systematic absences hk0: h=odd, 0kl: k=odd, and h0l: l=odd) with a=11.7278(5)Å, b=18.4783(8)Å, c=23.7323(11)Å, V=5143.0(4)Å^3, Z=8, and d_{calc}=1.339 g/cm^3. X-ray intensity data were collected on a Bruker APEXII CCD area detector employing graphite-monochromated Mo-Kα radiation (λ=0.71073 Å) at a temperature of 143(1)K. Preliminary indexing was performed from a series of thirty-six 0.5° rotation frames with exposures of 10 seconds. A total of 1201 frames were collected with a crystal to detector distance of 37.542 mm, rotation widths of 0.5° and exposures of 20 seconds:

scan type	2θ	ω	ϕ	X	frames
ϕ	-15.50	258.48	8.28	19.46	739
ω	-5.50	57.85	351.14	-31.86	64
ω	-10.50	345.67	80.80	-60.33	101
ω	-15.50	340.80	341.11	-63.64	97
ϕ	22.00	14.84	76.38	97.50	200

Rotation frames were integrated using SAINT[144], producing a listing of unaveraged F^2 and $\sigma(F^2)$ values which were then passed to the SHELXTL[145] program package for further processing and structure solution. A total of 54071 reflections were measured over the ranges $1.72 \leq \theta \leq 25.09°$, $-13 \leq h \leq 13$, $-22 \leq k \leq 22$, $-28 \leq l \leq 28$ yielding 4571 unique reflections (Rint = 0.0262). The intensity data were corrected for Lorentz and polarization effects and for absorption using SADABS[146] (minimum and maximum transmission 0.6949, 0.7452).

The structure was solved by direct methods (SHELXS-97[147]). Refinement was by full-matrix least squares based on F^2 using SHELXL-97.[147] All reflections were used during refinement. The weighting scheme used was $w=1/[\sigma^2(F_o^2)+ (0.0436P)^2 + 1.8674P]$ where $P = (F_o^2 + 2F_c^2)/3$. Non-hydrogen atoms were refined anisotropically and hydrogen atoms were refined using a riding model. Refinement converged to R1=0.0334 and wR2=0.0824 for 3768 observed reflections for which $F > 4\sigma(F)$ and R1=0.0443 and wR2=0.0906 and GOF =1.039 for all 4571 unique, non-zero reflections and 364 variables.[148] The maximum Δ/σ in the final cycle of least squares was 0.001 and the two most prominent peaks in the final difference Fourier were +0.178 and -0.176 e/Å^3.

Table B.31 lists cell information, data collection parameters, and refinement data. Final positional and equivalent isotropic thermal parameters are given in Table B.32 and Table B.33. Anisotropic thermal parameters are in Table B.34. Table B.35 and Table B.36 list bond distances and bond angles. Figure B.6 is an ORTEP[149] representation of the molecule with 30% probability thermal ellipsoids displayed.

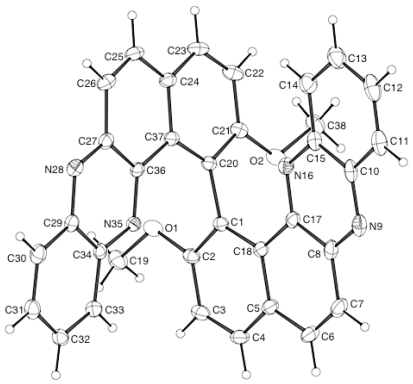

Figure B.6 ORTEP drawing of compound *rac*-**6.35a** with 30% probability thermal ellipsoids.

Table B.31 Summary of Structure Determination of Compound *rac*-**6.35a.**

Empirical formula	$C_{34}H_{22}N_4O_2$
Formula weight	518.56
Temperature	143(1) K
Wavelength	0.71073 Å
Crystal system	orthorhombic
Space group	Pbca
Cell constants:	
a	11.7278(5) Å
b	18.4783(8) Å
c	23.7323(11) Å
Volume	5143.0(4) $Å^3$
Z	8
Density (calculated)	1.339 Mg/m^3
Absorption coefficient	0.085 mm^{-1}
F(000)	2160
Crystal size	0.45 x 0.20 x 0.03 mm^3
Theta range for data collection	1.72 to 25.09°
Index ranges	$-13 \le h \le 13$, $-22 \le k \le 22$, $-28 \le l \le 28$
Reflections collected	54071
Independent reflections	4571 [R(int) = 0.0262]
Completeness to theta = 25.09°	100.0 %
Absorption correction	Semi-empirical from equivalents
Max. and min. transmission	0.7452 and 0.6949
Refinement method	Full-matrix least-squares on F^2
Data / restraints / parameters	4571 / 0 / 364
Goodness-of-fit on F^2	1.039
Final R indices [I>2sigma(I)]	R1 = 0.0334, wR2 = 0.0824
R indices (all data)	R1 = 0.0443, wR2 = 0.0906
Largest diff. peak and hole	0.178 and -0.176 $e.Å^{-3}$

Table B.32 Refined Positional Parameters for Compound *rac*-**6.35a.**

Atom	x	y	z	U_{eq}, Å^2
C1	0.50149(11)	0.69432(6)	0.65553(5)	0.0226(3)
C2	0.47972(11)	0.71386(7)	0.71121(6)	0.0255(3)
C3	0.37804(12)	0.69520(7)	0.73779(6)	0.0304(3)
C4	0.29758(12)	0.65718(8)	0.70843(6)	0.0332(3)
C5	0.31532(11)	0.63589(7)	0.65279(6)	0.0299(3)
C6	0.22972(12)	0.59493(9)	0.62377(7)	0.0390(4)
C7	0.24375(13)	0.57132(8)	0.57095(7)	0.0393(4)
C8	0.34740(12)	0.58643(7)	0.54116(6)	0.0307(3)
C10	0.45791(13)	0.57468(7)	0.46240(6)	0.0322(3)
C11	0.47606(15)	0.54730(8)	0.40755(7)	0.0411(4)
C12	0.57273(16)	0.56379(9)	0.37943(7)	0.0470(4)
C13	0.65710(15)	0.60823(10)	0.40399(7)	0.0455(4)
C14	0.64288(13)	0.63531(9)	0.45702(6)	0.0395(4)
C15	0.54277(12)	0.61892(7)	0.48749(6)	0.0295(3)
C17	0.43481(11)	0.62949(7)	0.56755(6)	0.0255(3)
C18	0.41899(11)	0.65472(7)	0.62543(6)	0.0243(3)
C19	0.55217(14)	0.76632(9)	0.79606(6)	0.0384(4)
C20	0.61221(11)	0.71835(7)	0.63020(5)	0.0220(3)
C21	0.61377(12)	0.78617(7)	0.60467(6)	0.0267(3)
C22	0.71075(13)	0.81231(8)	0.57778(6)	0.0337(3)
C23	0.80542(12)	0.76907(8)	0.57423(6)	0.0341(3)
C24	0.80752(11)	0.70010(7)	0.59823(6)	0.0273(3)
C25	0.90511(12)	0.65417(8)	0.59090(6)	0.0314(3)
C26	0.90880(12)	0.58651(8)	0.61132(6)	0.0316(3)
C27	0.81672(11)	0.55918(7)	0.64456(6)	0.0262(3)
C29	0.74334(11)	0.47153(7)	0.70239(6)	0.0262(3)
C30	0.75039(13)	0.40298(8)	0.72884(6)	0.0334(3)
C31	0.66962(13)	0.38292(8)	0.76680(6)	0.0341(3)
C32	0.57689(12)	0.42845(8)	0.77972(6)	0.0310(3)
C33	0.56633(11)	0.49409(7)	0.75416(6)	0.0280(3)
C34	0.64952(11)	0.51707(7)	0.71483(5)	0.0231(3)
C36	0.71877(10)	0.60414(7)	0.65497(5)	0.0217(3)
C37	0.71095(11)	0.67539(7)	0.62859(5)	0.0226(3)
C38	0.50381(14)	0.88596(8)	0.57144(7)	0.0399(4)
N9	0.35959(11)	0.55963(6)	0.48954(5)	0.0345(3)
N16	0.52946(9)	0.64575(6)	0.53993(5)	0.0278(3)

N28	0.82676(9)	0.49345(6)	0.66698(5)	0.0293(3)
N35	0.63752(9)	0.58260(6)	0.69006(4)	0.0228(2)
O1	0.56483(8)	0.75152(5)	0.73737(4)	0.0320(2)
O2	0.51317(8)	0.82374(5)	0.60637(4)	0.0333(2)

$U_{eq}={}^{1}/_{3}[U_{11}(aa^*)^2+U_{22}(bb^*)^2+U_{33}(cc^*)^2+2U_{12}aa^*bb^*\cos\gamma+2U_{13}aa^*cc^*\cos\beta+2U_{23}bb^*cc^*\cos\alpha]$

Table B.33 Positional Parameters for Hydrogens in Compound *rac*-**6.35a.**

Atom	x	y	z	U_{iso}, Å^2
H3	0.3650	0.7084	0.7751	0.040
H4	0.2293	0.6452	0.7260	0.044
H6	0.1619	0.5844	0.6424	0.052
H7	0.1861	0.5450	0.5535	0.052
H11	0.4214	0.5179	0.3908	0.055
H12	0.5839	0.5456	0.3433	0.063
H13	0.7229	0.6191	0.3839	0.060
H14	0.6989	0.6644	0.4730	0.053
H19a	0.4877	0.7975	0.8017	0.058
H19b	0.6197	0.7897	0.8099	0.058
H19c	0.5406	0.7218	0.8161	0.058
H22	0.7114	0.8586	0.5624	0.045
H23	0.8697	0.7860	0.5554	0.045
H25	0.9679	0.6719	0.5714	0.042
H26	0.9715	0.5573	0.6038	0.042
H30	0.8101	0.3718	0.7202	0.044
H31	0.6757	0.3382	0.7846	0.045
H32	0.5226	0.4136	0.8058	0.041
H33	0.5046	0.5238	0.7625	0.037
H38a	0.5570	0.9221	0.5839	0.060
H38b	0.4277	0.9049	0.5737	0.060
H38c	0.5204	0.8729	0.5332	0.060

Table B.34 Refined Thermal Parameters (U's) for Compound *rac*-**6.35a.**

Atom	U_{11}	U_{22}	U_{33}	U_{23}	U_{13}	U_{12}
C1	0.0226(6)	0.0183(6)	0.0269(7)	0.0041(5)	0.0027(5)	0.0020(5)
C2	0.0284(7)	0.0212(6)	0.0270(7)	0.0035(5)	0.0038(6)	0.0017(5)
C3	0.0325(7)	0.0291(7)	0.0296(7)	0.0051(6)	0.0100(6)	0.0048(6)
C4	0.0255(7)	0.0354(8)	0.0389(8)	0.0115(6)	0.0100(6)	0.0023(6)
C5	0.0212(7)	0.0284(7)	0.0400(8)	0.0096(6)	0.0002(6)	-0.0003(6)
C6	0.0215(7)	0.0453(9)	0.0504(10)	0.0110(8)	-0.0021(7)	-0.0069(6)
C7	0.0277(8)	0.0384(8)	0.0518(10)	0.0076(7)	-0.0134(7)	-0.0104(6)
C8	0.0315(7)	0.0248(7)	0.0356(8)	0.0042(6)	-0.0125(6)	0.0003(6)
C10	0.0424(8)	0.0246(7)	0.0295(7)	0.0005(6)	-0.0153(7)	0.0088(6)
C11	0.0568(10)	0.0336(8)	0.0329(8)	-0.0048(6)	-0.0175(8)	0.0083(7)
C12	0.0681(12)	0.0474(10)	0.0256(8)	-0.0073(7)	-0.0123(8)	0.0189(9)
C13	0.0490(10)	0.0596(11)	0.0279(8)	0.0000(7)	0.0007(7)	0.0137(8)
C14	0.0396(8)	0.0509(9)	0.0282(8)	-0.0045(7)	-0.0023(7)	0.0031(7)
C15	0.0335(7)	0.0296(7)	0.0253(7)	-0.0007(6)	-0.0067(6)	0.0069(6)
C17	0.0232(7)	0.0217(6)	0.0315(7)	0.0051(5)	-0.0048(5)	0.0018(5)
C18	0.0217(6)	0.0208(6)	0.0305(7)	0.0052(5)	-0.0009(5)	0.0011(5)
C19	0.0456(9)	0.0450(9)	0.0245(7)	-0.0035(6)	0.0038(7)	0.0010(7)
C20	0.0242(7)	0.0232(6)	0.0185(6)	-0.0018(5)	0.0007(5)	-0.0046(5)
C21	0.0313(7)	0.0240(7)	0.0248(7)	-0.0021(5)	0.0031(6)	-0.0018(6)
C22	0.0407(8)	0.0258(7)	0.0346(8)	0.0041(6)	0.0083(6)	-0.0076(6)
C23	0.0322(8)	0.0333(8)	0.0369(8)	0.0013(6)	0.0117(6)	-0.0103(6)
C24	0.0246(7)	0.0314(7)	0.0259(7)	-0.0028(6)	0.0021(5)	-0.0076(6)
C25	0.0225(7)	0.0391(8)	0.0327(8)	-0.0027(6)	0.0063(6)	-0.0076(6)
C26	0.0218(7)	0.0363(8)	0.0368(8)	-0.0047(6)	0.0043(6)	0.0002(6)
C27	0.0227(7)	0.0296(7)	0.0262(7)	-0.0028(6)	-0.0033(5)	-0.0022(6)
C29	0.0242(7)	0.0272(7)	0.0272(7)	-0.0017(5)	-0.0057(6)	-0.0011(5)
C30	0.0311(7)	0.0277(7)	0.0415(8)	0.0024(6)	-0.0071(7)	0.0034(6)
C31	0.0383(8)	0.0257(7)	0.0383(8)	0.0071(6)	-0.0107(7)	-0.0036(6)
C32	0.0331(8)	0.0308(7)	0.0290(7)	0.0050(6)	-0.0036(6)	-0.0075(6)
C33	0.0276(7)	0.0285(7)	0.0279(7)	0.0014(6)	-0.0004(6)	-0.0021(6)
C34	0.0240(7)	0.0233(6)	0.0221(6)	-0.0010(5)	-0.0058(5)	-0.0032(5)
C36	0.0194(6)	0.0258(7)	0.0200(6)	-0.0031(5)	-0.0023(5)	-0.0039(5)
C37	0.0228(6)	0.0259(7)	0.0190(6)	-0.0034(5)	-0.0003(5)	-0.0055(5)
C38	0.0487(9)	0.0316(8)	0.0393(9)	0.0111(7)	-0.0011(7)	0.0030(7)
N9	0.0394(7)	0.0259(6)	0.0382(7)	0.0034(5)	-0.0163(6)	0.0007(5)
N16	0.0269(6)	0.0307(6)	0.0257(6)	-0.0016(5)	-0.0032(5)	0.0008(5)

N28	0.0242(6)	0.0297(6)	0.0339(6)	-0.0008(5)	-0.0021(5)	0.0013(5)
N35	0.0224(5)	0.0240(5)	0.0220(5)	0.0002(4)	-0.0013(4)	-0.0026(4)
O1	0.0380(6)	0.0338(5)	0.0242(5)	-0.0042(4)	0.0051(4)	-0.0073(4)
O2	0.0366(6)	0.0250(5)	0.0382(6)	0.0081(4)	0.0078(4)	0.0033(4)

The form of the anisotropic displacement parameter is:
$\exp[-2\pi^2(a^{*2}U_{11}h^2+b^{*2}U_{22}k^2+c^{*2}U_{33}l^2+2b^*c^*U_{23}kl+2a^*c^*U_{13}hl+2a^*b^*U_{12}hk)]$

Table B.35 Bond Distances in Compound *rac*-**6.35a**, Å

C1-C2	1.3935(19)	C1-C18	1.4077(18)	C1-C20	1.4982(17)
C2-O1	1.3660(16)	C2-C3	1.3924(19)	C3-C4	1.367(2)
C4-C5	1.393(2)	C5-C18	1.4216(18)	C5-C6	1.434(2)
C6-C7	1.337(2)	C7-C8	1.434(2)	C8-N9	1.3290(19)
C8-C17	1.4410(19)	C10-N9	1.350(2)	C10-C11	1.413(2)
C10-C15	1.419(2)	C11-C12	1.350(3)	C12-C13	1.412(2)
C13-C14	1.364(2)	C14-C15	1.412(2)	C15-N16	1.3488(18)
C17-N16	1.3237(17)	C17-C18	1.4623(19)	C19-O1	1.4273(17)
C20-C21	1.3921(18)	C20-C37	1.4045(18)	C21-O2	1.3695(17)
C21-C22	1.3908(19)	C22-C23	1.370(2)	C23-C24	1.396(2)
C24-C37	1.4180(18)	C24-C25	1.435(2)	C25-C26	1.342(2)
C26-C27	1.4295(19)	C27-N28	1.3313(18)	C27-C36	1.4390(18)
C29-N28	1.3518(18)	C29-C30	1.4160(19)	C29-C34	1.4164(19)
C30-C31	1.359(2)	C31-C32	1.409(2)	C32-C33	1.362(2)
C33-C34	1.4154(19)	C34-N35	1.3533(17)	C36-N35	1.3265(16)
C36-C37	1.4607(18)	C38-O2	1.4216(17)		

Table B.36 Bond Angles in Compound *rac*-**6.35a**, °

C2-C1-C18	119.33(12)	C2-C1-C20	117.55(11)	C18-C1-C20	123.11(11)
O1-C2-C3	123.09(12)	O1-C2-C1	115.41(11)	C3-C2-C1	121.50(13)
C4-C3-C2	119.16(13)	C3-C4-C5	121.66(13)	C4-C5-C18	119.44(13)
C4-C5-C6	119.99(13)	C18-C5-C6	120.57(14)	C7-C6-C5	122.44(14)
C6-C7-C8	120.20(14)	N9-C8-C7	118.25(13)	N9-C8-C17	121.99(13)
C7-C8-C17	119.76(13)	N9-C10-C11	119.65(14)	N9-C10-C15	121.18(13)
C11-C10-C15	119.16(15)	C12-C11-C10	120.08(15)	C11-C12-C13	121.03(15)
C14-C13-C12	120.56(16)	C13-C14-C15	119.70(15)	N16-C15-C14	119.35(13)
N16-C15-C10	121.18(13)	C14-C15-C10	119.47(13)	N16-C17-C8	120.45(13)
N16-C17-C18	119.94(12)	C8-C17-C18	119.61(12)	C1-C18-C5	118.90(12)
C1-C18-C17	123.72(12)	C5-C18-C17	117.36(12)	C21-C20-C37	119.10(12)
C21-C20-C1	116.93(11)	C37-C20-C1	123.90(11)	O2-C21-C22	122.83(12)
O2-C21-C20	115.61(11)	C22-C21-C20	121.53(13)	C23-C22-C21	119.23(13)
C22-C23-C24	121.42(13)	C23-C24-C37	119.16(13)	C23-C24-C25	120.29(12)
C37-C24-C25	120.53(12)	C26-C25-C24	122.21(13)	C25-C26-C27	120.27(13)
N28-C27-C26	118.43(12)	N28-C27-C36	121.91(12)	C26-C27-C36	119.60(12)
N28-C29-C30	120.09(12)	N28-C29-C34	120.91(12)	C30-C29-C34	118.98(12)
C31-C30-C29	119.81(13)	C30-C31-C32	121.30(13)	C33-C32-C31	120.35(13)
C32-C33-C34	119.88(13)	N35-C34-C33	118.89(12)	N35-C34-C29	121.46(12)
C33-C34-C29	119.65(12)	N35-C36-C27	120.54(12)	N35-C36-C37	119.62(11)
C27-C36-C37	119.79(11)	C20-C37-C24	119.35(12)	C20-C37-C36	123.34(11)
C24-C37-C36	117.26(12)	C8-N9-C10	117.07(12)	C17-N16-C15	118.07(12)
C27-N28-C29	117.25(12)	C36-N35-C34	117.80(11)	C2-O1-C19	117.73(11)
C21-O2-C38	117.34(11)				

B.7 X-Ray Structure Determination of Compound (*S*)-6.36c

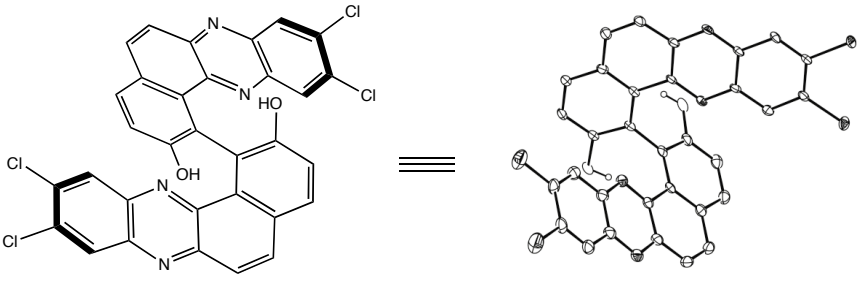

Compound (*S*)-**6.36c**, $C_{137}H_{77}N_{16}O_8Cl_{16}$, crystallizes in the monoclinic space group $P2_1$ (systematic absences 0k0: k=odd) with a=11.6724(11)Å, b=24.209(2)Å, c=22.364(2)Å, β=103.811(3)°, V=6136.9(9)Å^3, Z=2, and d_{calc}=1.430 g/cm^3. X-ray intensity data were collected on a Bruker APEXII CCD area detector employing graphite-monochromated Mo-Kα radiation (l=0.71073 Å) at a temperature of 143(1)K. Preliminary indexing was performed from a series of thirty-six 0.5° rotation frames with exposures of 10 seconds. A total of 2013 frames were collected with a crystal to detector distance of 37.6 mm, rotation widths of 0.5° and exposures of 30 seconds:

scan type	2θ	ω	ϕ	X	frames
ϕ	-15.50	258.48	9.96	19.46	704
ϕ	19.50	327.79	58.99	36.30	570
ϕ	22.00	321.06	18.69	41.79	739

The crystal grew as a non-merohedral twin; the program CELL_NOW[151] was used to index the diffraction images and to determine the twinning mechanism. The crystal was twinned by a rotation of 180° about the 100 direct direction. Rotation frames were integrated using SAINT[144], producing a listing of unaveraged F^2 and $\sigma(F^2)$ values which were then passed to the SHELXTL[145] program package for further processing and structure solution. A total of 116203 reflections were measured over the ranges $1.26 \leq \theta \leq 25.53°$, $-14 \leq h \leq 14$, $-29 \leq k \leq 29$, $-27 \leq l \leq 27$ yielding 22753 unique reflections (Rint = 0.0651). The intensity data were corrected for Lorentz and polarization effects and for

absorption using TWINABS[150] (minimum and maximum transmission 0.6093, 0.7452).

The structure was solved by direct methods (SHELXS-97[147]). The asymmetric unit includes four molecules of the title compound. During the early stages of refinement, it was noticed that Cl2 had a rather large thermal parameter that, during anisotropic refinement, developed a very anisotropic ellipsoid with the major vibrational component perpendicular to the molecular plane. This suggested that there was some flexibility in the C8,C9,C10,C11,C12,C13 ring. A disorder model was devised that postulated a slight rotation about the line connecting C10 and C13. Relative occupancies of 0.55/0.45 were assigned to the two disordered C11-C12-Cl2 moieties. In addition, two instances of hexane solvent molecules were found in the asymmetric unit. Both hexanes were disordered; thus, they were refined as rigid groups. One of the hexanes (C129-C134) displayed larger than expected thermal parameters; thus, it was postulated that these atoms had only 50% occupancy. Refinement was by full-matrix least squares based on F^2 using SHELXL-97.[147] All reflections were used during refinement. The weighting scheme used was $w=1/[\sigma^2(F_o^2)+ (0.1085P)^2 + 5.2981P]$ where $P = (F_o^2 + 2F_c^2)/3$. Non-hydrogen atoms were refined anisotropically and hydrogen atoms were refined using a riding model. Refinement converged to R1=0.0626 and wR2=0.1601 for 18243 observed reflections for which $F > 4\sigma(F)$ and R1=0.0871 and wR2=0.1787 and GOF =1.005 for all 22753 unique, non-zero reflections and 1633 variables.[148] The maximum Δ/σ in the final cycle of least squares was 0.001 and the two most prominent peaks in the final difference Fourier were +0.640 and -0.340 e/Å^3. The Flack absolute structure parameter[157] was estimated as 0.10(6), corroborating the assignment of absolute structure.

Table B.37 lists cell information, data collection parameters, and refinement data.

(157) Flack H.D. (1983). *Acta. Cryst.,* **A39**, 876-881.

Final positional and equivalent isotropic thermal parameters are given in Table B.38 and Table B.39. Anisotropic thermal parameters are in Table B.40. Table B.41 and Table B.42 list bond distances and bond angles. Figure B.7 displays ORTEP[149] representations of the four molecules in the asymmetric unit with 30% probability thermal ellipsoids displayed.

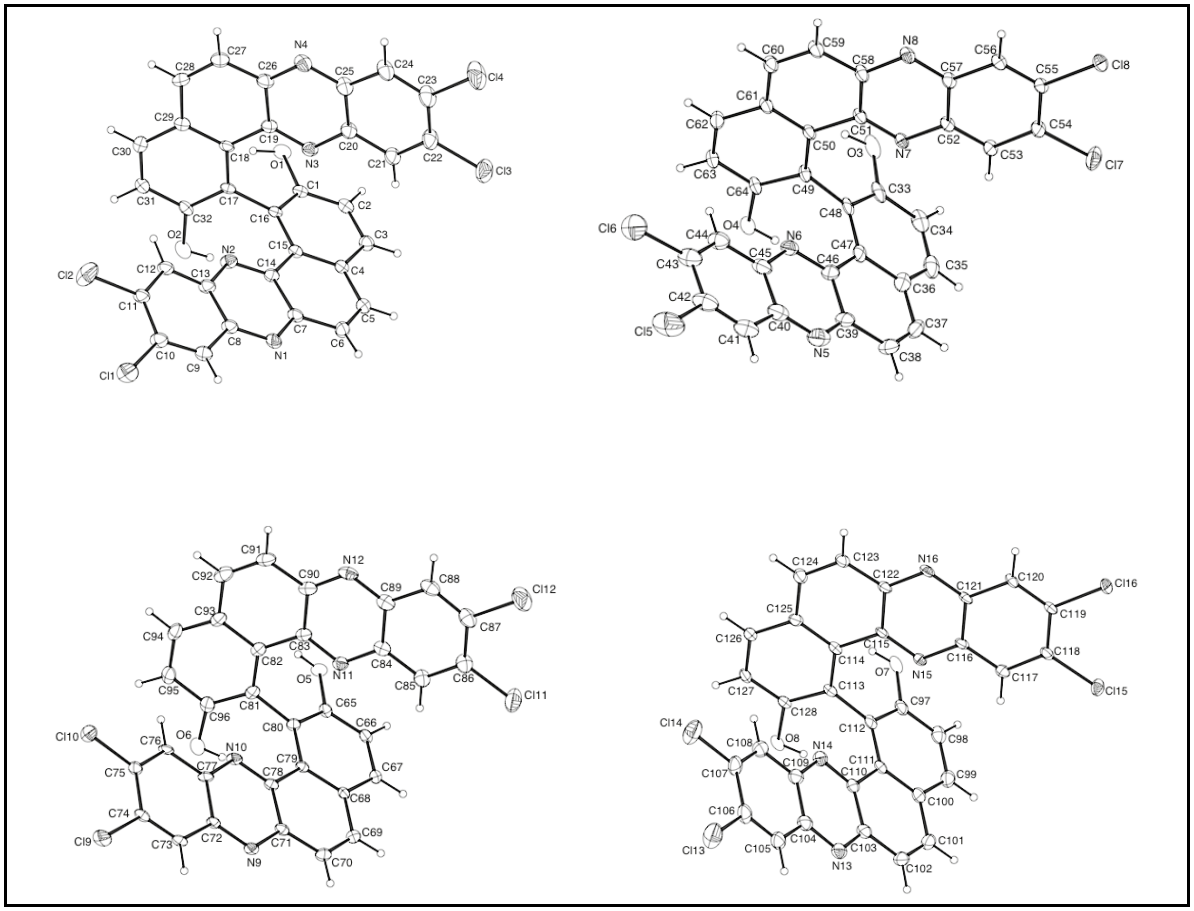

Figure B.7 ORTEP drawings of the four molecules of *(S)*-**6.36c** in the asymmetric unit with 30% probability thermal ellipsoids.

Table B.37 Summary of Structure Determination of Compound *(S)*-**6.36c.**

Empirical formula	$C_{137}H_{77}N_{16}O_8Cl_{16}$
Formula weight	2642.35
Temperature	143(1) K
Wavelength	0.71073 Å
Crystal system	monoclinic
Space group	$P2_1$
Cell constants:	
a	11.6724(11) Å
b	24.209(2) Å
c	22.364(2) Å
b	103.811(3)°
Volume	6136.9(9) $Å^3$
Z	2
Density (calculated)	1.430 Mg/m^3
Absorption coefficient	0.425 mm^{-1}
F(000)	2694
Crystal size	0.30 x 0.18 x 0.04 mm^3
Theta range for data collection	1.26 to 25.53°
Index ranges	$-14 \le h \le 14$, $-29 \le k \le 29$, $-27 \le l \le 27$
Reflections collected	116203
Independent reflections	22753 [R(int) = 0.0651]
Completeness to theta = 25.53°	98.6 %
Absorption correction	Semi-empirical from equivalents
Max. and min. transmission	0.7452 and 0.6093
Refinement method	Full-matrix least-squares on F^2
Data / restraints / parameters	22753 / 2341 / 1633
Goodness-of-fit on F^2	1.005
Final R indices [I>2sigma(I)]	R1 = 0.0626, wR2 = 0.1601
R indices (all data)	R1 = 0.0871, wR2 = 0.1787
Absolute structure parameter	0.10(6)
Largest diff. peak and hole	0.640 and -0.340 $e.Å^{-3}$

Table B.38 Refined Positional Parameters for Compound *(S)*-**6.36c**

Atom	x	y	Z	U_{eq}, Å^2
Cl1	-0.22805(15)	0.40618(10)	0.83621(9)	0.0560(6)
Cl3	0.6167(3)	0.54306(9)	1.22181(9)	0.0671(7)
Cl4	0.6537(3)	0.66392(9)	1.17646(11)	0.0834(9)
O1	0.7324(4)	0.3665(2)	0.9762(2)	0.0369(11)
O2	0.4325(4)	0.29803(18)	0.8826(2)	0.0340(10)
N1	0.1251(4)	0.3811(2)	1.0146(2)	0.0326(11)
N2	0.2834(4)	0.3891(2)	0.9360(2)	0.0318(11)
N3	0.5573(5)	0.4799(2)	1.0010(2)	0.0313(11)
N4	0.5940(6)	0.5870(2)	0.9601(3)	0.0389(12)
C1	0.6472(5)	0.3629(2)	1.0095(3)	0.0253(11)
C2	0.6886(6)	0.3525(3)	1.0719(3)	0.0312(12)
C3	0.6096(6)	0.3508(3)	1.1081(3)	0.0313(12)
C4	0.4867(5)	0.3595(3)	1.0825(3)	0.0269(11)
C5	0.4054(6)	0.3570(3)	1.1204(3)	0.0350(13)
C6	0.2872(6)	0.3661(3)	1.0996(3)	0.0359(13)
C7	0.2427(5)	0.3758(3)	1.0355(3)	0.0302(12)
C8	0.0863(5)	0.3905(3)	0.9542(3)	0.0313(12)
C9	-0.0389(6)	0.3944(3)	0.9283(3)	0.0333(13)
C10	-0.0780(6)	0.4026(3)	0.8679(3)	0.0386(13)
Cl2	-0.0508(6)	0.4370(4)	0.7564(3)	0.082(2)
C11	0.0005(16)	0.4174(5)	0.8332(7)	0.035(2)
C12	0.1248(15)	0.4133(6)	0.8558(7)	0.034(2)
Cl2'	-0.0554(7)	0.4022(4)	0.7450(3)	0.072(2)
C11'	-0.001(2)	0.3992(6)	0.8228(9)	0.037(2)
C12'	0.1173(19)	0.3942(7)	0.8455(9)	0.034(2)
C13	0.1646(5)	0.3954(3)	0.9148(3)	0.0323(12)
C14	0.3231(5)	0.3788(3)	0.9948(3)	0.0252(11)
C15	0.4477(5)	0.3693(2)	1.0191(3)	0.0240(10)
C16	0.5308(5)	0.3721(2)	0.9827(3)	0.0229(10)
C17	0.5000(5)	0.3900(2)	0.9154(3)	0.0220(10)
C18	0.5154(5)	0.4449(3)	0.8977(3)	0.0259(10)
C19	0.5484(6)	0.4897(3)	0.9425(3)	0.0296(11)
C20	0.5829(6)	0.5231(3)	1.0414(3)	0.0343(12)
C21	0.5890(7)	0.5129(3)	1.1045(3)	0.0389(14)
C22	0.6092(8)	0.5562(3)	1.1439(3)	0.0462(16)
C23	0.6269(8)	0.6089(3)	1.1247(3)	0.0508(17)

C24	0.6240(8)	0.6205(3)	1.0636(3)	0.0500(17)
C25	0.6019(7)	0.5772(3)	1.0198(3)	0.0383(13)
C26	0.5675(7)	0.5454(3)	0.9205(3)	0.0369(13)
C27	0.5491(7)	0.5550(3)	0.8568(3)	0.0443(15)
C28	0.5132(7)	0.5144(3)	0.8168(3)	0.0416(14)
C29	0.4915(6)	0.4587(3)	0.8344(3)	0.0317(12)
C30	0.4515(6)	0.4173(3)	0.7906(3)	0.0361(13)
C31	0.4349(6)	0.3648(3)	0.8085(3)	0.0351(13)
C32	0.4585(5)	0.3504(3)	0.8706(3)	0.0290(11)
Cl5	-0.1065(3)	0.45005(11)	1.16816(13)	0.0891(9)
Cl6	-0.0666(3)	0.57120(11)	1.21869(10)	0.0771(8)
Cl7	0.34755(16)	0.70114(12)	0.76001(8)	0.0644(7)
Cl8	0.60001(13)	0.71017(7)	0.84797(7)	0.0357(4)
O3	-0.0217(5)	0.8219(2)	0.8998(2)	0.0460(12)
O4	-0.2386(4)	0.7490(2)	0.9878(2)	0.0368(11)
N5	-0.1264(6)	0.5285(3)	0.9550(3)	0.0547(14)
N6	-0.0785(5)	0.6348(2)	1.0035(2)	0.0352(11)
N7	0.1779(4)	0.7239(2)	0.9464(2)	0.0283(10)
N8	0.4043(4)	0.7315(2)	1.0261(2)	0.0285(11)
C33	-0.0562(5)	0.7696(3)	0.8831(3)	0.0361(12)
C34	-0.0801(6)	0.7592(4)	0.8199(3)	0.0450(14)
C35	-0.1077(6)	0.7049(4)	0.7988(3)	0.0491(14)
C36	-0.1097(6)	0.6624(3)	0.8397(3)	0.0408(12)
C37	-0.1352(6)	0.6060(4)	0.8170(3)	0.0491(15)
C38	-0.1404(7)	0.5633(4)	0.8537(4)	0.0558(16)
C39	-0.1200(6)	0.5712(4)	0.9191(3)	0.0449(13)
C40	-0.1081(7)	0.5367(3)	1.0154(4)	0.0471(14)
C41	-0.1159(8)	0.4938(4)	1.0578(4)	0.0559(17)
C42	-0.0979(8)	0.5040(4)	1.1184(4)	0.0570(17)
C43	-0.0777(8)	0.5592(4)	1.1414(4)	0.0523(16)
C44	-0.0720(7)	0.6009(3)	1.1027(3)	0.0464(15)
C45	-0.0868(6)	0.5912(3)	1.0401(3)	0.0422(13)
C46	-0.0944(6)	0.6268(3)	0.9439(3)	0.0374(12)
C47	-0.0882(5)	0.6730(3)	0.9039(3)	0.0326(11)
C48	-0.0591(5)	0.7278(3)	0.9260(3)	0.0299(11)
C49	-0.0304(5)	0.7411(3)	0.9929(3)	0.0262(11)
C50	0.0846(5)	0.7422(3)	1.0311(3)	0.0253(11)
C51	0.1905(5)	0.7336(3)	1.0061(3)	0.0268(11)

C52	0.2752(5)	0.7185(3)	0.9244(3)	0.0266(11)
C53	0.2632(5)	0.7109(3)	0.8624(3)	0.0314(13)
C54	0.3635(5)	0.7080(3)	0.8390(3)	0.0323(13)
C55	0.4786(5)	0.7124(3)	0.8788(3)	0.0254(11)
C56	0.4925(5)	0.7191(3)	0.9400(3)	0.0271(12)
C57	0.3883(5)	0.7233(3)	0.9651(3)	0.0258(11)
C58	0.3056(5)	0.7357(3)	1.0477(3)	0.0308(12)
C59	0.3174(6)	0.7432(3)	1.1119(3)	0.0373(14)
C60	0.2207(6)	0.7510(3)	1.1339(3)	0.0363(14)
C61	0.1042(5)	0.7507(3)	1.0949(3)	0.0297(11)
C62	0.0042(6)	0.7595(3)	1.1204(3)	0.0342(13)
C63	-0.1066(6)	0.7599(3)	1.0841(3)	0.0329(13)
C64	-0.1250(5)	0.7510(3)	1.0209(3)	0.0298(12)
C129	0.2256(16)	0.5484(10)	0.8994(8)	0.111(6)
C130	0.2410(18)	0.5805(7)	0.9593(8)	0.125(5)
C131	0.2374(13)	0.5407(6)	1.0116(8)	0.121(5)
C132	0.2529(14)	0.5728(7)	1.0716(8)	0.126(5)
C133	0.2492(18)	0.5329(8)	1.1238(8)	0.130(6)
C134	0.2647(19)	0.5650(11)	1.1839(8)	0.147(8)
Cl9	-0.10940(14)	0.87551(8)	0.66877(8)	0.0395(4)
Cl10	0.14093(14)	0.83987(8)	0.74730(7)	0.0371(4)
Cl11	0.4831(3)	0.74786(9)	0.28136(9)	0.0655(7)
Cl12	0.6012(3)	0.63507(9)	0.33105(11)	0.0771(8)
O5	0.7204(3)	0.92447(19)	0.52559(19)	0.0315(10)
O6	0.4881(4)	0.9919(2)	0.6188(2)	0.0336(10)
N9	0.0807(4)	0.9184(2)	0.4930(2)	0.0245(10)
N10	0.3077(4)	0.8971(2)	0.5671(2)	0.0244(10)
N11	0.5520(5)	0.8120(2)	0.5026(2)	0.0312(10)
N12	0.6540(5)	0.7098(2)	0.5467(3)	0.0369(11)
C65	0.6085(5)	0.9289(3)	0.4935(3)	0.0234(11)
C66	0.5889(5)	0.9416(2)	0.4319(3)	0.0256(11)
C67	0.4765(5)	0.9455(3)	0.3962(3)	0.0262(11)
C68	0.3787(5)	0.9363(2)	0.4219(2)	0.0218(10)
C69	0.2611(6)	0.9426(3)	0.3847(3)	0.0298(12)
C70	0.1651(5)	0.9362(3)	0.4075(3)	0.0290(12)
C71	0.1793(5)	0.9228(2)	0.4703(3)	0.0230(10)
C72	0.0965(5)	0.9022(2)	0.5520(3)	0.0212(10)
C73	-0.0031(5)	0.8972(3)	0.5791(3)	0.0235(11)

C74	0.0108(5)	0.8808(3)	0.6370(3)	0.0253(11)
C75	0.1240(5)	0.8655(3)	0.6735(3)	0.0266(11)
C76	0.2236(5)	0.8710(3)	0.6500(3)	0.0249(11)
C77	0.2096(5)	0.8897(3)	0.5885(3)	0.0242(11)
C78	0.2922(5)	0.9135(2)	0.5092(3)	0.0207(10)
C79	0.3980(5)	0.9236(2)	0.4854(2)	0.0196(10)
C80	0.5129(5)	0.9189(2)	0.5209(2)	0.0223(10)
C81	0.5440(5)	0.9018(3)	0.5877(3)	0.0251(10)
C82	0.5850(5)	0.8482(3)	0.6056(3)	0.0266(10)
C83	0.5926(5)	0.8036(3)	0.5618(3)	0.0280(11)
C84	0.5627(6)	0.7700(3)	0.4635(3)	0.0324(12)
C85	0.5224(7)	0.7791(3)	0.3994(3)	0.0370(13)
C86	0.5329(7)	0.7373(3)	0.3598(3)	0.0408(14)
C87	0.5852(7)	0.6869(3)	0.3822(4)	0.0432(14)
C88	0.6264(7)	0.6767(3)	0.4432(4)	0.0402(13)
C89	0.6155(6)	0.7192(3)	0.4860(3)	0.0352(12)
C90	0.6427(6)	0.7500(3)	0.5845(3)	0.0337(11)
C91	0.6780(6)	0.7412(3)	0.6499(3)	0.0394(13)
C92	0.6648(6)	0.7812(3)	0.6893(3)	0.0416(13)
C93	0.6187(5)	0.8355(3)	0.6698(3)	0.0315(11)
C94	0.6090(6)	0.8746(3)	0.7122(3)	0.0383(13)
C95	0.5662(6)	0.9279(3)	0.6944(3)	0.0369(13)
C96	0.5334(5)	0.9404(3)	0.6321(3)	0.0306(11)
Cl13	-0.2241(3)	0.86076(9)	0.33645(11)	0.0749(8)
Cl14	-0.1726(2)	0.75086(9)	0.27307(9)	0.0660(6)
Cl15	0.58878(13)	0.61833(7)	0.71867(6)	0.0331(3)
Cl16	0.76316(12)	0.58882(7)	0.63564(7)	0.0323(3)
O7	0.1086(4)	0.47494(19)	0.5823(2)	0.0325(9)
O8	-0.1997(3)	0.5516(2)	0.4989(2)	0.0330(10)
N13	-0.0862(5)	0.7658(2)	0.5418(3)	0.0369(11)
N14	-0.0437(5)	0.6663(2)	0.4854(2)	0.0302(10)
N15	0.2519(4)	0.5747(2)	0.5365(2)	0.0222(9)
N16	0.4074(4)	0.5535(2)	0.4607(2)	0.0274(10)
C97	0.0849(5)	0.5262(3)	0.6018(3)	0.0306(11)
C98	0.1159(6)	0.5342(3)	0.6642(3)	0.0339(12)
C99	0.1014(6)	0.5869(3)	0.6878(3)	0.0389(13)
C100	0.0526(5)	0.6303(3)	0.6487(3)	0.0327(11)
C101	0.0331(6)	0.6834(3)	0.6750(3)	0.0396(13)

C102	-0.0142(6)	0.7251(3)	0.6399(3)	0.0390(13)
C103	-0.0418(5)	0.7204(3)	0.5744(3)	0.0350(12)
C104	-0.1073(6)	0.7608(3)	0.4797(3)	0.0350(12)
C105	-0.1509(6)	0.8072(3)	0.4427(3)	0.0421(14)
C106	-0.1712(7)	0.8039(3)	0.3811(4)	0.0438(14)
C107	-0.1469(6)	0.7532(3)	0.3517(3)	0.0394(13)
C108	-0.1064(6)	0.7089(3)	0.3868(3)	0.0376(13)
C109	-0.0838(6)	0.7119(3)	0.4514(3)	0.0330(11)
C110	-0.0247(5)	0.6701(3)	0.5460(3)	0.0282(11)
C111	0.0210(5)	0.6220(3)	0.5841(3)	0.0279(10)
C112	0.0361(5)	0.5681(3)	0.5598(3)	0.0240(10)
C113	0.0021(5)	0.5544(2)	0.4930(3)	0.0232(10)
C114	0.0846(5)	0.5491(2)	0.4552(3)	0.0219(10)
C115	0.2117(5)	0.5589(2)	0.4790(3)	0.0230(11)
C116	0.3673(5)	0.5801(2)	0.5579(3)	0.0231(11)
C117	0.4119(5)	0.5956(3)	0.6199(3)	0.0251(11)
C118	0.5337(5)	0.5989(3)	0.6426(3)	0.0272(12)
C119	0.6120(5)	0.5862(3)	0.6050(3)	0.0234(11)
C120	0.5723(5)	0.5715(3)	0.5452(3)	0.0243(11)
C121	0.4487(5)	0.5685(3)	0.5196(3)	0.0230(11)
C122	0.2917(5)	0.5488(3)	0.4387(3)	0.0247(11)
C123	0.2437(6)	0.5342(3)	0.3761(3)	0.0315(13)
C124	0.1268(6)	0.5272(3)	0.3549(3)	0.0298(12)
C125	0.0447(5)	0.5346(3)	0.3935(3)	0.0267(11)
C126	-0.0773(5)	0.5269(3)	0.3685(3)	0.0284(12)
C127	-0.1571(5)	0.5325(3)	0.4051(3)	0.0256(11)
C128	-0.1170(5)	0.5462(3)	0.4654(3)	0.0239(11)
C135	0.3050(9)	0.7344(4)	0.5902(3)	0.097(3)
C136	0.2610(9)	0.7588(3)	0.5260(3)	0.108(3)
C137	0.2565(7)	0.7136(3)	0.4780(3)	0.108(3)
C138	0.2124(7)	0.7380(3)	0.4138(3)	0.108(3)
C139	0.2079(10)	0.6928(4)	0.3658(3)	0.128(4)
C140	0.1639(11)	0.7172(6)	0.3016(3)	0.161(6)

$U_{eq}={}^{1}/_{3}[U_{11}(aa^*)^2+U_{22}(bb^*)^2+U_{33}(cc^*)^2+2U_{12}aa^*bb^*\cos\gamma+2U_{13}aa^*cc^*\cos\beta+2U_{23}bb^*cc^*\cos\alpha]$

Table B.39 Positional Parameters for Hydrogens in Compound *(S)*-**6.36c.**

Atom	X	y	z	U_{iso}, Å^2
H1a	0.7011	0.3640	0.9393	0.055
H2a	0.4625	0.2908	0.9187	0.051
H2	0.7686	0.3468	1.0888	0.042
H3	0.6363	0.3440	1.1501	0.042
H5	0.4342	0.3487	1.1619	0.047
H6	0.2374	0.3659	1.1264	0.048
H9	-0.0917	0.3912	0.9534	0.044
H12	0.1764	0.4224	0.8314	0.045
H12'	0.1678	0.3902	0.8193	0.045
H21	0.5793	0.4774	1.1185	0.052
H24	0.6365	0.6563	1.0516	0.067
H27	0.5622	0.5900	0.8427	0.059
H28	0.5013	0.5223	0.7751	0.055
H30	0.4363	0.4258	0.7488	0.048
H31	0.4073	0.3380	0.7788	0.047
H3a	-0.0158	0.8258	0.9368	0.069
H4a	-0.2405	0.7384	0.9527	0.055
H34	-0.0779	0.7876	0.7923	0.060
H35	-0.1249	0.6976	0.7568	0.065
H37	-0.1484	0.5997	0.7749	0.065
H38	-0.1573	0.5283	0.8369	0.074
H41	-0.1337	0.4581	1.0433	0.074
H44	-0.0578	0.6366	1.1179	0.062
H53	0.1886	0.7076	0.8362	0.042
H56	0.5676	0.7211	0.9659	0.036
H59	0.3918	0.7428	1.1388	0.050
H60	0.2301	0.7567	1.1759	0.048
H62	0.0156	0.7651	1.1626	0.045
H63	-0.1705	0.7661	1.1013	0.044
H129a	0.2268	0.5736	0.8664	0.166
H129b	0.1515	0.5292	0.8909	0.166
H129c	0.2887	0.5223	0.9031	0.166
H130a	0.1785	0.6076	0.9555	0.166
H130b	0.3159	0.5999	0.9682	0.166
H131a	0.3000	0.5136	1.0155	0.161
H131b	0.1625	0.5213	1.0027	0.161

H132a	0.3278	0.5921	1.0805	0.167
H132b	0.1903	0.5999	1.0678	0.167
H133a	0.3117	0.5058	1.1277	0.173
H133b	0.1743	0.5135	1.1150	0.173
H134a	0.2624	0.5399	1.2168	0.220
H134b	0.2022	0.5915	1.1800	0.220
H134c	0.3393	0.5838	1.1927	0.220
H5a	0.7223	0.9099	0.5589	0.047
H6a	0.5093	1.0042	0.5890	0.050
H66	0.6526	0.9476	0.4144	0.034
H67	0.4643	0.9543	0.3546	0.035
H69	0.2507	0.9515	0.3433	0.040
H70	0.0900	0.9405	0.3821	0.039
H73	-0.0782	0.9057	0.5557	0.031
H76	0.2981	0.8627	0.6742	0.033
H85	0.4894	0.8128	0.3845	0.049
H88	0.6608	0.6429	0.4568	0.053
H91	0.7102	0.7074	0.6650	0.052
H92	0.6864	0.7737	0.7313	0.055
H94	0.6313	0.8658	0.7538	0.051
H95	0.5600	0.9542	0.7238	0.049
H7a	0.0891	0.4737	0.5446	0.049
H8a	-0.1671	0.5521	0.5357	0.050
H98	0.1461	0.5053	0.6907	0.045
H99	0.1247	0.5930	0.7300	0.052
H101	0.0544	0.6880	0.7175	0.053
H102	-0.0297	0.7580	0.6580	0.052
H105	-0.1656	0.8400	0.4611	0.056
H108	-0.0931	0.6760	0.3681	0.050
H117	0.3610	0.6034	0.6450	0.033
H120	0.6252	0.5635	0.5212	0.032
H123	0.2936	0.5294	0.3497	0.042
H124	0.0977	0.5173	0.3139	0.040
H126	-0.1044	0.5179	0.3271	0.038
H127	-0.2373	0.5270	0.3886	0.034
H135a	0.3077	0.7628	0.6204	0.146
H135b	0.3826	0.7194	0.5942	0.146
H135c	0.2525	0.7056	0.5964	0.146

H136a	0.3135	0.7881	0.5197	0.144
H136b	0.1829	0.7744	0.5219	0.144
H137a	0.2040	0.6843	0.4844	0.144
H137b	0.3345	0.6980	0.4822	0.144
H138a	0.1344	0.7536	0.4097	0.144
H138b	0.2649	0.7673	0.4074	0.144
H139a	0.2860	0.6772	0.3700	0.170
H139b	0.1555	0.6635	0.3722	0.170
H140a	0.1611	0.6888	0.2714	0.241
H140b	0.2165	0.7459	0.2954	0.241
H140c	0.0864	0.7322	0.2976	0.241

Table B.40 Refined Thermal Parameters (U's) for Compound *(S)*-**6.36c**

Atom	U_{11}	U_{22}	U_{33}	U_{23}	U_{13}	U_{12}
Cl1	0.0189(8)	0.0885(16)	0.0571(11)	0.0188(11)	0.0020(8)	0.0045(9)
Cl3	0.109(2)	0.0532(12)	0.0399(10)	-0.0146(9)	0.0198(12)	-0.0085(13)
Cl4	0.140(3)	0.0398(12)	0.0580(13)	-0.0192(10)	-0.0015(15)	-0.0044(15)
O1	0.0138(19)	0.055(3)	0.043(2)	0.002(2)	0.0084(18)	-0.003(2)
O2	0.030(2)	0.031(2)	0.036(2)	-0.0007(18)	-0.004(2)	0.004(2)
N1	0.018(2)	0.047(3)	0.032(2)	-0.005(2)	0.0051(18)	-0.004(2)
N2	0.017(2)	0.042(3)	0.037(2)	0.009(2)	0.0079(17)	0.004(2)
N3	0.035(3)	0.026(2)	0.034(2)	-0.0028(18)	0.010(2)	-0.003(2)
N4	0.045(3)	0.024(2)	0.042(2)	0.0045(19)	-0.001(3)	0.000(3)
C1	0.023(2)	0.021(3)	0.034(2)	-0.002(2)	0.010(2)	-0.005(2)
C2	0.027(3)	0.028(3)	0.037(2)	-0.003(2)	0.005(2)	-0.002(3)
C3	0.028(2)	0.033(3)	0.030(3)	0.004(2)	0.002(2)	0.000(3)
C4	0.025(2)	0.027(3)	0.027(2)	-0.001(2)	0.0040(19)	-0.005(2)
C5	0.032(2)	0.044(4)	0.028(3)	0.000(3)	0.005(2)	-0.009(3)
C6	0.028(2)	0.055(4)	0.026(2)	-0.007(3)	0.009(2)	-0.007(3)
C7	0.017(2)	0.039(3)	0.035(2)	-0.003(3)	0.0071(18)	-0.005(2)
C8	0.019(2)	0.040(3)	0.036(2)	0.003(3)	0.0072(19)	-0.002(3)
C9	0.021(2)	0.039(3)	0.041(2)	0.002(3)	0.008(2)	0.002(3)
C10	0.022(2)	0.050(4)	0.042(2)	0.010(3)	0.005(2)	-0.003(3)
Cl2	0.030(2)	0.167(7)	0.045(3)	0.041(4)	-0.003(2)	0.000(4)
C11	0.022(3)	0.045(5)	0.034(4)	0.008(4)	0.001(3)	-0.008(5)
C12	0.021(3)	0.046(6)	0.034(4)	0.004(4)	0.003(3)	-0.009(5)

Cl2'	0.029(3)	0.146(7)	0.038(2)	0.032(4)	0.000(2)	0.012(5)
C11'	0.024(3)	0.047(6)	0.037(3)	0.008(5)	0.004(3)	-0.007(5)
C12'	0.022(3)	0.044(6)	0.035(3)	0.005(5)	0.006(3)	-0.007(5)
C13	0.018(2)	0.042(3)	0.037(2)	0.007(2)	0.0062(18)	-0.003(3)
C14	0.021(2)	0.027(3)	0.029(2)	-0.001(2)	0.0088(18)	0.000(2)
C15	0.022(2)	0.020(3)	0.029(2)	-0.001(2)	0.0051(18)	-0.002(2)
C16	0.022(2)	0.021(3)	0.026(2)	-0.003(2)	0.0070(19)	-0.005(2)
C17	0.009(2)	0.026(2)	0.032(2)	-0.0004(18)	0.0063(19)	-0.001(2)
C18	0.017(2)	0.030(2)	0.031(2)	-0.0008(18)	0.006(2)	-0.006(2)
C19	0.031(3)	0.025(2)	0.034(2)	0.0009(19)	0.010(2)	-0.002(2)
C20	0.042(3)	0.025(2)	0.035(2)	-0.0037(19)	0.008(3)	0.000(3)
C21	0.053(4)	0.027(3)	0.035(2)	-0.004(2)	0.006(3)	-0.002(3)
C22	0.065(4)	0.037(3)	0.035(3)	-0.012(2)	0.009(3)	0.001(3)
C23	0.073(5)	0.030(3)	0.044(3)	-0.012(2)	0.003(3)	0.005(3)
C24	0.070(4)	0.025(3)	0.045(3)	-0.003(2)	-0.007(3)	-0.003(3)
C25	0.047(3)	0.024(2)	0.038(2)	0.001(2)	-0.001(3)	0.004(3)
C26	0.041(3)	0.028(2)	0.040(2)	0.002(2)	0.007(3)	-0.007(3)
C27	0.061(4)	0.027(3)	0.046(3)	0.007(2)	0.013(3)	-0.011(3)
C28	0.051(4)	0.039(3)	0.038(3)	0.007(2)	0.016(3)	-0.010(3)
C29	0.033(3)	0.029(2)	0.035(2)	0.0014(19)	0.011(2)	-0.003(2)
C30	0.041(3)	0.042(3)	0.025(2)	0.001(2)	0.007(3)	-0.004(3)
C31	0.038(3)	0.037(3)	0.030(2)	-0.007(2)	0.009(3)	-0.009(3)
C32	0.021(3)	0.034(3)	0.030(2)	-0.005(2)	0.003(2)	-0.004(2)
Cl5	0.109(2)	0.0562(14)	0.0928(18)	0.0308(13)	0.0053(17)	-0.0237(15)
Cl6	0.103(2)	0.0783(16)	0.0446(10)	0.0242(10)	0.0072(12)	-0.0153(15)
Cl7	0.0326(9)	0.128(2)	0.0337(9)	-0.0264(11)	0.0097(8)	0.0061(12)
Cl8	0.0232(7)	0.0477(10)	0.0397(8)	-0.0063(7)	0.0141(7)	0.0003(7)
O3	0.044(3)	0.058(3)	0.044(3)	0.020(2)	0.025(3)	0.006(2)
O4	0.0200(19)	0.056(3)	0.036(2)	-0.002(2)	0.0093(17)	0.001(2)
N5	0.044(3)	0.051(3)	0.066(3)	-0.009(2)	0.007(3)	-0.008(3)
N6	0.033(3)	0.038(3)	0.033(2)	-0.0008(19)	0.005(2)	-0.005(2)
N7	0.016(2)	0.037(3)	0.033(2)	-0.004(2)	0.0080(18)	0.000(2)
N8	0.015(2)	0.041(3)	0.028(2)	0.005(2)	0.0026(17)	0.000(2)
C33	0.013(3)	0.063(3)	0.034(2)	0.015(2)	0.009(2)	0.008(3)
C34	0.019(3)	0.081(3)	0.032(2)	0.020(3)	0.002(3)	0.012(3)
C35	0.027(3)	0.090(4)	0.031(3)	0.003(2)	0.009(3)	0.012(4)
C36	0.018(3)	0.070(3)	0.031(2)	-0.004(2)	0.000(2)	0.009(3)
C37	0.032(3)	0.080(4)	0.033(3)	-0.026(2)	0.004(3)	-0.003(3)

C38	0.042(4)	0.072(4)	0.050(3)	-0.028(3)	0.005(3)	-0.019(4)
C39	0.030(3)	0.057(3)	0.045(3)	-0.016(2)	0.003(3)	-0.011(3)
C40	0.038(3)	0.043(3)	0.061(3)	-0.002(2)	0.012(3)	-0.009(3)
C41	0.051(4)	0.040(3)	0.073(3)	0.003(3)	0.009(4)	-0.012(4)
C42	0.052(4)	0.046(3)	0.065(3)	0.017(2)	0.000(4)	-0.014(4)
C43	0.052(4)	0.047(3)	0.049(3)	0.013(2)	-0.005(3)	-0.009(3)
C44	0.051(4)	0.039(3)	0.044(2)	0.008(2)	0.002(3)	-0.010(3)
C45	0.037(3)	0.041(3)	0.047(3)	0.004(2)	0.008(3)	-0.013(3)
C46	0.027(3)	0.050(3)	0.033(2)	-0.008(2)	0.003(3)	-0.006(3)
C47	0.016(2)	0.054(3)	0.029(2)	-0.0052(19)	0.008(2)	0.006(3)
C48	0.011(2)	0.053(3)	0.029(2)	0.004(2)	0.010(2)	0.003(2)
C49	0.022(2)	0.034(3)	0.026(2)	0.004(2)	0.0106(19)	0.004(2)
C50	0.018(2)	0.031(3)	0.028(2)	0.001(2)	0.0077(18)	-0.002(2)
C51	0.019(2)	0.036(3)	0.026(2)	0.005(2)	0.0062(18)	0.002(2)
C52	0.011(2)	0.037(3)	0.031(2)	-0.001(2)	0.0035(18)	0.004(2)
C53	0.011(2)	0.051(4)	0.031(2)	-0.009(3)	0.003(2)	0.004(3)
C54	0.017(2)	0.050(4)	0.029(2)	-0.004(3)	0.0039(19)	0.006(3)
C55	0.013(2)	0.031(3)	0.033(2)	-0.002(2)	0.0065(19)	0.005(2)
C56	0.014(2)	0.035(3)	0.031(2)	0.004(2)	0.0025(19)	0.006(2)
C57	0.018(2)	0.032(3)	0.027(2)	0.001(2)	0.0048(18)	0.004(2)
C58	0.020(2)	0.047(3)	0.026(2)	0.007(2)	0.0068(18)	0.003(3)
C59	0.023(2)	0.063(4)	0.023(2)	0.008(3)	0.001(2)	-0.009(3)
C60	0.031(2)	0.057(4)	0.020(2)	0.006(3)	0.005(2)	-0.009(3)
C61	0.026(2)	0.039(3)	0.026(2)	0.006(2)	0.0086(19)	-0.005(3)
C62	0.034(3)	0.043(3)	0.028(3)	-0.001(3)	0.013(2)	0.000(3)
C63	0.029(2)	0.042(3)	0.033(2)	0.002(3)	0.017(2)	0.000(3)
C64	0.024(2)	0.039(3)	0.030(2)	0.006(3)	0.014(2)	0.000(3)
C129	0.051(10)	0.100(14)	0.187(10)	-0.005(10)	0.037(12)	0.003(11)
C130	0.071(8)	0.116(10)	0.184(9)	-0.007(8)	0.024(9)	0.016(9)
C131	0.059(7)	0.121(10)	0.182(9)	-0.006(7)	0.028(8)	0.021(8)
C132	0.057(7)	0.133(10)	0.186(9)	-0.012(7)	0.029(8)	0.026(8)
C133	0.066(8)	0.146(11)	0.180(9)	-0.015(8)	0.034(9)	0.022(9)
C134	0.079(13)	0.172(18)	0.179(10)	-0.028(11)	0.012(14)	0.006(14)
Cl9	0.0194(7)	0.0554(11)	0.0484(9)	0.0081(8)	0.0171(7)	0.0012(7)
Cl10	0.0284(8)	0.0528(10)	0.0323(8)	0.0069(7)	0.0114(7)	-0.0030(8)
Cl11	0.111(2)	0.0504(12)	0.0365(9)	-0.0033(9)	0.0212(11)	0.0040(13)
Cl12	0.124(2)	0.0444(12)	0.0701(14)	-0.0104(10)	0.0366(15)	0.0179(14)
O5	0.0149(17)	0.049(3)	0.031(2)	0.007(2)	0.0069(16)	0.0053(19)

O6	0.026(2)	0.044(2)	0.036(2)	-0.0035(19)	0.0160(19)	-0.005(2)
N9	0.0102(19)	0.031(3)	0.029(2)	-0.0050(19)	-0.0027(17)	-0.001(2)
N10	0.0079(18)	0.033(3)	0.032(2)	0.005(2)	0.0047(17)	-0.001(2)
N11	0.029(3)	0.033(2)	0.032(2)	0.0081(18)	0.008(2)	0.004(2)
N12	0.023(2)	0.035(3)	0.055(2)	0.010(2)	0.012(2)	0.006(2)
C65	0.018(2)	0.026(3)	0.026(2)	-0.006(2)	0.0066(19)	-0.004(2)
C66	0.025(2)	0.024(3)	0.029(2)	-0.006(2)	0.010(2)	0.002(2)
C67	0.029(2)	0.030(3)	0.022(2)	0.002(2)	0.0099(19)	0.003(3)
C68	0.019(2)	0.024(3)	0.022(2)	-0.002(2)	0.0057(18)	0.004(2)
C69	0.029(2)	0.035(3)	0.023(2)	0.000(2)	0.002(2)	0.006(3)
C70	0.017(2)	0.036(3)	0.030(2)	0.000(2)	-0.003(2)	0.000(2)
C71	0.015(2)	0.025(3)	0.028(2)	-0.004(2)	0.0039(18)	0.001(2)
C72	0.0094(19)	0.027(3)	0.026(2)	-0.005(2)	0.0013(18)	-0.002(2)
C73	0.007(2)	0.029(3)	0.034(2)	-0.002(2)	0.0029(19)	0.002(2)
C74	0.014(2)	0.027(3)	0.037(2)	-0.002(2)	0.011(2)	-0.001(2)
C75	0.016(2)	0.035(3)	0.028(2)	-0.003(2)	0.0048(19)	0.002(2)
C76	0.011(2)	0.033(3)	0.031(2)	0.005(2)	0.0048(19)	0.008(2)
C77	0.012(2)	0.030(3)	0.029(2)	0.004(2)	0.0014(18)	0.004(2)
C78	0.0109(19)	0.025(3)	0.027(2)	-0.002(2)	0.0047(17)	0.000(2)
C79	0.0150(19)	0.018(2)	0.025(2)	-0.003(2)	0.0022(17)	0.000(2)
C80	0.0158(19)	0.028(3)	0.022(2)	-0.001(2)	0.0034(18)	-0.001(2)
C81	0.012(2)	0.040(2)	0.022(2)	0.0017(19)	0.0016(19)	-0.004(2)
C82	0.012(2)	0.042(2)	0.026(2)	0.0055(18)	0.005(2)	-0.004(2)
C83	0.021(3)	0.034(2)	0.030(2)	0.0096(19)	0.008(2)	0.002(2)
C84	0.030(3)	0.028(3)	0.040(2)	0.003(2)	0.011(2)	0.001(2)
C85	0.047(4)	0.026(3)	0.040(2)	0.000(2)	0.015(3)	-0.002(3)
C86	0.051(4)	0.032(3)	0.043(3)	-0.001(2)	0.018(3)	-0.004(3)
C87	0.054(4)	0.027(3)	0.056(3)	-0.005(2)	0.026(3)	0.000(3)
C88	0.039(3)	0.025(3)	0.061(3)	0.004(2)	0.020(3)	0.003(3)
C89	0.035(3)	0.027(3)	0.049(2)	0.008(2)	0.020(3)	0.000(2)
C90	0.022(3)	0.037(3)	0.043(2)	0.016(2)	0.010(2)	0.004(2)
C91	0.028(3)	0.044(3)	0.045(3)	0.021(2)	0.008(3)	0.008(3)
C92	0.031(3)	0.057(3)	0.038(3)	0.020(2)	0.009(3)	-0.001(3)
C93	0.014(2)	0.053(3)	0.027(2)	0.009(2)	0.003(2)	-0.002(2)
C94	0.026(3)	0.067(3)	0.022(2)	0.004(2)	0.006(2)	0.000(3)
C95	0.027(3)	0.058(3)	0.028(2)	-0.005(2)	0.011(2)	-0.006(3)
C96	0.016(2)	0.048(3)	0.029(2)	-0.004(2)	0.009(2)	-0.004(2)
Cl13	0.0984(19)	0.0416(12)	0.0640(13)	-0.0017(10)	-0.0218(13)	0.0098(12)

Cl14	0.0931(17)	0.0510(12)	0.0405(9)	-0.0005(9)	-0.0106(11)	-0.0015(13)
Cl15	0.0238(7)	0.0505(10)	0.0248(7)	-0.0044(7)	0.0055(6)	-0.0084(7)
Cl16	0.0146(6)	0.0489(10)	0.0320(7)	-0.0064(7)	0.0032(6)	-0.0005(7)
O7	0.016(2)	0.040(2)	0.038(2)	0.0031(18)	0.001(2)	0.0004(19)
O8	0.0120(18)	0.052(3)	0.036(2)	-0.002(2)	0.0071(17)	0.003(2)
N13	0.026(3)	0.039(3)	0.044(2)	-0.010(2)	0.005(2)	-0.002(2)
N14	0.024(2)	0.033(2)	0.033(2)	-0.0052(18)	0.005(2)	-0.004(2)
N15	0.0151(18)	0.027(2)	0.026(2)	-0.0008(19)	0.0093(16)	-0.0002(19)
N16	0.0192(19)	0.036(3)	0.030(2)	0.003(2)	0.0123(17)	0.008(2)
C97	0.016(3)	0.045(3)	0.031(2)	0.002(2)	0.007(2)	0.003(2)
C98	0.023(3)	0.047(3)	0.031(2)	0.005(2)	0.006(2)	-0.003(3)
C99	0.030(3)	0.058(3)	0.028(3)	-0.004(2)	0.006(2)	-0.002(3)
C100	0.016(2)	0.048(3)	0.034(2)	-0.006(2)	0.007(2)	-0.004(2)
C101	0.030(3)	0.054(3)	0.035(3)	-0.015(2)	0.007(3)	-0.007(3)
C102	0.029(3)	0.048(3)	0.041(3)	-0.018(2)	0.009(3)	-0.002(3)
C103	0.021(3)	0.043(3)	0.041(2)	-0.011(2)	0.007(2)	0.002(2)
C104	0.025(3)	0.036(3)	0.044(2)	-0.007(2)	0.007(2)	-0.002(2)
C105	0.034(3)	0.036(3)	0.050(3)	-0.011(2)	-0.004(3)	0.004(3)
C106	0.035(3)	0.034(3)	0.053(3)	-0.002(2)	-0.009(3)	0.000(3)
C107	0.033(3)	0.034(3)	0.043(2)	-0.005(2)	-0.006(3)	-0.011(3)
C108	0.037(3)	0.034(3)	0.039(2)	-0.004(2)	0.004(3)	0.000(3)
C109	0.027(3)	0.030(3)	0.041(2)	-0.007(2)	0.007(2)	-0.002(2)
C110	0.013(2)	0.038(2)	0.034(2)	-0.0081(19)	0.005(2)	-0.003(2)
C111	0.011(2)	0.043(2)	0.031(2)	-0.0048(19)	0.007(2)	0.003(2)
C112	0.008(2)	0.038(2)	0.028(2)	-0.0007(19)	0.0073(18)	-0.004(2)
C113	0.016(2)	0.027(3)	0.028(2)	0.002(2)	0.0089(18)	0.006(2)
C114	0.017(2)	0.022(3)	0.028(2)	0.004(2)	0.0074(18)	0.003(2)
C115	0.015(2)	0.027(3)	0.027(2)	0.000(2)	0.0065(18)	0.009(2)
C116	0.016(2)	0.025(3)	0.031(2)	-0.002(2)	0.0106(18)	0.004(2)
C117	0.020(2)	0.030(3)	0.029(2)	0.001(2)	0.0113(18)	0.000(2)
C118	0.022(2)	0.032(3)	0.027(2)	0.004(2)	0.0035(19)	0.013(2)
C119	0.016(2)	0.026(3)	0.028(2)	0.003(2)	0.0063(19)	0.007(2)
C120	0.013(2)	0.034(3)	0.029(2)	0.005(2)	0.0097(18)	0.003(2)
C121	0.015(2)	0.030(3)	0.026(2)	0.006(2)	0.0107(17)	0.006(2)
C122	0.019(2)	0.029(3)	0.029(2)	0.000(2)	0.0108(18)	0.005(2)
C123	0.023(2)	0.049(3)	0.026(2)	0.001(2)	0.011(2)	0.007(3)
C124	0.025(2)	0.038(3)	0.026(2)	0.003(2)	0.005(2)	0.001(3)
C125	0.025(2)	0.027(3)	0.030(2)	-0.002(2)	0.011(2)	0.004(2)

C126	0.024(2)	0.036(3)	0.025(2)	-0.001(2)	0.004(2)	0.007(3)
C127	0.013(2)	0.030(3)	0.032(2)	0.002(2)	0.0010(19)	0.003(2)
C128	0.018(2)	0.024(3)	0.030(2)	0.001(2)	0.0072(19)	0.004(2)
C135	0.068(7)	0.073(7)	0.154(6)	0.005(6)	0.034(7)	0.008(6)
C136	0.086(6)	0.082(6)	0.158(6)	0.005(5)	0.034(6)	0.019(6)
C137	0.084(6)	0.097(6)	0.153(6)	0.001(5)	0.045(6)	0.003(5)
C138	0.079(6)	0.107(7)	0.152(6)	0.010(5)	0.054(6)	-0.006(5)
C139	0.108(7)	0.139(8)	0.147(6)	0.003(5)	0.050(7)	-0.001(7)
C140	0.144(12)	0.200(14)	0.146(6)	0.023(8)	0.051(10)	-0.017(12)

The form of the anisotropic displacement parameter is:
$\exp[-2\pi^2(a^{*2}U_{11}h^2+b^{*2}U_{22}k^2+c^{*2}U_{33}l^2+2b^*c^*U_{23}kl+2a^*c^*U_{13}hl+2a^*b^*U_{12}hk)]$

Table B.41 Bond Distances in Compound *(S)*-**6.36c**, Å

Cl1-C10	1.728(7)	Cl3-C22	1.752(7)	Cl4-C23	1.745(7)
O1-C1	1.381(7)	O2-C32	1.345(8)	N1-C8	1.336(8)
N1-C7	1.347(8)	N2-C14	1.308(8)	N2-C13	1.363(8)
N3-C19	1.309(8)	N3-C20	1.366(8)	N4-C26	1.327(9)
N4-C25	1.337(9)	C1-C16	1.366(8)	C1-C2	1.386(9)
C2-C3	1.365(9)	C3-C4	1.428(9)	C4-C15	1.402(8)
C4-C5	1.417(9)	C5-C6	1.364(9)	C6-C7	1.422(9)
C7-C14	1.458(8)	C8-C13	1.419(9)	C8-C9	1.440(9)
C9-C10	1.335(9)	C10-C11	1.381(19)	C10-C11'	1.51(2)
Cl2-C11	1.744(16)	C11-C12	1.42(2)	C12-C13	1.362(17)
Cl2'-C11'	1.70(2)	C11'-C12'	1.36(3)	C12'-C13	1.52(2)
C14-C15	1.444(8)	C15-C16	1.409(8)	C16-C17	1.524(8)
C17-C32	1.388(8)	C17-C18	1.410(9)	C18-C29	1.416(9)
C18-C19	1.465(9)	C19-C26	1.471(9)	C20-C21	1.418(9)
C20-C25	1.431(10)	C21-C22	1.353(10)	C22-C23	1.377(11)
C23-C24	1.386(11)	C24-C25	1.415(10)	C26-C27	1.407(10)
C27-C28	1.327(10)	C28-C29	1.444(10)	C29-C30	1.401(9)
C30-C31	1.362(10)	C31-C32	1.394(9)	Cl5-C42	1.734(8)
Cl6-C43	1.726(9)	Cl7-C54	1.739(6)	Cl8-C55	1.718(6)
O3-C33	1.354(9)	O4-C64	1.356(8)	N5-C40	1.331(11)
N5-C39	1.321(11)	N6-C46	1.316(8)	N6-C45	1.355(9)
N7-C51	1.329(8)	N7-C52	1.348(7)	N8-C57	1.345(8)
N8-C58	1.356(8)	C33-C34	1.397(10)	C33-C48	1.400(9)

C34-C35	1.407(12)	C35-C36	1.381(11)	C36-C47	1.421(9)
C36-C37	1.462(12)	C37-C38	1.329(12)	C38-C39	1.438(10)
C39-C46	1.459(11)	C40-C41	1.424(12)	C40-C45	1.429(11)
C41-C42	1.345(12)	C42-C43	1.431(12)	C43-C44	1.342(11)
C44-C45	1.388(10)	C46-C47	1.444(10)	C47-C48	1.428(10)
C48-C49	1.487(8)	C49-C50	1.409(9)	C49-C64	1.415(8)
C50-C61	1.405(8)	C50-C51	1.487(8)	C51-C58	1.440(9)
C52-C53	1.373(8)	C52-C57	1.418(8)	C53-C54	1.394(8)
C54-C55	1.428(8)	C55-C56	1.350(8)	C56-C57	1.460(8)
C58-C59	1.423(8)	C59-C60	1.348(9)	C60-C61	1.429(9)
C61-C62	1.432(9)	C62-C63	1.353(10)	C63-C64	1.395(9)
C129-C130	1.5224	C130-C131	1.5233	C131-C132	1.5241
C132-C133	1.5225	C133-C134	1.5236	Cl9-C74	1.721(6)
Cl10-C75	1.730(6)	Cl11-C86	1.731(7)	Cl12-C87	1.738(7)
O5-C65	1.336(7)	O6-C96	1.358(8)	N9-C72	1.347(7)
N9-C71	1.367(7)	N10-C78	1.323(7)	N10-C77	1.355(7)
N11-C83	1.312(8)	N11-C84	1.366(9)	N12-C90	1.317(9)
N12-C89	1.345(9)	C65-C66	1.378(8)	C65-C80	1.415(8)
C66-C67	1.366(9)	C67-C68	1.414(8)	C68-C79	1.416(8)
C68-C69	1.434(8)	C69-C70	1.346(9)	C70-C71	1.413(8)
C71-C78	1.412(8)	C72-C77	1.409(8)	C72-C73	1.438(7)
C73-C74	1.328(8)	C74-C75	1.426(8)	C75-C76	1.392(8)
C76-C77	1.419(8)	C78-C79	1.478(7)	C79-C80	1.390(8)
C80-C81	1.509(8)	C81-C96	1.391(9)	C81-C82	1.409(9)
C82-C93	1.427(8)	C82-C83	1.475(9)	C83-C90	1.463(9)
C84-C85	1.416(9)	C84-C89	1.414(9)	C85-C86	1.370(10)
C86-C87	1.401(10)	C87-C88	1.356(11)	C88-C89	1.432(10)
C90-C91	1.436(9)	C91-C92	1.344(11)	C92-C93	1.447(10)
C93-C94	1.364(10)	C94-C95	1.406(11)	C95-C96	1.388(9)
Cl13-C106	1.726(8)	Cl14-C107	1.712(7)	Cl15-C118	1.734(6)
Cl16-C119	1.735(6)	O7-C97	1.364(8)	O8-C128	1.363(7)
N13-C104	1.357(9)	N13-C103	1.351(9)	N14-C110	1.323(8)
N14-C109	1.358(9)	N15-C115	1.315(7)	N15-C116	1.324(7)
N16-C121	1.338(8)	N16-C122	1.328(8)	C97-C98	1.371(9)
C97-C112	1.409(9)	C98-C99	1.406(11)	C99-C100	1.398(10)
C100-C111	1.417(8)	C100-C101	1.453(10)	C101-C102	1.315(11)
C102-C103	1.427(9)	C103-C110	1.410(9)	C104-C109	1.400(10)
C104-C105	1.415(10)	C105-C106	1.344(10)	C106-C107	1.453(11)

C107-C108	1.345(10)	C108-C109	1.407(9)	C110-C111	1.467(9)
C111-C112	1.440(9)	C112-C113	1.489(8)	C113-C128	1.395(8)
C113-C114	1.430(8)	C114-C125	1.392(8)	C114-C115	1.471(8)
C115-C122	1.465(8)	C116-C117	1.409(8)	C116-C121	1.451(7)
C117-C118	1.393(8)	C118-C119	1.416(8)	C119-C120	1.355(8)
C120-C121	1.422(8)	C122-C123	1.424(8)	C123-C124	1.344(9)
C124-C125	1.445(8)	C125-C126	1.413(9)	C126-C127	1.386(8)
C127-C128	1.357(8)	C135-C136	1.5234	C136-C137	1.5235
C137-C138	1.5242	C138-C139	1.5234	C139-C140	1.5233

Table B.42 Bond Angles in Compound *(S)*-**6.36c**, °

C8-N1-C7	116.1(5)	C14-N2-C13	117.3(5)	C19-N3-C20	118.3(6)
C26-N4-C25	118.8(6)	C16-C1-C2	122.8(5)	C16-C1-O1	121.5(5)
C2-C1-O1	115.6(5)	C3-C2-C1	118.7(6)	C2-C3-C4	120.9(6)
C15-C4-C5	120.7(6)	C15-C4-C3	118.8(5)	C5-C4-C3	120.4(5)
C6-C5-C4	123.8(6)	C5-C6-C7	117.9(6)	N1-C7-C6	117.6(5)
N1-C7-C14	122.2(5)	C6-C7-C14	120.2(5)	N1-C8-C13	121.9(6)
N1-C8-C9	118.9(5)	C13-C8-C9	119.2(6)	C10-C9-C8	119.0(6)
C9-C10-C11	119.7(9)	C9-C10-C11'	123.8(10)	C11-C10-C11'	19.2(7)
C9-C10-Cl1	119.4(5)	C11-C10-Cl1	120.0(8)	C11'-C10-Cl1	116.0(9)
C10-C11-C12	122.7(13)	C10-C11-Cl2	120.3(12)	C12-C11-Cl2	116.8(12)
C13-C12-C11	116.7(13)	C12'-C11'-C10	118.1(16)	C12'-C11'-Cl2'	119.0(16)
C10-C11'-Cl2'	122.9(15)	C11'-C12'-C13	118.1(17)	C12-C13-N2	117.2(9)
C12-C13-C8	120.5(9)	N2-C13-C8	121.8(6)	C12-C13-C12'	19.7(8)
N2-C13-C12'	116.5(10)	C8-C13-C12'	120.1(10)	N2-C14-C15	119.5(5)
N2-C14-C7	120.7(5)	C15-C14-C7	119.8(5)	C4-C15-C16	119.4(5)
C4-C15-C14	117.5(5)	C16-C15-C14	123.0(5)	C1-C16-C15	119.2(5)
C1-C16-C17	117.1(5)	C15-C16-C17	123.4(5)	C32-C17-C18	119.6(5)
C32-C17-C16	118.4(5)	C18-C17-C16	122.0(5)	C29-C18-C17	119.6(6)
C29-C18-C19	117.8(6)	C17-C18-C19	122.4(5)	N3-C19-C18	119.6(6)
N3-C19-C26	121.3(6)	C18-C19-C26	119.1(6)	N3-C20-C21	118.5(6)
N3-C20-C25	120.3(6)	C21-C20-C25	121.3(6)	C22-C21-C20	118.3(7)
C21-C22-C23	121.9(7)	C21-C22-Cl3	117.8(6)	C23-C22-Cl3	120.3(5)
C24-C23-C22	121.7(7)	C24-C23-Cl4	117.2(6)	C22-C23-Cl4	121.0(6)
C23-C24-C25	119.3(7)	N4-C25-C24	121.2(6)	N4-C25-C20	121.3(6)

C24-C25-C20	117.5(6)	N4-C26-C27	120.4(6)	N4-C26-C19	120.0(6)
C27-C26-C19	119.4(6)	C28-C27-C26	120.5(7)	C27-C28-C29	123.8(6)
C30-C29-C18	119.0(6)	C30-C29-C28	121.8(6)	C18-C29-C28	119.1(6)
C31-C30-C29	120.5(6)	C30-C31-C32	121.3(6)	O2-C32-C17	124.4(5)
O2-C32-C31	115.7(5)	C17-C32-C31	119.9(6)	C40-N5-C39	118.7(7)
C46-N6-C45	119.0(6)	C51-N7-C52	118.9(5)	C57-N8-C58	116.6(5)
O3-C33-C34	114.9(6)	O3-C33-C48	122.8(6)	C34-C33-C48	122.1(7)
C33-C34-C35	118.8(7)	C36-C35-C34	120.9(7)	C35-C36-C47	120.5(7)
C35-C36-C37	120.0(7)	C47-C36-C37	119.4(7)	C38-C37-C36	123.1(6)
C37-C38-C39	120.3(8)	N5-C39-C38	119.7(8)	N5-C39-C46	121.9(7)
C38-C39-C46	118.4(8)	N5-C40-C41	123.0(8)	N5-C40-C45	120.2(7)
C41-C40-C45	116.6(7)	C42-C41-C40	121.2(8)	C41-C42-C43	120.5(8)
C41-C42-Cl5	119.3(7)	C43-C42-Cl5	120.2(7)	C44-C43-C42	119.9(8)
C44-C43-Cl6	121.1(7)	C42-C43-Cl6	118.9(6)	C43-C44-C45	120.7(8)
N6-C45-C44	118.0(7)	N6-C45-C40	121.1(7)	C44-C45-C40	121.0(7)
N6-C46-C47	119.7(6)	N6-C46-C39	119.2(7)	C47-C46-C39	121.1(6)
C36-C47-C48	119.1(6)	C36-C47-C46	117.6(7)	C48-C47-C46	123.3(6)
C33-C48-C47	118.5(6)	C33-C48-C49	119.7(6)	C47-C48-C49	121.8(6)
C50-C49-C64	117.3(5)	C50-C49-C48	124.6(5)	C64-C49-C48	118.0(5)
C61-C50-C49	121.3(5)	C61-C50-C51	117.0(5)	C49-C50-C51	121.7(5)
N7-C51-C58	121.1(5)	N7-C51-C50	120.0(5)	C58-C51-C50	118.9(5)
C53-C52-N7	119.3(5)	C53-C52-C57	121.0(5)	N7-C52-C57	119.6(5)
C52-C53-C54	119.6(5)	C53-C54-C55	120.8(5)	C53-C54-Cl7	119.4(5)
C55-C54-Cl7	119.8(4)	C56-C55-C54	120.5(5)	C56-C55-Cl8	120.0(4)
C54-C55-Cl8	119.4(4)	C55-C56-C57	119.3(5)	N8-C57-C52	123.1(5)
N8-C57-C56	118.2(5)	C52-C57-C56	118.7(5)	N8-C58-C59	119.0(6)
N8-C58-C51	120.6(5)	C59-C58-C51	120.4(5)	C60-C59-C58	119.9(6)
C59-C60-C61	122.3(6)	C50-C61-C60	121.4(5)	C50-C61-C62	118.4(6)
C60-C61-C62	120.2(5)	C63-C62-C61	121.0(6)	C62-C63-C64	120.1(6)
O4-C64-C63	117.0(5)	O4-C64-C49	121.1(5)	C63-C64-C49	121.8(6)
C129-C130-C131	109.5	C130-C131-C132	109.5	C133-C132-C131	109.5
C132-C133-C134	109.5	C72-N9-C71	117.1(5)	C78-N10-C77	117.1(5)
C83-N11-C84	117.6(6)	C90-N12-C89	117.6(6)	O5-C65-C66	117.5(5)
O5-C65-C80	121.7(5)	C66-C65-C80	120.7(5)	C67-C66-C65	120.5(5)
C66-C67-C68	120.5(5)	C79-C68-C69	120.4(5)	C79-C68-C67	119.4(5)
C69-C68-C67	120.0(5)	C70-C69-C68	122.4(5)	C69-C70-C71	119.5(6)
N9-C71-C70	118.5(5)	N9-C71-C78	120.2(5)	C70-C71-C78	121.3(5)

N9-C72-C77	121.3(5)	N9-C72-C73	120.1(5)	C77-C72-C73	118.5(5)
C74-C73-C72	120.9(5)	C73-C74-C75	121.0(5)	C73-C74-Cl9	120.2(4)
C75-C74-Cl9	118.7(4)	C76-C75-C74	120.2(5)	C76-C75-Cl10	118.6(5)
C74-C75-Cl10	121.2(4)	C75-C76-C77	118.9(5)	N10-C77-C72	121.3(5)
N10-C77-C76	118.3(5)	C72-C77-C76	120.3(5)	N10-C78-C71	122.6(5)
N10-C78-C79	118.1(5)	C71-C78-C79	119.3(5)	C80-C79-C68	119.4(5)
C80-C79-C78	123.7(5)	C68-C79-C78	116.8(5)	C79-C80-C65	119.4(5)
C79-C80-C81	124.1(5)	C65-C80-C81	116.5(5)	C96-C81-C82	119.9(5)
C96-C81-C80	118.8(6)	C82-C81-C80	121.3(5)	C81-C82-C93	118.6(6)
C81-C82-C83	123.7(5)	C93-C82-C83	117.7(6)	N11-C83-C90	120.5(6)
N11-C83-C82	119.5(6)	C90-C83-C82	120.0(5)	N11-C84-C85	118.2(6)
N11-C84-C89	121.4(6)	C85-C84-C89	120.5(6)	C86-C85-C84	118.7(7)
C85-C86-C87	120.7(7)	C85-C86-Cl11	119.0(6)	C87-C86-Cl11	120.2(5)
C88-C87-C86	122.5(7)	C88-C87-Cl12	117.5(6)	C86-C87-Cl12	119.9(6)
C87-C88-C89	118.3(7)	N12-C89-C84	121.2(6)	N12-C89-C88	119.5(6)
C84-C89-C88	119.3(6)	N12-C90-C91	119.7(6)	N12-C90-C83	121.7(6)
C91-C90-C83	118.6(6)	C92-C91-C90	120.7(7)	C91-C92-C93	123.3(6)
C94-C93-C82	120.0(7)	C94-C93-C92	120.5(6)	C82-C93-C92	119.5(6)
C93-C94-C95	121.6(6)	C96-C95-C94	118.6(6)	O6-C96-C95	114.8(6)
O6-C96-C81	123.8(5)	C95-C96-C81	121.3(7)	C104-N13-C103	115.6(6)
C110-N14-C109	117.9(6)	C115-N15-C116	118.6(5)	C121-N16-C122	118.9(5)
O7-C97-C98	115.5(6)	O7-C97-C112	121.6(5)	C98-C97-C112	122.9(6)
C97-C98-C99	119.0(6)	C100-C99-C98	121.1(6)	C99-C100-C111	119.9(6)
C99-C100-C101	119.5(6)	C111-C100-C101	120.6(6)	C102-C101-C100	121.5(6)
C101-C102-C103	120.7(7)	N13-C103-C110	122.4(6)	N13-C103-C102	117.0(6)
C110-C103-C102	120.6(7)	N13-C104-C109	122.1(6)	N13-C104-C105	118.6(6)
C109-C104-C105	119.3(6)	C106-C105-C104	120.2(7)	C105-C106-C107	120.6(7)
C105-C106-Cl13	119.8(6)	C107-C106-Cl13	119.6(6)	C108-C107-C106	119.2(7)
C108-C107-Cl14	121.7(6)	C106-C107-Cl14	119.2(6)	C107-C108-C109	120.9(7)
N14-C109-C108	119.3(6)	N14-C109-C104	120.8(6)	C108-C109-C104	119.8(6)
N14-C110-C103	121.0(6)	N14-C110-C111	119.2(6)	C103-C110-C111	119.7(6)
C100-C111-	119.3(6)	C100-C111-C110	116.7(6)	C112-C111-	124.1(5)

C112				C110	
C97-C112-C111	117.9(5)	C97-C112-C113	118.4(6)	C111-C112-C113	123.7(5)
C128-C113-C114	117.8(5)	C128-C113-C112	118.3(5)	C114-C113-C112	123.9(5)
C125-C114-C113	119.7(5)	C125-C114-C115	118.0(5)	C113-C114-C115	122.3(5)
N15-C115-C122	121.2(5)	N15-C115-C114	119.7(5)	C122-C115-C114	119.1(5)
N15-C116-C117	119.2(5)	N15-C116-C121	121.3(5)	C117-C116-C121	119.5(5)
C118-C117-C116	118.7(5)	C117-C118-C119	121.2(5)	C117-C118-Cl15	118.8(4)
C119-C118-Cl15	120.1(5)	C120-C119-C118	121.8(5)	C120-C119-Cl16	118.4(4)
C118-C119-Cl16	119.8(4)	C119-C120-C121	119.1(5)	N16-C121-C120	120.1(5)
N16-C121-C116	120.0(5)	C120-C121-C116	119.8(5)	N16-C122-C123	120.8(5)
N16-C122-C115	119.9(5)	C123-C122-C115	119.2(5)	C124-C123-C122	120.4(5)
C123-C124-C125	122.4(6)	C114-C125-C126	119.4(5)	C114-C125-C124	120.7(5)
C126-C125-C124	119.9(5)	C127-C126-C125	120.7(5)	C128-C127-C126	119.3(6)
C127-C128-O8	116.6(5)	C127-C128-C113	123.1(5)	O8-C128-C113	120.3(5)
C135-C136-C137	109.5	C136-C137-C138	109.5	C139-C138-C137	109.5
C140-C139-C138	109.5				

BIBLIOGRAPHY

Aguirre, D. H.; Neumann, R. A. "Intoxicación por 'Cegadera' (*Heterophyllaea pustulata*) en Caprinos del Noroeste Argentino" *Med. Vet.* **2001**, *18*, 487–490.

Agusta, A.; Ohashi, K.; Shibuya, H. "Bisanthraquinone Metabolites Produced by the Endophytic Fungus *Diaporthe* sp" *Chem. Pharm. Bull.* **2006**, *54*, 579–582.

Aldakov, D.; Palacios, M. A.; Anzenbacher, Jr., P. "Benzothiadiazoles and Dipyrrolyl Quinoxalines with Extended Conjugated Chromophores-Fluorophores and Anion Sensors." *Chem. Mater.* **2005**, *17*, 5238–5241.

Ali, M. H.; Niedbalski, M.; Bohnert, G.; Bryant, D. "Silica-Gel-Supported Ceric Ammonium Nitrate (CAN): A Simple and Efficient Solid-Supported Reagent for Oxidation of Oxygenated Aromatic Compounds to Quinones" *Synth. Commun.* **2006**, *36*, 1751–1759.

Alonso, A. M.; Horcajada, R.; Motevalli, M.; Utley, J. H.; Wyatt, P. B. "The Reactivity, as Electrogenerated Bases, of Chiral and Achiral Phenazine Radical-anions, Including Application in Asymmetric Deprotonation." *Org. Biomol. Chem*. **2005**, *3*, 2842–2847.

Altomare, A., M. Burla, M. Camalli, G. Cascarano, C. Giacovazzo, A. Guagliardi, A. Moliterni, G. Polidori & R. Spagna (1999). J. Appl. Cryst., 32, 115-119.

Anderson, K. W.; Ikawa, T.; Tundel, R. E.; Buchwald, S. L. "The Selective Reaction of Aryl Halides With KOH: Synthesis of Phenols, Aromatic Ethers, and Benzofurans" *J. Am. Chem. Soc.* **2006**, *128*, 10694–10695.

Asche, C. "Antitumour Quinones" *Mini-Rev. Med. Chem.* **2005**, *5*, 449–467.

Aullón, G.; Bellamy, D.; Brammer, L.; Bruton, E. A.; Orpen, A. G. "Metal-Bound Chlorine Often Accepts Hydrogen Bonds" Chem. Commun., 1998 653–654.

Ballart, B.; Martí, J.; Velasco, D.; López-Calahorra, F.; Pascual, J.; García, M. L.; Cabré, F.; Mauleón, D. "Synthesis and Pharmacological Evaluation of New 4-[2-(7-Heterocycle-methoxynaphtalen-2-ylmethoxy)ethyl]benzoic Acids as LTD4-Antagonists" *Eur. J. Med. Chem.* **2000**, *35*, 439–447.

Bamfield, P.; Hutchings, M. G. *Chromic Phenomena. Technological Applications of Colour Chemistry,* 2nd ed., The Royal Society of Chemistry: Cambridge, UK, 2010.

Banerjee, R.; Desiraju, G. R.; Mondal, R.; Howard, J. A. K. "Organic Chlorine as a Hydrogen-Bridge Acceptor: Evidence for the Existence of Intramolecular O–H···Cl–C Interactions in Some *gem*-Alkynols" *Chem. Eur. J.* **2004**, *10*, 3373–3383.

Banks, H. J.; Cameron, D. W.; Crossley, M. J.; Samuel, E. L. "Synthesis of 5,7-Dihydroxynaphthoquinone Derivatives and Their Reactions with Nucleophiles: Nitration of 2,3-Dimethylnaphthalene and Subsequent Transformations" *Aust. J. Chem.* **1976**, *29,* 2247–2256.

Banks, H. J.; Cameron, D. W.; Raverty, W. D. "Chemistry of Coccoidea II. Condensed Polycyclic Pigments from Two Australian Pseudococcids (Hemiptera)" *Aust. J. Chem.* **1976**, *29*, 1509–1521.

Banville, J.; Grandmaison, J.- L.; Lang, G.; Brassard, P. "Reactions of Keten Acetals. Part I. A Simple Synthesis of Some Naturally Occurring Anthraquinones" *Can. J. Chem.* **1974**, *52*, 80–87.

Barret, R.; Daudon, M. "Oxidation of Phenols to Quinones by Bis(trifluoroacetoxy)iodobenzene" *Tetrahedron Lett.* **1990**, *31*, 4871–4872.

Bergquist, P. R. "A Revision of the Supraspecific Classification of the Orders Dictyoceratida, Dendroceratida and Verongida (Class Demospongiae)" *New Zeal. J. Zool.* **1980**, *7*, 443–503.

Berneth, H. "Azine Dyes." *Ullmann's Encyclopedia of Industrial Chemistry*, Electronic Release, Wiley-VCH, Weinheim Jun. 2000.

Bien, H.-S.; Stawitz, J.; Wunderlich, K. "Anthraquinone Dyes and Intermediates" *Ullmann's Encyclopedia of Industrial Chemistry*, Electronic Release, Wiley-VCH, Weinheim Jun. 2000.

Blackburn, G. M.; Cameron, D. W.; Chan, H. W.-S. "Colouring Matters of the Aphididae. Part XXX. Coupling Reactions Involving the Quinone A Derived by Reduction of Protoaphin-*fb*" *J. Chem. Soc. C* **1966**, 1836–1842.

Blackmore, K. J.; Ziller, J. W.; Heyduk, A. F. ""Oxidative Addition" to a Zirconium(IV) Redox-Active Ligand Complex " *Inorg. Chem.* **2005**, *44,* 5559-5561.

Boeckman, R. K.; Dolak, T. M.; Culos, K. O. "Diels-Alder Cycloaddition of Juglone Derivatives: Elucidation of Factors Influencing Regiochemical Control" *J. Am. Chem. Soc.* **1978**, *100*, 7098–7100.

Bozell, J. J.; Hames, B. R.; Dimmel, D. R. "Cobalt-Schiff Base Complex Catalyzed Oxidation of *Para*-Substituted Phenolics. Preparation of Benzoquinones" *J. Org. Chem.* **1995**, *60,* 2398–2404.

Bringmann, G.; Gulder, T.; Gulder, T. A. M.; Breuning, M. "Atroposelective Total Synthesis of Axially Chiral Biaryl Natural Products" *Chem. Rev.* **2011**, *111*, 563–639.

Brisson, C.; Brassard, P. "Regiospecific Reactions of Some Vinylogous Ketene Acetals with Haloquinones and Their Regioselective Formation by Dienolization" *J. Org. Chem.* **1981**, *46*, 1810–1814.

Bruker (2009) SAINT. Bruker AXS Inc., Madison, Wisconsin, USA.

Bruker (2009) SHELXTL. Bruker AXS Inc., Madison, Wisconsin, USA.

Brunel, J. M. "BINOL: A Versatile Chiral Reagent." *Chem. Rev.* **2005**, *105*, 857–897.

Cameron, D. W.; Chan, H. W.-S. "Colouring Matters of the Aphididae. Part XXVIII. A Coupling Reaction Involving Phenols and Quinones. Reconstruction of the Protoaphins, and Synthesis of the Chrysoaphin Chromophore" *J. Chem. Soc. C* **1966**, 1825–1832.

Cameron, D. W.; Chan, H. W.-S.; Hildyard, E. M. "Colouring Matters of the Aphididae. Part XXIX. Partial Synthesis of Erythroaphin and Related Systems by Oxidative Coupling" *J. Chem. Soc. C* **1966**, 1832–1836.

Cameron, D. W.; Edmonds, J. S.; Raverty, W. D. "Oxidation of Emodin Anthrone and Stereochemistry of Emodin Bianthrone" *Aust. J. Chem.* **1976**, *29*, 1535–1548.

Cameron, D. W.; Riches, A. G. "Reaction of 2-Acetoxy-3-chloro and 2,3-Diacetoxy Naphthoquinones with 1,3-Dioxy and 1,1,3-Trioxy Butadienes" *Aust. J. Chem*. **1999**, *52*, 1165–1171.

Campos-Martin, J. M.; Blanco-Brieva, G.; Fierro, J. L. G. "Hydrogen Peroxide Synthesis: An Outlook Beyond the Anthraquinone Process" *Angew. Chem. Int. Ed.* **2006**, *45*, 6962–6984.

Chen, Y.; Yekta, S.; Yudin, A. K. "Modified BINOL Ligands in Asymmetric Catalysis." *Chem. Rev.* **2003**, *103*, 3155–3211.

Chirik, P. J.; Wieghardt, K. *Science* **2010**, *327*, 794-795.

Cho, A. K., Di Stefano, E.; You, Y.; Rodriguez, C. E.; Schmitz, D. A.; Kumagai, Y.; Miguel, A. H.; Eiguren-Fernandez, A.; Kobayashi, T.; Avol, E.; Froines, J. R. "Determination of Four Quinones in Diesel Exhaust Particles SRM 1649a, and Atmospheric $PM_{2.5}$" *Aerosol. Sci. Tech.* **2004**, *38*, 68–81.

Comini, L. R.; Núñez Montoya, S. C.; Páez, P. L.; Argüello, G. A.; Albesa, I.; Cabrera, J. L. "Antibacterial Activity of Anthraquinone Derivatives From *Heterophyllaea pustulata*" *J. Photochem. Photobiol., B* **2011**, *102*, 108–114.

Comini, L. R.; Núñez Montoya, S. C.; Sarmiento, M.; Cabrera, J. L.; Argüello, G. A. "Characterizing Some Photophysical, Photochemical, and Photobiological Properties, of Photosensitizing Anthraquinones" *J. Photochem. Photobiol., A* **2007**, *188*, 185–191.

Cornella, J.; Sanchez, C.; Banawa, D.; Larrosa, I. "Silver-Catalysed Protodecarboxylation of *Ortho*-Substituted Benzoic Acids" *Chem. Commun.* **2009**, 7176–7178.

CrystalClear: Rigaku Corporation, 1999.

CrystalStructure: Crystal Structure Analysis Package, Rigaku Corp. Rigaku/MSC (2002).

Dai, J.; Liu, Y.; Zhou, Y.-D.; Nagle, D. G. "Cytotoxic Metabolites From an Indonesian Sponge *Lendenfeldia* sp" *J. Nat. Prod.* **2007**, *70,* 1824–1826.

Dai, J.; Punchihewa, C.; Mistry, P.; Ooi, A. T.; Yang, D. "Novel DNA Bis-intercalation by MLN944, a Potent Clinical Bisphenazine Anticancer Drug." *J. Biol. Chem.* **2004**, *279*, 46096–46103.

Danishefsky, S.; Kitaharai, T. "Useful Diene for the Diels-Alder Reaction" *J. Am. Chem. Soc.* **1974**, *96,* 7807–7808.

Danishefsky, S.; Uang, B. J.; Quallich, G. "Total Synthesis of Vineomycinone B2 Methyl Ester" *J. Am. Chem. Soc.* **1985**, *107*, 1285–1293.

Delle Monache, F.; D'Albuquerque, I. L.; De Andrade Chiappeta, A.; De Mello, J. F. "A Bianthraquinone and 4'-O-Methyl-*Ent*-gallocatechin from *Cassia Trachypus*" *Phytochemistry* **1992**, *31*, 259–261.

Dickstein, J. S.; Mulrooney, C. A.; O'Brien, E. M.; Morgan, B. J.; Kozlowski, M. C. "Development of a Catalytic Aromatic Decarboxylation Reaction" *Org. Lett.* **2007**, *9*, 2441-2444.

DiVirgilio, E. S.; Dugan, E. C.; Mulrooney, C. A.; Kozlowski, M. C. "Asymmetric Total Synthesis of Nigerone" *Org. Lett.* **2007**, *9*, 385–388.

Dolmans, D. E.; Fukumara, D.; Jain, R. K. "Photodynamic Therapy for Cancer" *Nat. Rev. Cancer* **2003**, *3*, 380–387.

Don, M.-J.; Huang, Y.-J.; Huang, R.-L.; Lin, Y.-L. "New Phenolic Principles From *Hypericum sampsonii*" *Chem. Pharm. Bull.* **2004**, *52*, 866–869.

Dougherty, T. J.; Gomer, C. J.; Henderson, B. W.; Jori, G.; Kessel, D; Korbelik, M.; Moan, J.; Peng, Q. "Photodynamic Therapy" *J. Natl. Cancer Inst.* **1998**, *90*, 889–905.

Esser, B.; Swager, T. M. "Detection of Ethylene Gas by Fluorescence Turn-on of a Conjugated Polymer." *Angew. Chem. Int. Ed.* **2010**, *49*, 8872–8875.

Evangelio, E.; Ruiz-Molina, D. "Valence Tautomerism: New Challenges for Electroactive Ligands" *Eur. J. Inorg. Chem.* **2005**, 2957-2971.

Evans, D. H.; Fitch, A. "Measurement of the Thermochromic Equilibrium Constant of a Nonthermochromic Compound: 1,1'-Dimethylbianthrone" *J. Am. Chem. Soc.* **1984**, *106*, 3039–3041.

Fernández, I.; Comini, L.; Nigra, A.; Núñez, S.; Rumie Vittar, B.; Cabrera, J.; Rivarola, V. A. "Photodynamic Action and Localization of Anthraquinones in Cancerous Cells" *Biocell* **2009**, *33*, A266.

Flack H.D. (1983). *Acta. Cryst.,* **A39**, 876-881.

Fotie, J. "Quinones and Malaria." *Anti-Infect. Agents Med. Chem.* **2006**, *5*, 357–366.

Fox, J. M.; Katz, T. J. "Conversion of a [6]Helicene into an [8]Helicene and a Helical 1,10-Phenanthroline Ligand." *J. Org. Chem.* **1999**, *64*, 302–305.

Franck, B.; Chahin, R.; Eckert, H.-G.; Langenberg, R.; Radtke, V. ""Natural Products From Fungi. 27. Biomimetic Synthesis of Skyrin" *Angew. Chem., Int. Ed.* **1975**, *14*, 819–820.

Fujitake, N.; Suzuki, T.; Fukumoto, M.; Oji, Y. "Predomination of Dimers Over Naturally Occurring Anthraquinones in Soil" *J. Nat. Prod*. **1998**, *61*, 189–192.

Georghiou, P. E.; Ashram, M.; Clase, H. J.; Bridson, J. N. "Spirodienone and Bis(spirodienone) Derivatives of Calix[4]naphthalenes" *J. Org. Chem.* **1998**, *63,* 1819–1826.

Gill, M.; Gimenez, A.; McKenzie, R. W. "Pigments of Fungi, Part 8. Bianthraquinones From *Dermocybe Austroveneta*" *J. Nat. Prod.* **1988**, *51*, 1251-1256.

Gingras, M.; Dubois, F. "Synthesis of Carbohelicenes and Derivatives by 'Carbenoid Couplings'" *Tetrahedron Lett.* **1999**, *40*, 1309–1312.

Grandmaison, J.-L.; Brassard, P. "Reactions of Ketene Acetals. 10. Total Syntheses of the Anthraquinones Rubrocomatulin Pentamethyl Ether, 2-Acetylemodin, 2-Acetyl-5-hydroxyemodin Tetramethyl Ether, and Xanthorin" *J. Org. Chem*. **1978**, *43*. 1435–1438.

Griffiths, J. "Benzoquinone and Naphthoquinone Dyes" *Ullmann's Encyclopedia of Industrial Chemistry*, Electronic Release, Wiley-VCH, Weinheim Jan. 2006.

Grove, C. I.; Fettinger, J. C.; Shaw, J. T. "Second-Generation Synthesis of (–)-Viriditoxin" *Synthesis*, **2012**, *44*, 362–371.

Guo, Q.-X.; Wu, Z.-J.; Luo, Z.-B.; Liu, Q.-Z.; Ye, J.-L.; Luo, S.-W.; Cun, L.-F.; Gong, L.-Z. "Highly Enantioselective Oxidative Couplings of 2-Naphthols Catalyzed by Chiral Bimetallic Oxovanadium Complexes with Either Oxygen or Air as Oxidant" *J. Am. Chem. Soc.* **2007**, *129*, 13927–13938.

Hamblin, M. R.; Hasan, T. "Photodynamic Therapy: A New Antimicrobial Approach to Infectious Disease?" *Photochem. Photobiol. Sci.* **2004**, *3*, 436–450.

Hattori, T.; Konno, A.; Adachi, K.; Shizuri, Y. "Four New Bioactive Bromophenols From the Palauan Sponge *Phyllospongia dendyi*" *Fisheries Sci.* **2001**, *67,* 899–903.

Hauser, F. M.; Gauuan, P. J. F. "Total Synthesis of (+/-)-Biphyscion" *Org. Lett.* **1999**, *1*, 671–672.

Hewgley, J. B.; Stahl, S. S.; Kozlowski, M. C. "Mechanistic Study of Asymmetric Oxidative Biaryl Coupling: Evidence for Self-processing of the Copper Catalyst to Achieve Control of Oxidase vs. Oxygenase Activity" *J. Am. Chem. Soc.* **2008**, *130,* 12232–12233.

Hoey, M. D.; Dittmer, D. C. "A Convenient Synthesis of 1,4-Dihydro-2,3-benzoxathiin 3-oxide, a Useful Precursor of *o*-Quinodimethane" *J. Org. Chem.* **1991**, *56*, 1947–1940.

Howard, B. H.; Raistrick, H. "Studies in Biochemistry of Microorganisms. The Colouring Matters of *Penicillum islandicum* Sopp. Part 3. Skyrin and Flavoskyrin" *Biochem. J.* **1954**, *56*, 56–65.

Hussain, H.; Specht, S.; Sarite, S. R.; Saeftel, M.; Hoerauf, A.; Schulz, B.; Krohn, K. "A New Class of Phenazines with Activity against a Chloroquine Resistant Plasmodium falciparum Strain and Antimicrobial Activity." *J. Med. Chem.* **2011**, *54*, 4913–4917.

Iida, H.; Iwahana, S.; Mizoguchi, T.; Yashima, E. "Main-Chain Optically Active Riboflavin Polymer for Asymmetric Catalysis and Its Vapochromic Behavior." *J. Am. Chem. Soc.* **2012**, *134*, 15103–15113.

Iio, H.; Zenfuku, K.; Tokoroyama, T. "A Facile Synthesis of Stentorin, the Photoreceptor of *Stentor coeruleus*" *Tetrahedron Lett.* **1995**, *36*, 5921–5924.

Ikekawa, T. "Isoskyrin" *Chem. Pharm. Bull.* **1963**, *11*, 749–751.

Iwao, M.; Kuraishi, T. "Utilization of Sulfide, Sulfoxide, and Sulfone Groups as Regiochemical Control Elements in the Diels–Alder Reaction of Naphthoquinones" *Bull. Chem. Soc. Jpn.* **1987**, *60*, 4051–4060.

Jang, K.; Brownell, L. V.; Forster, P. M.; Lee, D.-C. "Self-Assembly of Pyrazine-Containing Tetrachloroacenes." *Langmuir* **2011**, *27*, 14615–14620.

Jierry, L.; Harthong, S.; Aronica, C.; Mulatier, J.-C.; Guy, L.; Guy, S. "Efficient Dibenzo[c]acridine Helicene-like Synthesis and Resolution: Scaleup, Structural Control, and High Chiroptical Properties." *Org. Lett.* **2012**, *14*, 288–291.

Kamlet, M. J.; Abboud, J.-L. M.; Abraham, M. H.; Taft, R. W. "Linear Solvation Energy Relationships. 23. A Comprehensive Collection of the Solvatochromic Parameters, π^*, α, and β, and Some Methods for Simplifying the Generalized Solvatochromic Equation." *J. Org. Chem.* **1983**, *48*, 2877–2887.

Kamlet, M. J.; Taft, R. W. “The solvatochromic comparison method. I. The .beta.-scale of solvent hydrogen-bond acceptor (HBA) basicities.” *J. Am. Chem. Soc.* **1976**, *98*, 377–383.

Karikomi, M.; Yamada, M.; Ogawa, Y.; Houjou, H.; Seki, K.; Hiratani, K.; Haga, K.; Uyehara, T. “Novel Synthesis of a Unique Helical Quinone Derivative by Coupling Reaction of 2-Hydroxybenzo[c]phenanthrene” *Tetrahedron Lett.* **2005**, *46*, 5867–5870.

Kasturi, T. R.; Sattigeri, J. A.; Pragnacharyulu, P. V. P. “Reaction of Spironaphthalenones with Hydroxylamine Hydrochloride: Part IV” *Tetrahedron*, **1995**, *51*, 3051–3060.

Kelly, T. R. “Regiochemical Control in the Diels Alder Reactions of Substituted Naphthoquinones: Orientational Manipulation in the Synthesis of Anthraquinones” *Tetrahedron Lett.* **1978**, *19*, 1387–1390.

Kelly, T. R.; Parekh, N. D. "Regiochemical Control in the Diels-Alder Reaction of Substituted Naphthoquinones. The Directing Effects of C-6 Oxygen Substituents" *J. Org. Chem.* **1982**, *47,* 5009–5013.

Khan, A. T.; Blessing, B.; Schmidt, R. R. “An Expedient and Efficient Synthesis of Naturally Occurring Hydroxy Substituted Anthraquinones” *Synthesis* **1994**, 254–257.

Khoramabadi-zad, A.; Yavari, I.; Shiri, A.; Bani, A. “Oxidation of Bisnaphthols to Spironaphthalenones, Revisited” *J. Heterocyclic Chem.* **2008**, *45,* 1351–1358.

Khurana, J. M.; Chaudhary, A.; Lumb, A.; Nand, B. “An Expedient Four-Component Domino Protocol for the Synthesis of Novel Benzo[*a*]phenazine Annulated Heterocycles and Their Photophysical Studies.” *Green Chem.* **2012**, *14*, 2321–2327.

Kim, G. T.; Wenz, M.; Park, J. I.; Hasserodt, J.; Janda, K. D. “Polyene Substrates With Unusual Methylation Patterns to Probe the Active Sites of Three Catalytic Antibodies” *Bioorg. Med. Chem.* **2002**, *10*, 1249–1262.

Kizek, R.; Adam, V.; Hrabeta, J.; Eckschlager, T.; Smutny, S.; Burda, J. V.; Frei, E.; Stiborova, M. “Anthracyclines and Ellipticines as DNA-damaging Anticancer Drugs: Recent Advances” *Pharmacology and Therapeutics* **2012**, *133*, 26–39.

Kozlowski, M. C.; Dugan, E. C.; DiVirgilio, E. S.; Maksimenka, K.; Bringmann, G. “Asymmetric Total Synthesis of Nigerone and *ent*-Nigerone: Enantioselective Oxidative Biaryl Coupling of Highly Hindered Naphthols” *Adv. Synth. Catal.* **2007**, *349*, 583–594.

Kozlowski, M. C.; Li, X.; Carroll, P. J.; Xu, Z. “Copper(II) Complexes of Novel 1,5-Diaza-cis-decalin Diamine Ligands: An Investigation of Structure and Reactivity” *Organometallics* **2002**, *21,* 4513–4522.

Kozlowski, M. C.; Morgan, B. J.; Linton, E. C. "Total Synthesis of Chiral Biaryl Natural Products by Asymmetric Biaryl Coupling" *Chem. Soc. Rev.* **2009**, *38,* 3193–3207.

Kraus, G. A.; Woo, S. H. "Total Synthesis of 11-Deoxydaunomycinone and Analogs by a Tandem Claisen-Diels-Alder Strategy" *J. Org. Chem*. **1987**, *52*, 4841–4846.

Kumagai, Y.; Shinkai, Y.; Miura, T.; Cho, A. K. "The Chemical Biology of Naphthoquinones and its Environmental Implications" *Ann. Rev. Pharmacol. Toxicol.* **2012**, *52*, 221–247.

Laatsch, H. "Synthese von Maritonon und Anderen 8,8'-Bijuglomen" *Liebigs Ann. Chem*. **1985**, 2420–2442.

Lakowicz, J. R. *Principles of Fluorescence Spectroscopy*, 3rd ed.; Springer: New York, 2006.

Laursen, J. B.; Nielsen, J. "Phenazine Natural Products: Biosynthesis, Synthetic Analogues, and Biological Activity." *Chem. Rev.* **2004**, *104*, 1663–1685.

Le, T. P.; Rogers, J. E.; Kelly, L. A. "Photoinduced Electron Transfer in Covalently Linked 1,8-Naphthalimide/Viologen Systems" *J. Phys. Chem. A* **2000**, *104*, 6778–6785.

Lee, D.-C.; Cao, B.; Jang, K.; Forster, P. M. "Self-Assembly of Halogen Substituted Phenazines." *J. Mater. Chem.* **2010**, *20*, 867–873.

Li, X.; Hewgley, J. B.; Mulrooney, C. A.; Yang, J.; Kozlowski, M. C. "Enantioselective Oxidative Biaryl Coupling Reactions Catalyzed by 1,5-Diazadecalin Metal Complexes: Efficient Formation of Chiral Functionalized BINOL Derivatives" *J. Org. Chem.* **2003**, *68,* 5500–5511.

Li, X.; Yang, J.; Kozlowski, M. C. "Enantioselective Oxidative Biaryl Coupling Reactions Catalyzed by 1,5-Diazadecalin Metal Complexes" *Org. Lett.* **2001**, *3,* 1137–1140.

Lin, L.-C.; Chou, C.-J.; Kuo, Y.-C. "Cytotoxic Principles from *Ventilago leiocarpa*" *J. Nat. Prod.* **2001**, *64*, 674–676.

Litwak, A. M.; Grynszpan, F.; Aleksiuk, O.; Chen, S.; Biali, S. E. "Preparation, Stereochemistry, and Reactions of the Bis(spirodienone) Derivatives of *p-tert*-Butylcalix[4larene" *J. Org. Chem.* **1993**, *58*, 393–402.

Long, S.; Parkin, S.; Siegler, M. A.; Cammers, A.; Li, T. "Polymorphism and Phase Behaviors of 2-(Phenylamino)nicotinic Acid." *Cryst. Growth Des.* **2008**, *8*, 4006–4013.

Lou, S.; Moquist, P. N.; Schaus, S. E. "Asymmetric Allylboration of Ketones Catalyzed by Chiral Diols." *J. Am. Chem. Soc.* **2006**, *128*, 12660–12661.

Magdziak, D.; Rodriguez, A. A.; Van De Water, R. W.; Pettus, T. R. R. "Regioselective Oxidation of Phenols to *o*-Quinones with *o*-Iodoxybenzoic Acid" *Org. Lett.* **2002**, *4*, 285–288.

Makgatho, M. E.; Anderson, R.; O'Sullivan, J. F.; Egan, T. J.; Freese, J. A.; Cornelius, N.; van Rensburg, C. E. J. "Tetramethylpiperidine-substituted Phenazines as Novel Anti-plasmodial Agents. *Drug Dev. Res.* **2000**, *50*, 195–202.

Martyn, L. J. P.; Pandiaraju, S.; Yudin, A. K. "Catalytic Applications of F_8BINOL: Asymmetric Oxidation of Sulfides to Sulfoxides." *J. Organomet. Chem.* **2000**, *603*, 98–104.

Mataka, S.; Moriyama, H.; Sawada, T.; Takahashi, K.; Sakashita, H.; Tashiro, M. "Conformational Polymorphism of Mechanochromic 5,6-Di(*p*-chlorobenzoyl)-1,3,4,7-tetraphenylbenzo[*c*]thiophene." *Chem. Lett.* **1996**, 363–364.

McDonald, L. A.; Abbanat, D. R.; Barbieri, L. R.; Bernan, V. S.; Discafani, C. M.; Greenstein, M.; Janota, K.; Korshalla, J. D.; Lassota, P.; Tischler, M.; Carter, G. T. "Spiroxins, DNA Cleaving Antitumor Antibiotics From a Marine-Derived Fungus" *Tetrahedron Lett.* **1999**, *40*, 2489–2492.

McOmie, J. F. W.; Blatchly, J. M. The Thiele-Winter Acetoxylation of Quinones. In *Organic Reactions*, Wiley: New York, **1972**, 19, 199–203.

Mercep, M.; Mesic, M., Hrvacic, B.; Elenkov, I. J.; Malnar, I.; Markovic, S.; Simicic, L.; Klonkay, A. C.; Filipovic, A.; PCI Int. Appl. WO2005010006-A1, Feb. 3, 2005.

Mercep, M.; Mesic, M., Hrvacic, B.; Elenkov, I. J.; Malnar, I.; Markovic, S.;; Klonkay, A. C.; Filipovic, A., Simicic, L.; "Substituted Furochromene Compounds of Antiinflammatory Action" PCI Int. Appl. WO2005/10006-A1, Feb. 3, 2005.

Minatti, A.; Dötz, K. H. "Quinoid BINOL-type Compounds as a Novel Class of Chiral Ligands." *Tetrahedron: Asymmetry* **2005**, *16*, 3256–3267.

Morgan, B. J.; Dey, S.; Johnson, S. W.; Kozlowski, M. C. "Total Synthesis of Cercosporin and New Photodynamic Perylenequinones: Inhibition of the Protein Kinase C Regulatory Domain" *J. Am. Chem. Soc.* **2009**, *131,* 9413–9425.

Morgan, B. J.; Mulrooney, C. A.; Kozlowski, M. C. "Perylenequinone Natural Products: Evolution of the Total Synthesis of Cercosporin" *J. Org. Chem.* **2010**, *75,* 44–56.

Morgan, B. J.; Mulrooney, C. A.; O'Brien, E. M.; Kozlowski, M. C. "Perylenequinone Natural Products: Total Synthesis of the Diastereomers (+)-Phleichrome and (+)-Calphostin D by Assembly of Centrochiral and Axial Chiral Fragments" *J. Org. Chem.* **2010**, *75,* 30–43.

Motoyoshiya, J.; Kameda, T; Asari, M.; Miyamoto, M.; Narita, S.; Aoyama, H.; Hayashi, S. "Importance of the Role of Secondary Orbital Interactions in the

Diels–Alder Reaction. Regioselectivity in the Catalyzed and Uncatalyzed Reactions of Juglone and Aliphatic Dienes" *J. Chem. Soc., Perkin Trans. 2* **1997**, 1845–1850.

Motoyoshiya, J.; Masue, Y.; Nishi, Y.; Aoyama, H. "Synthesis of Hypericin via Emodin Anthrone Derived From a Two-Fold Diels-Alder Reaction of 1,4-Benzoquinone" *Nat. Prod. Commun.* **2007**, *2*, 67–70.

Mulrooney, C. A.; Li, X.; DiVirgilio, E. S.; Kozlowski, M. C. "General Approach for the Synthesis of Chiral Perylenequinones via Catalytic Enantioselective Oxidative Biaryl Coupling" *J. Am. Chem. Soc.* **2003**, *125,* 6856–6857.

Mulrooney, C. A.; Morgan, B. J.; Li, X.; Kozlowski, M. C. "Perylenequinone Natural Products: Asymmetric Synthesis of the Oxidized Pentacyclic Core" *J. Org. Chem.* **2010**, *75,* 16–29.

Mulrooney, C. A.; O'Brien, E. M.; Morgan, B. J.; Kozlowski, M. C. "Perylenequinones: Isolation, Synthesis and Biological Activity" *Eur. J. Org. Chem*. **2012**, 3887–3904.

Murphy, A. R.; Fréchet, J. M. J. "Organic Semiconducting Oligomers for Use in Thin Film Transistors." *Chem. Rev.* **2007**, *107*, 1066–1096.

Nakano, D.; Hirano, R.; Yamaguchi, M.; Kabuto, C. "Synthesis of Optically Active Bihelicenols" *Tetrahedron Lett.* **2003**, *44*, 3683–3686.

Nakano, K.; Hidehira, Y.; Takahashi, K.; Hiyama, T.; Nozaki, K. "Stereospecific Synthesis of Hetero[7]helicenes by Pd-Catalyzed Double *N*-Arylation and Intramolecular *O*-Arylation" *Angew. Chem. Int. Ed.* **2005**, *44*, 7136–7138.

Nicolaou, K. C.; Lim, Y. H.; Piper, J. L.; Papageorgiou, C. D. "Total Syntheses of 2,2 '-*Epi*-Cytoskyrin A, Rugulosin, and the Alleged Structure of Rugulin" *J. Am. Chem. Soc*. **2007**, *129*, 4001–4013.

Nicolaou, K. C.; Papageorgiou, C. D.; Piper, J. L.; Chadha, R. K. "The Cytoskyrin Cascade: A Facile Entry into Cytoskyrin A, Deoxyrubroskyrin, Rugulin, Skyrin, and Flavoskyrin Model Systems" *Angew. Chem. Int. Ed*. **2005**, *44*, 5846–5851.

Norton, R. S.; Croft, K. D.; Wells, R. J. "Polybrominated Oxydiphenol Derivatives From the Sponge *Dysidea herbacea*" *Tetrahedron* **1981**, *37,* 2341–2349.

Núñez Montoya, S. C.; Agnese, A. M.; Cabrera, J. L. "Anthraquinone Derivatives from *Heterophyllaea pustulata*" *J. Nat. Prod.* **2006**, *69*, 801–803.

Núñez Montoya, S. C.; Comini, L. R.; Rumie Vittar, B.; Fernández, I. M.; Rivarola, V. A.; Cabrera, J. L. "Phototoxic Effects of *Heterophyllaea pustulata* (Rubiaceae)" *Toxicon* **2008**, *51*, 1409–1415.

O'Brien, E. M.; Li, J.; Carroll, P. J.; Kozlowski, M. C. "Synthesis of the Cores of Hypocrellin and Shiraiachrome: Diastereoselective 1,8-Diketone Aldol Cyclization" *J. Org. Chem.* **2010**, *75*, 69–73.

O'Brien, E. M.; Morgan, B. J.; Kozlowski, M. C. "Dynamic Stereochemistry Transfer in a Transannular Aldol Reaction: Total Synthesis of Hypocrellin A" *Angew. Chem. Int. Ed.* **2008**, *47*, 6877–6880.

O'Brien, E. M.; Morgan, B. J.; Mulrooney, C. A.; Carroll, P. J.; Kozlowski, M. C. "Perylenequinone Natural Products: Total Synthesis of Hypocrellin A" *J. Org. Chem.* **2010**, *75*, 57–68.

O'Brien, P. J. "Molecular Mechanisms of Quinone Cytotoxicity" *Chem.-Biol. Interact.* **1991**, *80*, 1–41. (c) Medentsev, A. G.; Akimenko, V. K. "Naphthoquinone Metabolites of the Fungi" *Phytochemistry* **1998**, *47*, 935–959.

Okamoto, I.; Doi, H.; Kotani, E.; Takeya, T. "The Aryl-Aryl Coupling Reaction of 1-Naphthol With $SnCl_4$ for 2,2'-Binaphthol Synthesis and its Application to the Biomimetic Synthesis of Binaphthoquinone Isolated From *Plumbago zeylanica*" *Tetrahedron Lett.* **2001**, *42,* 2987–2989.

Okuyama, E.; Hossain, C. F.; Yamazaki, M. "Monomine Oxidase Inhibitors from a Lichen, *Solorina crocea* (L.) ACH" *Shoyakugaku Zasshi*, **1991**, *45*, 159–162.

ORTEP-II: A Fortran Thermal Ellipsoid Plot Program for Crystal Structure Illustrations". C.K. Johnson (1976) ORNL-5138.

Park, Y. S.; Grove, C. I.; González-López, M.; Urgaonkar, S.; Fettinger, J. C.; Shaw, J. T. "Synthesis of (–)-Viriditoxin: A 6,6'-Binaphthopyran-2-one that Targets the Bacterial Cell Division Protein FtsZ" *Angew. Chem. Int. Ed.* **2011**, *50*, 3730–3733.

Parker, J. C.; McPherson, R. K.; Andrews, K. M.; Levy, C. B.; Dubins, J. S.; Chin, J. E.; Perry, P. V.; Hulin, B.; Perry, D. A.; Inagaki, T.; Dekker, K. A.; Tachikawa, K.; Sugie, Y.; Treadway, J. L. "Effects of Skyrin, a Receptor-Selective Glucagon Antagonist, in Rat and Human Hepatocytes" *Diabetes* **2000**, *49*, 2079–2086.

Pauliukaite, R.; Ghica, M. E.; Barsan, M. M.; Brett, C. M. A. "Phenazines and Polyphenazines in Electrochemical Sensors and Biosensors." *Anal. Lett.* **2010**, 1588–1608.

Pelter, A.; Ward, R. S. "Two-Electron Phenolic Oxidations Using Phenyliodonium Dicarboxylates" *Tetrahedron* **2001**, *57*, 273–282.

Pinto, A. V.; de Castro, S. L. "The Trypanocidal Activity of Naphthoquinones: A Review" *Molecules* **2009**, *14*, 4570–4590.

Podlesny, E. E.; Carroll, P. J.; Kozlowski, M. C. "Selective Oxidation of 8,8'-Hydroxylated Binaphthols to Bis-spironaphthalenones or Binaphtho-*para*- and Binaphtho-*ortho*-quinones" *Org. Lett*. **2012**, *14*, 4862–4865.

Podlesny, E. E.; Kozlowski, M. C. "A Divergent Approach to the Bisanthraquinone Natural Products: Total Synthesis of (*S*)-Bisoranjidiol and Derivatives From Binaphtho-*para*-quinones" *J. Org. Chem.* Submitted for review.

Podlesny, E. E.; Kozlowski, M. C. "Enantioselective Total Synthesis of (*S*)-Bisoranjidiol, an Axially Chiral Bisanthraquinone" *Org. Lett.* **2012**, *14*, 1408–1411.

Podlesny, E. E.; Kozlowski, M. C. "Structural Reassignment of a Marine Metabolite from a Binaphthalenetetrol to a Tetrabrominated Diphenyl Ether" *J. Nat. Prod*. **2012**, *75*, 1125–1129.

Pouységu, L.; Sylla, T.; Garnier, T.; Rojas, L. B.; Charris, J.; Deffieux, D.; Quideau, S. "Hypervalent Iodine-Mediated Oxygenative Phenol Dearomatization Reactions" *Tetrahedron* **2010**, *66*, 5908–5917.

Pozzo, J.-L.; Clavier, G. M.; Desvergne, J. P. "Rational Design of New Acid-Sensitive Organogelators." *J. Mater. Chem*. **1998**, *8*, 2575–2577.

Pu, L. "1,1'-Binaphthyl Dimers, Oligomers, and Polymers: Molecular Recognition, Asymmetric Catalysis, and New Materials." *Chem. Rev.* **1998**, *98*, 2405–2494.

R1 = $S||F_o| - |F_c|| / S|F_o|$; wR2 = $[Sw(F_o^2 - F_c^2)^2/Sw(F_o^2)^2]^{½}$; GOF = $[Sw(F_o^2 - F_c^2)^2/(n - p)]^{½}$ where n = the number of reflections and p = the number of parameters refined.

Reeder, J.; Castro, P. P.; Knobler, C. B. "Chiral Recognition of Cinchona Alkaloids at the Minor and Major Grooves of 1,l'-Binaphthyl Receptors." *J. Org. Chem*. **1994**, *59*, 3151–3160.

Reichardt, C.; Welton, T. *Solvents and Solvent Effects in Organic Chemistry*, 4th ed.; Wiley-VCH: Germany, 2011.

REQAB4: R.A. Jacobsen, (1994). Private Communication.

Roberge, G.; Brassard, P. "Reactions of Ketene Acetals. 12. A Regiospecific Synthesis of Anthragallols" *Synthesis* **1981**, 381–384.

Rodrigues de Almeida, E. "Preclinical and Clinical Studies of Lapachol and Beta-Lapachone" *The Open Natural Products Journal* **2009**, *2*, 42–47.

Rüedi, P.; Uchida, M.; Eugster, C. H. "Partialsynthese der Grandidone A, B, 7-Epi-B, C, D und 7-Epi-D aus 14-Hydroxytaxodion" *Helv. Chim. Acta* **1981**, *64*, 2251–2256.

Santesson, J. “Anthraquinonoid Pigments of *Trypetheliopsis boninensis* and *Ocellularia domingensis*” *Acta Chem. Scand.* **1970**, *24*, 3331–3334.

Savard, J.; Brassard, P. “Reactions of Ketene Acetals-14. The Use of Simple Mixed Vinylketene Acetals in the Annulation of Quinones” *Tetrahedron* **1984**, *40*, 3455–3464.

Savard, J.; Brassard, P. “Regiospecific Syntheses of Quinones Using Vinylketene Acetals Derived From Unsaturated Esters” *Tetrahedron Lett.* **1979**, *20*, 4911–4914.

Schneider, J. F.; Nieger, M.; Nättinen, K.; Lewall, B.; Niecke, E.; Dötz, K. H. “Novel [6]- and [7]Helicene-Like Quinones via Mono- and Bidirectional Chromium-Templated Benzannulation of Bridged Binaphthyl Carbene Complexes.” *Eur. J. Org. Chem.* **2005**, 1541–1560.

Scholl, R.; Liese, K.; Michelson, K.; Grunewald, E. “Eine neue Synthese des 4,4'-Dimethyl-pyranthrons” *Ber.* **1910**, *43*, 512–518.

Sheldrick, G.M. (2007) SADABS. University of Gottingen, Germany.

Sheldrick, G.M. (2008) Acta Cryst. A64,112-122.

Sheldrick, G.M. (2008) CELL_NOW. University of Gottingen, Germany.

Sheldrick, G.M. (2008) TWINABS. University of Gottingen, Germany.

Sheth, A. R.; Lubach, J. W.; Munson, E. J.; Muller, F. X.; Grant, D. J. W. “Mechanochromism of Piroxicam Accompanied by Intermolecular Proton Transfer Probed by Spectroscopic Methods and Solid-Phase Changes.” *J. Am. Chem. Soc.* **2005**, *127*, 6641–6651.

Shibata, S.; Tanaka, O.; Kitagawa, I. “Metabolic Products of Fungi V. The Structure of Skyrin” *Pharm. Bull.* **1955**, *3*, 278–283.

Shultz, D. A. "Structure-Property Relationships in New Serniquinone-Type Ligands: Past, Present, and Future Research Efforts" *Comments Inorg. Chem.* **2002**, *23,* 1-21.

Singh, J.; Singh, J. “A Bianthraquinone and a Triterpenoid From the Seeds of *Cassia Hirsuta*” *Phytochemistry*, **1986**, *25*, 1985–1987.

Singh, P.; Baheti, A.; Thomas, K. R. J. “Synthesis and Optical Properties of Acidochromic Amine-Substituted Benzo[*a*]phenazines.” *J. Org. Chem.* **2011**, *76*, 6134–6145.

Singh, V.; Singh, J.; Sharma, J. P. “Anthraquinones From Heartwood of *Cassia Siamea*” *Phytochemistry* **1992**, *31*, 2176–2177.

Somei, H.; Asano, Y.; Yoshida, T.; Takizawa, S.; Yamataka, H.; Sasai, H. "Dual Activation in a Hemolytic Coupling Reaction Promoted by an Enantioselective Dinuclear Vanadium(IV) Catalyst." *Tetrahedron Lett.* **2004**, *45,* 1841–1844.

Son, H.-O.; Han, W.-S.; Wee, K.-R.; Yoo, D.-H.; Lee, J.-H.; Kwon, S. N.; Ko, J.; Kang, S. O. "Turning on Fluorescent Emission from C-Alkylation on Quinoxaline Derivatives." *Org. Lett*. **2008**, *10*, 5401–5404.

Son, H.-O.; Han, W.-S.; Yoo, D.-H.; Min, K.-T.; Kwon, S.-N.; Ko, J.; Kang, S. O. "Fluorescence Control on Panchromatic Spectra via C-Alkylation on Arylated Quinoxalines." *J. Org. Chem.* **2009**, *74*, 3175–3178.

Spyroudis, S. "Hydroxyquinones: Synthesis and Reactivity" *Molecules* **2000**, *5*, 1291–1330.

Steglich, W.; Jedtke, K.-F. "Novel Anthraquinone Pigments from *Solorina crocea*" *Z. Naturforsch.* **1976**, *31C*, 197–198.

Steiner, T. "The Hydrogen Bond in the Solid State" *Angew. Chem. Int. Ed.* **2002**, *41*, 48–76.

Sucunza, D.; Dembkowski, D.; Neufeind, S.; Velder, J.; Lex, J.; Schmalz, H.- G. "Synthesis of a Mumbaistatin Analogue Through Cross-Coupling" *Synlett* **2007**, 2569–2573.

Sunassee, S. N.; Davies-Coleman, M. T. "Cytotoxic and Antioxidant Marine Prenylated Quinones and Hydroquinones" *Nat. Prod. Rep.* **2012**, *29*, 513–535.

Taft, R. W.; Abboud, J.-L. M.; Kamlet, M. J. "Linear Solvation Energy Relationships. 28. An Analysis of Swain's Solvent 'Acity' and 'Basity' Scales." *J. Org. Chem.* **1984**, *49*, 2001–2005.

Takeya, T.; Doi, H.; Ogata, T.; Okamoto, I.; Kotani, E. "Aerobic Oxidative Dimerization of 1-Naphthols to 2,2'-Binaphthoquinones Mediated by $SnCl_4$ and its Application to Natural Product Synthesis" *Tetrahedron* **2004**, *60,* 9049–9060.

Takeya, T.; Otsuka, T.; Okamoto, I.; Kotani, E. "Semiconductor-Mediated Oxidative Dimerization of 1-Naphthols with Dioxygen and *o*-Demethylation of the Enol-Ethers by SnO_2 Without Dioxygen" *Tetrahedron* **2004**, *60,* 10681–10693.

Takizawa, S.; Katayama, T.; Kameyama, C.; Onitsuka, K.; Suzuki, T.; Yanagida, T.; Kawai, T.; Sasai, H. "Chiral Dinuclear Vanadium(V) Catalysts for Oxidative Coupling of 2-Naphthols" *Chem. Commun.* **2008**, 1810–1812.

Takizawa, S.; Katayama, T.; Sasai, H. "Dinuclear Chiral Vanadium Catalysts for Oxidative Coupling of 2-Naphthols *via* a Dual Activation Mechanism" *Chem. Commun.* **2008**, 4113–4122.

Takizawa, S.; Katayama, T.; Somei, H.; Asano, Y.; Yoshida, T.; Kameyama, C.; Rajesh, D.; Onitsuka, K.; Suzuki, T.; Mikami, M.; Yamataka, H.; Jayaprakash, D.; Sasai, H. "Dual Activation in Oxidative Coupling of 2-Naphthols Catalyzed by Chiral Dinuclear Vanadium Complexes" *Tetrahedron* **2008**, *64,* 3361–3371.

Tanaka, O. "Metabolic Products of Fungi. XIV. The Structure of Skyrin. (3). On Pseudoskyrin" *Chem. Pharm. Bull.* **1958**, *6,* 203–208.

Tanaka, O. "Metabolic Products of Fungi. XIV. The Structure of Skyrin (3). On Pseudoskyrin" *Chem. Pharm. Bull.* **1958**, *2*, 203–208.

Tanaka, O.; Kaneko, C. "Metabolic Products of Fungi. VI. The Structure of Skyrin. II. Synthesis of Skyrin Beta, Beta'-Dimethyl Ether" *Pharm. Bull.* **1955**, *3*, 284–286.

Tapuhi, Y.; Kalisky, O.; Agranat, I. "Thermochromism and Thermal E,Z Isomerizations in Bianthrones" *J. Org. Chem.* **1979**, *44*, 1949–1952.

Thomas III, S.W.; Joly, G. D.; Swager, T. M. "Chemical Sensors Based on Amplifying Fluorescent Conjugated Polymers." *Chem. Rev.* **2007**, *107*, 1339–1386.

Thomson, R. H. *Naturally Occurring Quinones III: Recent Advances*, 3rd ed.; Chapman and Hall: New York, 1987.

Tietz, L. F.; Gericke, K. M.; Schuberth, I. "Synthesis of Highly Functionalized Anthraquinones and Evaluation of Their Antitumor Activity" *Eur. J. Org. Chem.* **2007**, 4563–4577.

Tietz, L. F.; Gericke, K. M.; Singidi, R. R.; Schuberth, I. "Novel Strategies for the Synthesis of Anthrapyran Antibiotics: Discovery of a New Antitumor Agent and Total Synthesis of (*S*)-Espicufolin" *Org. Biomol. Chem.* **2007**, *5*, 1191–1200.

Turner, H. M.; Patel, J.; Niljianskul, N.; Chong, J. M. "Binaphthol-Catalyzed Asymmetric Conjugate Arylboration of Enones." *Org. Lett.* **2011**, *13*, 5796–5799.

Uchida, M.; Miyase, T.; Yoshizaki, F.; Bieri, J. H.; Rüedi, P.; Eugster, C. H. "14-Hydroxytaxodion als Hauptditerpen in *Plectranthus grandiden tatus* GÜRKE; Isolierung von Sieben Neuen Dimeren Diterpenen aus *P. grandidentatus, P. myrianthus* BRIQ. und *Coleus carnosus* HASSK.: Strukturen der Grandidone A, 7-Epi-A, B, 7-Epi-B, C, D und 7-Epi-D" *Helv. Chim. Acta* **1981**, *64*, 2227–2250.

Uliana, M. P.; Vieira, Y. W.; Donatoni, M. C.; Corrêa, A. G.; Brocksom, U.; Brocksom, T. J. "Oxidation of Mono-Phenols to *Para*-Benzoquinones: A Comparative Study" *J. Braz. Chem. Soc.* **2008**, *19*, 1484–1489.

Upadhyay, S. I.; Karnik, A. V. "Enantioselective Synthesis of (*R*) and (*S*)-[9,9']Bi[naphtha(2,1-*b*)furanyl]-8,8'-diol: A Furo-Fused BINOL Derivative" *Tetrahedron Lett.* **2007**, *48*, 317–318.

Urleb, U. Phenazines. In *Houben-Weyl Methods of Organic Chemistry* **1998**, Vol. E 9b2; pp 266–303.

v.d. Sluis, P. & A.L. Spek (1990). *Acta. Cryst.*, A46, 194.

Van Dort, H. M.; Guersen, H. J. "Salcomine-Catalyzed Oxidations of Some Phenols: A New Method for the Preparation of a Number of *Para*-Benzoquinones" *Recl. Trav. Chim. Pays-Bas* **1967**, *86*, 520–526.

Vargas, F.; Rivas, C.; Zoltan, T.; Lopez, V.; Ortega, J.; Izzo, C.; Pineda, M.; Medina, J.; Medina, E.; Rosales, L. "Antioxidant and Scavenging Activity of Skyrin on Free Radical and Some Reactive Oxygen Species" *Avances en Química* **2008**, *3*, 7–14.

Wakamatsu, T.; Nishi, T.; Ohnuma, T.; Ban, Y. "A Convenient Synthesis of Juglone Via Neutral Salcomine Oxidation" *Synth. Commun.* **1984**, *14*, 1167–1173.

Wang, D.-Y.; Wang, J.-L.; Zhang, D.-W.; Li, Z.-T. "NH···X (X = F, Cl, Br, and I) hydrogen bonding in aromatic amide derivatives in crystal structures" *Sci. China Chem.* **2012**, *55*, 2018–2026.

West, K. R.; Ludlow, R. F.; Corbett, P. T.; Besenius, P.; Mansfeld, F. M.; Cormack, P. A. G.; Sherrington, D. C.; Goodman, J. M.; Stuart, M. C. A.; Otto, S. "Dynamic Combinatorial Discovery of a [2]-Catenane and its Guest-Induced Conversion into a Molecular Square Host" *J. Am. Chem. Soc.*, **2008**, *130*, 10834–10835).

Wirz, A.; Simmen, U.; Heilmann, J.; Calis, I.; Meier, B.; Sticher, O. "Bisanthraquinone Glycosides of *Hypericum perforatum* With Binding Inhibition to CRH-1 Receptors" *Phytochemistry* **2000**, *55*, 941–947.

Yamamoto, K.; Noda, K.; Okamoto, Y. "Synthesis and Chiral Recognition of Optically Active Crown Ethers incorporating a 4,4'-Biphenanthryl Moiety as the Chiral Centre" *J. Chem. Soc., Chem. Commun.* **1985**, 1065–1066.

Yamamoto, K.; Noda, K.; Okamoto, Y. "Synthesis and Chiral Recognition of Optically Active Crown Ethers Incorporating a 4,4'-Biphenanthryl Moiety as the Chiral Centre" *J. Chem. Soc., Chem. Commun.* **1985**, 1065–1066.

Yamamura, K.; Ono, S.; Ogoshi, H.; Masuda, H.; Kuroda, Y. "Chiral Liquid Crystal Mesogens. Synthesis and Determination of Absolute Configuration of Mesogens with 4,4'-Biphenanthryl Cores" *Synlett*, **1989**, 18–19.

Yano, S.; Hirohara, S.; Obata, M.; Hagiya, Y.; Ogura, S.; Ikeda, A.; Kataoka, H.; Tanaka, M.; Joh, T. J. "Current States and Future Views in Photodynamic Therapy" *Photochem. Photobiol., C* **2011**, *12*, 46–67.

Yu, L. "Color Changes Caused by Conformational Polymorphism: Optical-Crystallography, Single-Crystal Spectroscopy, and Computational Chemistry." *J. Phys. Chem. A*. **2002**, *106*, 544–550.

Zimmer, H.; Lankin, D. C.; Horgan, S. W. “Oxidations with Potassium Nitrosodisulfonate (Fremy’s Radical). The Teuber Reaction” *Chem. Rev.* **1971**, *71*, 229–246.